

function of the relative distance  $D/r$  between two identical loops with  $r = 30\text{cm}$  and  $a = 2\text{cm}$ .

Fig. 22(b) illustrates the strong-coupling factor  $U$  and the strong-interference factor  $V$  as a curve in the  $U - V$  plane, parametrized with the relative distance  $D/r$  between the two loops, for the cases with interference and eigenfrequency  $f_\eta$  (solid), with interference and eigenfrequency  $f_U$  (dashed), and without interference and eigenfrequency  $f_U$  (dotted).

Fig. 22(c) shows the efficiency enhancement ratio of the solid curve in Fig. 22(b) relative to the dashed and dotted curves in Fig. 22(b).

Fig. 23 shows the radiation efficiency as a function of the resonant eigenfrequency of two identical capacitively-loaded conducting single-turn loops. Results for two different loop dimensions are shown and for two relative distances between the identical loops. For each loops dimension and distance, four different cases are examined: without far-field interference (dotted), with far-field interference but no driving-frequency detuning (dashed) and with driving-frequency detuning to maximize either the efficiency (solid) or the ratio of efficiency over radiation (dash-dotted).

Fig. 24 shows CMT results for (a) the coupling factor  $k$  and (b) the strong-coupling factor  $U$ , for three different  $m$  values of subwavelength resonant modes of two same dielectric disks at distance  $D/r = 5$  (and also a couple more distances for  $m = 2$ ), when varying their  $\epsilon$  in the range  $250 \geq \epsilon \geq 35$ . Note that disk-material loss-tangent  $\tan \delta = 6 \cdot 10^{-6} \epsilon - 2 \cdot 10^{-4}$  was used. (c) Relative  $U$  error between CMT and numerical FEFD calculations of part (b).

Fig. 25 shows Antenna Theory (AT) results for (a) the normalized interference term  $2\Lambda / \sqrt{\omega_1 \omega_2}$  and (b) magnitude of the strong-interference factor  $|V|$ , as a function of frequency, for the exact same parameters as in Fig.24. (c) Relative  $V$  error between AT and numerical FEFD calculations of part (b).

Fig. 26 shows results for the overall power transmission as a function of frequency, for the same set of resonant modes and distances as in Figs.24 and 25, based on the predictions including interference (solid lines) and without interference, just from  $U$  (dotted lines).

Fig. 27 (a) shows the frequencies  $f_U$  and  $f_\eta$ , where the strong-coupling factor  $U$  and the power-transmission efficiency  $\eta$  are respectively maximized, as a function of the transfer distance between the  $m = 2$  disks of Fig. 15. Fig. 27(b) shows the efficiencies achieved at the frequencies of (a) and, in inset, the enhancement ratio of the optimal (by definition) efficiency for  $f_\eta$  versus the achievable efficiency at  $f_U$ . Fig. 27(c) shows the  $D$ -parametrized path of the transmission efficiency for the frequency choices of (a) on the  $U - V$  efficiency map.

Fig. 28 shows results for the radiation efficiency as a function of the transfer distance at resonant frequency  $f_U$ , when the operating frequency is detuned (solid line), when it is not (dashed line), and when there is no interference whatsoever (dotted line). In the inset, we show the corresponding radiation suppression factors.

Figs. 29(a)-(b) show schematics for frequency control mechanisms.

Figs. 30(a)-(c) illustrate a wireless energy transfer scheme using two dielectric disks in the presence of various extraneous objects.

## DETAILED DESCRIPTION

### 1. Efficient energy-transfer by ‘strongly coupled’ resonances

Fig. 1 shows a schematic that generally describes one example of the invention, in which energy is transferred wirelessly between two resonant objects. Referring to Fig. 1, energy is transferred, over a distance  $D$ , between a resonant source object having a characteristic size  $r_1$  and a resonant device object of characteristic size  $r_2$ . Both objects are resonant objects. The wireless non-radiative energy transfer is performed using the field (e.g. the electromagnetic field or acoustic field) of the system of two resonant objects.

The characteristic size of an object can be regarded as being equal to the radius of the smallest sphere which can fit around the entire object. The characteristic thickness of an object can be regarded as being, when placed on a flat surface in any arbitrary configuration, the smallest possible height of the highest point of the object above a flat surface. The characteristic width of an object can be regarded as being the radius of the

smallest possible circle that the object can pass through while traveling in a straight line. For example, the characteristic width of a cylindrical object is the radius of the cylinder.

It is to be understood that while two resonant objects are shown in the example of Fig. 1, and in many of the examples below, other examples can feature three or more resonant objects. For example, in some examples, a single source object can transfer energy to multiple device objects. In some examples, energy can be transferred from a first resonant object to a second resonant object, and then from the second resonant object to a third resonant object, and so forth.

Initially, we present a theoretical framework for understanding non-radiative wireless energy transfer. Note however that it is to be understood that the scope of the invention is not bound by theory.

Different temporal schemes can be employed, depending on the application, to transfer energy between two resonant objects. Here we will consider two particularly simple but important schemes: a one-time finite-amount energy-transfer scheme and a continuous finite-rate energy-transfer (power) scheme.

### 1.1 Finite-amount energy-transfer efficiency

Let the source and device objects be 1, 2 respectively and their resonance eigemodes, which we will use for the energy exchange, have angular frequencies  $\omega_{1,2}$ , frequency-widths due to intrinsic (absorption, radiation etc.) losses  $\Gamma_{1,2}$  and (generally) vector fields  $\mathbf{F}_{1,2}(\mathbf{r})$ , normalized to unity energy. Once the two resonant objects are brought in proximity, they can interact and an appropriate analytical framework for modeling this resonant interaction is that of the well-known coupled-mode theory (CMT). In this picture, the field of the system of the two resonant objects 1, 2 can be approximated by  $\mathbf{F}(\mathbf{r}, t) = a_1(t)\mathbf{F}_1(\mathbf{r}) + a_2(t)\mathbf{F}_2(\mathbf{r})$ , where  $a_{1,2}(t)$  are the field amplitudes, with  $|a_{1,2}(t)|^2$  equal to the energy stored inside the object 1, 2 respectively, due to the normalization. Then, using  $e^{-i\omega t}$  time dependence, the field amplitudes can be shown to satisfy, to lowest order:

$$\begin{aligned}\frac{d}{dt}a_1(t) &= -i(\omega_1 - i\Gamma_1)a_1(t) + i\kappa_{11}a_1(t) + i\kappa_{12}a_2(t) \\ \frac{d}{dt}a_2(t) &= -i(\omega_2 - i\Gamma_2)a_2(t) + i\kappa_{21}a_1(t) + i\kappa_{22}a_2(t)\end{aligned}\quad (1)$$

where  $\kappa_{11,22}$  are the shifts in each object's frequency due to the presence of the other, which are a second-order correction and can be absorbed into the eigenfrequencies by setting  $\omega_{1,2} \rightarrow \omega_{1,2} + \kappa_{11,22}$ , and  $\kappa_{12,21}$  are the coupling coefficients, which from the reciprocity requirement of the system must satisfy  $\kappa_{21} = \kappa_{12} \equiv \kappa$ .

The normal modes of the combined system are found, by substituting  $[a_1(t), a_2(t)] = [A_1, A_2]e^{-i\bar{\omega}t}$ , to have complex frequencies

$$\bar{\omega}_{\pm} = \frac{\omega_1 + \omega_2}{2} - i\frac{\Gamma_1 + \Gamma_2}{2} \pm \sqrt{\left(\frac{\omega_1 - \omega_2}{2} - i\frac{\Gamma_1 - \Gamma_2}{2}\right)^2 + \kappa^2}\quad (2)$$

whose splitting we denote as  $\delta_E \equiv \bar{\omega}_+ - \bar{\omega}_-$ . Note that, at exact resonance  $\omega_1 = \omega_2$  and for  $\Gamma_1 = \Gamma_2$ , we get  $\delta_E = 2\kappa$ .

Assume now that at time  $t = 0$  the source object 1 has finite energy  $|a_1(0)|^2$ , while the device object has  $|a_2(0)|^2 = 0$ . Since the objects are coupled, energy will be transferred from 1 to 2. With these initial conditions, Eqs.(1) can be solved, predicting the evolution of the device field-amplitude to be

$$\frac{a_2(t)}{|a_1(0)|} = \frac{2\kappa}{\delta_E} \sin\left(\frac{\delta_E t}{2}\right) e^{-\frac{\Gamma_1 + \Gamma_2}{2}t}\quad (3)$$

The energy-transfer efficiency will be  $\eta_E \equiv |a_2(t)|^2/|a_1(0)|^2$ . Note that, at exact resonance  $\omega_1 = \omega_2$  and in the special case  $\Gamma_1 = \Gamma_2 \equiv \Gamma_0$ , Eq.(3) can be written as

$$\frac{a_2(T)}{|a_1(0)|} = \sin(UT)e^{-T}\quad (4)$$

where  $T \equiv \Gamma_0 t$  and  $U = \kappa/\Gamma_0$ .

In some examples, the system designer can adjust the duration of the coupling  $t$  at will. In some examples, the duration  $t$  can be adjusted to maximize the device energy (and thus efficiency  $\eta_E$ ). Then, in the special case  $\Gamma_1 = \Gamma_2 = \Gamma_o$ , it can be inferred from Eq.(4) that  $\eta_E$  is maximized for

$$T_* = \frac{\tan^{-1} U}{U} \tag{5}$$

resulting in an optimal energy-transfer efficiency

$$\eta_{E^*} \equiv \eta_E(T_*) = \frac{U^2}{1+U^2} \exp\left(-\frac{2 \tan^{-1} U}{U}\right) \tag{6}$$

which is only a function of the coupling-to-loss ratio  $U = \kappa/\Gamma_o$  and tends to unity when  $U \gg 1$ , as depicted in Fig.2(c). In general, also for  $\Gamma_1 \neq \Gamma_2$ , the energy transfer is nearly perfect, when the coupling rate is much faster than all loss rates ( $\kappa/\Gamma_{1,2} \gg 1$ ).

In a real wireless energy-transfer system, the source object can be connected to a power generator (not shown in Fig.1), and the device object can be connected to a power consuming load (e.g. a resistor, a battery, an actual device, not shown in Fig.1). The generator will supply the energy to the source object, the energy will be transferred wirelessly and non-radiatively from the source object to the device object, and the load will consume the energy from the device object. To incorporate such supply and consumption mechanisms into this temporal scheme, in some examples, one can imagine that the generator is very briefly but very strongly coupled to the source at time  $t = 0$  to almost instantaneously provide the energy, and the load is similarly very briefly but very strongly coupled to the device at the optimal time  $t = t_*$  to almost instantaneously drain the energy. For a constant powering mechanism, at time  $t = t_*$  also the generator can again be coupled to the source to feed a new amount of energy, and this process can be repeated periodically with a period  $t_*$ .

1.2 Finite-rate energy-transfer (power-transmission) efficiency

Let the generator be continuously supplying energy to the source object 1 at a rate  $\kappa_1$  and the load continuously draining energy from the device object 2 at a rate  $\kappa_2$ . Field amplitudes  $s_{\pm 1,2}(t)$  are then defined, so that  $|s_{\pm 1,2}(t)|^2$  is equal to the power ingoing to

(for the + sign) or outgoing from (for the - sign) the object 1, 2 respectively, and the CMT equations are modified to

$$\begin{aligned}
\frac{d}{dt}a_1(t) &= -i(\omega_1 - i\Gamma_1)a_1(t) + i\kappa_{11}a_1(t) + i\kappa_{12}a_2(t) - \kappa_1a_1(t) + \sqrt{2\kappa_1}s_{+1}(t) \\
\frac{d}{dt}a_2(t) &= -i(\omega_2 - i\Gamma_2)a_2(t) + i\kappa_{21}a_1(t) + i\kappa_{22}a_2(t) - \kappa_2a_2(t) \\
s_{-1}(t) &= \sqrt{2\kappa_1}a_1(t) - s_{+1}(t) \\
s_{-2}(t) &= \sqrt{2\kappa_2}a_2(t)
\end{aligned} \tag{7}$$

where again we can set  $\omega_{1,2} \rightarrow \omega_{1,2} + \kappa_{11,22}$  and  $\kappa_{21} = \kappa_{12} \equiv \kappa$ .

Assume now that the excitation is at a fixed frequency  $\omega$ , namely has the form  $s_{+1}(t) = S_{+1}e^{-i\omega t}$ . Then the response of the linear system will be at the same frequency, namely  $a_{1,2}(t) = A_{1,2}e^{-i\omega t}$  and  $s_{-1,2}(t) = S_{-1,2}e^{-i\omega t}$ . By substituting these into Eqs.(7), using  $\delta_{1,2} \equiv \omega - \omega_{1,2}$ , and solving the system, we find the field-amplitude transmitted to the load ( $S_{21}$  scattering-matrix element)

$$\begin{aligned}
S_{21} \equiv \frac{S_{-2}}{S_{+1}} &= \frac{2i\kappa\sqrt{\kappa_1\kappa_2}}{(\Gamma_1 + \kappa_1 - i\delta_1)(\Gamma_2 + \kappa_2 - i\delta_2) + \kappa^2} \\
&= \frac{2iU\sqrt{U_1U_2}}{(1+U_1 - iD_1)(1+U_2 - iD_2) + U^2}
\end{aligned} \tag{8}$$

and the field-amplitude reflected to the generator ( $S_{11}$  scattering-matrix element)

$$\begin{aligned}
S_{11} \equiv \frac{S_{-1}}{S_{+1}} &= \frac{(\Gamma_1 - \kappa_1 - i\delta_1)(\Gamma_2 + \kappa_2 - i\delta_2) + \kappa^2}{(\Gamma_1 + \kappa_1 - i\delta_1)(\Gamma_2 + \kappa_2 - i\delta_2) + \kappa^2} \\
&= \frac{(1-U_1 - iD_1)(1+U_2 - iD_2) + U^2}{(1+U_1 - iD_1)(1+U_2 - iD_2) + U^2}
\end{aligned} \tag{9}$$

where  $D_{1,2} \equiv \delta_{1,2}/\Gamma_{1,2}$ ,  $U_{1,2} \equiv \kappa_{1,2}/\Gamma_{1,2}$  and  $U \equiv \kappa/\sqrt{\Gamma_1\Gamma_2}$ . Similarly, the scattering-matrix elements  $S_{12}$ ,  $S_{22}$  are given by interchanging  $1 \leftrightarrow 2$  in Eqs.(8),(9) and, as expected from reciprocity,  $S_{21} = S_{12}$ . The coefficients for power transmission (efficiency) and reflection and loss are respectively  $\eta_p \equiv |S_{21}|^2 = |S_{-2}|^2/|S_{+1}|^2$  and  $|S_{11}|^2 = |S_{-1}|^2/|S_{+1}|^2$  and  $1 - |S_{21}|^2 - |S_{11}|^2 = (2\Gamma_1|A_1|^2 + 2\Gamma_2|A_2|^2)/|S_{+1}|^2$ .

In practice, in some implementations, the parameters  $D_{1,2}$ ,  $U_{1,2}$  can be designed (engineered), since one can adjust the resonant frequencies  $\omega_{1,2}$  (compared to the desired

operating frequency  $\omega$ ) and the generator/load supply/drain rates  $\kappa_{1,2}$ . Their choice can target the optimization of some system performance-characteristic of interest:

In some examples, a goal can be to maximize the power transmission (efficiency)  $\eta_P \equiv |S_{21}|^2$  of the system, so one would require

$$\eta'_P(D_{1,2}) = \eta'_P(U_{1,2}) = 0 \quad (10)$$

Since  $S_{21}$  (from Eq.(8)) is symmetric upon interchanging  $1 \leftrightarrow 2$ , the optimal values for  $D_{1,2}$  (determined by Eqs.(10)) will be equal, namely  $D_1 = D_2 \equiv D_o$ , and similarly  $U_1 = U_2 \equiv U_o$ . Then,

$$S_{21} = \frac{2iUU_o}{(1+U_o - iD_o)^2 + U^2} \quad (11)$$

and from the condition  $\eta'_P(D_o) = 0$  we get that, for fixed values of  $U$  and  $U_o$ , the efficiency can be maximized for the following values of the symmetric detuning

$$D_o = \begin{cases} \pm\sqrt{U^2 - (1+U_o)^2}, & \text{if } U > 1+U_o, \\ 0, & \text{if } U \leq 1+U_o, \end{cases} \quad (12)$$

which, in the case  $U > 1 + U_o$ , can be rewritten for the two frequencies at which the efficiency peaks as

$$\omega_{\pm} = \frac{\omega_1\Gamma_2 + \omega_2\Gamma_1}{\Gamma_1 + \Gamma_2} \pm \frac{2\sqrt{\Gamma_1\Gamma_2}}{\Gamma_1 + \Gamma_2} \sqrt{\kappa^2 - (\Gamma_1 + \kappa_1)(\Gamma_2 + \kappa_2)}, \quad (13)$$

whose splitting we denote as  $\delta_P \equiv \bar{\omega}_+ - \bar{\omega}_-$ . Note that, at exact resonance  $\omega_1 = \omega_2$ , and for  $\Gamma_1 = \Gamma_2 \equiv \Gamma_o$  and  $\kappa_1 = \kappa_2 \equiv \kappa_o$ , we get  $\delta_P = 2\sqrt{\kappa^2 - (\Gamma_o + \kappa_o)^2} < \delta_E$ , namely the transmission-peak splitting is smaller than the normal-mode splitting. Then, by substituting  $D_o$  into  $\eta_P$  from Eq.(12), from the condition  $\eta'_P(U_o) = 0$  we get that, for fixed value of  $U$ , the efficiency can be maximized for

$$U_{o*} = \sqrt{1+U^2} \stackrel{\text{Eq.(12)}}{\Rightarrow} D_{o*} = 0 \quad (14)$$

which is known as ‘critical coupling’ condition, whereas for  $U_o < U_{o*}$  the system is called ‘undercoupled’ and for  $U_o > U_{o*}$  it is called ‘overcoupled’. The dependence of the efficiency on the frequency detuning  $D_o$  for different values of  $U_o$  (including the

‘critical-coupling’ condition) are shown in Fig. 2(a,b). The overall optimal power efficiency using Eqs.(14) is

$$\eta_{P^*} \equiv \eta_P(D_{o^*}, U_{o^*}) = \frac{U_{o^*} - 1}{U_{o^*} + 1} = \left( \frac{U}{1 + \sqrt{1 + U^2}} \right)^2, \quad (15)$$

which is again only a function of the coupling-to-loss ratio  $U = \kappa/\sqrt{\Gamma_1\Gamma_2}$  and tends to unity when  $U \gg 1$ , as depicted in Fig. 2(c).

In some examples, a goal can be to minimize the power reflection at the side of the generator  $|S_{11}|^2$  and the load  $|S_{22}|^2$ , so one would then need

$$S_{11,22} = 0 \Rightarrow (1 \mp U_1 - iD_1)(1 \pm U_2 - iD_2) + U^2 = 0, \quad (16)$$

The equations above present ‘impedance matching’ conditions. Again, the set of these conditions is symmetric upon interchanging  $1 \leftrightarrow 2$ , so, by substituting  $D_1 = D_2 \equiv D_o$  and  $U_1 = U_2 \equiv U_o$  into Eqs.(16), we get

$$(1 - iD_o)^2 - U_o^2 + U^2 = 0, \quad (17)$$

from which we easily find that the values of  $D_o$  and  $U_o$  that cancel all reflections are again exactly those in Eqs.(14).

It can be seen that, for this particular problem, the two goals and their associated sets of conditions (Eqs.(10) and Eqs.(16)) result in the same optimized values of the intra-source and intra-device parameters  $D_{1,2}$ ,  $U_{1,2}$ . Note that for a lossless system this would be an immediate consequence of power conservation (Hermiticity of the scattering matrix), but this is not apparent for a lossy system.

Accordingly, for any temporal energy-transfer scheme, once the parameters specific only to the source or to the device (such as their resonant frequencies and their excitation or loading rates respectively) have been optimally designed, the efficiency monotonically increases with the ratio of the source-device coupling-rate to their loss rates. Using the definition of a resonance quality factor  $Q = \omega/2\Gamma$  and defining by analogy the coupling factor  $k \equiv 1/Q_\kappa \equiv 2\kappa/\sqrt{\omega_1\omega_2}$ , it is therefore exactly this ratio



$$U = \frac{\kappa}{\sqrt{\Gamma_1 \Gamma_2}} = k \sqrt{Q_1 Q_2} \quad (18)$$

that has been set as a figure-of-merit for any system under consideration for wireless energy-transfer, along with the distance over which this ratio can be achieved (clearly,  $U$  will be a decreasing function of distance). The desired optimal regime  $U > 1$  is called ‘strong-coupling’ regime and it is a necessary and sufficient condition for efficient energy-transfer. In particular, for  $U > 1$  we get, from Eq.(15),  $\eta_{P*} > 17\%$ , large enough for practical applications. The figure-of-merit  $U$  is called the strong-coupling factor. We will further show how to design systems with a large strong-coupling factor.

To achieve a large strong-coupling factor  $U$ , in some examples, the energy-transfer application preferably uses resonant modes of high quality factors  $Q$ , corresponding to low (i.e. slow) intrinsic-loss rates  $\Gamma$ . This condition can be satisfied by designing resonant modes where all loss mechanisms, typically radiation and absorption, are sufficiently suppressed.

This suggests that the coupling be implemented using, not the lossy radiative far-field, which should rather be suppressed, but the evanescent (non-lossy) stationary near-field. To implement an energy-transfer scheme, usually more appropriate are finite objects, namely ones that are topologically surrounded everywhere by air, into where the near field extends to achieve the coupling. Objects of finite extent do not generally support electromagnetic states that are exponentially decaying in *all* directions in air away from the objects, since Maxwell's Equations in free space imply that  $\mathbf{k}^2 = \omega^2 / c^2$ , where  $\mathbf{k}$  is the wave vector,  $\omega$  the angular frequency, and  $c$  the speed of light, because of which one can show that such finite objects cannot support states of infinite  $Q$ , rather there always is some amount of radiation. However, very long-lived (so-called ‘high- $Q$ ’) states can be found, whose tails display the needed exponential or exponential-like decay away from the resonant object over long enough distances before they turn oscillatory (radiative). The limiting surface, where this change in the field behavior happens, is called the ‘radiation caustic’, and, for the wireless energy-transfer scheme to be based on the near field rather than the far/radiation field, the distance between the coupled objects must be such that one lies within the radiation caustic of the other. One typical way of achieving a high radiation- $Q$  ( $Q_{\text{rad}}$ ) is to design subwavelength resonant objects. When

the size of an object is much smaller than the wavelength of radiation in free space, its electromagnetic field couples to radiation very weakly. Since the extent of the near-field into the area surrounding a finite-sized resonant object is set typically by the wavelength, in some examples, resonant objects of subwavelength size have significantly longer evanescent field-tails. In other words, the radiation caustic is pushed far away from the object, so the electromagnetic mode enters the radiative regime only with a small amplitude.

Moreover, most realistic materials exhibit some nonzero amount of absorption, which can be frequency dependent, and thus cannot support states of infinite  $Q$ , rather there always is some amount of absorption. However, very long-lived (“high- $Q$ ”) states can be found, where electromagnetic modal energy is only weakly dissipated. Some typical ways of achieving a high absorption- $Q$  ( $Q_{\text{abs}}$ ) is to use materials which exhibit very small absorption at the resonant frequency and/or to shape the field to be localized more inside the least lossy materials.

Furthermore, to achieve a large strong-coupling factor  $U$ , in some examples, the energy-transfer application preferably uses systems that achieve a high coupling factor  $k$ , corresponding to strong (i.e. fast) coupling rate  $\kappa$ , over distances larger than the characteristic sizes of the objects.

Since finite-sized subwavelength resonant objects can often be accompanied with a high  $Q$ , as was discussed above and will be seen in examples later on, such an object will typically be the appropriate choice for the possibly-mobile resonant device-object. In these cases, the electromagnetic field is, in some examples, of quasi-static nature and the distance, up to which sufficient coupling can be achieved, is dictated by the decay-law of this quasi-static field.

Note, though, that in some examples, the resonant source-object will be immobile and thus less restricted in its allowed geometry and size. It can be therefore chosen large enough that the near-field extent is not limited by the wavelength, and can thus have nearly infinite radiation- $Q$ . Some objects of nearly infinite extent, such as dielectric waveguides, can support guided modes, whose evanescent tails are decaying exponentially in the direction away from the object, slowly if tuned close to cutoff,

therefore a good coupling can also be achieved over distances quite a few times larger than a characteristic size of the source- and/or device-object.

## 2 ‘Strongly-coupled’ resonances at mid-range distances for realistic systems

In the following, examples of systems suitable for energy transfer of the type described above are described. We will demonstrate how to compute the CMT parameters  $\omega_{1,2}$ ,  $Q_{1,2}$  and  $k$  described above and how to choose or design these parameters for particular examples in order to produce a desirable figure-of-merit  $U = \kappa/\sqrt{\Gamma_1\Gamma_2} = k\sqrt{Q_1Q_2}$  at a desired distance  $D$ . In some examples, this figure-of-merit is maximized when  $\omega_{1,2}$  are tuned close to a particular angular frequency  $\omega_U$ .

### 2.1 Self-resonant conducting coils

In some examples, one or more of the resonant objects are self-resonant conducting coils. Referring to Fig. 3, a conducting wire of length  $l$  and cross-sectional radius  $a$  is wound into a helical coil of radius  $r$  and height  $h$  (namely with  $N = \sqrt{l^2 - h^2} / 2\pi r$  number of turns), surrounded by air. As described below, the wire has distributed inductance and distributed capacitance, and therefore it supports a resonant mode of angular frequency  $\omega$ . The nature of the resonance lies in the periodic exchange of energy from the electric field within the capacitance of the coil, due to the charge distribution  $\rho(\mathbf{x})$  across it, to the magnetic field in free space, due to the current distribution  $\mathbf{j}(\mathbf{x})$  in the wire. In particular, the charge conservation equation  $\nabla \cdot \mathbf{j} = i\omega\rho$  implies that: (i) this periodic exchange is accompanied by a  $\pi/2$  phase-shift between the current and the charge density profiles, namely the energy  $W$  contained in the coil is at certain points in time completely due to the current and at other points in time completely due to the charge, and (ii) if  $\rho_l(x)$  and  $I(x)$  are respectively the linear charge and current densities in the wire, where  $x$  runs along the wire,  $q_o = \frac{1}{2} \int dx |\rho_l(x)|$  is the maximum amount of positive charge accumulated in one side of the coil (where an equal amount of negative charge always also accumulates in the other side to make the system neutral) and  $I_o = \max \{ |I(x)| \}$  is the maximum positive value of the linear current distribution, then

$I_o = \omega q_o$ . Then, one can define an effective total inductance  $L$  and an effective total capacitance  $C$  of the coil through the amount of energy  $W$  inside its resonant mode:

$$W \equiv \frac{1}{2} I_o^2 L \Rightarrow L = \frac{\mu_o}{4\pi I_o^2} \iint d\mathbf{x} d\mathbf{x}' \frac{\mathbf{j}(\mathbf{x}) \cdot \mathbf{j}(\mathbf{x}')}{|\mathbf{x} - \mathbf{x}'|}, \quad (19)$$

$$W \equiv \frac{1}{2} q_o^2 \frac{1}{C} \Rightarrow \frac{1}{C} = \frac{1}{4\pi \varepsilon_o q_o^2} \iint d\mathbf{x} d\mathbf{x}' \frac{\rho(\mathbf{x}) \rho(\mathbf{x}')}{|\mathbf{x} - \mathbf{x}'|}, \quad (20)$$

where  $\mu_o$  and  $\varepsilon_o$  are the magnetic permeability and electric permittivity of free space.

With these definitions, the resonant angular frequency and the effective impedance can be given by the formulas  $\omega = 1/\sqrt{LC}$  and  $Z = \sqrt{L/C}$  respectively.

Losses in this resonant system consist of ohmic (material absorption) loss inside the wire and radiative loss into free space. One can again define a total absorption resistance  $R_{abs}$  from the amount of power absorbed inside the wire and a total radiation resistance  $R_{rad}$  from the amount of power radiated due to electric- and magnetic-dipole radiation:

$$P_{abs} \equiv \frac{1}{2} I_o^2 R_{abs} \Rightarrow R_{abs} \approx \zeta_c \frac{l}{2\pi a} \cdot \frac{I_{rms}^2}{I_o^2} \quad (21)$$

$$P_{rad} \equiv \frac{1}{2} I_o^2 R_{rad} \Rightarrow R_{rad} \approx \frac{\zeta_o}{6\pi} \left[ \left( \frac{\omega |\mathbf{p}|}{c} \right)^2 + \left( \frac{\omega \sqrt{|\mathbf{m}|}}{c} \right)^4 \right], \quad (22)$$

where  $c = 1/\sqrt{\mu_o \varepsilon_o}$  and  $\zeta_o = \sqrt{\mu_o / \varepsilon_o}$  are the light velocity and light impedance in free space, the impedance  $\zeta_c$  is  $\zeta_c = 1/\sigma \delta = \sqrt{\mu_o \omega / 2\sigma}$  with  $\sigma$  the conductivity of the conductor and  $\delta$  the skin depth at the frequency  $\omega$ ,  $I_{rms}^2 = \frac{1}{l} \int dx |I(x)|^2$ ,  $\mathbf{p} = \int dx \mathbf{r} \rho_l(x)$  is the electric-dipole moment of the coil and  $\mathbf{m} = \frac{1}{2} \int dx \mathbf{r} \times \mathbf{j}(x)$  is the magnetic-dipole moment of the coil. For the radiation resistance formula Eq.(22), the assumption of operation in the quasi-static regime ( $h, r \ll \lambda = 2\pi c / \omega$ ) has been used, which is the desired regime of a subwavelength resonance. With these definitions, the absorption and

radiation quality factors of the resonance are given by  $Q_{abs} = Z / R_{abs}$  and  $Q_{rad} = Z / R_{rad}$  respectively.

From Eq.(19)-(22) it follows that to determine the resonance parameters one simply needs to know the current distribution  $\mathbf{j}$  in the resonant coil. Solving Maxwell's equations to rigorously find the current distribution of the resonant electromagnetic eigenmode of a conducting-wire coil is more involved than, for example, of a standard LC circuit, and we can find no exact solutions in the literature for coils of finite length, making an exact solution difficult. One could in principle write down an elaborate transmission-line-like model, and solve it by brute force. We instead present a model that is (as described below) in good agreement (~5%) with experiment. Observing that the finite extent of the conductor forming each coil imposes the boundary condition that the current has to be zero at the ends of the coil, since no current can leave the wire, we assume that the resonant mode of each coil is well approximated by a sinusoidal current profile along the length of the conducting wire. We shall be interested in the lowest mode, so if we denote by  $x$  the coordinate along the conductor, such that it runs from  $-l/2$  to  $+l/2$ , then the current amplitude profile would have the form

$I(x) = I_o \cos(\pi x / l)$ , where we have assumed that the current does not vary significantly along the wire circumference for a particular  $x$ , a valid assumption provided  $a \ll r$ . It immediately follows from the continuity equation for charge that the linear charge density profile should be of the form  $\rho_l(x) = \rho_o \sin(\pi x / l)$ , and thus

$q_o = \int_0^{l/2} dx \rho_o |\sin(\pi x / l)| = \rho_o l / \pi$ . Using these sinusoidal profiles we find the so-called "self-inductance"  $L_s$  and "self-capacitance"  $C_s$  of the coil by computing numerically the integrals Eq.(19) and (20); the associated frequency and effective impedance are  $\omega_s$  and  $Z_s$  respectively. The "self-resistances"  $R_s$  are given analytically by Eq.(21) and (22)

$$\text{using } I_{rms}^2 = \frac{1}{l} \int_{-l/2}^{l/2} dx |I_o \cos(\pi x / l)|^2 = \frac{1}{2} I_o^2, \quad |\mathbf{p}| = q_o \sqrt{\left(\frac{2}{\pi} h\right)^2 + \left(\frac{4N \cos(\pi N)}{(4N^2 - 1)\pi} r\right)^2} \quad \text{and}$$

$$|\mathbf{m}| = I_o \sqrt{\left(\frac{2}{\pi} N \pi r^2\right)^2 + \left(\frac{\cos(\pi N)(12N^2 - 1) - \sin(\pi N)\pi N(4N^2 - 1)}{(16N^4 - 8N^2 + 1)\pi} hr\right)^2},$$

and therefore the associated  $Q_s$  factors can be calculated.

The results for two examples of resonant coils with subwavelength modes of  $\lambda_s / r \geq 70$  (i.e. those highly suitable for near-field coupling and well within the quasi-static limit) are presented in Table 1. Numerical results are shown for the wavelength and absorption, radiation and total loss rates, for the two different cases of subwavelength-coil resonant modes. Note that, for conducting material, copper ( $\sigma = 5.998 \cdot 10^{-7}$  S/m) was used. It can be seen that expected quality factors at microwave frequencies are  $Q_{s,abs} \geq 1000$  and  $Q_{s,rad} \geq 5000$ .

**Table 1**

single coil	$\lambda_s / r$	f(MHz)	$Q_{s,rad}$	$Q_{s,abs}$	$Q_s$
r=30cm, h=20cm, a=1cm, N=4	74.7	13.39	4164	8170	2758
r=10cm, h=3cm, a=2mm, N=6	140	21.38	43919	3968	3639

Referring to Fig. 4, in some examples, energy is transferred between two self-resonant conducting-wire coils. The electric and magnetic fields are used to couple the different resonant conducting-wire coils at a distance  $D$  between their centers. Usually, the electric coupling highly dominates over the magnetic coupling in the system under consideration for coils with  $h \gg 2r$  and, oppositely, the magnetic coupling highly dominates over the electric coupling for coils with  $h \ll 2r$ . Defining the charge and current distributions of two coils 1,2 respectively as  $\rho_{1,2}(\mathbf{x})$  and  $\mathbf{j}_{1,2}(\mathbf{x})$ , total charges and peak currents respectively as  $q_{1,2}$  and  $I_{1,2}$ , and capacitances and inductances respectively as  $C_{1,2}$  and  $L_{1,2}$ , which are the analogs of  $\rho(\mathbf{x})$ ,  $\mathbf{j}(\mathbf{x})$ ,  $q_o$ ,  $I_o$ ,  $C$  and  $L$  for the single-coil case and are therefore well defined, we can *define* their mutual capacitance and inductance through the total energy:

$$W \equiv W_1 + W_2 + \frac{1}{2}(q_1^* q_2 + q_2^* q_1) / M_C + \frac{1}{2}(I_1^* I_2 + I_2^* I_1) M_L$$

$$\Rightarrow 1 / M_C = \frac{1}{4\pi\epsilon_0 q_1 q_2} \iint d\mathbf{x} d\mathbf{x}' \frac{\rho_1(\mathbf{x}) \rho_2(\mathbf{x}')}{|\mathbf{x} - \mathbf{x}'|} u, \quad M_L = \frac{\mu_0}{4\pi I_1 I_2} \iint d\mathbf{x} d\mathbf{x}' \frac{\mathbf{j}_1(\mathbf{x}) \cdot \mathbf{j}_2(\mathbf{x}')}{|\mathbf{x} - \mathbf{x}'|} u, \quad (23)$$

where  $W_1 = \frac{1}{2} q_1^2 / C_1 = \frac{1}{2} I_1^2 L_1$ ,  $W_2 = \frac{1}{2} q_2^2 / C_2 = \frac{1}{2} I_2^2 L_2$  and the retardation factor of  $u = \exp(i\omega|\mathbf{x} - \mathbf{x}'|/c)$  inside the integral can be ignored in the quasi-static regime  $D \ll \lambda$  of interest, where each coil is within the near field of the other. With this definition, the coupling factor is given by  $k = \sqrt{C_1 C_2} / M_C + M_L / \sqrt{L_1 L_2}$ .

Therefore, to calculate the coupling rate between two self-resonant coils, again the current profiles are needed and, by using again the assumed sinusoidal current profiles, we compute numerically from Eq.(23) the mutual capacitance  $M_{C,s}$  and inductance  $M_{L,s}$  between two self-resonant coils at a distance  $D$  between their centers, and thus  $k = 1/Q_\kappa$  is also determined.

**Table 2**

pair of coils	$D/r$	$Q$	$Q_\kappa = 1/k$	$U$
r=30cm, h=20cm, a=1cm, N=4 $\lambda/r \approx 75$ $Q_s^{abs} \approx 8170, Q_s^{rad} \approx 4164$	3	2758	38.9	70.9
	5	2758	139.4	19.8
	7	2758	333.0	8.3
	10	2758	818.9	3.4
r=10cm, h=3cm, a=2mm, N=6 $\lambda/r \approx 140$ $Q_s^{abs} \approx 3968, Q_s^{rad} \approx 43919$	3	3639	61.4	59.3
	5	3639	232.5	15.7
	7	3639	587.5	6.2
	10	3639	1580	2.3

Referring to Table 2, relevant parameters are shown for exemplary examples featuring pairs or identical self resonant coils. Numerical results are presented for the average wavelength and loss rates of the two normal modes (individual values not shown), and also the coupling rate and figure-of-merit as a function of the coupling distance  $D$ , for the two cases of modes presented in Table1. It can be seen that for

medium distances  $D/r = 10 - 3$  the expected coupling-to-loss ratios are in the range  $U \sim 2 - 70$ .

### 2.1.1 Experimental Results

An experimental realization of an example of the above described system for wireless energy transfer consists of two self-resonant coils of the type described above, one of which (the source coil) is coupled inductively to an oscillating circuit, and the second (the device coil) is coupled inductively to a resistive load, as shown schematically in Fig. 5. Referring to Fig. 5,  $A$  is a single copper loop of radius 25cm that is part of the driving circuit, which outputs a sine wave with frequency 9.9MHz.  $s$  and  $d$  are respectively the source and device coils referred to in the text.  $B$  is a loop of wire attached to the load ("light-bulb"). The various  $\kappa$ 's represent direct couplings between the objects. The angle between coil  $d$  and the loop  $A$  is adjusted so that their direct coupling is zero, while coils  $s$  and  $d$  are aligned coaxially. The direct coupling between  $B$  and  $A$  and between  $B$  and  $s$  is negligible.

The parameters for the two identical helical coils built for the experimental validation of the power transfer scheme were  $h = 20$  cm,  $a = 3$  mm,  $r = 30$  cm and  $N = 5.25$ . Both coils are made of copper. Due to imperfections in the construction, the spacing between loops of the helix is not uniform, and we have encapsulated the uncertainty about their uniformity by attributing a 10% (2 cm) uncertainty to  $h$ . The expected resonant frequency given these dimensions is  $f_0 = 10.56 \pm 0.3$  MHz, which is about 5% off from the measured resonance at around 9.90 MHz.

The theoretical  $Q$  for the loops is estimated to be  $\sim 2500$  (assuming perfect copper of resistivity  $\rho = 1/\sigma = 1.7 \times 10^{-8} \Omega \text{ m}$ ) but the measured value is  $950 \pm 50$ . We believe the discrepancy is mostly due to the effect of the layer of poorly conducting copper oxide on the surface of the copper wire, to which the current is confined by the short skin depth ( $\sim 20 \mu \text{ m}$ ) at this frequency. We have therefore used the experimentally observed  $Q$  (and  $\Gamma_1 = \Gamma_2 = \Gamma = \omega/(2Q)$  derived from it) in all subsequent computations.

The coupling coefficient  $\kappa$  can be found experimentally by placing the two self-resonant coils (fine-tuned, by slightly adjusting  $h$ , to the same resonant frequency when isolated) a distance  $D$  apart and measuring the splitting in the frequencies of the two



resonant modes in the transmission spectrum. According to Eq.(13) derived by coupled-mode theory, the splitting in the transmission spectrum should be  $\delta_p = 2\sqrt{\kappa^2 - \Gamma^2}$ , when  $\kappa_{A,B}$  are kept very small by keeping A and B at a relatively large distance. The comparison between experimental and theoretical results as a function of distance when the two the coils are aligned coaxially is shown in Fig. 6.

Fig. 7 shows a comparison of experimental and theoretical values for the strong-coupling factor  $U = \kappa / \Gamma$  as a function of the separation between the two coils. The theory values are obtained by using the theoretically obtained  $\kappa$  and the experimentally measured  $\Gamma$ . The shaded area represents the spread in the theoretical  $U$  due to the  $\sim 5\%$  uncertainty in  $Q$ . As noted above, the maximum theoretical efficiency depends only on the parameter  $U$ , which is plotted as a function of distance in Fig. 7.  $U$  is greater than 1 even for  $D = 2.4\text{m}$  (eight times the radius of the coils), thus the system is in the strongly-coupled regime throughout the entire range of distances probed.

The power-generator circuit was a standard Colpitts oscillator coupled inductively to the source coil by means of a single loop of copper wire 25cm in radius (see Fig. 5). The load consisted of a previously calibrated light-bulb, and was attached to its own loop of insulated wire, which was in turn placed in proximity of the device coil and inductively coupled to it. Thus, by varying the distance between the light-bulb and the device coil, the parameter  $U_B = \kappa_B / \Gamma$  was adjusted so that it matched its optimal value, given theoretically by Eq.(14) as  $U_{B*} = \sqrt{1 + U^2}$ . Because of its inductive nature, the loop connected to the light-bulb added a small reactive component to  $\kappa_B$  which was compensated for by slightly retuning the coil. The work extracted was determined by adjusting the power going into the Colpitts oscillator until the light-bulb at the load was at its full nominal brightness.

In order to isolate the efficiency of the transfer taking place specifically between the source coil and the load, we measured the current at the mid-point of each of the self-resonant coils with a current-probe (which was not found to lower the Q of the coils noticeably.) This gave a measurement of the current parameters  $I_1$  and  $I_2$  defined above. The power dissipated in each coil was then computed from  $P_{1,2} = \Gamma L |I_{1,2}|^2$ , and the

efficiency was directly obtained from  $\eta = P_B / (P_1 + P_2 + P_B)$ . To ensure that the experimental setup was well described by a two-object coupled-mode theory model, we positioned the device coil such that its direct coupling to the copper loop attached to the Colpitts oscillator was zero. The experimental results are shown in Fig. 8, along with the theoretical prediction for maximum efficiency, given by Eq.(15).

Using this example, we were able to transmit significant amounts of power using this setup from the source coil to the device coil, fully lighting up a 60W light-bulb from distances more than 2m away, for example. As an additional test, we also measured the total power going into the driving circuit. The efficiency of the wireless power-transmission itself was hard to estimate in this way, however, as the efficiency of the Colpitts oscillator itself is not precisely known, although it is expected to be far from 100%. Nevertheless, this gave an overly conservative lower bound on the efficiency. When transmitting 60W to the load over a distance of 2m, for example, the power flowing into the driving circuit was 400W. This yields an overall wall-to-load efficiency of  $\sim 15\%$ , which is reasonable given the expected  $\sim 40\%$  efficiency for the wireless power transmission at that distance and the low efficiency of the driving circuit.

From the theoretical treatment above, we see that in typical examples it is important that the coils be on resonance for the power transmission to be practical. We found experimentally that the power transmitted to the load dropped sharply as one of the coils was detuned from resonance. For a fractional detuning  $\Delta f/f_0$  of a few times the inverse loaded  $Q$ , the induced current in the device coil was indistinguishable from noise.

The power transmission was not found to be visibly affected as humans and various everyday objects, such as metallic and wooden furniture, as well as electronic devices large and small, were placed between the two coils, even when they drastically obstructed the line of sight between source and device. External objects were found to have an effect only when they were closer than 10cm from either one of the coils. While some materials (such as aluminum foil, styrofoam and humans) mostly just shifted the resonant frequency, which could in principle be easily corrected with a feedback circuit of the type described earlier, others (cardboard, wood, and PVC) lowered  $Q$  when placed

closer than a few centimeters from the coil, thereby lowering the efficiency of the transfer.

This method of power transmission is believed safe for humans. When transmitting 60W (more than enough to power a laptop computer) across 2m, we estimated that the magnitude of the magnetic field generated is much weaker than the Earth's magnetic field for all distances except for less than about 1cm away from the wires in the coil, an indication of the safety of the scheme even after long-term use. The power radiated for these parameters was  $\sim 5$  W, which is roughly an order of magnitude higher than cell phones but could be drastically reduced, as discussed below.

Although the two coils are currently of identical dimensions, it is possible to make the device coil small enough to fit into portable devices without decreasing the efficiency. One could, for instance, maintain the product of the characteristic sizes of the source and device coils constant.

These experiments demonstrated experimentally a system for power transmission over medium range distances, and found that the experimental results match theory well in multiple independent and mutually consistent tests.

The efficiency of the scheme and the distances covered can be appreciably improved by silver-plating the coils, which should increase their  $Q$ , or by working with more elaborate geometries for the resonant objects. Nevertheless, the performance characteristics of the system presented here are already at levels where they could be useful in practical applications.

## 2.2 Capacitively-loaded conducting loops or coils

In some examples, one or more of the resonant objects are capacitively-loaded conducting loops or coils. Referring to Fig. 9 a helical coil with  $N$  turns of conducting wire, as described above, is connected to a pair of conducting parallel plates of area  $A$  spaced by distance  $d$  via a dielectric material of relative permittivity  $\epsilon$ , and everything is surrounded by air (as shown,  $N=1$  and  $h=0$ ). The plates have a capacitance  $C_p = \epsilon_0 \epsilon A / d$ , which is added to the distributed capacitance of the coil and thus modifies its resonance. Note however, that the presence of the loading capacitor modifies significantly the current distribution inside the wire and therefore the total

effective inductance  $L$  and total effective capacitance  $C$  of the coil are different respectively from  $L_s$  and  $C_s$ , which are calculated for a self-resonant coil of the same geometry using a sinusoidal current profile. Since some charge is accumulated at the plates of the external loading capacitor, the charge distribution  $\rho$  inside the wire is reduced, so  $C < C_s$ , and thus, from the charge conservation equation, the current distribution  $\mathbf{j}$  flattens out, so  $L > L_s$ . The resonant frequency for this system is

$$\omega = 1/\sqrt{L(C + C_p)} < \omega_s = 1/\sqrt{L_s C_s}, \text{ and } I(x) \rightarrow I_o \cos(\pi x/l) \Rightarrow C \rightarrow C_s \Rightarrow \omega \rightarrow \omega_s, \text{ as } C_p \rightarrow 0.$$

In general, the desired CMT parameters can be found for this system, but again a very complicated solution of Maxwell's Equations is required. Instead, we will analyze only a special case, where a reasonable guess for the current distribution can be made.

When  $C_p \gg C_s > C$ , then  $\omega \approx 1/\sqrt{LC_p} \ll \omega_s$  and  $Z \approx \sqrt{L/C_p} \ll Z_s$ , while all the charge is on the plates of the loading capacitor and thus the current distribution is constant along the wire. This allows us now to compute numerically  $L$  from Eq.(19). In the case  $h = 0$  and  $N$  integer, the integral in Eq.(19) can actually be computed analytically, giving the formula  $L = \mu_o r [\ln(8r/a) - 2] N^2$ . Explicit analytical formulas are again available for  $R$  from Eq.(21) and (22), since  $I_{rms} = I_o$ ,  $|\mathbf{p}| \approx 0$  and  $|\mathbf{m}| = I_o N \pi r^2$  (namely only the magnetic-dipole term is contributing to radiation), so we can determine also  $Q_{abs} = \omega L / R_{abs}$  and  $Q_{rad} = \omega L / R_{rad}$ . At the end of the calculations, the validity of the assumption of constant current profile is confirmed by checking that indeed the condition  $C_p \gg C_s \Leftrightarrow \omega \ll \omega_s$  is satisfied. To satisfy this condition, one could use a large external capacitance, however, this would usually shift the operational frequency lower than the optimal frequency, which we will determine shortly; instead, in typical examples, one often prefers coils with very small self-capacitance  $C_s$  to begin with, which usually holds, for the types of coils under consideration, when  $N = 1$ , so that the self-capacitance comes from the charge distribution across the single turn, which is almost always very small, or when  $N > 1$  and

$h \gg 2Na$ , so that the dominant self-capacitance comes from the charge distribution across adjacent turns, which is small if the separation between adjacent turns is large.

The external loading capacitance  $C_p$  provides the freedom to tune the resonant frequency (for example by tuning  $A$  or  $d$ ). Then, for the particular simple case  $h = 0$ , for which we have analytical formulas, the total  $Q = \omega L / (R_{abs} + R_{rad})$  becomes highest at the optimal frequency

$$\omega_Q = \left[ \frac{c^4}{\pi} \sqrt{\frac{\epsilon_o}{2\sigma}} \cdot \frac{1}{aNr^3} \right]^{2/7}, \quad (24)$$

reaching the value

$$Q_{\max} = \frac{6}{7\pi} \left( 2\pi^2 \eta_o \frac{\sigma a^2 N^2}{r} \right)^{3/7} \cdot \left[ \ln \left( \frac{8r}{a} \right) - 2 \right]. \quad (25)$$

At lower frequencies it is dominated by ohmic loss and at higher frequencies by radiation. Note, however, that the formulas above are accurate as long as  $\omega_Q \ll \omega_s$  and, as explained above, this holds almost always when  $N = 1$ , and is usually less accurate when  $N > 1$ , since  $h = 0$  usually implies a large self-capacitance. A coil with large  $h$  can be used, if the self-capacitance needs to be reduced compared to the external capacitance, but then the formulas for  $L$  and  $\omega_Q$ ,  $Q_{\max}$  are again less accurate. Similar qualitative behavior is expected, but a more complicated theoretical model is needed for making quantitative predictions in that case.

The results of the above analysis for two examples of subwavelength modes of  $\lambda/r \geq 70$  (namely highly suitable for near-field coupling and well within the quasi-static limit) of coils with  $N = 1$  and  $h = 0$  at the optimal frequency Eq.(24) are presented in Table 3. To confirm the validity of constant-current assumption and the resulting analytical formulas, mode-solving calculations were also performed using another completely independent method: computational 3D finite-element frequency-domain (FEFD) simulations (which solve Maxwell's Equations in frequency domain exactly apart for spatial discretization) were conducted, in which the boundaries of the conductor were modeled using a complex impedance  $\zeta_c = \sqrt{\mu_o \omega / 2\sigma}$  boundary condition, valid as

long as  $\zeta_c / \zeta_o \ll 1$  ( $< 10^{-5}$  for copper in the microwave). Table 3 shows Numerical FEFD (and in parentheses analytical) results for the wavelength and absorption, radiation and total loss rates, for two different cases of subwavelength-loop resonant modes. Note that for conducting material copper ( $\sigma = 5.998 \cdot 10^7 S/m$ ) was used. Specific parameters of the plot in Fig. 4 are highlighted in bold in the table. The two methods (analytical and computational) are in good agreement and show that, in some examples, the optimal frequency is in the low-MHz microwave range and the expected quality factors are  $Q_{abs} \geq 1000$  and  $Q_{rad} \geq 10000$ .

**Table 3**

single coil	$\lambda / \tau$	f	$Q_{rad}$	$Q_{abs}$	Q
<b>r=30cm, a=2cm</b> <b><math>\epsilon=10, A=138cm^2,</math></b> <b>d=4mm</b>	<b>111.4 (112.4)</b>	<b>8.976 (8.897)</b>	<b>29546 (30512)</b>	<b>4886 (5117)</b>	<b>4193 (4381)</b>
r=10cm, a=2mm $\epsilon=10, A=3.14cm^2,$ d=1mm	69.7 (70.4)	43.04 (42.61)	10702 (10727)	1545 (1604)	1350 (1395)

Referring to Fig. 10, in some examples, energy is transferred between two capacitively-loaded coils. For the rate of energy transfer between two capacitively-loaded coils 1 and 2 at distance  $D$  between their centers, the mutual inductance  $M_L$  can be evaluated numerically from Eq.(23) by using constant current distributions in the case  $\omega \ll \omega_s$ . In the case  $h = 0$ , the coupling is only magnetic and again we have an analytical formula, which, in the quasi-static limit  $r \ll D \ll \lambda$  and for the relative orientation shown in Fig. 10, is  $M_L \approx \pi \mu_o / 2 \cdot (r_1 r_2)^2 N_1 N_2 / D^3$ , which means that  $k \propto (\sqrt{r_1 r_2} / D)^3$  is independent of the frequency  $\omega$  and the number of turns  $N_1, N_2$ . Consequently, the resultant coupling figure-of-merit of interest is

$$U = k \sqrt{Q_1 Q_2} \approx \left( \frac{\sqrt{r_1 r_2}}{D} \right)^3 \cdot \frac{\pi^2 \eta_o \frac{\sqrt{r_1 r_2}}{\lambda} \cdot N_1 N_2}{\prod_{j=1,2} \left( \sqrt{\frac{\pi \eta_o}{\lambda \sigma}} \cdot \frac{r_j}{a_j} N_j + \frac{8}{3} \pi^5 \eta_o \left( \frac{r_j}{\lambda} \right)^4 N_j^2 \right)^{1/2}}, \quad (26)$$

which again is more accurate for  $N_1 = N_2 = 1$ .

From Eq.(26) it can be seen that the optimal frequency  $\omega_U$ , where the figure-of-merit is maximized to the value  $U_{\max}$ , is close to the frequency  $\omega_{Q_1 Q_2}$  at which  $Q_1 Q_2$  is maximized, since  $k$  does not depend much on frequency (at least for the distances  $D \ll \lambda$  of interest for which the quasi-static approximation is still valid). Therefore, the optimal frequency  $\omega_U \approx \omega_{Q_1 Q_2}$  is mostly independent of the distance  $D$  between the two coils and lies between the two frequencies  $\omega_{Q_1}$  and  $\omega_{Q_2}$  at which the single-coil  $Q_1$  and  $Q_2$  respectively peak. For same coils, this optimal frequency is given by Eq.(24) and then the strong-coupling factor from Eq.(26) becomes

$$U_{\max} = kQ_{\max} \approx \left(\frac{r}{D}\right)^3 \cdot \frac{3}{7} \left(2\pi^2 \eta_o \frac{\sigma a^2 N^2}{r}\right)^{3/7}. \quad (27)$$

In some examples, one can tune the capacitively-loaded conducting loops or coils, so that their angular eigenfrequencies are close to  $\omega_U$  within  $\Gamma_U$ , which is half the angular frequency width for which  $U > U_{\max} / 2$ .

Referring to Table 4, numerical FEFD and, in parentheses, analytical results based on the above are shown for two systems each composed of a matched pair of the loaded coils described in Table 3. The average wavelength and loss rates are shown along with the coupling rate and coupling to loss ratio figure-of-merit  $U = \kappa / \Gamma$  as a function of the coupling distance  $D$ , for the two cases. Note that the average numerical  $\Gamma_{rad}$  shown are slightly different from the single-loop value of Figure 3, analytical results for  $\Gamma_{rad}$  are not shown but the single-loop value is used. (The specific parameters corresponding to the plot in Fig. 10 are highlighted with bold in the table.) Again we chose  $N = 1$  to make the constant-current assumption a good one and computed  $M_L$  numerically from Eq.(23). Indeed the accuracy can be confirmed by their agreement with the computational FEFD mode-solver simulations, which give  $\kappa$  through the frequency splitting of the two normal modes of the combined system ( $\delta_E = 2\kappa$  from Eq.(4)). The results show that for medium distances  $D/r = 10 - 3$  the expected coupling-to-loss ratios are in the range  $U \sim 0.5 - 50$ .

**Table 4**

pair of coils	$D/r$	$Q^{ms}$	$Q = \omega/\Xi$	$Q_c = \omega/2\kappa$	$\kappa/\Gamma$
$r=30\text{cm}, a=2\text{cm}$ $\varepsilon=10, A=138\text{cm}^2, d=4\text{mm}$ $\lambda/r \approx 112$ $Q^{ms} \approx 4886$	3	30729	4216	62.6 (63.7)	67.4 (68.7)
	5	29577	4194	235 (248)	17.8 (17.6)
	7	<b>29128</b>	<b>4185</b>	<b>589 (646)</b>	<b>7.1 (6.8)</b>
	10	28833	4177	1539 (1828)	2.7 (2.4)
$r=10\text{cm}, a=2\text{mm}$ $\varepsilon=10, A=3.14\text{cm}^2, d=1\text{mm}$ $\lambda/r \approx 70$ $Q^{ms} \approx 1546$	3	10955	1355	85.4 (91.3)	15.9 (15.3)
	5	10740	1351	313 (356)	4.32 (3.92)
	7	10759	1351	754 (925)	1.79 (1.51)
	10	10756	1351	1895 (2617)	0.71 (0.53)

2.2.1 Derivation of optimal power-transmission efficiency

Referring to Fig. 11, to rederive and express Eq.(15) in terms of the parameters which are more directly accessible from particular resonant objects, such as the capacitively-loaded conducting loops, one can consider the following circuit-model of the system, where the inductances  $L_s, L_d$  represent the source and device loops respectively,  $R_s, R_d$  their respective losses, and  $C_s, C_d$  are the required corresponding capacitances to achieve for both resonance at frequency  $\omega$ . A voltage generator  $V_g$  is considered to be connected to the source and a load resistance  $R_l$  to the device. The mutual inductance is denoted by  $M$ .

Then from the source circuit at resonance ( $\omega L_s = 1/\omega C_s$ ):

$$V_g = I_s R_s - j\omega M I_d \Rightarrow \frac{1}{2} V_g^* I_s = \frac{1}{2} |I_s|^2 R_s + \frac{1}{2} j\omega M I_d^* I_s, \tag{28}$$

and from the device circuit at resonance ( $\omega L_d = 1/\omega C_d$ ):

$$0 = I_d (R_d + R_l) - j\omega M I_s \Rightarrow j\omega M I_s = I_d (R_d + R_l) \tag{29}$$

So by substituting Eq.(29) to Eq.(28) and taking the real part (for time-averaged power) we get:

$$P_g = \text{Re} \left\{ \frac{1}{2} V_g^* I_s \right\} = \frac{1}{2} |I_s|^2 R_s + \frac{1}{2} |I_d|^2 (R_d + R_l) = P_s + P_d + P_l, \tag{30}$$

where we identified the power delivered by the generator  $P_g = \text{Re} \left\{ V_g^* I_s / 2 \right\}$ , the power



lost inside the source  $P_s = |I_s|^2 R_s / 2$ , the power lost inside the device  $P_d = |I_d|^2 R_d / 2$  and the power delivered to the load  $P_l = |I_d|^2 R_l / 2$ . Then, the power transmission efficiency is:

$$\eta_P \equiv \frac{P_l}{P_g} = \frac{R_l}{\left| \frac{I_s}{I_d} \right|^2 R_s + (R_d + R_l)} \stackrel{(29)}{=} \frac{R_l}{\frac{(R_d + R_l)^2}{(\omega M)^2} R_s + (R_d + R_l)}. \quad (31)$$

If we now choose the load impedance  $R_l$  to optimize the efficiency by  $\eta_P'(R_l) = 0$ , we get the optimal load impedance

$$\frac{R_{l^*}}{R_d} = \sqrt{1 + \frac{(\omega M)^2}{R_s R_d}} \quad (32)$$

and the maximum possible efficiency

$$\eta_{P^*} = \frac{R_{l^*} / R_d - 1}{R_{l^*} / R_d + 1} = \left[ \frac{\omega M / \sqrt{R_s R_d}}{1 + \sqrt{1 + (\omega M / \sqrt{R_s R_d})^2}} \right]^2. \quad (33)$$

To check now the correspondence with the CMT model, note that  $\kappa_l = R_l / 2L_d$ ,  $\Gamma_d = R_d / 2L_d$ ,  $\Gamma_s = R_s / 2L_s$ , and  $\kappa = \omega M / 2\sqrt{L_s L_d}$ , so then  $U_l = \kappa_l / \Gamma_d = R_l / R_d$  and  $U = \kappa / \sqrt{\Gamma_s \Gamma_d} = \omega M / \sqrt{R_s R_d}$ . Therefore, the condition Eq.(32) is identical to the condition Eq.(14) and the optimal efficiency Eq.(33) is identical to the general Eq.(15). Indeed, as the CMT analysis predicted, to get a large efficiency, we need to design a system that has a large strong-coupling factor  $U$ .

### 2.2.2 Optimization of $U$

The results above can be used to increase or optimize the performance of a wireless energy transfer system, which employs capacitively-loaded coils. For example, from the scaling of Eq.(27) with the different system parameters, one sees that to maximize the system figure-of-merit  $U$ , in some examples, one can:

-- Decrease the resistivity of the conducting material. This can be achieved, for example, by using good conductors (such as copper or silver) and/or lowering the temperature. At very low temperatures one could use also superconducting materials to achieve extremely good performance.

-- Increase the wire radius  $a$ . In typical examples, this action can be limited by physical size considerations. The purpose of this action is mainly to reduce the resistive losses in the wire by increasing the cross-sectional area through which the electric current is flowing, so one could alternatively use also a Litz wire or a ribbon instead of a circular wire.

-- For fixed desired distance  $D$  of energy transfer, increase the radius of the loop  $r$ . In typical examples, this action can be limited by physical size considerations, typically especially for the device.

-- For fixed desired distance vs. loop-size ratio  $D/r$ , decrease the radius of the loop  $r$ . In typical examples, this action can be limited by physical size considerations.

-- Increase the number of turns  $N$ . (Even though Eq.(27) is expected to be less accurate for  $N > 1$ , qualitatively it still provides a good indication that we expect an improvement in the coupling-to-loss ratio with increased  $N$ .) In typical examples, this action can be limited by physical size and possible voltage considerations, as will be discussed in following paragraphs.

-- Adjust the alignment and orientation between the two coils. The figure-of-merit is optimized when both cylindrical coils have exactly the same axis of cylindrical symmetry (namely they are "facing" each other). In some examples, particular mutual coil angles and orientations that lead to zero mutual inductance (such as the orientation where the axes of the two coils are perpendicular and the centers of the two coils are on one of the two axes) should be avoided.

-- Finally, note that the height of the coil  $h$  is another available design parameter, which can have an impact to the performance similar to that of its radius  $r$ , and thus the design rules can be similar.

The above analysis technique can be used to design systems with desired parameters. For example, as listed below, the above described techniques can be used to determine the cross sectional radius  $a$  of the wire which one should use when designing

as system two same single-turn loops with a given radius in order to achieve a specific performance in terms of  $U = \kappa / \Gamma$  at a given  $D/r$  between them, when the material is copper ( $\sigma=5.998 \cdot 10^7 S/m$ ):

$$\begin{aligned} D/r = 5, U \geq 10, r = 30cm &\Rightarrow a \geq 9mm \\ D/r = 5, U \geq 10, r = 5cm &\Rightarrow a \geq 3.7mm \\ D/r = 5, U \geq 20, r = 30cm &\Rightarrow a \geq 20mm \\ D/r = 5, U \geq 20, r = 5cm &\Rightarrow a \geq 8.3mm \\ D/r = 10, U \geq 1, r = 30cm &\Rightarrow a \geq 7mm \\ D/r = 10, U \geq 1, r = 5cm &\Rightarrow a \geq 2.8mm \\ D/r = 10, U \geq 3, r = 30cm &\Rightarrow a \geq 25mm \\ D/r = 10, U \geq 3, r = 5cm &\Rightarrow a \geq 10mm \end{aligned}$$

Similar analysis can be done for the case of two dissimilar loops. For example, in some examples, the device under consideration is very specific (e.g. a laptop or a cell phone), so the dimensions of the device object ( $r_d, h_d, a_d, N_d$ ) are very restricted.

However, in some such examples, the restrictions on the source object ( $r_s, h_s, a_s, N_s$ ) are much less, since the source can, for example, be placed under the floor or on the ceiling. In such cases, the desired distance is often well defined, based on the application (e.g.  $D \sim 1m$  for charging a laptop on a table wirelessly from the floor). Listed below are examples (simplified to the case  $N_s = N_d = 1$  and  $h_s = h_d = 0$ ) of how one can vary the dimensions of the source object to achieve the desired system performance in terms of

$U_{sd} = \kappa / \sqrt{\Gamma_s \Gamma_d}$ , when the material is again copper ( $\sigma=5.998 \cdot 10^7 S/m$ ):

$$\begin{aligned} D = 1.5m, U_{sd} \geq 15, r_d = 30cm, a_d = 6mm &\Rightarrow r_s = 1.158m, a_s \geq 5mm \\ D = 1.5m, U_{sd} \geq 30, r_d = 30cm, a_d = 6mm &\Rightarrow r_s = 1.15m, a_s \geq 33mm \\ D = 1.5m, U_{sd} \geq 1, r_d = 5cm, a_d = 4mm &\Rightarrow r_s = 1.119m, a_s \geq 7mm \\ D = 1.5m, U_{sd} \geq 2, r_d = 5cm, a_d = 4mm &\Rightarrow r_s = 1.119m, a_s \geq 52mm \\ D = 2m, U_{sd} \geq 10, r_d = 30cm, a_d = 6mm &\Rightarrow r_s = 1.518m, a_s \geq 7mm \\ D = 2m, U_{sd} \geq 20, r_d = 30cm, a_d = 6mm &\Rightarrow r_s = 1.514m, a_s \geq 50mm \\ D = 2m, U_{sd} \geq 0.5, r_d = 5cm, a_d = 4mm &\Rightarrow r_s = 1.491m, a_s \geq 5mm \\ D = 2m, U_{sd} \geq 1, r_d = 5cm, a_d = 4mm &\Rightarrow r_s = 1.491m, a_s \geq 36mm \end{aligned}$$

### 2.2.3 Optimization of $k$

As described below, in some examples, the quality factor  $Q$  of the resonant objects is limited from external perturbations and thus varying the coil parameters cannot lead to improvement in  $Q$ . In such cases, one can opt to increase the strong-coupling factor  $U$  by increasing the coupling factor  $k$ . The coupling does not depend on the frequency and the number of turns. Therefore, in some examples, one can:

-- Increase the wire radii  $a_1$  and  $a_2$ . In typical examples, this action can be limited by physical size considerations.

-- For fixed desired distance  $D$  of energy transfer, increase the radii of the coils  $r_1$  and  $r_2$ . In typical examples, this action can be limited by physical size considerations, typically especially for the device.

-- For fixed desired distance vs. coil-sizes ratio  $D/\sqrt{r_1 r_2}$ , only the weak (logarithmic) dependence of the inductance remains, which suggests that one should decrease the radii of the coils  $r_1$  and  $r_2$ . In typical examples, this action can be limited by physical size considerations.

-- Adjust the alignment and orientation between the two coils. In typical examples, the coupling is optimized when both cylindrical coils have exactly the same axis of cylindrical symmetry (namely they are "facing" each other). Particular mutual coil angles and orientations that lead to zero mutual inductance (such as the orientation where the axes of the two coils are perpendicular and the centers of the two coils are on one of the two axes) should obviously be avoided.

-- Finally, note that the heights of the coils  $h_1$  and  $h_2$  are other available design parameters, which can have an impact to the coupling similar to that of their radii  $r_1$  and  $r_2$ , and thus the design rules can be similar.

Further practical considerations apart from efficiency, e.g. physical size limitations, will be discussed in detail below.

### 2.2.4 Optimization of overall system performance

In many cases, the dimensions of the resonant objects will be set by the particular application at hand. For example, when this application is powering a laptop or a cell-phone, the device resonant object cannot have dimensions larger than those of the laptop

or cell-phone respectively. In particular, for a system of two loops of specified dimensions, in terms of loop radii  $r_{s,d}$  and wire radii  $a_{s,d}$ , the independent parameters left to adjust for the system optimization are: the number of turns  $N_{s,d}$ , the frequency  $f$ , the power-load consumption rate  $\kappa_l = R_l / 2L_d$  and the power-generator feeding rate  $\kappa_g = R_g / 2L_s$ , where  $R_g$  is the internal (characteristic) impedance of the generator.

In general, in various examples, the primary dependent variable that one wants to increase or optimize is the overall efficiency  $\eta$ . However, other important variables need to be taken into consideration upon system design. For example, in examples featuring capacitively-loaded coils, the design can be constrained by, for example, the currents flowing inside the wires  $I_{s,d}$  and the voltages across the capacitors  $V_{s,d}$ . These limitations can be important because for  $\sim Watt$  power applications the values for these parameters can be too large for the wires or the capacitors respectively to handle.

Furthermore, the total loaded (by the load) quality factor of the device

$Q_{d[l]} = \omega / 2(\Gamma_d + \Gamma_l) = \omega L_d / (R_d + R_l)$  and the total loaded (by the generator) quality factor of the source  $Q_{s[g]} = \omega / 2(\Gamma_s + \Gamma_g) = \omega L_s / (R_s + R_g)$  are quantities that should be preferably small, because to match the source and device resonant frequencies to within their  $Q$ 's, when those are very large, can be challenging experimentally and more sensitive to slight variations. Lastly, the radiated powers  $P_{s,rad}$  and  $P_{d,rad}$  should be minimized for concerns about far-field interference and safety, even though, in general, for a magnetic, non-radiative scheme they are already typically small. In the following, we examine then the effects of each one of the independent variables on the dependent ones.

We define a new variable  $wp$  to express the power-load consumption rate for some particular value of  $U$  through  $U_l = \kappa_l / \Gamma_d = \sqrt{1 + wp \cdot U^2}$ . Then, in some examples, values which impact the choice of this rate are:  $U_l = 1 \Leftrightarrow wp = 0$  to minimize the required energy stored in the source (and therefore  $I_s$  and  $V_s$ ),  $U_l = \sqrt{1 + U^2} > 1 \Leftrightarrow wp = 1$  to maximize the efficiency, as seen earlier, or  $U_l \gg 1 \Leftrightarrow wp \gg 1$  to decrease the required

energy stored in the device (and therefore  $I_d$  and  $V_d$ ) and to decrease or minimize  $Q_{d[l]}$ . Similar is the impact of the choice of the power-generator feeding rate  $U_g = \kappa_g / \Gamma_s$ , with the roles of the source/device and generator/load reversed.

In some examples, increasing  $N_s$  and  $N_d$  increases  $Q_s$  and  $Q_d$ , and thus  $U$  and the efficiency significantly, as seen before. It also decreases the currents  $I_s$  and  $I_d$ , because the inductance of the loops increases, and thus the energy  $W_{s,d} = L_{s,d} |I_{s,d}|^2 / 2$  required for given output power  $P_l$  can be achieved with smaller currents. However, in some examples, increasing  $N_d$  and thus  $Q_d$  can increase  $Q_{d[l]}$ ,  $P_{d,rad}$  and the voltage across the device capacitance  $V_d$ . Similar can be the impact of increasing  $N_s$  on  $Q_{s[g]}$ ,  $P_{s,rad}$  and  $V_s$ . As a conclusion, in some examples, the number of turns  $N_s$  and  $N_d$  should be chosen large enough (for high efficiency) but such that they allow for reasonable voltages, loaded  $Q$ 's and/or powers radiated.

With respect to the resonant frequency, again, there is an optimal one for efficiency. Close to that optimal frequency  $Q_{d[l]}$  and/or  $Q_{s[g]}$  can be approximately maximum. In some examples, for lower frequencies the currents typically get larger but the voltages and radiated powers get smaller. In some examples, one should pick either the frequency that maximizes the efficiency or somewhat lower.

One way to decide on an operating regime for the system is based on a graphical method. Consider two loops of  $r_s = 25cm$ ,  $r_d = 15cm$ ,  $h_s = h_d = 0$ ,  $a_s = a_d = 3mm$  and distance  $D = 2m$  between them. In Fig. 12, we plot some of the above dependent variables (currents, voltages and radiated powers normalized to 1Watt of output power) in terms of frequency  $f$  and  $N_d$ , given some choice for  $wp$  and  $N_s$ . Fig. 12 depicts the trend of system performance explained above. In Fig. 13, we make a contour plot of the dependent variables as functions of both frequency and  $wp$  but for both  $N_s$  and  $N_d$  fixed. For example, a reasonable choice of parameters for the system of two loops with the dimensions given above are:  $N_s = 2$ ,  $N_d = 6$ ,  $f = 10MHz$  and  $wp = 10$ , which gives the following performance characteristics:  $\eta = 20.6\%$ ,  $Q_{d[l]} = 1264$ ,  $I_s = 7.2A$ ,  $I_d = 1.4A$ ,

$V_s = 2.55kV$ ,  $V_d = 2.30kV$ ,  $P_{s,rad} = 0.15W$ ,  $P_{d,rad} = 0.006W$ . Note that the results in Figs. 12, 13 and the just above calculated performance characteristics are made using the analytical formulas provided above, so they are expected to be less accurate for large values of  $N_s$ ,  $N_d$ , but still they give a good estimate of the scalings and the orders of magnitude.

Finally, one could additionally optimize for the source dimensions, since usually only the device dimensions are limited, as discussed earlier. Namely, one can add  $r_s$  and  $a_s$  in the set of independent variables and optimize with respect to these too for all the dependent variables of the problem (we saw how to do this only for efficiency earlier). Such an optimization would lead to improved results.

In this description, we propose that, if one ensures operation in the strongly-coupled regime at mid-range distances, at least medium-power transmission ( $\sim W$ ) at mid-range distances with high efficiency is possible.

### 2.3 Inductively-loaded conducting rods

A straight conducting rod of length  $2h$  and cross-sectional radius  $a$  has distributed capacitance and distributed inductance, and therefore it supports a resonant mode of angular frequency  $\omega$ . Using the same procedure as in the case of self-resonant coils, one can define an effective total inductance  $L$  and an effective total capacitance  $C$  of the rod through formulas Eqs.(19) and (20). With these definitions, the resonant angular frequency and the effective impedance are given again by the common formulas  $\omega = 1/\sqrt{LC}$  and  $Z = \sqrt{L/C}$  respectively. To calculate the total inductance and capacitance, one can assume again a sinusoidal current profile along the length of the conducting wire. When interested in the lowest mode, if we denote by  $x$  the coordinate along the conductor, such that it runs from  $-h$  to  $+h$ , then the current amplitude profile would have the form  $I(x) = I_o \cos(\pi x/2h)$ , since it has to be zero at the open ends of the rod. This is the well-known half-wavelength electric dipole resonant mode.

In some examples, one or more of the resonant objects are inductively-loaded conducting rods. Referring to Fig. 14, a straight conducting rod of length  $2h$  and cross-sectional radius  $a$ , as in the previous paragraph, is cut into two equal pieces of length  $h$ ,

which are connected via a coil wrapped around a magnetic material of relative permeability  $\mu$ , and everything is surrounded by air. The coil has an inductance  $L_c$ , which is added to the distributed inductance of the rod and thus modifies its resonance. Note however, that the presence of the center-loading inductor modifies significantly the current distribution inside the wire and therefore the total effective inductance  $L$  and total effective capacitance  $C$  of the rod are different respectively from  $L_s$  and  $C_s$ , which are calculated for a self-resonant rod of the same total length using a sinusoidal current profile, as in the previous paragraph. Since some current is running inside the coil of the external loading inductor, the current distribution  $\mathbf{j}$  inside the rod is reduced, so  $L < L_s$ , and thus, from the charge conservation equation, the linear charge distribution  $\rho_l$  flattens out towards the center (being positive in one side of the rod and negative in the other side of the rod, changing abruptly through the inductor), so  $C > C_s$ . The resonant frequency for this system is  $\omega = 1/\sqrt{(L + L_c)C} < \omega_s = 1/\sqrt{L_s C_s}$ , and  $I(x) \rightarrow I_o \cos(\pi x/2h) \Rightarrow L \rightarrow L_s \Rightarrow \omega \rightarrow \omega_s$ , as  $L_c \rightarrow 0$ .

In general, the desired CMT parameters can be found for this system, but again a very complicated solution of Maxwell's Equations is generally required. In a special case, a reasonable estimate for the current distribution can be made. When  $L_c \gg L_s > L$ , then  $\omega \approx 1/\sqrt{L_c C} \ll \omega_s$  and  $Z \approx \sqrt{L_c/C} \gg Z_s$ , while the current distribution is triangular along the rod (with maximum at the center-loading inductor and zero at the ends) and thus the charge distribution is positive constant on one half of the rod and equally negative constant on the other side of the rod. This allows us to compute numerically  $C$  from Eq.(20). In this case, the integral in Eq.(20) can actually be computed analytically, giving the formula  $1/C = 1/(\pi\epsilon_o h) [\ln(h/a) - 1]$ . Explicit analytical formulas are again available for  $R$  from Eq.(21) and (22), since  $I_{rms} = I_o$ ,  $|\mathbf{p}| = q_o h$  and  $|\mathbf{m}| = 0$  (namely only the electric-dipole term is contributing to radiation), so we can determine also  $Q_{abs} = 1/\omega C R_{abs}$  and  $Q_{rad} = 1/\omega C R_{rad}$ . At the end of the calculations, the validity of the assumption of triangular current profile is confirmed by checking that indeed the



condition  $L_c \gg L_s \Leftrightarrow \omega \ll \omega_s$  is satisfied. This condition is relatively easily satisfied, since typically a conducting rod has very small self-inductance  $L_s$  to begin with.

Another important loss factor in this case is the resistive loss inside the coil of the external loading inductor  $L_c$  and it depends on the particular design of the inductor. In some examples, the inductor is made of a Brooks coil, which is the coil geometry which, for fixed wire length, demonstrates the highest inductance and thus quality factor. The Brooks coil geometry has  $N_{Bc}$  turns of conducting wire of cross-sectional radius  $a_{Bc}$  wrapped around a cylindrically symmetric coil former, which forms a coil with a square cross-section of side  $r_{Bc}$ , where the inner side of the square is also at radius  $r_{Bc}$  (and thus

the outer side of the square is at radius  $2r_{Bc}$ ), therefore  $N_{Bc} \approx (r_{Bc} / 2a_{Bc})^2$ . The inductance of the coil is then  $L_c = 2.0285\mu_o r_{Bc} N_{Bc}^2 \approx 2.0285\mu_o r_{Bc}^5 / 8a_{Bc}^4$  and its

resistance  $R_c \approx \frac{1}{\sigma} \frac{l_{Bc}}{\pi a_{Bc}^2} \sqrt{1 + \frac{\mu_o \omega \sigma}{2} \left(\frac{a_{Bc}}{2}\right)^2}$ , where the total wire length is

$l_{Bc} \approx 2\pi(3r_{Bc}/2)N_{Bc} \approx 3\pi r_{Bc}^3 / 4a_{Bc}^2$  and we have used an approximate square-root law for the transition of the resistance from the dc to the ac limit as the skin depth varies with frequency.

The external loading inductance  $L_c$  provides the freedom to tune the resonant frequency. For example, for a Brooks coil with a fixed size  $r_{Bc}$ , the resonant frequency can be reduced by increasing the number of turns  $N_{Bc}$  by decreasing the wire cross-sectional radius  $a_{Bc}$ . Then the desired resonant angular frequency  $\omega = 1/\sqrt{L_c C}$  is achieved for  $a_{Bc} \approx (2.0285\mu_o r_{Bc}^5 \omega^2 C)^{1/4}$  and the resulting coil quality factor is

$Q_c \approx 0.169\mu_o \sigma r_{Bc}^2 \omega / \sqrt{1 + \omega^2 \mu_o \sigma \sqrt{2.0285\mu_o} (r_{Bc}/4)^5 C}$ . Then, for the particular simple case  $L_c \gg L_s$ , for which we have analytical formulas, the total

$Q = 1/\omega C (R_c + R_{abs} + R_{rad})$  becomes highest at some optimal frequency  $\omega_Q$ , reaching the value  $Q_{\max}$ , both determined by the loading-inductor specific design. For example,

for the Brooks-coil procedure described above, at the optimal frequency

$Q_{\max} \approx Q_c \approx 0.8 \left( \mu_o \sigma^2 r_{Be}^3 / C \right)^{1/4}$ . At lower frequencies it is dominated by ohmic loss inside the inductor coil and at higher frequencies by radiation. Note, again, that the above formulas are accurate as long as  $\omega_Q \ll \omega_s$  and, as explained above, this is easy to design for by using a large inductance.

The results of the above analysis for two examples, using Brooks coils, of subwavelength modes of  $\lambda/h \geq 200$  (namely highly suitable for near-field coupling and well within the quasi-static limit) at the optimal frequency  $\omega_Q$  are presented in Table 5.

Table 5 shows in parentheses (for similarity to previous tables) analytical results for the wavelength and absorption, radiation and total loss rates, for two different cases of subwavelength-loop resonant modes. Note that for conducting material copper ( $\sigma=5.998 \cdot 10^7 S/m$ ) was used. The results show that, in some examples, the optimal frequency is in the low-MHz microwave range and the expected quality factors are  $Q_{abs} \geq 1000$  and  $Q_{rad} \geq 100000$ .

**Table 5**

single rod	$\lambda/h$	f (MHz)	$Q_{rad}$	$Q_{abs}$	$Q$
h=30cm, a=2cm $\mu=1, r_{Be}=2cm, a_{Be}=0.88mm, N_{Be}=129$	(403.8)	(2.477)	( $2.72 \cdot 10^6$ )	(7400)	(7380)
h=10cm, a=2mm $\mu=1, r_{Be}=5mm, a_{Be}=0.25mm,$ $N_{Be}=103$	(214.2)	(14.010)	( $6.92 \cdot 10^5$ )	(3908)	(3886)

In some examples, energy is transferred between two inductively-loaded rods. For the rate of energy transfer between two inductively-loaded rods 1 and 2 at distance  $D$  between their centers, the mutual capacitance  $M_C$  can be evaluated numerically from Eq.(23) by using triangular current distributions in the case  $\omega \ll \omega_s$ . In this case, the coupling is only electric and again we have an analytical formula, which, in the quasi-static limit  $h \ll D \ll \lambda$  and for the relative orientation  $h$  such that the two rods are aligned on the same axis, is  $1/M_C \approx 1/2\pi\epsilon_o \cdot (h_1 h_2)^2 / D^3$ , which means that  $k \propto \left( \sqrt{h_1 h_2} / D \right)^3$  is independent of the frequency  $\omega$ . One can then get the resultant strong-coupling factor  $U$ .

It can be seen that the optimal frequency  $\omega_U$ , where the figure-of-merit is maximized to the value  $U_{\max}$ , is close to the frequency  $\omega_{Q_1 Q_2}$ , where  $Q_1 Q_2$  is maximized, since  $k$  does not depend much on frequency (at least for the distances  $D \ll \lambda$  of interest for which the quasi-static approximation is still valid). Therefore, the optimal frequency  $\omega_U \approx \omega_{Q_1 Q_2}$  is mostly independent of the distance  $D$  between the two rods and lies between the two frequencies  $\omega_{Q_1}$  and  $\omega_{Q_2}$  at which the single-rod  $Q_1$  and  $Q_2$  respectively peak. In some typical examples, one can tune the inductively-loaded conducting rods, so that their angular eigenfrequencies are close to  $\omega_U$  within  $\Gamma_U$ , which is half the angular frequency width for which  $U > U_{\max} / 2$ .

Referring to Table 6, in parentheses (for similarity to previous tables) analytical results based on the above are shown for two systems each composed of a matched pair of the loaded rods described in Table 5. The average wavelength and loss rates are shown along with the coupling rate and coupling to loss ratio figure-of-merit  $U = \kappa / \Gamma$  as a function of the coupling distance  $D$ , for the two cases. Note that for  $\Gamma_{rod}$  the single-rod value is used. Again we chose  $L_c \gg L_s$  to make the triangular-current assumption a good one and computed  $M_C$  numerically from Eq.(23). The results show that for medium distances  $D/h = 10 - 3$  the expected coupling-to-loss ratios are in the range  $U \sim 0.5 - 100$ .

**Table 6**

pair of rods	$D/h$	$Q_{\kappa} = 1/k$	$U$
h=30cm, a=2cm $\mu=1, r_{Bc}=2\text{cm}, a_{Bc}=0.88\text{mm}, N_{Bc}=129$ $\lambda/h \approx 404$ $Q \approx 7380$	3	(70.3)	(105.0)
	5	(389)	(19.0)
	7	(1115)	(6.62)
	10	(3321)	(2.22)
h=10cm, a=2mm $\mu=1, r_{Bc}=5\text{mm}, a_{Bc}=0.25\text{mm}, N_{Bc}=103$ $\lambda/h \approx 214$ $Q \approx 3886$	3	(120)	(32.4)
	5	(664)	(5.85)
	7	(1900)	(2.05)
	10	(5656)	(0.69)

2.4 Dielectric disks

In some examples, one or more of the resonant objects are dielectric objects, such as disks. Consider a two dimensional dielectric disk object, as shown in Fig. 15(a), of radius  $r$  and relative permittivity  $\epsilon$  surrounded by air that supports high- $Q$  “whispering-gallery” resonant modes. The loss mechanisms for the energy stored inside such a resonant system are radiation into free space and absorption inside the disk material. High- $Q_{rad}$  and long-tailed subwavelength resonances can be achieved when the dielectric permittivity  $\epsilon$  is large and the azimuthal field variations are slow (namely of small principal number  $m$ ). Material absorption is related to the material loss tangent:  $Q_{abs} \sim \text{Re}\{\epsilon\} / \text{Im}\{\epsilon\}$ . Mode-solving calculations for this type of disk resonances were performed using two independent methods: numerically, 2D finite-difference frequency-domain (FDFD) simulations (which solve Maxwell’s Equations in frequency domain exactly apart for spatial discretization) were conducted with a resolution of  $30pts/r$ ; analytically, standard separation of variables (SV) in polar coordinates was used.

Table 7

single disk	$\lambda/r$	$Q_{abs}$	$Q_{rad}$	$Q$
<b>Re{<math>\epsilon</math>}=147.7, m=2</b>	<b>20.01 (20.00)</b>	<b>10103 (10075)</b>	<b>1988 (1992)</b>	<b>1661 (1663)</b>
Re{ $\epsilon$ }=65.6, m=3	9.952 (9.950)	10098 (10037)	9078 (9168)	4786 (4802)

The results for two TE-polarized dielectric-disk subwavelength modes of  $\lambda/r \geq 10$  are presented in Table 7. Table 7 shows numerical FDFD (and in parentheses analytical SV) results for the wavelength and absorption, radiation and total loss rates, for two different cases of subwavelength-disk resonant modes. Note that disk-material loss-tangent  $\text{Im}\{\epsilon\}/\text{Re}\{\epsilon\}=10^{-4}$  was used. (The specific parameters corresponding to the plot in Fig. 15(a) are highlighted with bold in the table.) The two methods have excellent agreement and imply that for a properly designed resonant low-loss-dielectric object values of  $Q_{rad} \geq 2000$  and  $Q_{abs} \sim 10000$  are achievable. Note that for the 3D case the computational complexity would be immensely increased, while the physics would not be significantly different. For example, a spherical object of  $\epsilon=147.7$  has a whispering gallery mode with  $m=2$ ,  $Q_{rad}=13962$ , and  $\lambda/r=17$ .

The required values of  $\varepsilon$ , shown in Table 7, might at first seem unrealistically large. However, not only are there in the microwave regime (appropriate for approximately meter-range coupling applications) many materials that have both reasonably high enough dielectric constants and low losses (e.g. Titania, Barium tetratitanate, Lithium tantalite etc.), but also  $\varepsilon$  could signify instead the effective index of other known subwavelength surface-wave systems, such as surface modes on surfaces of metallic materials or plasmonic (metal-like, negative- $\varepsilon$ ) materials or metallo-dielectric photonic crystals or plasmono-dielectric photonic crystals.

To calculate now the achievable rate of energy transfer between two disks 1 and 2, as shown in Fig. 15(b) we place them at distance  $D$  between their centers. Numerically, the FDFD mode-solver simulations give  $\kappa$  through the frequency splitting of the normal modes of the combined system ( $\delta_E = 2\kappa$  from Eq.(4)), which are even and odd superpositions of the initial single-disk modes; analytically, using the expressions for the separation-of-variables eigenfields  $\mathbf{E}_{1,2}(\mathbf{r})$  CMT gives  $\kappa$  through

$$\kappa = \omega_1 / 2 \cdot \int d^3r \varepsilon_2(\mathbf{r}) E_2^*(\mathbf{r}) E_1(\mathbf{r}) / \int d^3r \varepsilon(\mathbf{r}) |E_1(\mathbf{r})|^2,$$

where  $\varepsilon_j(\mathbf{r})$  and  $\varepsilon(\mathbf{r})$  are the dielectric functions that describe only the disk  $j$  (minus the constant  $\varepsilon_0$  background) and the whole space respectively. Then, for medium distances  $D/r = 10^{-3}$  and for non-radiative coupling such that  $D < 2r_c$ , where  $r_c = m\lambda / 2\pi$  is the radius of the radiation caustic, the two methods agree very well, and we finally find, as shown in Table 8, strong-coupling factors in the range  $U \sim 1 - 50$ . Thus, for the analyzed examples, the achieved figure-of-merit values are large enough to be useful for typical applications, as discussed below.

**Table 8**

two disks	$D/r$	$Q^{rad}$	$Q = \omega/2\Gamma$	$\omega/2\kappa$	$\kappa/\Gamma$
$\text{Re}\{\epsilon\}=147.7, m=2$ $\lambda/r = 20$ $Q^{abs} = 10093$	3	2478	1989	46.9 (47.5)	42.4 (35.0)
	5	2411	1946	298.0 (298.0)	8.5 (5.6)
	7	2196	1804	769.7 (770.2)	2.3 (2.2)
	<b>10</b>	<b>2017</b>	<b>1681</b>	<b>1714 (1601)</b>	<b>0.98 (1.04)</b>
$\text{Re}\{\epsilon\}=85.6, m=3$ $\lambda/r = 10$ $Q^{abs} = 10096$	3	7972	4455	144 (140)	30.9 (34.3)
	5	9240	4824	2242 (2083)	2.2 (2.3)
	7	9187	4810	7485 (7417)	0.64 (0.65)

Note that even though particular examples are presented and analyzed above as examples of systems that use resonant electromagnetic coupling for wireless energy transfer, those of self-resonant conducting coils, capacitively-loaded resonant conducting coils, inductively-loaded resonant conducting rods and resonant dielectric disks, any system that supports an electromagnetic mode with its electromagnetic energy extending much further than its size can be used for transferring energy. For example, there can be many abstract geometries with distributed capacitances and inductances that support the desired kind of resonances. In some examples, the resonant structure can be a dielectric sphere. In any one of these geometries, one can choose certain parameters to increase and/or optimize  $U$  or, if the  $Q$ 's are limited by external factors, to increase and/or optimize for  $k$  or, if other system performance parameters are of importance, to optimize those.

3 Coupled-Mode Theory for prediction of far-field radiation interference

The two objects in an energy-transfer system generate radiation, which can sometimes be a significant part of the intrinsic losses, and can interfere in the far field. In the previous Sections, we analyzed systems, where this interference phenomenon was not in effect. In this description, we will repeat the analysis, including the interference effects and will show how it can be used to further enhance the power transmission efficiency and/or the radiated power.

The coupled-mode equations of Eqs.(1) fail to predict such an interference phenomenon. In fact, the inability to predict interference phenomena has often been considered inherent to coupled-mode theory (CMT). However, we show here that making only a simple extension to this model, it can actually very successfully predict such interference. The root of the problem stems from the fact that the coupling coefficients were tacitly assumed to be real. This is usually the case when dealing with proper (real) eigenmodes of a Hermitian (lossless) operator. However, this assumption fails when losses are included, as is for example the current case dealing with generally non-proper (leaky, radiative) eigenmodes of a non-Hermitian (lossy) operator. In this case, the coupling-matrix elements will generally be complex and their imaginary parts will be shown to be directly related to far-field radiation interference.

Imagine a system of many resonators in proximity to each other. When their resonances have close enough frequencies compared to their coupling rates, the CMT assumption is that the total-system field  $\psi$  is approximately determined only by these resonances as the superposition  $\psi(t) = \sum_n a_n(t)\psi_n$ , where  $\psi_n$  is the eigenfield of the resonance  $n$  normalized to unity energy, and  $a_n$  is the field amplitude inside it, which corresponds, due to the normalization, to  $|a_n|^2$  stored energy. The fundamental Coupled-Mode Equations (CME) of CMT are then those of the evolution of the vector  $\mathbf{a} = \{a_n\}$

$$\frac{d}{dt}\mathbf{a} = -i\bar{\mathbf{\Omega}} \cdot \mathbf{a} + i\bar{\mathbf{K}} \cdot \mathbf{a} \quad (34)$$

where the frequency matrix  $\bar{\mathbf{\Omega}}$  and the coupling matrix  $\bar{\mathbf{K}}$  are found usually using a Perturbation Theory (PT) approach.

We restate here one of the many perturbative formulations of CMT in a system of ElectroMagnetic (EM) resonators: Let  $\mu = \mu_o$  and  $\epsilon = \epsilon_o + \sum_n \epsilon_n$  be the magnetic-permeability and dielectric-permittivity functions of space that describe the whole system, where  $\epsilon_n$  is the permittivity of only the dielectric, reciprocal and generally anisotropic object  $n$  of volume  $V_n$ , in excess to the constant  $\mu_o, \epsilon_o$  background space. Each resonator  $n$ , when alone in the background space, supports a resonant eigenmode of complex frequency  $\Omega_n = \omega_n - i\Gamma_n$  and field profiles  $\psi_n = [\mathbf{E}_n, \mathbf{H}_n]$  normalized to unity energy, satisfying the equations  $\nabla \times \mathbf{E}_n = i\Omega_n\mu_o\mathbf{H}_n$  and  $\nabla \times \mathbf{H}_n = -i\Omega_n(\epsilon_o + \epsilon_n)\mathbf{E}_n$ ,

and the boundary condition  $\hat{\mathbf{n}} \times \mathbf{E}_n = 0$  on the potential metallic surface  $S_n$  of object  $n$ . The whole system fields  $\psi = [\mathbf{E}, \mathbf{H}]$  satisfy the equations  $\nabla \times \mathbf{E} = -\mu \frac{\partial}{\partial t} \mathbf{H}$  and  $\nabla \times \mathbf{H} = \epsilon \frac{\partial}{\partial t} \mathbf{E}$ , and the boundary condition  $\hat{\mathbf{n}} \times \mathbf{E} = 0$  on  $S = \sum_n S_n$ . Then, start by expanding  $\nabla \cdot (\mathbf{E} \times \mathbf{H}_n^- - \mathbf{E}_n^- \times \mathbf{H})$  and integrating over all space, apply the CMT superposition assumption, and finally use the PT argument that, when the coupling-rates between the resonators are small compared to their frequencies, within a sum only terms of lowest order in this small perturbation need to be kept. The result is the CME of Eq.(34), with  $\bar{\Omega} = \bar{\mathbf{W}}^{-1} \cdot \bar{\Omega}_o \cdot \bar{\mathbf{W}}$ ,  $\bar{\mathbf{K}} = \bar{\mathbf{W}}^{-1} \cdot \mathbf{K}_o$ , where  $\bar{\Omega}_o = \text{diag}\{\Omega_n\}$ ,

$$K_{o,nm} = \frac{\Omega_n}{4} \int_{V_m} dv (\mathbf{E}_n^- \cdot \boldsymbol{\epsilon}_m \cdot \mathbf{E}_m) + \frac{i}{4} \oint_{S_m} da \hat{\mathbf{n}} \cdot (\mathbf{E}_n^- \times \mathbf{H}_m) \quad (35)$$

$$W_{nm} = \frac{1}{4} \int_{V_m} dv (\mathbf{E}_n^- \cdot \boldsymbol{\epsilon} \cdot \mathbf{E}_m + \mathbf{H}_n^- \cdot \boldsymbol{\mu} \cdot \mathbf{H}_m) \quad (36)$$

and where  $\psi_n = [\mathbf{E}_n^-, \mathbf{H}_n^-]$  satisfy the time-reversed equations (where  $\Omega_n \rightarrow -\Omega_n$ ). The choice of these fields in the analysis rather than  $\psi_n^* = [\mathbf{E}_n^*, \mathbf{H}_n^*]$  allows to treat also lossy (due to absorption and/or radiation) but reciprocal systems (so  $\bar{\mathbf{K}}$  is complex symmetric but non-Hermitian). In the limit, though, of weak loss (high- $Q$  resonances), these two sets of fields can be approximately equal. Therefore, again to lowest order,  $\bar{\mathbf{W}} \approx \bar{\mathbf{I}}$ , due to the unity-energy normalization, so  $\bar{\Omega} \approx \bar{\Omega}_o$  and for  $\bar{\mathbf{K}}$  the off-diagonal terms

$$K_{nm} \approx K_{o,mn} \approx \frac{i}{4} \int_{V_m} dv (\mathbf{E}_n^* \cdot \mathbf{J}_m); \quad n \neq m \quad (37)$$

where  $\mathbf{J}_m$  includes both the volume-polarization currents  $\mathbf{J}_{p,m} = -i\Omega_m \epsilon_m \mathbf{E}_m$  in  $V_m$  and the surface electric currents  $\mathbf{J}_{s,m} = \hat{\mathbf{n}} \times \mathbf{H}_m$  on  $S_m$ , while the diagonal terms  $K_{nn}$  are higher-order small and can often lead to anomalous coupling-induced frequency shifts. The term of Eq.(37) can generally be complex  $K_{nm} = \kappa_{nm} + i\Lambda_{nm}$  and, even though the physical interpretation of its real part is well understood, as describing the coupling between the resonators, it is not so the case for its imaginary part



$$\begin{aligned}
 \Lambda_{nm} &= \frac{1}{4} \operatorname{Re} \left\{ \int_{V_m} dv [i\omega \mathbf{A}_n - \nabla \phi_n]^* \cdot \mathbf{J}_m \right\} \\
 &= \frac{1}{4} \operatorname{Re} \left\{ \int_{V_m} dv \left[ \int_{V_n} dv \frac{e^{ik|\mathbf{r}_m - \mathbf{r}_n|}}{4\pi|\mathbf{r}_m - \mathbf{r}_n|} \left( i\omega\mu_0 \mathbf{J}_n + \frac{\rho_n}{\epsilon_0} \nabla \right) \right]^* \cdot \mathbf{J}_m \right\} \quad (38) \\
 &= \frac{\omega}{16\pi} \int_{V_m} dv \int_{V_n} dv \operatorname{Re} \left\{ \left( \frac{\rho_n^* \rho_m}{\epsilon_0} - \mu_0 \mathbf{J}_n^* \cdot \mathbf{J}_m \right) \frac{e^{ik|\mathbf{r}_m - \mathbf{r}_n|}}{4\pi|\mathbf{r}_m - \mathbf{r}_n|} \right\}
 \end{aligned}$$

where integration by parts was used for the  $\nabla \phi_n$  term and the continuity equation  $\nabla \cdot \mathbf{J} = i\omega\rho$ , with  $\rho$  being the volume charge density.

Towards understanding this term, let us consider two resonators 1, 2 and evaluate from Eqs.(34) the total power lost from the system

$$\begin{aligned}
 P_{loss} &= -\frac{d}{dt} (|a_1|^2 + |a_2|^2) \\
 &= 2\Gamma_1 |a_1|^2 + 2\Gamma_2 |a_2|^2 + 4\Lambda_{12} \operatorname{Re} \{ a_1^* a_2 \} \quad (39)
 \end{aligned}$$

Clearly, the term involving an interaction between the two objects should not relate to material absorption, since this is a very localized process inside each object. We therefore split this lost power into absorbed and radiated in the following way

$$P_{abs} = 2\Gamma_{1,abs} |a_1|^2 + 2\Gamma_{2,abs} |a_2|^2 \quad (40)$$

$$P_{rad} = 2\Gamma_{1,rad} |a_1|^2 + 2\Gamma_{2,rad} |a_2|^2 + 4\Lambda_{12} \operatorname{Re} \{ a_1^* a_2 \} \quad (41)$$

so  $\Lambda_{12}$  is associated with the radiation from the two-object system. However, we have a tool to compute this radiated power separately: Antenna Theory (AT).

Let  $\zeta_o = \sqrt{\mu_o/\epsilon_o}$  and  $c_o = 1/\sqrt{\mu_o\epsilon_o}$  be the background impedance and light-velocity, and  $f = (g, \mathbf{f}) = \int_V dv' J^\nu(\mathbf{r}') e^{-ik \cdot \mathbf{r}'}$  the moment of the current-distribution 4-vector  $J^\nu = (c_o\rho, \mathbf{J})$  of an electromagnetic resonator, where unity-energy normalization is

again assumed for  $J^\nu$  and  $g = \hat{\mathbf{k}} \cdot \mathbf{f}$ , as can be shown using the continuity equation and integration by parts. The power radiated from one EM resonator is:

$$P_{rad} = 2\Gamma_{rad} |a|^2 = \frac{\zeta_o k^2}{32\pi^2} \left( \oint d\Omega |f|^2 \right) |a|^2 \quad (42)$$

where  $|f|^2 = f^* \cdot f \equiv |\mathbf{f}|^2 - |g|^2$ . The power radiated from an ‘array’ of two resonators 1 and 2, at vector-distance  $\mathbf{D}$  between their centers, is given by:

$$\begin{aligned} P_{rad} &= \frac{\zeta_o k^2}{32\pi^2} \oint d\Omega \left| a_1 f_1 + a_2 f_2 e^{-i\mathbf{k} \cdot \mathbf{D}} \right|^2 \\ &= \frac{\zeta_o k^2}{32\pi^2} \left[ \left( \oint d\Omega |f_1|^2 \right) |a_1|^2 + \left( \oint d\Omega |f_2|^2 \right) |a_2|^2 \right. \\ &\quad \left. + 2 \operatorname{Re} \left\{ \oint d\Omega f_1^* \cdot f_2 e^{-i\mathbf{k} \cdot \mathbf{D}} a_1^* a_2 \right\} \right] \end{aligned} \quad (43)$$

where  $f_1^* \cdot f_2 \equiv \mathbf{f}_1^* \cdot \mathbf{f}_2 - g_1^* \cdot g_2$ . Thus, by comparing Eqs.(41) and (43), using Eq.(42),

$$\Lambda_{12} = \frac{\zeta_o k^2 \operatorname{Re} \left\{ \oint d\Omega f_1^* \cdot f_2 e^{-i\mathbf{k} \cdot \mathbf{D}} a_1^* a_2 \right\}}{64\pi^2 \operatorname{Re} \left\{ a_1^* a_2 \right\}} \quad (44)$$

namely  $\Lambda_{12}$  is exactly the interference term in AT. By substituting for the 4-vector current-moments and making the change of variables  $\mathbf{r}_1 = \mathbf{r}'_1$ ,  $\mathbf{r}_2 = \mathbf{r}'_2 + \mathbf{D}$ ,

$$\begin{aligned} \Lambda_{12} &= \frac{\zeta_o k^2 \operatorname{Re} \left\{ \int_{V_1} dv \int_{V_2} dv J_1^* \cdot J_2 \oint d\Omega e^{-i\mathbf{k} \cdot (\mathbf{r}_2 - \mathbf{r}_1)} a_1^* a_2 \right\}}{64\pi^2 \operatorname{Re} \left\{ a_1^* a_2 \right\}} \\ &= \frac{\zeta_o k \operatorname{Re} \left\{ \int_{V_1} dv \int_{V_2} dv J_1^* \cdot J_2 \frac{\sin(k|\mathbf{r}_2 - \mathbf{r}_1|)}{|\mathbf{r}_2 - \mathbf{r}_1|} a_1^* a_2 \right\}}{16\pi \operatorname{Re} \left\{ a_1^* a_2 \right\}} \end{aligned} \quad (45)$$

where we evaluated the integral over all angles of  $\mathbf{k}$  with  $\mathbf{r}_2 - \mathbf{r}_1$ .

Note now that Eqs.(38) and (45) will become identical, if we can take the currents  $J_{1,2}'$  to be real. This is indeed the case for eigenmodes, where the field solution in bounded regions (such as those where the currents are flowing) is always stationary (in contrast to the leaky part of the eigenmode, which is radiative) and for high enough  $Q$  it can be chosen so that it is approximately real in the entire bounded region. Therefore, from either Eq.(38) or (45) we can write

$$\Lambda_{12} = \frac{\zeta_o k}{16\pi} \int_{V_1} dv \int_{V_2} dv J_1 \cdot J_2 \frac{\sin(k|\mathbf{r}_2 - \mathbf{r}_1|)}{|\mathbf{r}_2 - \mathbf{r}_1|} \quad (46)$$

and from Eq.(44), using Eq.(42), we can define the interference factor

$$V_{\text{rad},12} \equiv \frac{\Lambda_{12}}{\sqrt{\Gamma_{1,\text{rad}} \Gamma_{2,\text{rad}}}} = \frac{\oint d\Omega f_1^* \cdot f_2 e^{-ik \cdot \mathbf{D}}}{\sqrt{\oint d\Omega |f_1|^2 \oint d\Omega |f_2|^2}} \quad (47)$$

We have shown that, in the high- $Q$  limit, both PT and AT give the same expression for the imaginary part  $\Lambda_{nm}$  of the coupling coefficient, which thus physically describes within CMT the effects of far-field radiation interference. Again, this phenomenon was so far not considered to be predictable from CMT.

#### 4 Efficiency enhancement and radiation suppression by far-field destructive interference

Physically, one can expect that far-field radiation interference can in principle be engineered to be destructive, resulting in reduced overall radiation losses for the two-object system and thus in enhanced system efficiency. In this section, we show that, indeed, in the presence of far-field interference, energy transfer can be more efficient and with less radiated power than what our previous model predicts.

Once more, we will treat the same temporal energy-transfer schemes as before (finite-amount and finite-rate), so that a direct comparison can be made.

##### 4.1 Finite-amount energy-transfer efficiency

Considering again the source and device objects 1,2 to include the interference effects, the same CMT equations as in Eq.(1) can be used, but with the substitutions  $\kappa_{nm} \rightarrow K_{nm} = \kappa_{nm} + i\Lambda_{nm}$ ;  $n, m = 1, 2$ . The real parts  $\kappa_{11,22}$  can describe, as before, the shift in each object's resonance frequency due to the presence of the other; the imaginary parts  $\Lambda_{11,22}$  can describe the change in the losses of each object due to the

presence of the other (due to absorption in it or scattering from it, in which latter case losses could be either increased or decreased); both of these are second-order effects and, for the purposes of our mathematical analysis, can again be absorbed into the complex eigenfrequencies by setting  $\omega_{1,2} \rightarrow \omega_{1,2} + \kappa_{11,22}$  and  $\Gamma_{1,2} \rightarrow \Gamma_{1,2} - \Lambda_{11,22}$ . The real parts  $\kappa_{12,21}$  can denote, as before, the coupling coefficients; the imaginary parts  $\Lambda_{12,21}$  can describe the far-field interference, as was shown in Section 3; again, from reciprocity  $K_{12} = K_{21} \equiv K \equiv \kappa + i\Lambda$  (note that for a Hermitian problem, the additional requirement  $K_{12} = K_{21}^*$  would impose  $K$  to be real, which makes sense, since without losses there cannot be any radiation interference).

Substituting  $\kappa \rightarrow \kappa + i\Lambda$  into Eq.(2), we can find the normal modes of the system including interference effects. Note that, when the two objects are at exact resonance  $\omega_1 = \omega_2 \equiv \omega_o$  and  $\Gamma_1 = \Gamma_2 \equiv \Gamma_o$ , the normal modes are found to be

$$\Omega_+ = (\omega_o + \kappa) - i(\Gamma_o - \Lambda) \quad \text{and} \quad \Omega_- = (\omega_o - \kappa) - i(\Gamma_o + \Lambda), \quad (48)$$

which is exactly the typical case for respectively the odd and even normal modes of a system of two coupled objects, where for the even mode the objects' field-amplitudes have the same sign and thus the frequency is lowered and the radiative far-fields interfere constructively so loss is increased, while for the odd mode the situation is the opposite. This is another confirmation for the fact that the coefficient  $\Lambda$  can describe the far-field interference phenomenon under examination.

To treat now again the problem of energy transfer to object 2 from 1, but in the presence of radiative interference, again simply substitute  $\kappa \rightarrow \kappa + i\Lambda$  into Eq.(3). Note that, at exact resonance  $\omega_1 = \omega_2$  and, in the special case  $\Gamma_1 = \Gamma_2 \equiv \Gamma_o$ , we can just substitute into Eq.(4)  $U \rightarrow U + iV$ , where  $U \equiv \kappa/\Gamma_o$  and  $V \equiv \Lambda/\Gamma_o$ , and then, with  $T \equiv \Gamma_o t$ , the evolution of the device field-amplitude becomes

$$\frac{a_2(T)}{|a_1(0)|} = \sin[(U + iV)T] \cdot e^{-T} \quad (49)$$

Now the efficiency  $\eta_E \equiv |a_2(t)|^2/|a_1(0)|^2$  can be optimized for the normalized time  $T_*$  which is the solution of the transcendental equation

$$\operatorname{Re}\{(U + iV) \cdot \cot[(U + iV)T_*]\} = 1 \quad (50)$$

and the resulting optimal energy-transfer efficiency depends only on  $U$ ,  $V$  and is depicted in Fig. 16(c), evidently increasing with  $V$  for a fixed  $U$ .

#### 4.2 Finite-rate energy-transfer (power-transmission) efficiency

Similarly, to treat the problem of continuous powering of object 2 by 1, in the presence of radiative interference, simply substitute  $U \rightarrow U + iV$  into the equations of Section 1.2, where  $V \equiv \Lambda/\sqrt{\Gamma_1\Gamma_2}$  we call the strong-interference factor and quantifies the degree of far-field interference that the system experiences compared to loss. In practice, the parameters  $D_{1,2}$ ,  $U_{1,2}$  can be designed (engineered), since one can adjust the resonant frequencies  $\omega_{1,2}$  (compared to the desired operating frequency  $\omega$ ) and the generator/load supply/drain rates  $\kappa_{1,2}$ . Their choice can target the optimization of some system performance-characteristic of interest.

In some examples, a goal can be to maximize the power transmission (efficiency)  $\eta_P \equiv |S_{21}|^2$  of the system. The symmetry upon interchanging  $1 \leftrightarrow 2$  is then preserved and, using Eq.(11), the field-amplitude transmission coefficient becomes

$$S_{21} = \frac{2i(U + iV)U_0}{(1 + U_0 - iD_0)^2 + (U + iV)^2} \quad (51)$$

and from  $\eta'_P(D_0) = 0$  we get that, for fixed  $U$ ,  $V$  and  $U_0$ , the efficiency can be maximized for the symmetric detuning

$$D_0 = \begin{cases} 2\sqrt{\alpha} \cos\left(\frac{\theta + 2v\pi}{3}\right); v = 0, 1, & \text{if } U^{2/3} - V^{2/3} > (1 + U_0)^{2/3} \\ \sqrt[3]{\beta + \sqrt{\beta^2 - \alpha^3}} + \sqrt[3]{\beta - \sqrt{\beta^2 - \alpha^3}} & \text{if } U^{2/3} - V^{2/3} \leq (1 + U_0)^{2/3} \end{cases} \quad (52)$$

where  $\alpha \equiv [U^2 - V^2 - (1 + U_0)^2]/3$ ,  $\beta \equiv UV(1 + U_0)$ ,  $\theta \equiv \tan^{-1}\sqrt{\alpha^3/\beta^2 - 1}$  and  $U^{2/3} - V^{2/3} > (1 + U_0)^{2/3} \Leftrightarrow \alpha^3 - \beta^2 > 0 \Leftrightarrow \alpha > 0$ . Note that, in the first case, the two peaks of the transmission curve are not equal for  $V > 0$ , but the one at higher frequencies ( $v = 0 \Rightarrow$  positive detuning) corresponding to the odd system normal mode is higher, as should be expected, since the odd mode is the one that radiates less. Finally,

by substituting  $D_o$  into  $\eta_P$  from Eq.(52), then from  $\eta'_P(U_o) = 0$  we get that, for fixed  $U$  and  $V$ , the efficiency can be maximized for

$$U_{0*} = \sqrt{(1 + U^2)(1 - V^2)} \quad \text{and} \quad D_{0*} = UV. \quad (53)$$

The dependence of the efficiency on  $D_o$  for different  $U_o$  (including the new 'critical-coupling' condition) are shown in Figs. 16(a,b). The overall optimal power efficiency using Eqs.(53) is

$$\eta_{P*} \equiv \eta_P(D_{0*}, U_{0*}) = \frac{U^2 + V^2}{(U_{0*} + 1)^2 + U^2V^2} \quad (54)$$

which depends only on  $U$ ,  $|V|$  and is depicted in Figs. 16 (c,d), increasing with  $|V|$  for a fixed  $U$ , and actually  $\eta_P \rightarrow 1$  as  $|V| \rightarrow 1$  for all values of  $U$ .

In some examples, a goal can be to minimize the power reflection at the side of the generator  $|S_{11}|^2$  and the load  $|S_{22}|^2$ . The symmetry upon interchanging  $1 \leftrightarrow 2$  is again preserved and, using then Eq.(17), one would require the 'impedance matching' condition

$$(1 - iD_o)^2 - U_o^2 + (U + iV)^2 = 0 \quad (55)$$

from which again we easily find that the values of  $D_o$  and  $U_o$  that cancel all reflections are exactly those in Eqs.(53).

In some examples, it can be of interest to minimize the power radiated from the system, since e.g. it can be a cause of interference to other communication systems, while still maintaining good efficiency. In some examples, the two objects can be the same, and then, using Eq.(41), we find

$$\eta_{rad} \equiv \frac{P_{rad}}{|S_{+1}|^2} = \frac{4U_o(|1 + U_o - iD_o|^2 + |U + iV|^2) \frac{Q}{Q_{rad}} - 2V(V + VU_o + UD_o)}{|(1 + U_o - iD_o)^2 + (U + iV)^2|^2} \quad (56)$$

Then, to achieve our goal, we maximize  $\eta_P/\eta_{rad}$  and find that this can be achieved for

$$U_{0**} = \sqrt{1 + U^2 - V_{rad}^2 U^2 + V^2 - 2VV_{rad}} \quad \text{and} \quad D_{0**} = UV_{rad},$$

(57)

where  $V_{\text{rad}} \equiv \Lambda/\sqrt{\Gamma_{1,\text{rad}}\Gamma_{2,\text{rad}}}$ , as defined in Eq.(47), we call the interference factor and quantifies the degree of far-field interference that the system experiences compared to the radiative loss, thus  $V_{\text{rad}} = V \sqrt{\frac{Q_{1,\text{rad}}}{Q_1} \frac{Q_{2,\text{rad}}}{Q_2}} \geq V$ , and  $V = V_{\text{rad}}$  when all loss is radiative, in which case Eq.(57) reduces to Eq.(53).

In this description, we suggest that, for any temporal energy-transfer scheme and given some achieved coupling-to-loss ratio, the efficiency can be enhanced and the radiation can be suppressed by shifting the operational frequency away from exact resonance with each object's eigenfrequency and closer to the frequency of the odd normal-mode, which suffers less radiation due to destructive far-field interference. It is the parameters

$$U = \frac{\kappa}{\sqrt{\Gamma_1\Gamma_2}} = k\sqrt{Q_1Q_2} \quad \text{and} \quad V = \frac{\Lambda}{\sqrt{\Gamma_1\Gamma_2}} = V_{\text{rad}} \sqrt{\frac{Q_1}{Q_{1,\text{rad}}} \frac{Q_2}{Q_{2,\text{rad}}}} \quad (58)$$

that are the figures-of-merit for any system under consideration for wireless energy-transfer, along with the distance over which large  $U$ ,  $|V|$  can be achieved. Clearly, also  $|V|$  can be a decreasing function of distance, since two sources of radiation distant by more than a few wavelengths do not interfere substantially. It is important also to keep in mind that the magnitude of  $V$  depends on the degree to which radiation dominates the objects' losses, since it is only these radiative losses that can contribute to interference, as expressed from  $V_{\text{rad}} \geq V$ .

To achieve a large strong-interference factor  $V$ , in some examples, the energy-transfer application preferably uses again subwavelength resonances, because, for a given source-device distance, the interference factor  $V_{\text{rad}}$  will increase as frequency decreases, since naturally the odd mode of two coupled objects, distant much closer than a wavelength, will not radiate at all.

To achieve a large strong-interference factor  $V$ , in some examples, the energy-transfer application preferably uses resonant modes of high factors  $Q/Q_{\text{rad}}$ . This condition can be satisfied by designing resonant modes where the dominant loss

mechanism is radiation. As frequency decreases, radiation losses always decrease and typically systems are limited by absorption losses, as discussed earlier, so  $Q/Q_{\text{rad}}$  decreases; thus, the advantage of interference can be insignificant at some point compared to the deterioration of absorption- $Q$ .

Therefore,  $|V|$  will be maximized at some frequency  $\omega_V$ , dependent on the source-device distance, and this optimal frequency will typically be different than  $\omega_U$ , the optimal frequency for  $U$ . As seen above, the problem of maximizing the energy-transfer efficiency can require a modified treatment in the presence of interference. The choice of eigenfrequency for the source and device objects as  $\omega_U$ , where  $U$  is maximum, can not be a good one anymore, but also  $V$  needs to be considered. The optimization of efficiency occurs then at a frequency  $\omega_\eta$  between  $\omega_U$  and  $\omega_V$  and is a combined problem, which will be demonstrated below for few examples of electromagnetic systems.

Moreover, note that, at some fixed distance between the source and device objects, the figures  $U, V$  can not be maximized for the same set of system parameters; in that case, these parameters could be chosen so that the efficiency of Eq.(54) is maximized.

In the following section, we calculate a magnitude of efficiency improvement and radiation reduction for realistic systems at mid-range distances between two objects, by employing this frequency detuning and by doing a joint optimization for  $U, V$ .

#### 5 Far-field interference at mid-range distances for realistic systems

In the case of two objects 1, 2 supporting radiative electromagnetic resonant modes of the same eigenfrequency  $\omega_1 = \omega_2 \equiv \omega_o$  and placed at distance  $D$  between their arbitrarily-chosen centers, so that they couple in the near field and interfere in the far field, the interference factor  $V_{\text{rad}}$  is predicted from antenna theory (AT) to be that in Eq.(47).

We have also seen above how to compute the resonance quality factors  $Q$  and  $Q_{\text{rad}}$ , for some example structures, and thus we can compute the factor  $Q/Q_{\text{rad}}$ .

We will demonstrate the efficiency enhancement and the radiation suppression due to interference for the two examples of capacitively-loaded conducting loops and



dielectric disks. The degree of improvement will be shown to depend on the nature of the system.

### 5.1 Capacitively-loaded conducting loops

Consider two loops 1, 2 of radius  $r$  with  $N$  turns of conducting wire with circular cross-section of radius  $a$  at distance  $D$ , as shown in Fig. 10. It was shown in Section 2.2 how to calculate the quality, coupling and strong-coupling factors for such a system.

Their coupling factor is shown in Fig. 17(a) as a function of the relative distance  $D/r$ , for three different dimensions of single-turn ( $N = 1$ ) loops. Their strong-coupling factor at the eigenfrequency  $\omega_{Q_1Q_2}$  is shown in Fig. 17(b). The approximate scaling

$k, U \propto (r/D)^3$ , indicated by Eqs.(26) and (27), is apparent.

We compute the interference parameter between two coupled loops at distance  $D$ , using the AT analysis Eq.(47), leading to

Consider two loops 1, 2 of radius  $r$  with  $N$  turns of conducting wire with circular cross-section of radius  $a$  at distance  $D$ , as shown in Fig. 10. It was shown in Section 2.2 how to calculate the quality, coupling and strong-coupling factors for such a system. Their coupling factor is shown in Fig. 17(a) as a function of the relative distance  $D/r$ , for three different dimensions of single-turn ( $N = 1$ ) loops. Their strong-coupling factor at the eigenfrequency  $\omega_{Q_1Q_2}$  is shown in Fig. 17(b). The approximate scaling

$k, U \propto (r/D)^3$ , indicated by Eqs.(26) and (27), is apparent. We compute the interference parameter between two coupled loops at distance  $D$ , using the AT analysis Eq.(47), leading to

$$V_{\text{rad}} = \frac{3}{(kD)^3} [\sin(kD) - (kD)\cos(kD)], \quad (59)$$

for the orientation of optimal coupling, where one loop is above the other. Their interference factor is shown in Fig. 18 as a function of the normalized distance  $D/\lambda$ , where it can be seen that this factor has nulls only upon reaching the radiative regime. Since the resonant loops are highly subwavelength (in many examples  $\lambda/r \geq 50$ ), at mid-range distances ( $D/r \leq 10$ ), we expect  $D/\lambda \leq 0.2$  and thus the interference factor to be very large ( $V_{\text{rad}} \geq 0.8$ ).

At a fixed resonant frequency, in some examples, the factor  $Q/Q_{\text{rad}}$  can be increased by increasing the radii  $r$  of the loops. In some examples, the factor  $Q/Q_{\text{rad}}$  can be increased by increasing the number  $N$  of turns of the loops. In some examples, the factor  $Q/Q_{\text{rad}}$  can be increased by increasing the radius  $a$  of the conducting wire of the loops or by using Litz wire or a ribbon to reduce the absorption losses and thus make radiation more dominant loss mechanism.

We also plot in Fig. 19, for the example  $r = 30\text{cm}$  and  $a = 2\text{cm}$ , the strong-coupling factor  $U$ , the interference factor  $V_{\text{rad}}$  and the strong-interference factor  $V$  as a function of the resonant eigenfrequency of the loops, for a fixed distance  $D = 5r$ . Indeed, for this example,  $V_{\text{rad}}$  decreases monotonically with frequency in this subwavelength regime and is always great than 0.8, but  $V$  exhibits a maximum, since the term  $Q/Q_{\text{rad}}$  is increasing towards  $\infty$  with frequency, as losses become more and more radiation dominated. It can be seen that the resonant eigenfrequencies  $f_U$  and  $f_V$ , at which  $U$  and  $V$  become maximum respectively, are different. This implies that the efficiency will now not necessarily peak at the eigenfrequency  $f_U$ , at which  $U$  is maximized, as would be the assumption based on prior knowledge, but at a different one  $f_\eta$  between  $f_U$  and  $f_V$ . This is shown below.

In Fig. 20 the efficiency  $\eta_P$  is plotted as a function of the resonant eigenfrequency of the loops for two different examples of loop dimensions  $r = 30\text{cm}$ ,  $a = 2\text{cm}$  and  $r = 1\text{m}$ ,  $a = 2\text{cm}$ , at two different loop distances  $D = 5r$  and  $D = 10r$ , and for the cases:

- (i) (solid lines) including interference effects and detuning the driving frequency from the resonant frequency by  $D_o = UV$  from Eq.(53) to maximize the power-transmission efficiency and similarly using  $U_o$  from Eq.(53), which thus implies optimal efficiency as in Eq.(54).
- (ii) (dash-dotted lines) including interference effects and detuning the driving frequency from the resonant frequency by  $D_o = UV_{\text{rad}}$  from Eq.(57) to maximize the ratio of power transmitted over power radiated and similarly using  $U_o$  from Eq.(57).
- (iii) (dashed lines) including interference effects but not detuning the driving frequency from the resonant frequency and using  $U_o$  from Eq.(14), as one would do to maximize

efficiency in the absence of interference.

(iv) (dotted lines) truly in the absence of interference effects and thus maximizing efficiency by not detuning the driving frequency from the resonant frequency and using  $U_o$  from Eq.(14), which thus implies efficiency as in Eq.(15).

In Fig. 21 we show the amount of driving-frequency detuning that is used in the presence of interference either to maximize efficiency (case (i) (solid lines) of Fig. 20 -  $D_o = UV$ ) or to maximize the ratio of power transmitted over power radiated (case (ii) (dash-dotted lines) of Fig. 20 -  $D_o = UV_{\text{rad}}$ ). Clearly, this driving-frequency detuning can be a non-trivial amount.

It can be seen from Fig. 20 that, for all frequencies, the efficiency of case (i) (solid lines) is larger than the efficiency of case (iii) (dashed lines) which is in turn larger than the efficiency of case (iv) (dotted lines). Therefore, in this description, we suggest that employing far-field interference improves on the power-transmission efficiency (improvement from (iv) (dotted) to (iii) (dashed)) and, furthermore, employing destructive far-field interference, by detuning the driving frequency towards the low-radiation-loss odd normal mode, improves on the power-transmission efficiency even more (improvement from (iii) (dashed) to (i) (solid)).

If  $f_\eta$  is the eigenfrequency, at which the efficiency of case (i) (solid) is optimized, then, in some examples, the resonant eigenfrequency can be designed to be larger than  $f_\eta$ , namely in a regime where the system is more radiation dominated. In this description, we suggest that at such eigenfrequencies, there can be a significant improvement in efficiency by utilizing the destructive far-field interference effects and driving the system at a frequency close to the odd normal mode. This can be seen again from Fig. 20 by comparing the solid lines to the corresponding dashed lines and the dotted lines.

In general, one would tend to design a system resonant at the frequency  $f_U$  where the strong-coupling factor  $U$  is maximal. However, as suggested above, in the presence of interference, Fig. 20 shows that the maximum of  $\eta_P$  is at an eigenfrequency  $f_\eta$  different than  $f_U$ . In some examples,  $f_\eta > f_U$ . This is because at higher eigenfrequencies, losses are determined more by radiation than absorption, therefore destructive radiation interference can play a more significant role in reducing overall losses and thus  $f_V > f_U$  and the efficiency is increased at  $f_\eta > f_U$ . In this description, we

suggest that, in some examples, the resonant eigenfrequency can be designed to be close to the frequency  $f_\eta$  that optimizes the efficiency rather than the different  $f_U$ . In particular, in Fig. 22(a) are plotted these two frequencies  $f_\eta$  (solid line) and  $f_U$  (dashed line) as a function of relative distance  $D/r$  of two  $r = 30\text{cm}$  loops. In Fig. 22(b) we show a graded plot of the optimal efficiency from Eq.(54) in the  $U - V$  plane. Then, we superimpose the  $U - V$  curve of case (i) (solid), parametrized with distance  $D$ , for two  $r = 30\text{cm}$  loops resonant at the optimal frequency  $f_\eta$  for each  $D$ . From the path of this curve onto the graded plot the efficiency as a function of distance can be extracted for case (i) (solid). We then also superimpose in Fig. 22(b) the  $U - V$  curve of case (iii) (dashed), parametrized with distance  $D$ , for two  $r = 30\text{cm}$  loops resonant at  $f_U$ , and the  $U$  range of case (iv) (dotted), parametrized with distance  $D$ , for two  $r = 30\text{cm}$  loops resonant at  $f_U$  (note that in this last case there is no interference and thus  $V = 0$ ). In Fig. 22(c) we then show the efficiency enhancement factor achieved by the solid curve of Fig. 22(b), as a function of distance  $D/r$ , compared to best that can be achieved without driving-frequency detuning (dashed) and without interference whatsoever (dotted). The improvement by employing interference can reach a factor of 2 at large separation between the loops.

In Fig. 23 we plot the radiation efficiency  $\eta_{\text{rad}}$ , using Eq.(39), as a function of the eigenfrequency of the loops for the two different loop dimensions, the two different distances and the four different cases examined in Fig. 20. It can be seen from Fig. 23 that, for all frequencies,  $\eta_{\text{rad}}$  of case (ii) (dash-dotted lines) is smaller than  $\eta_{\text{rad}}$  of case (i) (solid lines) which is in turn smaller than  $\eta_{\text{rad}}$  of case (iii) (dashed lines) and this smaller than  $\eta_{\text{rad}}$  of case (iv) (dotted lines). Therefore, in this description, we suggest that employing far-field interference suppresses radiation (improvement from (iv) (dotted) to (iii) (dashed)) and, furthermore, employing destructive far-field interference, by detuning the driving frequency towards the low-radiation-loss odd normal mode, suppress radiation efficiency even more (improvement from (iii) (dashed) to (i) (solid) and (ii) (dash-dotted)), more so in case (ii), specifically optimized for this purpose.

In some examples, the resonant eigenfrequency can be designed to be larger than  $f_\eta$ , namely in a regime where the system is more radiation dominated. In this description, we suggest that at such eigenfrequencies, there can be a significant suppression in

radiation by utilizing the destructive far-field interference effects and driving the system at a frequency close to the odd normal mode. The case (ii)=(dash-dotted) accomplishes the greatest suppression in radiation and, as can be seen in Fig. 20, there is a range of eigenfrequencies (close to  $f_V$ ), for which the efficiency that this configuration can achieve is only little compromised compared to the maximum possible of configuration (i).

In one example, two single-turn loops of  $r = 30\text{cm}$  and  $a = 2\text{cm}$  are at a distance  $D/r = 5$  in the orientation shown in Fig. 10 and they are designed to resonate at 30MHz. In the absence of interference, the power-transmission efficiency is 59% and the radiation efficiency is 38%. In the presence of interference and without detuning the driving frequency from 30MHz, the power-transmission efficiency is 62% and the radiation efficiency is 32%. In the presence of interference and detuning the driving frequency from 30MHz to 31.3MHz to maximize efficiency, the power-transmission efficiency is increased to 75% and the radiation efficiency is suppressed to 18%.

In another example, two single-turn loops of  $r = 30\text{cm}$  and  $a = 2\text{cm}$  are at a distance  $D/r = 5$  in the orientation shown in Fig. 10 and they are designed to resonate at 10MHz. In the absence of interference or in the presence of interference and without detuning the driving frequency from 10MHz, the power-transmission efficiency is approximately 81% and the radiation efficiency is approximately 4%. In the presence of interference and detuning the driving frequency from 10MHz to 10.22MHz to maximize transmission over radiation, the power-transmission efficiency is 42%, reduced by less than a factor of 2, while the radiation efficiency is 0.4%, suppressed by an order of magnitude.

In another example, two single-turn loops of  $r = 1\text{m}$  and  $a = 2\text{cm}$  are at a distance  $D/r = 5$  in the orientation shown in Fig. 10 and they are designed to resonate at 10MHz. In the absence of interference, the power-transmission efficiency is 48% and the radiation efficiency is 47%. In the presence of interference and without detuning the driving frequency from 10MHz, the power-transmission efficiency is 54% and the radiation efficiency is 37%. In the presence of interference and detuning the driving frequency from 10MHz to 14.8MHz to maximize efficiency, the power-transmission efficiency is increased to 66% and the radiation efficiency is suppressed to 24%.

In another example, two single-turn loops of  $r = 1m$  and  $a = 2cm$  are at a distance  $D/r = 5$  in the orientation shown in Fig. 10 and they are designed to resonate at 4MHz. In the absence of interference or in the presence of interference and without detuning the driving frequency from 4MHz, the power-transmission efficiency is approximately 71% and the radiation efficiency is approximately 8%. In the presence of interference and detuning the driving frequency from 4MHz to 5.06MHz to maximize transmission over radiation, the power-transmission efficiency is 40%, reduced by less than a factor of 2, while the radiation efficiency is approximately 1%, suppressed by almost an order of magnitude.

### 5.2 Dielectric disks

Consider two dielectric disks 1 and 2 of radius  $r$  and dielectric permittivity  $\epsilon$  placed at distance  $D$  between their centers, as shown in Fig. 15(b). Their coupling as a function of distance was calculated in Section 2.4, using analytical and finite-element-frequency-domain (FEFD) methods, and is shown in Fig. 24.

To compute the interference factor between two coupled disks at distance  $D$ , we again use two independent methods to confirm the validity of our results: numerically, the FEFD calculations again give  $\Lambda$  (and thus  $V$ ) by the splitting of the loss-rates of the two normal modes; analytically, calculation of the AT prediction of Eq.(47) gives

$$\begin{aligned}
 m=1: \quad V_{\text{rad}} &= \frac{2}{(kD)} J_1(kD) \\
 m=2: \quad V_{\text{rad}} &= \frac{8}{(kD)^3} \left\{ 3(kD)J_0(kD) + [(kD)^2 - 6]J_1(kD) \right\} \\
 m=3: \quad V_{\text{rad}} &= \frac{6}{(kD)^5} \left\{ [24(kD)^3 - 320(kD)]J_0(kD) + [3(kD)^4 - 128(kD)^2 + 640]J_1(kD) \right\}
 \end{aligned} \tag{60}$$

The results for the interference of two same disks, for exactly the same parameters for which the coupling was calculated in Fig. 24, are presented in Fig. 25, as a function of frequency (due to varying  $\epsilon$ ) at fixed distances. It can be seen that also the strong-interference factor  $\tilde{\gamma}$  can have nulls, which can occur even before the system enters the radiative-coupling regime, namely at smaller frequencies than those of  $U$  at the same distances, and it decreases with frequency, since then the objects become more and more absorption dominated, so the benefit from radiative interference is suppressed. Both the

above effects result into the fact that, for most distances,  $U$  (from Fig. 24(b)) and  $V$  (from Fig. 25(b)) can be maximized at different values of the frequency ( $f_U$  and  $f_V$  respectively), and thus different can also be the optimal frequency  $f_\eta$  for the final energy-transfer efficiency of Eq.(54), which is shown in Fig. 26 again for the same set of parameters. From this plot, it can be seen that interference can significantly improve the transfer efficiency, compared to what Eq.(15) would predict from the calculated values of the coupling figure-of-merit  $U$ .

Furthermore, not only does a given energy-transfer system perform better than what a prediction which ignores interference would predict, but also our optimization design will typically lead to different optimal set of parameters in the presence of interference. For example, for the particular distance  $D/r = 5$ , it turns out from Fig. 26 that the  $m = 1$  resonant modes can achieve better efficiency than the  $m = 2$  modes within the available range of  $\epsilon$ , by making use of strong interference which counteracts their weaker  $U$ , as viewed in Fig. 24, from which one would have concluded the opposite performance. Moreover, even within the same  $m$ -branch, one would naively design the system to operate at the frequency  $f_U$ , at which  $U$  is maximum. However, the optimization design changes in the presence of interference, since the system should be designed to operate at the different frequency  $f_\eta$ , where the overall efficiency  $\eta$  peaks. In Fig. 27(a), we first calculate those different frequencies where the strong-coupling factor  $U$  and the efficiency  $\eta$  (which includes interference) peak, as distance  $D$  is changing for the choice of the  $m = 2$  disk of Fig. 24, and observe that their difference is actually significant. Then, in Fig. 27(b) we show the peak efficiency for the various frequency choices. For large distances, where efficiency is small and could use a boost, the improvement factor reaches a significant 2 for the particular system under examination. The same result is shown in Fig. 27(c) as a plot of the path of the efficiency on the  $U - V$  map, as distance is changing. Similar results are derived for the modes of different  $m$ -order. Physically, moving to higher frequencies increases role of radiative losses compared to absorption and thus interference can have a greater influence. At the optimal frequency  $f_\eta$  radiated power including interference is close to what it is at  $f_U$ , but absorbed power is much less, therefore the efficiency has been improved.

In some examples, instead of improving efficiency, one might care more about minimizing radiation. In that case, we calculate at the frequency  $f_U$  how much power is radiated when optimized under the conditions Eq.(57) compared to the power radiated when simply operating on resonance ( $D_o = 0$ ) in the cases with and without interference (the latter case can be describing a case where the two disks do not interfere, because they are dissimilar, or due to decoherence issues etc.). We find in Fig. 28 that radiation can be suppressed by a factor of 1.6 by detuning the operating frequency towards the odd sub-radiant mode.

## 6 System Sensitivity to Extraneous Objects

In general, the overall performance of an example of the resonance-based wireless energy-transfer scheme depends strongly on the robustness of the resonant objects' resonances. Therefore, it is desirable to analyze the resonant objects' sensitivity to the near presence of random non-resonant extraneous objects. One appropriate analytical model is that of "perturbation theory" (PT), which suggests that in the presence of an extraneous perturbing object  $p$  the field amplitude  $a_1(t)$  inside the resonant object 1 satisfies, to first order:

$$\frac{da_1}{dt} = -i(\omega_1 - i\Gamma_1)a_1 + i\left(\delta\kappa_{11(p)} + i\delta\Gamma_{1(p)}\right)a_1 \quad (61)$$

where again  $\omega_1$  is the frequency and  $\Gamma_1$  the intrinsic (absorption, radiation etc.) loss rate, while  $\delta\kappa_{11(p)}$  is the frequency shift induced onto 1 due to the presence of  $p$  and  $\delta\Gamma_{1(p)}$  is the extrinsic due to  $p$  (absorption inside  $p$ , scattering from  $p$  etc.) loss rate.  $\delta\Gamma_{1(p)}$  is defined as  $\delta\Gamma_{1(p)} \equiv \Gamma_{1(p)} - \Gamma_1$ , where  $\Gamma_{1(p)}$  is the total perturbed loss rate in the presence of  $p$ . The first-order PT model is valid only for small perturbations. Nevertheless, the parameters  $\delta\kappa_{11(p)}$ ,  $\delta\Gamma_{1(p)}$  are well defined, even outside that regime, if  $a_1$  is taken to be the amplitude of the exact perturbed mode. Note also that interference effects between the radiation field of the initial resonant-object mode and the field scattered off the extraneous object can for strong scattering (e.g. off metallic objects) result in total  $\Gamma_{1,\text{rad}(p)}$  that are smaller than the initial  $\Gamma_{1,\text{rad}}$  (namely  $\delta\Gamma_{1,\text{rad}(p)}$  is negative).



It has been shown that a specific relation is desired between the resonant frequencies of the source and device-objects and the driving frequency. In some examples, all resonant objects must have the same eigenfrequency and this must be equal to the driving frequency. In some examples, when trying to optimize efficiency or suppress radiation by employing far-field interference, all resonant objects must have the same eigenfrequency and the driving frequency must be detuned from them by a particular amount. In some implementations, this frequency-shift can be “fixed” by applying to one or more resonant objects and the driving generator a feedback mechanism that corrects their frequencies. In some examples, the driving frequency from the generator can be fixed and only the resonant frequencies of the objects can be tuned with respect to this driving frequency.

The resonant frequency of an object can be tuned by, for example, adjusting the geometric properties of the object (e.g. the height of a self-resonant coil, the capacitor plate spacing of a capacitively-loaded loop or coil, the dimensions of the inductor of an inductively-loaded rod, the shape of a dielectric disc, etc.) or changing the position of a non-resonant object in the vicinity of the resonant object.

In some examples, referring to Fig. 29a, each resonant object is provided with an oscillator at fixed frequency and a monitor which determines the eigenfrequency of the object. At least one of the oscillator and the monitor is coupled to a frequency adjuster which can adjust the frequency of the resonant object. The frequency adjuster determines the difference between the fixed driving frequency and the object frequency and acts, as described above, to bring the object frequency into the required relation with respect to the fixed frequency. This technique assures that all resonant objects operate at the same fixed frequency, even in the presence of extraneous objects.

In some examples, referring to Fig. 29(b), during energy transfer from a source object to a device object, the device object provides energy or power to a load, and an efficiency monitor measures the efficiency of the energy-transfer or power-transmission. A frequency adjuster coupled to the load and the efficiency monitor acts, as described above, to adjust the frequency of the object to maximize the efficiency.

In other examples, the frequency adjusting scheme can rely on information exchange between the resonant objects. For example, the frequency of a source object

can be monitored and transmitted to a device object, which is in turn synched to this frequency using frequency adjusters, as described above. In other embodiments the frequency of a single clock can be transmitted to multiple devices, and each device then synched to that frequency using frequency adjusters, as described above.

Unlike the frequency shift, the extrinsic perturbing loss due to the presence of extraneous perturbing objects can be detrimental to the functionality of the energy-transfer scheme, because it is difficult to remedy. Therefore, the total perturbed quality factors  $Q_{(p)}$  (and the corresponding perturbed strong-coupling factor  $U_{(p)}$  and the perturbed strong-interference factor  $V_{(p)}$ ) should be quantified.

In some examples, a system for wireless energy-transfer uses primarily magnetic resonances, wherein the energy stored in the near field in the air region surrounding the resonator is predominantly magnetic, while the electric energy is stored primarily inside the resonator. Such resonances can exist in the quasi-static regime of operation ( $r \ll \lambda$ ) that we are considering: for example, for coils with  $h \ll 2r$ , most of the electric field is localized within the self-capacitance of the coil or the externally loading capacitor and, for dielectric disks, with  $\epsilon \gg 1$  the electric field is preferentially localized inside the disk. In some examples, the influence of extraneous objects on magnetic resonances is nearly absent. The reason is that extraneous non-conducting objects  $p$  that could interact with the magnetic field in the air region surrounding the resonator and act as a perturbation to the resonance are those having significant magnetic properties (magnetic permeability  $Re\{\mu\} > 1$  or magnetic loss  $Im\{\mu\} > 0$ ). Since almost all every-day non-conducting materials are non-magnetic but just dielectric, they respond to magnetic fields in the same way as free space, and thus will not disturb the resonance of the resonator. Extraneous conducting materials can however lead to some extrinsic losses due to the eddy currents induced inside them or on their surface (depending on their conductivity). However, even for such conducting materials, their presence will not be detrimental to the resonances, as long as they are not in very close proximity to the resonant objects.

The interaction between extraneous objects and resonant objects is reciprocal, namely, if an extraneous object does not influence a resonant object, then also the resonant object does not influence the extraneous object. This fact can be viewed in light of safety considerations for human beings. Humans are also non-magnetic and can

sustain strong magnetic fields without undergoing any risk. A typical example, where magnetic fields  $B \sim IT$  are safely used on humans, is the Magnetic Resonance Imaging (MRI) technique for medical testing. In contrast, the magnetic near-field required in typical embodiments in order to provide a few Watts of power to devices is only  $B \sim 10^{-4}T$ , which is actually comparable to the magnitude of the Earth’s magnetic field. Since, as explained above, a strong electric near-field is also not present and the radiation produced from this non-radiative scheme is minimal, the energy-transfer apparatus, methods and systems described herein is believed safe for living organisms.

6.1 Capacitively-loaded conducting loops or coils

In some examples, one can estimate the degree to which the resonant system of a capacitively-loaded conducting-wire coil has mostly magnetic energy stored in the space surrounding it. If one ignores the fringing electric field from the capacitor, the electric and magnetic energy densities in the space surrounding the coil come just from the electric and magnetic field produced by the current in the wire; note that in the far field, these two energy densities must be equal, as is always the case for radiative fields. By using the results for the fields produced by a subwavelength ( $r \ll \lambda$ ) current loop (magnetic dipole) with  $h = 0$ , we can calculate the ratio of electric to magnetic energy densities, as a function of distance  $D_p$  from the center of the loop (in the limit  $r \ll D_p$ ) and the angle  $\theta$  with respect to the loop axis:

$$\frac{w_e(x)}{w_m(x)} = \frac{\epsilon_o |E(x)|^2}{\mu_o |H(x)|^2} = \frac{\left(1 + \frac{1}{x^2}\right) \sin^2 \theta}{\left(\frac{1}{x^2} + \frac{1}{x^4}\right) 4 \cos^2 \theta + \left(1 - \frac{1}{x^2} + \frac{1}{x^4}\right) \sin^2 \theta}; \quad x = 2\pi \frac{D_p}{\lambda} \tag{62}$$

$$\Rightarrow \frac{\oint_{S_p} w_e(x) dS}{\oint_{S_p} w_m(x) dS} = \frac{1 + \frac{1}{x^2}}{1 + \frac{1}{x^2} + \frac{3}{x^4}}; \quad x = 2\pi \frac{D_p}{\lambda}$$

where the second line is the ratio of averages over all angles by integrating the electric and magnetic energy densities over the surface of a sphere of radius  $D_p$ . From Eq.(62) it is obvious that indeed for all angles in the near field ( $x \ll 1$ ) the magnetic energy density

is dominant, while in the far field ( $x \gg 1$ ) they are equal as they should be. Also, the preferred positioning of the loop is such that objects which can interfere with its resonance lie close to its axis ( $\theta = 0$ ), where there is no electric field. For example, using the systems described in Table 4, we can estimate from Eq.(62) that for the loop of  $r = 30cm$  at a distance  $D_p = 10r = 3m$  the ratio of average electric to average magnetic energy density would be  $\sim 12\%$  and at  $D_p = 3r = 90cm$  it would be  $\sim 1\%$ , and for the loop of  $r = 10cm$  at a distance  $D_p = 10r = 1m$  the ratio would be  $\sim 33\%$  and at  $D_p = 3r = 30cm$  it would be  $\sim 2.5\%$ . At closer distances this ratio is even smaller and thus the energy is predominantly magnetic in the near field, while in the radiative far field, where they are necessarily of the same order (ratio  $\rightarrow 1$ ), both are very small, because the fields have significantly decayed, as capacitively-loaded coil systems are designed to radiate very little. Therefore, this is the criterion that qualifies this class of resonant system as a magnetic resonant system.

To provide an estimate of the effect of extraneous objects on the resonance of a capacitively-loaded loop including the capacitor fringing electric field, we use the perturbation theory formula, stated earlier,

$$\delta\Gamma_{1,abs(p)} = \omega_1 / 4 \cdot \int d^3\mathbf{r} \operatorname{Im} \{ \varepsilon_p(\mathbf{r}) \} | \mathbf{E}_1(\mathbf{r}) |^2 / W$$

with the computational FEFD results for the field of an example like the one shown in the plot of Fig. 5 and with a rectangular object of dimensions  $30cm \times 30cm \times 1.5m$  and permittivity  $\varepsilon = 49 + 16i$  (consistent with human muscles) residing between the loops and almost standing on top of one capacitor ( $\sim 3cm$  away from it) and find  $\delta Q_{abs(human)} \sim 10^5$  and for  $\sim 10cm$  away

$\delta Q_{abs(human)} \sim 5 \cdot 10^5$ . Thus, for ordinary distances ( $\sim 1m$ ) and placements (not immediately on top of the capacitor) or for most ordinary extraneous objects  $p$  of much smaller loss-tangent, we conclude that it is indeed fair to say that  $\delta Q_{abs(p)} \rightarrow \infty$ . The only perturbation that is expected to affect these resonances is a close proximity of large metallic structures.

Self-resonant coils can be more sensitive than capacitively-loaded coils, since for the former the electric field extends over a much larger region in space (the entire coil)

rather than for the latter (just inside the capacitor). On the other hand, self-resonant coils can be simple to make and can withstand much larger voltages than most lumped capacitors. Inductively-loaded conducting rods can also be more sensitive than capacitively-loaded coils, since they rely on the electric field to achieve the coupling.

## 6.2 Dielectric disks

For dielectric disks, small, low-index, low-material-loss or far-away stray objects will induce small scattering and absorption. In such cases of small perturbations these extrinsic loss mechanisms can be quantified using respectively the analytical first-order perturbation theory formulas

$$\left[ \delta Q_{1,rad(p)} \right]^{-1} \equiv 2\delta\Gamma_{1,rad(p)} / \omega_1 \propto \int d^3\mathbf{r} \left[ \text{Re}\{\varepsilon_p(\mathbf{r})\} |\mathbf{E}_1(\mathbf{r})|^2 \right] / W$$

$$\left[ \delta Q_{1,abs(p)} \right]^{-1} \equiv 2\delta\Gamma_{1,abs(p)} / \omega_1 = \int d^3\mathbf{r} \text{Im}\{\varepsilon_p(\mathbf{r})\} |\mathbf{E}_1(\mathbf{r})|^2 / 2W$$

where  $W = \int d^3\mathbf{r} \varepsilon(\mathbf{r}) |\mathbf{E}_1(\mathbf{r})|^2 / 2$  is the total resonant electromagnetic energy of the unperturbed mode. As one can see, both of these losses depend on the square of the resonant electric field tails  $\mathbf{E}_1$  at the site of the extraneous object. In contrast, the coupling factor from object 1 to another resonant object 2 is, as stated earlier,

$$k_{12} = 2\kappa_{12} / \sqrt{\omega_1\omega_2} \approx \int d^3\mathbf{r} \varepsilon_2(\mathbf{r}) E_2^*(\mathbf{r}) E_1(\mathbf{r}) / \int d^3\mathbf{r} \varepsilon(\mathbf{r}) |\mathbf{E}_1(\mathbf{r})|^2$$

and depends *linearly* on the field tails  $\mathbf{E}_1$  of 1 inside 2. This difference in scaling gives us confidence that, for, for example, exponentially small field tails, coupling to other resonant objects should be much faster than all extrinsic loss rates ( $\kappa_{12} \gg \delta\Gamma_{1,2(p)}$ ), at least for small perturbations, and thus the energy-transfer scheme is expected to be sturdy for this class of resonant dielectric disks.

However, we also want to examine certain possible situations where extraneous objects cause perturbations too strong to analyze using the above first-order perturbation theory approach. For example, we place a dielectric disk close to another off-resonance object of large  $\text{Re}\{\varepsilon\}$ ,  $\text{Im}\{\varepsilon\}$  and of same size but different shape (such as a human being  $h$ ), as shown in Fig. 30a, and a roughened surface of large extent but of small  $\text{Re}\{\varepsilon\}$ ,

$\text{Im}\{\varepsilon\}$  (such as a wall  $w$ ), as shown in Fig. 30b. For distances  $D_{h,w}/r = 10 - 3$  between the disk-center and the “human”-center or “wall”, the numerical FDFD simulation results presented in Figs. 30a and 30b suggest that, the disk resonance seems to be fairly robust, since it is not detrimentally disturbed by the presence of extraneous objects, with the exception of the *very* close proximity of high-loss objects. To examine the influence of large perturbations on an entire energy-transfer system we consider two resonant disks in the close presence of both a “human” and a “wall”. Comparing Table 8 to the table in Figure 30c, the numerical FDFD simulations show that the system performance deteriorates from  $U \sim 1 - 50$  to  $U_{(hw)} \sim 0.5 - 10$ , i.e. only by acceptably small amounts.

In general, different examples of resonant systems have different degree of sensitivity to external perturbations, and the resonant system of choice depends on the particular application at hand, and how important matters of sensitivity or safety are for that application. For example, for a medical implantable device (such as a wirelessly powered artificial heart) the electric field extent must be minimized to the highest degree possible to protect the tissue surrounding the device. In such cases where sensitivity to external objects or safety is important, one should design the resonant systems so that the ratio of electric to magnetic energy density  $w_e/w_m$  is reduced or minimized at most of the desired (according to the application) points in the surrounding space.

## 7 Applications

The non-radiative wireless energy transfer techniques described above can enable efficient wireless energy-exchange between resonant objects, while suffering only modest transfer and dissipation of energy into other extraneous off-resonant objects. The technique is general, and can be applied to a variety of resonant systems in nature. In this Section, we identify a variety of applications that can benefit from or be designed to utilize wireless power transmission.

Remote devices can be powered directly, using the wirelessly supplied power or energy to operate or run the devices, or the devices can be powered by or through or in addition to a battery or energy storage unit, where the battery is occasionally being charged or re-charged wirelessly. The devices can be powered by hybrid battery/energy storage devices such as batteries with integrated storage capacitors and the like.

Furthermore, novel battery and energy storage devices can be designed to take advantage of the operational improvements enabled by wireless power transmission systems.

Devices can be turned off and the wirelessly supplied power or energy used to charge or recharge a battery or energy storage unit. The battery or energy storage unit charging or recharging rate can be high or low. The battery or energy storage units can be trickle charged or float charged. It would be understood by one of ordinary skill in the art that there are a variety of ways to power and/or charge devices, and the variety of ways could be applied to the list of applications that follows.

Some wireless energy transfer examples that can have a variety of possible applications include for example, placing a source (e.g. one connected to the wired electricity network) on the ceiling of a room, while devices such as robots, vehicles, computers, PDAs or similar are placed or move freely within the room. Other applications can include powering or recharging electric-engine buses and/or hybrid cars and medical implantable devices. Additional example applications include the ability to power or recharge autonomous electronics (e.g. laptops, cell-phones, portable music players, house-hold robots, GPS navigation systems, displays, etc), sensors, industrial and manufacturing equipment, medical devices and monitors, home appliances (e.g. lights, fans, heaters, displays, televisions, counter-top appliances, etc.), military devices, heated or illuminated clothing, communications and navigation equipment, including equipment built into vehicles, clothing and protective-wear such as helmets, body armor and vests, and the like, and the ability to transmit power to physically isolated devices such as to implanted medical devices, to hidden, buried, implanted or embedded sensors or tags, to and/or from roof-top solar panels to indoor distribution panels, and the like.

In some examples, far-field interference can be utilized by a system designer to suppress total radiation loss and/or to increase the system efficiency. In some examples, systems operating optimally closer to the radiative regime can benefit more from the presence of far-field interference, which leads to reduced losses for the sub-radiant normal mode of the coupled objects, and this benefit can be substantial.

A number of examples of the invention have been described. Nevertheless, it will be understood that various modifications can be made without departing from the spirit and scope of the invention.

**WHAT IS CLAIMED IS:**

1. An apparatus for use in wireless energy transfer, the apparatus comprising:  
a first resonator structure configured for energy transfer with a second resonator structure, over a distance  $D$  larger than a characteristic size  $L_1$  of said first resonator structure and larger than a characteristic size  $L_2$  of said second resonator structure,  
wherein the energy transfer has a rate  $\kappa$  and is mediated by evanescent-tail coupling of a resonant field of the first resonator structure and a resonant field of the second resonator structure, wherein  
said resonant field of the first resonator structure has a resonance angular frequency  $\omega_1$ , a resonance frequency-width  $\Gamma_1$ , and a resonance quality factor  $Q_1 = \omega_1 / 2\Gamma_1$  at least larger than 300, and  
said resonant field of the second resonator structure has a resonance angular frequency  $\omega_2$ , a resonance frequency-width  $\Gamma_2$ , and a resonance quality factor  $Q_2 = \omega_2 / 2\Gamma_2$  at least larger than 300,  
wherein the absolute value of the difference of said angular frequencies  $\omega_1$  and  $\omega_2$  is smaller than the broader of said resonant widths  $\Gamma_1$  and  $\Gamma_2$ , and the quantity  $\kappa / \sqrt{\Gamma_1\Gamma_2}$  is at least larger than 20,  
and further comprising a power supply coupled to the first structure and configured to drive the first resonator structure or the second resonator structure at an angular frequency away from the resonance angular frequencies and shifted towards a frequency corresponding to an odd normal mode for the resonator structures to reduce radiation from the resonator structures by destructive far-field interference.
2. The apparatus of claim 1, wherein the power supply is configured to drive the first resonator structure or the second resonator structure at the angular frequency away from the resonance angular frequencies and shifted towards the frequency corresponding to an odd normal mode for the resonator structures to substantially suppress radiation from the resonator structures by destructive far-field interference.



3. A method for wireless energy transfer involving a first resonator structure configured for energy transfer with a second resonator structure, over a distance  $D$  larger than a characteristic size  $L_1$  of said first resonator structure and larger than a characteristic size  $L_2$  of said second resonator structure, wherein the energy transfer has a rate  $\kappa$  and is mediated by evanescent-tail coupling of a resonant field of the first resonator structure and a resonant field of the second resonator structure, wherein said resonant field of the first resonator structure has a resonance angular frequency  $\omega_1$ , a resonance frequency-width  $\Gamma_1$ , and a resonance quality factor  $Q_1 = \omega_1 / 2\Gamma_1$  at least larger than 300, and said resonant field of the second resonator structure has a resonance angular frequency  $\omega_2$ , a resonance frequency-width  $\Gamma_2$ , and a resonance quality factor  $Q_2 = \omega_2 / 2\Gamma_2$  at least larger than 300, wherein the absolute value of the difference of said angular frequencies  $\omega_1$  and  $\omega_2$  is smaller than the broader of said resonant widths  $\Gamma_1$  and  $\Gamma_2$ , and the quantity  $\kappa / \sqrt{\Gamma_1 \Gamma_2}$  is at least larger than 20, the method comprising:

driving the first resonator structure or the second resonator structure at an angular frequency away from the resonance angular frequencies and shifted towards a frequency corresponding to an odd normal mode for the resonator structures to reduce radiation from the resonator structures by destructive far-field interference.

4. The method of claim 3, wherein the first resonator structure or the second resonator structure is driven at the angular frequency away from the resonance angular frequencies and shifted towards the frequency corresponding to an odd normal mode for the resonator structures to substantially suppress radiation from the resonator structures by destructive far-field interference.

5. An apparatus for use in wireless energy transfer, the apparatus comprising:  
a first resonator structure configured for energy transfer with a second resonator structure, over a distance  $D$  larger than a characteristic size  $L_1$  of said first resonator structure and larger than a characteristic size  $L_2$  of said second resonator structure,  
wherein the energy transfer has a rate  $\kappa$  and is mediated by evanescent-tail

coupling of a resonant field of the first resonator structure and a resonant field of the second resonator structure, wherein

said resonant field of the first resonator structure has a resonance angular frequency  $\omega_1$ , a resonance frequency-width  $\Gamma_1$ , and a resonance quality factor  $Q_1 = \omega_1 / 2\Gamma_1$  at least larger than 300, and

said resonant field of the second resonator structure has a resonance angular frequency  $\omega_2$ , a resonance frequency-width  $\Gamma_2$ , and a resonance quality factor  $Q_2 = \omega_2 / 2\Gamma_2$  at least larger than 300,

wherein the absolute value of the difference of said angular frequencies  $\omega_1$  and  $\omega_2$  is smaller than the broader of said resonant widths  $\Gamma_1$  and  $\Gamma_2$ , and the quantity  $\kappa / \sqrt{\Gamma_1 \Gamma_2}$  is at least larger than 20,

and wherein for a desired range of the distances  $D$ , the resonance angular frequencies for the resonator structures increase transmission efficiency  $T$  by accounting for radiative interference, wherein the increase is relative to a transmission efficiency  $T$  calculated without accounting for the radiative interference.

6. The apparatus of claim 5, wherein the resonance angular frequencies for the resonator structures are selected by optimizing the transmission efficiency  $T$  to account for both a resonance quality factor  $U$  and an interference factor  $V$ .

7. A method for designing a wireless energy transfer apparatus, the apparatus including a first resonator structure configured for energy transfer with a second resonator structure, over a distance  $D$  larger than a characteristic size  $L_1$  of said first resonator structure and larger than a characteristic size  $L_2$  of said second resonator structure, wherein the energy transfer has a rate  $\kappa$  and is mediated by evanescent-tail coupling of a resonant field of the first resonator structure and a resonant field of the second resonator structure, wherein said resonant field of the first resonator structure has a resonance angular frequency  $\omega_1$ , a resonance frequency-width  $\Gamma_1$ , and a resonance quality factor  $Q_1 = \omega_1 / 2\Gamma_1$  at least larger than 300, and said resonant field of the second

resonator structure has a resonance angular frequency  $\omega_2$ , a resonance frequency-width  $\Gamma_2$ , and a resonance quality factor  $Q_2 = \omega_2 / 2\Gamma_2$  at least larger than 300, wherein the absolute value of the difference of said angular frequencies  $\omega_1$  and  $\omega_2$  is smaller than the broader of said resonant widths  $\Gamma_1$  and  $\Gamma_2$ , and the quantity  $\kappa / \sqrt{\Gamma_1 \Gamma_2}$  is at least larger than 20, the method comprising:

selecting the resonance angular frequencies for the resonator structures to substantially optimize the transmission efficiency by accounting for radiative interference between the resonator structures.

8. The method of claim 7, wherein the resonance angular frequencies for the resonator structures are selected by optimizing the transmission efficiency  $T$  to account for both a resonance quality factor  $U$  and an interference factor  $V$ .

9. An apparatus for use in wireless energy transfer, the apparatus comprising:

a first resonator structure configured for energy transfer with a second resonator structure over a distance  $D$ ,

wherein the energy transfer is mediated by evanescent-tail coupling of a resonant field of the first resonator structure and a resonant field of the second resonator structure, with a coupling factor  $k$ , wherein

said resonant field of the first resonator structure has a resonance angular frequency  $\omega_1$ , a resonance frequency-width  $\Gamma_1$ , and a resonance quality factor  $Q_1 = \omega_1 / 2\Gamma_1$ , and is radiative in the far field, with an associated radiation quality factor  $Q_{1,\text{rad}} \geq Q_1$ , and

said resonant field of the second resonator structure has a resonance angular frequency  $\omega_2$ , a resonance frequency-width  $\Gamma_2$ , and a resonance quality factor  $Q_2 = \omega_2 / 2\Gamma_2$ , and is radiative in the far field, with an associated radiation quality factor  $Q_{2,\text{rad}} \geq Q_2$ ,

wherein an absolute value of a difference of said angular frequencies  $\omega_1$  and  $\omega_2$

is smaller than broader of said resonant widths  $\Gamma_1$  and  $\Gamma_2$ , and an average resonant angular frequency is defined as  $\omega_o = \sqrt{\omega_1 \omega_2}$ , corresponding to an average resonant wavelength  $\lambda_o = 2\pi c / \omega_o$ , where  $c$  is the speed of light in free space, and a strong-coupling factor being defined as  $U = k\sqrt{Q_1 Q_2}$ ,

wherein the apparatus is configured to employ interference between said radiative far fields of the resonant fields of the first and second resonator, with an interference factor  $V_{\text{rad}}$ , to reduce a total amount of radiation from the apparatus compared to an amount of radiation from the apparatus in the absence of interference, a strong-interference factor being defined as  $V = V_{\text{rad}} \sqrt{(Q_1 / Q_{1,\text{rad}})(Q_2 / Q_{2,\text{rad}})}$ .

10. The apparatus of claim 9, wherein  $Q_1 / Q_{1,\text{rad}} \geq 0.01$  and  $Q_2 / Q_{2,\text{rad}} \geq 0.01$ .
11. The apparatus of claim 9, wherein  $Q_1 / Q_{1,\text{rad}} \geq 0.1$  and  $Q_2 / Q_{2,\text{rad}} \geq 0.1$ .
12. The apparatus of claim 9, wherein  $D / \lambda_o$  is larger than 0.001 and the strong-interference factor  $V$  is larger than 0.01.
13. The apparatus of claim 9, wherein  $D / \lambda_o$  is larger than 0.001 and the strong-interference factor  $V$  is larger than 0.1.
14. The apparatus of claim 9, further comprising the second resonator structure.
15. The apparatus of claim 9, wherein, during operation, a power generator is coupled to one of the first and second resonant structure, with a coupling rate  $\kappa_g$ , and is configured to drive the resonator structure, to which it is coupled, at a driving frequency  $f$ , corresponding to a driving angular frequency  $\omega = 2\pi f$ ,

wherein  $U_g$  is defined as  $\kappa_g / \Gamma_1$ , if the power generator is coupled to the first resonator structure and defined as  $\kappa_g / \Gamma_2$ , if the power generator is coupled to the second

resonator structure.

16. The apparatus of claim 15, wherein the driving frequency is different from the resonance frequencies of the first and second resonator structures and is closer to a frequency corresponding to an odd normal mode of the system of the two resonator structures,

wherein the detuning of the first resonator from the driving frequency is defined as  $D_1 = (\omega - \omega_1) / \Gamma_1$  and the detuning of the second resonator structure from the driving frequency is defined as  $D_2 = (\omega - \omega_2) / \Gamma_2$ .

17. The apparatus of claim 16, wherein  $D_1$  is approximately equal to  $UV_{\text{rad}}$  and  $D_2$  is approximately equal to  $UV_{\text{rad}}$ .

18. The apparatus of claim 15, wherein  $U_g$  is chosen to maximize the ratio of the energy-transfer efficiency to the radiation efficiency.

19. The apparatus of claim 17, wherein  $U_g$  is approximately equal to

$$\sqrt{1 + U^2 - V_{\text{rad}}^2 U^2 + V^2 - 2VV_{\text{rad}}}.$$

20. The apparatus of claim 15, wherein  $f$  is at least larger than 100 kHz and smaller than 500MHz.

21. The apparatus of claim 15, wherein  $f$  is at least larger than 1MHz and smaller than 50MHz.

22. The apparatus of claim 15, further comprising the power generator.

23. The apparatus of claim 15, wherein, during operation, a power load is coupled to the resonant structure to which the power generator is not coupled, with a coupling rate

$\kappa_l$ , and is configured to receive from the resonator structure, to which it is coupled, a usable power,

wherein  $U_l$  is defined as  $\kappa_l / \Gamma_1$ , if the power load is coupled to the first resonator structure and defined as  $\kappa_l / \Gamma_2$ , if the power load is coupled to the second resonator structure.

24. The apparatus of claim 23, wherein  $U_l$  is chosen to maximize the ratio of the energy-transfer efficiency to the radiation efficiency.

25. The apparatus of claim 24, wherein the driving frequency is different from the resonance frequencies of the first and second resonator structures and is closer to a frequency corresponding to an odd normal mode of the system of the two resonator structures,

wherein the detuning of the first resonator from the driving frequency is defined as  $D_1 = (\omega - \omega_1) / \Gamma_1$  and is approximately equal to  $UV_{\text{rad}}$ , and the detuning of the second resonator structure from the driving frequency is defined as  $D_2 = (\omega - \omega_2) / \Gamma_2$  and is approximately equal to  $UV_{\text{rad}}$ ,

and  $U_l$  is approximately equal to  $\sqrt{1 + U^2 - V_{\text{rad}}^2 U^2 + V^2 - 2VV_{\text{rad}}}$ .

26. The apparatus of claim 9, wherein at least one of the first and second resonator structures comprises a capacitively loaded loop or coil of at least one of a conducting wire, a conducting Litz wire, and a conducting ribbon.

27. The apparatus of claim 26, where the characteristic size of said loop or coil is less than 30 cm and the width of said conducting wire or Litz wire or ribbon is less than 2cm.

28. The apparatus of claim 26, where the characteristic size of said loop or coil is less than 1m and the width of said conducting wire or Litz wire or ribbon is less than 2cm.

29. The apparatus of claim 9, further comprising a feedback mechanism for maintaining the resonant frequency of one or more of the resonant objects.

30. The apparatus of claim 29, wherein the feedback mechanism comprises an oscillator with a fixed driving frequency and is configured to adjust the resonant frequency of the one or more resonant objects to be detuned by a fixed amount with respect to the fixed frequency.

31. An apparatus for use in wireless energy transfer, the apparatus comprising:  
a first resonator structure configured for energy transfer with a second resonator structure over a distance  $D$ ,

wherein the energy transfer is mediated by evanescent-tail coupling of a resonant field of the first resonator structure and a resonant field of the second resonator structure, with a coupling factor  $k$ , wherein

said resonant field of the first resonator structure has a resonance angular frequency  $\omega_1$ , a resonance frequency-width  $\Gamma_1$ , and a resonance quality factor  $Q_1 = \omega_1 / 2\Gamma_1$ , and is radiative in the far field, with an associated radiation quality factor  $Q_{1,\text{rad}} \geq Q_1$ , and

said resonant field of the second resonator structure has a resonance angular frequency  $\omega_2$ , a resonance frequency-width  $\Gamma_2$ , and a resonance quality factor  $Q_2 = \omega_2 / 2\Gamma_2$ , and is radiative in the far field, with an associated radiation quality factor  $Q_{2,\text{rad}} \geq Q_2$ ,

wherein an absolute value of a difference of said angular frequencies  $\omega_1$  and  $\omega_2$  is smaller than the broader of said resonant widths  $\Gamma_1$  and  $\Gamma_2$ , and an average resonant angular frequency is defined as  $\omega_o = \sqrt{\omega_1\omega_2}$ , corresponding to an average resonant wavelength  $\lambda_o = 2\pi c / \omega_o$ , where  $c$  is the speed of light in free space, and a strong-coupling factor is defined as  $U = k\sqrt{Q_1Q_2}$ ,

wherein the apparatus is configured to employ interference between said radiative far fields of the resonant fields of the first and second resonator, with an interference

factor  $V_{\text{rad}}$ , to increase efficiency of energy transfer for the apparatus compared to efficiency for the apparatus in the absence of interference, the strong-interference factor being defined as  $V = V_{\text{rad}} \sqrt{(Q_1 / Q_{1,\text{rad}})(Q_2 / Q_{2,\text{rad}})}$ .

32. The apparatus of claim 31, wherein  $Q_1 / Q_{1,\text{rad}} \geq 0.05$  and  $Q_2 / Q_{2,\text{rad}} \geq 0.05$ .

33. The apparatus of claim 31, wherein  $Q_1 / Q_{1,\text{rad}} \geq 0.5$  and  $Q_2 / Q_{2,\text{rad}} \geq 0.5$ .

34. The apparatus of claim 31, wherein  $D / \lambda_o$  is larger than 0.01 and the strong-interference factor  $V$  is larger than 0.05.

35. The apparatus of claim 31, wherein  $D / \lambda_o$  is larger than 0.01 and the strong-interference factor  $V$  is larger than 0.5.

36. The apparatus of claim 31, further comprising the second resonator structure.

37. The apparatus of claim 31, wherein, during operation, a power generator is coupled to one of the first and second resonant structure, with a coupling rate  $\kappa_g$ , and is configured to drive the resonator structure, to which it is coupled, at a driving frequency  $f$ , corresponding to a driving angular frequency  $\omega = 2\pi f$ ,

wherein  $U_g$  is defined as  $\kappa_g / \Gamma_1$ , if the power generator is coupled to the first resonator structure and defined as  $\kappa_g / \Gamma_2$ , if the power generator is coupled to the second resonator structure.

38. The apparatus of claim 37, wherein the driving frequency is different from the resonance frequencies of the first and second resonator structures and is closer to a frequency corresponding to an odd normal mode of the system of the two resonator structures,

wherein the detuning of the first resonator from the driving frequency is defined



as  $D_1 = (\omega - \omega_1) / \Gamma_1$  and the detuning of the second resonator structure from the driving frequency is defined as  $D_2 = (\omega - \omega_2) / \Gamma_2$ .

39. The apparatus of claim 38, wherein  $D_1$  is approximately equal to  $UV$  and  $D_2$  is approximately equal to  $UV$ .

40. The apparatus of claim 37, wherein  $U_g$  is chosen to maximize the energy-transfer efficiency.

41. The apparatus of claim 39, wherein  $U_g$  is approximately equal to

$$\sqrt{(1+U^2)(1-V^2)}.$$

42. The apparatus of claim 37, wherein  $f$  is at least larger than 100 kHz and smaller than 500MHz.

43. The apparatus of claim 37, wherein  $f$  is at least larger than 1MHz and smaller than 50MHz.

44. The apparatus of claim 37, further comprising the power generator.

45. The apparatus of claim 37, wherein, during operation, a power load is coupled to the resonant structure to which the power generator is not coupled, with a coupling rate  $\kappa_l$ , and is configured to receive from the resonator structure, to which it is coupled, a usable power,

wherein  $U_l$  is defined as  $\kappa_l / \Gamma_1$ , if the power load is coupled to the first resonator structure and defined as  $\kappa_l / \Gamma_2$ , if the power load is coupled to the second resonator structure.

46. The apparatus of claim 45, wherein  $U_1$  is chosen to maximize the energy-transfer efficiency.

47. The apparatus of claim 46, wherein the driving frequency is different from the resonance frequencies of the first and second resonator structures and is closer to a frequency corresponding to an odd normal mode of the system of the two resonator structures,

wherein the detuning of the first resonator from the driving frequency is defined as  $D_1 = (\omega - \omega_1) / \Gamma_1$  and is approximately equal to  $UV$ , and the detuning of the second resonator structure from the driving frequency is defined as  $D_2 = (\omega - \omega_2) / \Gamma_2$  and is approximately equal to  $UV$ ,

and  $U_1$  is approximately equal to  $\sqrt{(1+U^2)(1-V^2)}$ .

48. The apparatus of claim 31, wherein at least one of the first and second resonator structures comprises a capacitively loaded loop or coil of at least one of a conducting wire, a conducting Litz wire, and a conducting ribbon.

49. The apparatus of claim 48, where the characteristic size of said loop or coil is less than 30 cm and the width of said conducting wire or Litz wire or ribbon is less than 2cm.

50. The apparatus of claim 48, where the characteristic size of said loop or coil is less than 1m and the width of said conducting wire or Litz wire or ribbon is less than 2cm.

51. The apparatus of claim 31, further comprising a feedback mechanism for maintaining the resonant frequency of one or more of the resonant objects.

52. The apparatus of claim 51, wherein the feedback mechanism comprises an oscillator with a fixed driving frequency and is configured to adjust the resonant frequency of the one or more resonant objects to be detuned by a fixed amount with

respect to the fixed frequency.

53. The apparatus of claim 51, where the feedback mechanism is configured to monitor an efficiency of the energy transfer, and adjust the resonant frequency of the one or more resonant objects to maximize the efficiency.

54. The apparatus of claim 31, wherein the resonance angular frequencies for the resonator structures are selected to optimize the energy-transfer efficiency by accounting for both the strong-coupling factor  $U$  and the strong-interference interference factor  $V$ .

55. A method for wireless energy transfer, the method comprising:

providing a first resonator structure configured for energy transfer with a second resonator structure over a distance  $D$ ,

wherein the energy transfer is mediated by evanescent-tail coupling of a resonant field of the first resonator structure and a resonant field of the second resonator structure, with a coupling factor  $k$ , wherein

said resonant field of the first resonator structure has a resonance angular frequency  $\omega_1$ , a resonance frequency-width  $\Gamma_1$ , and a resonance quality factor  $Q_1 = \omega_1 / 2\Gamma_1$ , and is radiative in the far field, with an associated radiation quality factor  $Q_{1,\text{rad}} \geq Q_1$ , and

said resonant field of the second resonator structure has a resonance angular frequency  $\omega_2$ , a resonance frequency-width  $\Gamma_2$ , and a resonance quality factor  $Q_2 = \omega_2 / 2\Gamma_2$ , and is radiative in the far field, with an associated radiation quality factor  $Q_{2,\text{rad}} \geq Q_2$ ,

wherein an absolute value of a difference of said angular frequencies  $\omega_1$  and  $\omega_2$  is smaller than broader of said resonant widths  $\Gamma_1$  and  $\Gamma_2$ , and an average resonant angular frequency is defined as  $\omega_o = \sqrt{\omega_1 \omega_2}$ , corresponding to an average resonant wavelength  $\lambda_o = 2\pi c / \omega_o$ , where  $c$  is the speed of light in free space, and the strong-coupling factor is defined as  $U = k\sqrt{Q_1 Q_2}$ , and

employing interference between said radiative far fields of the resonant fields of the first and second resonator, with an interference factor  $V_{\text{rad}}$ , to reduce a total amount of radiation from the first and second resonator compared to an amount of radiation from the first and second resonator in the absence of interference, a strong-interference factor being defined as  $V = V_{\text{rad}} \sqrt{(Q_1 / Q_{1,\text{rad}})(Q_2 / Q_{2,\text{rad}})}$ .

56. The method of claim 55, wherein  $Q_1 / Q_{1,\text{rad}} \geq 0.01$  and  $Q_2 / Q_{2,\text{rad}} \geq 0.01$ .

57. The method of claim 55, wherein, during operation, a power generator is coupled to one of the first and second resonant structure and is configured to drive the resonator structure, to which it is coupled, at a driving frequency  $f$ , corresponding to a driving angular frequency  $\omega = 2\pi f$ ,

wherein the driving frequency is different from the resonance frequencies of the first and second resonator structures and is closer to a frequency corresponding to an odd normal mode of the system of the two resonator structures.

58. The method of claim 57, wherein, during operation, a power load is coupled to the resonant structure to which the power generator is not coupled and is configured to receive from the resonator structure, to which it is coupled, a usable power.

59. A method for wireless energy transfer, the method comprising:

providing a first resonator structure configured for energy transfer with a second resonator structure over a distance  $D$ ,

wherein the energy transfer is mediated by evanescent-tail coupling of a resonant field of the first resonator structure and a resonant field of the second resonator structure, with a coupling factor  $k$ , wherein

said resonant field of the first resonator structure has a resonance angular frequency  $\omega_1$ , a resonance frequency-width  $\Gamma_1$ , and a resonance quality factor

$Q_1 = \omega_1 / 2\Gamma_1$ , and is radiative in the far field, with an associated radiation quality factor

$Q_{1,rad} \geq Q_1$ , and

said resonant field of the second resonator structure has a resonance angular frequency  $\omega_2$ , a resonance frequency-width  $\Gamma_2$ , and a resonance quality factor  $Q_2 = \omega_2 / 2\Gamma_2$ , and is radiative in the far field, with an associated radiation quality factor  $Q_{2,rad} \geq Q_2$ ,

wherein an absolute value of the difference of said angular frequencies  $\omega_1$  and  $\omega_2$  is smaller than the broader of said resonant widths  $\Gamma_1$  and  $\Gamma_2$ , and an average resonant angular frequency is defined as  $\omega_o = \sqrt{\omega_1 \omega_2}$ , corresponding to an average resonant wavelength  $\lambda_o = 2\pi c / \omega_o$ , where  $c$  is the speed of light in free space, and the strong-coupling factor is defined as  $U = k\sqrt{Q_1 Q_2}$ , and

employing interference between said radiative far fields of the resonant fields of the first and second resonator, with an interference factor  $V_{rad}$ , to increase efficiency of energy transfer between the first and second resonator compared to efficiency of energy transfer between the first and second resonator in the absence of interference, a strong-interference factor being defined as  $V = V_{rad} \sqrt{(Q_1 / Q_{1,rad})(Q_2 / Q_{2,rad})}$ .

60. The method of claim 59, wherein  $Q_1 / Q_{1,rad} \geq 0.05$  and  $Q_2 / Q_{2,rad} \geq 0.05$ .

61. The method of claim 59, wherein, during operation, a power generator is coupled to one of the first and second resonant structure and is configured to drive the resonator structure, to which it is coupled, at a driving frequency  $f$ , corresponding to a driving angular frequency  $\omega = 2\pi f$ ,

wherein the driving frequency is different from the resonance frequencies of the first and second resonator structures and is closer to a frequency corresponding to an odd normal mode of the system of the two resonator structures.

62. The method of claim 61, wherein, during operation, a power load is coupled to the resonant structure to which the power generator is not coupled and is configured to

receive from the resonator structure, to which it is coupled, a usable power.

63. The method of claim 59, wherein the resonance angular frequencies for the resonator structures are selected to optimize the energy-transfer efficiency by accounting for both the strong-coupling factor  $U$  and the strong-interference interference factor  $V$ .

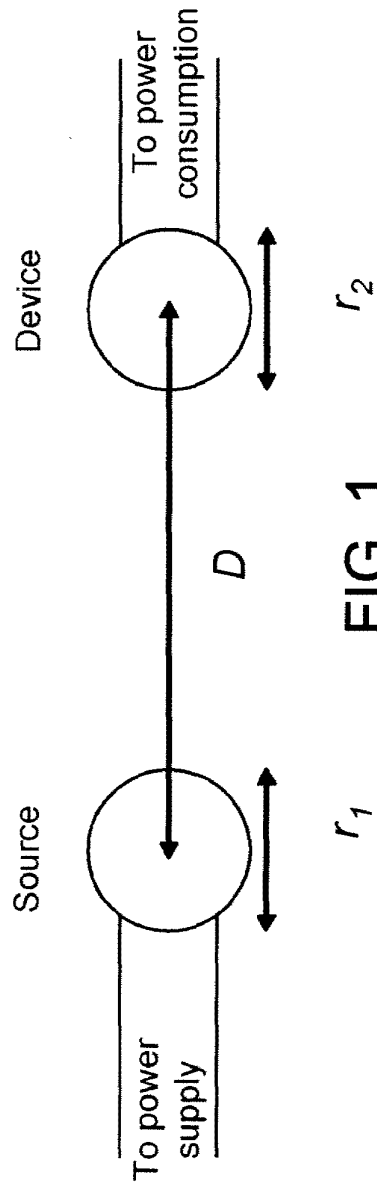


FIG. 1

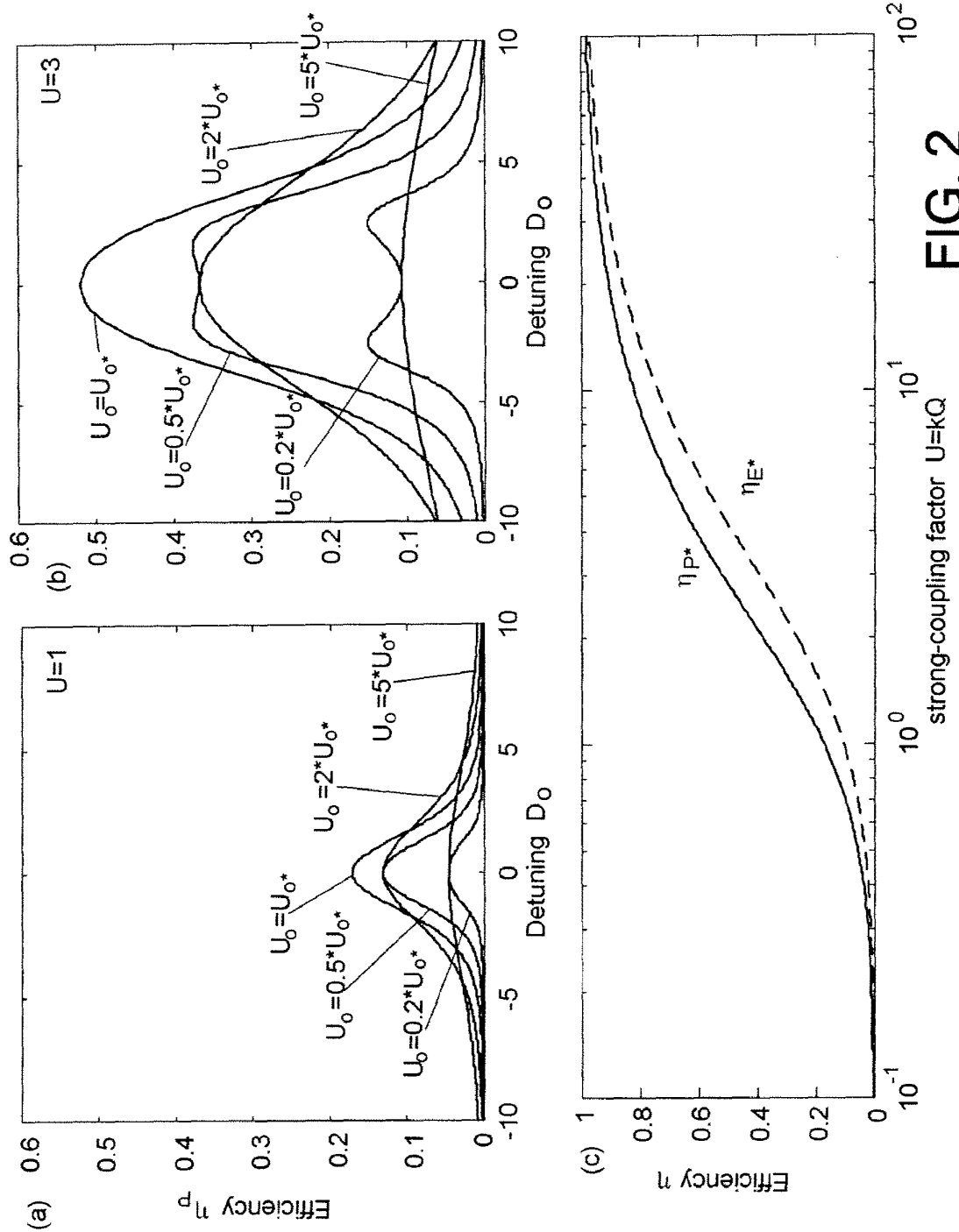


FIG. 2

SUBSTITUTE SHEET (RULE 26)



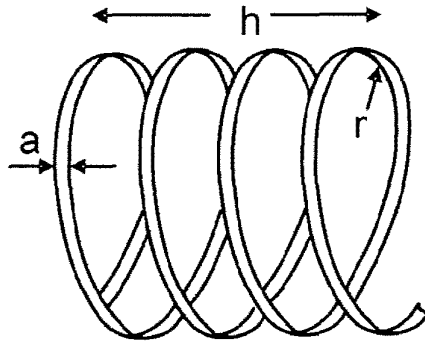


FIG. 3

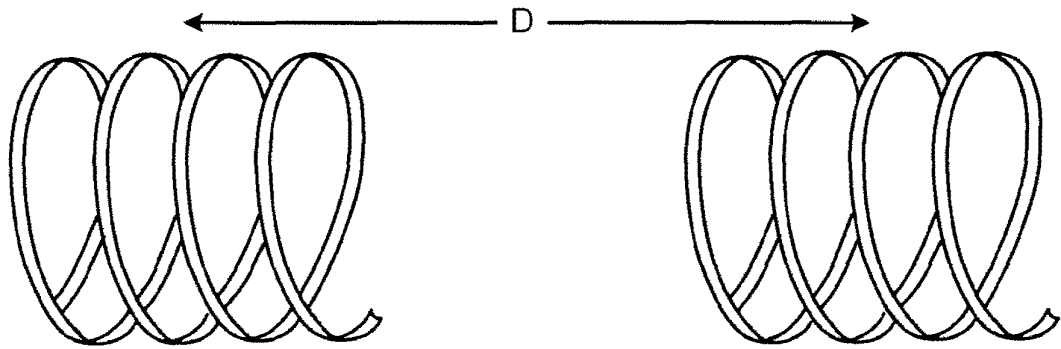


FIG. 4

4/30

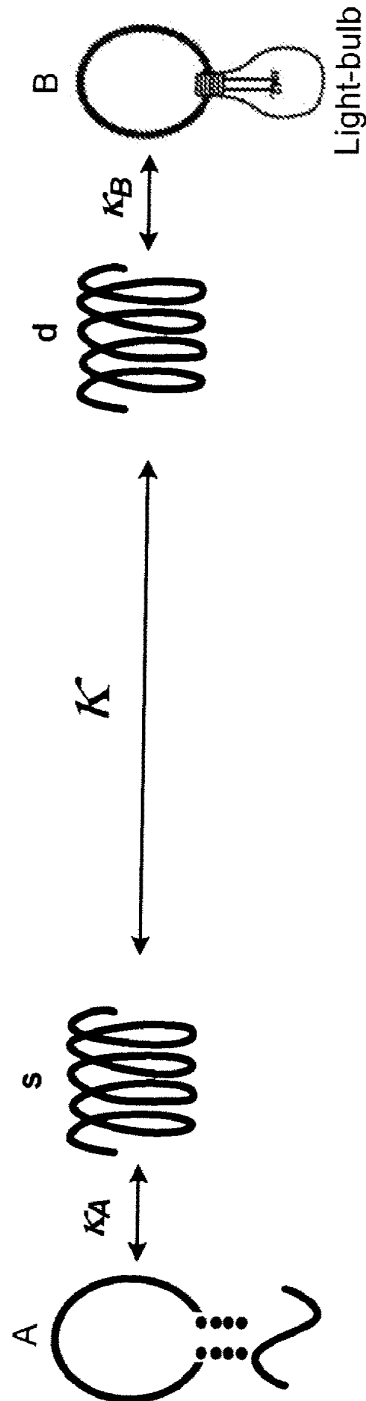
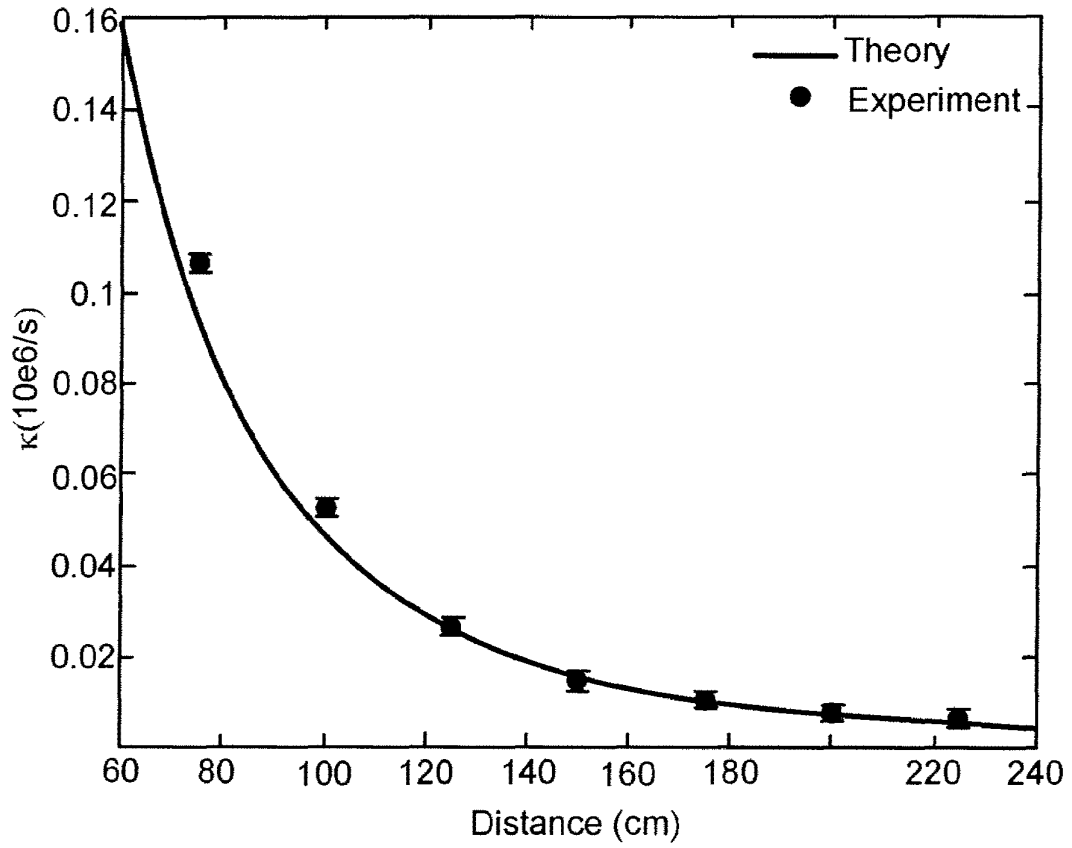


FIG. 5

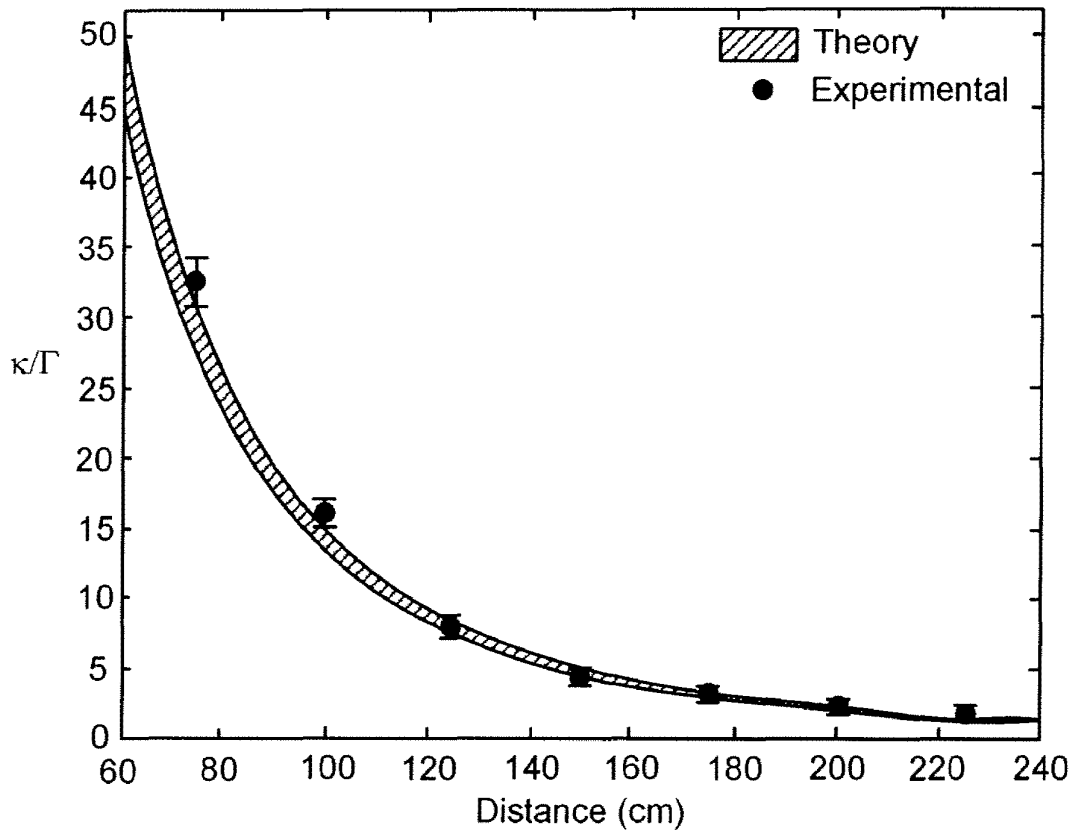
5/30



Comparison of experimental and theoretical values for  $\kappa$  as a function of the separation between the source and device coils.

FIG. 6

6/30



Comparison of experimental and theoretical values for the parameter  $\kappa/\Gamma$  as a function of the separation between the two coils. The theory values are obtained by using the theoretically obtained  $\kappa$  and the experimentally measured  $\Gamma$ . The shaded area represents the spread in the theoretical  $\kappa/\Gamma$  due to the ~5% uncertainty in  $Q$ .

FIG.7

7/30

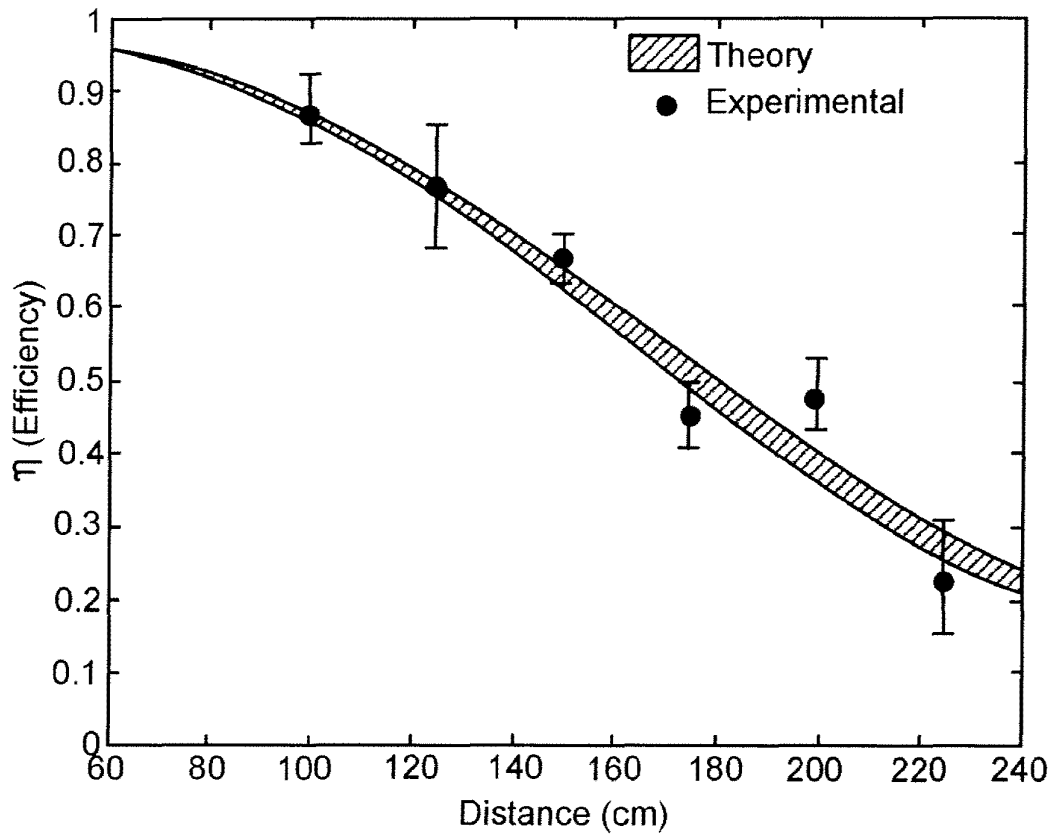


FIG. 8

SUBSTITUTE SHEET (RULE 26)

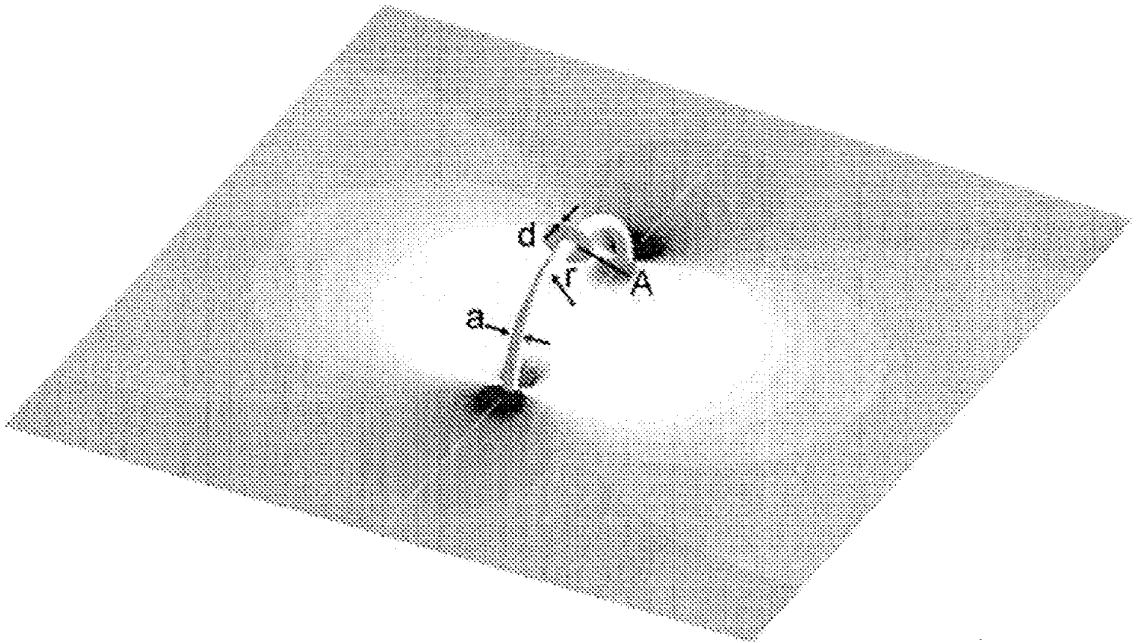


FIG. 9

9/30

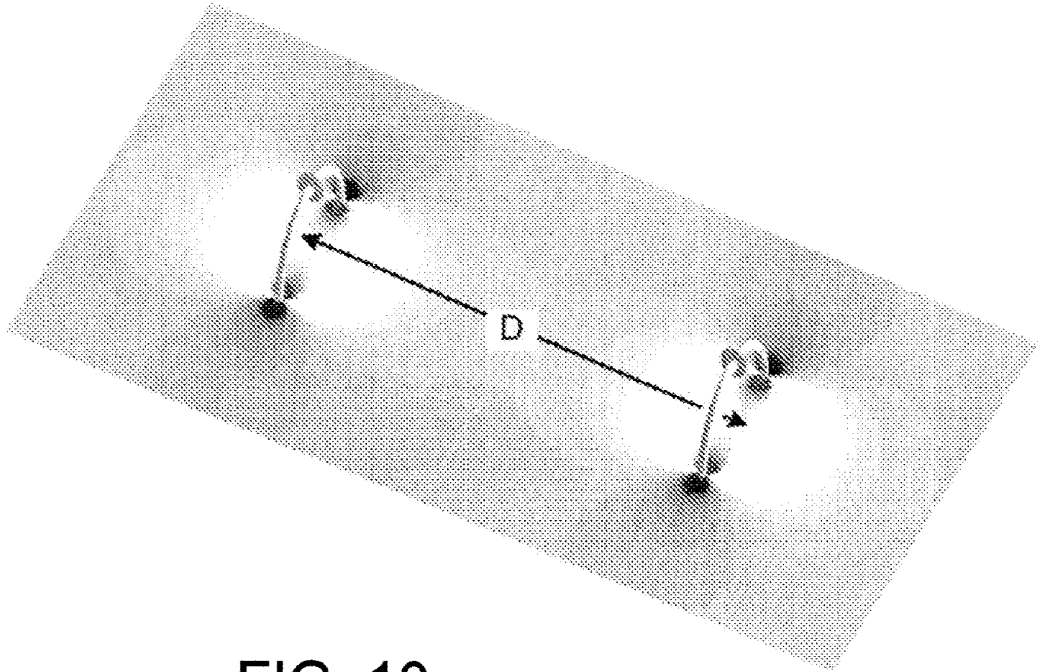


FIG. 10

10/30

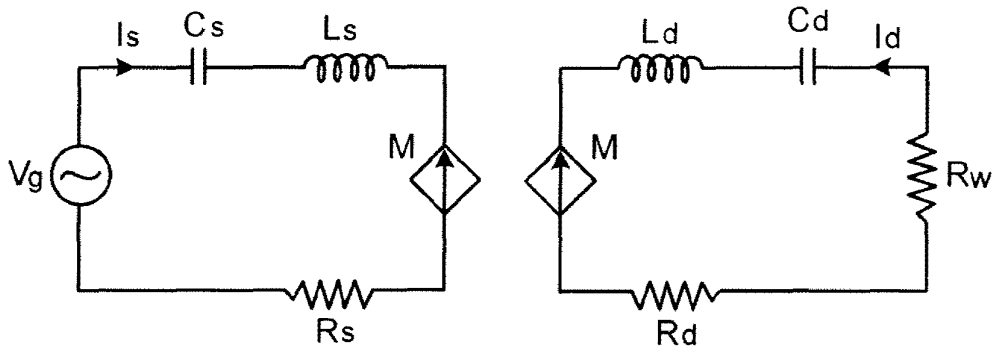


FIG. 11

SUBSTITUTE SHEET (RULE 26)



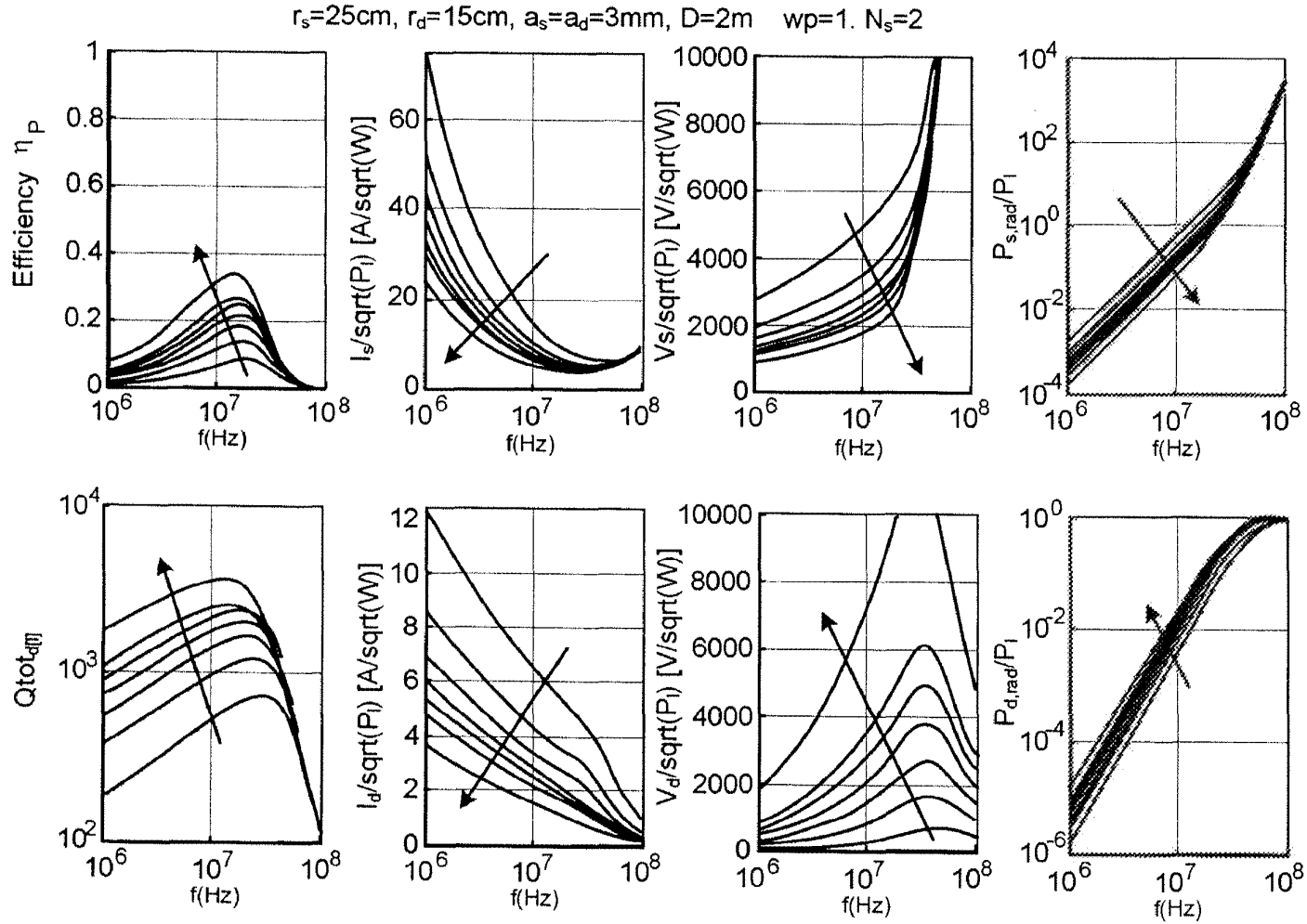


FIG. 12

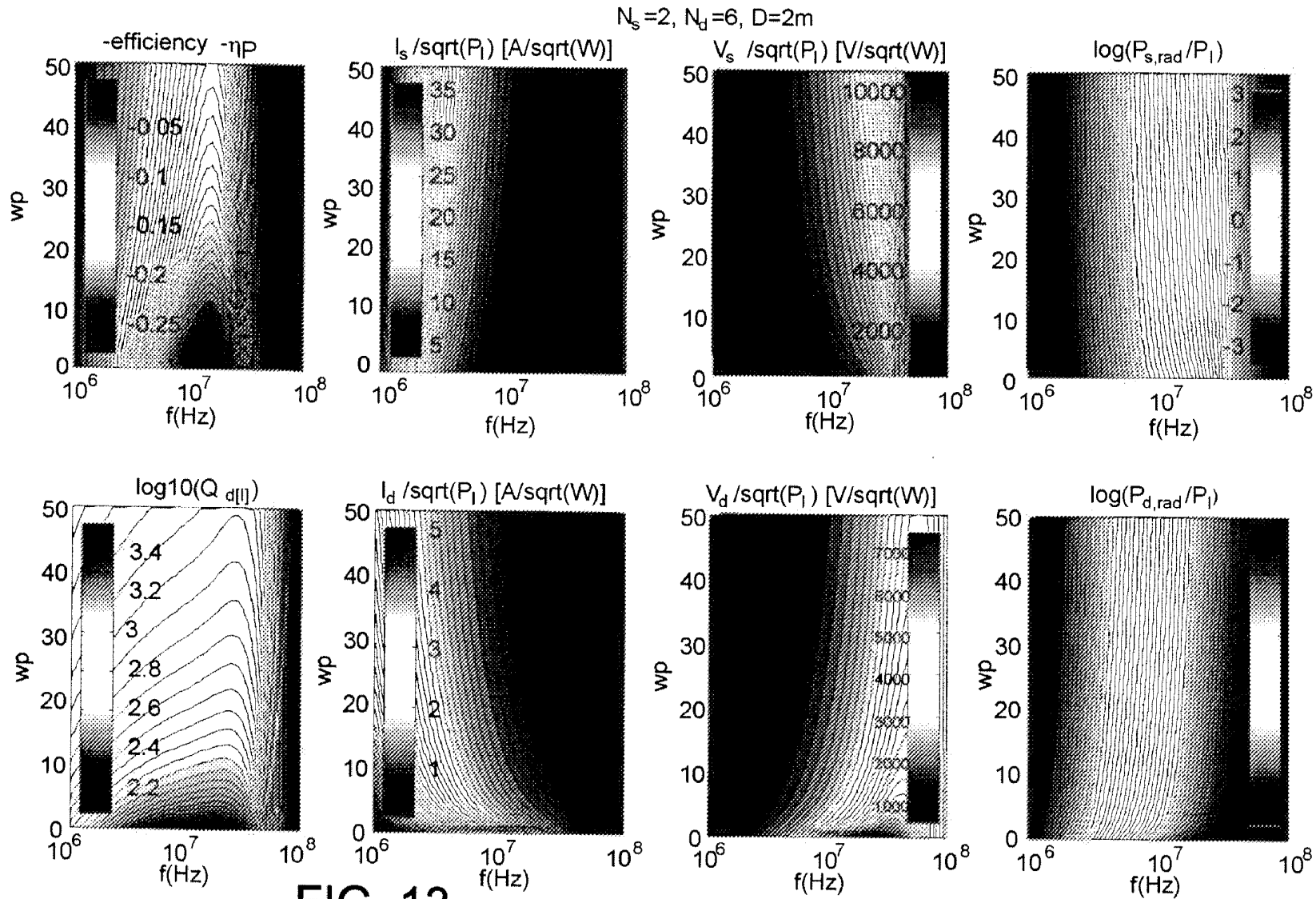


FIG. 13

13/30

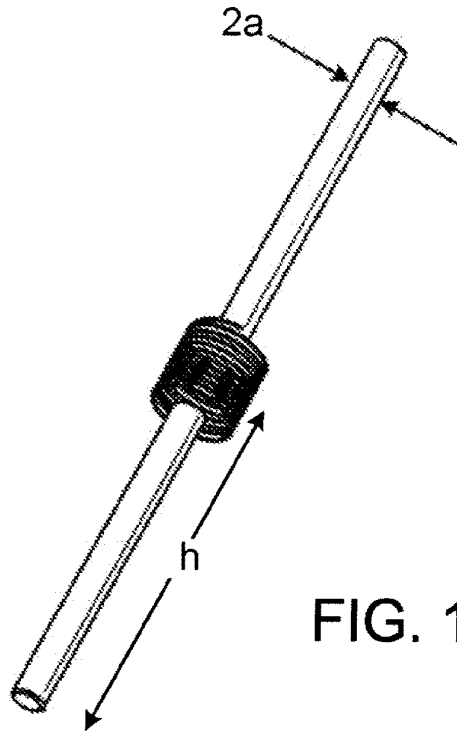


FIG. 14

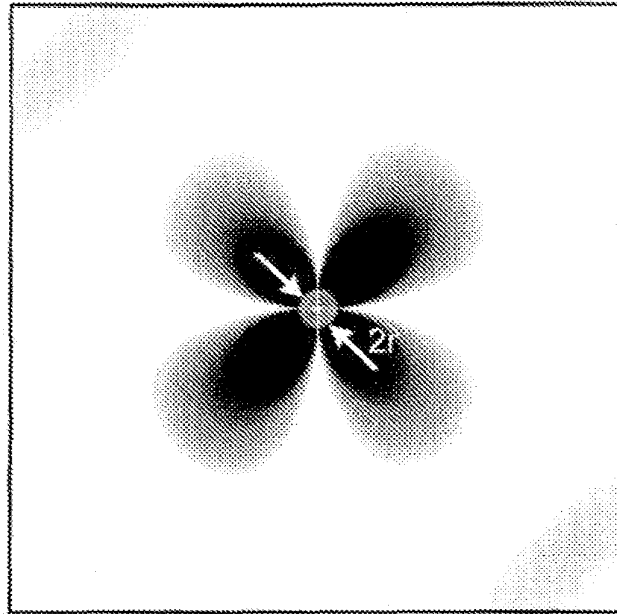


FIG. 15A

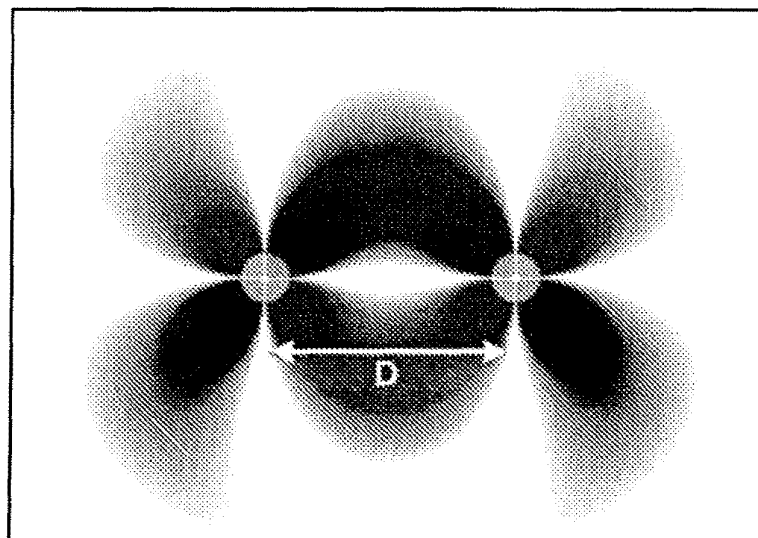


FIG. 15B

SUBSTITUTE SHEET (RULE 26)

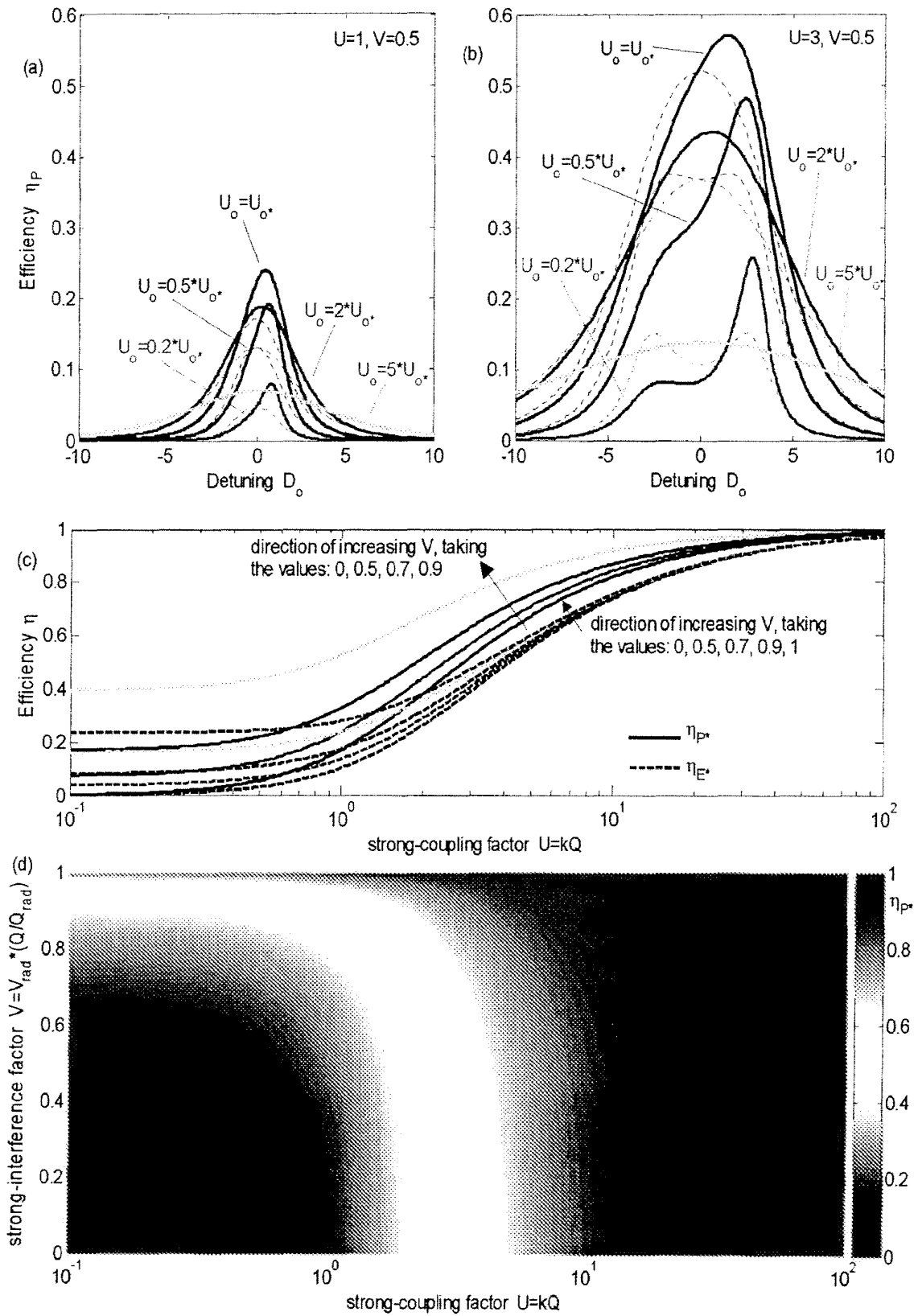


FIG. 16

SUBSTITUTE SHEET (RULE 26)

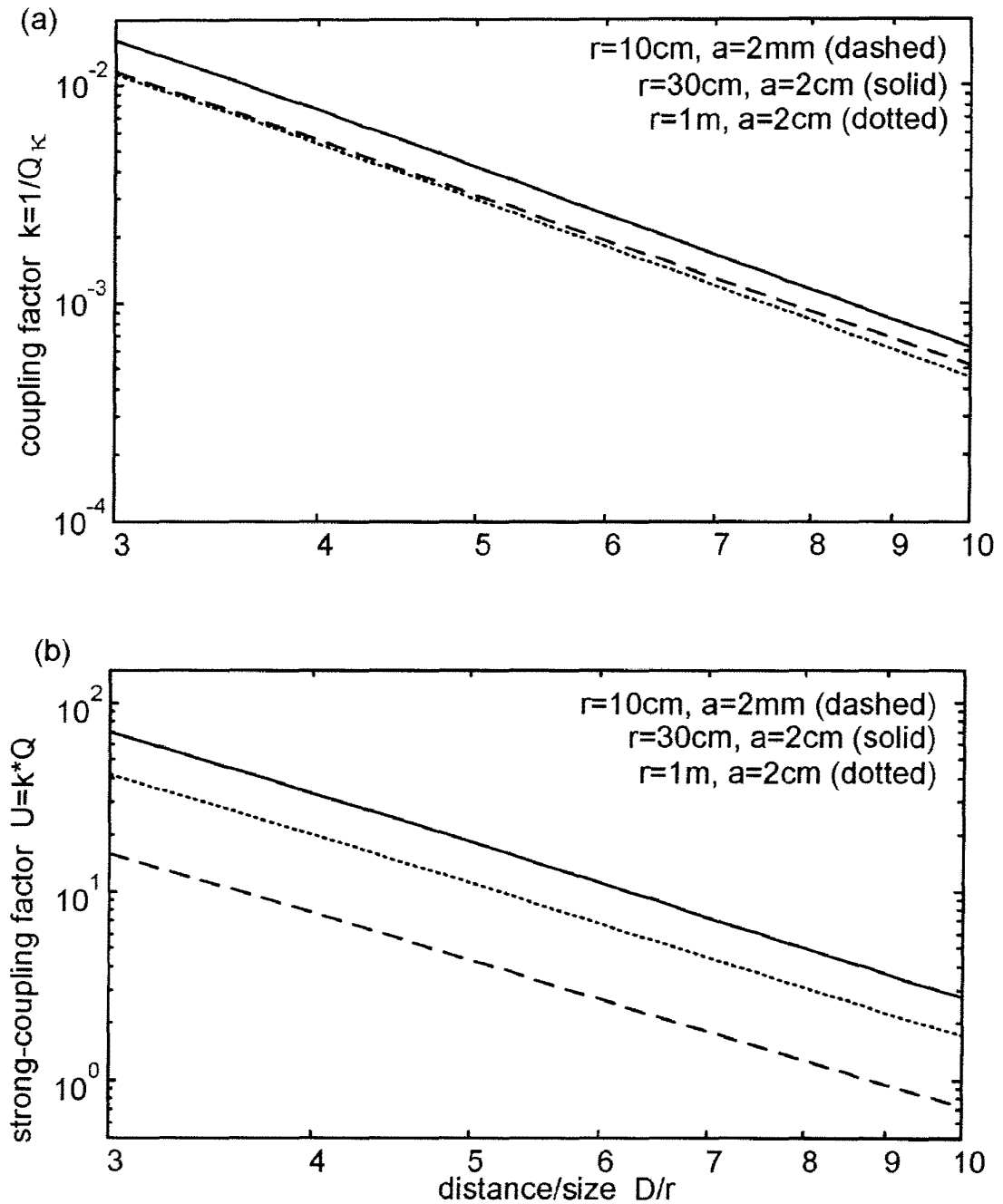


FIG. 17

SUBSTITUTE SHEET (RULE 26)

17/30

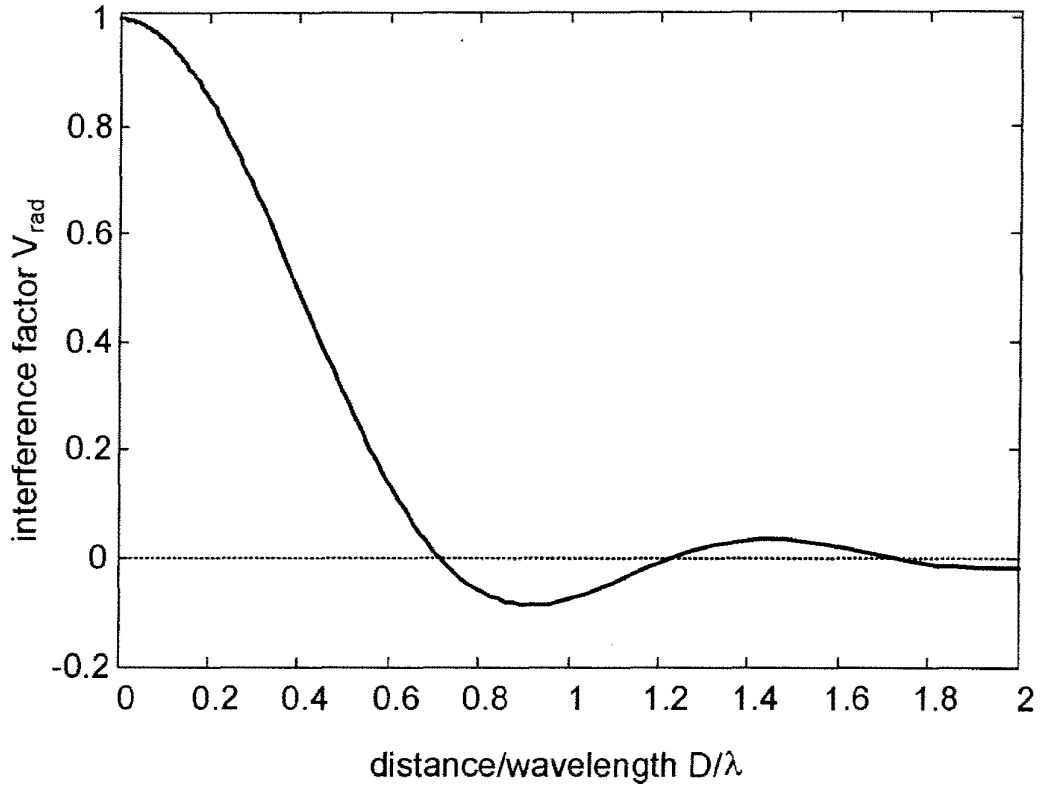


FIG. 18

SUBSTITUTE SHEET (RULE 26)

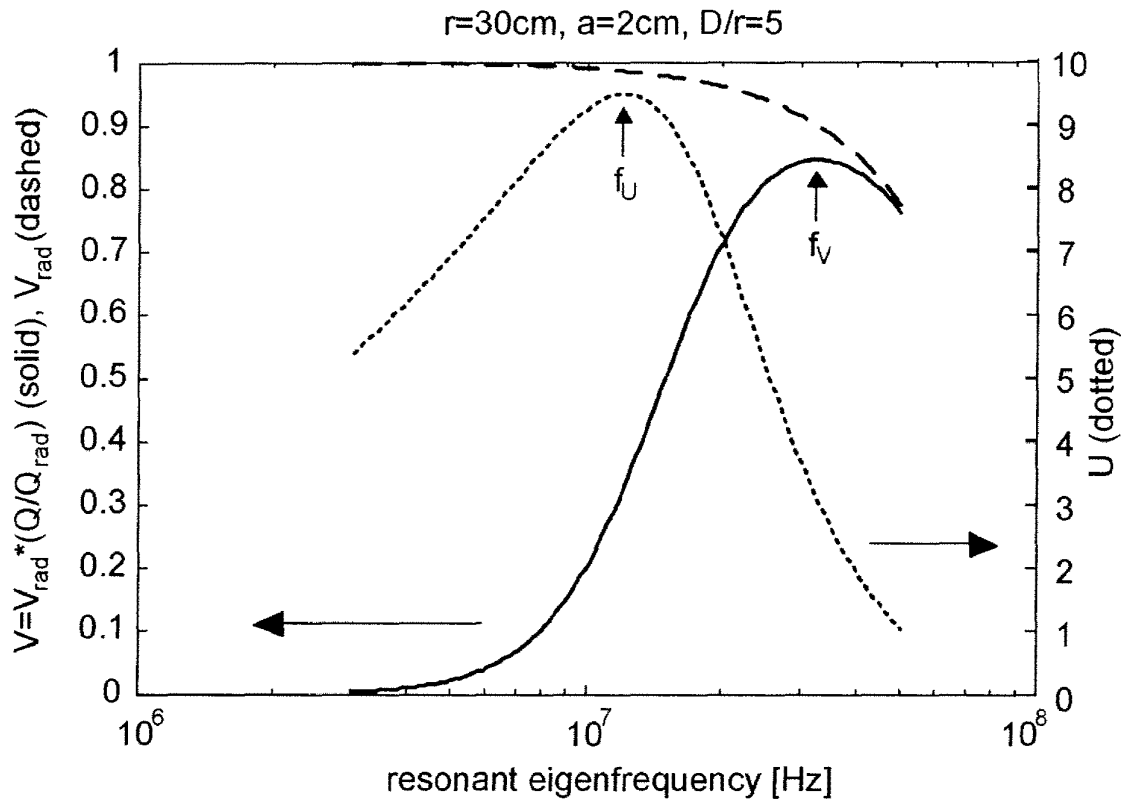


FIG. 19



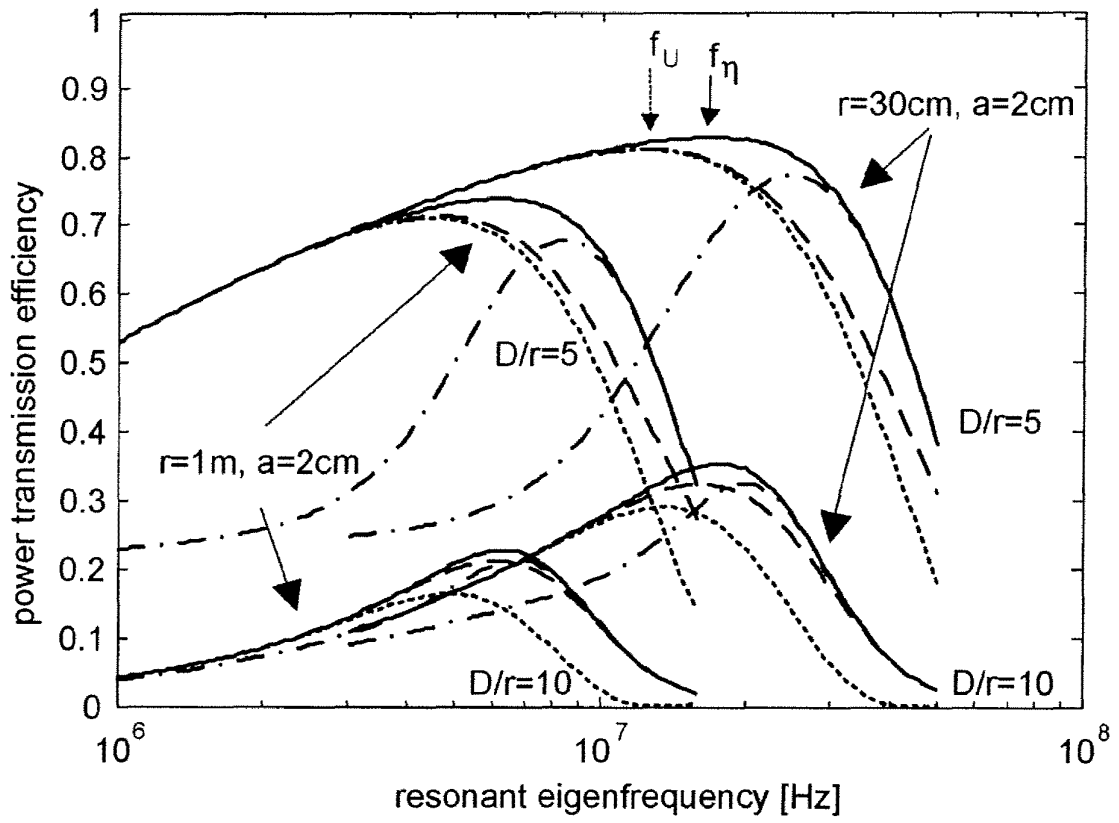


FIG. 20

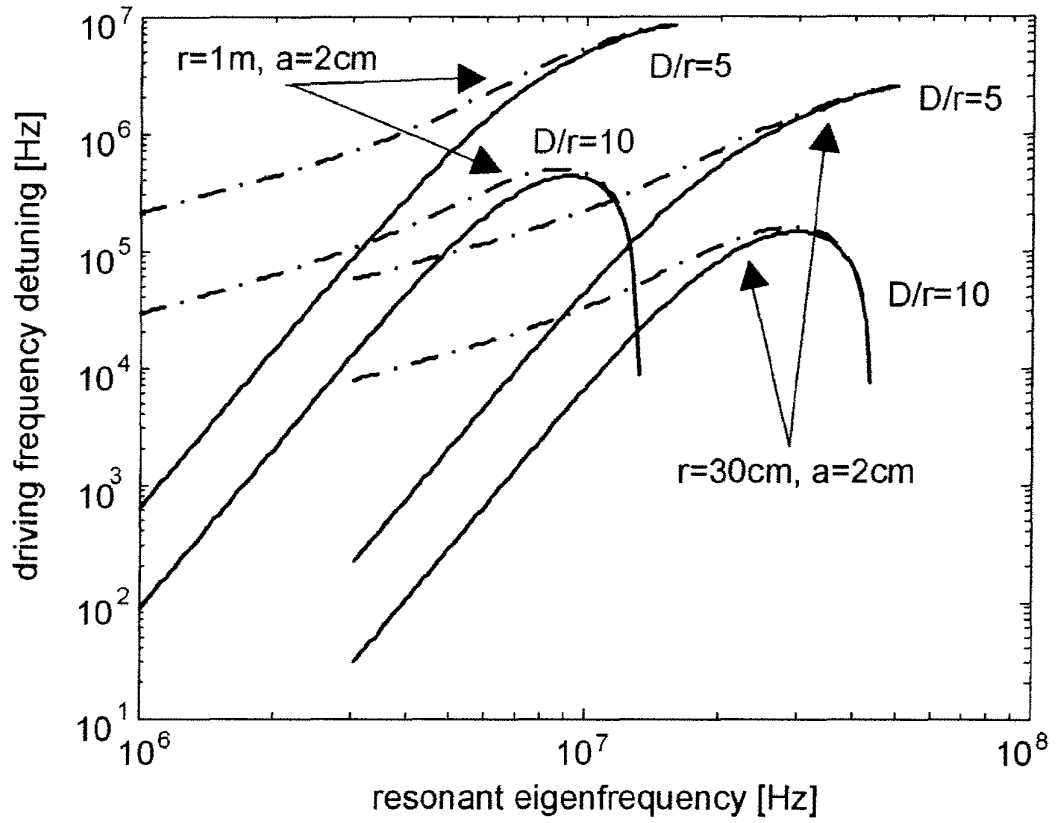


FIG. 21

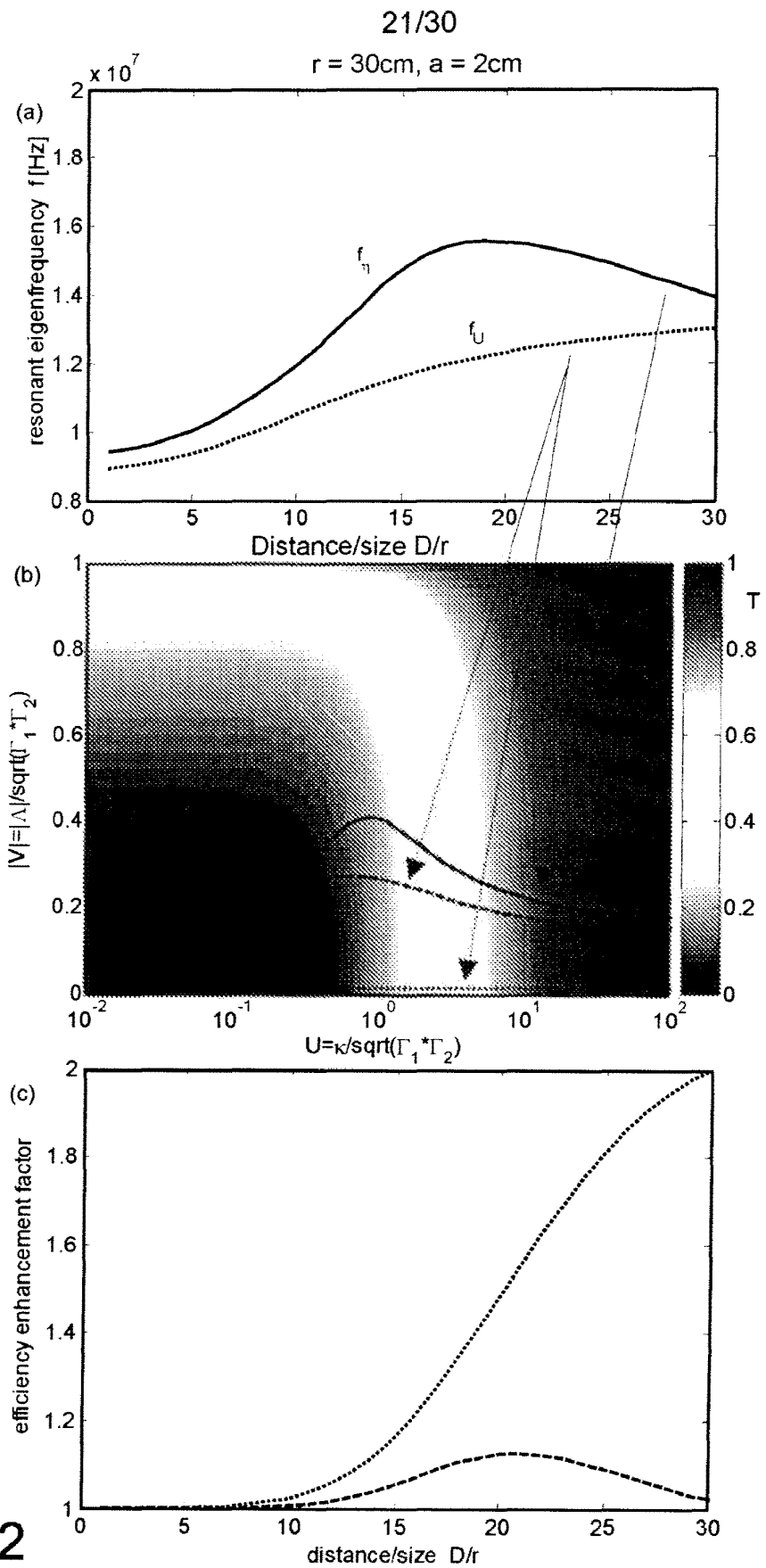


FIG. 22

SUBSTITUTE SHEET (RULE 26)

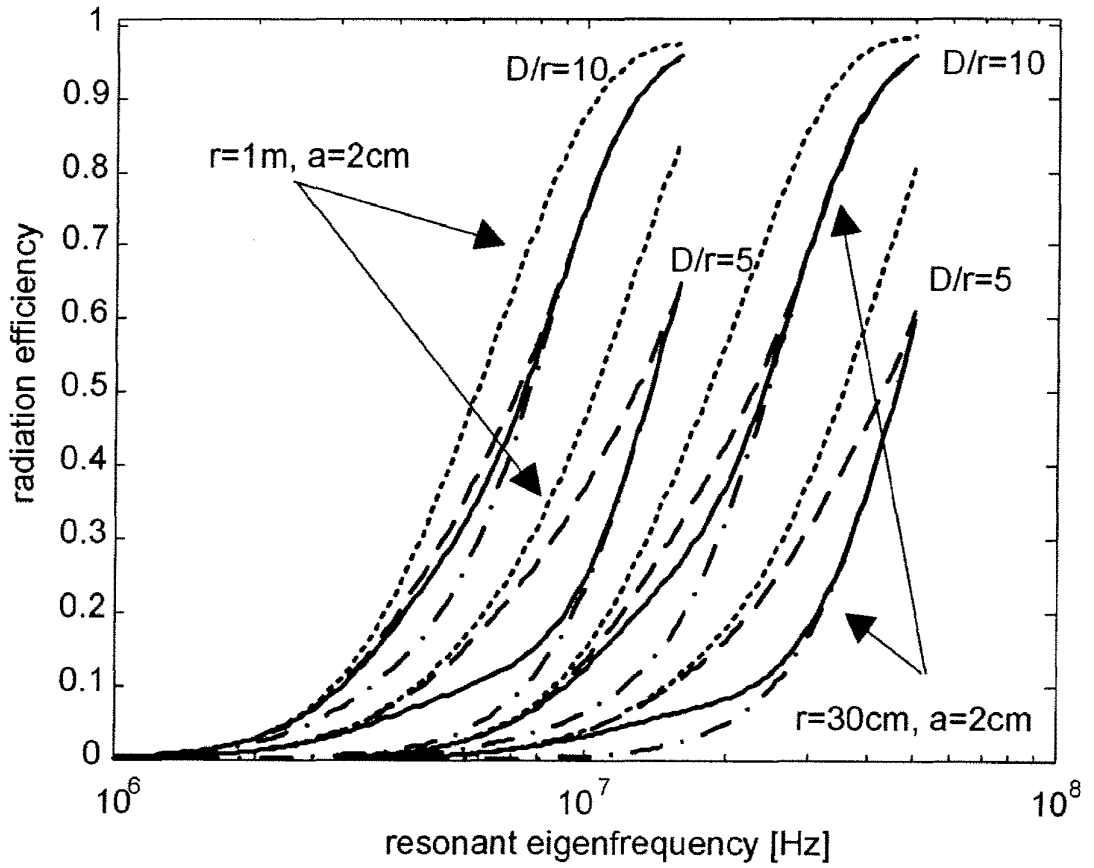


FIG. 23

23/30

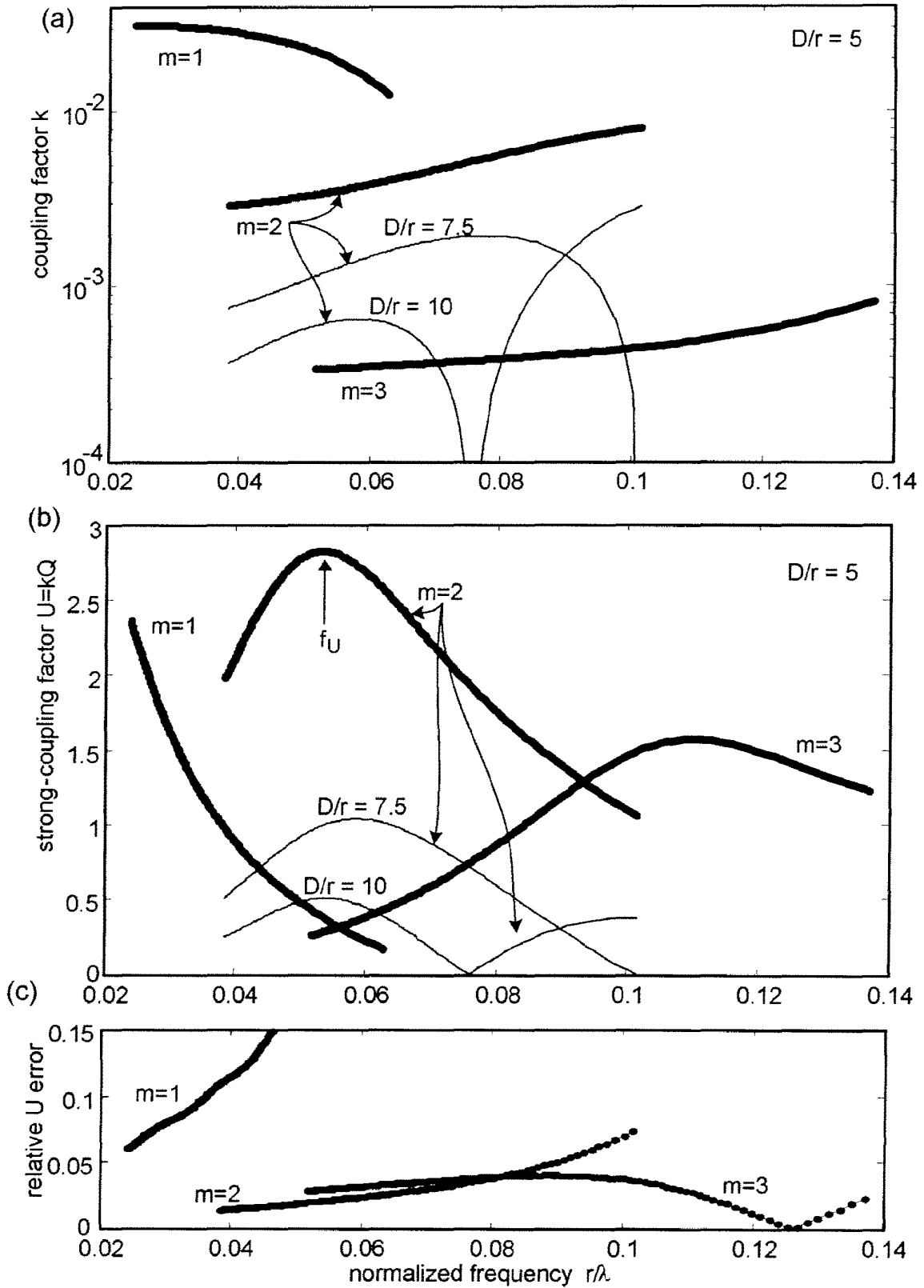


FIG. 24

SUBSTITUTE SHEET (RULE 26)

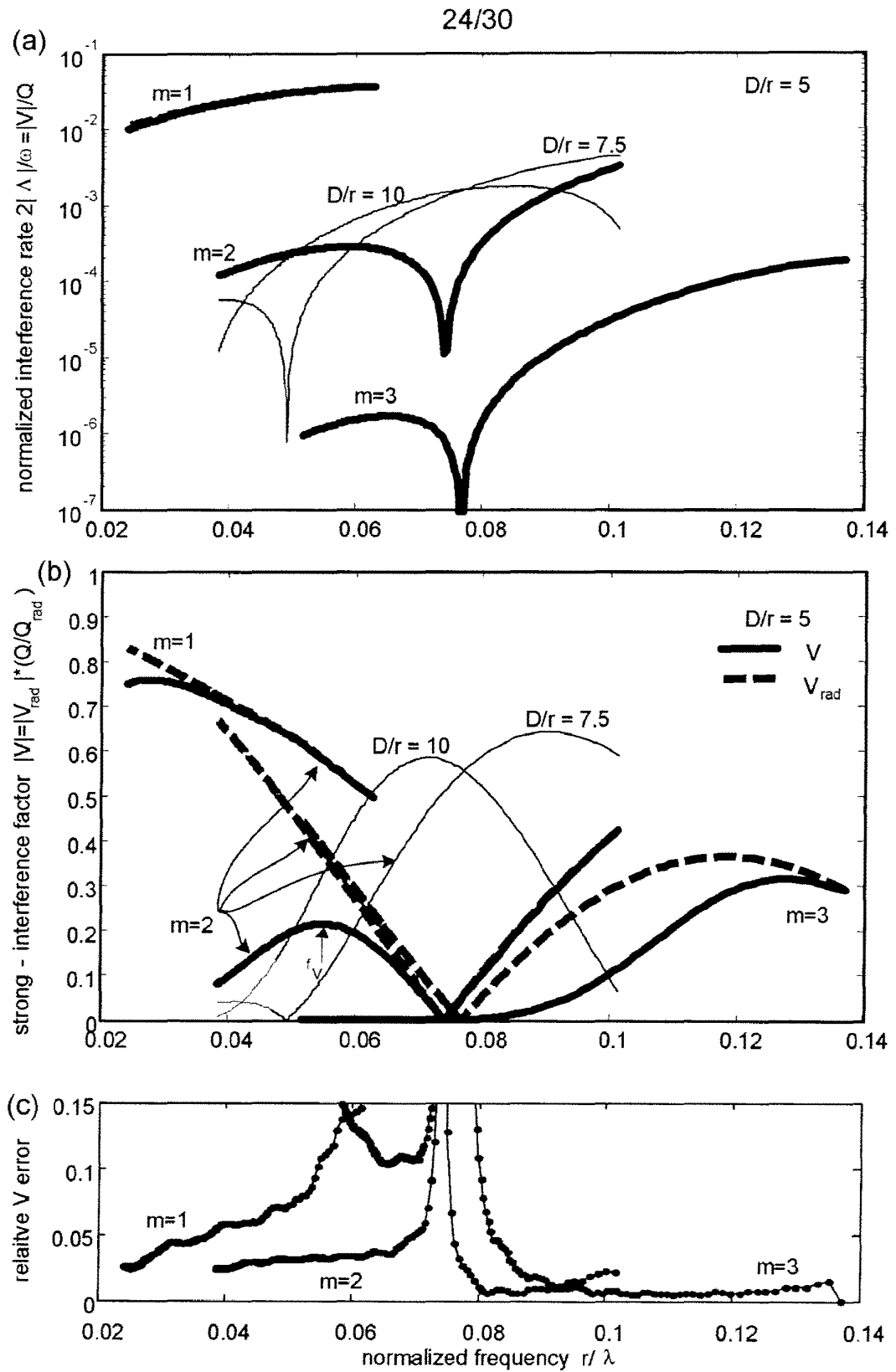


FIG. 25

SUBSTITUTE SHEET (RULE 26)

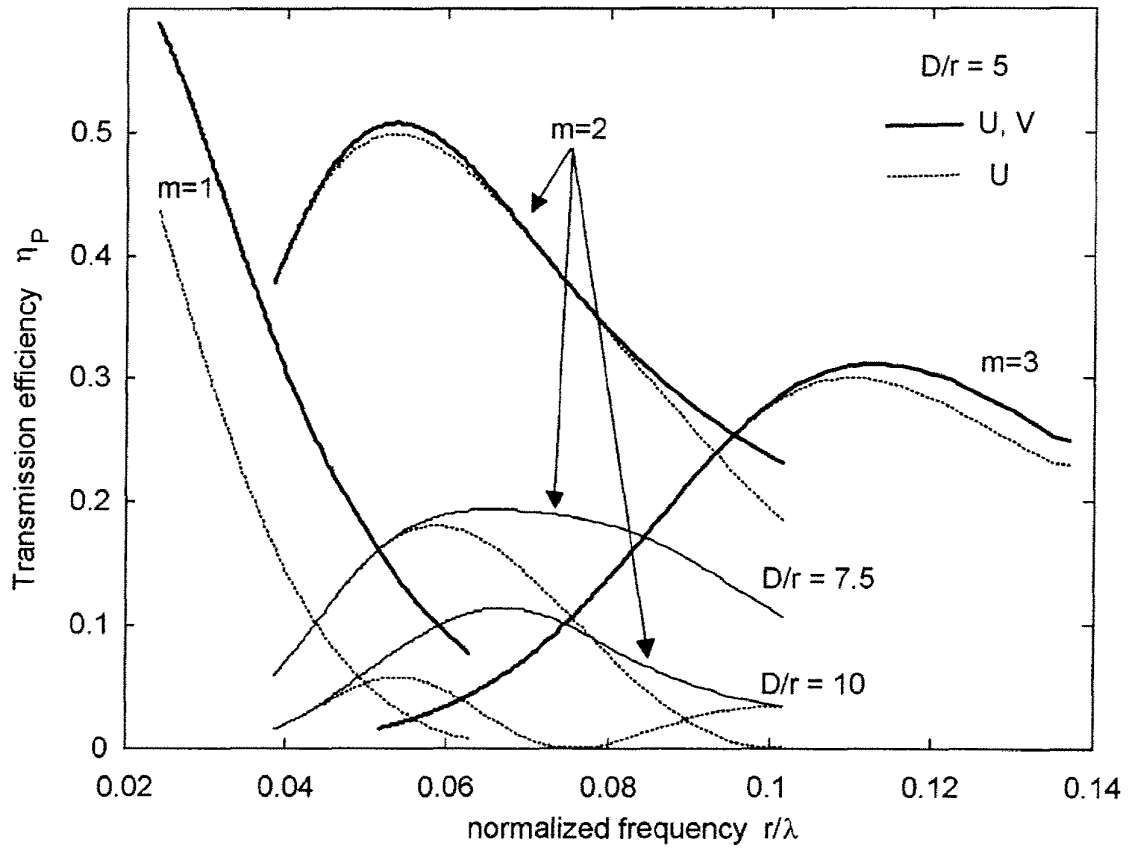


FIG. 26

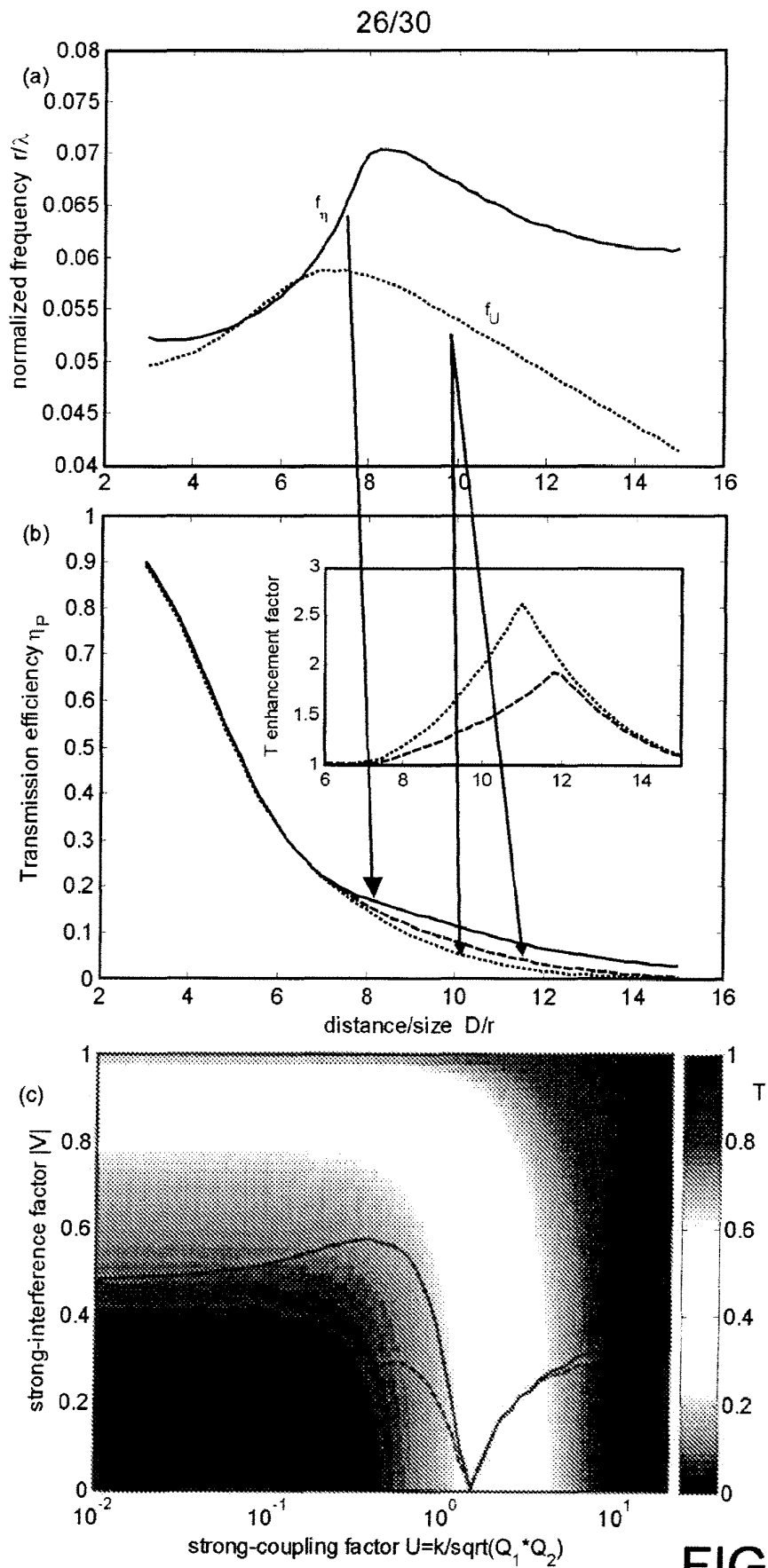


FIG. 27

SUBSTITUTE SHEET (RULE 26)



27/30

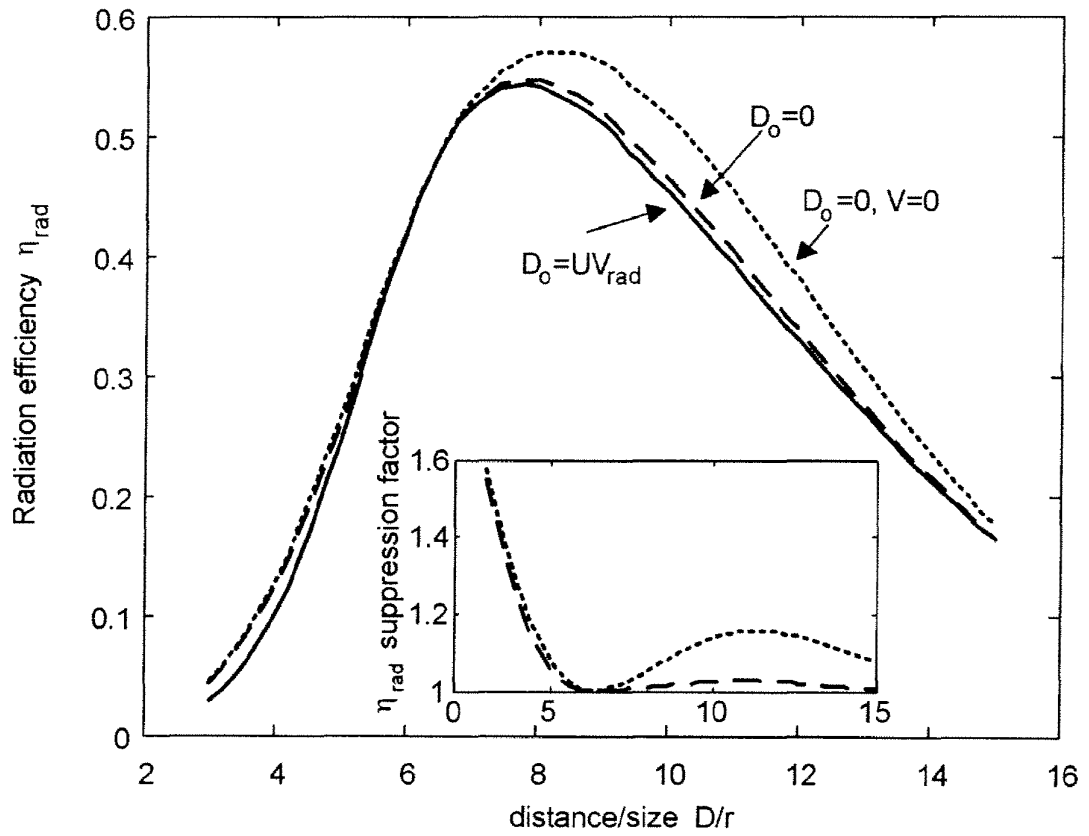


FIG. 28

SUBSTITUTE SHEET (RULE 26)

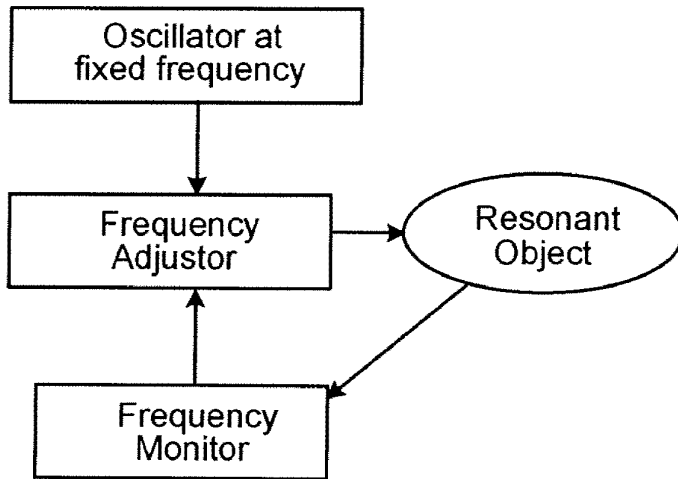


FIG. 29A

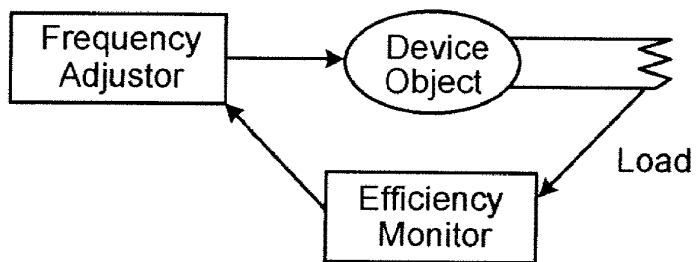
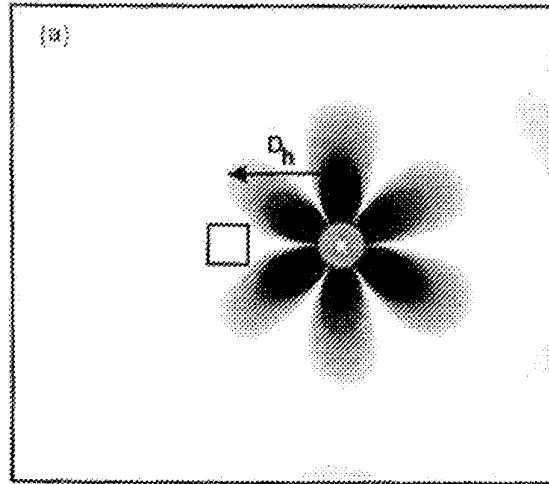
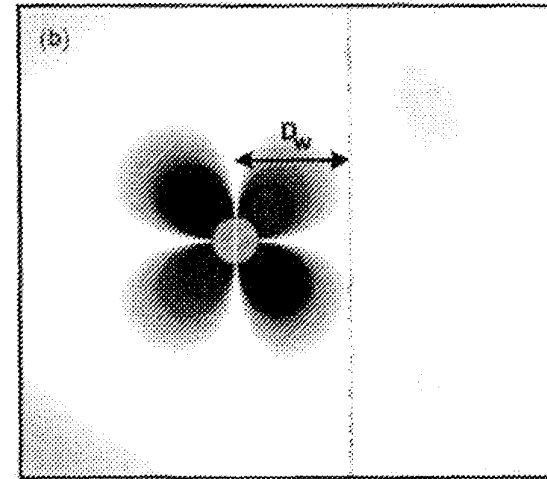


FIG. 29B



Disk with "human"	$D_h/r$	$Q_{c-h}^{abc}$	$Q_{c[h]}^{rad}$	$Q_{c[h]}$
$Re\{\epsilon\}=147.7, m=2$ $\lambda/r \approx 20$ $Q_c^{abc} \approx 10096$	3	230	981	
	5	2917	1984	
	7	11573	2230	
	10	41496	2201	
$Re\{\epsilon\}=65.6, m=3$ $\lambda/r \approx 10$ $Q_c^{abc} \approx 10096$	3	1827	6197	
	<b>5</b>	<b>58431</b>	<b>11808</b>	
	7	249748	9931	
	10	867552	9078	

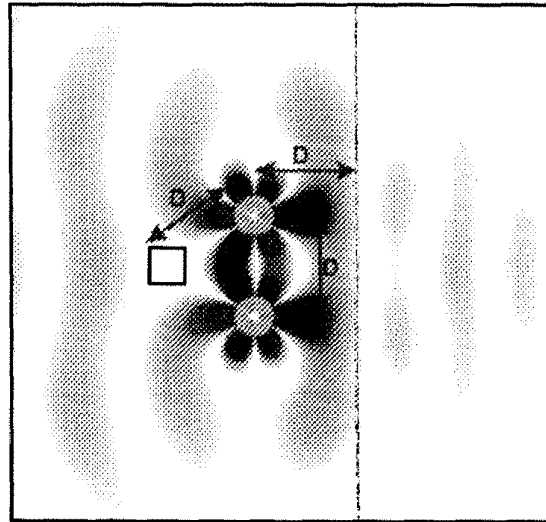
FIG. 30A



Disk with "human"	$D_w/r$	$Q_{c-w}^{abc}$	$Q_{c[w]}^{rad}$	$Q_{c[w]}$
$Re\{\epsilon\}=147.7, m=2$ $\lambda/r \approx 20$ $Q_c^{abc} \approx 10098$	3	16725	1235	1033
	<b>5</b>	<b>31659</b>	<b>1922</b>	<b>1536</b>
	7	49440	2389	1859
	10	82839	2140	1729
$Re\{\epsilon\}=65.6, m=3$ $\lambda/r \approx 10$ $Q_c^{abc} \approx 10097$	3	53154	6228	3592
	<b>5</b>	<b>127402</b>	<b>10988</b>	<b>5053</b>
	7	159192	10168	4910
	10	191506	9510	4775

FIG. 30B

29/30



Two disks with "human" and "wall"	$D/r$	$Q_{c-h}^{abc}$	$Q_{c-w}^{abc}$	$Q_{c[hw]}^{rad}$	$Q_{w[hw]} = \omega/2\Gamma$	$\omega/2\kappa[hw]$	$\kappa[hw]/\Gamma_{c[hw]}$
$Re\{\epsilon\}=147.7, m=2$	3	3300	12774	536	426	48	8.8
$\lambda/r \approx 20$	5	5719	26333	1600	1068	322	3.3
$Q_c^{abc} \approx 10100$	7	13248	50161	3542	2097	973	2.2
	10	18447	68460	3624	2254	1768	1.3
$Re\{\epsilon\}=65.6, m=3$	3	2088	36661	6764	1328	141	9.4
$\lambda/r \approx 10$	5	<b>72137</b>	<b>90289</b>	<b>11945</b>	<b>4815</b>	<b>2114</b>	<b>2.3</b>
$Q_c^{abc} \approx 10100$	7	237822	129094	12261	5194	8307	0.6

FIG. 30C

## INTERNATIONAL SEARCH REPORT

International application No.  
PCT/US 09/43970

<b>A. CLASSIFICATION OF SUBJECT MATTER</b> IPC(8) - H01P 7/00 (2009.01) USPC - 333/219 According to International Patent Classification (IPC) or to both national classification and IPC		
<b>B. FIELDS SEARCHED</b> Minimum documentation searched (classification system followed by classification symbols) IPC(8) - H01P 7/00 (2009.01) USPC - 333/219 Documentation searched other than minimum documentation to the extent that such documents are included in the fields searched USPC - 333/219, 230 Electronic data base consulted during the international search (name of data base and, where practicable, search terms used) PubWEST ( PGPB,USPT,EPAB,JPAB); Google Patents; Google Scholar Search Terms Used: resonance, resonator, energy, electricity, power, transfer, wireless, frequency, wavelength, angular, width, quality, factor, far, field, interference, generator, source, driving, drive		
<b>C. DOCUMENTS CONSIDERED TO BE RELEVANT</b>		
Category*	Citation of document, with indication, where appropriate, of the relevant passages	Relevant to claim No.
X	US 2007/0222542 A1 (JOANNOPOULOS et al.) 27 September 2007 (27.09.2007), para [0005], [0006], [0012], [0015], [0016], [0019], [0021], [0022], [0024], [0027], [0028], [0029], [0031], [0035], [0042]	1-8 ---
Y	US 2004/0113847 A1 (QI et al.) 17 June 2004 (17.06.2004), para [0015], [0023]	9-63
Y	US 5,437,057 A (RICHEY et al.) 25 July 1995 (25.07.1995), col 9, ln 6-18	9-63 15-25, 37-47, 57, 58, 61, 62
<input type="checkbox"/> Further documents are listed in the continuation of Box C. <input type="checkbox"/>		
* Special categories of cited documents: "A" document defining the general state of the art which is not considered to be of particular relevance "E" earlier application or patent but published on or after the international filing date "L" document which may throw doubts on priority claim(s) or which is cited to establish the publication date of another citation or other special reason (as specified) "O" document referring to an oral disclosure, use, exhibition or other means "P" document published prior to the international filing date but later than the priority date claimed "T" later document published after the international filing date or priority date and not in conflict with the application but cited to understand the principle or theory underlying the invention "X" document of particular relevance; the claimed invention cannot be considered novel or cannot be considered to involve an inventive step when the document is taken alone "Y" document of particular relevance; the claimed invention cannot be considered to involve an inventive step when the document is combined with one or more other such documents, such combination being obvious to a person skilled in the art "&" document member of the same patent family		
Date of the actual completion of the international search 07 July 2009 (07.07.2009)		Date of mailing of the international search report <b>14 JUL 2009</b>
Name and mailing address of the ISA/US Mail Stop PCT, Attn: ISA/US, Commissioner for Patents P.O. Box 1450, Alexandria, Virginia 22313-1450 Facsimile No. 571-273-3201		Authorized officer: Lee W. Young PCT Helpdesk: 571-272-4300 PCT OSP: 571-272-7774

Form PCT/ISA/210 (second sheet) (April 2007)



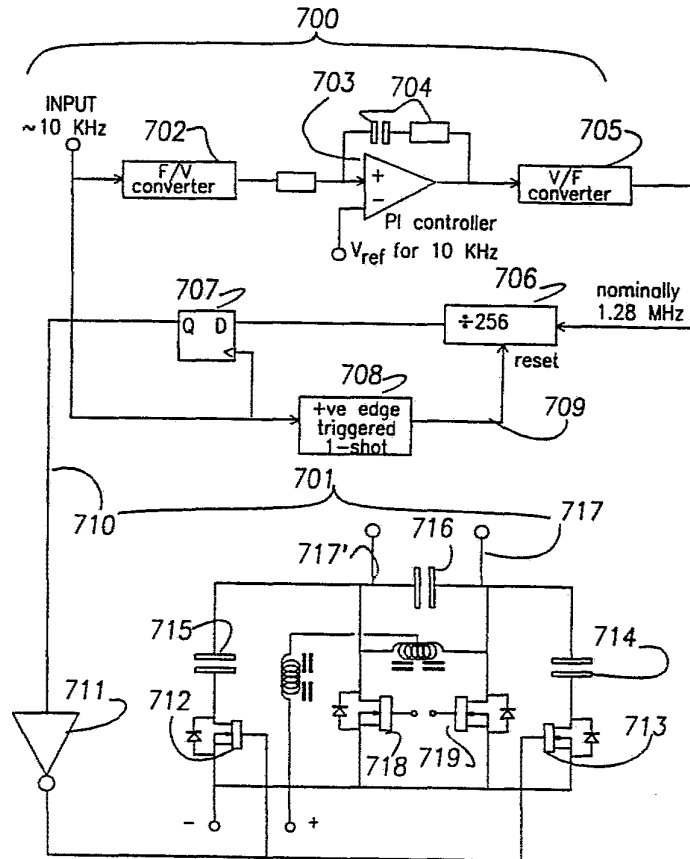
INTERNATIONAL APPLICATION PUBLISHED UNDER THE PATENT COOPERATION TREATY (PCT)

<p>(51) International Patent Classification <sup>5</sup> : <b>H02J 17/00, B60L 9/00, 9/08</b></p>	<p><b>A1</b></p>	<p>(11) International Publication Number: <b>WO 93/23908</b> (43) International Publication Date: 25 November 1993 (25.11.93)</p>											
<p>(21) International Application Number: PCT/NZ93/00031 (22) International Filing Date: 5 May 1993 (05.05.93)</p> <p>(30) Priority data:</p> <table border="0"> <tr> <td>241380</td> <td>10 May 1992 (10.05.92)</td> <td>NZ</td> </tr> <tr> <td>243102</td> <td>10 June 1992 (10.06.92)</td> <td>NZ</td> </tr> <tr> <td>245956</td> <td>22 February 1993 (22.02.93)</td> <td>NZ</td> </tr> <tr> <td>247268</td> <td>26 March 1993 (26.03.93)</td> <td>NZ</td> </tr> </table> <p>(71) Applicants (for all designated States except US): AUCKLAND UNISERVICES LIMITED [NZ/NZ]; UniServices House, 58 Symonds Street, Auckland 1001 (NZ). DAIFUKU, CO., LTD. [JP/JP]; 2-11, 3-chome, Mitejima, Nishiyodogawa-ku, Osaka 555 (JP).</p> <p>(72) Inventors; and (75) Inventors/Applicants (for US only) : NISHINO, Shuzo [JP/JP]; 2-11, 3-chome, Mitejima, Nishiyodogawa-ku, Osaka 555 (JP). BOYS, John, Talbot [NZ/NZ]; 15A Island Bay Road, Birkdale, Auckland 1310 (NZ).</p>	241380	10 May 1992 (10.05.92)	NZ	243102	10 June 1992 (10.06.92)	NZ	245956	22 February 1993 (22.02.93)	NZ	247268	26 March 1993 (26.03.93)	NZ	<p>(74) Agents: PIPER, James, William et al.; James W. Piper &amp; Co., 46 Brown Street, Ponsonby, Auckland 1002 (NZ).</p> <p>(81) Designated States: AT, AU, BB, BG, BR, CA, CH, CZ, DE, DK, ES, FI, GB, HU, JP, KP, KR, KZ, LK, LU, MG, MN, MW, NL, NO, NZ, PL, PT, RO, RU, SD, SE, SK, UA, US, VN, European patent (AT, BE, CH, DE, DK, ES, FR, GB, GR, IE, IT, LU, MC, NL, PT, SE), OAPI patent (BF, BJ, CF, CG, CI, CM, GA, GN, ML, MR, NE, SN, TD, TG).</p> <p><b>Published</b> <i>With international search report. Before the expiration of the time limit for amending the claims and to be republished in the event of the receipt of amendments.</i></p>
241380	10 May 1992 (10.05.92)	NZ											
243102	10 June 1992 (10.06.92)	NZ											
245956	22 February 1993 (22.02.93)	NZ											
247268	26 March 1993 (26.03.93)	NZ											

(54) Title: A NON-CONTACT POWER DISTRIBUTION SYSTEM

(57) Abstract

An inductively coupled power distribution system for moving vehicles, in which resonating primary circuits distribute power for resonating secondary circuits to collect and use in an optimised manner. In order to have all circuits resonating at substantially the same frequency, means to detect and adjust resonating components are used, for example the circuit (700) illustrates a frequency drift compensator applicable to several embodiments wherein elements (702-709) compare the present frequency to a reference voltage and cause the driver (711) to be ON or OFF accordingly. Switches (712 and 713) are thereby driven CLOSED or OPEN respectively and when CLOSED, the supplementary capacitors (714 and 715) are included with the main capacitor (716) in the primary resonant circuit. Dithering or pulsed control provides a continuous control of resonance as the system takes some milliseconds to respond.



**FOR THE PURPOSES OF INFORMATION ONLY**

Codes used to identify States party to the PCT on the front pages of pamphlets publishing international applications under the PCT.

AT	Austria	FR	France	MR	Mauritania
AU	Australia	GA	Gabon	MW	Malawi
BB	Barbados	GB	United Kingdom	NL	Netherlands
BE	Belgium	GN	Guinea	NO	Norway
BF	Burkina Faso	GR	Greece	NZ	New Zealand
BG	Bulgaria	HU	Hungary	PL	Poland
BJ	Benin	IE	Ireland	PT	Portugal
BR	Brazil	IT	Italy	RO	Romania
CA	Canada	JP	Japan	RU	Russian Federation
CF	Central African Republic	KP	Democratic People's Republic of Korea	SD	Sudan
CG	Congo	KR	Republic of Korea	SE	Sweden
CH	Switzerland	KZ	Kazakhstan	SK	Slovak Republic
CI	Côte d'Ivoire	LJ	Liechtenstein	SN	Senegal
CM	Cameroon	LK	Sri Lanka	SU	Soviet Union
CS	Czechoslovakia	LU	Luxembourg	TD	Chad
CZ	Czech Republic	MC	Monaco	TG	Togo
DE	Germany	MG	Madagascar	UA	Ukraine
DK	Denmark	ML	Mali	US	United States of America
ES	Spain	MN	Mongolia	VN	Viet Nam
FI	Finland				

5       **A NON-CONTACT POWER DISTRIBUTION SYSTEM**

**TECHNICAL FIELD OF THE INVENTION**

10       This invention relates to the provision of inductively coupled electric power across a gap to mobile or portable power consuming devices such as vehicles. It more particularly relates to those inductively coupled systems that employ resonant circuits, and most particularly to ways to maintain mutually consistent resonant frequencies in both primary and secondary circuits.

15

**BACKGROUND**

Modern semiconductor developments have made feasible the provision of inductively coupled power to moving vehicles, and have permitted the use of resonant LC circuits in either or both the primary and the secondary circuits. Resonance provides - among other advantages - (a) large circulating currents despite relatively small power supplies, (b) relatively low emission of electromagnetic fields at harmonics of the operating frequency, (c) small ferromagnetic cores, if any, and (d) novel means for control of the electromagnetic coupling across spaces.

25

Clearly the system will be most efficient when all resonant circuits resonate naturally at substantially the same frequency, and substantially in phase. Despite careful tuning at the time of installation, effects on inductance and also on the operating parameters of switches caused by varying loads can cause operating frequencies to change. This variability owes its origin in part to combined use in preferred embodiments of the invention of the trackway conductor as both the resonating inductor and as the emitter of changing magnetic fields. The resonant inductor is actually the distributed inductance of the trackway and is inherently vulnerable to induced currents in adjacent secondary coils, which vary according to consumption. The preferred prior-art switching power supply simply detects each zero crossing within the current in the resonant circuit and causes immediate switching transitions. It has no means to

35



determine the actual operating frequency - apart from a momentarily applied start-up oscillator.

- 5 The tightness of primary-secondary coupling may give rise to more than one condition for which the entire system appears to be in resonance but generally only one of these conditions correlates to a frequency at which optimal power transfer can take place.

- 10 Because the efficiency of power transfer will fall if the resonant frequencies are not well matched, it is hence desirable to maintain a relatively constant operating frequency during all reasonable conditions of use.

### **OBJECT**

- 15 It is an object of the present invention to provide an improved system for the maintenance of consistent resonating frequencies within an inductively coupled power transfer system, or one which will at least provide the public with a useful choice.

### **STATEMENT OF INVENTION**

- 20 In one aspect the invention provides a non-contact power distribution system for causing electric power to be transferred from a primary resonant circuit capable of generating an alternating magnetic field to at least one movable body provided with at least one secondary resonant circuit incorporating an inductive coil for intercepting said  
25 magnetic field and thereby generating an electromotive force, characterised in that said power distribution system includes means to maintain the resonant frequency of the primary resonant circuit and the secondary resonant circuits at or close to a consistent frequency.

- 30 In another aspect the invention provides a non-contact power supply for causing electric power to be transferred from a primary resonant circuit to at least one movable body provided with at least one secondary resonant circuit incorporating an inductive coil for intercepting a magnetic field and thereby generating an electromotive force, said power supply comprising a switching power supply which generates a high-frequency  
35 resonant current, characterised in that there is means to maintain the frequency of the resonant current at or close to a predetermined frequency.

**DRAWINGS**

5 The following is a description of several preferred forms of the invention, given by way of example only, with reference to the accompanying diagrams. These examples relate in particular to a system for distributing power to moving trolleys running on rails adjacent to primary conductors, though it is of course applicable to other power consumers such as lamps or battery chargers.

10 Fig 1: is a circuit diagram illustrating an induction line which can be tuned by a tuning capacitor.

Fig 2: is a circuit diagram of an induction line which can be tuned by means of adjustable coils.

15 Fig 3: is an illustration of a solution using switched inductors to vary the resonant inductance by small increments.

Fig 4: is an illustration of a system to provide a frequency-stable source for the primary power supply rather than allowing it to drift in frequency.

20 Fig 5: is an illustration of one means for tuning (or frequency-tracking) within the secondary circuits- such as the trolleys themselves.

25 Fig 6: is an illustration of a "dummy trolley" or artificial secondary resonant circuit within or near the power supply, used to effect control and optionally act as a sensor of induction line parameters.

Fig 7: is a circuit that tests the present operating frequency and continually adjusts tuning of the power supply. It is based on a proportional-integral controller and uses capacitors and switches in parallel with the main resonant capacitor.

30 Fig 8a-c: shows diagrammatic graphs of phase angle (Y axis) against frequency (X axis) in circuits that are (8a) under-coupled, (8b) critically coupled, and (8c) over-coupled.

35 Fig 9a-c: shows the use of zero-inductance cables in principle (9a), and in practice (9b and 9c) to link spaced-apart nodes of a circuit

having multiple resonant elements, and thereby restrict oscillation modes.

## **PREFERRED EMBODIMENTS**

5

All embodiments have the common objective of providing a consistent resonant frequency across the power distribution system. Advantages of providing a system-wide resonant frequency include:

- 10
1. all resonant circuits have substantially zero power factor - they act like pure resistances.
  2. The Q of the system is raised.
  3. Aberrant modes of oscillation are inhibited.
  4. Coupling is enhanced.
  - 15 5. Power transfer is enhanced.

Some of a number of possible solutions to the problem of ensuring a consistent resonant frequency across an entire system are illustrated by the preferred embodiments described herein. In summary the embodiments to be described are:-

20

1. Tune the primary loop with a small switched capacitor across the main resonant capacitor. This method endeavours to keep the system resonant frequency constant. (Fig 1, Fig 7)
- 25 2. Tune the primary loop using a pair of variable inductances; one in series with each side of the primary loop. This method also endeavours to keep the system resonant frequency constant. (Fig 2)
- 30 3. Using switched inductors, (eg switched by SCR devices) to vary the resonant inductance by small increments. This solution endeavours to keep the system resonant frequency constant. (Fig 3)
- 35 4. Render the primary power supply a frequency-stable source rather than drift in frequency as set by track inductance parameters. This approach will keep the system resonant frequency constant. (Fig 4)

5. Add tuning (or frequency-tracking) means on the secondary circuits- the trolleys themselves. This system has a variable overall frequency. (Fig 5)
- 5 6. Use a "dummy trolley" or artificial secondary resonant circuit at or near the power supply to effect control. This system also has a variable overall frequency. (Fig 6)
- 10 7. Use switched capacitances within the power supply to vary the resonant capacitance by small increments. (Dithering or pulsed control provides finer control). (Fig 7)
- 15 8. Use zero-inductance cables to link spaced-apart nodes having similar amplitude and phase of a circuit, usually at capacitors, and thereby restrict oscillation modes. (Fig 9a-c)

Embodiments shown in Figs 1, 2, 3 and 6 assume the presence of a master controller, not illustrated therein, to monitor the frequency of the resonant current in the primary circuit and take suitable steps to alter specific lumped circuit parameters (one or both of L and C) should the frequency drift away from a target range. This controller may be a type of phase-locked loop, although a preferable form is a proportional controller of the type shown in Fig 7.

**Embodiment 1 - see Fig 1.**

25

An induction line 100 is provided by a pair of litz wire cables 101 and 102, together with a coil 103 and a main capacitor 104. (The power source is not shown but would be connected across inductor 103). In this example an auxiliary capacitor 116 is provided in parallel with the main capacitor, and can be switched in or out of the circuit by an appropriate switch 117, in order to vary the resonant frequency of the induction line. By providing an auxiliary capacitor 116, it is possible to tune the resonant frequency of the induction line in order to accommodate changes to the frequency resulting from the number of movement of movable bodies, (typically electrically powered trolleys) on the induction line. The frequency change is a result of changing inductance, hence a shift in the frequency of resonance. If a substantially constant primary frequency is maintained, secondary circuits should not require re-tuning.

35

**SUBSTITUTE SHEET**

It will be appreciated that the capacitor 116 can be in series, instead of in parallel with the main capacitor (where a switch would instead bypass it), and it could comprise one or more variable capacitors, so that the resonant frequency of the line can be tuned by varying the capacitance of the auxiliary capacitor 116. In another version the two capacitors may be replaced by one variable capacitor.

### Embodiment 2

Fig 2 shows a similar induction line 200, having a pair of litz wire cables 201 and 202 forming a loop, a main coil 203, and a main capacitor 204. A tuning coil arrangement 205 and 206 is provided, so that the resonant frequency of the induction line can be tuned by varying the mutual inductance of coils 205 and 206. This can be achieved in a number of ways; using either electrical or mechanical adjustments. The simplest solution is to provide one coil within the other, each wound on a cylindrical (preferably plastics) former, with the inner coil capable of being moved relative to the outer coil. This can be achieved in a number of different ways. For example, the inner coil could be telescoped in or out with respect to the outer coil, so that there is a different degree of overlap, and hence a different resulting frequency of the induction line as the inductance of the coils is varied. Alternatively, the resonant frequency can be tuned, by rotating the inner coil with respect to the outer coil. This is the preferred arrangement, in which the length of the inner coil is shorter than the internal diameter of the outer coil, so that the inner coil can be rotated about its midpoint relative to the position of the outer coil. Thus maximum inductance can be achieved when the inner coil has its longitudinal axis aligned with the longitudinal axis of the outer coil, and minimum inductance can be achieved when the inner coil has its longitudinal axis at right angles to the longitudinal axis of the outer coil.

By this means, the resonant frequency of the induction line 201-202 can be varied, to take account of an increase or decrease in the number of vehicles on the induction line, and the amount of power that the or each vehicle draws from the induction line.

### Embodiment 3

Fig 3 illustrates the principles of this modification, in which part of the main resonant conductor is illustrated as 301, having a group of discrete inductances (302, 302', 302''

etc) placed in series with it. Each inductance has a shorting switch, such as a solid-state switch 303, 303', 303'' etc) in series with it. Here we show the use of back-to-back SCR devices as the solid-state switches, although other devices are usable, such as TRIACs, or MOSFET devices (preferable on the grounds of a low ON resistance and therefore a low  $I^2R$  heat loss). A gate power supply (304, 304', 304'' etc) is provided for each SCR device and an isolated drive input is used to connect a control signal. Preferably the values of the inductances are graded in an increasing series, so that a wider range of compensating inductance is available yet with fine increments.

Preferably, track symmetry is maintained by making equal changes to the inductance of both legs of the track. In use, a steady gate current is caused to flow through a particular SCR 303x whenever a particular incremental inductance 302x is not required, as determined by a frequency monitoring device.

#### Embodiment 4

The prior-art method of allowing the resonant power supply to detect zero-crossing points of the resonant current in the primary circuit, and switch over at that moment, resulting in a resonant power supply whose actual operating frequency is set by instantaneous values of L and C and therefore can drift may be replaced by a method in which the switch-over points are determined by an external, independent, and stable clock. Although the resonant circuit may no longer emulate a pure resistance whenever the operating frequency is not the same as its resonant frequency, and therefore a power factor component will arise, this is minimal when measured at the switching devices on a single-cycle basis. In order to compensate for possibly troublesome power factor effects, switched inductances or capacitances may also be introduced into the circuit as per embodiments in Figs 3 or 7 above. This method does not require any re-tuning on the part of individual trolleys, and it is insensitive to the effects of over-critical damping on the power factor around resonance (See Fig 8). It has the further advantage for airports and the like that any radiated electromagnetic interference is of a constant frequency, which may be placed where it does not interfere with identified devices.

In more detail, Fig 4 shows a simplified diagram 400 of a constant-frequency resonant power supply, with two solid-state switches 401, 401' alternately connecting each side

of the resonant line 402 to one power rail 403; meanwhile a DC return is provided through the centre-tapped choke 404. A capacitor 405 is the resonating capacitor. A crystal-controlled oscillator with an optional divider chain 406 (crystal: 409) generates complementary 10 KHz drive pulses to the solid-state switches. (10 KHz is a preferred frequency; some other frequency may be used.) Optionally, to take account of thermal effects on resonant components for example, a frequency may be generated which is stable in the short term but is varied in accordance with (for example) ambient or local temperatures.

10

### **Embodiment 5**

In this embodiment the primary circuit resonant frequency is allowed to find its own stable level, while the onus is put on each of the consumer devices to individually track that frequency by causing their own secondary resonant circuit parameters to change in order to match it.

15

Advantages of this approach include (a) smaller currents are involved, (b) the system is more robust in that it has inherent redundancy, (c) the sensing process is located within the devices responsible for variations in load and (d) possible voltage limits are less likely to be exceeded - especially by transients - as the secondary resonant circuit will tend to minimise the peak amplitude of any transients generated by switching capacitors.

20

Fig 5 shows a secondary resonant circuit 500, together with a frequency monitor 510 (which may comprise a phase-locked loop, a circuit like that shown in Fig 7, or a pre-programmed set of cause/effect combinations - a lookup table), a series of incremental capacitors 502, 502', 502'' etc, and series switches 504, 504', 504'' etc, which in use are switched by the controller so that the resonant frequency of the entire circuit 500 is caused to closely track the operating frequency of the primary circuit 501.

30

### **Embodiment 6**

The specialised secondary circuit or "dummy trolley" embodiment shown in Fig 6 is a hybrid in that it is like an on-trolley frequency shifter as in the previous embodiment, but, being located adjacent to the switching power supply it may be under the control of

35

a master controller and furthermore can be used as a line monitoring device.

5 While secondary circuits are normally provided about a resonant inductive power transfer system as mobile consumers, a dedicated and fixed secondary circuit, preferably located at or within the main switching power supply and inductively coupled to the power supply output can be used to (a) monitor system performance and (b) modify the characteristics of the primary loop with relatively little cost.

10 Fig. 6 shows a typical specialised secondary resonant circuit or "dummy trolley" (611-613), coupled to an inductively powered track system 600. (603 is the main resonant capacitor, 604 is the centre-tapped powering inductor, while the inductor 605 provides a constant current supply from the DC source 606. 607 and 608, the switching devices, are controlled by a controller 609). Secondary inductor 611 is coupled at primary  
15 inductor 610 to the primary resonant circuit 601, and the tuning capacitor 612 completes the resonant circuit in this secondary resonant circuit. Capacitor 612 is shown as a variable device; a master controller may vary this capacitor as for embodiments 1, 5 and 7, in order to tune the "dummy trolley" and thereby affect resonance in the primary circuit. As this circuit is electrically isolated from the  
20 primary, one side of it may be connected or referenced to system ground, and a test point 613 can be used to provide signals proportional to the resonant circuit current. Means may be provided to cause the input power to the switching or resonant power supply to be cut if the circulating resonant current becomes too high. The preferred turns ratio of inductance 611 compared to inductance 600 is preferably greater than 1,  
25 to provide for relatively low-current switching in the dummy trolley, to effect a varying capacitance 612 by, for example, switching in or out increments of capacitance.

This mode of coupling can give a relatively high-voltage induced resonating current which is rather more amenable to control in a low-loss manner with solid-state switches  
30 such as MOSFET devices or high-voltage bipolar transistors. The  $I$  of  $I^2R$  losses is made smaller for a given power. As these active devices are incorporated within a secondary resonant circuit they are relatively speaking better protected from transients in the primary resonant circuit. This method is generally preferable over methods that modify frequency by action directly within the primary circuit.

35

This method, involving a resonant circuit adjacent to and under direct control of the



5 master frequency controller, also has the advantage that changes can be caused to happen rapidly, thus immediately compensating for shifts in primary frequency because the slave resonant circuit is within or close to the resonant power supply and its controller.

*Calculations on the "effective capacitance" that can be provided by a dummy trolley.*

10 For a realistic example (see Fig. 5) in which the secondary inductance 611 of the dummy trolley is 300  $\mu\text{H}$ , tuned to resonance by a capacitor 612 of 0.9  $\mu\text{F}$ , the mutual inductance M is 10  $\mu\text{H}$ ,  $\omega$  (frequency) is  $2 * \pi * 10^4$ , and in which a switch 614 can render the resonant circuit open-circuit...

15 The impedance reflected into the track is

$$Z2' = (\omega^2 m^2) / Z2$$

where  $Z2 = j(\omega L2 - 1/\omega C2)$

20 In the case where C2 (612) is switched out of circuit (open circuit)...

$$Z2' = -j. 20.9 \times 10^{-3}$$

$$\Rightarrow C2' = 759 \mu\text{F}$$

25

In comparison to the case where C2 is switched into circuit ...

$$Z2' = -j. 1.165$$

30

$$\Rightarrow C2' = 46.9 \mu\text{F}$$

Thus a 0.9 microfarad capacitor can simulate a very much greater capacitor to the primary track.

35 **Embodiment 7**

One embodiment of frequency control includes a plurality of capacitor pairs placed across the solid-state switches of the switching power supply. These capacitors are provided with values in an arithmetic series, so that a digital approximation to a given value could be created and held.

Surprisingly it has been found that, as the frequency of the resonating system takes some time to adjust to a new frequency, it is possible to use just one additional capacitor pair across the solid-state switches and vary the duty cycle over which the pair is connected into the circuit in order to achieve a fine control over frequency. The time course of frequency change, as a result of an imposed step alteration in L or C in this type of resonant inductive power distribution system, is relatively long - at least several to ten milliseconds - especially where one or more secondary resonant circuits are carrying resonant current at a first frequency and will tend to continue to resonate at that first frequency.

In order to gain a finer and more continuous control of frequency than might be provided by long-term introduction of relatively large increments of inductance or capacitance, these increments may be repetitively switched in and out of the system for even single-cycle durations whereupon the mean frequency will assume an intermediate value.

Fig 7 illustrates at 701 a resonant power supply similar to that of Fig 6 in which one additional pair of semiconductor switches 712, 713 are switched ON or OFF by gate control buffer 711 (e.g. integrated circuit type ICL 7667) in order to insert capacitors 714 and 715 into the resonant circuit.

The control section is illustrated at 700. A square-wave version of the resonant voltage picked off from across the capacitor 716 (typically converted by limiting and a Schmitt trigger, as is well known in the art) is applied to the input. This will be approximately 10 KHz for preferred systems. The signal is fed to a frequency-to-voltage converter 702, preferably having a time constant of about 10 mS. The frequency-dependent output of this stage is taken to a proportional-integral controller section 703 for which feedback components 704 determine its response characteristics. A steady voltage is fed in at Vref to provide a reference for the circuit. The output is fed to a voltage-to-frequency converter 705; the output of which is at nominally 1.28 MHz and which is

fed to an 8-bit binary divider 706 for a division of 256. A reset input to this divider is created from the positive-going edges of the input square-wave signal, as a brief pulse (preferably less than 0.5 $\mu$ S) within a one-shot device 708.

5

Thus the divider 706 creates a square-wave signal of nominally 5 KHz frequency. This is fed to the D input of a flip flop 707, while the original signal is fed to the clock input. Thus the Q output of the flipflop is either high (when the track frequency is too low and capacitance is to be removed) or low (when the track frequency is too high and extra capacitance is required). This signal is fed to the buffer 711 and on to both MOSFET or IGBT transistors 712 and 713 and hence causes the capacitors 714 and 715 to be brought into or out of circuit.

10

15

There are, of course, many other ways in which frequency control might be implemented.

20

Fig 8a, b, and c illustrate measurements of the relationship of phase angle (Y axis) against frequency (X axis) for a resonant power distribution system having both resonant primary and resonant secondary circuits. The nominal resonant frequency is 10 KHz. Points where the zero phase angle line is crossed represent true or false resonant modes.

25

30

Measurements and computer modelling of an inductive power transfer system show that as the coupling between primary and secondary circuits rises (e.g. from that shown in Fig 8a towards Fig 8b) towards a critical value (Fig 8b), the phase angle against frequency graph develops a kink, tending to the horizontal. With over-critical coupling, a graph of phase (Y) against frequency (X) will show a brief reversal of direction about the zero point (Fig 8c) if the circuit under test is swept through resonance. Critical coupling is defined as the condition wherein the plot runs horizontally about the resonance point, while in under-critical coupling the plot crosses the zero phase line once. The switching resonant power supply may, with critical coupling conditions, show an instability in operating frequency since the "pure resistance" or zero power-factor conditions are satisfied at more than one frequency.)

35

## Embodiment 8

In this embodiment a primary circuit having more than one resonating capacitor spaced apart from one another (a practice used to extend track length among other reasons) has been constrained to minimise a possible variety of oscillation frequencies. Any L and C pair may form a resonant circuit, and if typical manufacturing tolerances or track inductance variations are considered, it will be apparent that a number of possible resonant frequencies may be adopted, by various combinations of adjacent inductance and capacitance. If the capacitors were to be tied together, more particularly at points where the amplitude and phase are similar, the possible modes of oscillation would be restricted. Zero-inductance cables may be used to link spaced-apart nodes of the power supply and thereby restrict possible modes of oscillation.

A zero-inductance cable (e.g. 910 or 924) is typically one having a pair of physically symmetrical conductors, electrically insulated from one another yet closely coupled magnetically. A close approach to the ideal is a length of litz wire with conductors randomly allocated to one group or the other, hence interspersed. Multiple-conductor telephone cable, for which colour-coding facilitates grouping, is a more realistic type of cable. In use, a current in one conductor flows against a current of opposite sense in the other conductor so that the magnetic fields are substantially cancelled out by each other and the conductor appears to have substantially no intrinsic inductance.

Fig 9 shows three examples of the use of zero-inductance cables to link spaced-apart nodes of a circuit and thereby restrict oscillation modes. Fig 9a illustrates a single primary conductor module having two capacitors 906 and 907 separated by intrinsic inductance 905 and 909 within primary conductors. The zero-inductance cable 910 joins the capacitors, and a crossover at 911 is provided because the phase of the current at top left (see the vectors labelled V) will be opposite to the phase of the current at top right, in resonance, but the same as the phase of the current at bottom right. Preferably capacitors are matched reasonably well at the time of assembly, so that difference currents flowing through the zero-inductance cable are minimised, and so that remaining currents in the zero-inductance cable comprise dynamic corrections to cancel out imbalances.

Fig 9b illustrates an extended zero-inductance cable joining the ends of a modular primary track so that the capacitor/generator pair 922 is effectively locked to the voltage across the far capacitor 923. Intermediate modules (like 921) are shown with

connectors to adjacent modules.

5 Fig 9c illustrates a special case of 9b, in which an almost continuous loop track 940 forms a ring and is energised by a power supply 949. (Typical manufacturing processes commonly have conveyer devices travelling in a closed circuit of this style). In order to match the nodes at the capacitors at the beginning (943) and the end (947), a simple connection or cable including a cross-over 950, completes the circuit of the entire track conductors 941 and 942. Intermediate primary conductor modules are not shown here.

10

Finally, it will be appreciated that various alterations and modifications may be made to the foregoing without departing from the scope of this invention as set forth in the following claims.

15

20

25

30

35

**CLAIMS**

1. A non-contact power distribution system for causing electric power to be transferred from a primary resonant circuit capable of generating an alternating magnetic field to at least one movable body provided with at least one secondary resonant circuit incorporating an inductive coil for intercepting said magnetic field and thereby generating an electromotive force, characterised in that said power distribution system includes means to maintain the resonant frequency of the primary resonant circuit and the secondary resonant circuits at or close to a consistent frequency.
2. A non-contact power supply for causing electric power to be transferred from a primary resonant circuit to at least one movable body provided with at least one secondary resonant circuit incorporating an inductive coil for intercepting a magnetic field and thereby generating an electromotive force, said power supply comprising a switching power supply which generates a high-frequency resonant current, characterised in that there is means to maintain the frequency of the resonant current at or close to a predetermined frequency.
3. A non-contact power supply as claimed in claim 2, characterised in that the switching power supply is driven by a stable oscillator.
4. A non-contact power distribution system as claimed in claim 1, in which the primary resonant circuit comprises one or more elongated primary conductors having more than one resonating capacitor for each elongated primary conductor, located at physically separated sites about the elongated primary conductor(s), characterised in that the capacitors are electrically connected at nodes of like phase by a zero-inductance cable.
5. A non-contact power distribution system as claimed in claim 1, characterised in that the primary resonant circuit includes means to vary the resonating inductance included in the circuit so that the resonant frequency remains substantially stable.
6. A non-contact power distribution system as claimed in claim 5, characterised in that the means to vary the resonating inductance in the primary inductive circuit comprise a first inductance in series with one primary conductor, mutually coupled by a

variable amount to a second inductance in series with a second primary inductor.

- 5 7. A non-contact power distribution system as claimed in claim 5, characterised in that the means to vary the resonating inductance in the primary inductive circuit comprises one or more discrete inductances in series with each primary conductor, each discrete inductance being capable of being switched in or out of circuit with an associated switch driven by a controlling device.
- 10 8. A non-contact power distribution system as claimed in claim 1, characterised in that the primary resonant circuit includes means to vary the resonating capacitance included in the circuit so that the resonant frequency remains substantially stable.
- 15 9. A non-contact power distribution system as claimed in claim 8, characterised in that the means to vary the resonating capacitance comprises one or more extra capacitances capable of being connected by a corresponding switch into the primary resonant circuit.
- 20 10. A non-contact power distribution equipment as claimed in claim 1, characterised in that a dedicated secondary resonant circuit having inductance and capacitance is coupled to the primary circuit and is capable of having its resonant frequency altered by adjustments to the inductance or the capacitance so as to cause, via the coupling to the primary circuit, the resonant frequency of the primary circuit to be maintained at a substantially constant value.
- 25 11. A non-contact power distribution equipment as claimed in claim 1, characterised in that the or each secondary resonant circuit is provided with means to detect the frequency of the primary resonant circuit and means to alter the resonant frequency of the secondary circuit(s) to substantially match the frequency of the primary circuit.
- 30 12. A non-contact power distribution system as claimed in claim 11, characterised in that the secondary circuit is equipped with means for including or excluding additional resonating capacitance.
- 35 13. A non-contact power distribution system as claimed in claim 11, characterised in that the secondary circuit is equipped with means for including or excluding

additional resonating inductance.

5 14. A non-contact power distribution system as claimed in claim 11, characterised  
in that the secondary circuit is equipped with means for determining the power factor of  
the secondary circuit, together with resonance altering means capable of controlling the  
inclusion or exclusion of additional resonating capacitance or inductance.

10 15. A non-contact power distribution system as claimed in claim 11, characterised  
in that the secondary circuit is equipped with means for determining the power factor of  
the secondary circuit, together with resonance altering means capable of controlling the  
inclusion or inclusion or exclusion of additional resonating inductance.

15

20

25

30

35



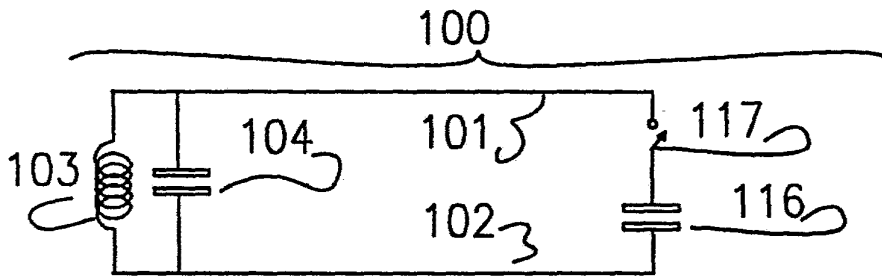


Fig 1

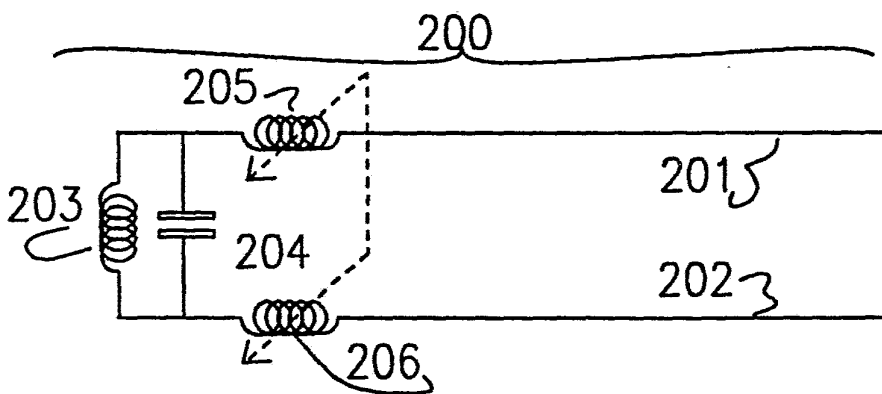


Fig 2

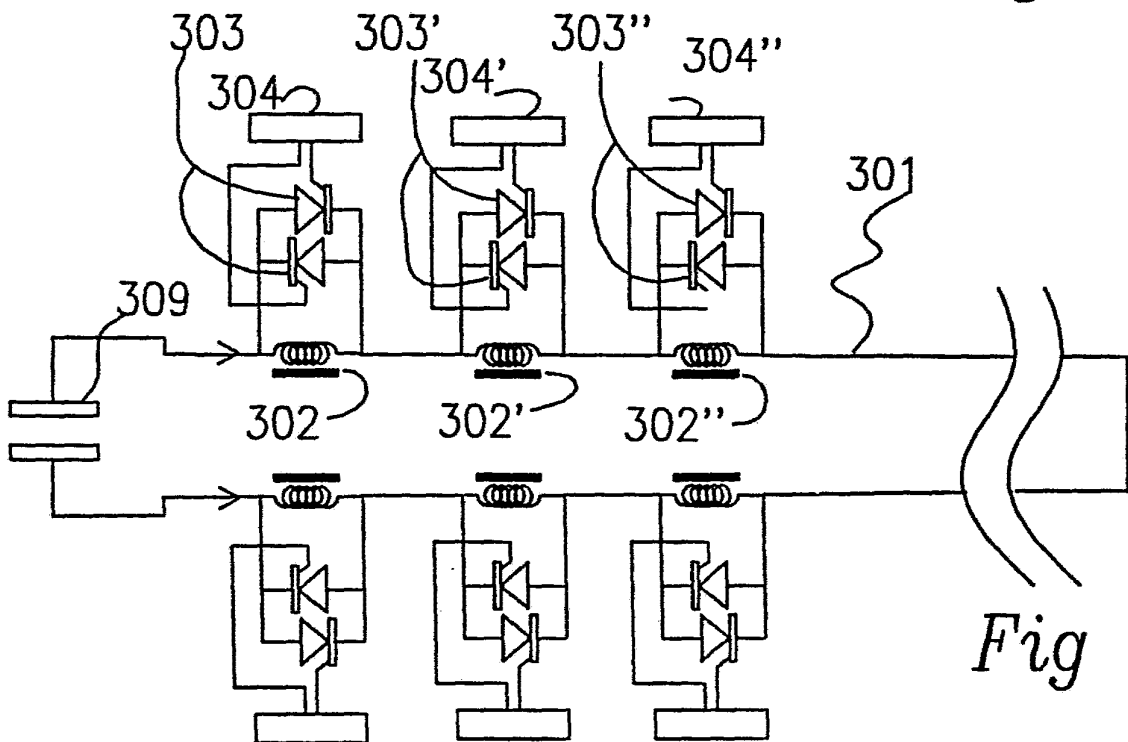


Fig 3

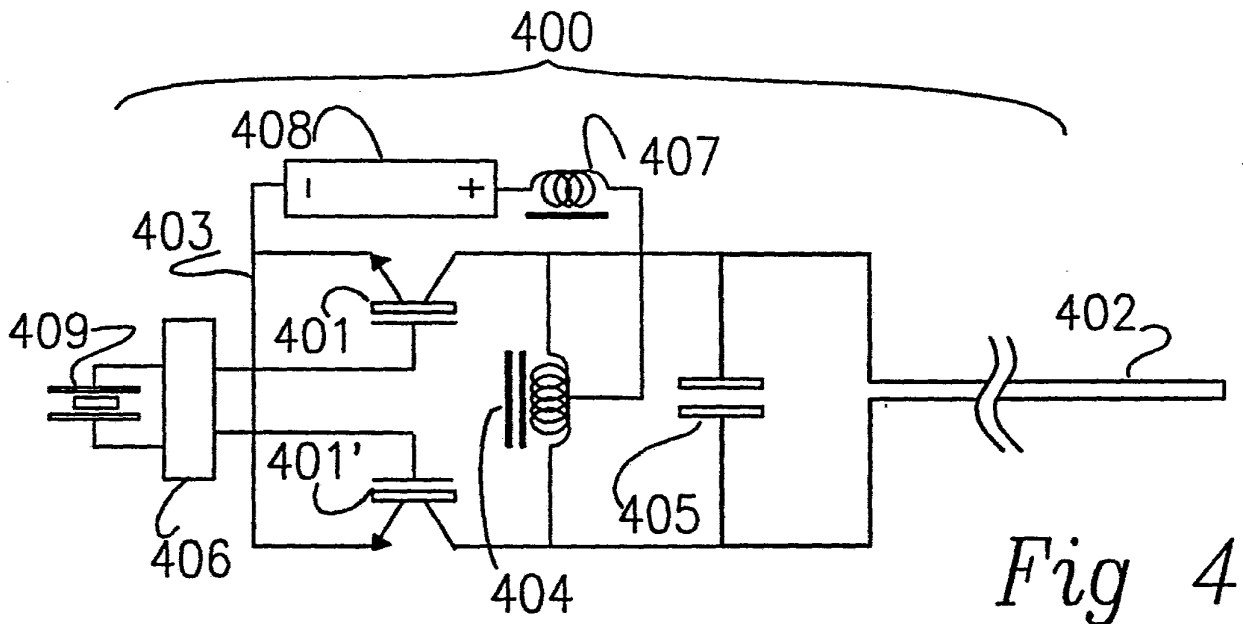


Fig 4

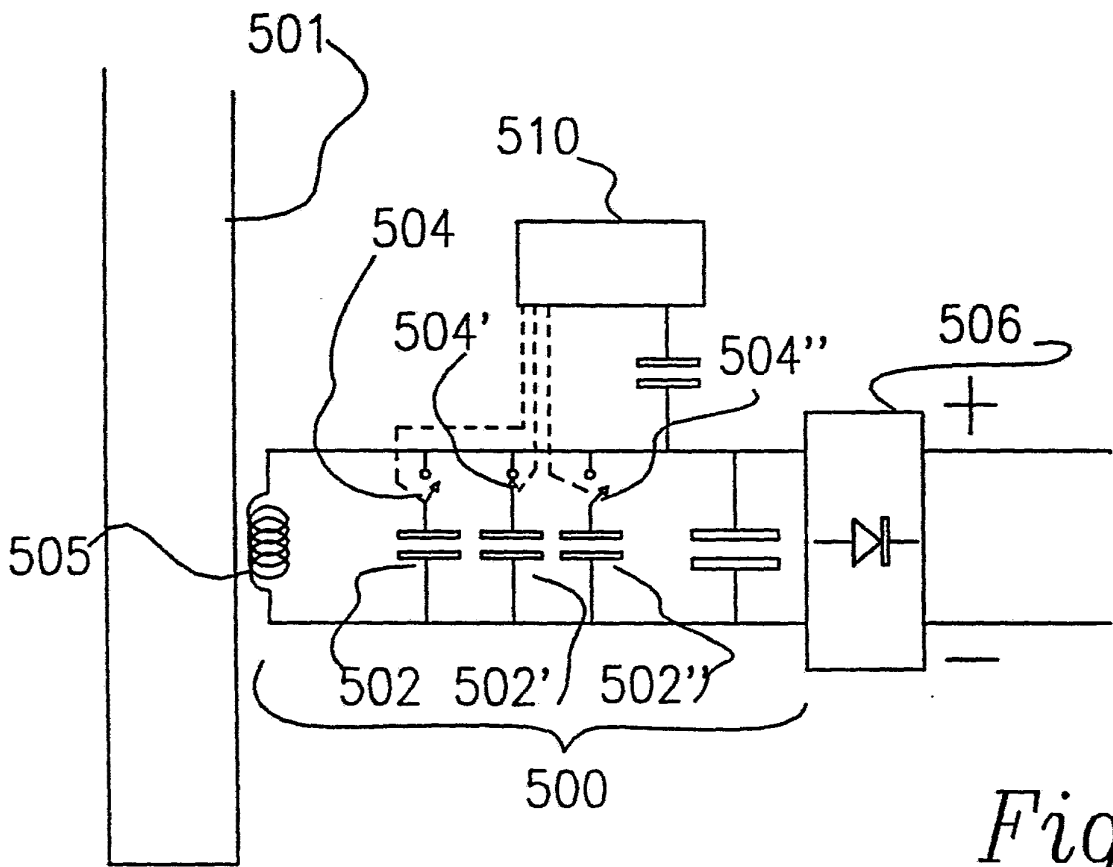


Fig 5

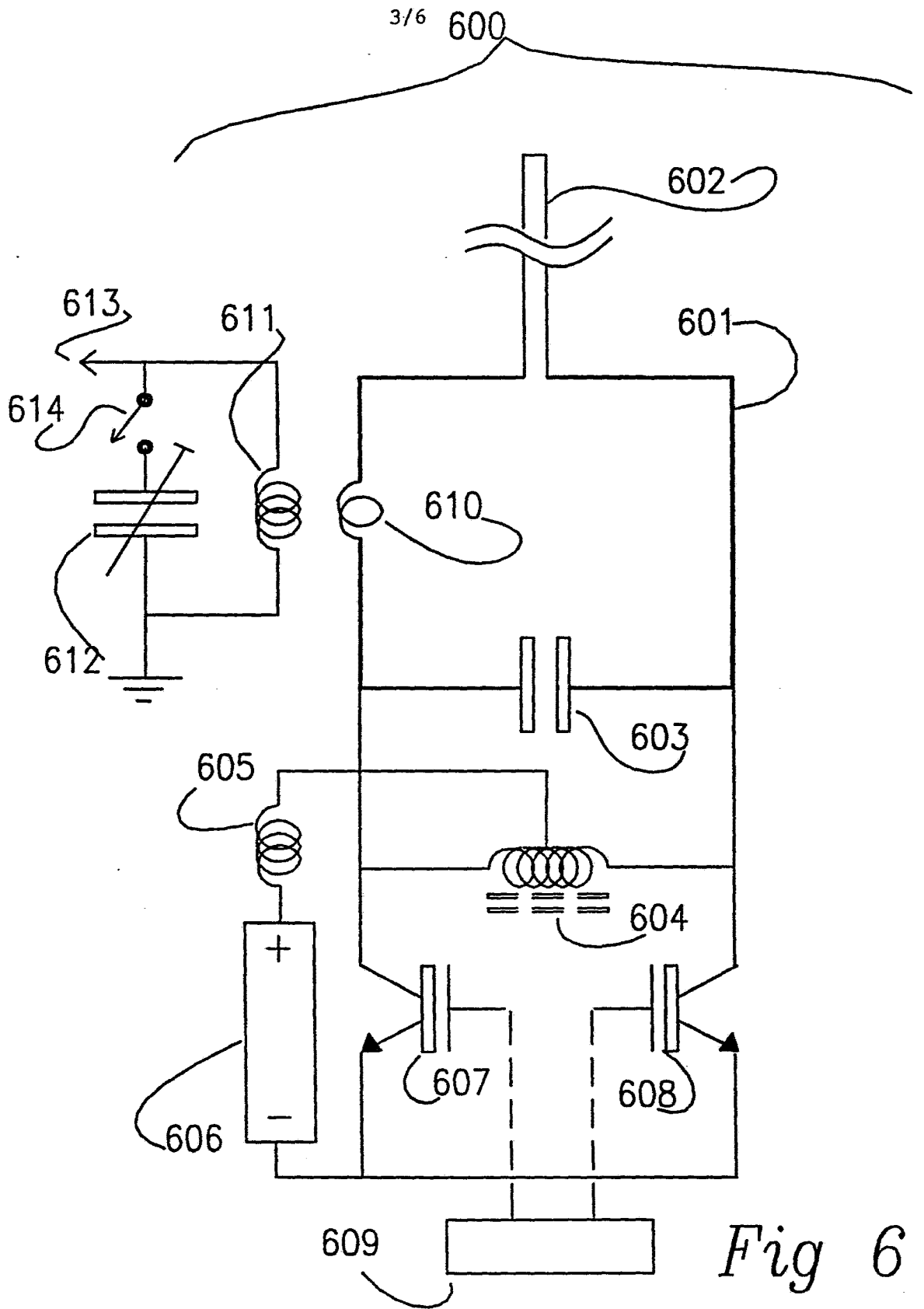


Fig 6

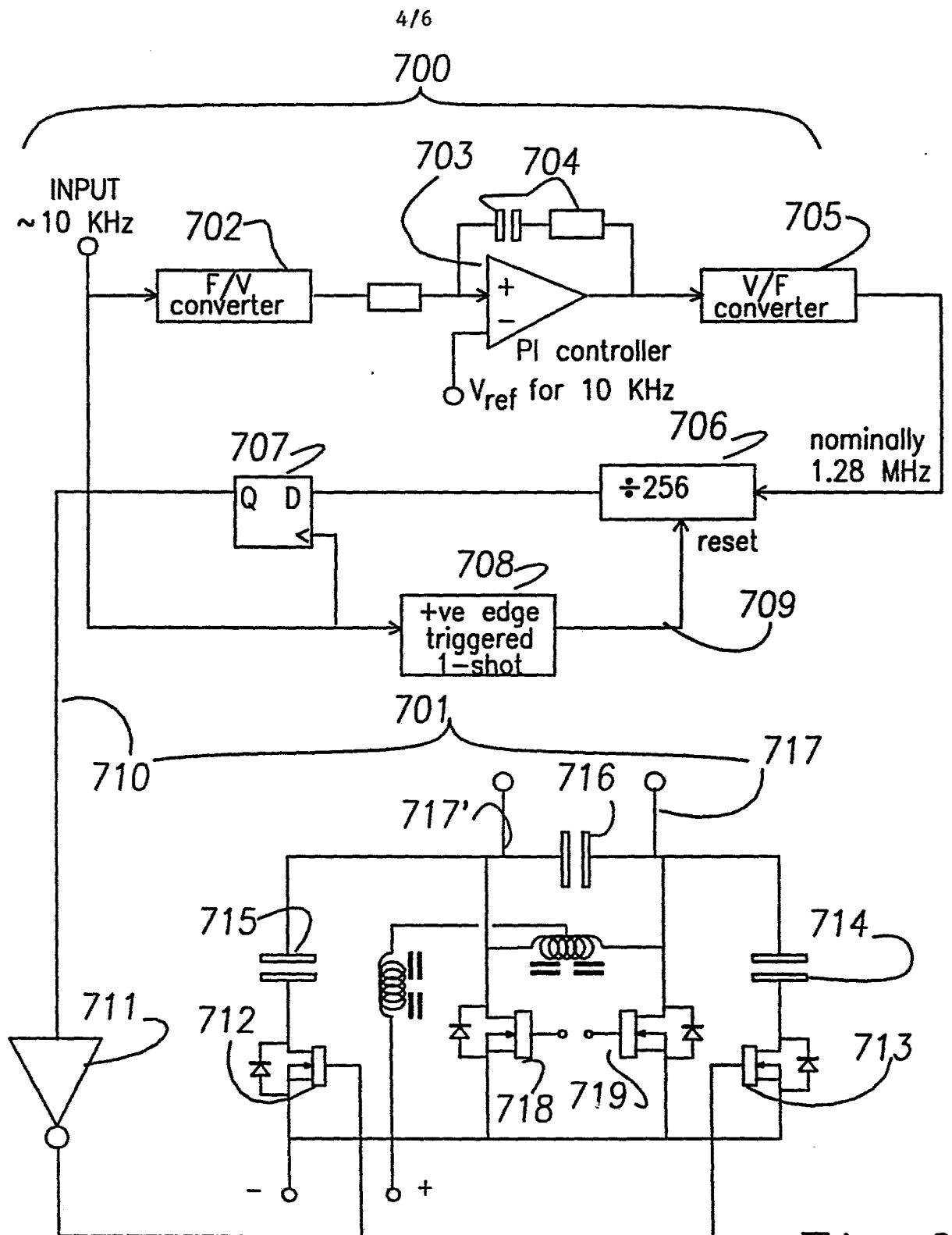
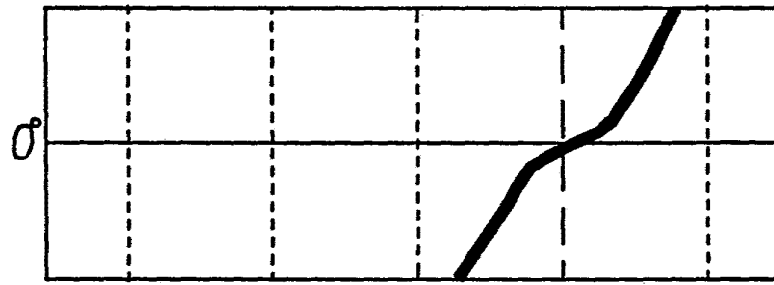
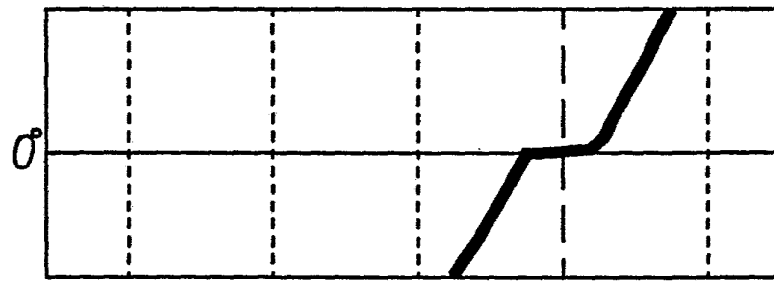


Fig 7



*Fig 8a*




*Fig 8b*

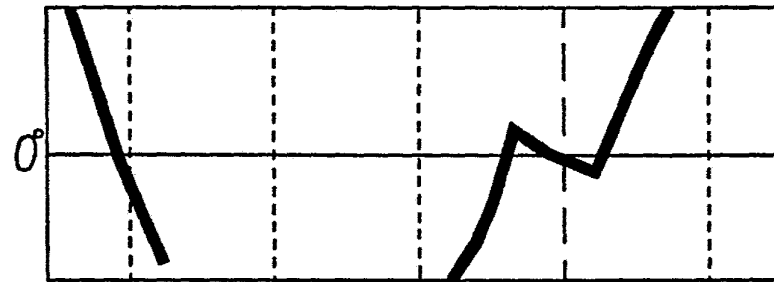
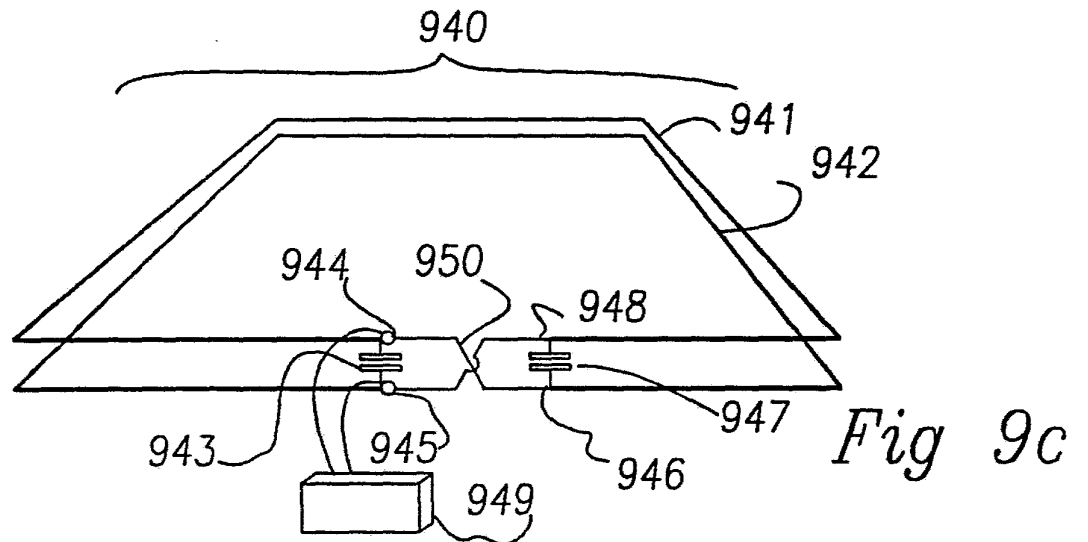
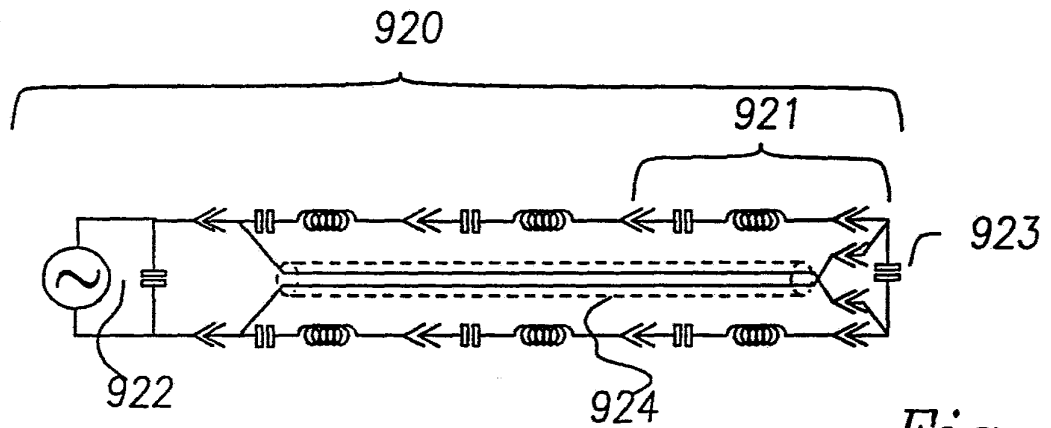
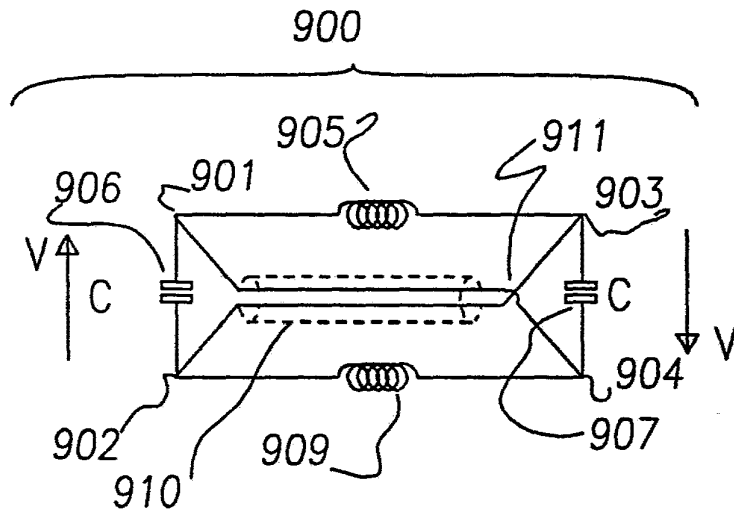


*Fig 8c*

9.7 9.8 9.9 10.1  
10 KHz



<b>A. CLASSIFICATION OF SUBJECT MATTER</b>				
Int. Cl. <sup>5</sup> H02J 17/00, B60L 9/00, 9/08				
According to International Patent Classification (IPC) or to both national classification and IPC				
<b>B. FIELDS SEARCHED</b>				
Minimum documentation searched (classification system followed by classification symbols) IPC H02J 17/00, 5/00, B60L 9/00, 9/08				
Documentation searched other than minimum documentation to the extent that such documents are included in the fields searched AU : IPC as above				
Electronic data base consulted during the international search (name of data base, and where practicable, search terms used) DERWENT, CAPRI, INPADOC				
<b>C. DOCUMENTS CONSIDERED TO BE RELEVANT</b>				
Category*	Citation of document, with indication, where appropriate, of the relevant passages	Relevant to Claim No.		
X,P	AU,A, 12373/92 (PIPER) 15 October 1992 (15.10.92) page 13, lines 6-16, Figs 6,7	1-3, 5-9		
X	EP,A, 334804 (ANGEWANDTE DIGITAL ELEKTRONIK GmbH) 27 September 1989 (27.09.89) Abstract, Fig. 1	1,2		
X	EP,A, 473957 (SIEMENS ELEMA AB) 11 March 1992 (11.03.92) Abstract, Fig. 1	1,2		
<input checked="" type="checkbox"/> Further documents are listed in the continuation of Box C. <input checked="" type="checkbox"/> See patent family annex.				
* Special categories of cited documents : <table border="0" style="width:100%"> <tr> <td style="width:50%">           "A" document defining the general state of the art which is not considered to be of particular relevance            "E" earlier document but published on or after the international filing date            "L" document which may throw doubts on priority claim(s) or which is cited to establish the publication date of another citation or other special reason (as specified)            "O" document referring to an oral disclosure, use, exhibition or other means            "P" document published prior to the international filing date but later than the priority date claimed         </td> <td style="width:50%">           "T" later document published after the international filing date or priority date and not in conflict with the application but cited to understand the principle or theory underlying the invention            "X" document of particular relevance; the claimed invention cannot be considered novel or cannot be considered to involve an inventive step when the document is taken alone            "Y" document of particular relevance; the claimed invention cannot be considered to involve an inventive step when the document is combined with one or more other such documents, such combination being obvious to a person skilled in the art            "&amp;" document member of the same patent family         </td> </tr> </table>			"A" document defining the general state of the art which is not considered to be of particular relevance "E" earlier document but published on or after the international filing date "L" document which may throw doubts on priority claim(s) or which is cited to establish the publication date of another citation or other special reason (as specified) "O" document referring to an oral disclosure, use, exhibition or other means "P" document published prior to the international filing date but later than the priority date claimed	"T" later document published after the international filing date or priority date and not in conflict with the application but cited to understand the principle or theory underlying the invention "X" document of particular relevance; the claimed invention cannot be considered novel or cannot be considered to involve an inventive step when the document is taken alone "Y" document of particular relevance; the claimed invention cannot be considered to involve an inventive step when the document is combined with one or more other such documents, such combination being obvious to a person skilled in the art "&" document member of the same patent family
"A" document defining the general state of the art which is not considered to be of particular relevance "E" earlier document but published on or after the international filing date "L" document which may throw doubts on priority claim(s) or which is cited to establish the publication date of another citation or other special reason (as specified) "O" document referring to an oral disclosure, use, exhibition or other means "P" document published prior to the international filing date but later than the priority date claimed	"T" later document published after the international filing date or priority date and not in conflict with the application but cited to understand the principle or theory underlying the invention "X" document of particular relevance; the claimed invention cannot be considered novel or cannot be considered to involve an inventive step when the document is taken alone "Y" document of particular relevance; the claimed invention cannot be considered to involve an inventive step when the document is combined with one or more other such documents, such combination being obvious to a person skilled in the art "&" document member of the same patent family			
Date of the actual completion of the international search 2 September 1993 (02.09.93)		Date of mailing of the international search report 14 SEP 1993 (14.09.93)		
Name and mailing address of the ISA/AU AUSTRALIAN INDUSTRIAL PROPERTY ORGANISATION PO BOX 200 WODEN ACT 2606 AUSTRALIA Facsimile No. 06 2853929		Authorized officer  R. CHIA Telephone No. (06) 2832185		

C(Continuation). DOCUMENTS CONSIDERED TO BE RELEVANT		
Category*	Citation of document, with indication, where appropriate of the relevant passages	Relevant to Claim No.
A	GB,A, 1418128 (OTTO) 17 December 1975 (17.12.75)	
A	Patent Abstracts of Japan, E-1091, page 74, JP,A, 3-98432 (EITO DENSHI K.K.) 24 April 1991 (24.04.91)	
A	40th IEEE Vehicular Technology Conference, 6 May 1990, Orlando, Florida pages 100-104; MANOCHEHR EGHTESEADI: "Inductive Power Transfer to an electric vehicle - analytical model"	
A	US,A, 4802080 (BOSSI et al) 31 January 1989 (31.01.89)	



This Annex lists the known "A" publication level patent family members relating to the patent document cited in the above-mentioned international search report. The Australian Patent Office is in no way liable for these particulars which are merely given for the purpose of information.

Patent Document Cited in Search Report		Patent Family Member	
AU,A, 12373/92	WO,A, 92/17929	MX,A 9201100	
EP,A, 334804	DE,A, 3810702	JP,A, 1311391	
EP,A, 473957	AU,A, 81320/91	US,A, 5095224	JP,A, 4285436
US,A, 4802080	AU,A, 31468/89, KR,A, 9207372	JP,A, 2007838	EP,A, 333388



(43) International Publication Date  
10 December 2009 (10.12.2009)

(10) International Publication Number  
**WO 2009/149464 A2**

- (51) International Patent Classification:  
H02J 17/00 (2006.01)
- (21) International Application Number:  
PCT/US2009/046648
- (22) International Filing Date:  
8 June 2009 (08.06.2009)
- (25) Filing Language: English
- (26) Publication Language: English
- (30) Priority Data:  
61/059,663 6 June 2008 (06.06.2008) US
- (71) Applicant (for all designated States except US): **UNIVERSITY OF FLORIDA RESEARCH FOUNDATION, INC.** [US/US]; 223 Grinter Hall, Gainesville, FL 32611 (US).
- (72) Inventors; and
- (75) Inventors/Applicants (for US only): **LOW, Zhen, Ning** [SG/US]; 712 S.W. 16th Avenue, #311, Gainesville, FL 32601 (US). **LIN, Jenshan** [US/US]; 910 SW. 105th Terrace, Gainesville, FL 32607 (US). **CHINGA, Raul, Andres** [PE/US]; 1653 N.W. 16th Avenue, Gainesville, FL 32605 (US).
- (74) Agent: **PARKER, James, S.**; Saliwanchik, Lloyd, Saliwanchik, P.O. Box 142950, Gainesville, FL 32614-2950 (US).

(81) Designated States (unless otherwise indicated, for every kind of national protection available): AE, AG, AL, AM, AO, AT, AU, AZ, BA, BB, BG, BH, BR, BW, BY, BZ, CA, CH, CL, CN, CO, CR, CU, CZ, DE, DK, DM, DO, DZ, EC, EE, EG, ES, FI, GB, GD, GE, GH, GM, GT, HN, HR, HU, ID, IL, IN, IS, JP, KE, KG, KM, KN, KP, KR, KZ, LA, LC, LK, LR, LS, LT, LU, LY, MA, MD, ME, MG, MK, MN, MW, MX, MY, MZ, NA, NG, NI, NO, NZ, OM, PE, PG, PH, PL, PT, RO, RS, RU, SC, SD, SE, SG, SK, SL, SM, ST, SV, SY, TJ, TM, TN, TR, TT, TZ, UA, UG, US, UZ, VC, VN, ZA, ZM, ZW.

(84) Designated States (unless otherwise indicated, for every kind of regional protection available): ARIPO (BW, GH, GM, KE, LS, MW, MZ, NA, SD, SL, SZ, TZ, UG, ZM, ZW), Eurasian (AM, AZ, BY, KG, KZ, MD, RU, TJ, TM), European (AT, BE, BG, CH, CY, CZ, DE, DK, EE, ES, FI, FR, GB, GR, HR, HU, IE, IS, IT, LT, LU, LV, MC, MK, MT, NL, NO, PL, PT, RO, SE, SI, SK, TR), OAPI (BF, BJ, CF, CG, CI, CM, GA, GN, GQ, GW, ML, MR, NE, SN, TD, TG).

**Published:**

— without international search report and to be republished upon receipt of that report (Rule 48.2(g))

(54) Title: METHOD AND APPARATUS FOR CONTACTLESS POWER TRANSFER

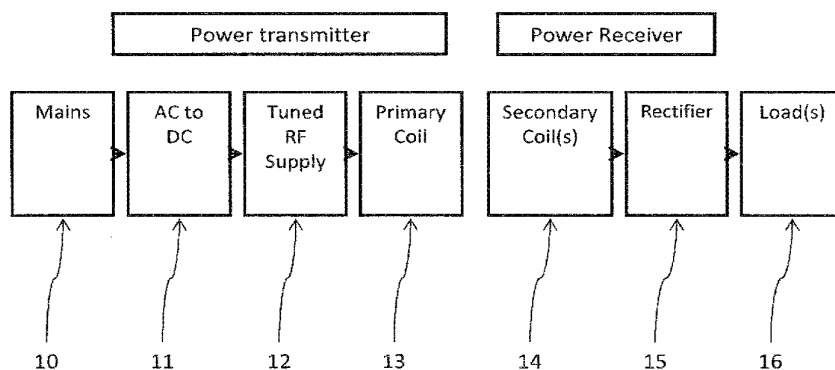


FIG. 1

(57) Abstract: Embodiments of the subject invention pertain to a method and apparatus for contactless power transfer. A specific embodiment relates to an impedance transformation network, a new class of load network for application to a contactless power system. Embodiments of the impedance transformation network enable a contactless power system to operate without encountering the common problems of: 1) over-voltage and/or under-voltage conditions; 2) over-power and/or under-power conditions; 3) power oscillations; and 4) high heat dissipation.

WO 2009/149464 A2

## DESCRIPTION

## METHOD AND APPARATUS FOR CONTACTLESS POWER TRANSFER

## 5 CROSS-REFERENCE TO RELATED APPLICATION

The present application claims the benefit of U.S. Provisional Application Serial No. 61/059,663, filed June 6, 2008, which is hereby incorporated by reference herein in its entirety, including any figures, tables, or drawings.

## 10 BACKGROUND OF INVENTION

In recent years, inductive charging technology has become a leading candidate to eliminate power cables. Inductive power systems and other contactless power systems typically use one or more transmitters to send power to one or more receivers. Electronic devices with contactless power receivers can be powered or charged by being positioned in close proximity to a contactless power transmitter. Such systems have been designed and implemented.

Contemporary contactless power systems are make use of switch-mode inverters, such as the Class, D, DE, E, E<sup>-1</sup>, F, F<sup>-1</sup>, EF, EF2, EF3, Phi. The switch-mode inverter converts DC voltage that is provided by a DC voltage source to into a high frequency signal that enables efficient coupling of one or more primary coils to one or more secondary coils. The secondary coils are ultimately connected to one more loads. In the case of a contactless power transfer system the load of an inverter is typically a portable electronic device or some other load device with a variable power requirement. In many instances the load has an input impedance that is variable. The load can use energy or it can be designed to store energy. The load can comprise a voltage regulator and / or a power management system for regulating and relaying the power to an energy consuming or energy storing element. The impedance of the load helps determine the loading condition.

A typical switch-mode inverter comprises an active device, a supply network, and a load network with output terminals for connecting to a load.

30 The active device is typically a transistor and operates as a switch. The switch alternates between a conductive and non-conductive state. A control signal from a gate drive or clock can be used to operate the switch. The switch is connected to a supply network and a load network. The switching of the active devices helps form an AC signal at the output of the load network.

The supply network relays power from a source the DC voltage source to a terminal of the active device. The DC voltage source can have an output voltage that is variable. The supply network can be a simple inductor and typically comprises passive components. In some cases it may comprise an active device or variable elements for active reconfiguration of the supply network. A reconfiguration of the supply network can be performed depending on the load conditions in order to optimize efficiency or regulate the power which is delivered from the source.

The load network relays power to the load device from a terminal of the active device and supply network. The load network typically comprises passive components. In some cases it may contain an active device or variable for active reconfiguration of the load network. A reconfiguration of the load network may be performed depending on the load conditions in order to optimize efficiency and / or regulate the power delivered to the load.

The load network includes one or more primary coils for inductively coupling to one or more secondary coils. Because of size mismatches and restrictions on the use of bulky core materials, the coupling between the primary and secondary coils can be weak thereby reducing efficiency, power delivery, or both.

In order to compensate for weak coupling between primary and secondary coils, typical inductive charge systems typically operate at frequencies greater than 50kHz. At these higher operating frequencies soft-switching inverters, such as the Class E,  $E^{-1}$ , are preferred because they are more efficient than hard-switching inverters. High efficiency is preferable for environmental and regulatory reasons as well as practical reasons such as minimizing heat dissipation.

Soft-switching describes a mode of operation where an active device, such as a transistor, will switch when either the voltage or current across the transistor is zero. Soft-switching eliminates losses that normally occur with hard switching due to switch capacitance and the overlap of voltage and current in the switch. For example, in the case of zero voltage switching, the voltage across a transistor swings to zero before the device turns on and current flows. Likewise, at turn-off, the voltage differential across the active device swings to zero before it is driven to a non-conductive state.

A practical system is preferably capable of matching the power supplied to the power demanded by a load device. This is important because many load devices have variable power requirements. If the power delivered does not match power required, the excess energy can be dissipated as heat. A load device can have an input impedance that is variable because of a power requirement that is variable (see Figure 5 for a graph of resistance versus changing

time for a typical cell phone battery). The input impedance of the load device can change by an order of magnitude. The input impedance of a voltage regulator connected to a portable electronic device can change by two orders of magnitude. The variable impedance of a load device makes the implementation of contactless power system difficult.

5           The following two characteristics of soft-switched inverters found in typical contactless power system make the adaptation to a load device with a variable impedance challenging: 1. Most switch-mode inverters have high efficiency over a narrow range of impedances. As an example, a class E inverter typically operates under, high-efficiency soft-switched conditions over a factor of two in load impedance (see Figure 3) (Raab, 1978). (see  
10 Figure 2 for a graph of efficiency versus normalized resistance for typical switch-mode inverters); 2. The output power vs. load impedance relationship of a switch-mode inverter is different than the output power vs. load impedance relationship of a DC supply (See figure 4 for a graph of power delivery vs. load resistance for a DC supply and an inverter). Because of this, a load device's pre-existing power management control system can fail to appropriately  
15 regulate the power delivered to the load device which can lead to component failure.

Due to the above described characteristics a contactless power system is likely to encounter one or more of the following problems: 1) over-voltage and/or under-voltage conditions throughout the circuit; 2) excess or inadequate power delivery to individual loads  
3) power oscillations; 4) heat problems; and 5) low efficiency.

20           Notably, a class D inverter architecture does not share the unfavorable characteristics and resulting problems of the other soft-switched inverters. Class D inverters are optimized for driving an impedance looking into the load network that has zero-phase angle (ZPA), and works for positive phase angles. Zero phase angle operation can be maintained by eliminating the reactance in a circuit of by using a combination of control functionalities, including, but  
25 not limited to, frequency, and tank circuit control (see Figures 7 and 8). A contactless power system with other soft-switched inverter architectures would be expected to make use of similar control functionality because of their sensitivity to the input impedance of the load(s). (Laouamer, R., *et al.*, "A multi-resonant converter for non-contact charging with electromagnetic coupling," in *Proc. 23rd International Conference on Electronics, Control and Instrumentation*, Nov 1997, Vol. 2, pp. 792 – 797; Abe, H., *et al.*, "A non-contact charger using a resonant converter with parallel capacitor of the secondary coil," in *Proc. Applied Power Electronics Conference and Exposition*, 15-19 Feb 1998, Vol. 1, pp. 136 –  
30 141; Joung, G. B. *et al.*, "An energy transmission system for an artificial heart using leakage inductance compensation of transcutaneous transformer," *IEEE Transactions on Power*

*Electronics*, Vol. 13, pp. 1013 – 1022 Nov 1998; Lu, Y., *et al.*, “Gapped air-cored power converter for intelligent clothing power transfer,” in *Proc. 7<sup>th</sup> International Conference on Power Electronics and Drive Systems*, 27-30 Nov. 2007, pp. 1578 – 1584; Jang, Y., *et al.*, “A contactless electrical energy transmission system for portable-telephone battery chargers,” *IEEE Transactions on Industrial Electronics*, Vol. 3, pp. 520 – 527, June 2003; Wang, C., *et al.*, “Power transfer capability and bifurcation phenomena of loosely coupled inductive power transfer system,” *IEEE Transactions on Industrial Electronics*, Vol. 51, pp. 148 – 157, Feb. 2004; Wang, C., *et al.*, “Investigating an LCL load resonant inverter for inductive power transfer applications,” *IEEE Transactions on Power Electronics*, Vol. 19, pp. 995 – 1002, July 2004; Wang, C., *et al.*, “Design consideration for a contactless electric vehicle battery charger,” *IEEE Transactions on Industrial Electronics*, Vol. 52, pp. 1308 – 1314, Oct. 2005) Control functionality adds to the cost and complexity of a system and detracts from the commercial viability.

To enable better control functionality and to ensure proper operation of the system, communication systems between the power supply and the load have been proposed (see Figures 6 and 9). Such communication systems also add undesirable cost to the system.

The previously described control functionality has been implemented in both contactless power transmitters and contactless power receivers. Control functionality in the receiver has been considered of particular importance when multiple loads require power from the same transmitter. To support multiple loads, it has been proposed that receiver units incorporate mechanisms such as, but not limited to, variable inductance and duty cycling. These mechanisms allow multiple loads to receive power from the same source by giving load devices a mechanism to protect themselves from over-voltage and/or current conditions (Figure 6). These mechanisms are of high importance because loads without such mechanisms will continue to receive power even when they no longer require power. The power will be dissipated as heat in the load device. Contemporary batteries will not charge at temperatures over 50°C. These systems also add undesirable cost to the system.

#### SUMMARY OF THE INVENTION

Embodiments of the subject invention pertain to a method and apparatus for contactless power transfer. A specific embodiment relates to an impedance transformation network, a new class of load network for application to a contactless power system. Embodiments of the impedance transformation network enables a contactless power system to operate without encountering the common problems of: 1) over-voltage and/or under-

voltage conditions; 2) over-power and/or under-power conditions; 3) power oscillations; and 4) high heat dissipation.

Embodiments of the impedance transformation network enables the contactless power system to avoid one or more of the four common problems described above, without any feedback, communication, and/or control functionality. The pre-existing power and battery charge management circuitry for a load, which may include a voltage regulator, can regulate the power output of a contactless power system under normal modes of operation. In accordance with embodiments of the invention, contactless power systems can be combined with very simple controls to improve the performance of the system. In this preferred mode of operation, a contactless power system can predictably and reliably deliver power to a load across a wide range of load impedances.

Embodiments of the invention provide one or more of, and a preferred embodiment of the invention provides each of, the following four functions:

1) Reactance shifting and phase angle control: a reactance is added to the resistance looking from the switch-mode supply through the load network. The reactance is shifted such that the phase angle looking from the switch-mode inverter into the load network is within a range that provides substantially soft-switching operation of the active device either when connected to or disconnected from one or more loads. Embodiments of the invention use the phase angle to control the power delivered by the inverter. Such embodiments can take advantage of the correlation between phase angle and load resistance. Changes in load resistance are transformed into a shift in the phase angle looking into the impedance transformation network. The output power response is more pronounced with respect to phase than with respect to load resistance (see Figure 12). This enables the invention to match power delivery and more closely mimic the response of a traditional DC supply (see Figure 13). In this method of operation, the contactless power system can deliver the necessary amount of power to the load. The soft-switching operation of the active device is preferably maintained for all load impedances.

If the inverter is designed for soft switching when the impedance looking into the load network from the active device is inductive, then the impedance transformation network is configured such that the impedance of the phase angle looking from the active device into the load network is positively correlated with the effective resistance of the load(s). If the effective resistance of the load increases, then the impedance transformation network is configured such that the phase angle looking from the active device through the load network increases. If the effective resistance of the load decreases, then the impedance transformation

network is configured such that the phase angle looking from the active device through the load network decreases. In a specific embodiment the reference phase angle is 40 degrees or greater, and in another 45 degrees or greater. In further embodiments, increases in load resistance can increase the phase angle up to 85 degrees.

5 If the inverter is designed for soft switching when the impedance looking into the load network from the active device is capacitive, than the impedance transformation network can be configured such that impedance of the phase angle looking from the active device into the load network is negatively correlated with the effective resistance requirement of the load. If the effective resistance of the load increases, then the impedance transformation network is  
 10 configured such that the phase angle looking from the active device through the load network decreases. If the effective resistance of the load decreases, then the impedance transformation network is configured such that the phase angle looking from the active device through the load network increases.

The effective resistance is a combination of the resistances of the loads looking from  
 15 the terminals of the secondary coils toward the load. The loads can be seen as in series or parallel. The loads can be seen as the series or parallel combination of the inverse of the individual load resistances. In the generalized form, the effective load resistance of any close proximity contactless power system via magnetic induction that incorporates m primary coils and n secondary coils can be described by:

$$Z_{in} = \{1_{1M} [Z^{IV} - (Z^{II})^T (Z^I)^{-1} Z^{II}]^{-1} 1_{M1}\}$$

$$Z = \begin{bmatrix} Z^{III} & (Z^{II})^T \\ Z^{II} & Z^I \end{bmatrix}$$

$$Z_{ab} = \begin{cases} j\omega L_a + R_a & \text{for } a = b \\ j\omega M_{ab} & \text{otherwise} \end{cases}$$

$$Z^{IV} = Z^{III} + Z_{in} 1_{MM}$$

20

Z<sub>in</sub>: Input impedance looking into the primary coil

1<sub>1M</sub>: Vector of 1's of length M



$1_{MM}$ : M X M matrix of 1's

Z: Impedance matrix

$Z_{ab}$ : Element ab of the impedance matrix

$Z^I$ : Sub-matrix of Z

5  $Z^{II}$ : Sub-matrix of Z

$Z^{III}$ : Sub-matrix of Z

$M_{ab}$ : Mutual inductance between the a<sup>th</sup> and b<sup>th</sup> coil

j: imaginary number

a: coil index

10 b: coil index

$\omega$ : radian frequency

$R_a$ : Parasitic resistance of the a<sup>th</sup> coil

$L_a$ : Self inductance of the a<sup>th</sup> coil

15 Typically, the power requirement of the device is negatively correlated with load resistance. As the resistance of the load increases the power required by the load decreases.

2) Resistance isolation: the resistance looking from the switch-mode supply through the load network can be minimally affected by changes in load resistance (see Figure 10);

20 Embodiments of the invention can isolate the switch-mode supply from changes in load resistance in order to improve the predictability and stability of the output power. The isolation from changes can be accomplished by the implementation one or more filter networks such that the range of resistances presented by load appear much narrower at the output terminals of a switch-mode inverter. The switch-mode supply should see a resistance such that it is in a high efficiency mode of operation (see Figure 2).

25 3) Frequency filtering: a filter removes extra harmonics, effectively "cleaning" the power signal before it enters the primary or secondary coil. In one embodiment this frequency filter incorporates an inductor and a capacitor with a "low Q" value. In another embodiment this frequency filter incorporates an inductor and a capacitor, the filter being considered to have a high Q value.

30 4) Coupling: at least one primary coil in the load network is inductively coupled to one or more secondary coils of the same load network. The primary coils can be configured in a spiral configuration and maybe designed with a variable pitch in order to create an even

magnetic field distribution. The primary coils can be arranged in an array pattern with each coil in the array wound with an irregular shape so that the array has a substantially even magnetic field distribution. The secondary coils can be coupled to the primary coil in any position or orientation. The secondary coil can be adapted to attach to a load. In a preferred embodiment the secondary coil is adapted to attach to a portable electronic device. In specific embodiments, both the primary coil and the secondary coil are the same size to maximize coupling. In this example, and other specific embodiments, the receiver coil is significantly smaller than the primary coil, in order to allow the user to place the device in any orientation. It is desirable for the secondary coil to be much smaller than the primary coil, but the efficiency and power transfer capabilities start to degrade significantly if the receiver is too small, due to poor coupling. In this example the secondary is wound along a single path with minimal spacing between turns in order to minimize the occupied volume and ease integration.

The voltage and current characteristics of the primary coil and the secondary coil can be described using the following equations [7][12]:

$$V_1 = M_{11} \frac{dI_1}{dt} + M_{12} \frac{dI_2}{dt} \quad (1)$$

$$V_2 = M_{21} \frac{dI_1}{dt} + M_{22} \frac{dI_2}{dt} \quad (2)$$

$$M_{12} = k\sqrt{M_{11}M_{22}} \quad (3)$$

Where

$V_1$  is the voltage at the transmitting coil

$I_1$  is the current at the transmitting coil

$V_2$  is the voltage at the receiving coil

$I_2$  is the current at the receiving coil

$M_{11}$  is the self inductance of the transmitting coil

$M_{22}$  is the self inductance of the receiving coil

$M_{12} = M_{21}$  is the mutual inductance of the two coils

$k$  is the coupling coefficient between the two coils

30

By Ohm's law:

$$\begin{aligned} Z_{rx} &= R_{rx} + jX_{rx} \\ &= \frac{V_1}{I_1} \end{aligned} \tag{4}$$

$$\begin{aligned} Z_{rx} &= R_{rx} + jX_{rx} \\ &= \frac{V_2}{I_2} \end{aligned} \tag{5}$$

5 Solving equations (1-3)

$$\begin{aligned} Z_{rx} &= \frac{\omega^2 M_{12}^2 R_{rx}}{R_{rx}^2 + (\omega M_{22} + X_{rx})^2} \\ &\quad + j \left( \omega M_{11} - \frac{\omega^2 M_{12}^2 (\omega M_{22} + X_{rx})}{R_{rx}^2 + (\omega M_{22} + X_{rx})^2} \right) \end{aligned} \tag{6}$$

The above equations neglect any 2<sup>nd</sup> order effects such as skin depth and proximity effects. A more in-depth analysis accounting for the above effects can be utilized. In an embodiment, litz wires can be used to mitigate such effects to the extent that they do not create significant discrepancies.

By using the combination of resistance isolation and phase angle control, a reliable, stable transmitter can power a variable load. First, the inverter preferably will not fail or overheat when the secondary coil is removed from the primary coil. Although a load detection scheme can be used to turn off the transmitter and reduce unloaded power losses, it can still be desirable for the unloaded power consumption to be sufficiently low. Since the coil voltage is unique to each load resistance as shown in Figure 49, load detection and status can be easily acquired. To avoid false detection, the load detection and status can be verified by analyzing the supply current via a current sense resistor. Limiting unloaded power loss can be achieved by ensuring the unloaded transmitting load network has effective impedance similar to a high load resistance case (high impedance with large phase angle). From the schematic of the class E circuit in Figure 44, it can be deduced that most of the power lost is due to the primary coil and inductor parasitic resistances as they are in the path of power transfer. Therefore, one way to reduce the unloaded power loss is to use an inductor with lower parasitic resistance.

## BRIEF DESCRIPTION OF DRAWINGS

The foregoing and other objects, features, and advantages of the present invention, as well as the invention itself, will be more fully understood from the following description of various embodiments, when read together with the accompanying drawings.

5           **Figure 1** shows a typical contactless power system that uses an inverter to drive a primary coil that may couple to one or more secondary coils and loads.

**Figure 2** shows the operating efficiency versus load resistance seen by an inverter (Class E) that is driving load resistances from .1 to 10, a span that reaches two orders of magnitude, where the high efficiency operating range for the inverter is identified, and the  
10           operating range of a typical portable electronic device is identified.

**Figure 3** shows the power in ( $P_i$ ) and power out ( $P_o$ ) versus load resistance seen by an inverter (Class E) that is driving load resistances from .1 to 10, a span that reaches two orders of magnitude, where the high efficiency operating range for the inverter is identified, and the operating range of a typical portable electronic device is identified.

15           **Figure 4** shows the power delivered to a variable load resistance from two different sources: a tuned switch-mode inverter supply and a fixed voltage DC supply, illustrating that power delivered to the load across a range of impedances is very different depending on the source, and that the range of output power can be much smaller with switch-mode inverters.

**Figure 5** shows the load resistance of a Motorola Razr during the charge cycle, illustrating that during the charge cycle, the resistance can change by greater than one order  
20           of magnitude.

**Figure 6** shows a block diagram of a typical prior art contactless power system, including commonly proposed and implemented communication and control functionality.

**Figure 7** shows a logic diagram, which is continued in Figure 8, of a typical prior art  
25           contactless power system, including commonly proposed and implemented control functionality.

**Figure 8** shows a continuation of the logic diagram of Figure 7.

**Figure 9** shows a block diagram of a typical prior art wireless power system with communication capability.

30           **Figure 10** shows the correlation between load resistance and the resistance looking from the inverter in accordance with an embodiment of the subject method, where the load resistance is transformed such that the resistance seen by the switch-mode supply is relatively constant, and in particular, the resistance from the supply is seen as between 2 and 6 ohms while the resistance of the load is varied from 5-500 ohms.

**Figure 11** shows the operating efficiency and power output of a class E inverter that is driving a fixed resistance with a phase angle ranging from -90 to 90 degrees, where the operating region for an embodiment of the invention is indicated.

**Figures 12A and 12B** show the power output of a class E inverter in response to variable load resistance and variable phase, respectively, showing a calculation of output range and compares them against each other.

**Figure 13** shows the power delivered to a variable load resistance from three different sources: an inverter, a fixed voltage DC supply, and a switch-mode inverter operating in accordance with an embodiment of the invention.

**Figure 14** shows the decoupling, or degradation of coupling efficiency between the load and the transmitter for various filter networks.

**Figure 15** shows a block diagram of a system in accordance with an embodiment of the subject invention, where the block diagram shows the direction of power flow and the various networks that can be used.

**Figure 16** shows a typical load resistance vs. time plot as seen from the input of a rectifier feeding into a device.

**Figure 17** shows the real and reactive components of the impedance as seen looking into the receiver side impedance transformation network, where the impedance characteristic at this point is measured from a system operating in accordance with a preferred embodiment of the invention.

**Figure 18** shows the real and reactive components of the impedance as looking into the primary coil, where the impedance characteristic at this point is measured from a system operating in accordance with a preferred embodiment of the invention .

**Figure 19** shows the real and reactive components of the impedance as seen from the transmitter side load-transformation network, where the impedance characteristic at this point is measured from a system operating in accordance with a preferred embodiment of the invention.

**Figure 20** shows the real and reactive components of the impedance as seen from the transmitter-side, phase shift network, where the impedance characteristic at this point is measured from a system operating in accordance with a preferred embodiment of the invention.

**Figure 21** shows the phase angle of the impedance as it is seen from the inverter, where the impedance characteristic at this point is measured from a system operating in accordance with a preferred embodiment of the invention.

**Figure 22** shows the actual power delivery and efficiency of a system that is operating in accordance with a preferred embodiment of the invention.

**Figures 23A-23C** show the actual power delivery and efficiency for another system in accordance with the invention. The experimental results are from a 12V supply system. Efficiency peaks at main power delivery band, which is approximately 25-100Ω load resistance, are shown. Power delivery drops rapidly after 100Ω, when the system goes into low load condition or trickle charge condition. Although the efficiency at high load resistance is poor, the absolute power loss is kept at about 1.75W, while power delivery continues to drop. This power loss is distributed in the system and little or no heat issues are observed (especially at the receiver) during the low load operation.

**Figure 24** shows the phase angle of the impedance as it is seen from the inverter, where the impedance characteristic at this point is measured from a system operating in the non-preferred mode of operation.

**Figure 25** shows the actual power delivery and efficiency of a system that is operating in the non-preferred mode of operation.

**Figures 26A-26B** show the instantaneous peak power loss for hard switching topologies, known in the art, as they are compared to soft-switching topologies, known in the art, where Figure 26A shows a “hard switching” topology power loss waveform for a bridge MOSFET (320 W/div) showing high instantaneous peak power loss during each switching cycle, and Figure 26B shows a “soft switching” topology power supply with the same rating as that in Figure 26A.

**Figure 27** shows the real and reactive components of the impedance as seen looking into the receiver side impedance transformation network, where the impedance characteristic at this point is measured from a system operating in an undesirable range.

**Figure 28** shows the real and reactive components of the impedance as looking into the primary coil, where the impedance characteristic at this point is measured from a system operating in an undesirable range.

**Figure 29** shows the real and reactive components of the impedance as seen from the transmitter side load-transformation network, where the impedance characteristic at this point is measured from a system operating in an undesirable range.

**Figure 30** shows the real and reactive components of the impedance as seen from the transmitter-side, phase shift network, where the impedance characteristic at this point is measured from a system operating in an undesirable range.

**Figure 31** shows the circuitry shown in Figure 68 with dotted lines, labeled A and B, around portions of the circuitry to show one embodiment of how the circuitry can be split between a transmitter unit, for example a transmitter pad, and a receiver unit.

**Figure 32** shows the block diagram of Figure 15 with dotted lines, labeled A and B, around portions of the block diagram elements to show how the block diagram elements can be split between a transmitter unit, for example a transmitter pad, and a receiver unit, in accordance with the embodiment shown in Figure 31.

**Figure 33** shows the circuitry shown in Figure 68 with dotted lines, labeled A, B, C, and D, around portions of the circuitry to show one embodiment of how the circuitry can be split between a transmitter unit, for example a transmitter pad, and a receiver unit.

**Figure 34** shows the block diagram of Figure 15 with dotted lines, labeled A, B, C, and D, around portions of the block diagram elements to show how the block diagram elements can be split between a transmitter unit, for example a transmitter pad, and a receiver unit, in accordance with the embodiment shown in Figure 33.

**Figure 35** shows the circuitry shown in Figure 68 with dotted lines, labeled A, B, C, and D, around portions of the circuitry to show one embodiment of how the circuitry can be split between a transmitter unit, for example a transmitter pad, and a receiver unit.

**Figure 36** shows the block diagram of Figure 15 with dotted lines, labeled A, B, C, and D, around portions of the block diagram elements to show how the block diagram elements can be split between a transmitter unit, for example a transmitter pad, and a receiver unit, in accordance with the embodiment shown in Figure 35.

**Figure 37** shows the circuitry shown in Figure 68 with dotted lines, labeled A, B, C, and D, around portions of the circuitry to show one embodiment of how the circuitry can be split between a transmitter unit, for example a transmitter pad, and a receiver unit.

**Figure 38** shows the block diagram of Figure 15 with dotted lines, labeled A, B, C, and D, around portions of the block diagram elements to show how the block diagram elements can be split between a transmitter unit, for example a transmitter pad, and a receiver unit, in accordance with the embodiment shown in Figure 37.

**Figure 39** shows the circuitry shown in Figure 68 with dotted lines, labeled A, B, C, and D, around portions of the circuitry to show one embodiment of how the circuitry can be split between a transmitter unit, for example a transmitter pad, and a receiver unit.

**Figure 40** shows the block diagram of Figure 15 with dotted lines, labeled A, B, C, and D, around portions of the block diagram elements to show how the block diagram

elements can be split between a transmitter unit, for example a transmitter pad, and a receiver unit, in accordance with the embodiment shown in Figure 39.

**Figure 41** shows a typical inductive coupling system.

5 **Figure 42** shows some of the possible topologies for a single-element transformation network.

**Figure 43** shows some of the possible topologies for a single-element transformation network.

**Figure 44** shows a typical Class E driver using parallel-parallel transformation network.

10 **Figure 45** shows a dual channel class E driver that can be used in accordance with an embodiment of the invention.

**Figure 46** shows an impedance response looking into receiver with different parallel capacitor value.

15 **Figure 47** shows an optimum receiver capacitor value across a range of load resistances to achieve maximum R looking into the transmitter coil.

**Figures 48A-48B** show a coupling efficiency and transformed impedance looking into the primary coil.

**Figure 49** shows a normalize primary coil voltage across a range of load resistances.

**Figure 50** shows a load network reactance with different transmitter capacitor.

20 **Figure 51** shows an amplitude and phase of impedance of unloaded transmitter load network with different  $C_{tx}$ .

**Figure 52** shows an impedance looking into transmitter load network.

**Figure 53** shows a phase looking into transmitter load network.

25 **Figure 54** shows a power delivered into the transmitting load network if transmitter is an ideal sine voltage source.

**Figure 55** shows a transistor drain voltage where  $C_{shunt} = 19nF$ .

**Figure 56** shows a dual channel class E driver.

**Figure 57** shows a primary coil – 10 turns (embedded into the table top) and secondary coil – 5 turns (taped up).

30 **Figure 58** shows a power delivery and efficiency of 120V system with a peak power of 295W.

**Figure 59** shows a temperature of transistor and inductor with natural convection cooling and forced cooling.

**Figure 60** shows a dual channel class E with forced air cooling.



**Figure 61** shows a waveform of the class E driver.

**Figures 62A-62B** show power delivered to load with respect to load resistance. Peak power occurs at approximately  $50\Omega$  load resistance for dual channel at 69W for dual channel and  $75\Omega$  for single channel at 10W for single channel.

5 **Figure 63** shows system efficiency with respect to load resistance with both peak efficiency of 64.5% for single channel and 76% of dual channel at approximately  $70\Omega$  load resistance.

**Figure 64** shows transmitter efficiency with respect to load resistance. Peak transmitter efficiency occurs across the band of  $60\Omega$  to  $100\Omega$  load resistance at 90% for dual  
10 channel and 79% for single channel.

**Figure 65** shows system efficiency with respect to load resistance with both cases achieving high efficiency at heavy load and also illustrating that a single channel mode is more efficient at low power delivery state.

**Figure 66** shows primary coil RMS voltage having a unique load resistance for each  
15 value.

**Figure 67** shows receiver DC voltage converging to approximately 70V for dual channel and 37V for single channel.

**Figure 68** shows a generalized contactless power system with a single transistor power amplifier in a single ended configuration.

20 **Figure 69** shows a generalized contactless power system with two, single transistor power amplifiers in a push-pull configuration.

**Figure 70** shows a generalized contactless power with a two transistor power amplifier in a single ended configuration.

**Figure 71** shows a generalized contactless power system with two, two transistor  
25 power amplifiers in a push-pull configuration.

**Figure 72** shows different supply network configurations that are used to connect a DC supply voltage to a terminal of the active device of a power amplifier.

**Figure 73** shows the functions of an impedance transformation network for a single ended system in block diagram format. The functional blocks are arranged in no particular  
30 order and there can be multiples of the same functional blocks.

**Figure 74** shows the functions of an impedance transformation network for a push-pull system in block diagram format. The functional blocks are arranged in no particular order and there can be multiples of the same functional blocks.

**Figure 75** shows various circuit elements arranged to achieve the function of reactance shifting. These circuit elements, or variants thereof, can add or remove the magnitude of reactance looking into the impedance transformation network. Inductive elements increase reactance. Capacitive elements decrease reactance.

5 **Figure 76** shows various circuit elements arranged to achieve the function of frequency filtering. Two notch filters are shown that can remove unwanted harmonics from the signal. A combination of other filter types can be used to achieve frequency filtering.

10 **Figure 77** shows various circuit elements arranged to adjust the correlation between the equivalent resistance and the phase of the load. Inductive elements will tend to result in a positive correlation between phase and load resistance. Capacitive elements will tend to result in a negative correlation between phase and load resistance. These elements can also serve the purpose of resistance compression.

15 **Figure 78** shows primary to secondary coil configurations. The impedance transformation network may comprise a single primary and a single secondary. Alternatively, the impedance transformation network may comprise one or more primary coils coupled to one or more secondary coils. The inductance of the primary and/or secondary coil(s) can be used to compress resistance and change the phase vs. resistance relationship.

20 **Figure 79** show various circuit elements arranged to compress the resistance seen looking into the impedance transformation network. Either capacitive or inductive elements can be used.

**Figure 80** shows a typical configuration of an impedance transformation network connected to an active device.

**Figure 81** shows a typical configuration of an impedance transformation network connected to an active device.

25 **Figure 82** shows a typical configuration of an impedance transformation network connected to an active device.

**Figure 83** shows a typical configuration of an impedance transformation network connected to an active device.

30

#### DETAILED DISCLOSURE

Contactless power systems typically use high frequency power electronics to deliver power to one or more loads. Figure 1 shows the fundamental components of many contactless power systems. A contactless power supply generally draws its power from the electrical grid through a standard wall outlet 10. The power from the wall is typically AC so it is generally

converted to DC voltage by an AC to DC converter 11. In order to shrink the size of components it is desirable to work at a high frequency, so the DC voltage is switched by an inverter 12. The high frequency signal, such as a high frequency voltage signal or high frequency current signal, is fed into one or more primary coils 13. The high frequency signal may pass through one or more filters before it feeds in to the primary 13. The primary coil 13 couples with one or more secondary coils 14. The secondary coil 14 will receive the high frequency power signal and will feed that into a rectifier 15, which will then output power to the load 16. One or more filter networks may be present between the secondary coil 14, rectifier 15, and load 16. Voltage regulation and battery charge management circuitry may be considered part of load 16.

The incorporation of a switch-mode inverter can make it difficult to deliver the correct amount of power to the load or loads. This is partially attributable to the limited range of load resistances that enable high-efficiency operation. Figure 2 shows the high efficiency operating range 20 of an inverter as it compares to the operating range 21 of a typical battery operated device. The operating range of resistances of the battery operated device is substantially wider than the high efficiency operating range or the inverter. Figure 3 shows the relation of input power 34 and output power 33 of an inverter across a range of resistances. The lost power can be calculated by subtracting output power 33 from input power 34. The power loss is significant outside the high efficiency operating region 31.

Switch-mode inverters are difficult to implement in contactless power systems with variable loads because the output power response relative to load resistance is very different than a DC supply's output power response relative to load resistance. Figure 3 shows output power 33 increasing with load resistance until it reaches a center value and decreases again. This is different than a typical constant-voltage DC supply whose power delivery follows the relationship  $P=V^2/R$ . The difference is illustrated in Figure 4 where we can see that the power delivery from a DC supply 41 will decrease rapidly with an increase in load resistance. By contrast, the output power from an inverter 42 will increase with load resistance and will later drop as load resistance continues to increase. The drop in power delivery 42 is markedly slower than the drop in power delivery 41. Although Figure 4 shows the curve for one example of a tuned switch-mode inverter supply, other tuned inverters can have different curves.

Portable electronic devices display a wide range of input resistances. Figure 5 shows the effective resistance 51 looking into a Motorola Razr during the charge cycle. Figure 5

shows the wide dynamic range of the load **52**, and in this case it is greater than one order of magnitude.

The aforementioned challenges of efficiency and power delivery can be overcome by implementing a variety of communications and controls. Figure 6 shows a contactless charging system that is an elaboration of the basic components and systems shown in Figure 1. The grayed blocks are components that are found in a basic contactless power system. The white boxes are components that enhance the performance of a typical contactless power system. It shows a transmitter control **60** which can alter the phase, duty cycle, frequency, tank circuit impedance, or rail voltage depending on loading conditions. There is a detection circuit **61** that draws information from various parts of the circuit and feeds that information back into the controller **60**. It shows contactless communication links **62** on both the transmitter side **66** and receiver side **67**. The communication link can work in conjunction with the detection mechanisms **61** to help the controller **60** make the most appropriate adjustments to the system. The receiver side **67** also has a controller **63** which can adjust the resonant frequency, duty cycle **65**, or perform other functionality to regulate power being delivered to the load. A front end regulator **64** is added to provide an additional level of protection to the load.

With a system such as the one in Figure 6 in place, designers can implement control logic such as that shown in Figure 7 and Figure 8 taken from a prior art system. We can see from Figure 8 **433, 434, 436, 438, 440, 442** some of the logic functionality that designers have built into contemporary contactless power systems. We can see from **432** that this system includes memory in order to achieve the desired functionality. Figure 9 shows another prior art system that uses a communication mechanism **91** on the receiver and a communication mechanism **90** on the transmitter. The communication, logic, and use of memory add additional cost to the system and require a large number of sensing points to be considered.

In order to stay within the high-efficiency operating region **20** and to match the power delivery of DC supply **41** several steps can be taken. Figure 10 shows the resistance seen by the switch-mode supply **100** as it compares to actual load resistance. From **100**, we can see that the resistance appears to vary from 2 to 6 ohms over a range from 5 to 500 ohms. This enables the switch-mode supply to stay in the high efficiency region **20** shown in Figure 2, regardless of load resistance.

Compressing the resistance will not solve the problem of improper power delivery. Figure 2 shows that if we keep the resistance in a narrowband, power output changes

minimally. In fact, the compression would exacerbate the power delivery discrepancy shown in Figure 4 where we see that power output response to load resistance from a switch-mode supply **42** does not match the power output response to load resistance from a constant voltage, DC supply. If too much power is delivered, the device may be destroyed, if too little is delivered it may not function.

In order to address the challenge, the phase angle of the load can be affected in order to affect the power output of the switch-mode supply, in accordance with embodiments of the invention. Figure 11 shows, for class E inverters, that an increase or decrease in phase correlates with an increase or decrease in output power. Input power **111** and output power **110** matched closely for a phase angle in the range of about +45 to +80 degrees. Even though efficiency **112** drops considerably as the phase angle approaches +90 degrees, the absolute power lost remains low. The use of phase angle control enables a +/-70% usable range of output power **113** with very low absolute power loss.

Embodiments of the invention use phase angle control to power a battery operated device. Conventional voltage regulators increase the resistance so that the power output of a DC supply is reduced **41**. Figures 12A-12B show, for class E inverters, the difference between using traditional resistance controlled output power vs. using phase controlled output power in accordance with embodiments of the invention. Referring to Figure 12A, in a resistance controlled scheme, input power **122** matches power out **123** for a very small dynamic range **125** of output power. This shows that varying the resistance is an ineffective way of controlling output power. The usable range of power levels for a resistance controlled scheme is only about +/- 9% **125** of the center value. Outside of this range the high absolute losses are high and can create harmful heat and wear and tear on components. Referring to Figure 12B, in a phase controlled scheme, input power **121** matches power out **120** for a much wider dynamic range of output power **124**. This shows that varying the phase dramatically increases the output power range. The usable range of power levels is +/- 70% **124** of the center value. Even though resistance may drop over this range, the absolute power losses are relatively low in this band **124**. Efficiency can be low, but total dissipated power is very low. The low absolute power loss avoids the problem of overheating and device damage.

By combining the resistance compression and the phase control, the contactless system can achieve a power output response to load resistance that is very similar to that of a conventional DC supply. Figure 13 shows the power output response of a DC supply **130**, an inverter **131**, and an inverter in accordance with an embodiment of the subject method of

operation 132. The output power in response to load resistance of the inverter in accordance with the embodiment of the subject method of operation 132 is much closer to the output power a device should expect from a constant voltage DC supply 130.

5 An additional challenge to designing and implementing a contactless power system is that multiple loads may draw power from a single source. This is problematic when different devices have different power requirements. For instance, a fully discharged cell phone may require 10-15 times the power of a fully charged cell phone. Embodiments of the subject method of operation can provide a mechanism to protect individual devices from damage if the power output exceeds the device requirement. Loads that no longer require power can be  
10 decoupled from the primary coil. De-coupling can include degradation in coupling efficiency so that the load is effectively isolated from the transmitter. This can be accomplished by using pre-existing voltage regulator behavior. As a voltage regulator increases the effective input resistance, coupling efficiency drops and vice-versa.

Figure 14 shows the decoupling effect for various receiver circuits. A parallel  
15 capacitor can be selected to tune the decoupling point, which is the point when efficiency of receiver is at 50%. For this case, the decoupling point for 100nF capacitor is at 700Ω, whereas the decoupling point for 150nF capacitor is at 320Ω. We can see that for various configurations 141, 142, 143 the rate of decoupling occurs at varying rates. 143 shows a curve that is a good fit for a single device charger that can regulate power output from the  
20 transmitter. 141 shows a curve that is good fit for a multi-device charger where individual loads may need to be isolated from the source. Although not shown in Figure 14, when the capacitor value is changed the power received is also changed.

In order to accomplish this method of operation without any communication and control functionality, other than the pre-existing control found in today's voltage regulators,  
25 embodiments of the subject system can use a series of carefully tuned transformation networks that transform, compress, and shift the impedance of the load. Through these filter networks the resistance can be compressed, the phase angle manipulated, and the loads allowed to decouple from the primary.

**Example 1:**

30 A high power, high-efficiency contactless power transfer system using the impedance transformation network and has been designed and fabricated using the subject impedance transformation network. The contactless transfer system requires minimal control to achieve the desired power delivery profile across a wide range of load resistances, while maintaining high efficiency to which helps to prevent overheating of components. This embodiment of the

subject system includes more than one active device with independent gate drive to control power delivery. The system is able to achieve power delivery of 295W to a load of 50Ω with a DC voltage of 121.5V and current of 2.43A. The input current was current-limited at 3.25A. The system efficiency at maximum power output is 75.7%. The system operates at a minimum of 77% efficiency across load resistances ranging from 60Ω to 140Ω which corresponds to a high output power state. The system can be scaled to achieve higher output power if the current limit is removed. Higher efficiency and better power delivery can be achieved by using components with lower parasitic resistance.

The DC source voltage is the 600W CS112005S power supply by Circuit Specialists, Inc rated at 120V at 5A. The active devices are transistors, specifically the transistors are part IRFP21N60L from International Rectifier.

A pair of coils was fabricated using 16 AWG magnet wire for the set-up. The primary coil is 21cm by 21cm with 10 turns with variable spacing between turns while the secondary coil is 13cm by 13cm with 5 turns wound along the same path. Figure 57 shows the primary coil embedded in plastic with the secondary coil placed on top. The primary and secondary coils are separated by a gap of 10mm. The primary coil is designed with the appropriate spacing between the turns to achieve only 5% power variation of the received power at all different locations. In this example, the coupling is approximately constant regardless of the receiver position provided that the entire secondary coil is within the outer perimeter of the primary coil. The self inductance of the primary coil is 31.95μH with a parasitic resistance of 0.32Ω and secondary coil is 12.52μH with a parasitic resistance of 0.2Ω. Mutual inductance between the coils is 7.454uH with a coupling coefficient of 0.373. The measurements were taken using the HP4192A LF Impedance Analyzer.

In order to reduce losses through parasitic resistance, low loss Polypropylene capacitors are used. In order to strike a balance between size and efficiency, 1140-101K-RC by Bourns Jw Miller is selected to be  $L_{out}$ . Since most of the losses of the transmitter are from the parasitic resistance of  $L_{out}$ , a larger and more efficient inductor can be replaced, if space permits. The fabricated dual channel driver with a dimension of 10cm x 8.5cm is shown in Figure 56. There are a lot of empty spaces; therefore its size can be further reduced.  $L_{out}$  takes up a significant amount of space due to the requirement for low parasitic resistance so as to maintain sufficiently high efficiency and power delivery.

Peak drain voltage is only 460V, which is approximately 25% lower than the rated voltage of the transistor used. Figure 58 shows the efficiency and power delivery of the 120V system with respect to load resistance. The power delivery of the system can be scaled by

varying the supply voltage as long as the DC power supply driving system is able to provide sufficient power and the drain voltage across the transistor stays within its breakdown voltage.

The efficiency of the single channel is approximately 10-15% lower for the same load  
5 resistance because the current is flowing through a single  $L_{out}$  inductor instead of a pair of  
them, which means the parasitic resistance is doubled, thus resulting in a low system and  
transmitter efficiency as shown in Figure 63 and Figure 64, respectively. However, when the  
system goes into light load mode or trickle charge mode, it would be desirable to go into the  
single channel mode. It can be seen from Figure 65 that the system efficiency is  
10 approximately 15% higher than the dual channel mode for delivering the same amount of  
power below 10W. Instead of operating at high load resistance for a dual channel mode  
resulting in high receiver DC voltage as shown in Figure 67, it is possible to achieve similar  
power delivery at much lower load resistance for a single channel mode resulting in lower  
receiver DC voltage as lower load resistance would result in higher system efficiency. In  
15 addition, a typical buck regulator has higher DC-DC efficiency when the input voltage is  
lower. Therefore, a load resistance detection scheme can be used to determine the switch over  
point from dual channel to single channel. It can be seen from Figure 62 that a power delivery  
of 10W occurs at 500 $\Omega$  load resistance of the dual channel mode making it a good switch  
over point. It can be concluded that a 500 $\Omega$  load resistance would translate to an approximate  
20 primary coil RMS voltage of 20V for the dual channel mode as shown in Figure 66.  
Likewise, if the power requirement for the single channel mode is too high, it can be switched  
to dual channel mode. It can be inferred from Figure 62 that the switch over point would be  
approximately 75 $\Omega$ , which translates to a RMS coil voltage of 22V from Figure 65. The coil  
voltage can be read using an ADC where the DC voltage at the input of the ADC can be  
25 transformed from the coil voltage by rectification and stepping down using a potential  
divider.

In a specific embodiment, for size and efficiency considerations, capacitors can be  
used for the network. This is because resistors dissipate power and a low loss inductor would  
be large in size. Alternative embodiments can incorporate resistors and inductors. Although, a  
30 multi-element transformation network might achieve a more appropriate response, for  
simplicity and low components count, an embodiment of the system uses a single-element  
transformation network. Four topologies are shown in Figures 42 and 43.

A series capacitor only introduces a negative reactance and does not change the real  
part of the impedance. A parallel capacitor affects both the real and imaginary part of the



impedance. For simplicity, the receiver input impedance can be modeled using a variable resistor load such that equation (7) illustrates the transformation performed by the parallel capacitor.

$$Z_m = \frac{R}{1 + \omega^2 C^2 R^2} - j \frac{\omega C R^2}{1 + \omega^2 C^2 R^2} \quad (7)$$

5 Equation (7) shows that the resistance is “compressed” non-linearly by a factor of  $1/(1 + \omega^2 C^2 R^2)$ . Thus, the effective resistance decreases with increasing load resistance. At high load resistance, the transformed resistance is small. Therefore, a significant part of the power received is dissipated across the secondary coil as heat. This phenomenon is actually desirable if the receiver is in a state that requires very little power or during trickle charge.

10 Therefore, it has a “decoupling” effect regulating the power delivery with increasing load resistance. However, this should preferably occur only when the transmitter is designed to use limited power at this state of operation as heating would become an issue if too much power is being dissipated across the secondary coil. By using a parallel capacitor, a reactive term can be introduced. The reactive term decreases nonlinearly from null with

15 increasing load resistance with an asymptote of  $-1/\omega C$ , which can be useful in compensating the secondary coil inductance.

From equation (6) it can be observed that the resistance looking into the transmitter coil can be reduced significantly with the increase of resistance looking from the receiver coil into the receiver. Due to loose coupling between the coils, the resistance looking into the

20 primary coil can be further reduced as the mutual inductance can be relatively low. If the total resistance looking into the primary coil is comparable to the parasitic resistance of the primary coil, limited power is transmitted to the receiver as most of the power would be dissipated across the primary coil as heat. Therefore, it would be preferred for a power transmission via loosely coupled coils to have a parallel capacitor on the secondary coil. By

25 substituting equation (7) into equation (6),

$$Z_x = \left( \frac{\omega^2 M_{12}^2 \left( \frac{R}{1 + \omega^2 C^2 R^2} \right)}{\left( \frac{R}{1 + \omega^2 C^2 R^2} \right)^2 + \left( \omega M_{22} - \frac{\omega C R^2}{1 + \omega^2 C^2 R^2} \right)^2} \right) \quad (8)$$

$$+ j \left( \omega M_{11} - \frac{\omega^2 M_{12}^2 \left( \omega M_{22} - \frac{\omega C R^2}{1 + \omega^2 C^2 R^2} \right)}{\left( \frac{R}{1 + \omega^2 C^2 R^2} \right)^2 + \left( \omega M_{22} - \frac{\omega C R^2}{1 + \omega^2 C^2 R^2} \right)^2} \right)$$

For the transmitter transformation network, a series or parallel topology can be used. However, to maintain an ideal efficiency above 95%, the allowable variation of load resistance of an ideal class E inverter can be kept within +55% and -37% [F. H. Raab, "Effects of circuit variations on the class E tuned power amplifier," *IEEE Journal of Solid-State Circuits*, vol. 13, pp. 239 – 247, Apr 1978.]. Therefore, if the variation of resistance with respect to load resistance looking into the transmitter is too large, it can be preferable to use a parallel capacitor instead of a series capacitor. A capacitor value can be selected that ensures that the transmitter would not suffer immediate failure when there is no secondary coil as well as having an increasing reactance trend with increasing load resistance. Having an increasing reactance trend with increasing load resistance can ensure the preferred power delivery trend.

Figure 15 shows an example configuration of a system that can work in this mode of operation in accordance with an embodiment of the subject invention. Other circuit configurations can also be utilized to work in this mode of operation in accordance with the subject invention. The grayed boxes, which include an AC/DC converter **150**, switch-mode inverter **151**, primary coil **154**, secondary coil **156**, rectifier stage **158**, regulator stage **159**, and load **1500**, are components of a typical contactless power system, for example, as shown in Figure 1. In order to achieve the method of operation in accordance with the subject invention, this system uses four transformation networks, including receiver-side impedance transformation network **157**, coupling network **155**, transmitter-side impedance transformation network **153**, phase shift network **152**. Measuring the impedance at probe points looking into the rectifier stage **1503**, receiver-side impedance transformation network **1504**, primary coil **1505**, transmitter-side impedance transformation network **1506**, and phase shift network **1507**, facilitate a better understanding of the operation.

Figure 16 shows a simulated load resistance vs. time **160** measured looking into the rectifier stage from probe **1503**. The swing from 0-500 ohms is well outside usable operating

range of an inverter **20** and **31**, shown in Figure 2 and Figure 3, respectively. It would be desirable to compress the resistance into a useable operating range **20, 31**. At this stage there is no reactive component which is introduced by the impedance transformation network **157** in order to use the phase angle method of power control in accordance with embodiments of the invention.

Figure 17 shows the transformed load resistance **170** looking into the receiver-side impedance transformation stage from probe **1504**. The objective of this stage is to achieve the decoupling effect shown in Figure 14. This decoupling effect is automatic decoupling where the degradation of coupling efficiency between the contactless power transmitter and the load(s) effectively decouples the receiver from the transmitter. Figure 17 also shows the reactive component **171** introduced by the impedance transformation network **157**. The introduction of the reactive component **171** compresses the resistance looking into the receiver in order to stay within the useable operating range of the inverter identified in Figure 2. Additional reactive components will be further added on the transmitter side for implementing the phase-angle method of control in accordance with the invention. At this stage the reactive component **171** decreases with respect to load resistances, which means that phase angle is decreasing with respect to load resistance. From Figure 11, we can see that the working range **114** requires an increase in phase angle for inductive load, to reduce power output. Impedance transformation networks **153** on the transmitter side can compensate from the phase angle introduced by the impedance transformation network **157**.

Figure 18 shows the impedance transformation that is the result of the coupling network **155** and is measured looking into the primary coil **154** from probe **1505**. The objective is to maximize the real part **170** shown in Figure 17, which has been compressed to the point where parasitic losses would become less dominant. Increasing the resistance can improve the efficiency of the circuit. The real part **180** is much greater at this stage and has been increased to maximize power delivery through to the secondary coil **156** and minimize the losses from other parasitic upstream stages closer to the wall outlet, or AC/DC **150**. The negative aspect, however, is that magnitude change of the real component **180** is too large when compared to the working region of a switch-mode supply **20** and **31**, shown in Figure 2 and Figure 3, respectively. This can be corrected by the upstream transformation networks, such as impedance transformation network **153**. The reactive component **181** still trends downward with load resistance and can also be corrected by upstream transformation networks.

Figure 19 shows the impedance transformation that is the result of impedance transformation network **153** and is measured looking into the impedance transformation network **153** from probe **1506**. The objective is to compress the real component **180** such that it falls within the operating range **20** and **31**, defined in Figure 2 and Figure 3, respectively.

5 The second objective is to transform the reactive component **181** such that the increase in load resistance increases the reactive component and phase angle. The real part **190** is compressed back within the operating range of a switch-mode inverter **20** and **31**. The reactive part **191** has been corrected such that it trends upward with increasing load resistance. This corresponds to an increasing phase angle and decreased power delivery as

10 load resistance increases. The reactive part **191** is negative at this stage and this would correspond to a negative phase angle. From Figure 11, it can be seen, for a class E inverter, that a negative phase angle corresponds with poor efficiency and high actual power losses. The same is true for class D and Phi inverters. The trend is undesirable at this stage because an increase in phase angle on the negative slope of **110** would increase power output. The

15 reactive component can be shifted by phase shift network **152**, for example, so that it falls within the working region **114**.

Figure 20 shows the impedance transformation that is the result of the phase shift network **152** and is measured looking into the phase shift network **152** from probe **1507**. The objective is to keep the real part **190** in the operating range of the switch-mode inverter and

20 shift the reactive part **191** into the operating range of the switch-mode inverter. The real part **200** is within the operating range of resistances of a switch-mode inverter **20** and **31**, from Figure 2 and Figure 3, respectively. The reactive part **201** now falls in the correct operating region **114** shown in Figure 11. Confirmation that the phase angle and trend are correct can be shown by converting **200** and **201** into a phase angle plot, as shown in Figure 21. The

25 phase angle **210** is within the operating region **114** and increases with respect to load resistance. The phase angle **210** has a dip at very low impedances and in specific embodiments the initial dip in phase can be avoided.

Figure 22 shows actual experimental data taken from the system shown in Figure 15. After the 30 Ohm inflection point **220**, power output decreases with load impedance and the

30 system achieves high operating efficiency. Because a typical portable electronic device will operate at impedances greater than 30 ohms when the supply voltage is sufficiently high, this is an example of a preferred power delivery vs. load resistance vs. efficiency plot.

### Example 2:

A primary coil parallel capacitor value in a specific embodiment can meet two

constraints.

Figure 24 offers a contrast to the preferred phase angle vs. load resistance trend shown in Figure 21. The reference phase angle is approximately 80 degrees and decreases with load resistance. The phase angle **240** decreases with load resistance.

5 Figure 25 shows the result of this mode of operation when there are no communication and control mechanisms in place. The power output increases with load resistance, which is exactly opposite the response of a fixed voltage DC supply **130** which is shown in Figure 13.

10 Figure 27 shows the real and reactive components of the impedance as seen looking into the receiver side impedance transformation network, where the impedance characteristic at this point is measured from a system operating in an undesirable range.

Figure 28 shows the real and reactive components of the impedance as looking into the primary coil, where the impedance characteristic at this point is measured from a system operating in an undesirable range.

15 Figure 29 shows the real and reactive components of the impedance as seen from the transmitter side load-transformation network, where the impedance characteristic at this point is measured from a system operating in an undesirable range.

20 Figure 30 shows the real and reactive components of the impedance as seen from the transmitter-side, phase shift network, where the impedance characteristic at this point is measured from a system operating in an undesirable range.

Figures 31-40 show a variety of ways that the components of various embodiments of the subject invention can be located, for example proximate the transmitter coil, proximate the receiver coil, or separate from both.

25 Figure 31 shows the circuitry shown in Figure 68 with dotted lines, labeled A and B, around portions of the circuitry to show one embodiment of how the circuitry can be split between a transmitter unit, for example a transmitter pad, and a receiver unit.

30 Figure 32 shows the block diagram of Figure 15 with dotted lines, labeled A and B, around portions of the block diagram elements to show how the block diagram elements can be split between a transmitter unit, for example a transmitter pad, and a receiver unit, in accordance with the embodiment shown in Figure 31.

Figure 33 shows the circuitry shown in Figure 68 with dotted lines, labeled A, B, C, and D, around portions of the circuitry to show one embodiment of how the circuitry can be split between a transmitter unit, for example a transmitter pad, and a receiver unit.

Figure 34 shows the block diagram of Figure 15 with dotted lines, labeled A, B, C, and D, around portions of the block diagram elements to show how the block diagram elements can be split between a transmitter unit, for example a transmitter pad, and a receiver unit, in accordance with the embodiment shown in Figure 33.

5 Figure 35 shows the circuitry shown in Figure 68 with dotted lines, labeled A, B, C, and D, around portions of the circuitry to show one embodiment of how the circuitry can be split between a transmitter unit, for example a transmitter pad, and a receiver unit.

10 Figure 36 shows the block diagram of Figure 15 with dotted lines, labeled A, B, C, and D, around portions of the block diagram elements to show how the block diagram elements can be split between a transmitter unit, for example a transmitter pad, and a receiver unit, in accordance with the embodiment shown in Figure 35.

Figure 37 shows the circuitry shown in Figure 68 with dotted lines, labeled A, B, C, and D, around portions of the circuitry to show one embodiment of how the circuitry can be split between a transmitter unit, for example a transmitter pad, and a receiver unit.

15 Figure 38 shows the block diagram of Figure 15 with dotted lines, labeled A, B, C, and D, around portions of the block diagram elements to show how the block diagram elements can be split between a transmitter unit, for example a transmitter pad, and a receiver unit, in accordance with the embodiment shown in Figure 37.

20 Figure 39 shows the circuitry shown in Figure 68 with dotted lines, labeled A, B, C, and D, around portions of the circuitry to show one embodiment of how the circuitry can be split between a transmitter unit, for example a transmitter pad, and a receiver unit.

25 Figure 40 shows the block diagram of Figure 15 with dotted lines, labeled A, B, C, and D, around portions of the block diagram elements to show how the block diagram elements can be split between a transmitter unit, for example a transmitter pad, and a receiver unit, in accordance with the embodiment shown in Figure 39.

Figure 41 shows a typical inductive coupling system.

Figures 42-83 show various components and systems or subsystems that can be utilized with various embodiments of the invention, and/or data corresponding to various embodiments of the invention.

30 Figure 42 shows some of the possible topologies for a single-element transformation network.

Figure 43 shows some of the possible topologies for a single-element transformation network.

Figure 44 shows a typical Class E driver using parallel-parallel transformation network.

Figure 45 shows a dual channel class E driver that can be used in accordance with an embodiment of the invention.

5 Figure 46 shows an impedance response looking into receiver with different parallel capacitor value.

Figure 47 shows an optimum receiver capacitor value across a range of load resistances to achieve maximum R looking into the transmitter coil.

10 Figures 48A-48B show a coupling efficiency and transformed impedance looking into the primary coil.

Figure 49 shows a normalize primary coil voltage across a range of load resistances.

Figure 50 shows a load network reactance with different transmitter capacitor.

Figure 51 shows an amplitude and phase of impedance of unloaded transmitter load network with different  $C_{tx}$ .

15 Figure 52 shows an impedance looking into transmitter load network.

Figure 53 shows a phase looking into transmitter load network.

Figure 54 shows a power delivered into the transmitting load network if transmitter is an ideal sine voltage source.

Figure 55 shows a transistor drain voltage where  $C_{shunt} = 19nF$ .

20 Figure 56 shows a dual channel class E driver.

Figure 57 shows a primary coil – 10 turns (embedded into the table top) and secondary coil – 5 turns (taped up).

Figure 58 shows a power delivery and efficiency of 120V system with a peak power of 295W.

25 Figure 59 shows a temperature of transistor and inductor with natural convection cooling and forced cooling.

Figure 60 shows a dual channel class E with forced air cooling.

Figure 61 shows a waveform of the class E driver.

30 Figures 62A-62B show power delivered to load with respect to load resistance. Peak power occurs at approximately  $50\Omega$  load resistance for dual channel at 69W for dual channel and  $75\Omega$  for single channel at 10W for single channel.

Figure 63 shows system efficiency with respect to load resistance with both peak efficiency of 64.5% for single channel and 76% of dual channel at approximately  $70\Omega$  load resistance.

Figure 64 shows transmitter efficiency with respect to load resistance. Peak transmitter efficiency occurs across the band of  $60\Omega$  to  $100\Omega$  load resistance at 90% for dual channel and 79% for single channel.

5 Figure 65 shows system efficiency with respect to load resistance with both cases achieving high efficiency at heavy load and also illustrating that a single channel mode is more efficient at low power delivery state.

Figure 66 shows primary coil RMS voltage having a unique load resistance for each value.

10 Figure 67 shows receiver DC voltage converging to approximately 70V for dual channel and 37V for single channel.

Figure 68 shows a generalized contactless power system with a single transistor power amplifier in a single ended configuration.

Figure 69 shows a generalized contactless power system with two, single transistor power amplifiers in a push-pull configuration.

15 Figure 70 shows a generalized contactless power with a two transistor power amplifier in a single ended configuration.

Figure 71 shows a generalized contactless power system with two, two transistor power amplifiers in a push-pull configuration.

20 Figure 72 shows different supply network configurations that are used to connect a DC supply voltage to a terminal of the active device of a power amplifier.

Figure 73 shows the functions of a impedance transformation network for a single ended system in block diagram format. The functional blocks are arranged in no particular order and there can be multiples of the same functional blocks.

25 Figure 74 shows the functions of a impedance transformation network for a push-pull system in block diagram format. The functional blocks are arranged in no particular order and there can be multiples of the same functional blocks.

30 Figure 75 shows various circuit elements arranged to achieve the function of reactance shifting. These circuit elements, or variants thereof, can add or remove the magnitude of reactance looking into the impedance transformation network. Inductive elements increase reactance. Capacitive elements decrease reactance.

Figure 76 shows various circuit elements arranged to achieve the function of frequency filtering. Two notch filters are shown that can remove unwanted harmonics from the signal. A combination of other filter types can be used to achieve frequency filtering.



Figure 77 shows various circuit elements arranged to adjust the correlation between the equivalent resistance and the phase of the load. Inductive elements will tend to result in a positive correlation between phase and load resistance. Capacitive elements will tend to result in a negative correlation between phase and load resistance. These elements can also serve the purpose of resistance compression.

Figure 78 shows primary to secondary coil configurations. The impedance transformation network may comprise a single primary and a single secondary. Alternatively, the impedance transformation network may comprise one or more primary coils coupled to one or more secondary coils. The inductance of the primary and/or secondary coil(s) can be used to compress resistance and change the phase vs. resistance relationship.

Figure 79 show various circuit elements arranged to compress the resistance seen looking into the impedance transformation network. Either capacitive or inductive elements can be used.

Figure 80 shows a typical configuration of an impedance transformation network connected to an active device.

Figure 81 shows a typical configuration of an impedance transformation network connected to an active device.

Figure 82 shows a typical configuration of an impedance transformation network connected to an active device.

Figure 83 shows a typical configuration of an impedance transformation network connected to an active device.

Specific embodiments pertain to a method and a circuit for inductive power transfer, incorporating an impedance transformation network, where the impedance transformation network has an input port for coupling to an active device for creating a signal at a selected operating frequency, an output port for coupling to a load having a variable impedance; and a reactive network coupled between the input port and the output port, where the reactive network includes a primary coil; and a secondary coil, where the primary coil is inductively coupled to the secondary coil, where when the output is coupled to the load having a variable impedance and the input port is coupled to the active device that creates a signal at the selected operating frequency, a phase angle of an impedance looking into the impedance transformation network through the input port is inductive and negatively correlated with the amount of power delivered to the load. A real part of the impedance looking into the impedance transformation network through the input port can be in a range between a minimum real part and a maximum real part. The maximum real part can be less than or

equal to one order of magnitude greater than the minimum real part. Further embodiments can incorporate at least one additional input port, at least one additional output port, at least one additional primary coil, and/or at least one additional secondary coil. The output port can be adapted for coupling to at least two loads.

- 5 In an embodiment, the phase angle of the impedance looking into the impedance transformation network through the input port is positively correlated with the resistance of the load. In another embodiment, the phase angle of the impedance looking into the impedance transformation network through the input port is positively correlated with an equivalent resistance of the load. In a specific embodiment, the phase angle of the impedance
- 10 looking into the impedance transformation network through the input port is positively correlated with an equivalent resistance of the load, wherein when the impedance looking to the primary coil,  $Z_{in}$ , is explained by:

$$Z_{in} = \{1_{1M} [Z^{IV} - (Z^{II})^T (Z^I)^{-1} Z^{II}]^{-1} 1_{M1}\}$$

$$Z = \begin{bmatrix} Z^{III} & (Z^{II})^T \\ Z^{II} & Z^I \end{bmatrix}$$

$$Z_{ab} = \begin{cases} j\omega L_a + R_a & \text{for } a = b \\ j\omega M_{ab} & \text{otherwise} \end{cases}$$

$$Z^{IV} = Z^{III} + Z_{in} 1_{MM}$$

$Z_{in}$ : Input impedance looking into the primary coil

- 15  $1_{1M}$ : Vector of 1's of length M

$1_{MM}$ : M X M matrix of 1's

Z: Impedance matrix

$Z_{ab}$ : Element ab of the impedance matrix

$Z^I$ : Sub-matrix of Z

- 20  $Z^{II}$ : Sub-matrix of Z

$Z^{III}$ : Sub-matrix of Z

$M_{ab}$ : Mutual inductance between the  $a^{\text{th}}$  and  $b^{\text{th}}$  coil

$j$ : imaginary number

$a$ : coil index

$b$ : coil index

5  $\omega$ : radian frequency

$R_a$ : Parasitic resistance of the  $a^{\text{th}}$  coil

$L_a$ : Self inductance of the  $a^{\text{th}}$  coil

The reactive network can have at least one shunt network with a negative reactance that is connected between a first terminal of the secondary coil and a second terminal of the  
10 secondary coil. The at least one shunt network with a negative reactance can have a capacitor. The active device can have a transistor. In a specific embodiment, active device includes a switching component that operates substantially as a switch; and a capacitance in parallel with the switching component. The input port can be coupled to a voltage source or input port can be coupled to a current source. A supply network can be connected between  
15 the input port and a voltage source, where the supply network includes at least one inductor. The supply network connected between the input port and a voltage source can be configured to reject harmonics not intended to reach the load. In specific embodiments, the supply network connected between the input port and a voltage source can include elements of the supply network, load network, and the active device so as to represent at least one class D  
20 inverter or variant, at least one class DE inverter or variant, at least one class E inverter or variant, at least one class  $E^{-1}$  inverter or variant at least one class F inverter or variant, at least one class  $F^{-1}$  inverter or variant, at least one class  $EF^{-1}$  inverter or variant, or at least one class Phi inverter or variant.

The signal from the active device can be an AC signal and/or a periodic signal. When  
25 the active device is coupled to the input port, a voltage source is coupled to the input port, and the load is coupled to the output port, the phase angle of the impedance looking into the impedance transformation network through the input port can be within a range such that substantially zero voltage-switching of the active device occurs. Regarding this range, in specific embodiments switching of the active device can occur when the voltage is within a  
30 range of 10% of a peak voltage and zero voltage, switching of the active device can occur when the voltage is within a range of 5% of a peak voltage and zero voltage, and/or switching

of the active device occurs when the voltage is within a range of 1% of a peak voltage and zero voltage.

In another embodiment, when the active device creating a signal at the selected operating frequency is coupled to the input port, a voltage source is coupled to the input port, and the load is coupled to the output port, the phase angle of the impedance looking into the impedance transformation network through the input port is within a range such that substantially zero voltage derivative switching of the active device occurs. Regarding this range, in specific embodiments, switching of the active device occurs when the slope of the voltage is within a range of -1 and +1, switching of the active device occurs when the slope of the voltage is within a range of -0.5 and +0.5, and/or switching of the active device occurs when the slope of the voltage is within a range of -0.1 and +0.1. In a further specific embodiment, when the active device creating a signal at the selected operating frequency is coupled to the input port, a voltage source is coupled to the input port, and the load is coupled to the output port, the phase angle of the impedance looking into the impedance transformation network through the input port is within a range such that substantially zero voltage-switching and substantially zero voltage derivation switching of the active device occurs. Such switching of the active device can occur when the voltage is within a range of 10% of a peak voltage and zero and when the slope of the voltage is within a range of -1 and +1, when the voltage is within a range of 5% of a peak voltage and zero and when the slope of the voltage is within a range of -0.5 and +0.5, and/or when the voltage is within a range of 1% of a peak voltage and zero and when the slope of the voltage is within a range of -0.1 and +0.1.

When the active device creating a signal at the selected operating frequency is coupled to the input port, a voltage source is coupled to the input port, and the load is coupled to the output port, a real component of the impedance looking into the impedance transformation network through the input port can be within a range such that substantially zero voltage-switching of the active device occurs. Switching of the active device occurs when the voltage is within a range of 10% of a peak voltage and zero voltage, switching of the active device occurs when the voltage is within a range of 5% of a peak voltage and zero voltage, and/or switching of the active device occurs when the voltage is within a range of 1% of a peak voltage and zero voltage. When the active device creating a signal at the selected operating frequency is coupled to the input port, a voltage source is coupled to the input port, and the load is coupled to the output port, the phase angle of the impedance looking into the impedance transformation network through the input port is within a range

such that substantially zero voltage derivative switching of the active device occurs. Switching of the active device occurs when the slope of the voltage is within a range of -1 and +1, switching of the active device occurs when the slope of the voltage is within a range of -0.5 and +0.5, and/or switching of the active device occurs when the slope of the voltage is within a range of -0.1 and +0.1.

When the active device creating a signal at the selected operating frequency is coupled to the input port, a voltage source is coupled to the input port, and the load is coupled to the output port, a phase angle of the impedance looking into the impedance transformation network through the input port can be within a range such that substantially zero current-switching of the active device occurs. Switching of the active device occurs when the current is within a range of 10% of a peak current and zero current, switching of the active device occurs when the current is within a range of 5% of a peak current and zero current, and/or switching of the active device occurs when the current is within a range of 1% of a peak current and zero current. When the active device creating a signal at the selected operating frequency is coupled to the input port, a voltage source is coupled to the input port, and the load is coupled to the output port, the phase angle of the impedance looking into the impedance transformation network through the input port can be within a range such that substantially zero current derivative switching of the active device occurs. Switching of the active device occurs when the slope of the current is within a range of -1 and +1, switching of the active device occurs when the slope of the current is within a range of -0.5 and +0.5, and/or switching of the active device occurs when the slope of the current is within a range of -0.1 and +0.1.

When the active device creating a signal at the selected operating frequency is coupled to the input port, a voltage source is coupled to the input port, and the load is coupled to the output port, a real component of the impedance looking into the impedance transformation network through the input port can be within a range such that substantially zero current-switching of the active device occurs. Switching of the active device occurs when the current is within a range of 10% of a peak current and zero current, switching of the active device occurs when the current is within a range of 5% of a peak current and zero current, and/or switching of the active device occurs when the current is within a range of 1% of a peak current and zero current. When the active device creating a signal at the selected operating frequency is coupled to the input port, a voltage source is coupled to the input port, and the load is coupled to the output port, the phase angle of the impedance looking into the impedance transformation network through the input port can be within a range such that

substantially zero current derivative switching of the active device occurs. Switching of the active device occurs when the slope of the current is within a range of -1 and +1, switching of the active device occurs when the slope of the current is within a range of -0.5 and +0.5, and/or switching of the active device occurs when the slope of the current is within a range of  
5 -0.1 and +0.1.

When the active device creating a signal at the selected operating frequency is coupled to the input port, a voltage is coupled to the input port, and the load is coupled to the output port, the real part of the impedance looking into the impedance transformation network through the input port can be within a range such that the maximum real part of the  
10 impedance looking into the impedance transformation network through the input port is no more than two orders of magnitude greater than the minimum real part of the impedance looking into the impedance transformation network through the input port. A supply network can be connected between the input port and a voltage source, where the supply network is configured to reject harmonics not intended to reach the load. At least one load having a  
15 time-dependent impedance connected to the output port. In another embodiment, the system can be adapted least one load having a time dependent non-negative real resistance can be connected to the output port. In a specific embodiment where the phase angle of the impedance looking into the impedance transformation network through the input port is inductive, the phase angle of the impedance looking into the impedance transformation  
20 network through the input port is between 40 and 85 degrees.

In an embodiment with a shunt network connected between the first terminal of the secondary coil and the second terminal of the secondary coil, where the shunt network has a negative reactance, the shunt network can be configured such that the resistance looking from the secondary coil towards the load is between an upper bound and a lower bound, wherein  
25 the difference between the upper bound and lower bound is less than the difference between the maximum load resistance and minimum resistance. In specific embodiments, the upper bound is 1000 ohms and the lower bound is .01 ohms when the maximum load resistance is 100,000 ohms and the minimum load resistance is 1 ohms, the upper bound is 10 ohms and the lower bound is 1 ohm when the maximum load resistance is 100,000 ohms and the  
30 minimum load resistance is 1 ohms, the upper bound is 10,000 ohms and the lower bound is 500 ohms when the maximum load resistance is 100,000 ohms and the minimum load resistance is 1 ohms, or the upper bound is 1,000,000 ohms and the lower bound is 800,000 ohms when the maximum load resistance is 10,000,000 ohms and the minimum load resistance is 1 ohms. In a further specific embodiment, the at least one shunt network has a

negative reactive value such that the phase angle looking into the primary coil is positively correlated with the load resistance. In a further specific embodiment, the at least one shunt network is configured to have a negative reactive value such that the phase angle looking into the primary coil is negatively correlated with the load resistance, where the reactive network further utilizes at least one additional shunt network connected between a first terminal of the primary coil and a second terminal of the primary coil, the at least one additional shunt network having a positive reactive value such that the phase angle looking into the impedance transformation network through the input port is positively correlated with the load resistance.

The reactive network can further include at least one additional shunt network connected between a first terminal of the primary coil and a second terminal of the primary coil.

The reactive network can include at least one reactive component connected to the primary coil, where the at least one reactive component has a reactance that shifts the phase angle looking into the impedance transformation network through the input port can be within a range such that substantially zero-voltage switching of the active device occurs. In specific embodiments, the impedance transformation network is configured such that the range of resistances looking into the impedance transformation network through the input port is between an upper bound and a lower bound, where the difference between the upper bound and lower bound is less than the difference between the maximum load resistance and the minimum load resistance. In various embodiments, the upper bound is 1000 ohms and the lower bound is .01 ohms when the maximum load resistance is 100,000 ohms and the minimum load resistance is 1 ohms, the upper bound is 10 ohms and the lower bound is 1 ohm when the maximum load resistance is 100,000 ohms and the minimum load resistance is 1 ohms, the upper bound is 10,000 ohms and the lower bound is 500 ohms when the maximum load resistance is 100,000 ohms and the minimum load resistance is 1 ohms, and the upper bound is 1,000,000 ohms and the lower bound is 800,000 ohms when the maximum load resistance is 10,000,000 ohms and the minimum load resistance is 1 ohms.

The at least one filter network having a positive reactance can be connected in series with the primary coil, where a reactance of the at least one filter network divided by a resistance looking from the filter network towards the load has a value between 1.5 and 10.

The impedance transformation network can be configured to couple to two active devices via a single input port. The input port can have at least two input ports for coupling to at least two active devices.

A rectifier can be positioned between the impedance transformation network and the load.

The primary coil can be connected in series with at least one reactive component and the secondary coil can be connected in series with at least one additional reactive component.

5 In another embodiment, the primary coil is connected in series with at least one reactive component and at least one additional reactive component is connected between a first terminal of the secondary coil and a second terminal of the secondary coil. In yet another embodiment, at least one other reactive component is connected between a first terminal of the primary and a second terminal of the primary coil and the secondary coil is connected in  
10 series with at least one additional reactive component. In further embodiments, at least one other reactive component is connected between a first terminal of the primary coil and a second terminal of the primary coil and at least one additional reactive component is connected between a first terminal of the secondary coil and a second terminal of the secondary coil.

15 The primary coil can be a single primary coil inductively coupled to at least two secondary coils. In another embodiment, at least two primary coils are inductively coupled to the secondary coils. In various other embodiments,  $m$  primary coils are inductively coupled to  $n$  secondary coils, where  $m > 1$  and  $n > 1$ .

A specific embodiment relates to a circuit for inductive power transfer having an  
20 impedance transformation network, incorporating an input port for coupling to an active device for creating a signal at a selected operating frequency, an output port for coupling to a load having a variable impedance; and a reactive network coupled between the input port and the output port, wherein the reactive network has a primary coil; and a secondary coil, where the primary coil is inductively coupled to the secondary coil, such that when the output is  
25 coupled to the load having a variable impedance and the input port is coupled to the active device that creates a signal at the selected operating frequency, a phase angle of an impedance looking into the impedance transformation network through the input port is capacitive and positively correlated with the amount of power delivered to the load.

Another embodiment pertains to a circuit for inductive power transfer, having a  
30 primary impedance transformation network, where the primary impedance transformation network has an input port for coupling to an active device that creates a signal at a selected operating frequency, a primary coil for coupling to a secondary coil, and a reactive network coupled to the input port and coupled to the primary coil, where the reactive network incorporates at least one capacitor, and at least one inductor, such that when the primary coil



is coupled to the secondary coil and the input port is coupled to the active device that creates a signal at the selected operating frequency, a phase angle of an impedance looking into the primary impedance transformation network through the input port is inductive and negatively correlated with the amount of power inductively transferred from the primary coil.

5           Another embodiment relates to a circuit for inductive power transfer, having a primary impedance transformation network, where the primary impedance transformation network includes an input port for coupling to an one active device that creates a signal at a selected operating frequency, a primary coil for coupling to a secondary coil, a reactive network coupled to the input port and coupled to the primary coil, where the reactive network  
10 incorporates at least one capacitor, at least one inductor, such that when the primary coil is coupled to the secondary coil and the input port is coupled to the active device that creates a signal at the selected operating frequency, a phase angle of an impedance looking into the primary impedance transformation network through the input port is capacitive and positively correlated with the amount of power inductively transferred from the primary coil.

15           A further embodiment pertains to a circuit for inductive power transfer, having a secondary side impedance transformation network, where the secondary side impedance transformation network incorporates at least one secondary coil for coupling to at least one primary coil, at least one output port for coupling to at least one load having a variable impedance; and a secondary side reactive network coupled to the output port and coupled to  
20 the secondary coil, where the reactive network incorporates at least one capacitor, such that when the secondary coil is coupled to the primary coil, where the primary coil is coupled to a primary side reactive network, where the primary side reactive network has an input port for connection to at least one active device that creates a signal at a selected operating frequency, the a phase angle of an impedance looking into the primary side reactive network through the  
25 input port is inductive and positively correlated with the amount of power inductively transferred from the primary coil.

          A further embodiment is directed to a circuit for inductive power transfer, having a secondary side impedance transformation network, wherein the secondary side impedance transformation network has at least one secondary coil for coupling to at least one primary  
30 coil, at least one output port for coupling to at least one load having a variable impedance; and a secondary side reactive network coupled to the at least one output port and coupled to the at least one secondary coil, wherein the reactive network includes at least one capacitor, such that when the secondary coil is coupled to the primary coil, where the primary coil is coupled to a primary side reactive network, where the primary side reactive network has an

input port for connection to at least one active device that creates a signal at a selected operating frequency, the a phase angle of an impedance looking into the primary side reactive network through the input port is capacitive and negatively correlated with the amount of power inductively transferred from the primary coil.

5           An embodiment of the invention is directed to an apparatus for wireless power transfer, having a rectifier stage, where the rectifier stage is adapted to interconnect with a load; a first impedance transformation network (FITN), where the first impedance transformation network interconnects with the rectifier stage and transforms the impedance looking into the rectifier stage such that the impedance looking into the FITN is such that the  
10 load decouples from the primary coil; a secondary coil, where the secondary coil is interconnected with the FITN such that the power coupled from the primary coil to the secondary coil is received by the FITN; a primary coil, where the primary coil is positioned with respect to the secondary coil such that the primary coil is coupled to the secondary coil, wherein the interaction between the primary coil and secondary coil is such that the  
15 impedance looking into the primary coil has a resistance large enough to maximize power delivery through to the secondary coil; a second impedance transformation network (SITN), where the SITN interconnects with the primary coil and transforms the impedance looking into the primary coil such that the resistance looking into the SITN toward the load is within a usable operating range of the tuned switch-mode inverter, large enough to maximize power  
20 delivery through to the secondary coil; a phase shifting network, where the phase shifting network interconnects with the SITN and transforms the impedance looking into the SITN such that the impedance looking into the phase shifting network has a resistance in the operating range of the tuned switch-mode inverter and a reactive part in the operating range of the tuned switch-mode inverter; a tuned switch-mode inverter, where the tuned switch-  
25 mode inverter is interconnected with the phase shifting network; and a power source, where the power source is interconnected with the tuned switch-mode inverter. In this embodiment, the load can have a load resistance that can range from 0 to 500 ohms.

          An embodiment is an apparatus for wireless power transfer, having a rectifier stage, where the rectifier stage is adapted to interconnect with a load; a secondary coil, where the  
30 secondary coil is interconnected with the rectifier stage; a primary coil, where the primary coil is coupled to the secondary coil; a tuned switch-mode supply, wherein the tuned switch-mode supply is interconnected to the primary coil; a power supply, where the power supply supplies power to the tuned switch-mode supply; a first circuitry interconnected between the tuned switch-mode supply and the primary coil; and a second circuitry interconnected

between the secondary coil and the rectifier stage, such that power output to the load decreases as the impedance of the load increases.

Another embodiment is an apparatus for wireless power transfer, having a rectifier stage, where the rectifier stage is adapted to interconnect with a load; a secondary coil, where  
5 the secondary coil is interconnected with the rectifier stage; a primary coil, where the primary coil is coupled to the secondary coil; a tuned switch-mode supply, where the tuned switch-mode supply is interconnected to the primary coil; a power supply, where the power supply supplies power to the tuned switch-mode supply; a first circuitry interconnected between the  
10 tuned switch-mode supply and the primary coil; and a second circuitry interconnected between the secondary coil and the rectifier stage, such that power output to the load is adjusted as the phase angle of the load changes.

All patents, patent applications, provisional applications, and publications referred to or cited herein are incorporated by reference in their entirety, including all figures and tables, to the extent they are not inconsistent with the explicit teachings of this specification.

15 It should be understood that the examples and embodiments described herein are for illustrative purposes only and that various modifications or changes in light thereof will be suggested to persons skilled in the art and are to be included within the spirit and purview of this application.

20

## CLAIMS

1. A circuit for inductive power transfer, comprising:  
an impedance transformation network, wherein the impedance transformation  
5 network comprises:  
an input port for coupling to an active device for creating a signal at a selected  
operating frequency,  
an output port for coupling to a load having a variable impedance; and  
a reactive network coupled between the input port and the output port, wherein the  
10 reactive network comprises:  
a primary coil;  
a secondary coil, wherein the primary coil is inductively coupled to the  
secondary coil, wherein when the output is coupled to the load having a variable  
impedance and the input port is coupled to the active device that creates a signal at the  
15 selected operating frequency, a phase angle of an impedance looking into the  
impedance transformation network through the input port is inductive and negatively  
correlated with the amount of power delivered to the load.
2. The circuit according to claim 1, wherein a real part of the impedance looking into  
20 the impedance transformation network through the input port is in a range between a  
minimum real part and a maximum real part.
3. The circuit according to claim 2, wherein the maximum real part is less than or  
equal to one order of magnitude greater than the minimum real part.
- 25
4. The circuit according to claim 1, further comprising at least one additional input  
port.
5. The circuit according to claim 1, further comprising at least one additional output  
30 port.
6. The circuit according to claim 1, further comprising at least one additional primary  
coil.

7. The circuit according to claim 1, further comprising at least one additional secondary coil.

8. The circuit according to claim 1, wherein the output port is for coupling to at least two loads.

9. The circuit according to claim 1, wherein the phase angle of the impedance looking into the impedance transformation network through the input port is positively correlated with the resistance of the load.

10

10. The circuit according to claim 1, wherein the phase angle of the impedance looking into the impedance transformation network through the input port is positively correlated with an equivalent resistance of the load.

15

11. The circuit according to claim 1, wherein the phase angle of the impedance looking into the impedance transformation network through the input port is positively correlated with an equivalent resistance of the load, wherein when the impedance looking to the primary coil,  $Z_{in}$ , is explained by:

$$Z_{in} = \{1_{1M} [Z^{IV} - (Z^{II})^T (Z^I)^{-1} Z^{II}]^{-1} 1_{M1}\}$$

$$Z = \begin{bmatrix} Z^{III} & (Z^{II})^T \\ Z^{II} & Z^I \end{bmatrix}$$

$$Z_{ab} = \begin{cases} j\omega L_a + R_a & \text{for } a = b \\ j\omega M_{ab} & \text{otherwise} \end{cases}$$

$$Z^{IV} = Z^{III} + Z_{in} 1_{MM}$$

20  $Z_{in}$ : Input impedance looking into the primary coil

$1_{1M}$ : Vector of 1's of length M

$1_{MM}$ : M X M matrix of 1's

Z: Impedance matrix

$Z_{ab}$ : Element ab of the impedance matrix

$Z^I$ : Sub-matrix of Z

$Z^{II}$ : Sub-matrix of Z

5  $Z^{III}$ : Sub-matrix of Z

$M_{ab}$ : Mutual inductance between the a<sup>th</sup> and b<sup>th</sup> coil

j: imaginary number

a: coil index

b: coil index

10  $\omega$ : radian frequency

$R_a$ : Parasitic resistance of the a<sup>th</sup> coil

$L_a$ : Self inductance of the a<sup>th</sup> coil

12. The circuit according to claim 1, wherein the reactive network further comprises  
 15 at least one shunt network with a negative reactance that is connected between a first terminal of the secondary coil and a second terminal of the secondary coil.

13. The circuit according to claim 12, wherein the at least one shunt network with a  
 20 negative reactance comprises a capacitor.

14. The circuit according to claim 1, wherein the active device comprises a transistor.

15. The circuit according to claim 1 wherein the active device comprises:  
 25 a switching component that operates substantially as a switch; and  
 a capacitance in parallel with the switching component.

16. The circuit according to claim 1 wherein the input port is coupled to a voltage  
 source.

30 17. The circuit according to claim 1, wherein the input port is coupled to a current  
 source.

18. The circuit according to claim 1 comprising a supply network connected between the input port and a voltage source, wherein the supply network comprises at least one inductor.

5

19. The circuit according to claim 1 comprising a supply network connected between the input port and a voltage source, wherein the supply network is configured to reject harmonics not intended to reach the load.

10

20. The circuit according to claim 1, comprising a supply network connected between the input port and a voltage source, wherein the elements of the supply network, load network, and the active device represent at least one class D inverter or variant.

15

21. The circuit according to claim 1, comprising a supply network connected between the input port and a voltage source, wherein the elements of the supply network, load network, and the active device represent at least one class DE inverter or variant.

20

22. The circuit according to claim 1, comprising a supply network connected between the input port and a voltage source, wherein the elements of the supply network, load network, and the active device represent at least one class E inverter or variant.

25

23. The circuit according to claim 1, comprising a supply network connected between the input port and a voltage source, wherein the elements of the supply network, load network, and the active device represent at least one class E<sup>-1</sup> inverter or variant.

30

24. The circuit according to claim 1, comprising a supply network connected between the input port and a voltage source, wherein the elements of the supply network, load network, and the active device represent at least one class F inverter or variant.

25. The circuit according to claim 1, comprising a supply network connected between the input port and a voltage source, wherein the elements of the supply network, load network, and the active device represent at least one class F<sup>-1</sup> inverter or variant.

26. The circuit according to claim 1, comprising a supply network connected between the input port and a voltage source, wherein the elements of the supply network, load network, and the active device represent at least one class  $EF^{-1}$  inverter or variant.

5 27. The circuit according to claim 1, comprising a supply network connected between the input port and a voltage source, wherein the elements of the supply network, load network, and the active device represent at least one class Phi inverter or variant.

28. The circuit according to claim 1, wherein the signal is an AC signal.

10

29. The circuit according to claim 1, wherein the signal is a periodic signal.

30. The circuit according to claim 1, wherein when the active device creating a signal at the selected operating frequency is coupled to the input port, a voltage source is coupled to the input port, and the load is coupled to the output port, the phase angle of the impedance looking into the impedance transformation network through the input port is within a range such that substantially zero voltage-switching of the active device occurs.

15

31. The circuit according to claim 30, wherein switching of the active device occurs when the voltage is within a range of 10% of a peak voltage and zero voltage.

20

32. The circuit according to claim 30, wherein switching of the active device occurs when the voltage is within a range of 5% of a peak voltage and zero voltage.

25 33. The circuit according to claim 30, wherein switching of the active device occurs when the voltage is within a range of 1% of a peak voltage and zero voltage.

25

34. The circuit according to claim 1, wherein when the active device creating a signal at the selected operating frequency is coupled to the input port, a voltage source is coupled to the input port, and the load is coupled to the output port, the phase angle of the impedance looking into the impedance transformation network through the input port is within a range such that substantially zero voltage derivative switching of the active device occurs.

30



35. The circuit according to claim 34, wherein switching of the active device occurs when the slope of the voltage is within a range of -1 and +1.

5 36. The circuit according to claim 34, wherein switching of the active device occurs when the slope of the voltage is within a range of -0.5 and +0.5.

37. The circuit according to claim 34, wherein switching of the active device occurs when the slope of the voltage is within a range of -0.1 and +0.1.

10 38. The circuit according to claim 1, wherein when the active device creating a signal at the selected operating frequency is coupled to the input port, a voltage source is coupled to the input port, and the load is coupled to the output port, the phase angle of the impedance looking into the impedance transformation network through the input port is within a range such that substantially zero voltage-switching and substantially zero voltage derivation  
15 switching of the active device occurs.

39. The circuit according to claim 38, wherein switching of the active device occurs when the voltage is within a range of 10% of a peak voltage and zero and when the slope of the voltage is within a range of -1 and +1.

20

40. The circuit according to claim 38, wherein switching of the active device occurs when the voltage is within a range of 5% of a peak voltage and zero and when the slope of the voltage is within a range of -0.5 and +0.5.

25

41. The circuit according to claim 38, wherein switching of the active device occurs when the voltage is within a range of 1% of a peak voltage and zero and when the slope of the voltage is within a range of -0.1 and +0.1.

30

42. The circuit according to claim 1, wherein when the active device creating a signal at the selected operating frequency is coupled to the input port, a voltage source is coupled to the input port, and the load is coupled to the output port, a real component of the impedance looking into the impedance transformation network through the input port is within a range such that substantially zero voltage-switching of the active device occurs.

43. The circuit according to claim 42, wherein switching of the active device occurs when the voltage is within a range of 10% of a peak voltage and zero voltage.

5 44. The circuit according to claim 42, wherein switching of the active device occurs when the voltage is within a range of 5% of a peak voltage and zero voltage.

45. The circuit according to claim 42, wherein switching of the active device occurs when the voltage is within a range of 1% of a peak voltage and zero voltage.

10 46. The circuit according to claim 1, wherein when the active device creating a signal at the selected operating frequency is coupled to the input port, a voltage source is coupled to the input port, and the load is coupled to the output port, the phase angle of the impedance looking into the impedance transformation network through the input port is within a range such that substantially zero voltage derivative switching of the active device occurs.

15

47. The circuit according to claim 46, wherein switching of the active device occurs when the slope of the voltage is within a range of -1 and +1.

20 48. The circuit according to claim 46, wherein switching of the active device occurs when the slope of the voltage is within a range of -0.5 and +0.5.

49. The circuit according to claim 46, wherein switching of the active device occurs when the slope of the voltage is within a range of -0.1 and +0.1.

25 50. The circuit according to claim 1, wherein when the active device creating a signal at the selected operating frequency is coupled to the input port, a voltage source is coupled to the input port, and the load is coupled to the output port, a phase angle of the impedance looking into the impedance transformation network through the input port is within a range such that substantially zero current-switching of the active device occurs.

30

51. The circuit according to claim 50, wherein switching of the active device occurs when the current is within a range of 10% of a peak current and zero current.

52. The circuit according to claim 50, wherein switching of the active device occurs when the current is within a range of 5% of a peak current and zero current.

53. The circuit according to claim 50, wherein switching of the active device occurs  
5 when the current is within a range of 1% of a peak current and zero current.

54. The circuit according to claim 1, wherein when the active device creating a signal at the selected operating frequency is coupled to the input port, a voltage source is coupled to the input port, and the load is coupled to the output port, the phase angle of the impedance  
10 looking into the impedance transformation network through the input port is within a range such that substantially zero current derivative switching of the active device occurs.

55. The circuit according to claim 54, wherein switching of the active device occurs when the slope of the current is within a range of -1 and +1.  
15

56. The circuit according to claim 54, wherein switching of the active device occurs when the slope of the current is within a range of -0.5 and +0.5.

57. The circuit according to claim 54, wherein switching of the active device occurs  
20 when the slope of the current is within a range of -0.1 and +0.1.

58. The circuit according to claim 1, wherein when the active device creating a signal at the selected operating frequency is coupled to the input port, a voltage source is coupled to the input port, and the load is coupled to the output port, a real component of the impedance  
25 looking into the impedance transformation network through the input port is within a range such that substantially zero current-switching of the active device occurs.

59. The circuit according to claim 58, wherein switching of the active device occurs when the current is within a range of 10% of a peak current and zero current.  
30

60. The circuit according to claim 58, wherein switching of the active device occurs when the current is within a range of 5% of a peak current and zero current.

61. The circuit according to claim 58, wherein switching of the active device occurs when the current is within a range of 1% of a peak current and zero current.

5 62. The circuit according to claim 1, wherein when the active device creating a signal at the selected operating frequency is coupled to the input port, a voltage source is coupled to the input port, and the load is coupled to the output port, the phase angle of the impedance looking into the impedance transformation network through the input port is within a range such that substantially zero current derivative switching of the active device occurs.

10 63. The circuit according to claim 62, wherein switching of the active device occurs when the slope of the current is within a range of -1 and +1.

64. The circuit according to claim 62, wherein switching of the active device occurs when the slope of the current is within a range of -0.5 and +0.5.

15

65. The circuit according to claim 62, wherein switching of the active device occurs when the slope of the current is within a range of -0.1 and +0.1.

20 66. The circuit according to claim 1, wherein when the active device creating a signal at the selected operating frequency is coupled to the input port, a voltage is coupled to the input port, and the load is coupled to the output port, the real part of the impedance looking into the impedance transformation network through the input port is within a range such that the maximum real part of the impedance looking into the impedance transformation network through the input port is no more than two orders of magnitude greater than the minimum real part of the impedance looking into the impedance transformation network through the input port.

25

30 67. The circuit according to any of claims 27 – 31, comprising a supply network connected between the input port and a voltage source, wherein the supply network is configured to reject harmonics not intended to reach the load.

68. The circuit according to claim 1, comprising at least one load connected to the output port, the load having a time-dependent impedance.

69. The circuit according to claim 1, comprising at least one load connected to the output port, the load having a time dependent non-negative real resistance.

5 70. The circuit according to claim 1, wherein the phase angle of the impedance looking into the impedance transformation network through the input port is inductive.

10 71. The circuit according to claim 1, wherein the phase angle of the impedance looking into the impedance transformation network through the input port is between 40 and 85 degrees.

15 72. The circuit according to claim 12, wherein the shunt network is configured such that the resistance looking from the secondary coil towards the load is between an upper bound and a lower bound, wherein the difference between the upper bound and lower bound is less than the difference between the maximum load resistance and minimum resistance.

20 73. The circuit according to claim 72, wherein the upper bound is 1000 ohms and the lower bound is .01 ohms when the maximum load resistance is 100,000 ohms and the minimum load resistance is 1 ohms.

25 74. The circuit according to claim 72, wherein the upper bound is 10 ohms and the lower bound is 1 ohm when the maximum load resistance is 100,000 ohms and the minimum load resistance is 1 ohms.

30 75. The circuit according to claim 72, wherein the upper bound is 10,000 ohms and the lower bound is 500 ohms when the maximum load resistance is 100,000 ohms and the minimum load resistance is 1 ohms.

76. The circuit according to claim 72, wherein the upper bound is 1,000,000 ohms and the lower bound is 800,000 ohms when the maximum load resistance is 10,000,000 ohms and the minimum load resistance is 1 ohms.

77. The circuit according to claim 12, wherein the at least one shunt network has a negative reactive value such that the phase angle looking into the primary coil is positively correlated with the load resistance.

78. The circuit according to claim 12, wherein the at least one shunt network is configured to have a negative reactive value such that the phase angle looking into the primary coil is negatively correlated with the load resistance, wherein the reactive network further comprises at least one additional shunt network connected between a first terminal of the primary coil and a second terminal of the primary coil, wherein the at least one additional shunt network has a positive reactive value such that the phase angle looking into the impedance transformation network through the input port is positively correlated with the load resistance.

10

79. The circuit according to claim 1, wherein the reactive network further comprises at least one additional shunt network connected between a first terminal of the primary coil and a second terminal of the primary coil.

15

80. The circuit according to claim 78, wherein the at least one additional shunt network has a positive reactive value such that the phase angle looking into the impedance transformation network through the input port is positively correlated with the load resistance.

20

81. The circuit according to claim 1, wherein the reactive network comprises at least one reactive component connected to the primary coil, wherein the at least one reactive component has a reactance that shifts the phase angle looking into the impedance transformation network through the input port is within a range such that substantially zero-voltage switching of the active device occurs.

25

82. The circuit according to claim 1, wherein impedance transformation network is configured such that the range of resistances looking into the impedance transformation network through the input port is between an upper bound and a lower bound, wherein the difference between the upper bound and lower bound is less than the difference between the maximum load resistance and the minimum load resistance.

30

83. The circuit according to claim 82, wherein the upper bound is 1000 ohms and the lower bound is .01 ohms when the maximum load resistance is 100,000 ohms and the minimum load resistance is 1 ohms.

84. The circuit according to claim 82, wherein the upper bound is 10 ohms and the lower bound is 1 ohm when the maximum load resistance is 100,000 ohms and the minimum load resistance is 1 ohms.

5

85. The circuit according to claim 82, wherein the upper bound is 10,000 ohms and the lower bound is 500 ohms when the maximum load resistance is 100,000 ohms and the minimum load resistance is 1 ohms.

10

86. The circuit according to claim 82, wherein the upper bound is 1,000,000 ohms and the lower bound is 800,000 ohms when the maximum load resistance is 10,000,000 ohms and the minimum load resistance is 1 ohms.

15

87. The circuit according to claim 1, wherein at least one filter network having a positive reactance is connected in series with the primary coil, wherein a reactance of the at least one filter network divided by a resistance looking from the filter network towards the load has a value between 1.5 and 10.

20

88. The circuit according to claim 1, wherein the impedance transformation network is configured to couple to two active devices via a single input port.

89. The circuit according to claim 1, wherein the input port comprises at least two input ports for coupling to at least two active devices.

25

90. The circuit according to claim 1, wherein the load is resistive.

91. The circuit according to claim 1, wherein the load is reactive.

30

92. The circuit according to claim 1, wherein the load comprises resistive and reactive components.

93. The circuit according to claim 1, wherein a rectifier is positioned between the impedance transformation network and the load.

94. The circuit according to claim 93, wherein the load comprises a portable electronic device.

95. The circuit according to claim 94, wherein the load comprises:

- 5 a voltage regulator;  
a power management system; and  
a battery.

10 96. The circuit according to claim 1, wherein the primary coil is connected in series with at least one reactive component and the secondary coil is connected in series with at least one additional reactive component.

15 97. The circuit according to claim 1, wherein the primary coil is connected in series with at least one reactive component and at least one additional reactive component is connected between a first terminal of the secondary coil and a second terminal of the secondary coil.

20 98. The circuit according to claim 1, wherein at least one other reactive component is connected between a first terminal of the primary and a second terminal of the primary coil and the secondary coil is connected in series with at least one additional reactive component.

25 99. The circuit according to claim 1, wherein at least one other reactive component is connected between a first terminal of the primary coil and a second terminal of the primary coil and at least one additional reactive component is connected between a first terminal of the secondary coil and a second terminal of the secondary coil.

100. The circuit according to claim 1, wherein the primary coil is a single primary coil inductively coupled to at least two secondary coils.

30 101. The circuit according to claim 1, wherein the at least two primary coils are inductively coupled to the secondary coils.

102. The circuit according to claim 1, wherein  $m$  primary coils are inductively coupled to  $n$  secondary coils, where  $m > 1$  and  $n > 1$ .



103. A circuit for inductive power transfer, comprising:

an impedance transformation network, wherein the impedance transformation  
5 network comprises:

an input port for coupling to an active device for creating a signal at a selected  
operating frequency,

an output port for coupling to a load having a variable impedance; and

10 a reactive network coupled between the input port and the output port, wherein the  
reactive network comprises:

a primary coil;

a secondary coil, wherein the primary coil is inductively coupled to the  
secondary coil, wherein when the output is coupled to the load having a variable  
impedance and the input port is coupled to the active device that creates a signal at the  
15 selected operating frequency, a phase angle of an impedance looking into the  
impedance transformation network through the input port is capacitive and positively  
correlated with the amount of power delivered to the load.

104. A circuit for inductive power transfer, comprising:

20 a primary impedance transformation network, wherein the primary impedance  
transformation network comprises:

an input port for coupling to a active device that creates a signal at a selected  
operating frequency,

a primary coil for coupling to a secondary coil

25 a reactive network coupled to the input port and coupled to the primary coil,  
wherein the reactive network comprises:

at least one capacitor

at least one inductor

30 wherein when the primary coil is coupled to the secondary coil and the input port is  
coupled to the active device that creates a signal at the selected operating frequency, a phase  
angle of an impedance looking into the primary impedance transformation network through  
the input port is inductive and negatively correlated with the amount of power inductively  
transferred from the primary coil.

105. A circuit for inductive power transfer, comprising:

a primary impedance transformation network, wherein the primary impedance transformation network comprises:

an input port for coupling to an one active device that creates a signal at a selected operating frequency,

a primary coil for coupling to a secondary coil

a reactive network coupled to the input port and coupled to the primary coil, wherein the reactive network comprises:

at least one capacitor

at least one inductor

wherein when the primary coil is coupled to the secondary coil and the input port is coupled to the active device that creates a signal at the selected operating frequency, a phase angle of an impedance looking into the primary impedance transformation network through the input port is capacitive and positively correlated with the amount of power inductively transferred from the primary coil.

106. A circuit for inductive power transfer, comprising:

a secondary side impedance transformation network, wherein the secondary side impedance transformation network comprises:

at least one secondary coil for coupling to at least one primary coil

at least one output port for coupling to at least one load having a variable impedance; and

a secondary side reactive network coupled to the output port and coupled to the secondary coil, wherein the reactive network comprises:

at least one capacitor

wherein when the secondary coil is coupled to the primary coil wherein the primary coil is coupled to a primary side reactive network

wherein the primary side reactive network comprises an input port for connection to at least one active device that creates a signal at a selected operating frequency

the a phase angle of an impedance looking into the primary side reactive network through the input port is inductive and positively correlated with the amount of power inductively transferred from the primary coil.

107. A circuit for inductive power transfer, comprising:

a secondary side impedance transformation network, wherein the secondary side impedance transformation network comprises:

at least one secondary coil for coupling to at least one primary coil

5 at least one output port for coupling to at least one load having a variable impedance; and

a secondary side reactive network coupled to the at least one output port and coupled to the at least one secondary coil, wherein the reactive network comprises:

at least one capacitor

10 wherein when the secondary coil is coupled to the primary coil wherein the primary coil is coupled to a primary side reactive network

wherein the primary side reactive network comprises an input port for connection to at least one active device that creates a signal at a selected operating frequency

15 the a phase angle of an impedance looking into the primary side reactive network through the input port is capacitive and negatively correlated with the amount of power inductively transferred from the primary coil.

108. An apparatus for wireless power transfer, comprising:

a rectifier stage, wherein the rectifier stage is adapted to interconnect with a load;

20 a first impedance transformation network (FITN), wherein the first impedance transformation network interconnects with the rectifier stage and transforms the impedance looking into the rectifier stage such that the impedance looking into the FITN is such that the load decouples from the primary coil;

25 a secondary coil, wherein the secondary coil is interconnected with the FITN such that the power coupled from the primary coil to the secondary coil is received by the FITN;

30 a primary coil, wherein the primary coil is positioned with respect to the secondary coil such that the primary coil is coupled to the secondary coil, wherein the interaction between the primary coil and secondary coil is such that the impedance looking into the primary coil has a resistance large enough to maximize power delivery through to the secondary coil;

a second impedance transformation network (SITN), wherein the SITN interconnects with the primary coil and transforms the impedance looking into the primary coil such that the resistance looking into the SITN toward the load is within a usable operating range of the

tuned switch-mode inverter, large enough to maximize power delivery through to the secondary coil;

5 a phase shifting network, wherein the phase shifting network interconnects with the SITN and transforms the impedance looking into the SITN such that the impedance looking into the phase shifting network has a resistance in the operating range of the tuned switch-mode inverter and a reactive part in the operating range of the tuned switch-mode inverter;

a tuned switch-mode inverter, wherein the tuned switch-mode inverter is interconnected with the phase shifting network; and

10 a power source, wherein the power source is interconnected with the tuned switch-mode inverter.

109. The apparatus according to claim 108, wherein the load has a load resistance that can range from 0 to 500 ohms.

15 110. An apparatus for wireless power transfer, comprising:

a rectifier stage, wherein the rectifier stage is adapted to interconnect with a load;

a secondary coil, wherein the secondary coil is interconnected with the rectifier stage;

a primary coil, wherein the primary coil is coupled to the secondary coil;

20 a tuned switch-mode supply, wherein the tuned switch-mode supply is interconnected to the primary coil;

a power supply, wherein the power supply supplies power to the tuned switch-mode supply;

a first circuitry interconnected between the tuned switch-mode supply and the primary coil; and

25 a second circuitry interconnected between the secondary coil and the rectifier stage, wherein power output to the load decreases as the impedance of the load increases.

111. An apparatus for wireless power transfer, comprising:

a rectifier stage, wherein the rectifier stage is adapted to interconnect with a load;

30 a secondary coil, wherein the secondary coil is interconnected with the rectifier stage;

a primary coil, wherein the primary coil is coupled to the secondary coil;

a tuned switch-mode supply, wherein the tuned switch-mode supply is interconnected to the primary coil;

a power supply, wherein the power supply supplies power to the tuned switch-mode supply;

a first circuitry interconnected between the tuned switch-mode supply and the primary coil; and

5 a second circuitry interconnected between the secondary coil and the rectifier stage, wherein power output to the load is adjusted as the phase angle of the load changes.

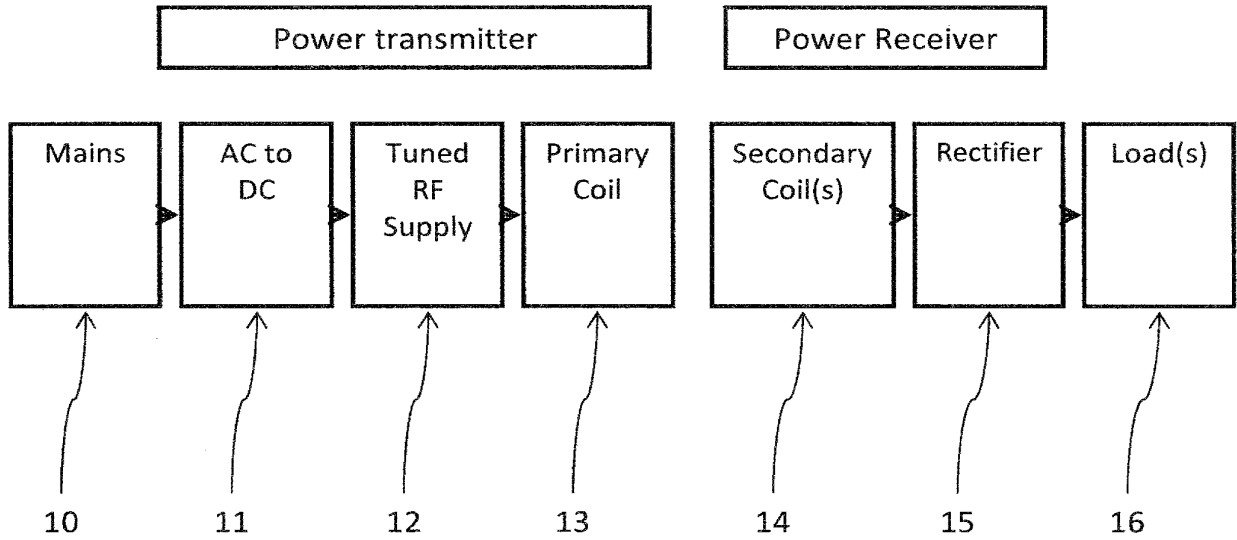


FIG. 1

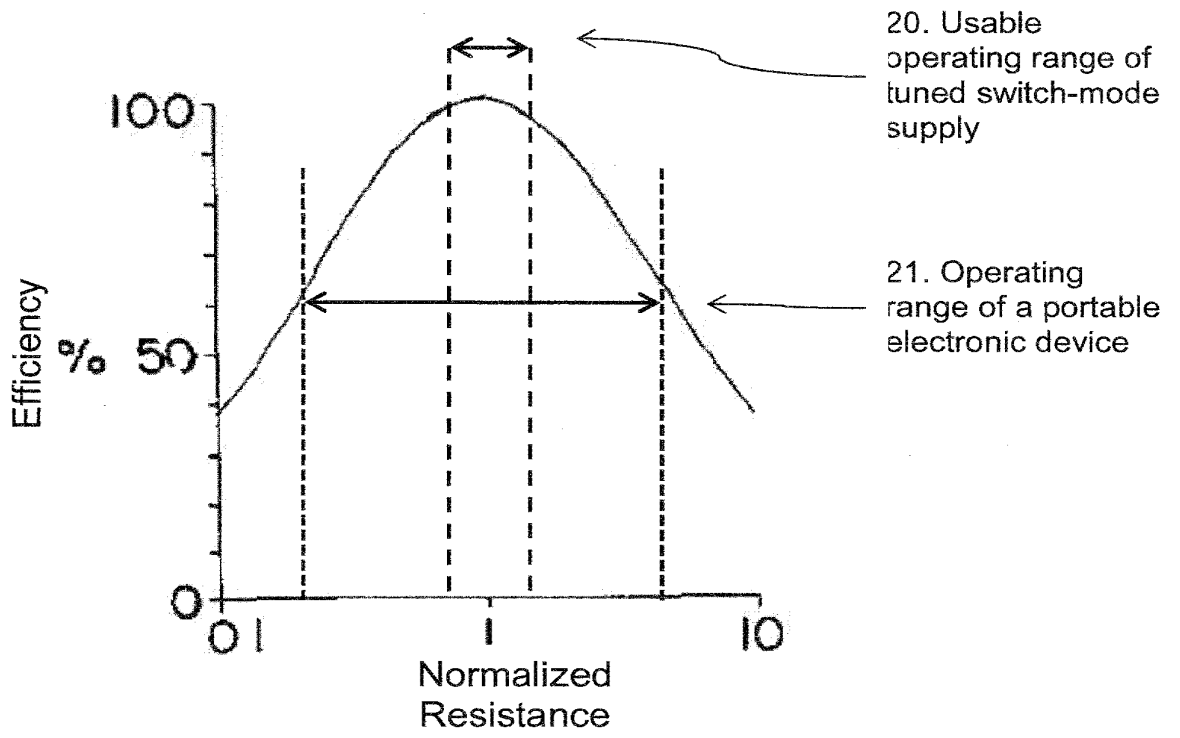


FIG. 2

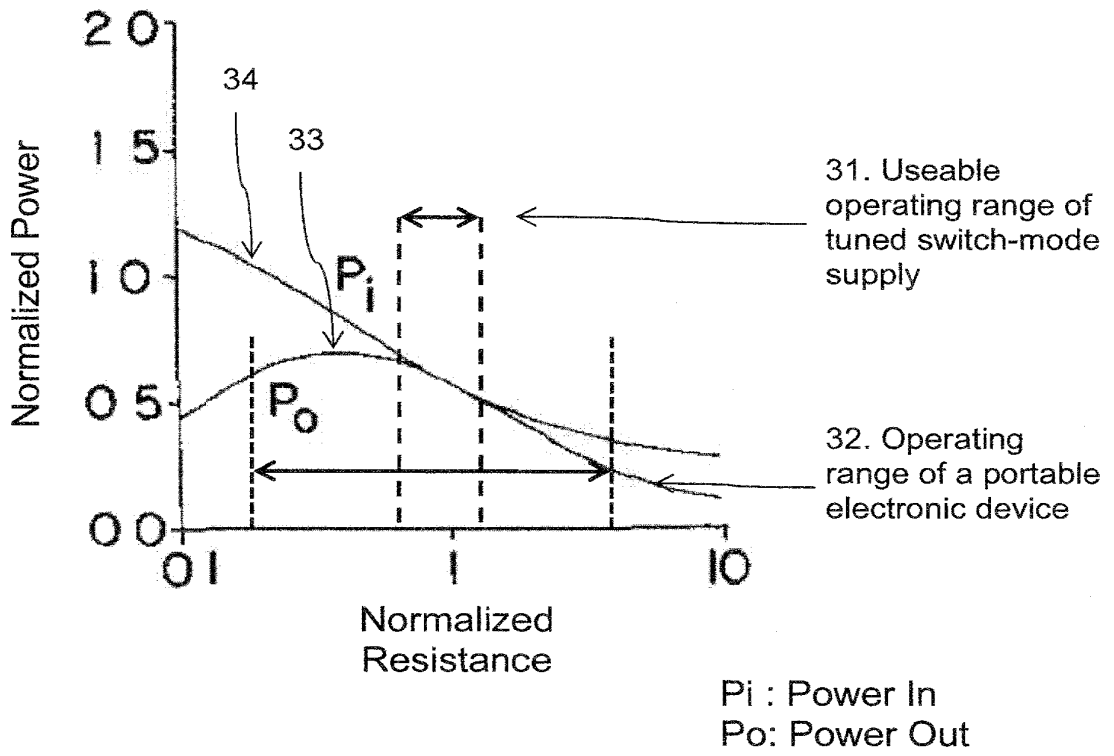


FIG. 3



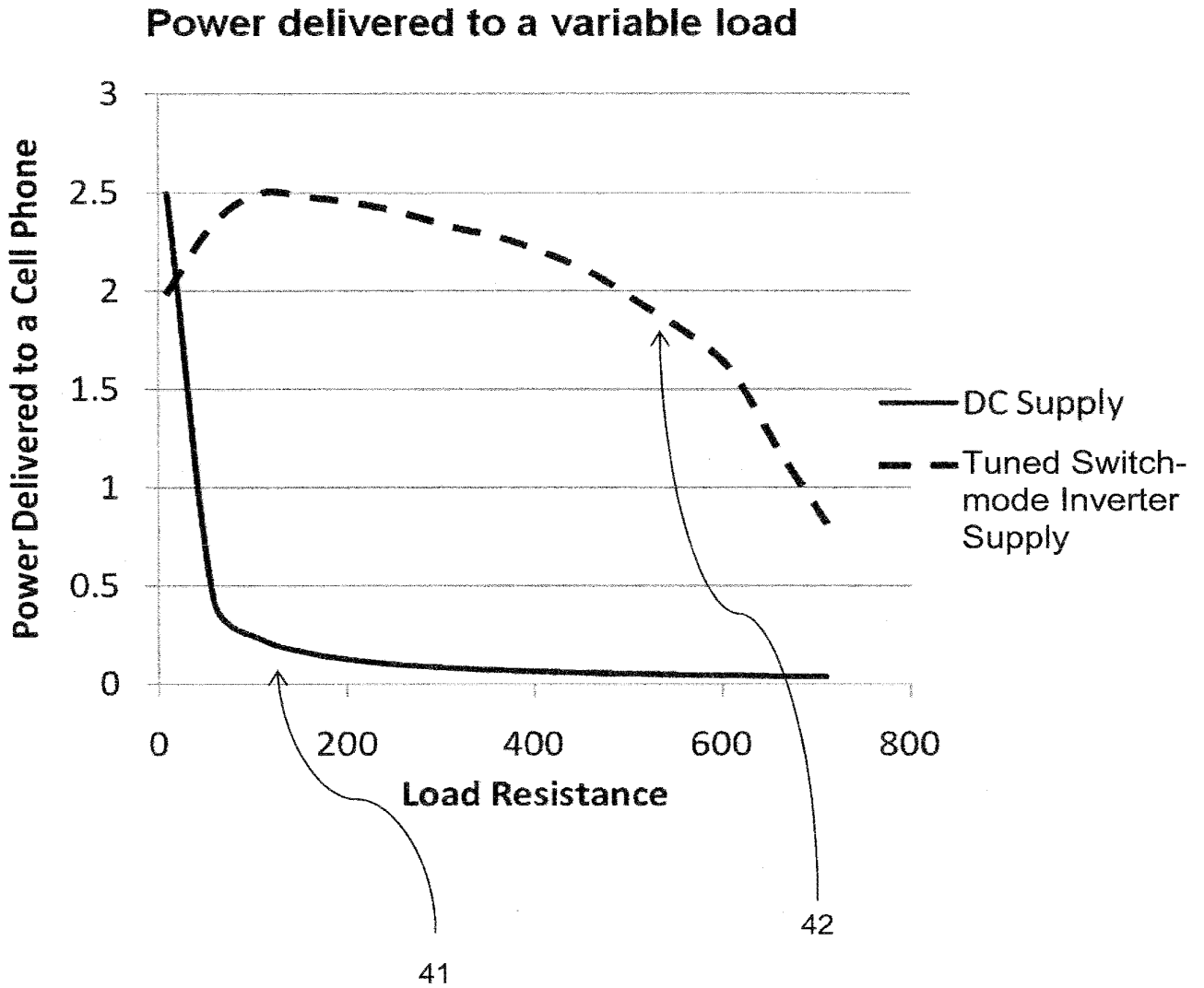
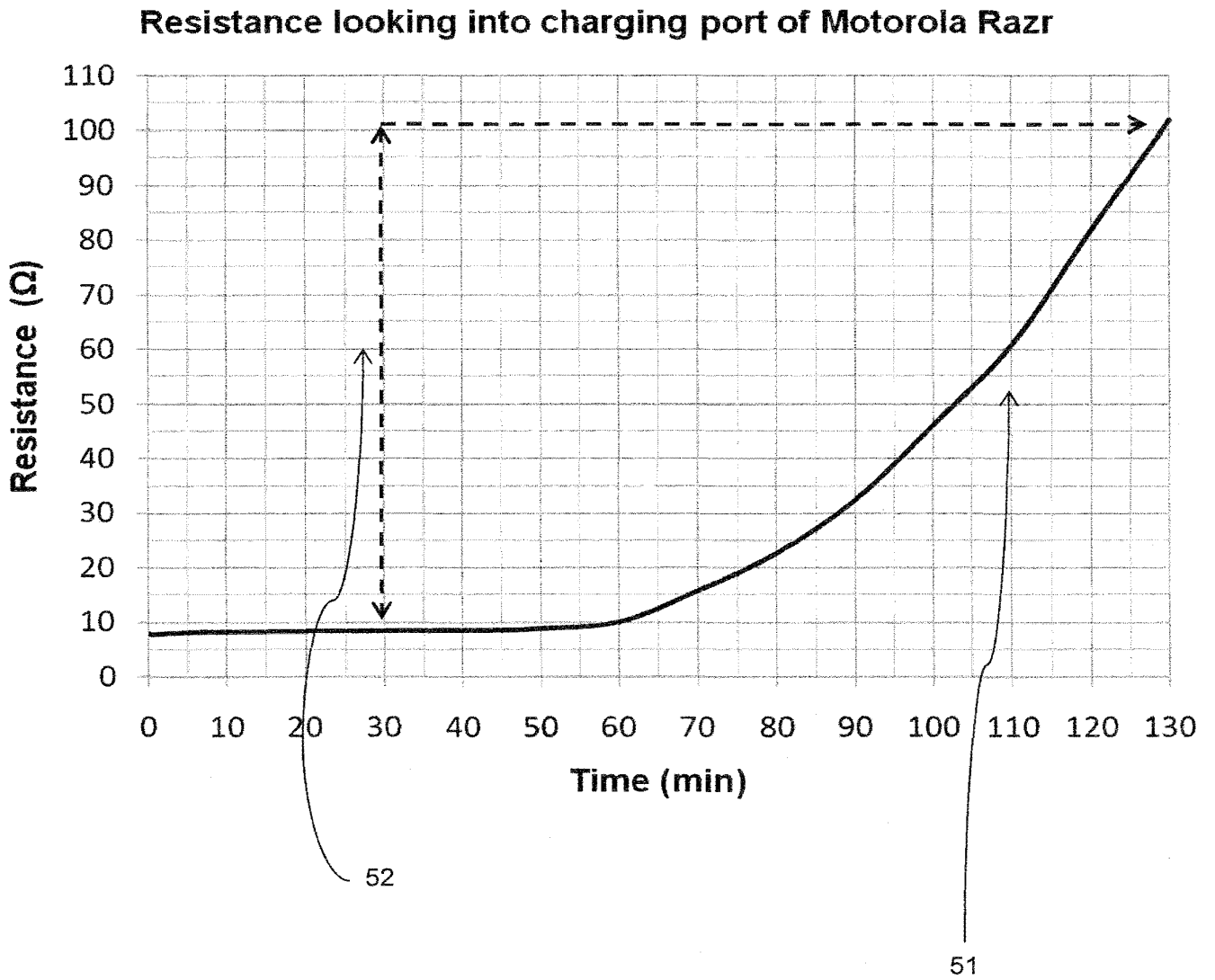


FIG. 4



**FIG. 5**

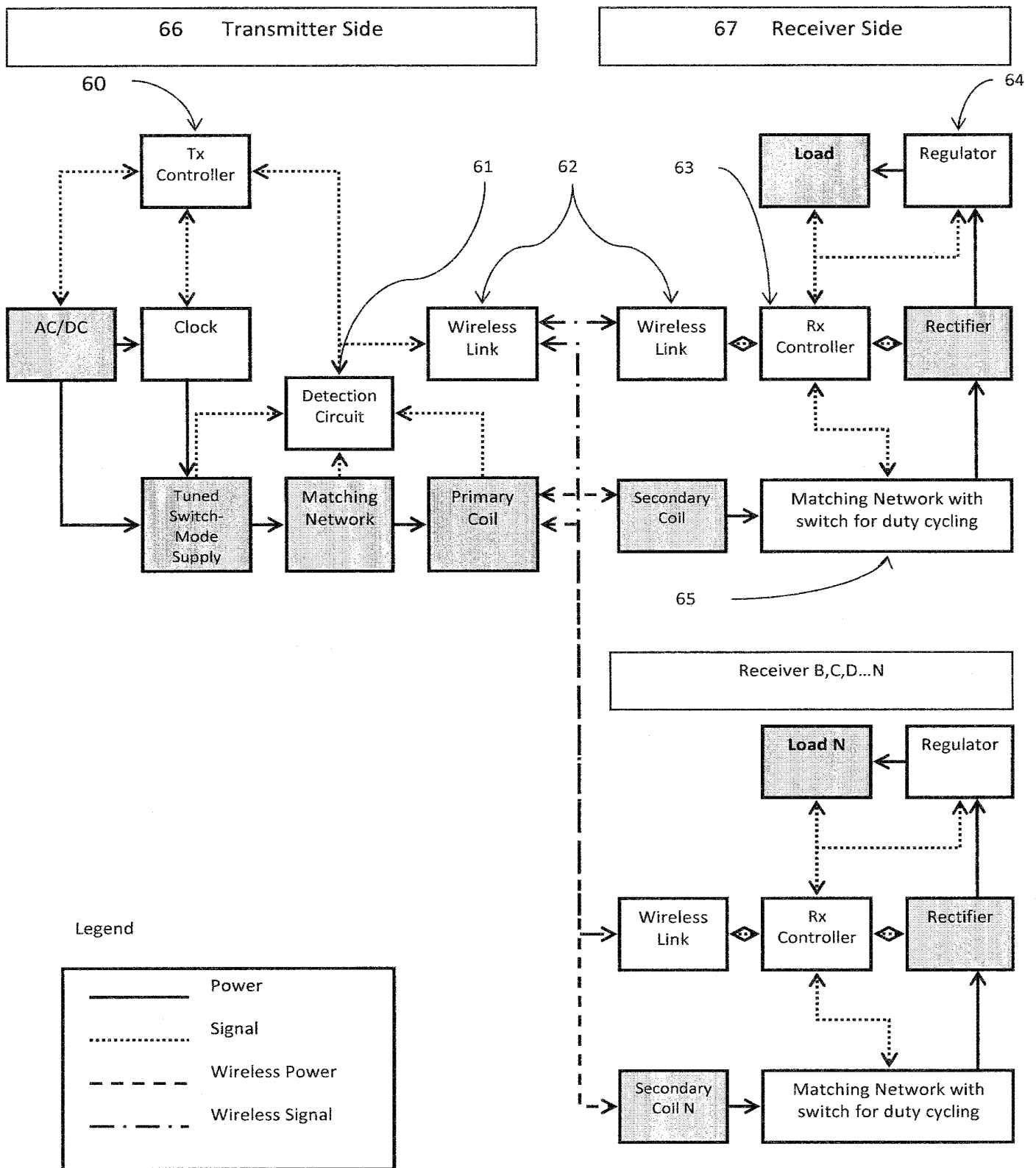
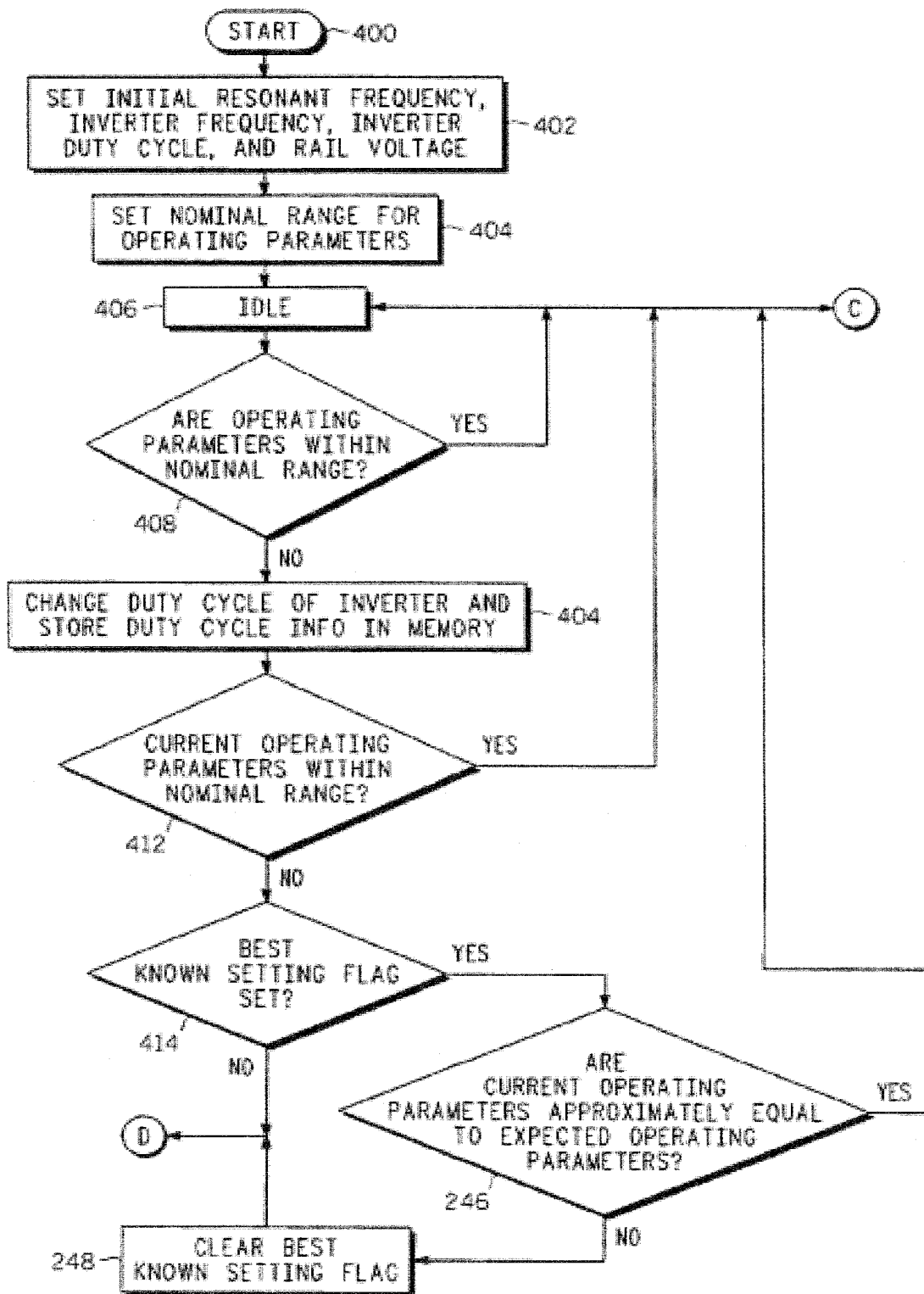
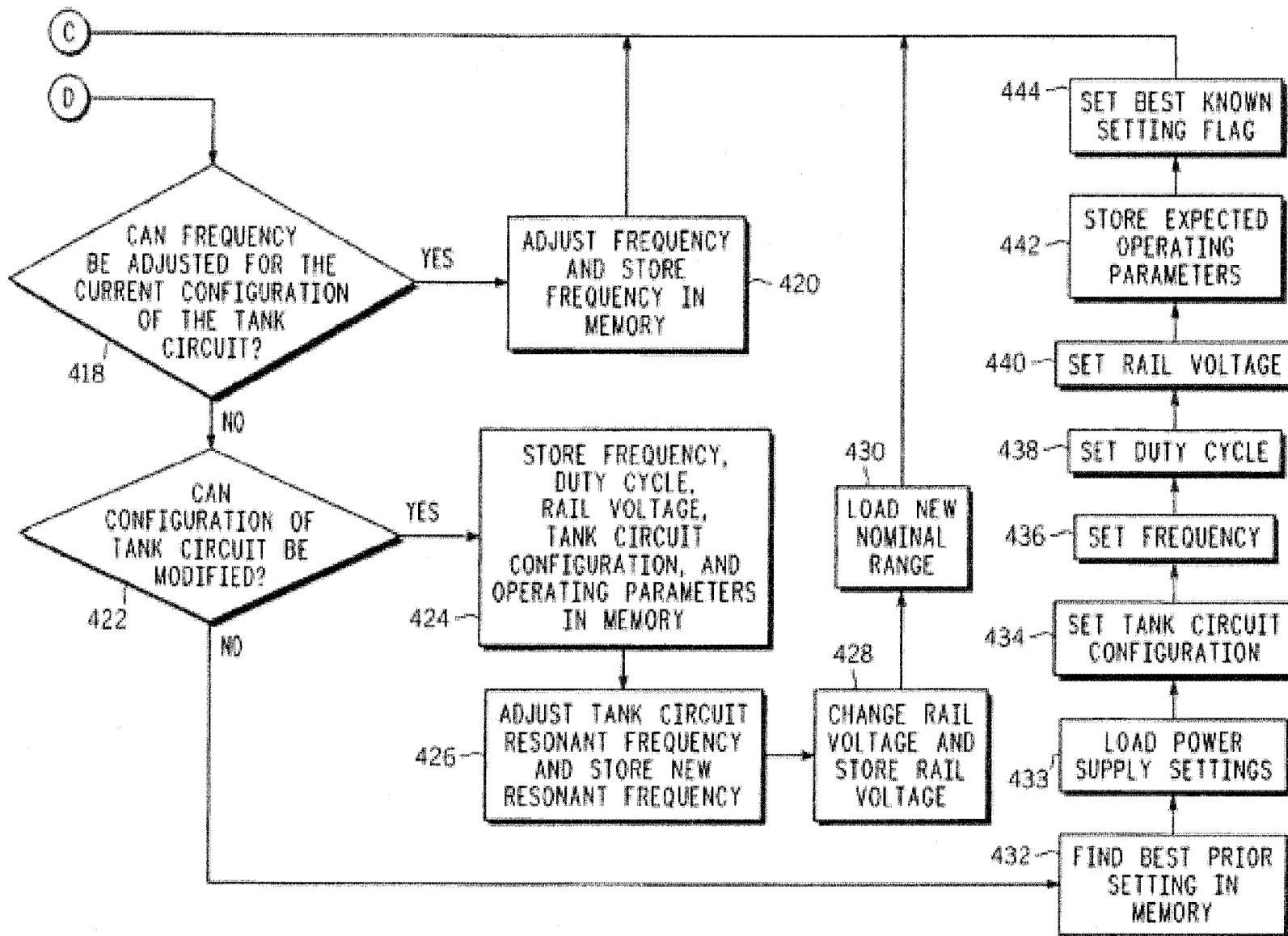


FIG. 6



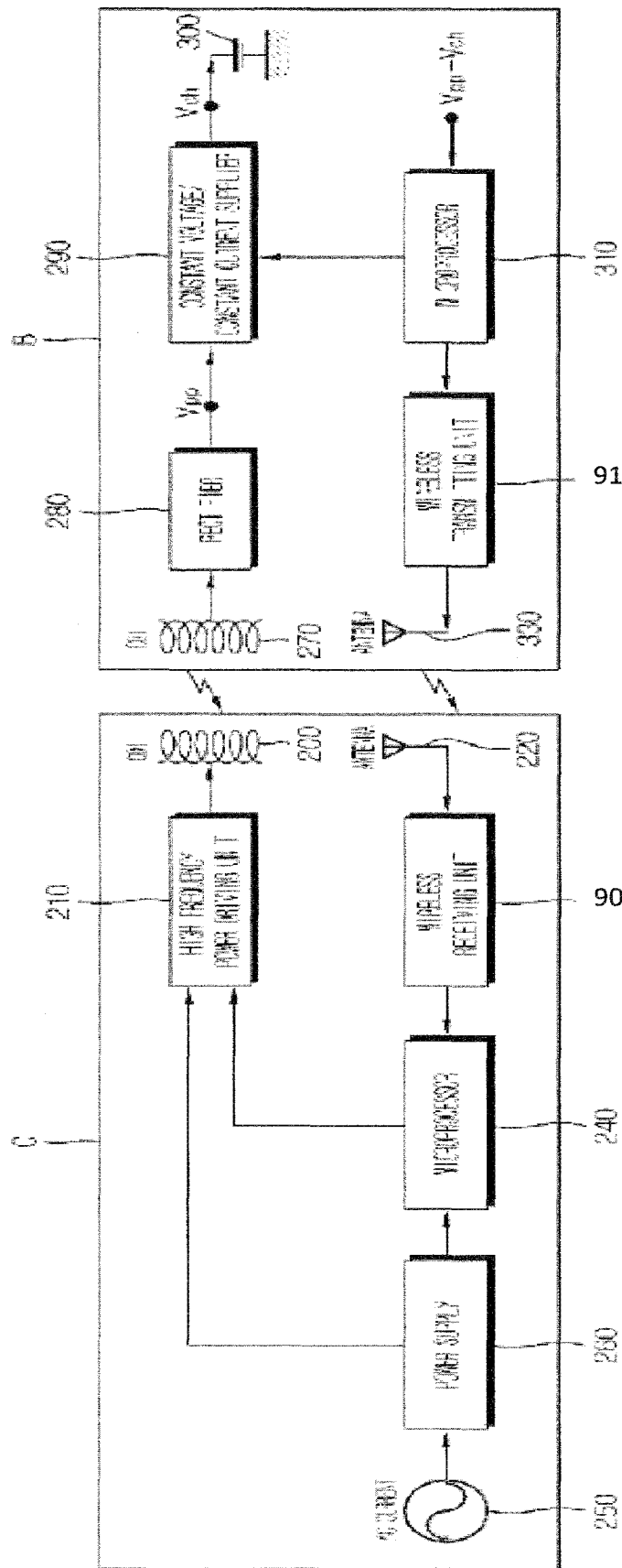
(PRIOR ART)

FIG. 7



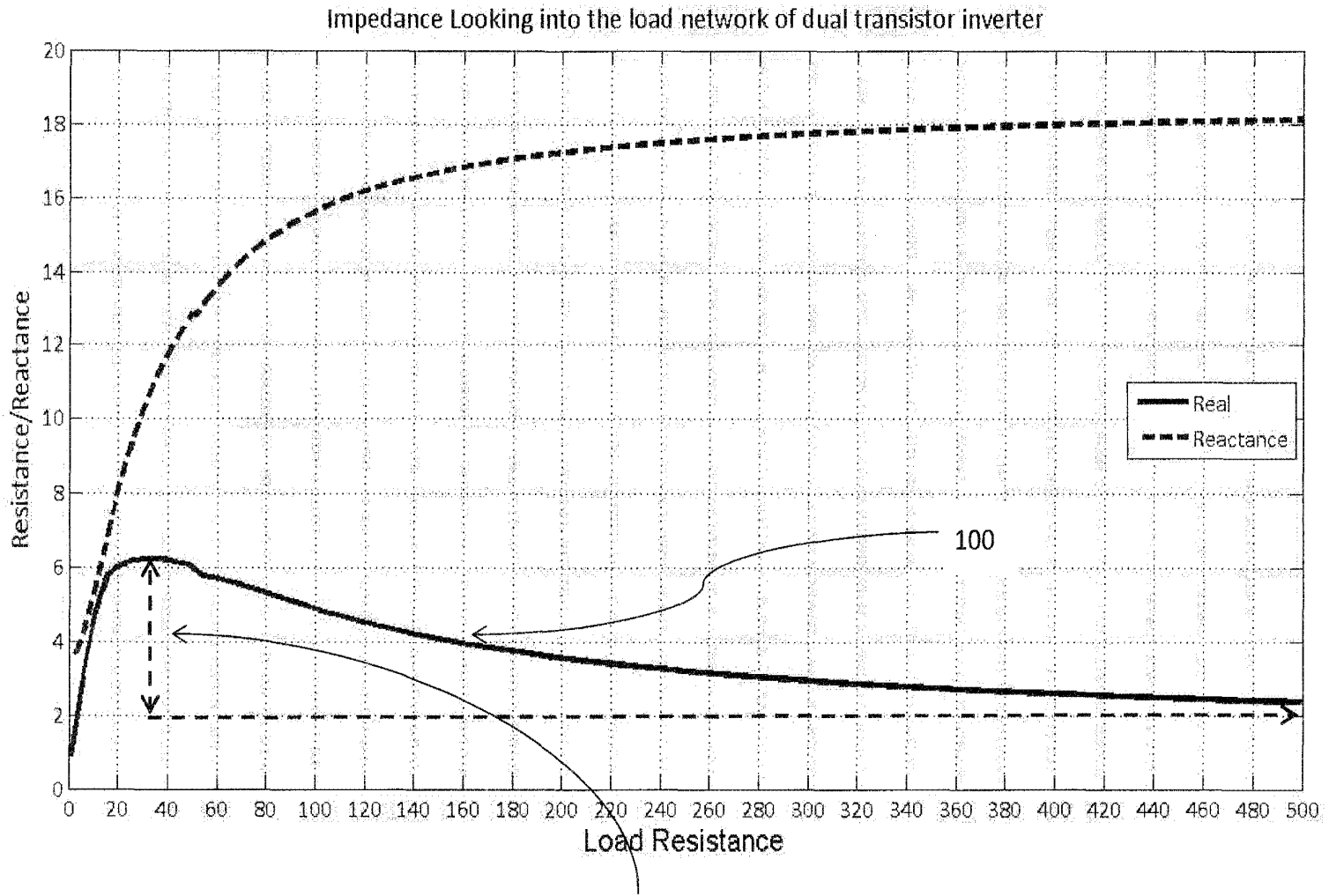
(PRIOR ART)

FIG. 8



(PRIOR ART)

FIG. 9



**FIG. 10**

11/84

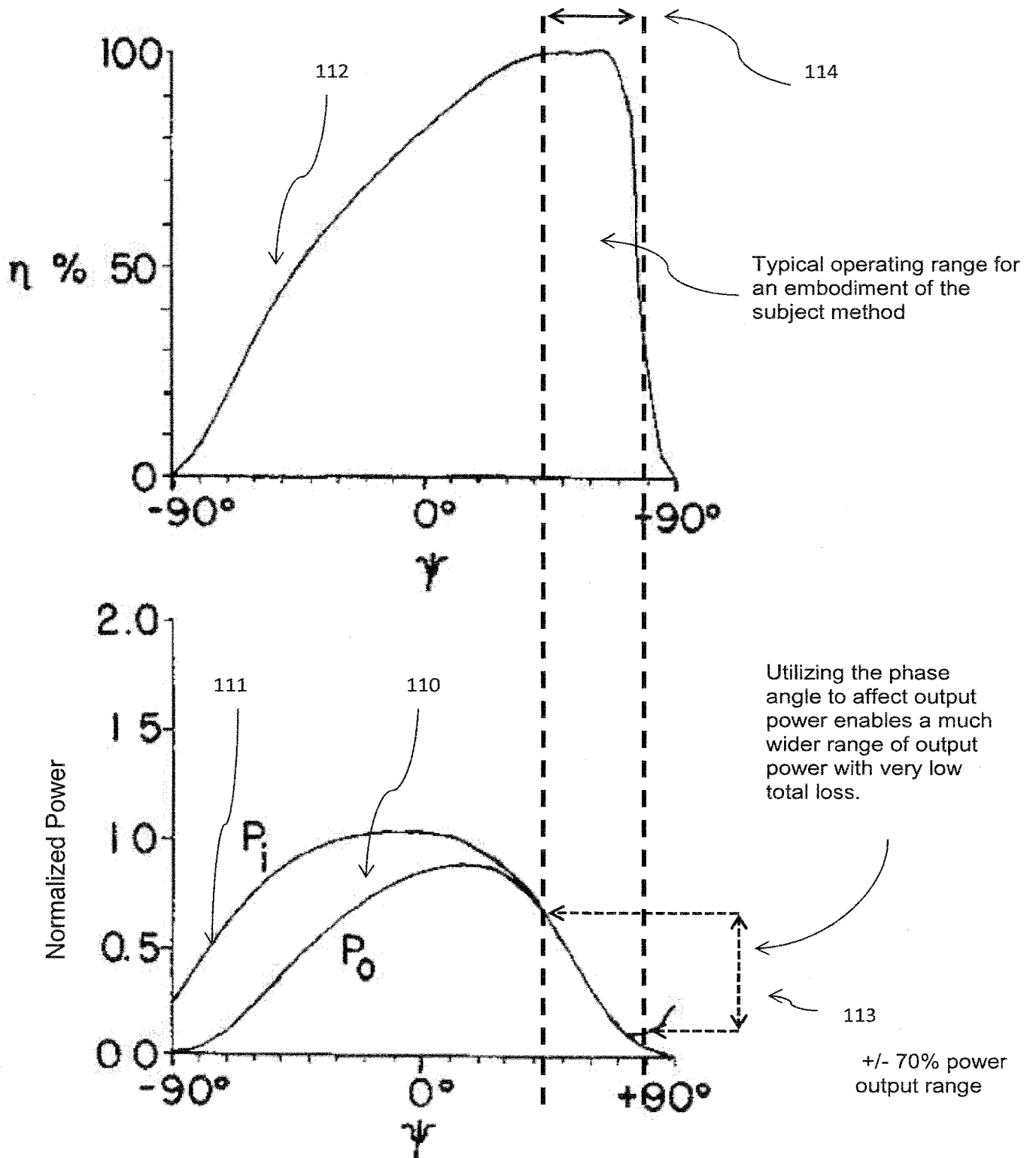


FIG. 11



12/84

127 Resistance controlled power delivery

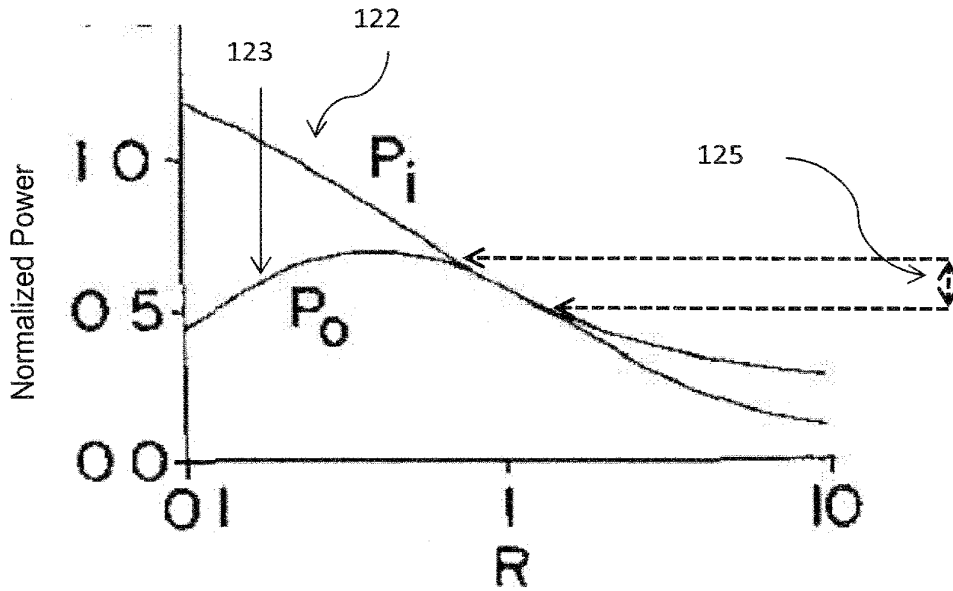


FIG. 12A

126 Phase controlled power delivery

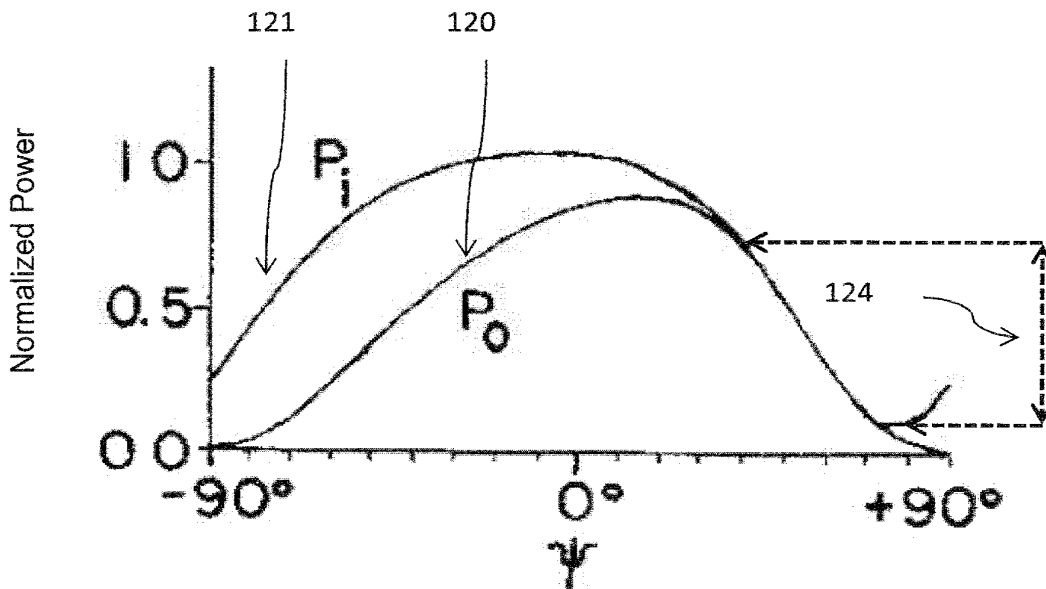


FIG. 12B

### Power delivered to a variable load

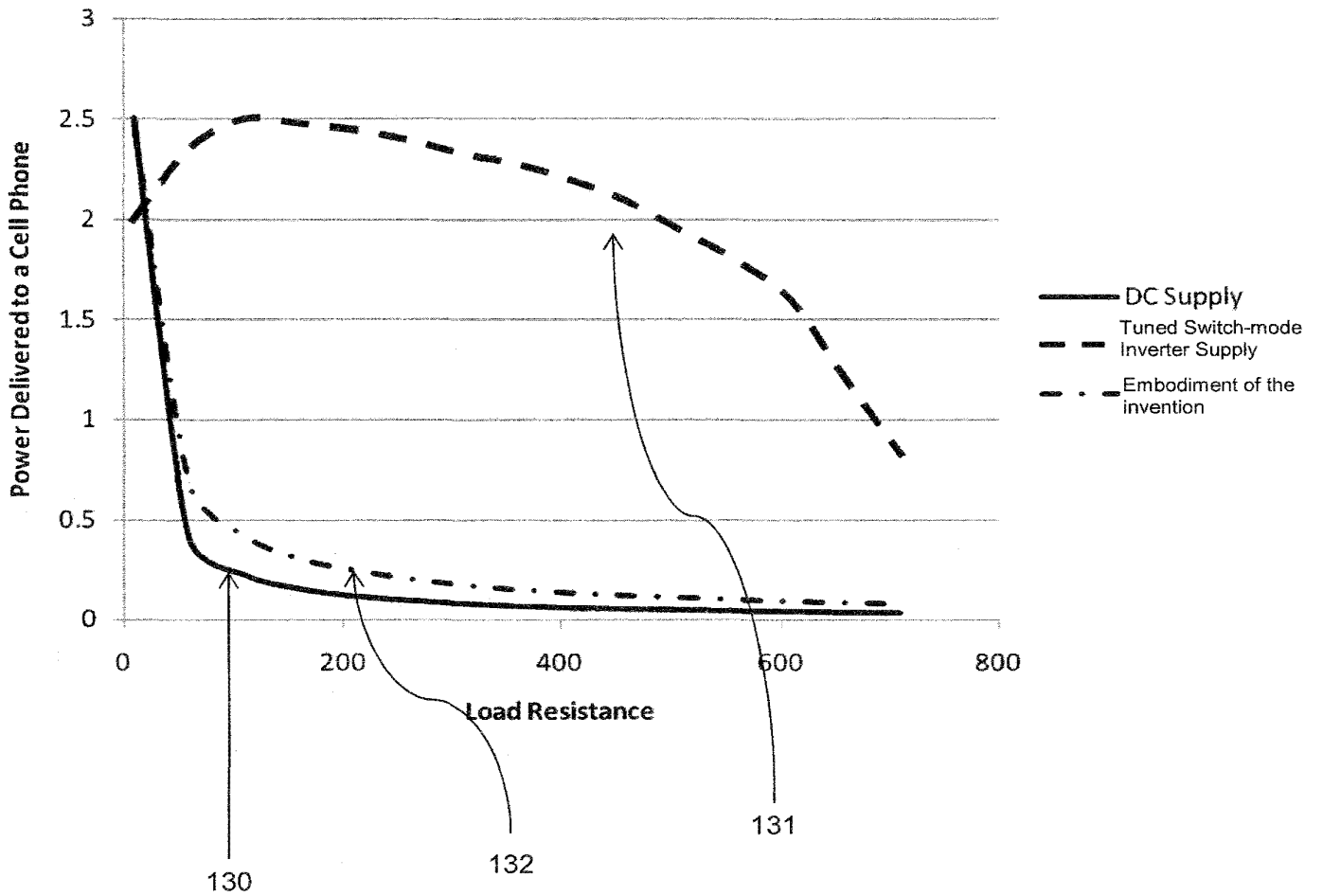


FIG. 13

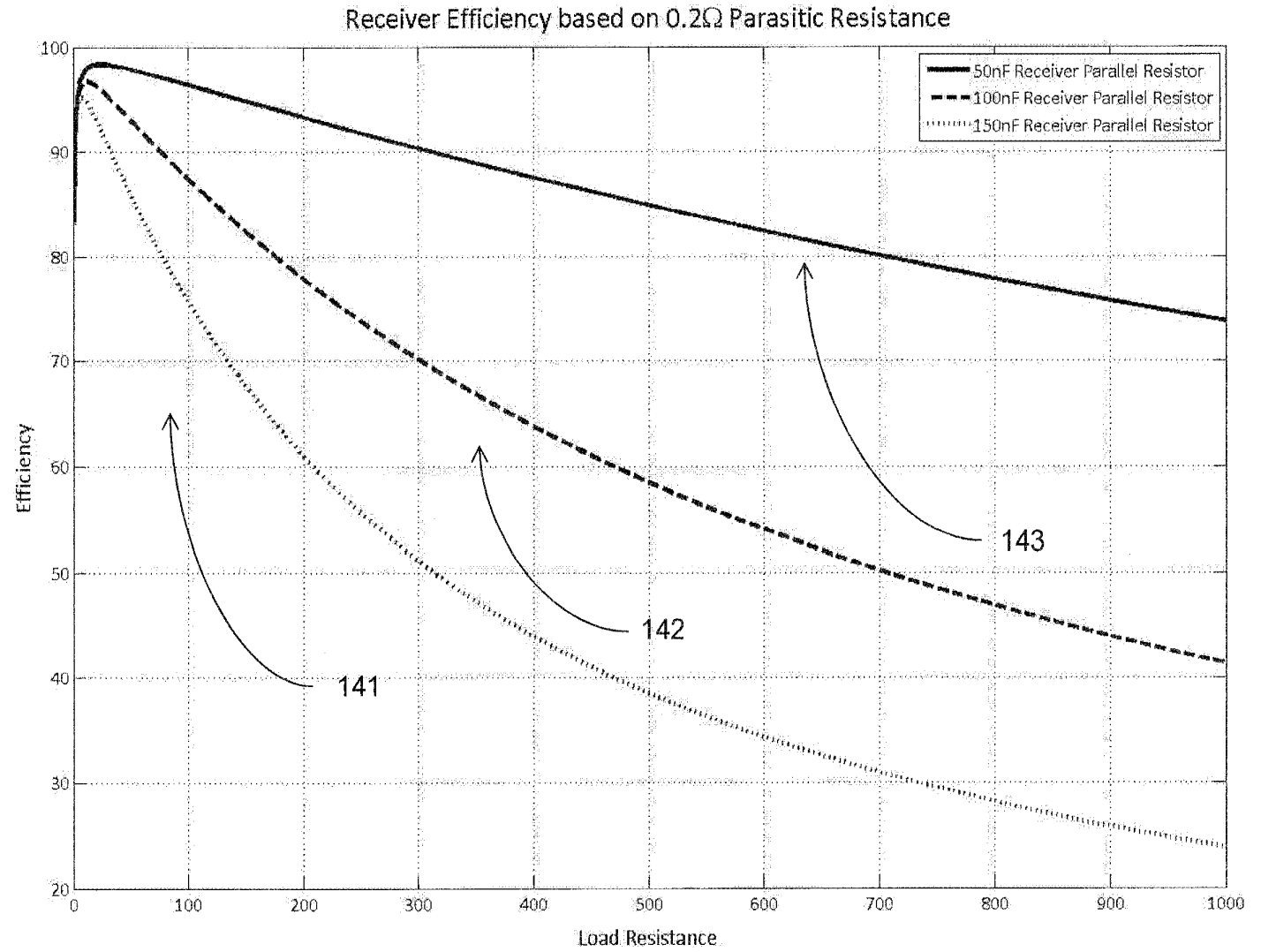


FIG. 14

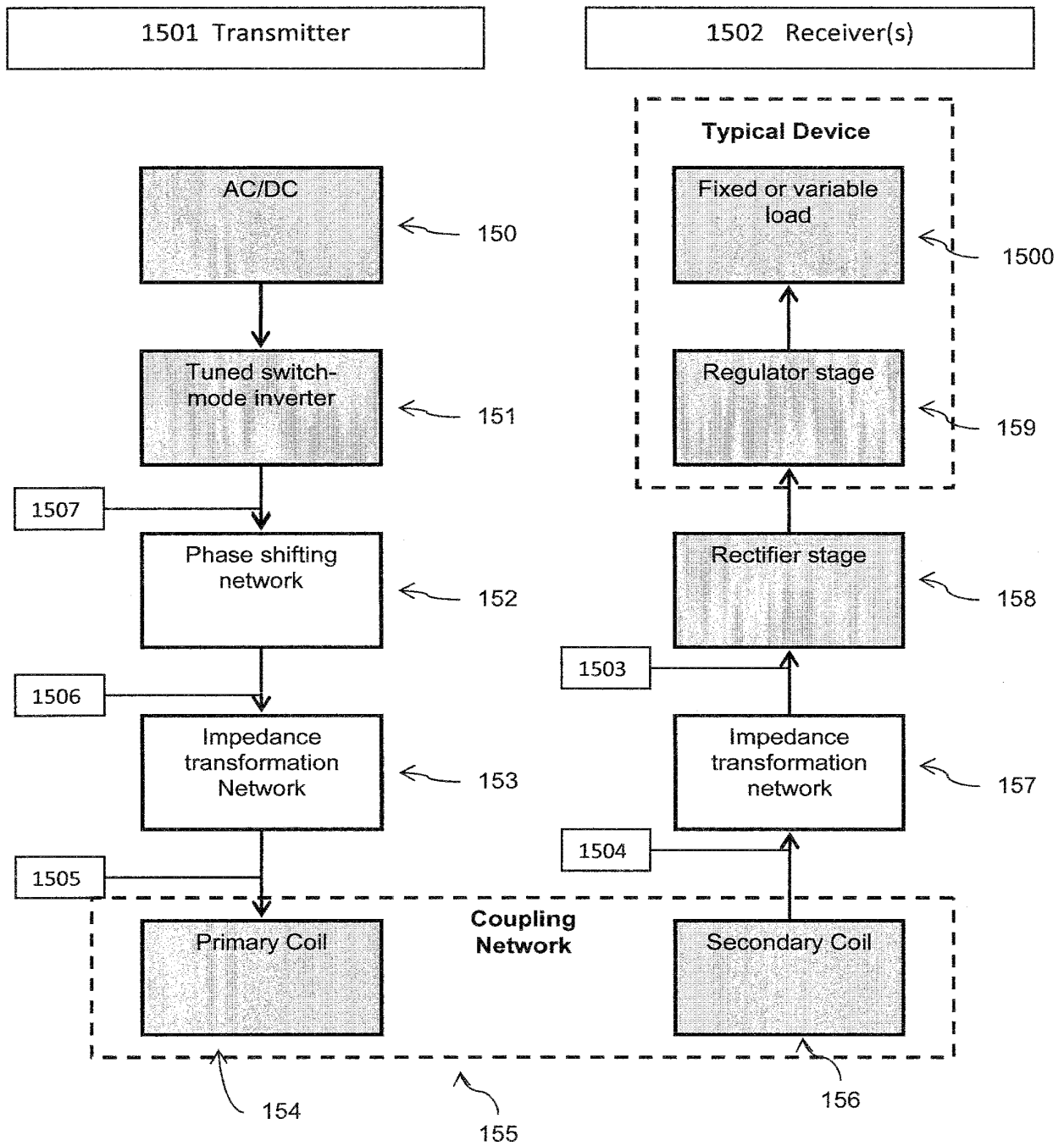


FIG. 15

16/84



**FIG. 16**

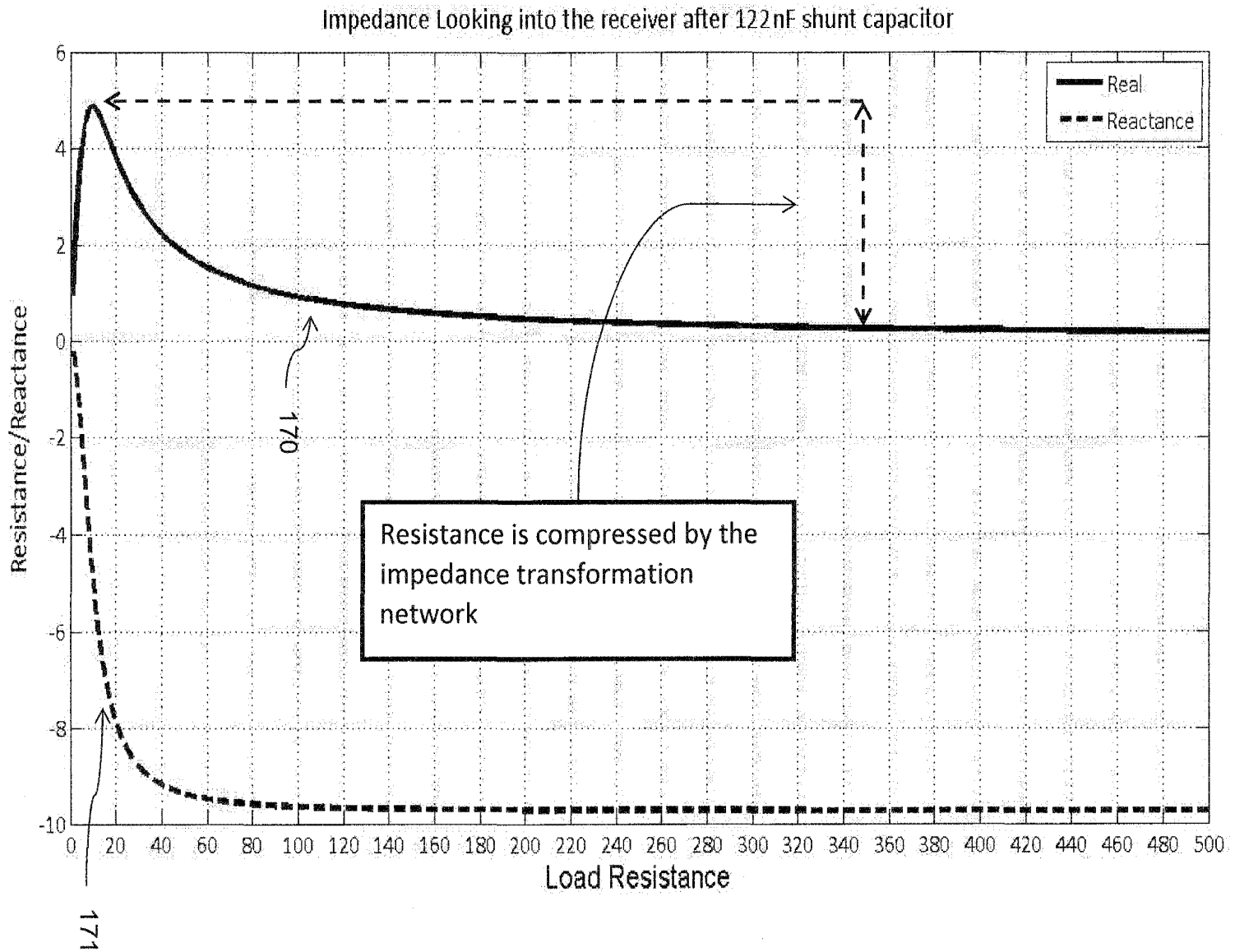


FIG. 17

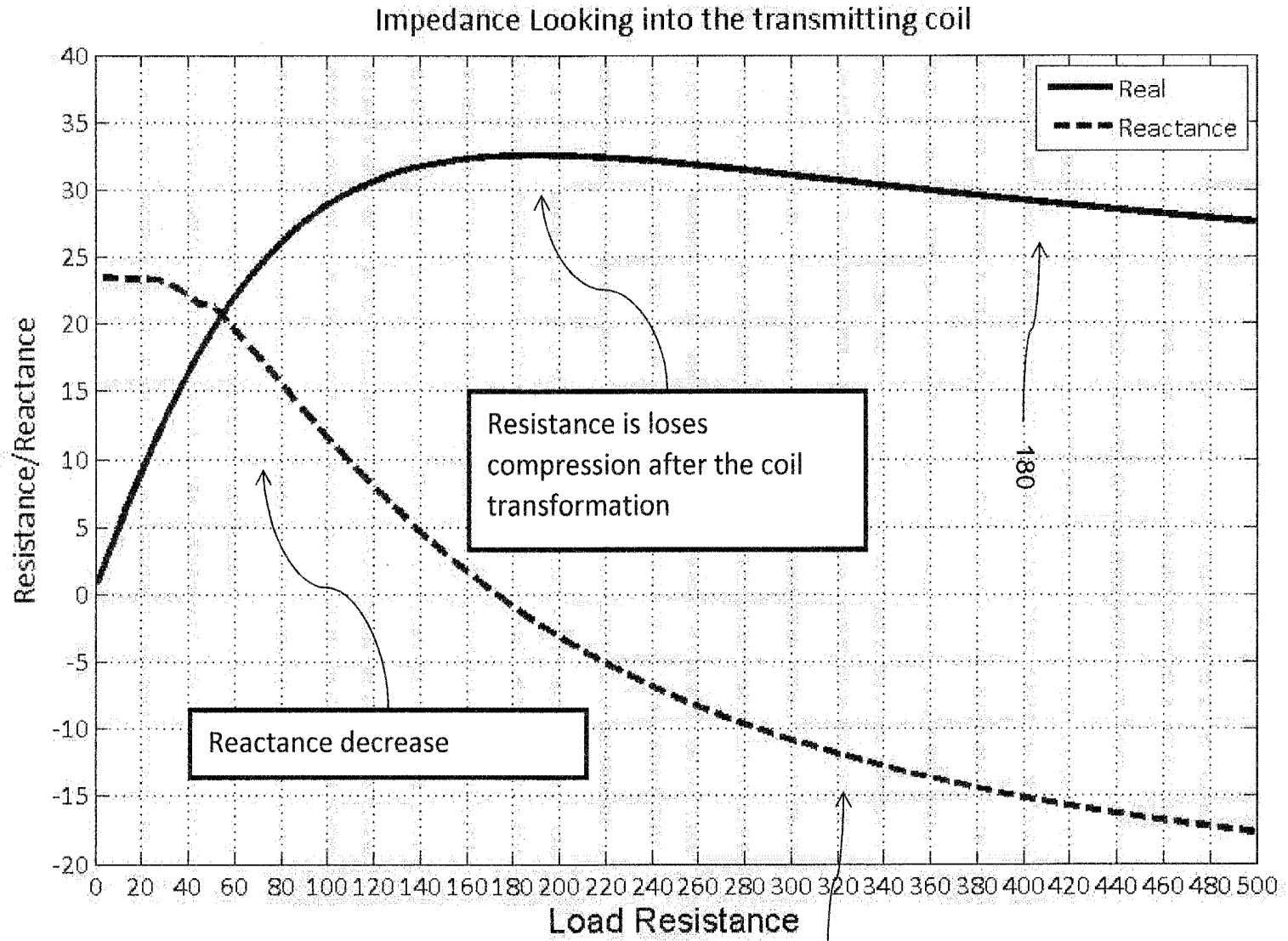


FIG. 18

181

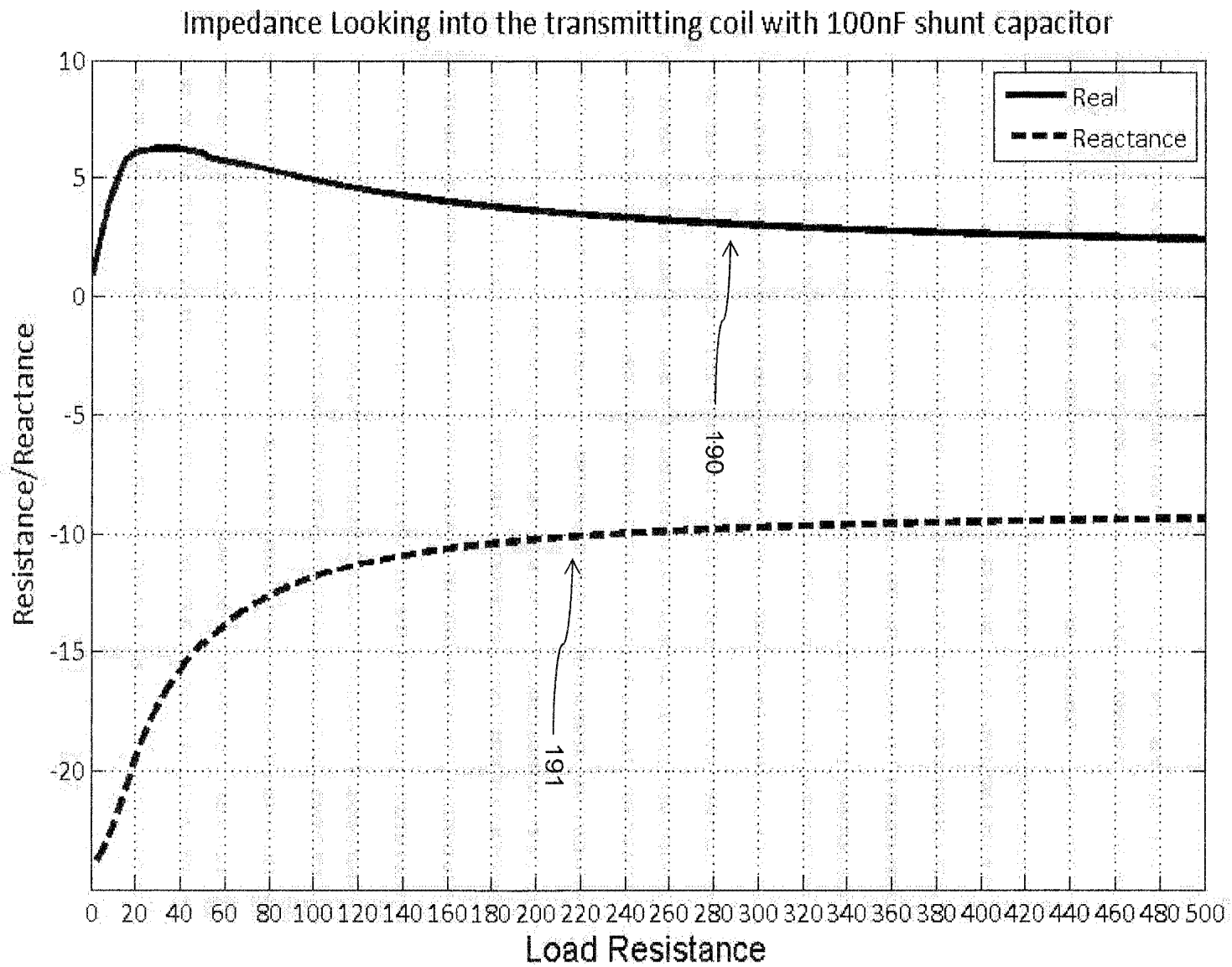
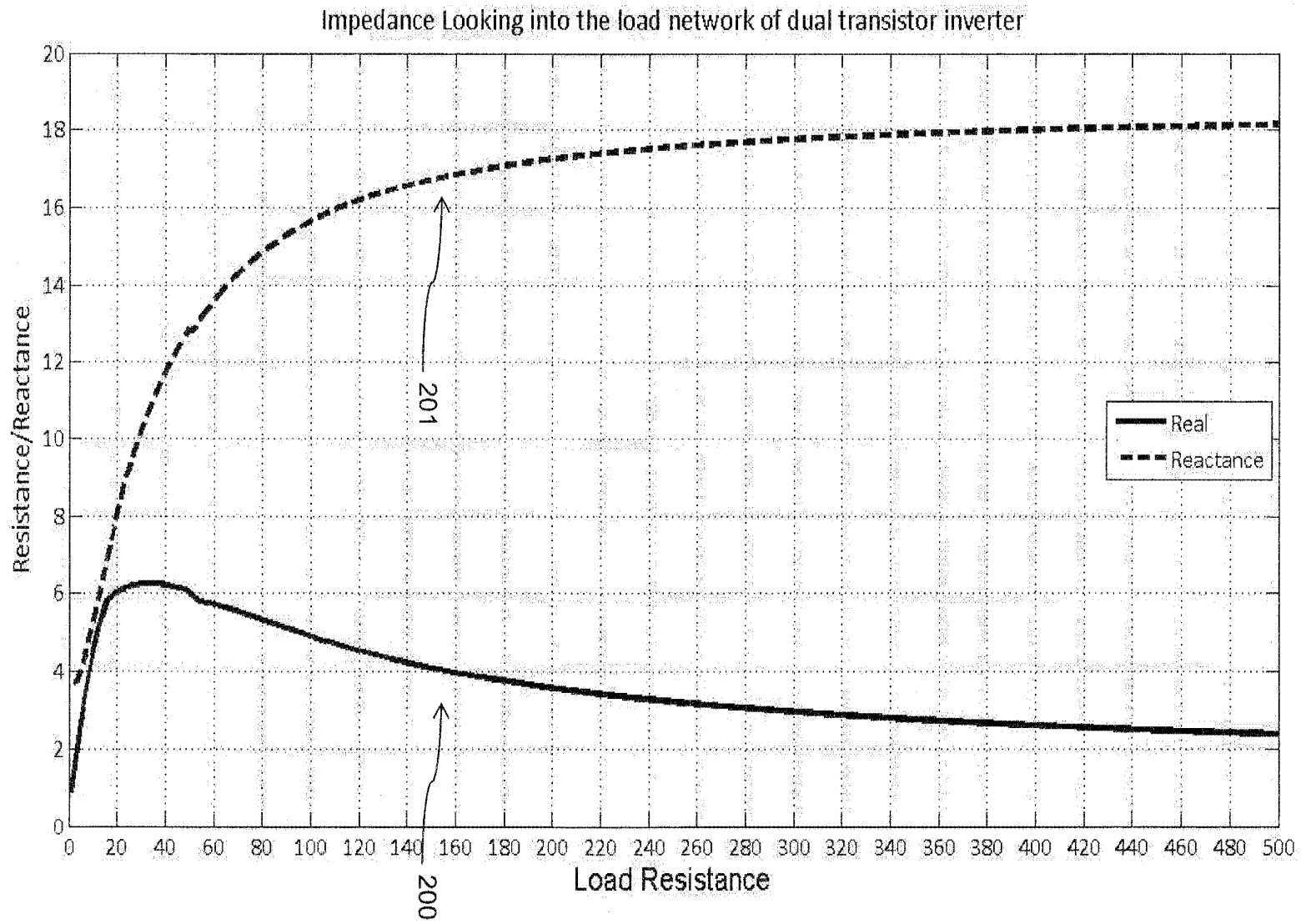


FIG. 19





**FIG. 20**

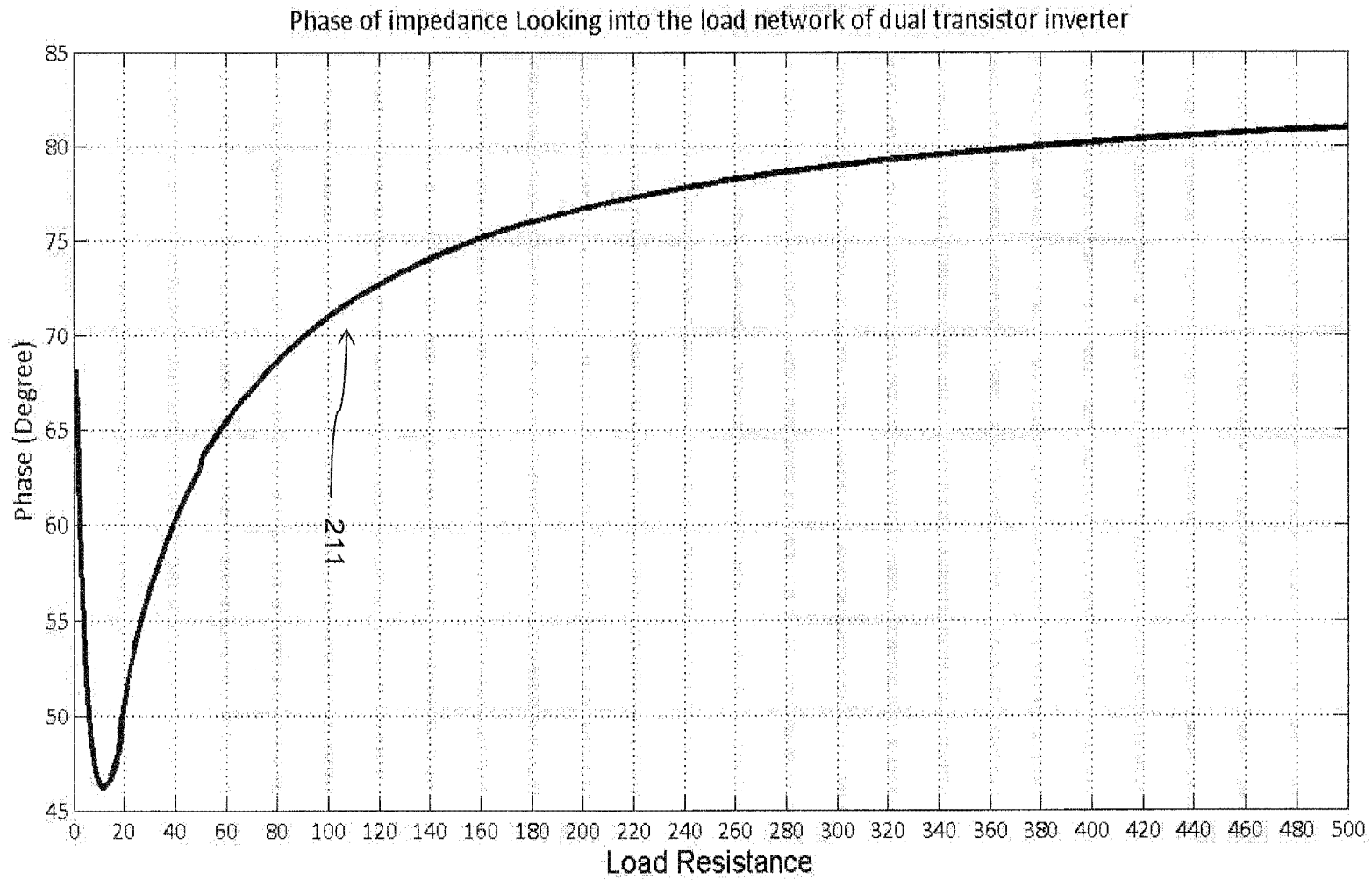


FIG. 21

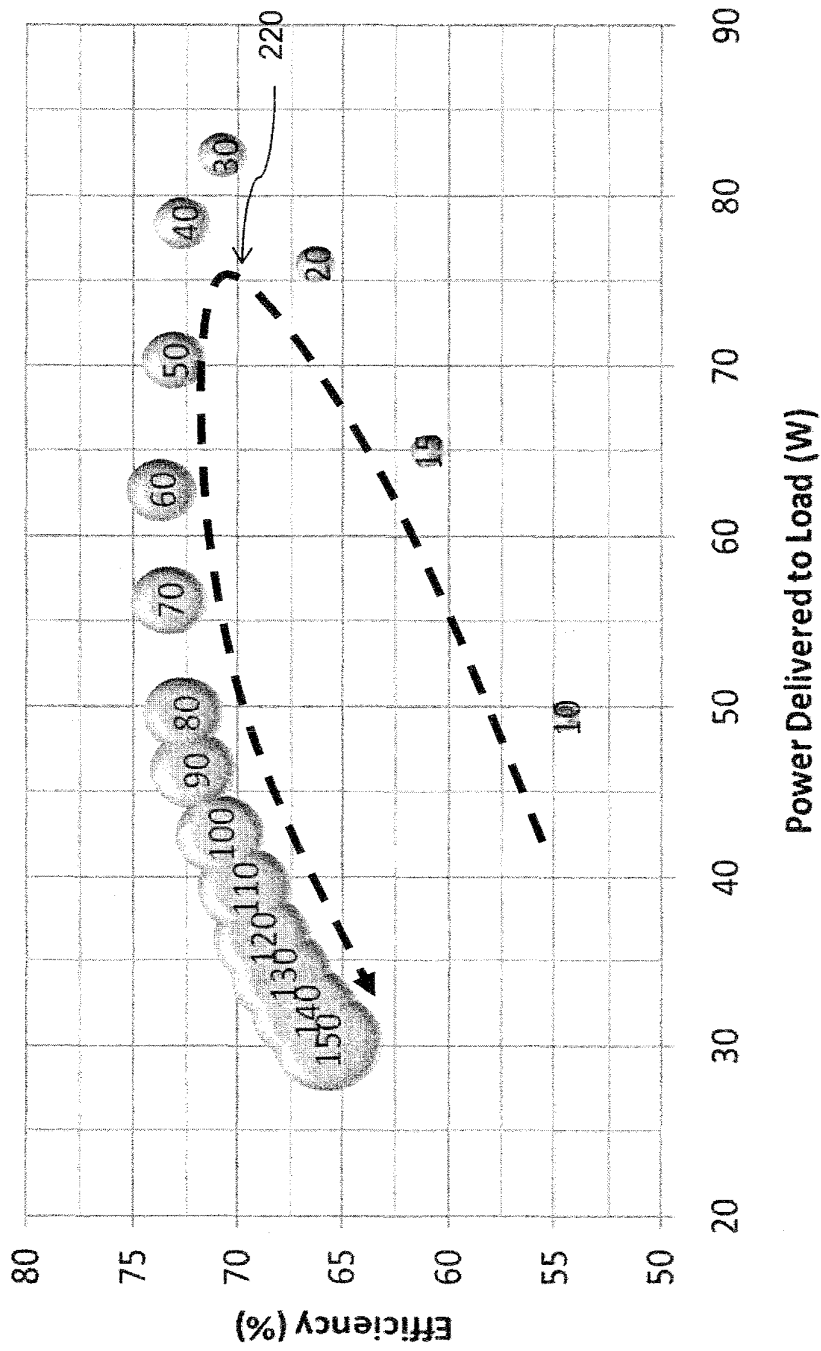


FIG. 22

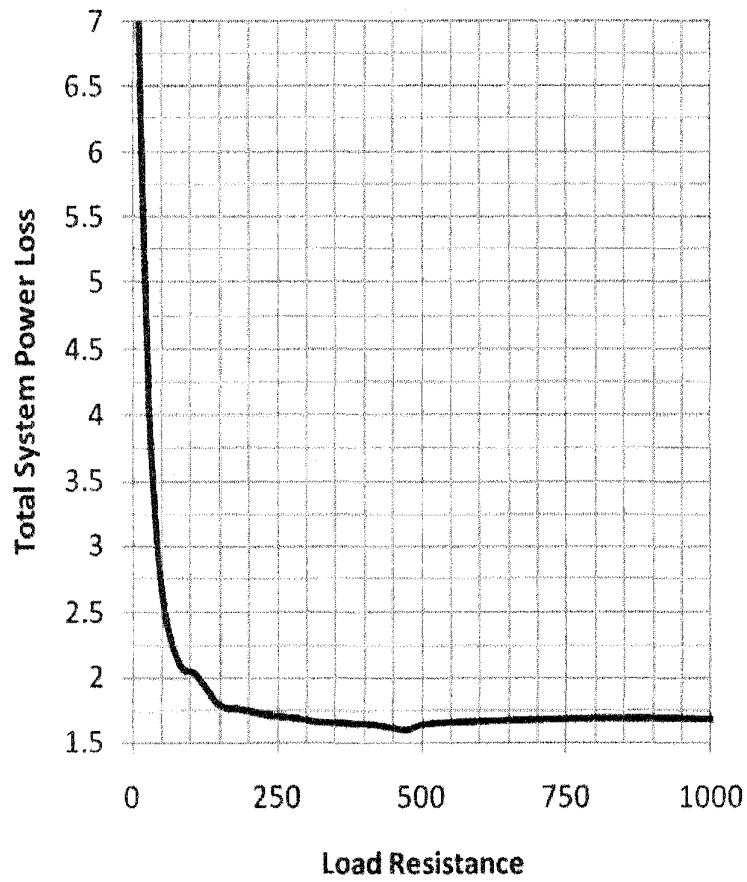


FIG. 23A

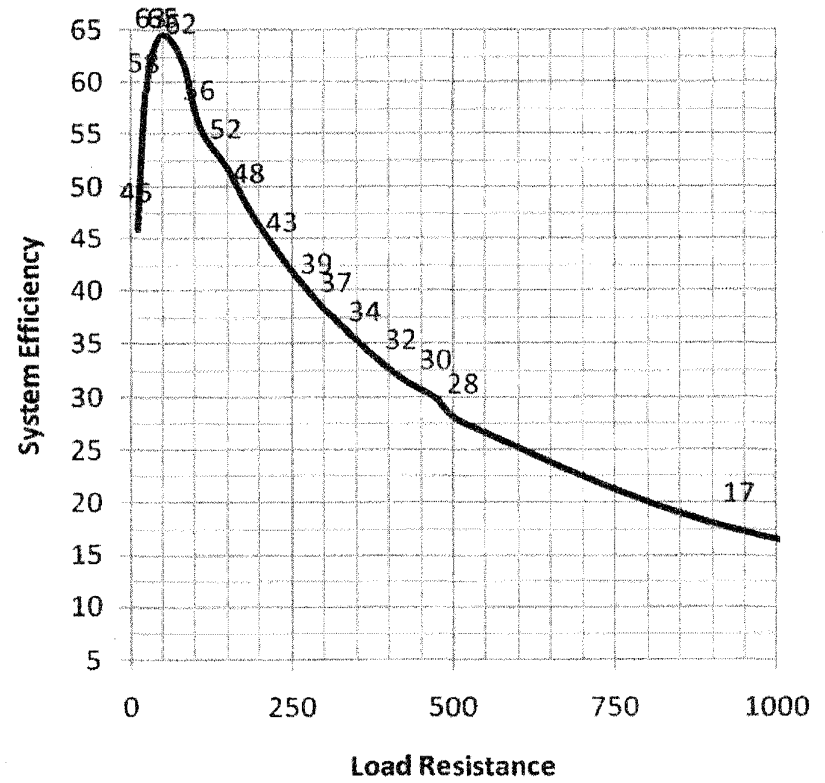


FIG. 23B

24/84

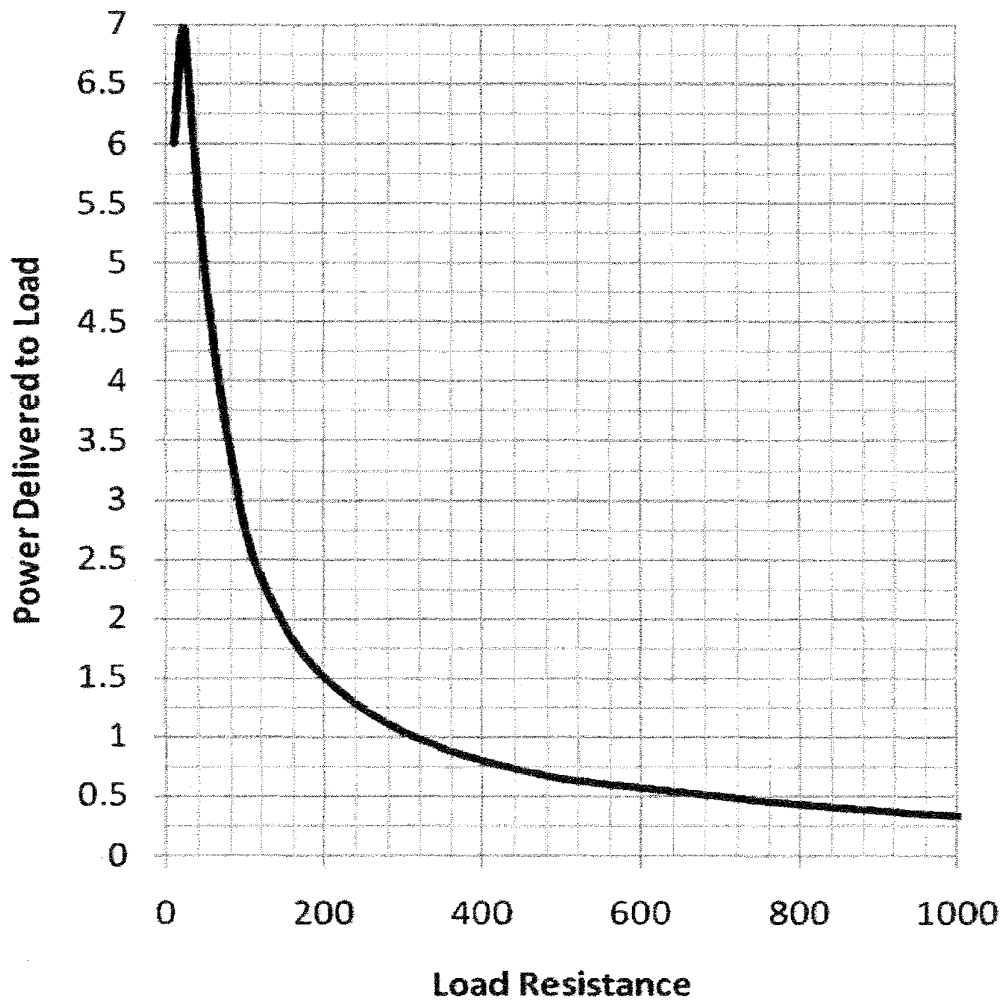


FIG. 23C

25/84

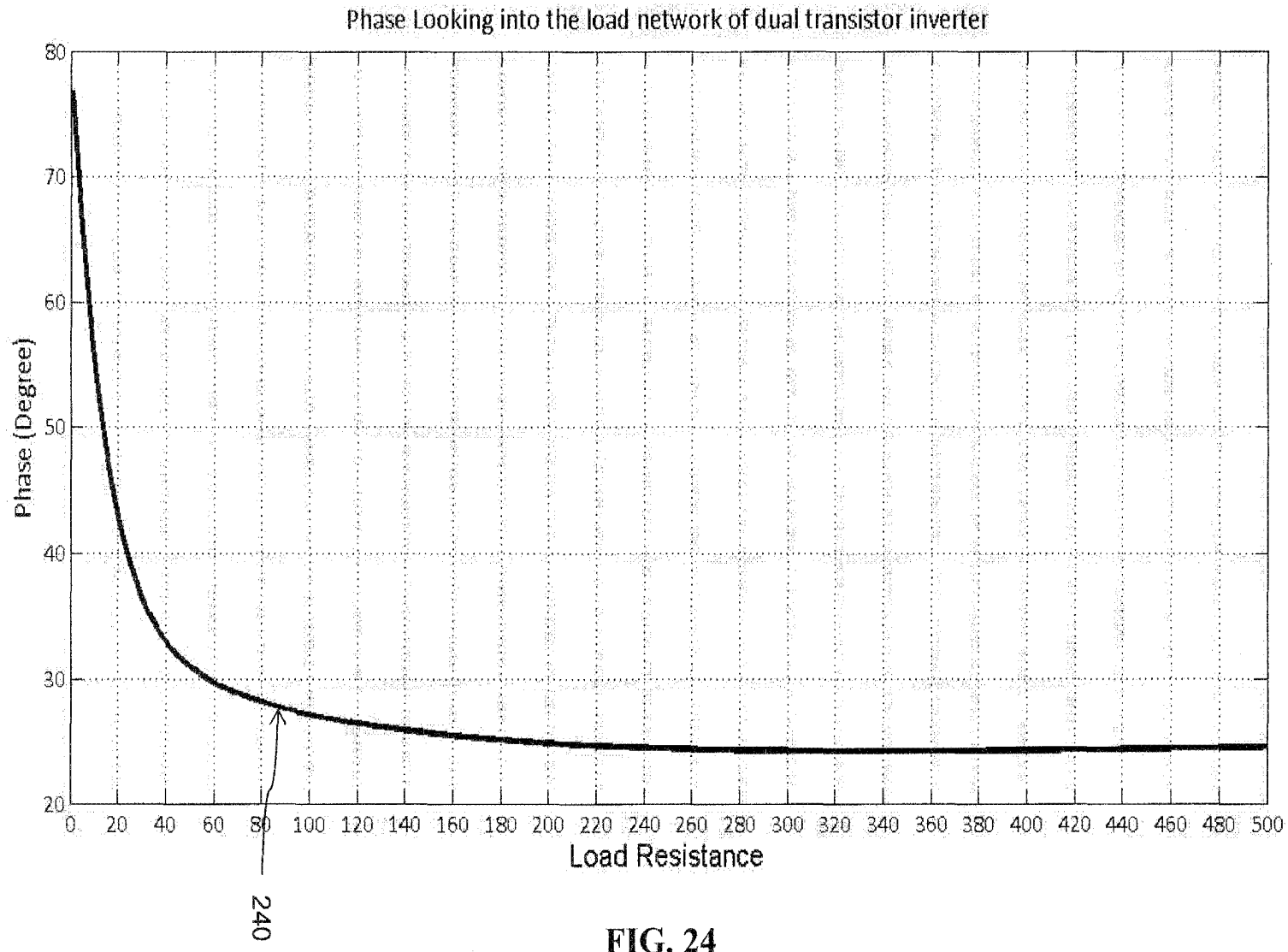


FIG. 24

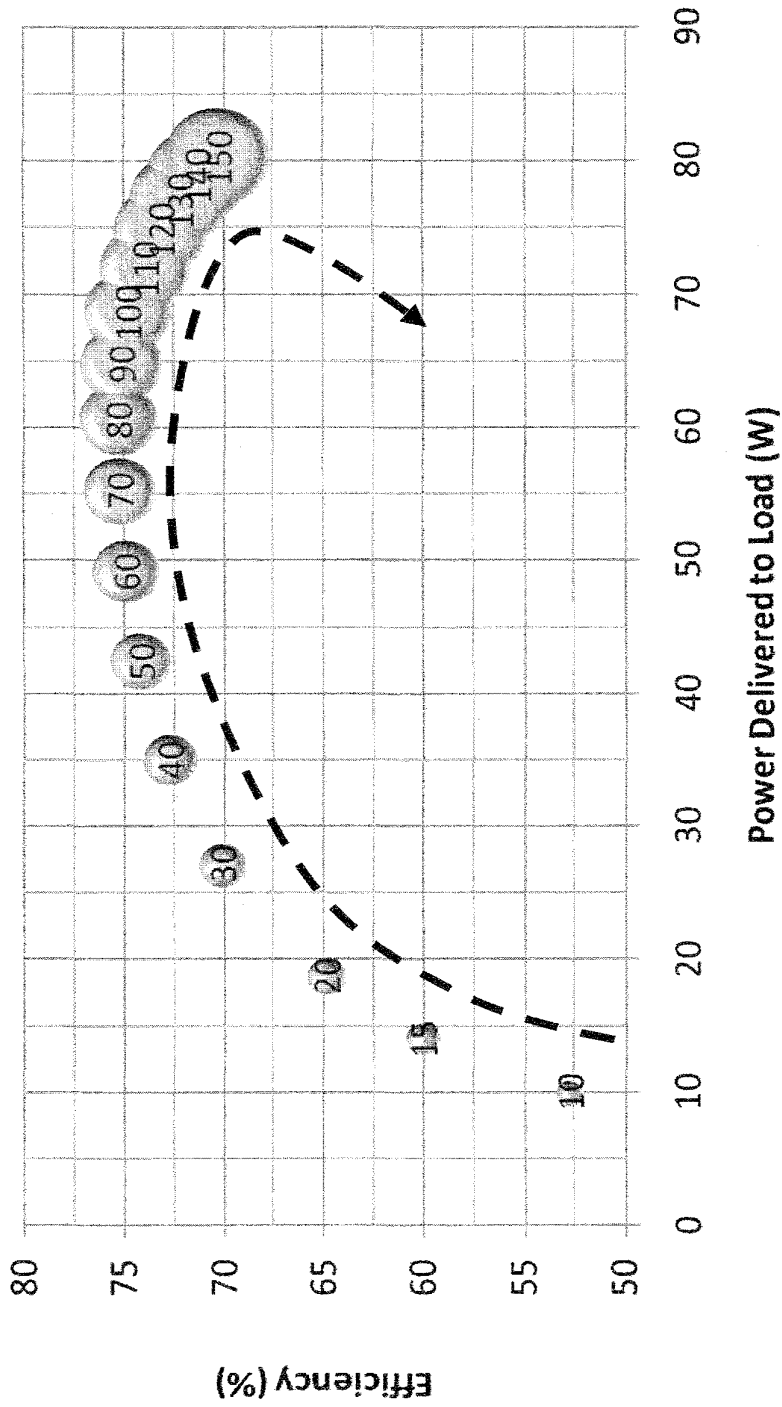


FIG. 25

27/84

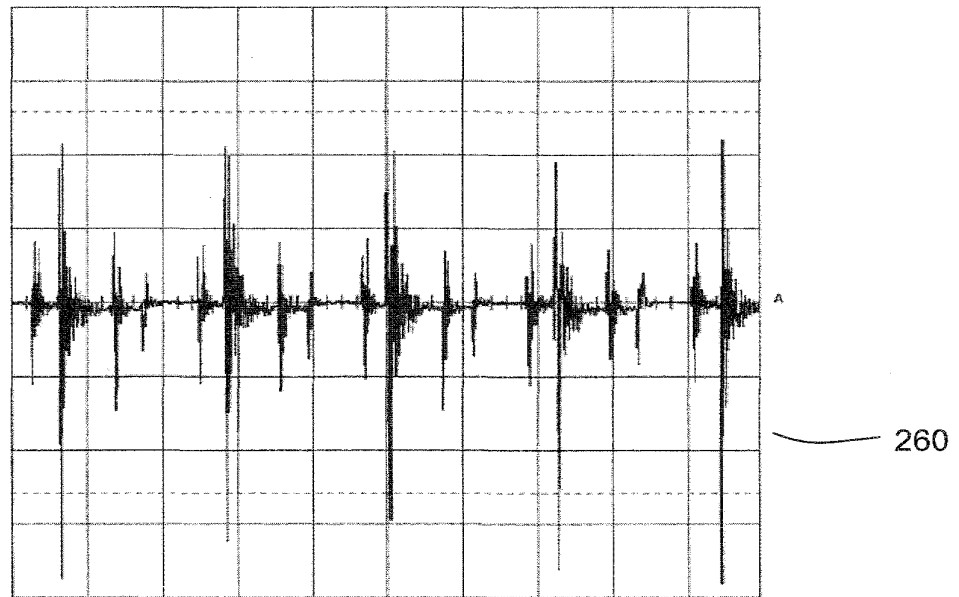


FIG. 26A

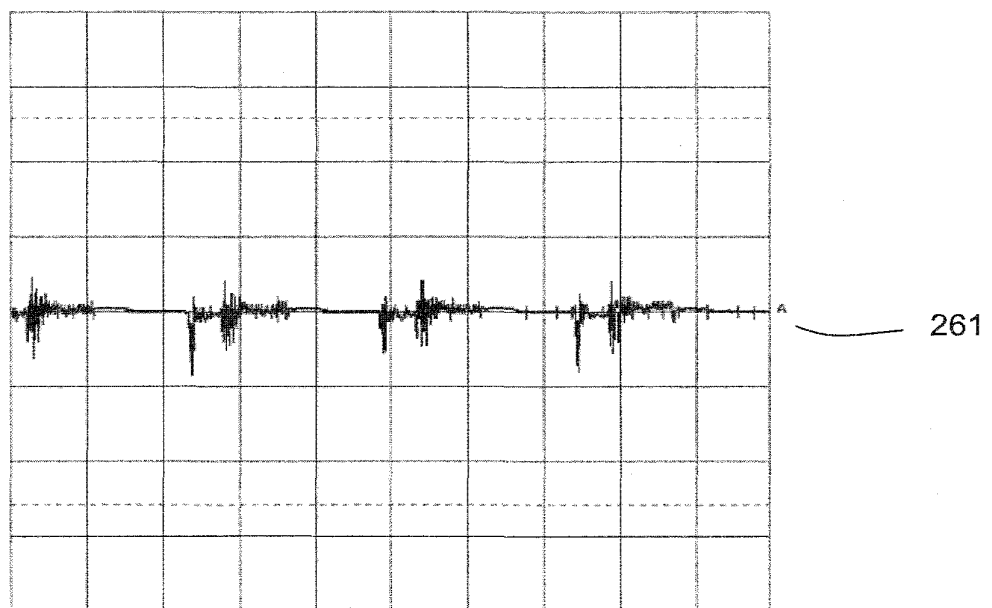


FIG. 26B



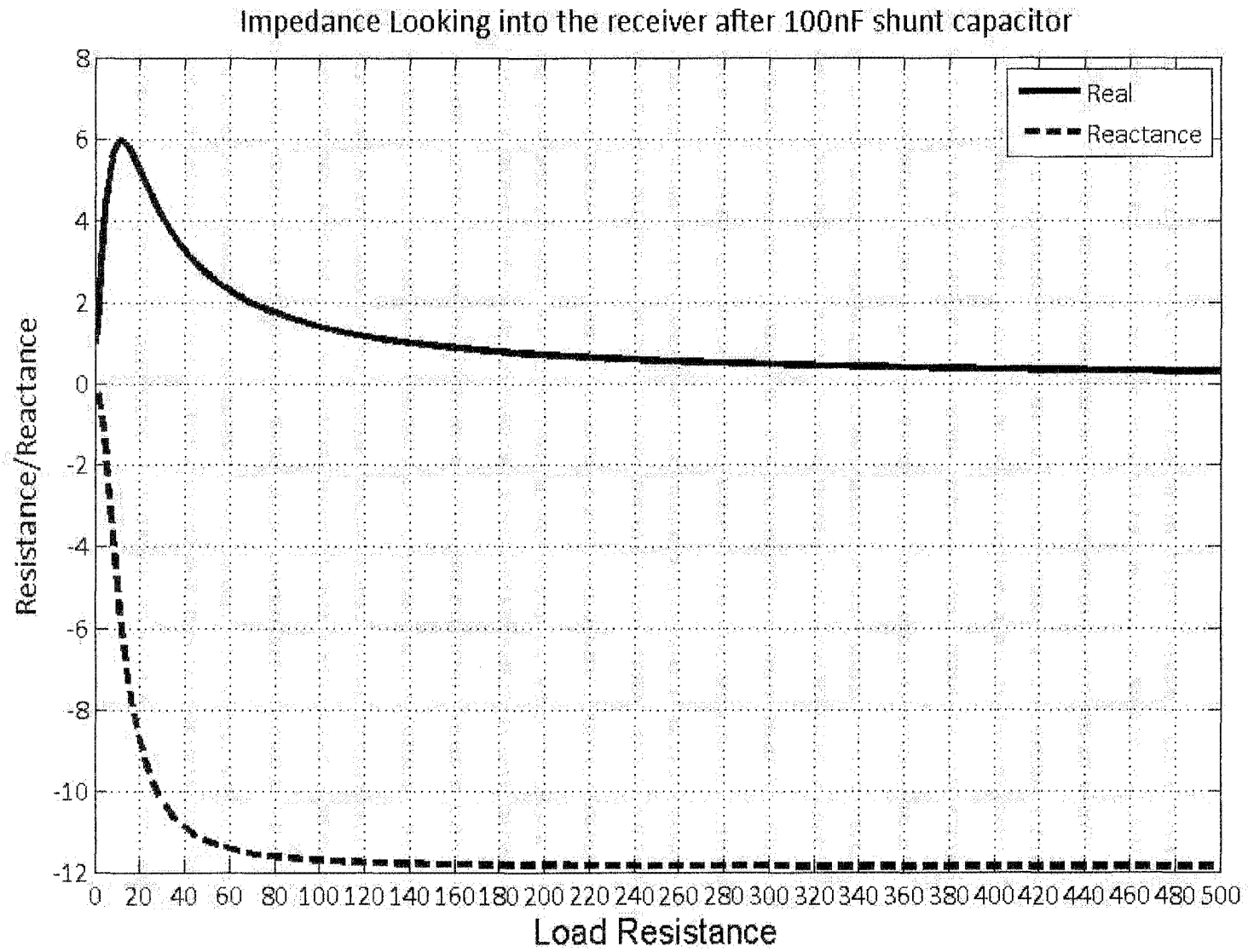


FIG. 27

28/84

29/84

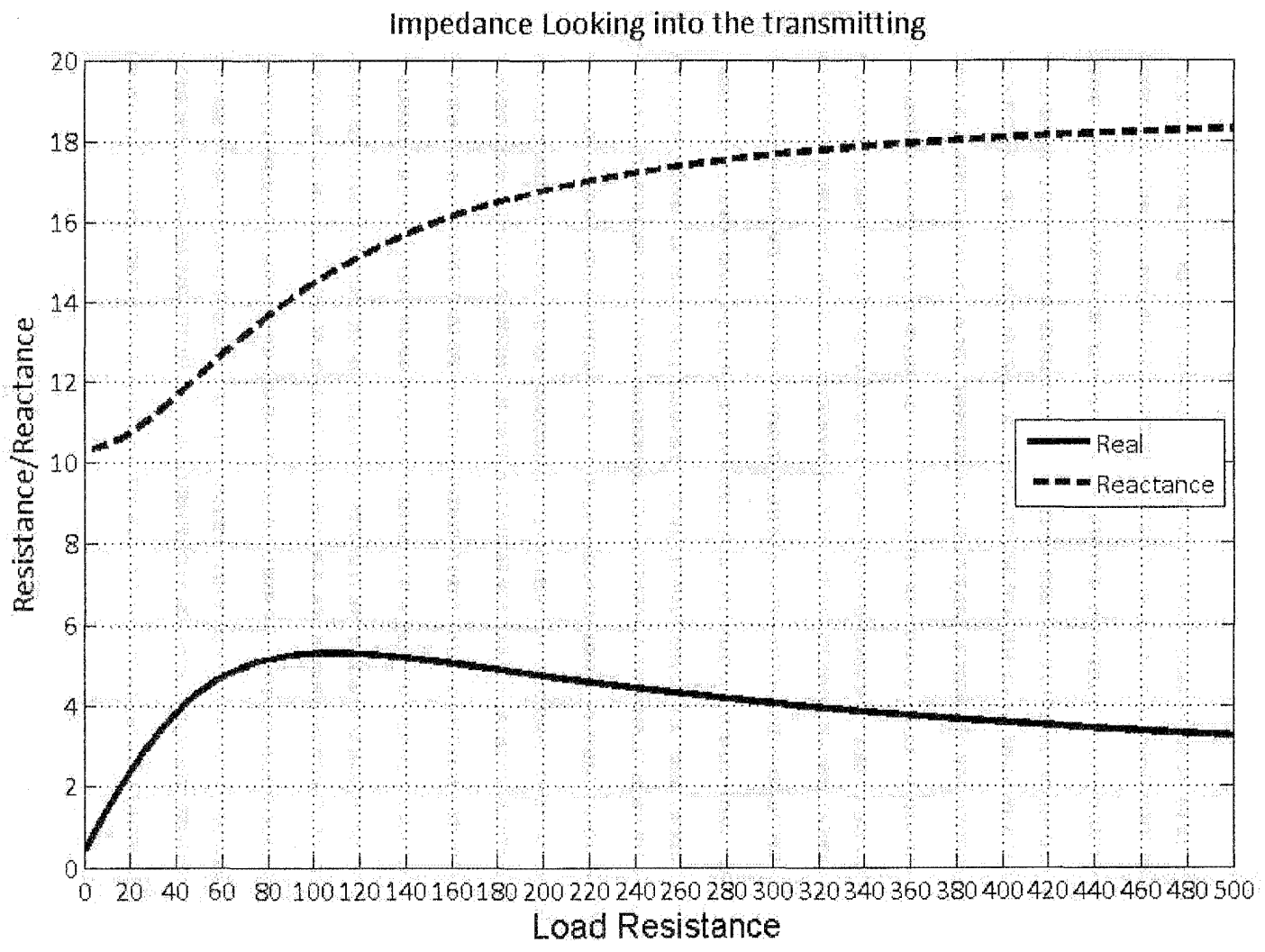
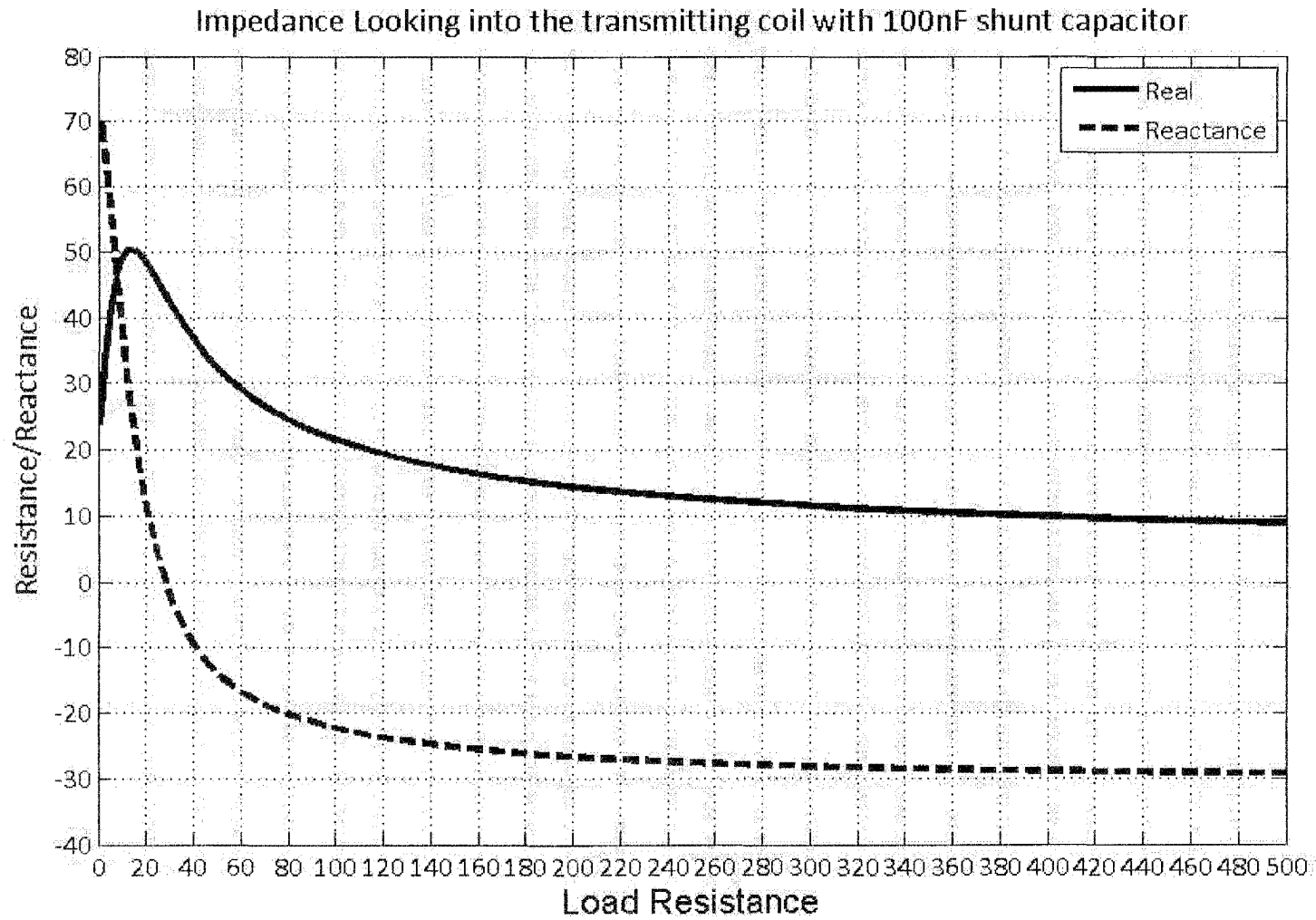


FIG. 28



30/84

FIG. 29

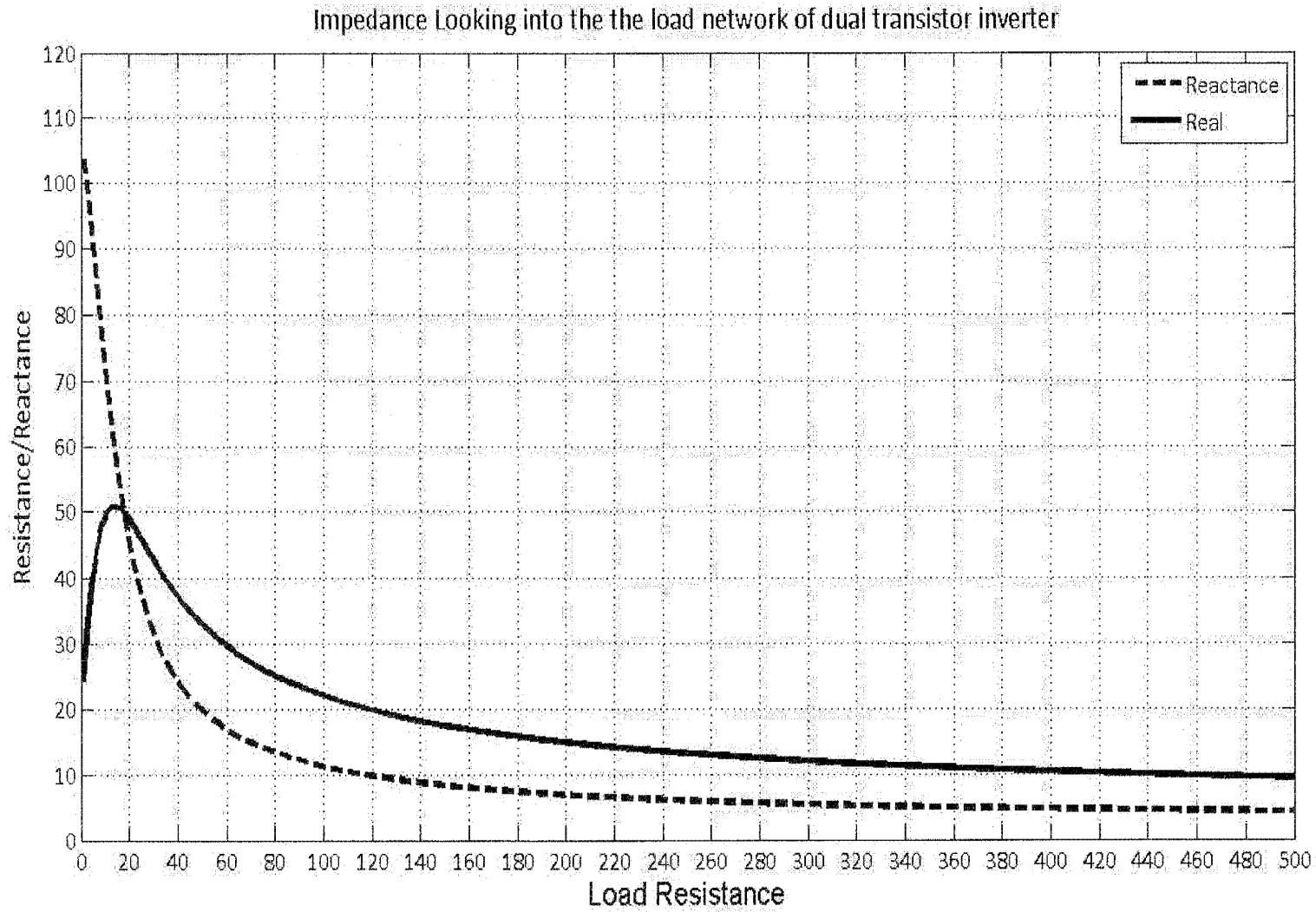
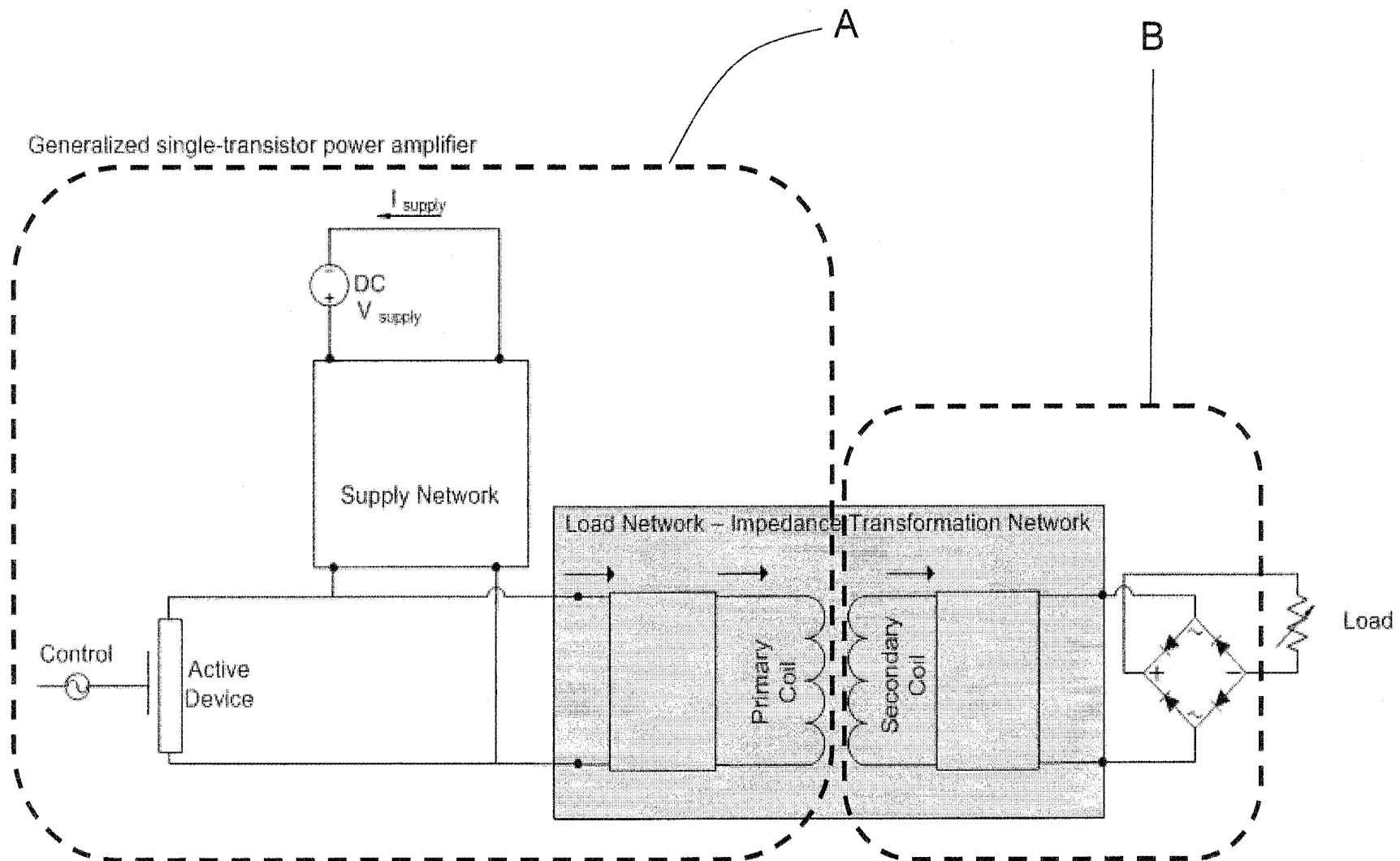


FIG. 30



32/84

FIG. 31

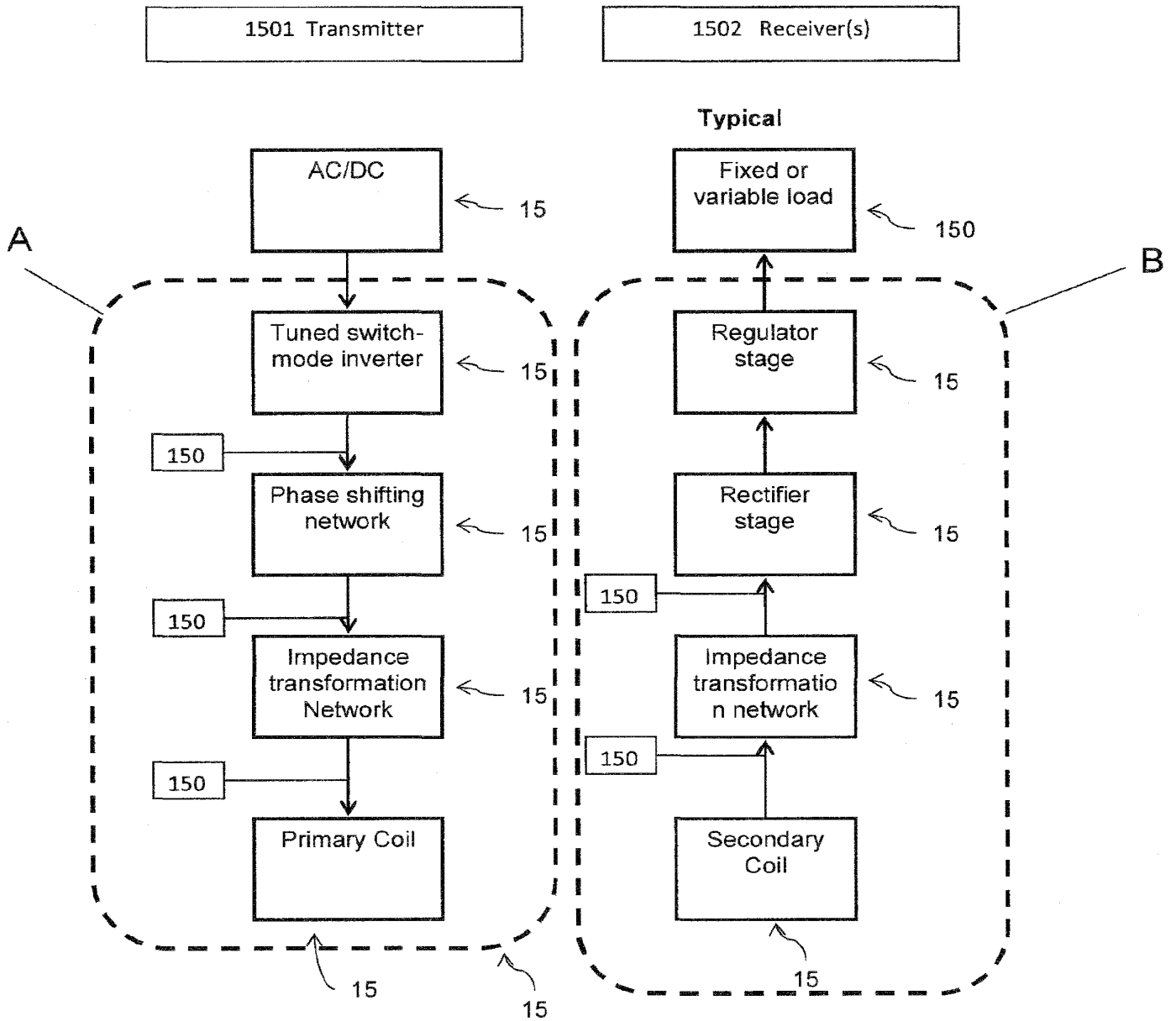


FIG. 32

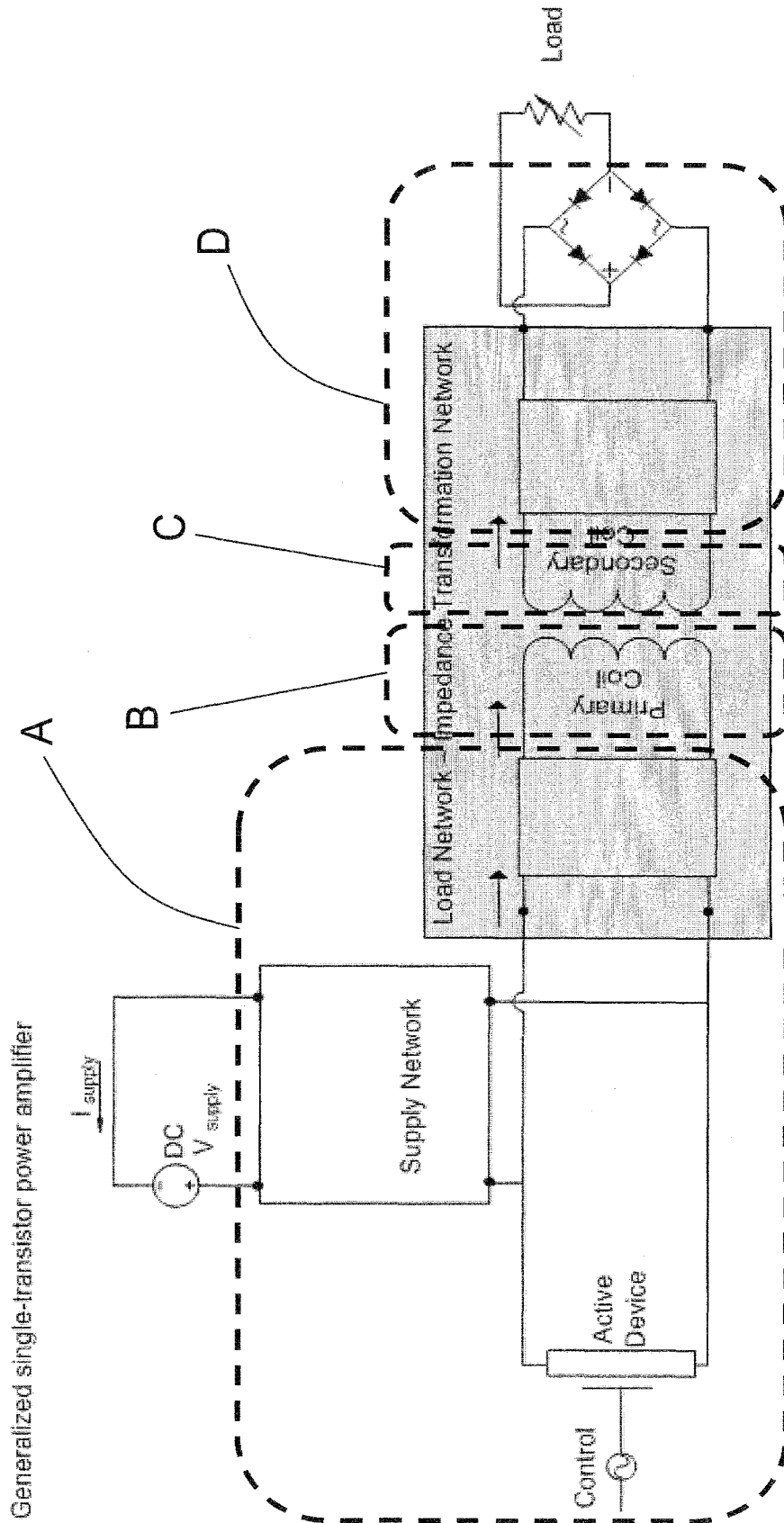


FIG. 33

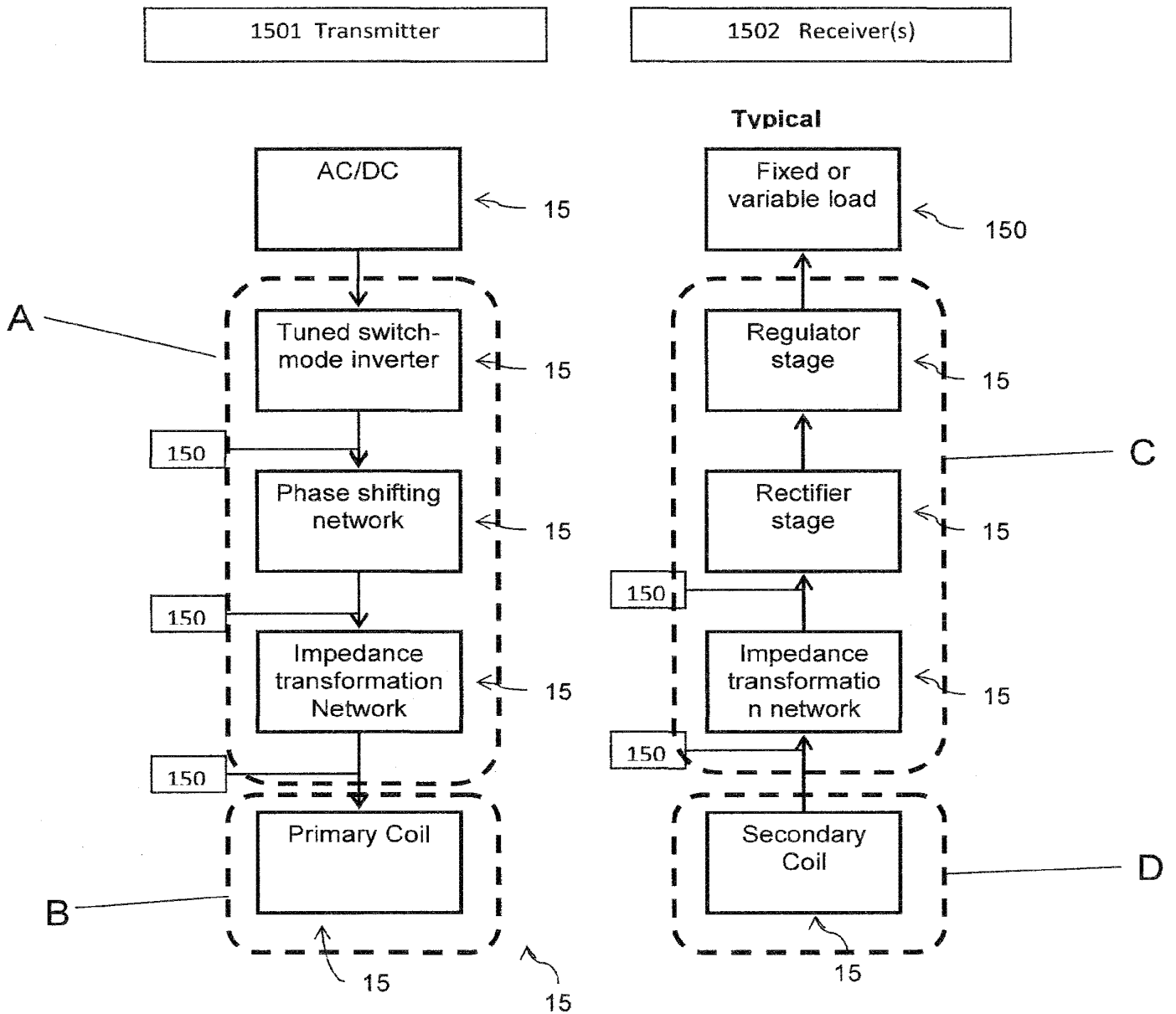


FIG. 34



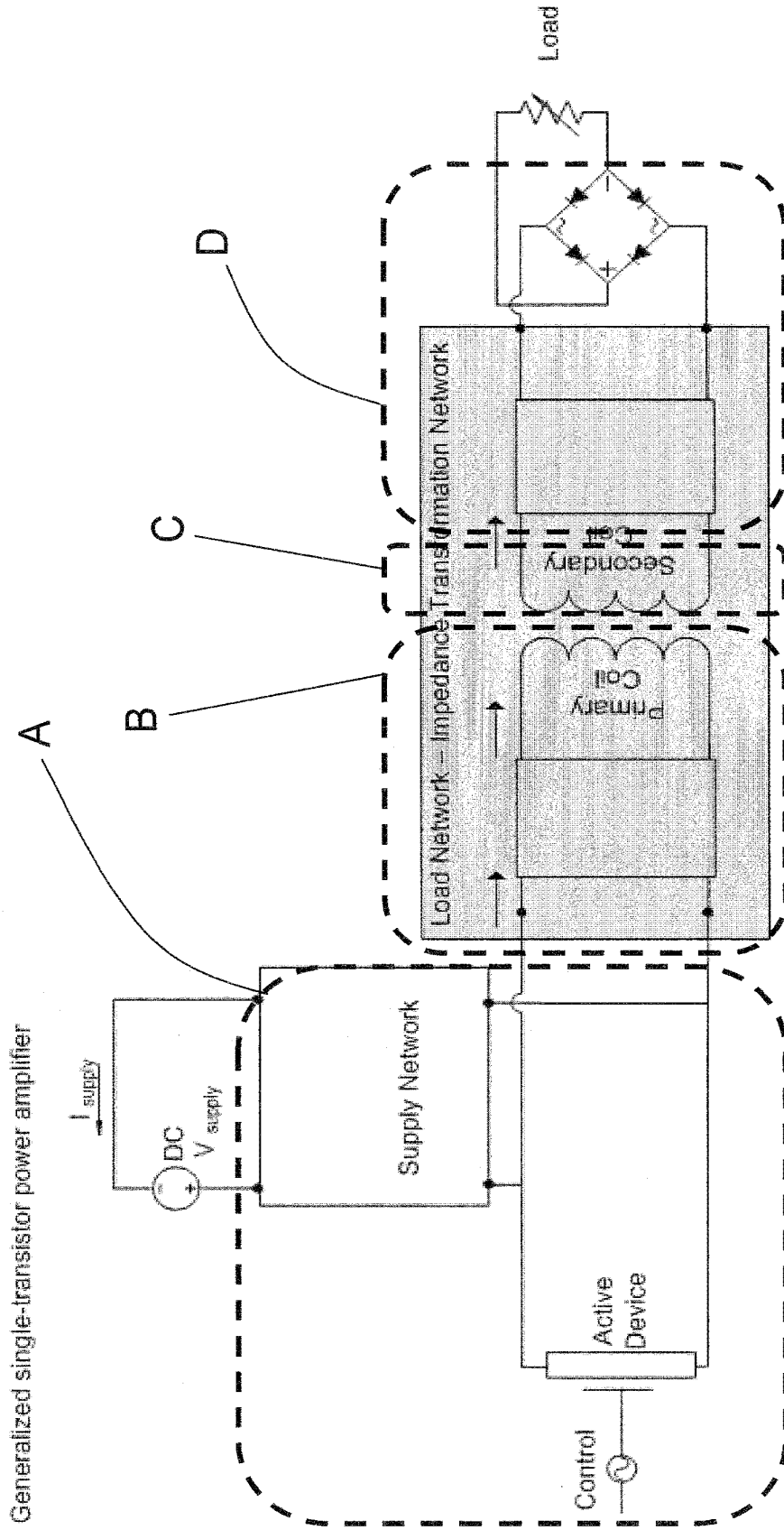


FIG. 35

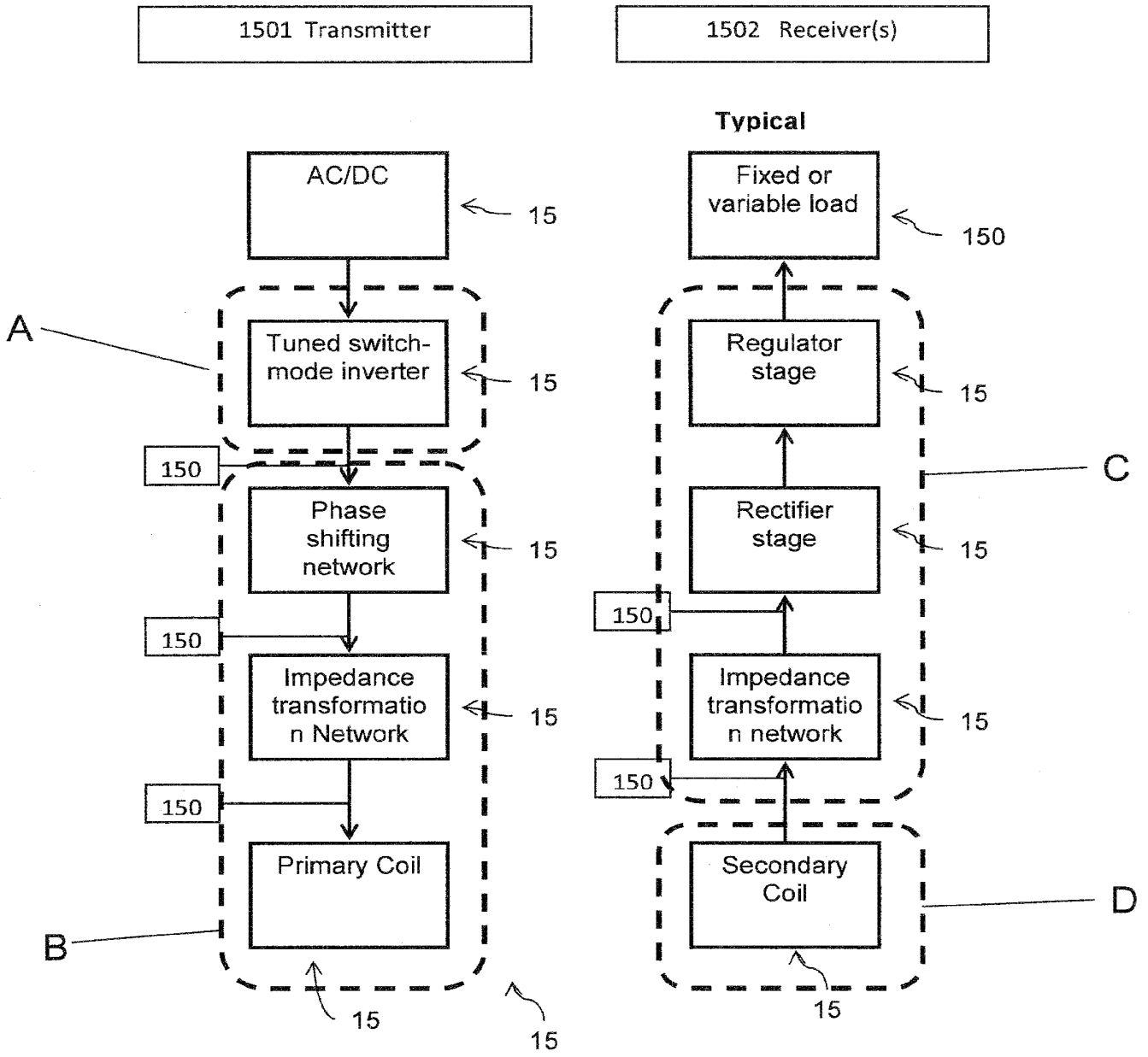


FIG. 36

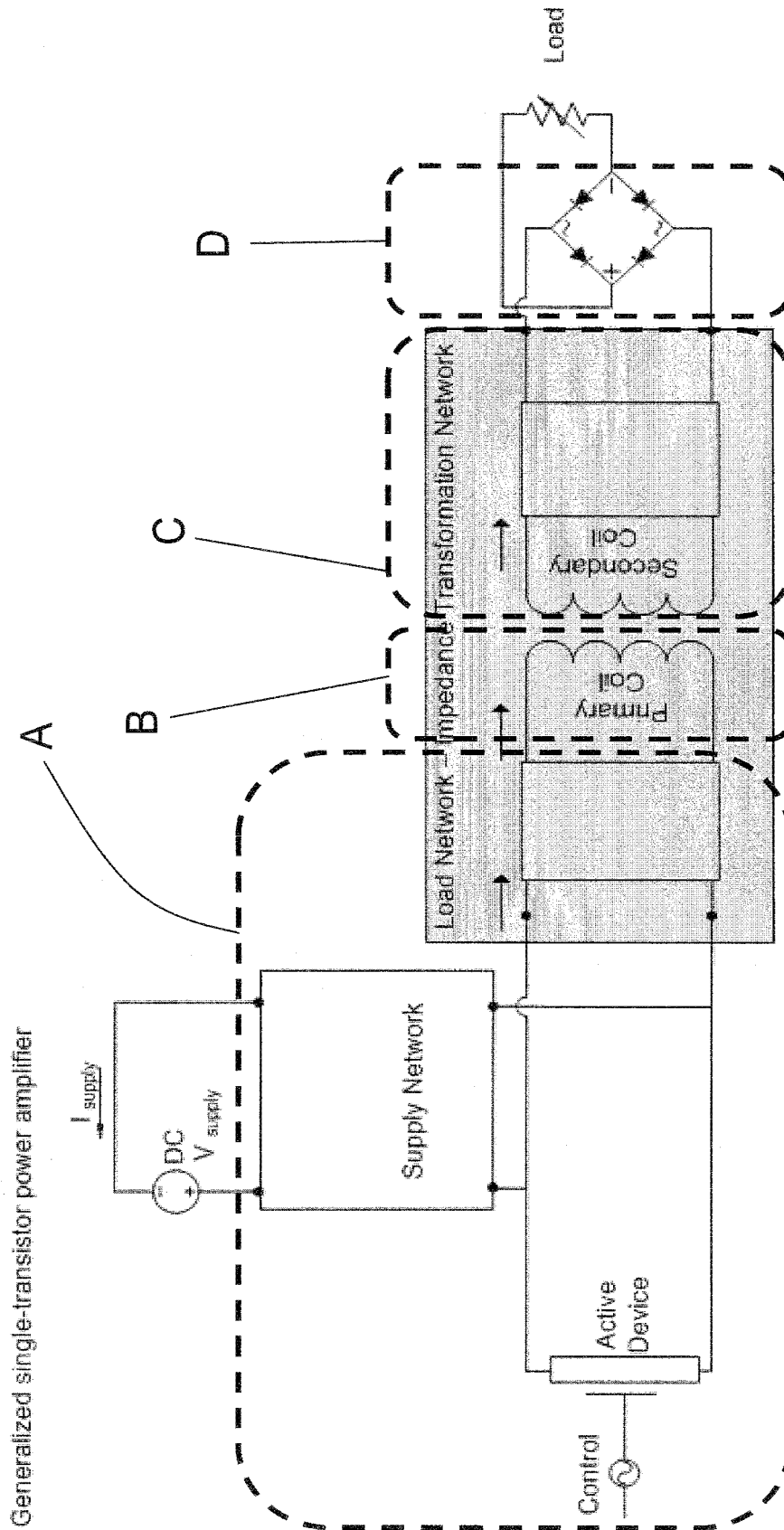


FIG. 37

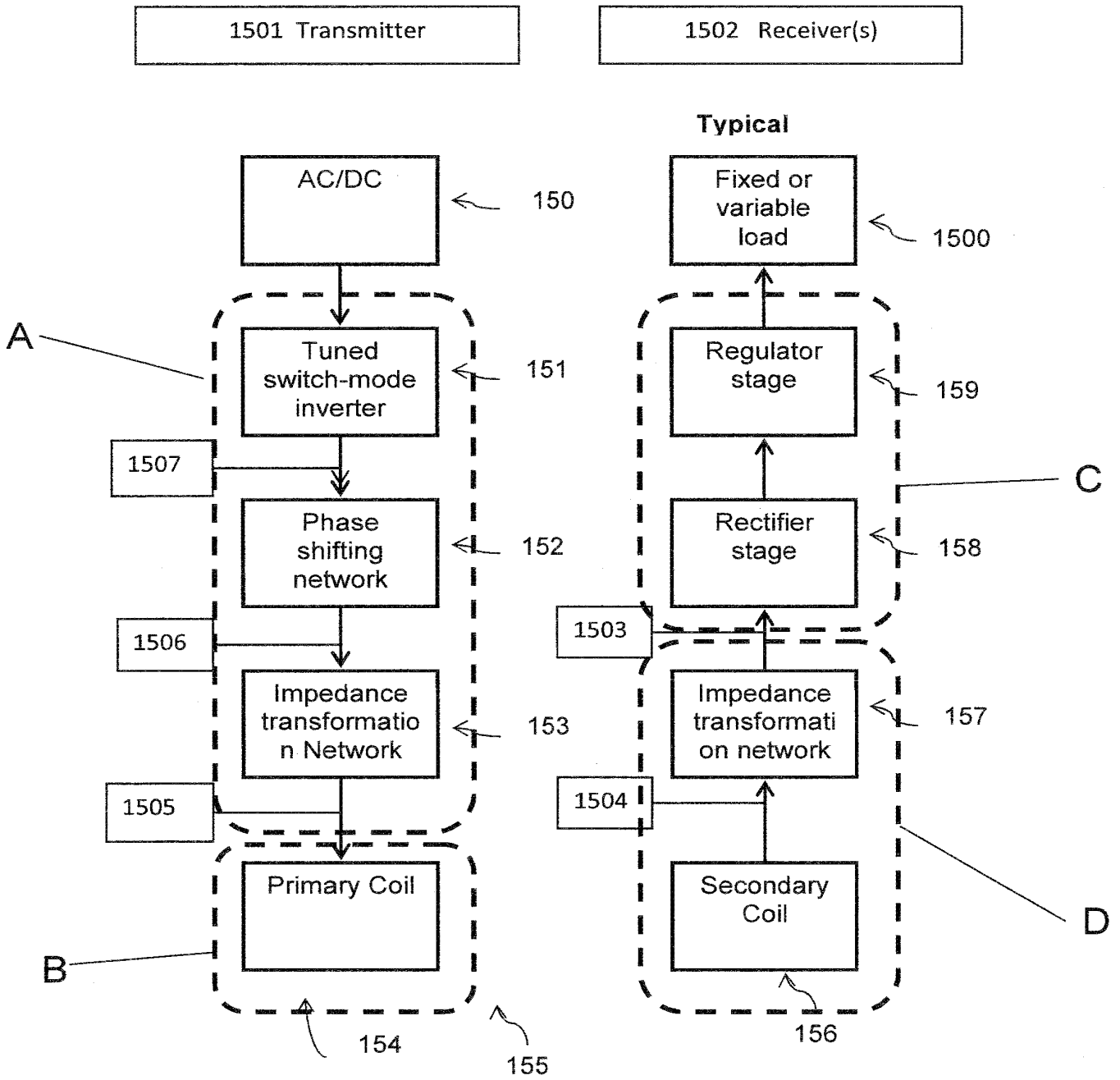


FIG. 38

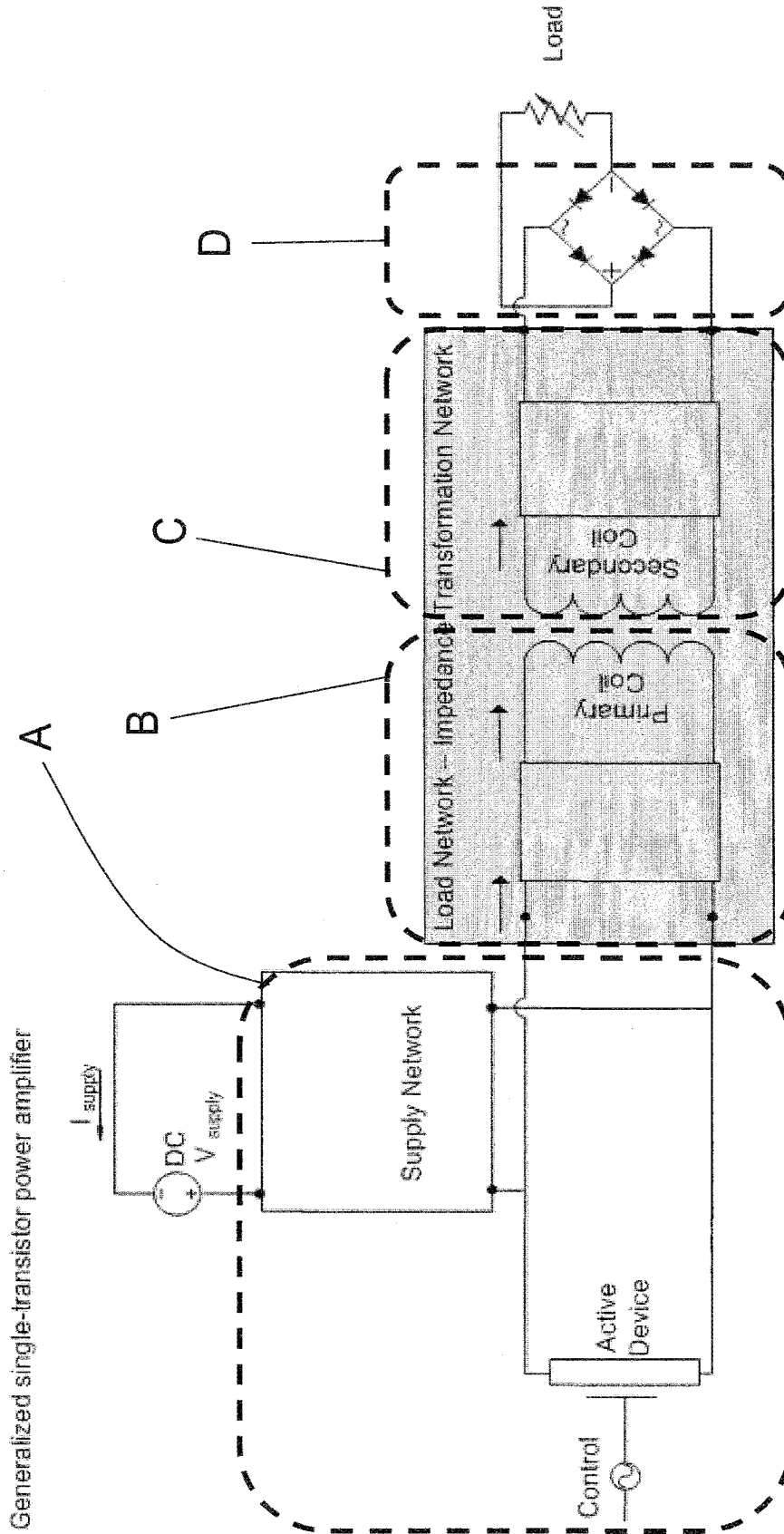


FIG. 39

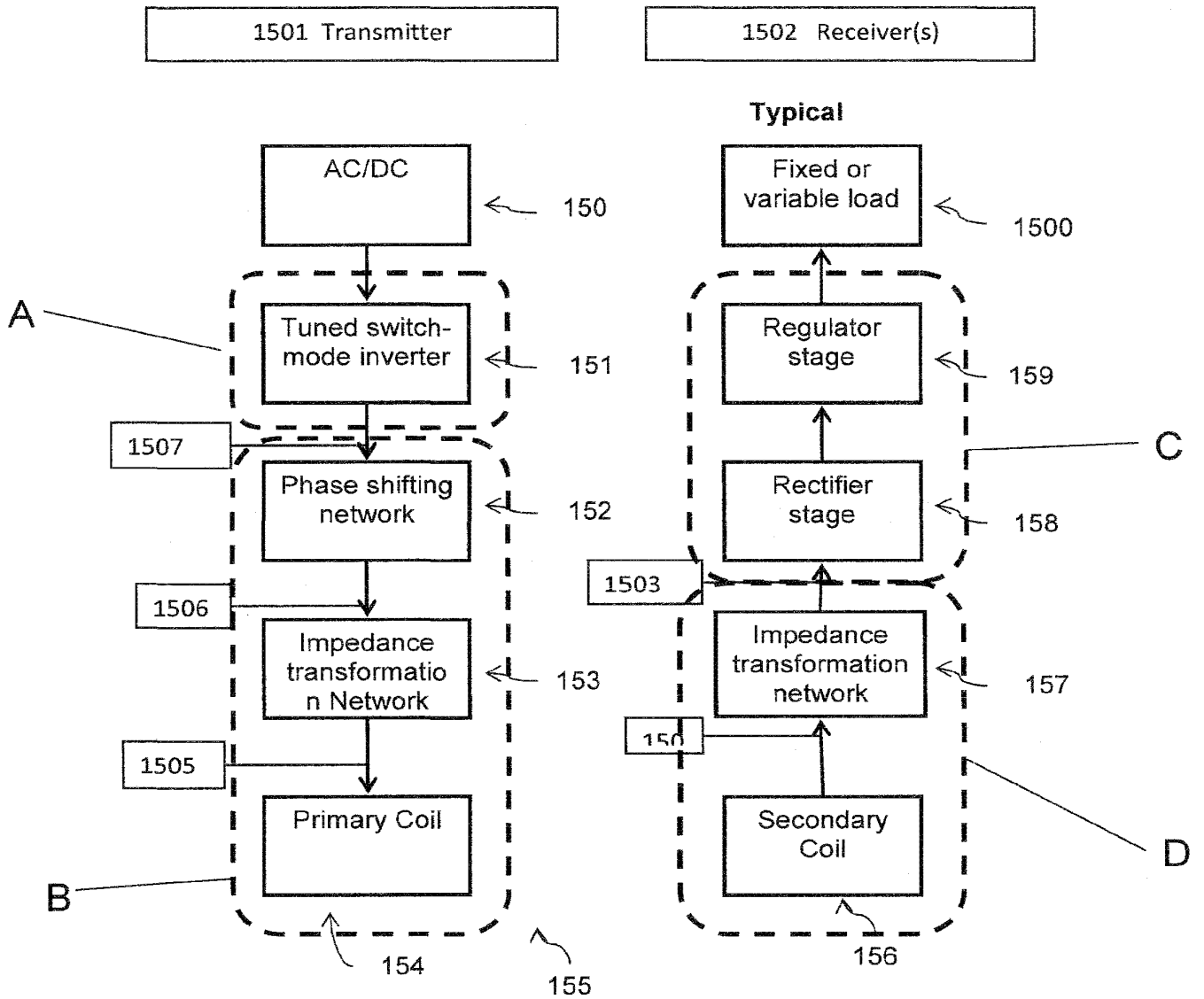


FIG. 40

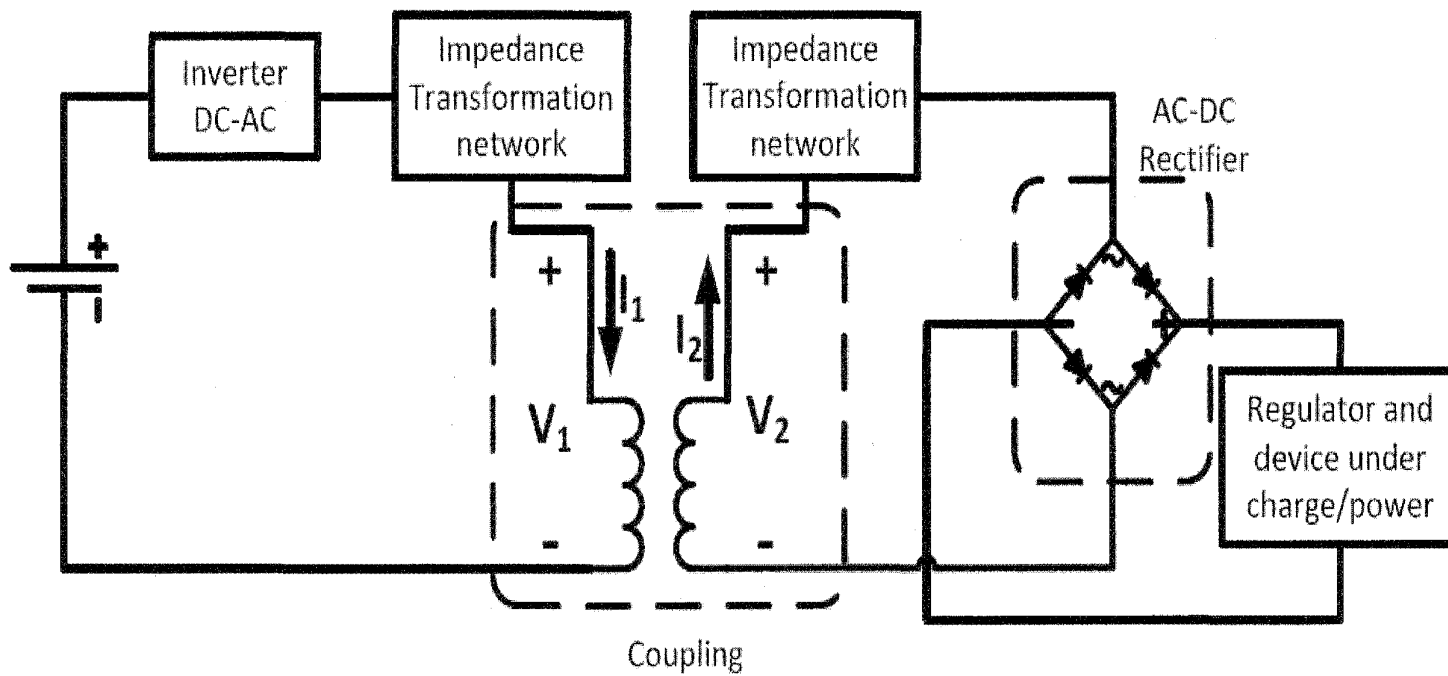


FIG. 41

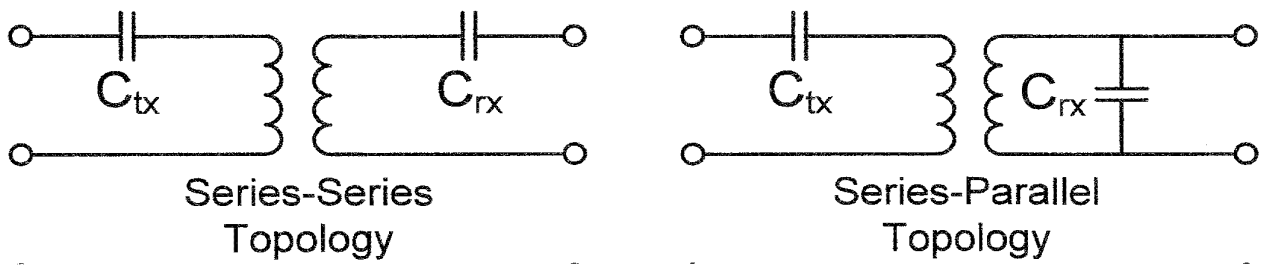


FIG. 42

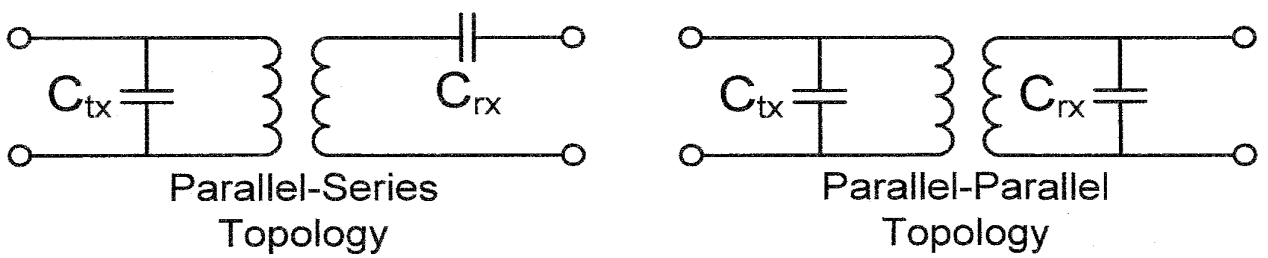
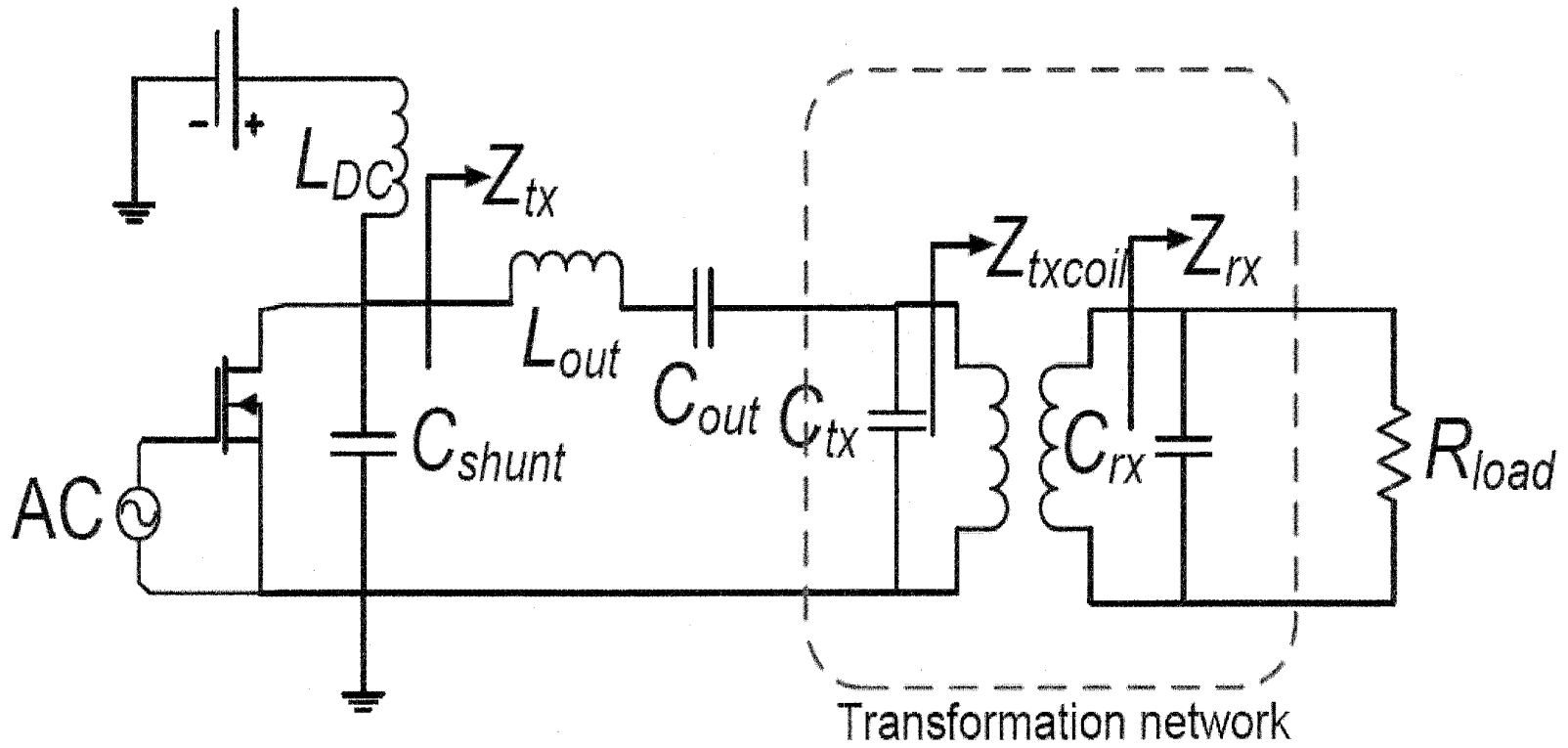


FIG. 43





44/84

FIG. 44

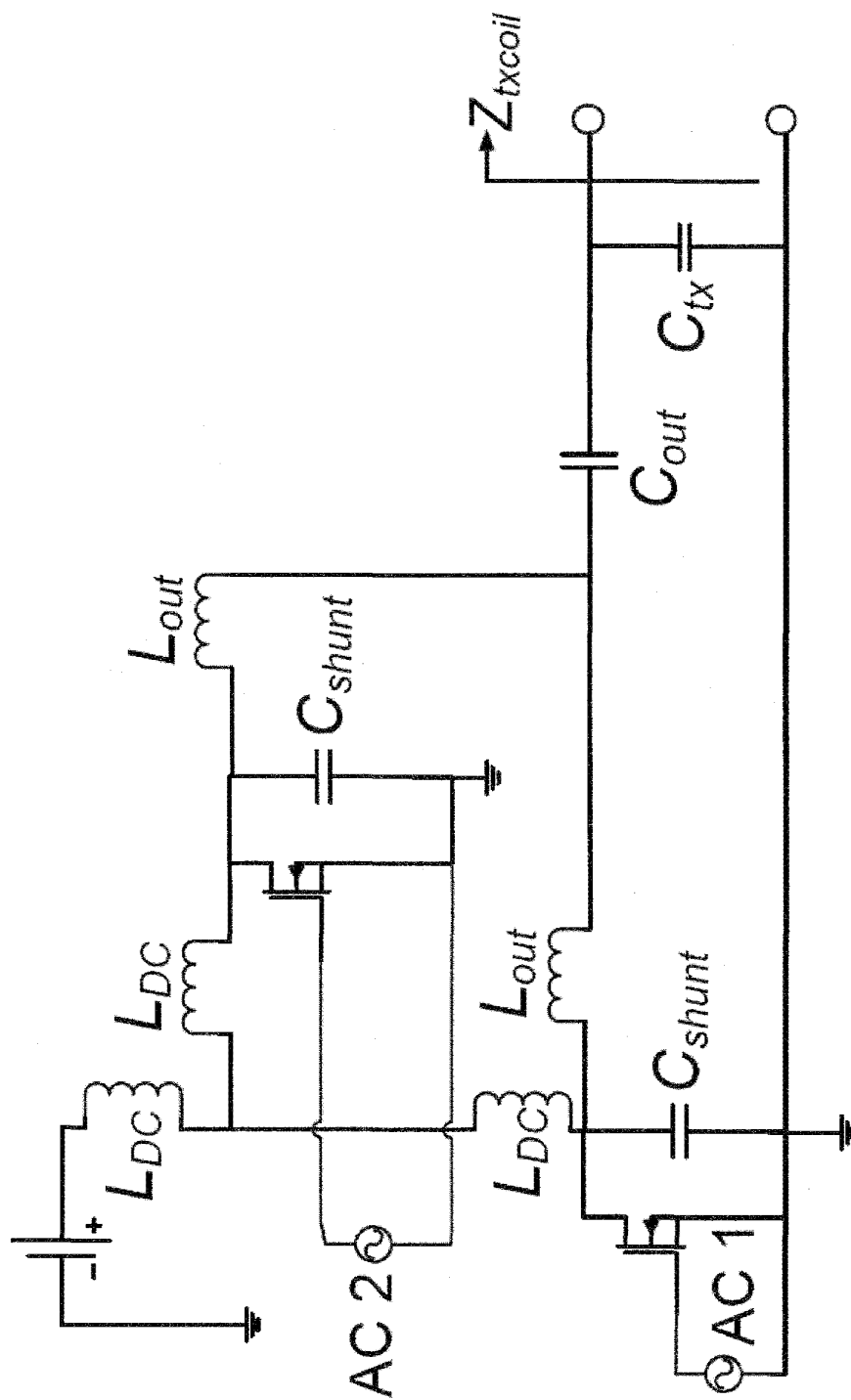


FIG. 45

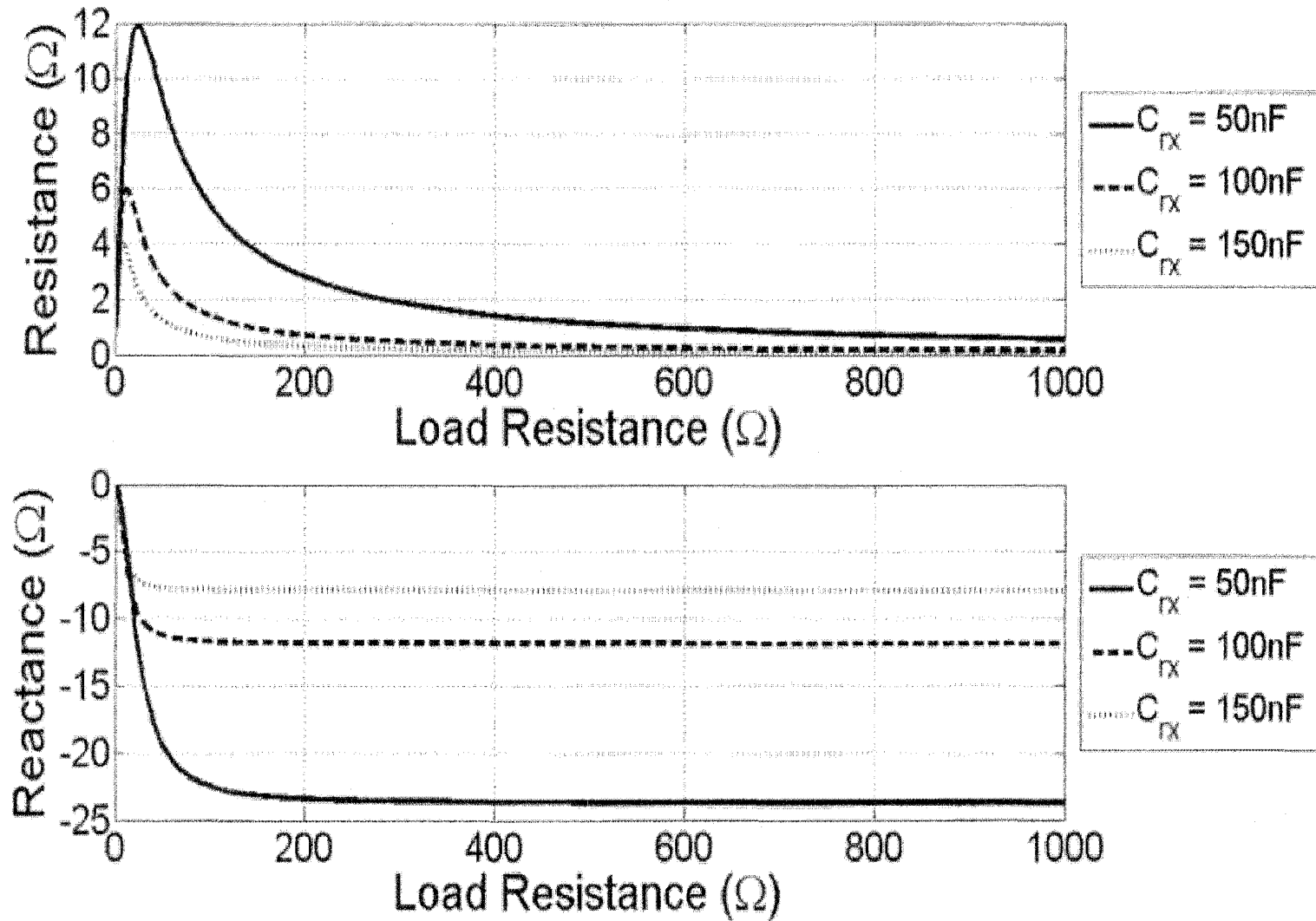


FIG. 46

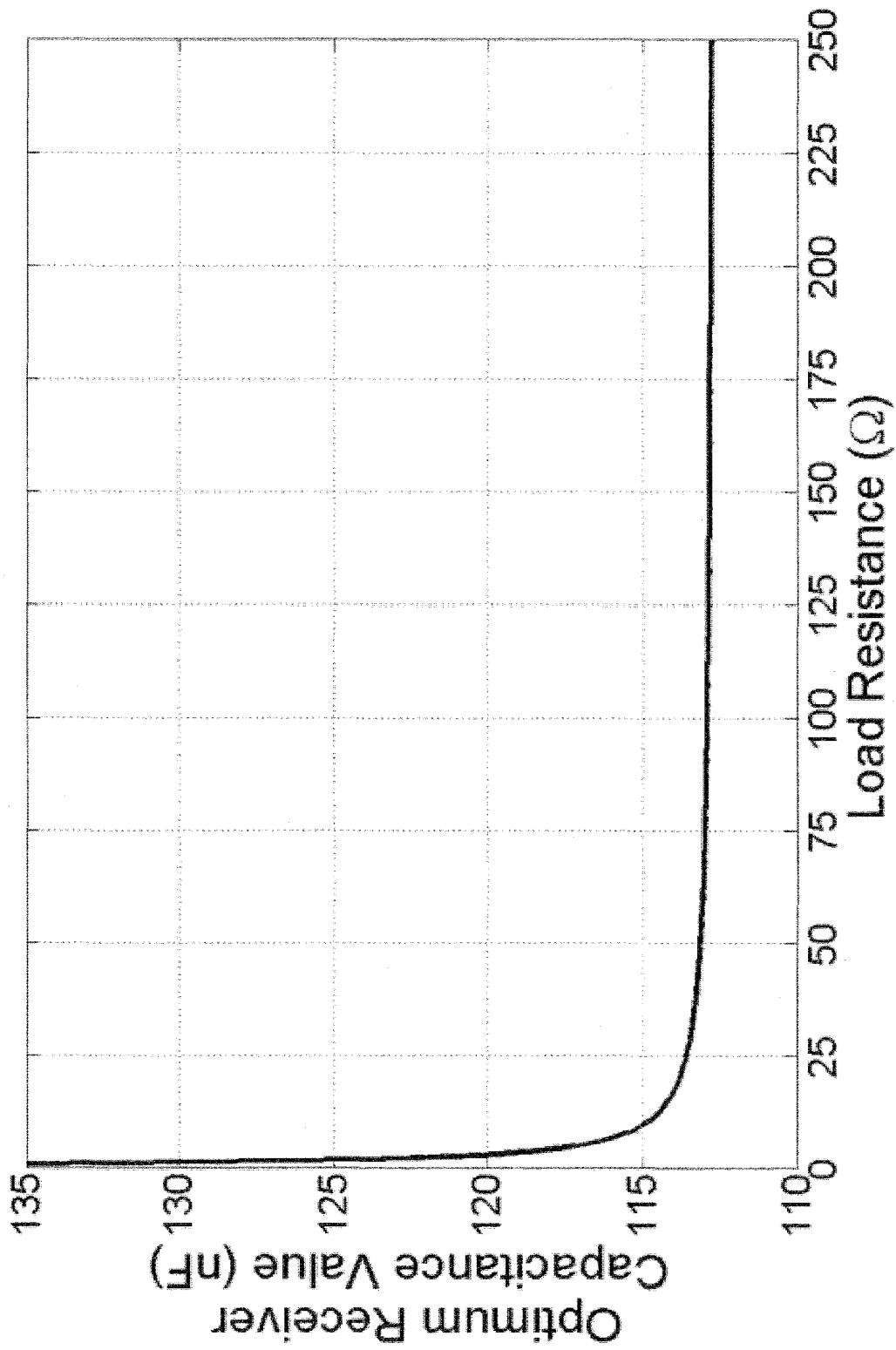


FIG. 47

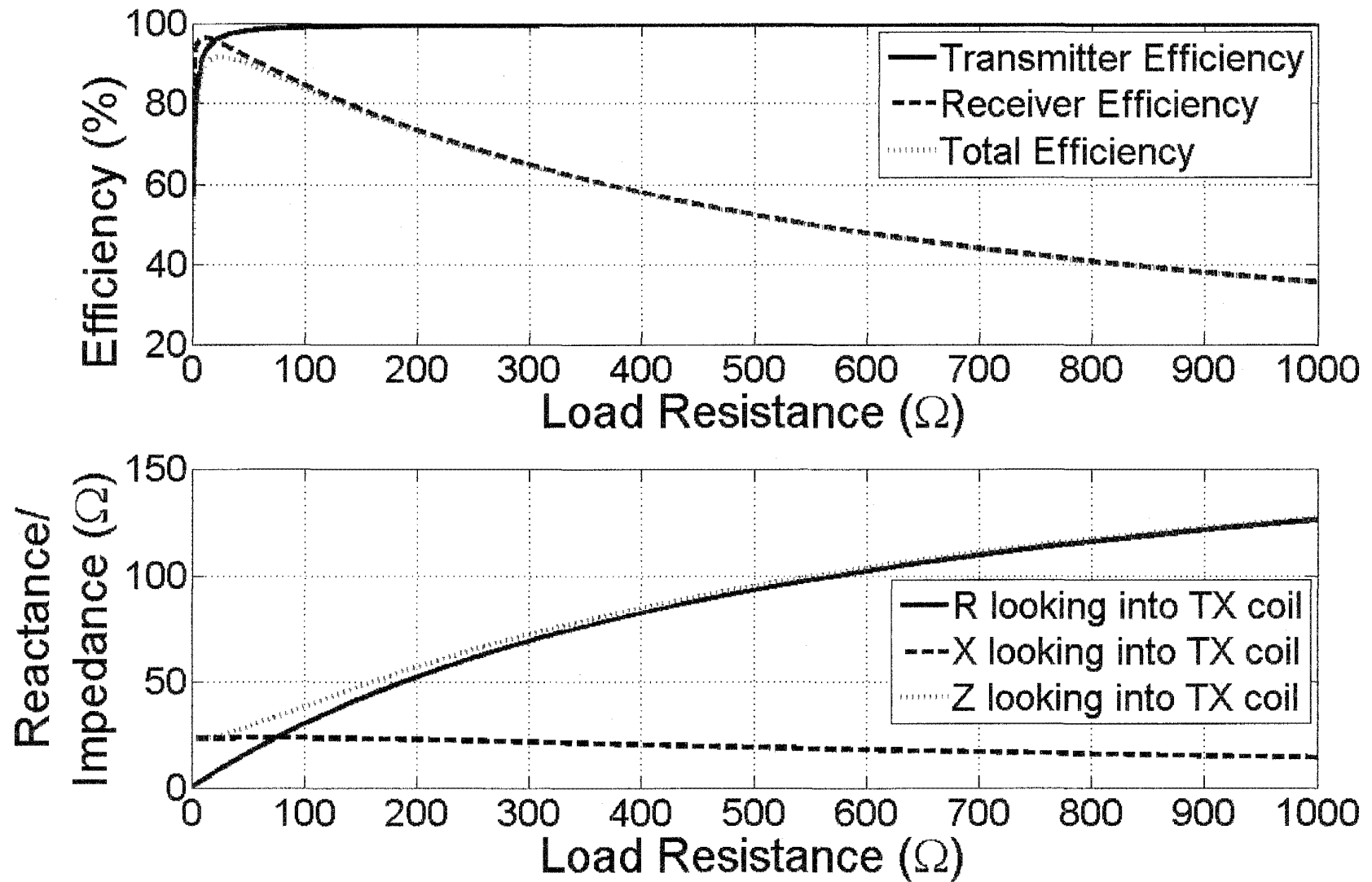


FIG. 48A

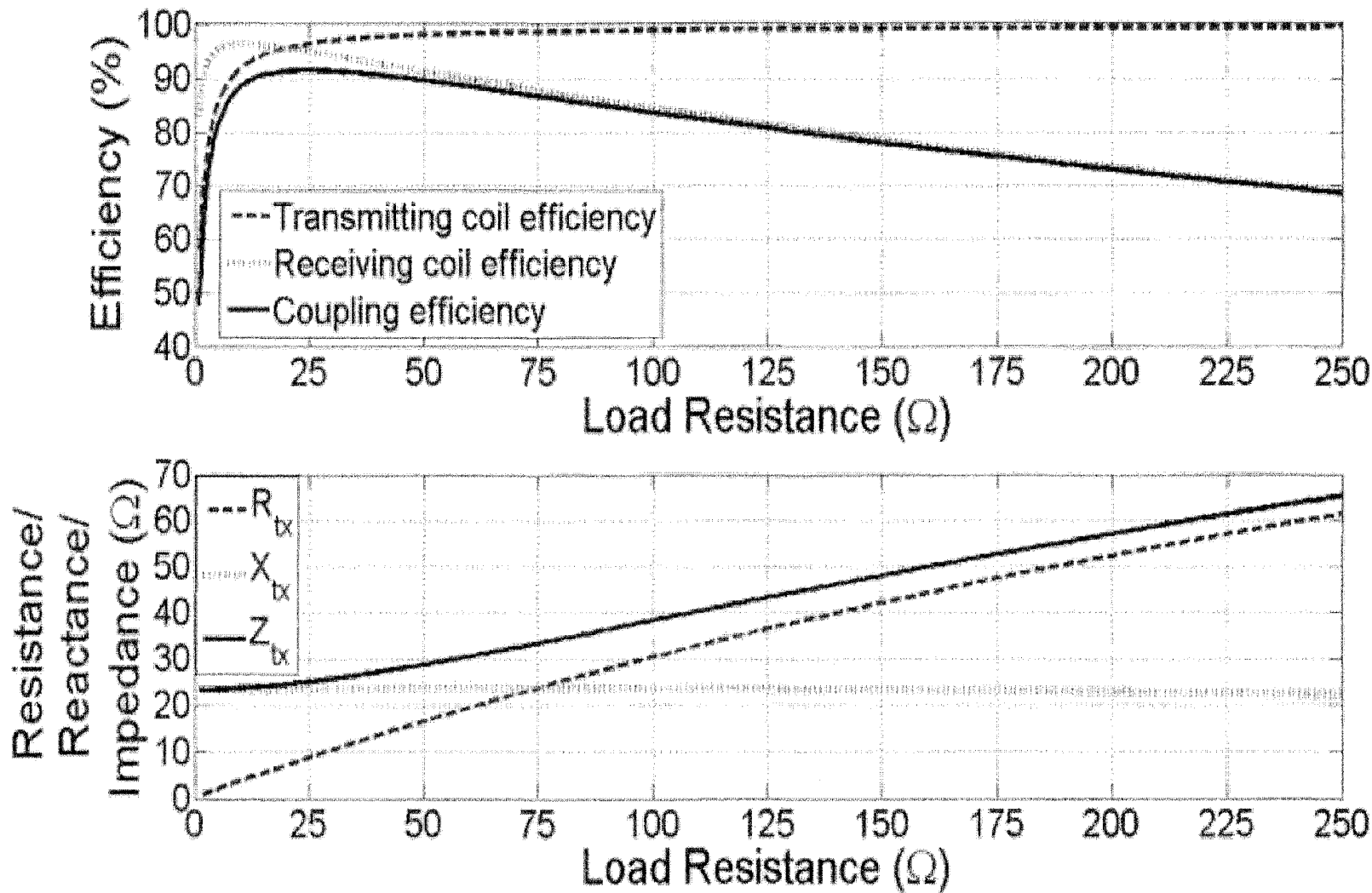


FIG. 48B

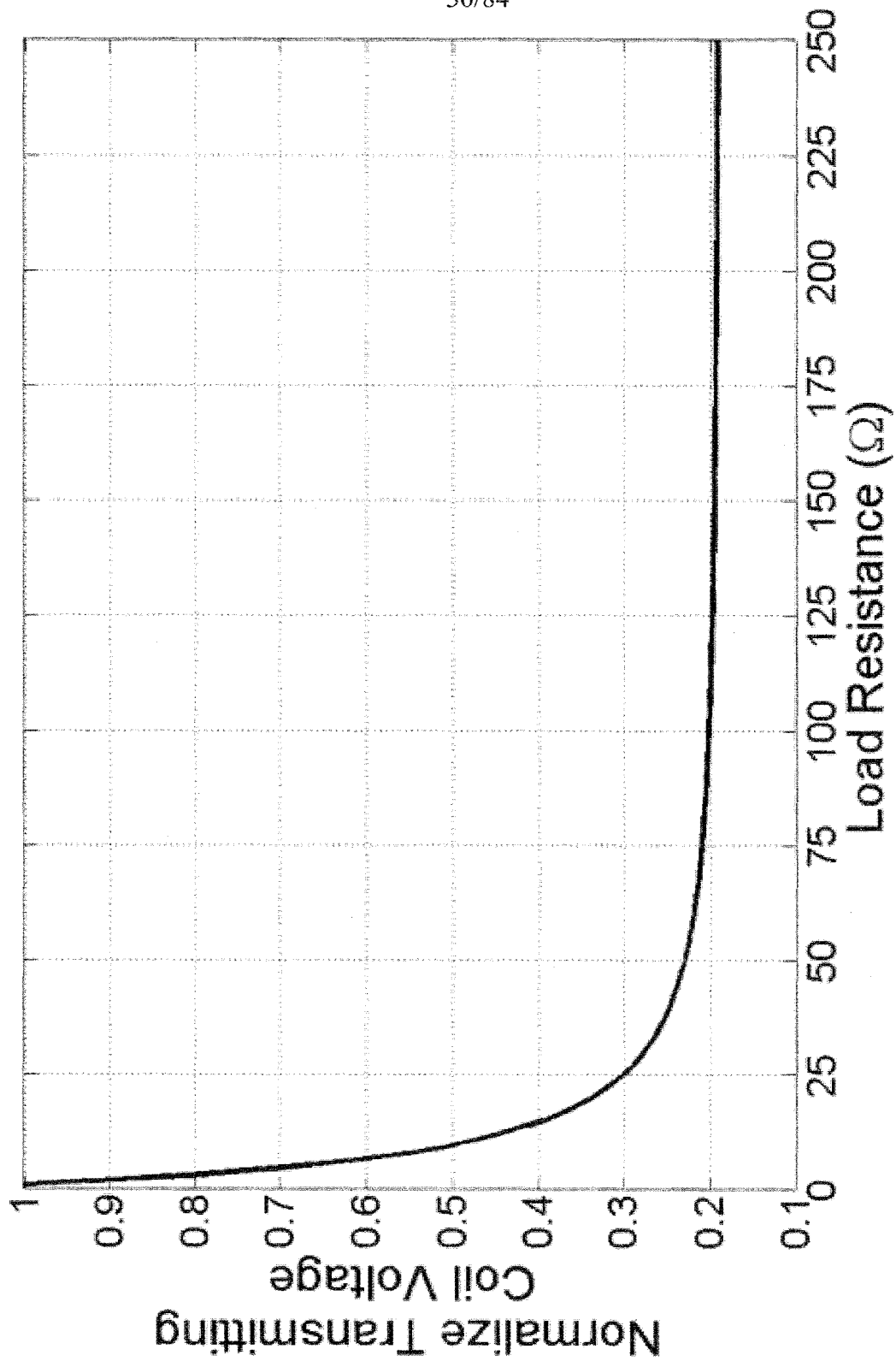


FIG. 49

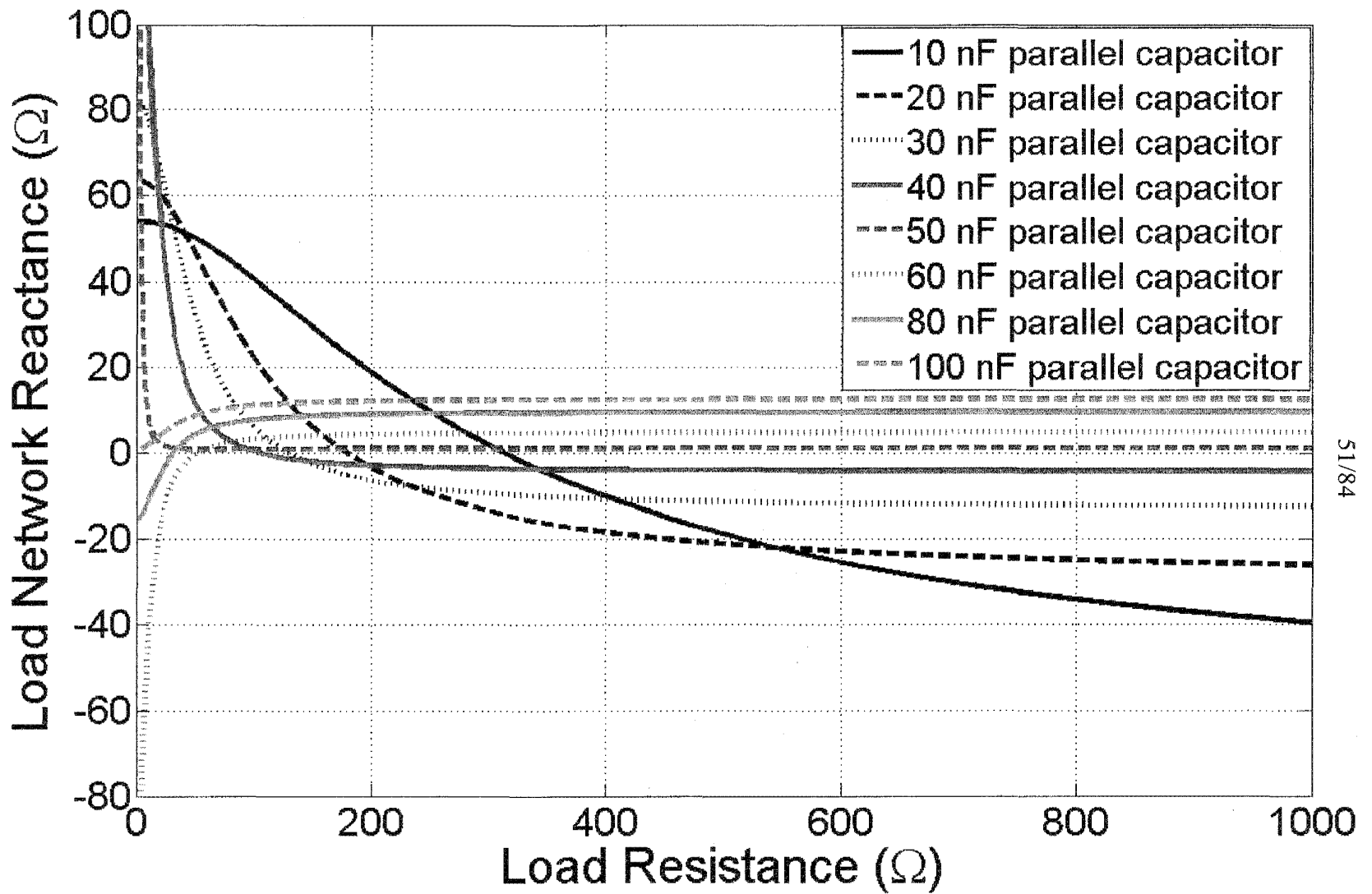


FIG. 50



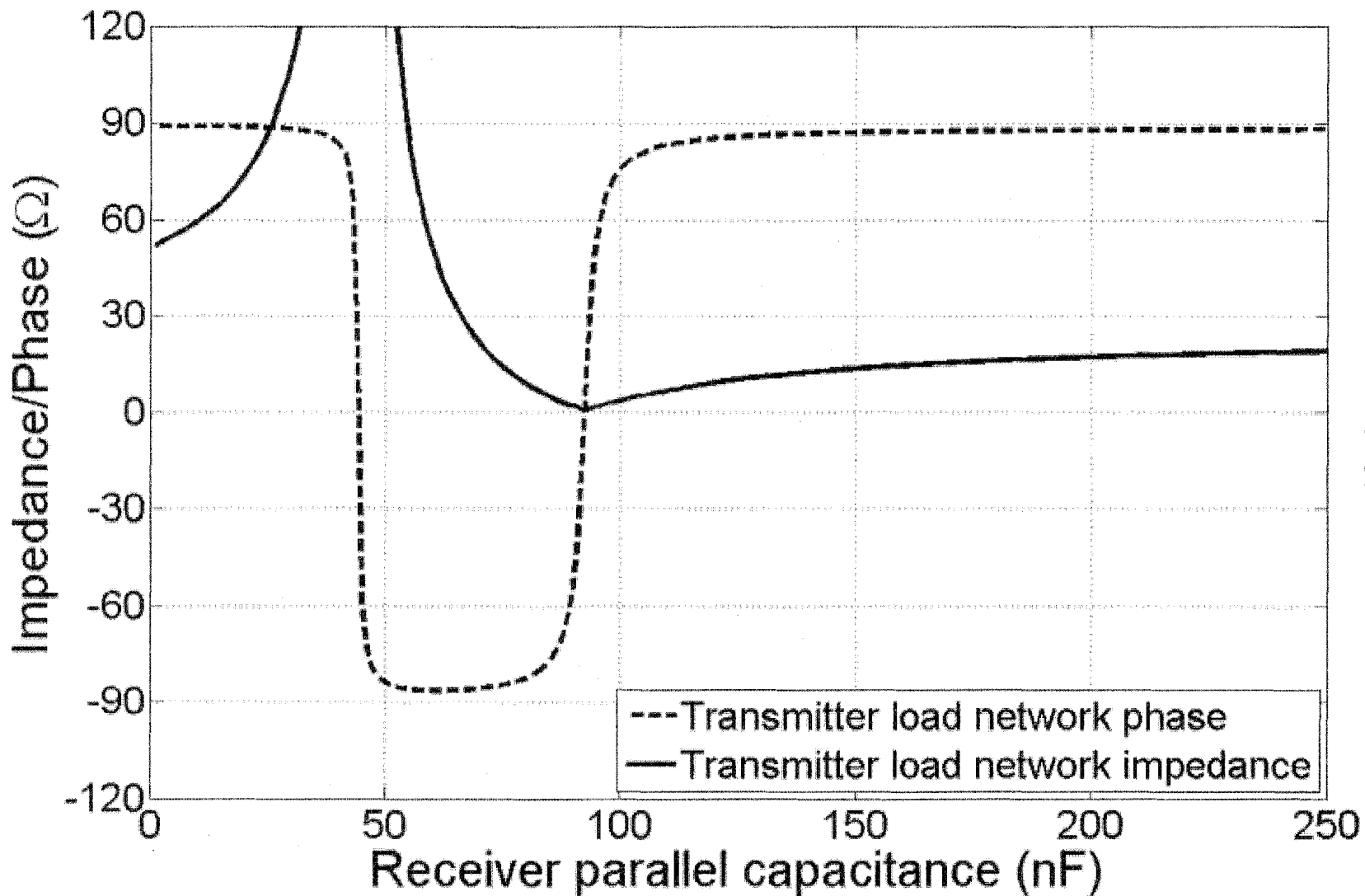


FIG. 51

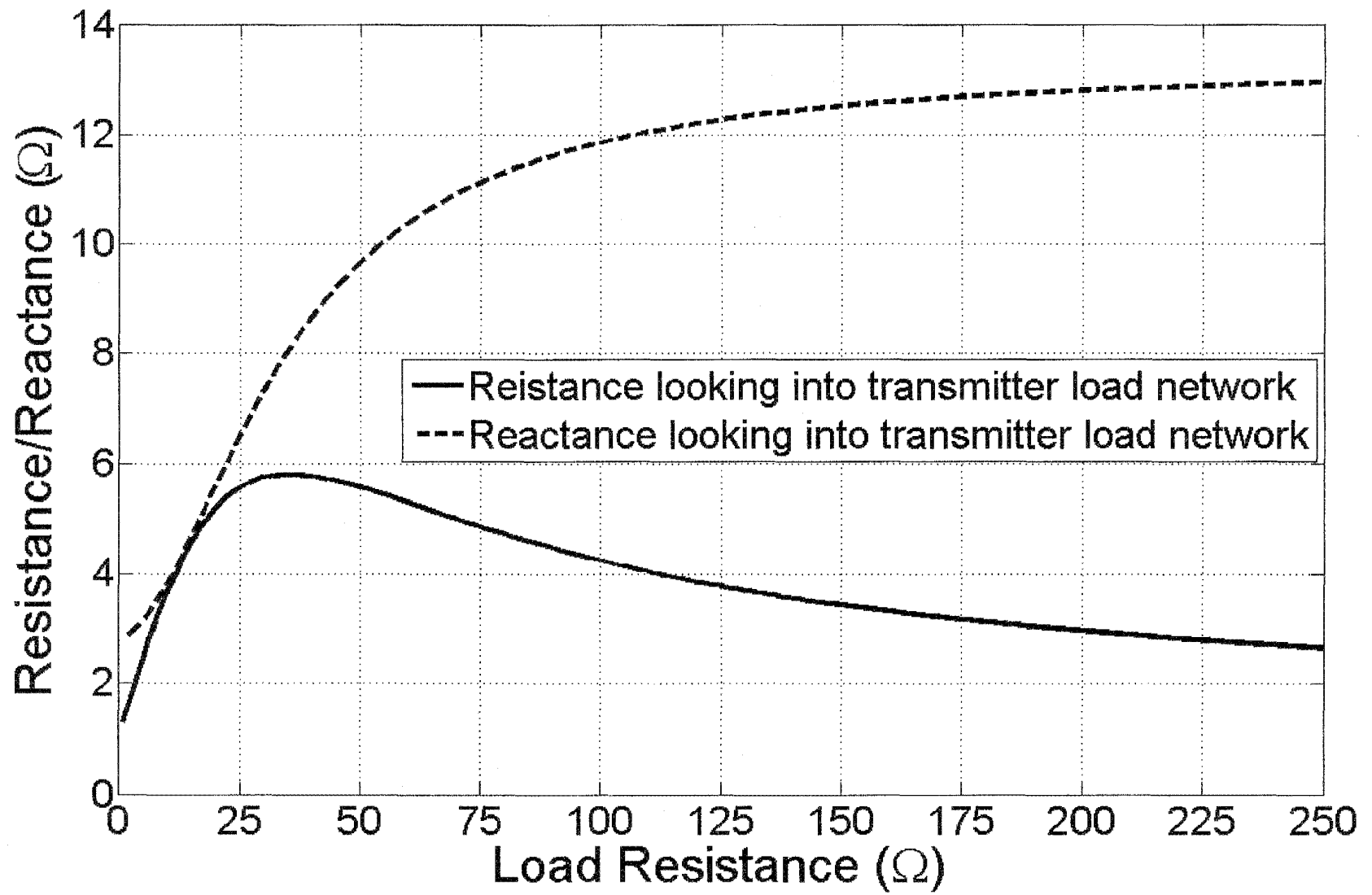


FIG. 52

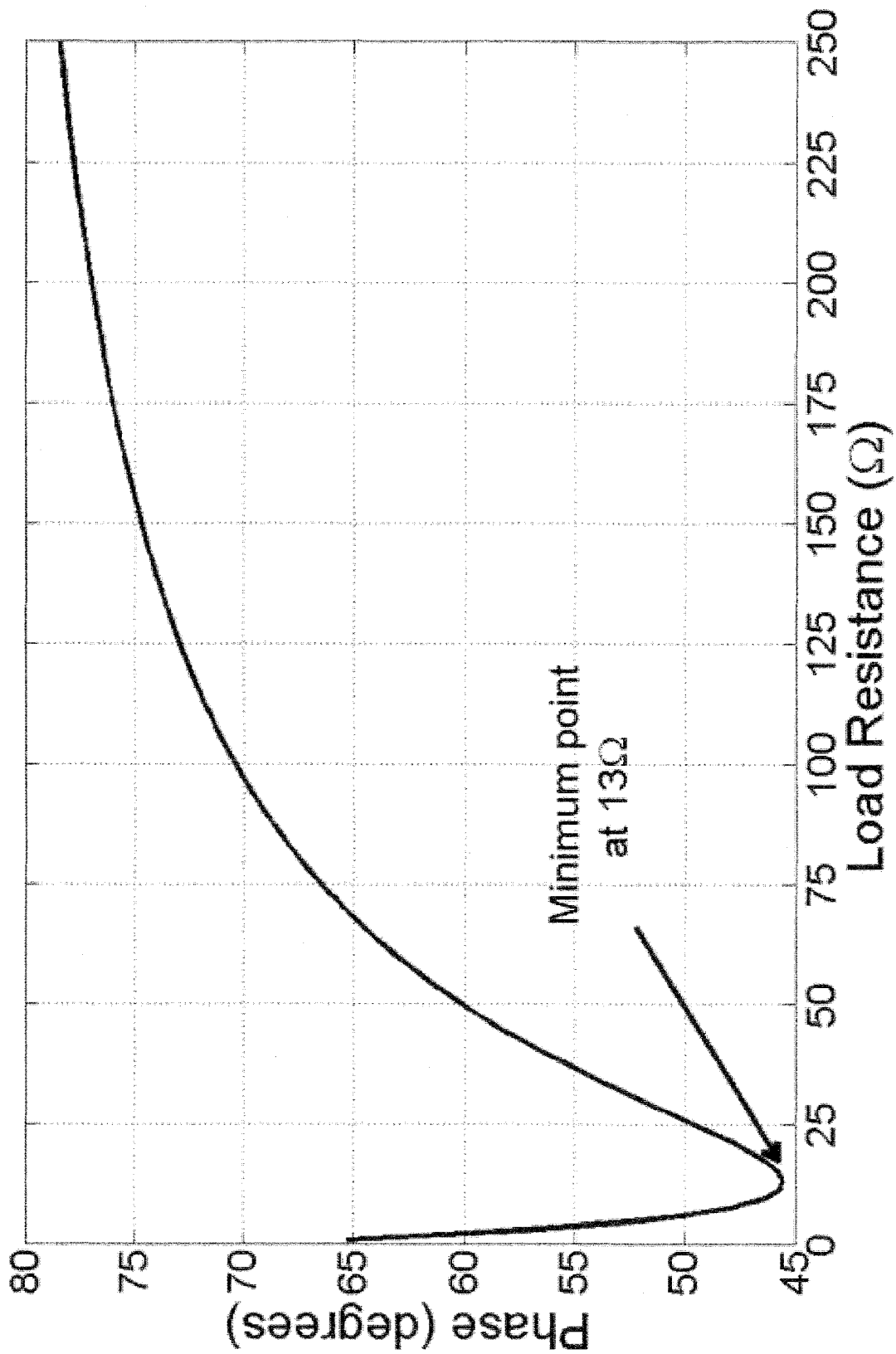


FIG. 53

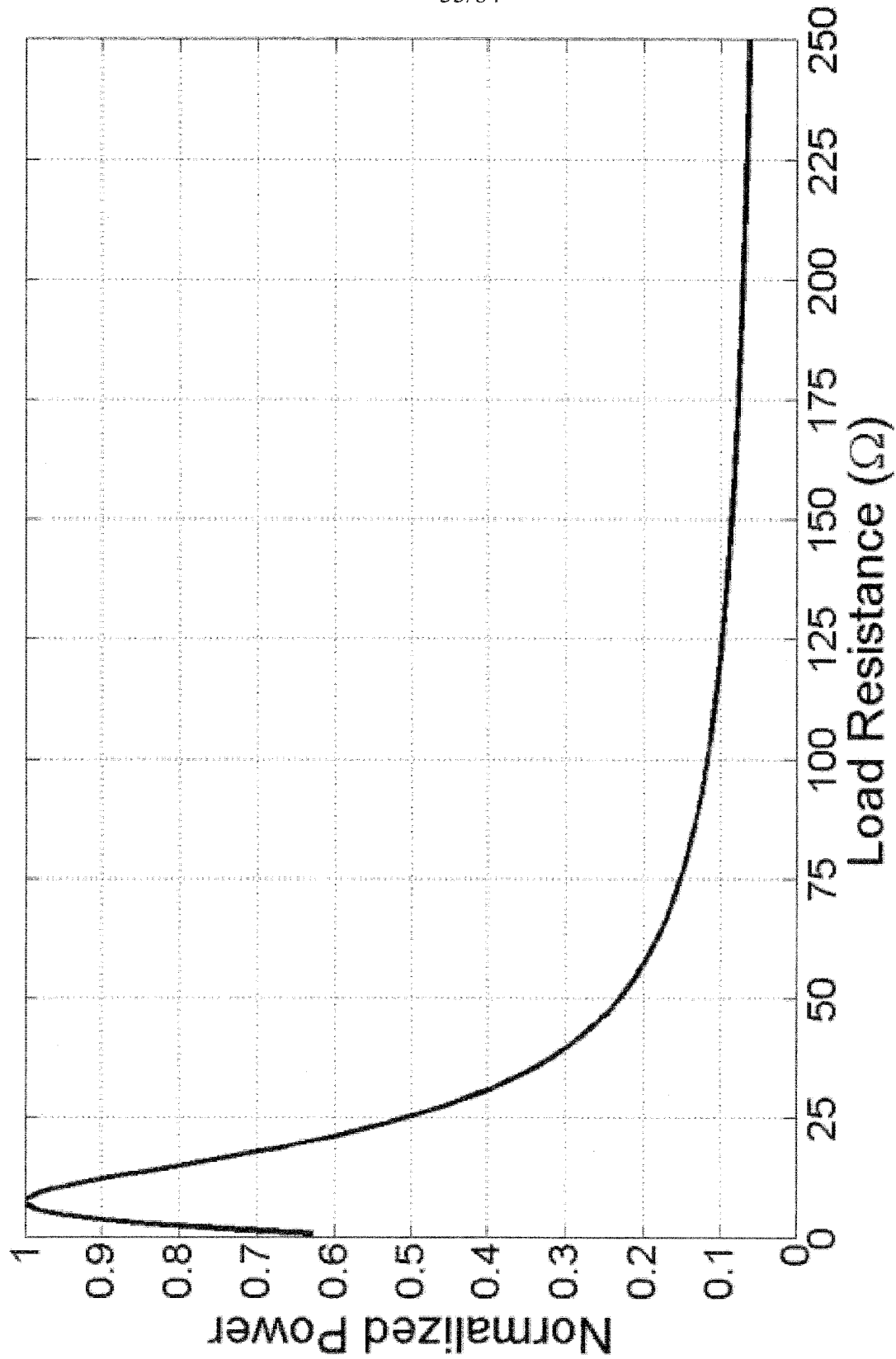


FIG. 54

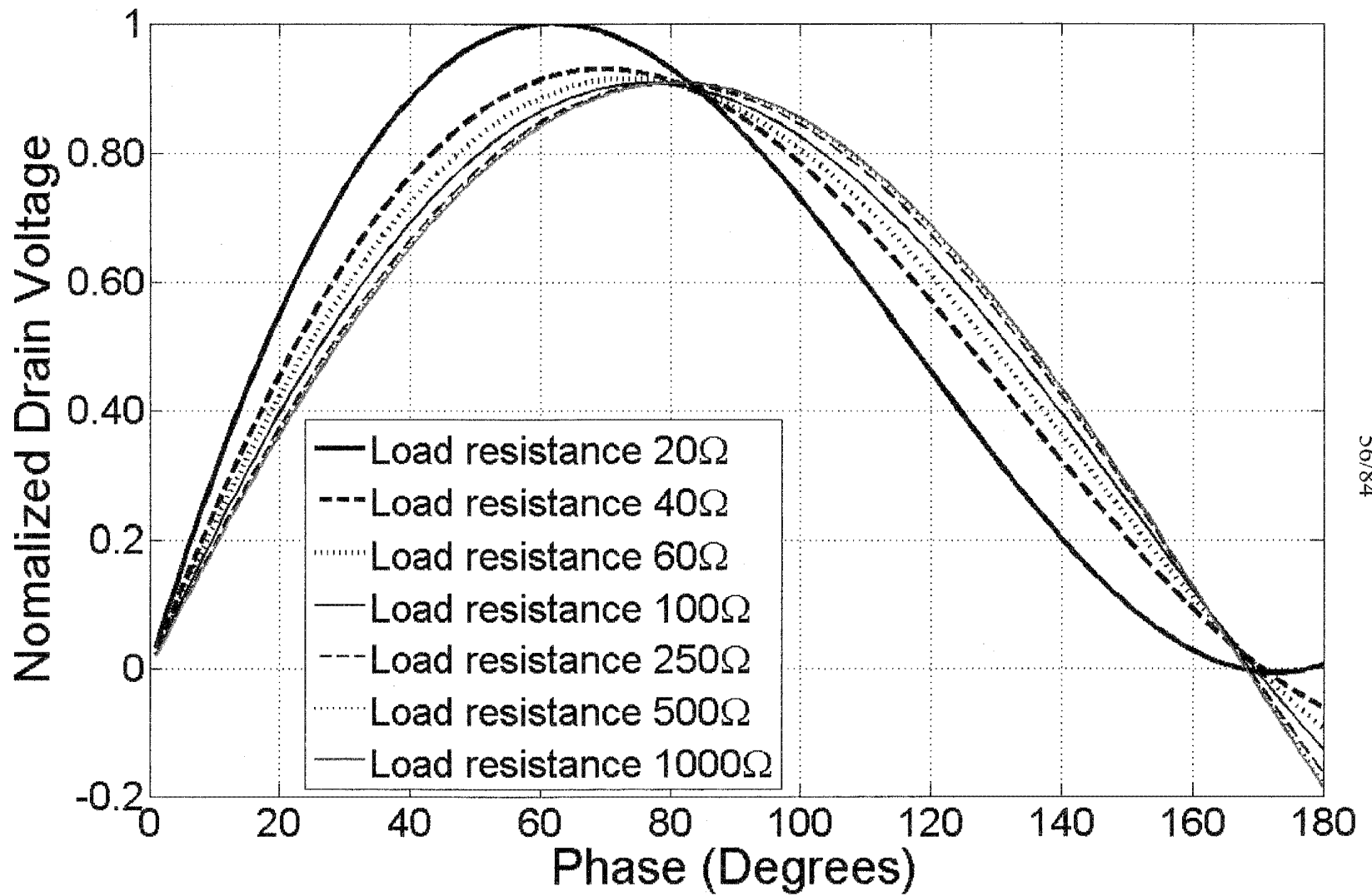
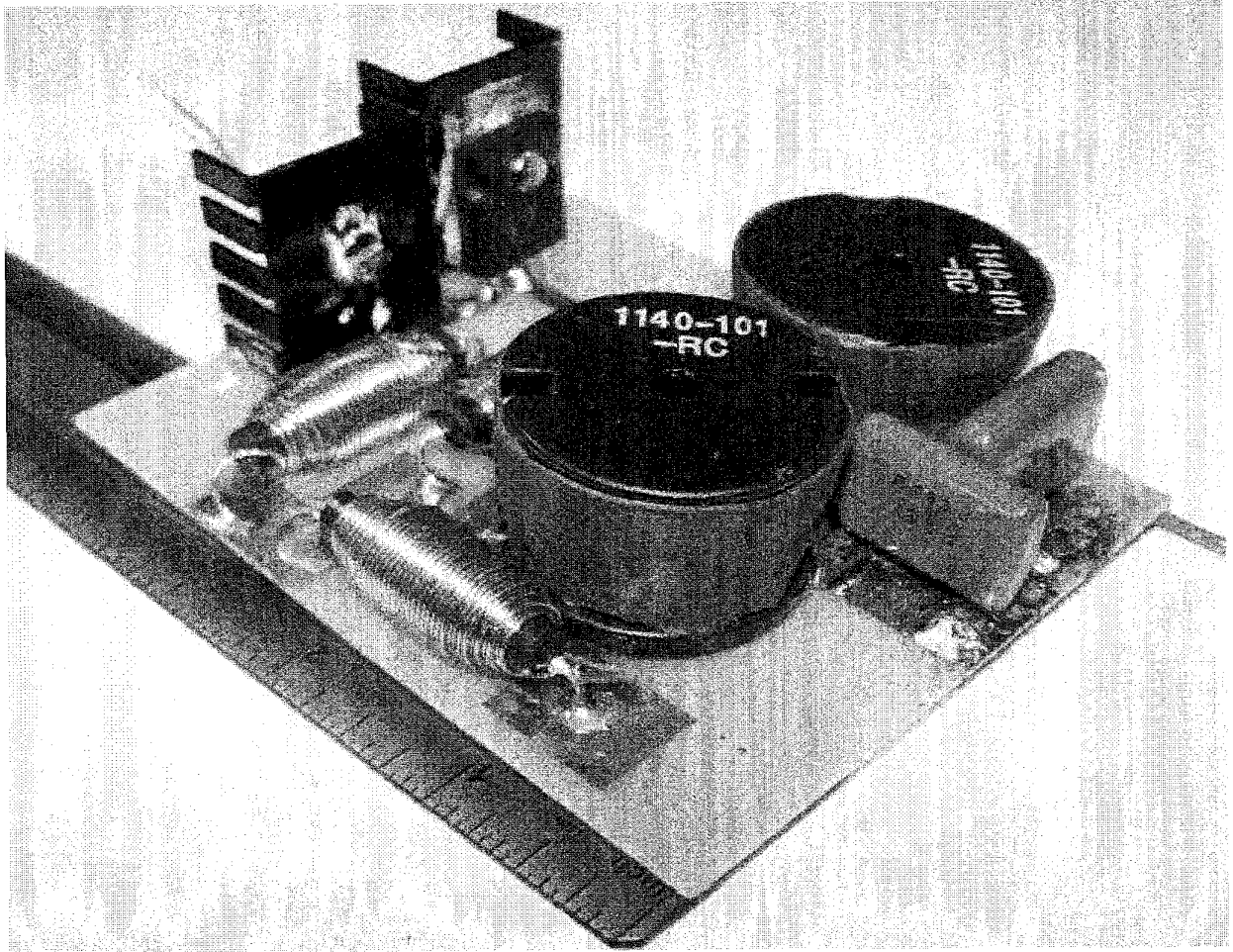
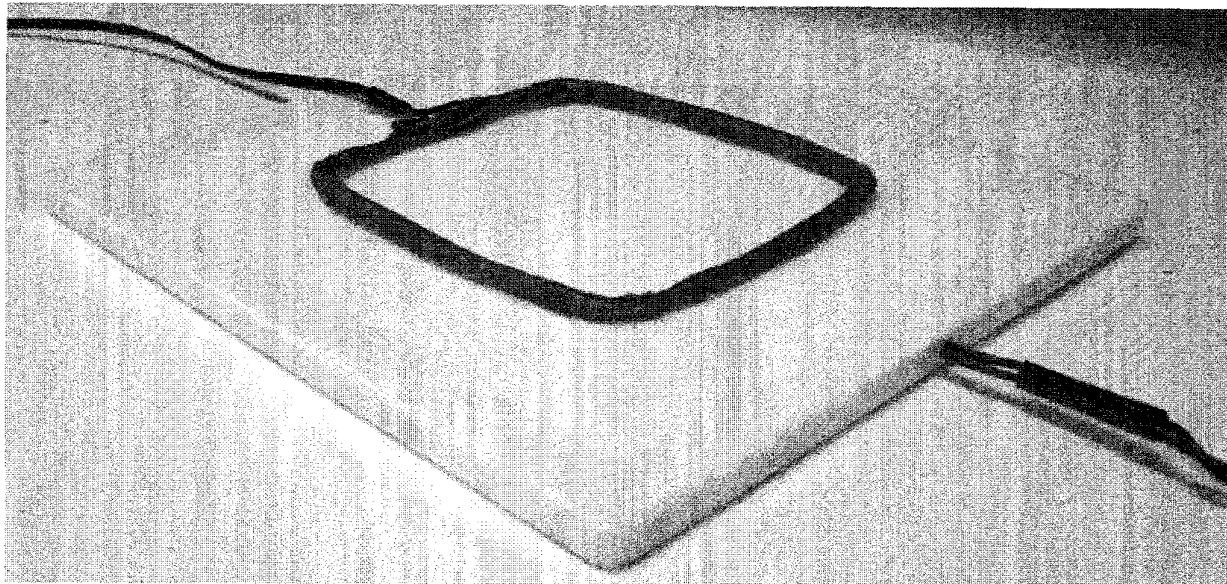


FIG. 55

57/84





**FIG. 57**

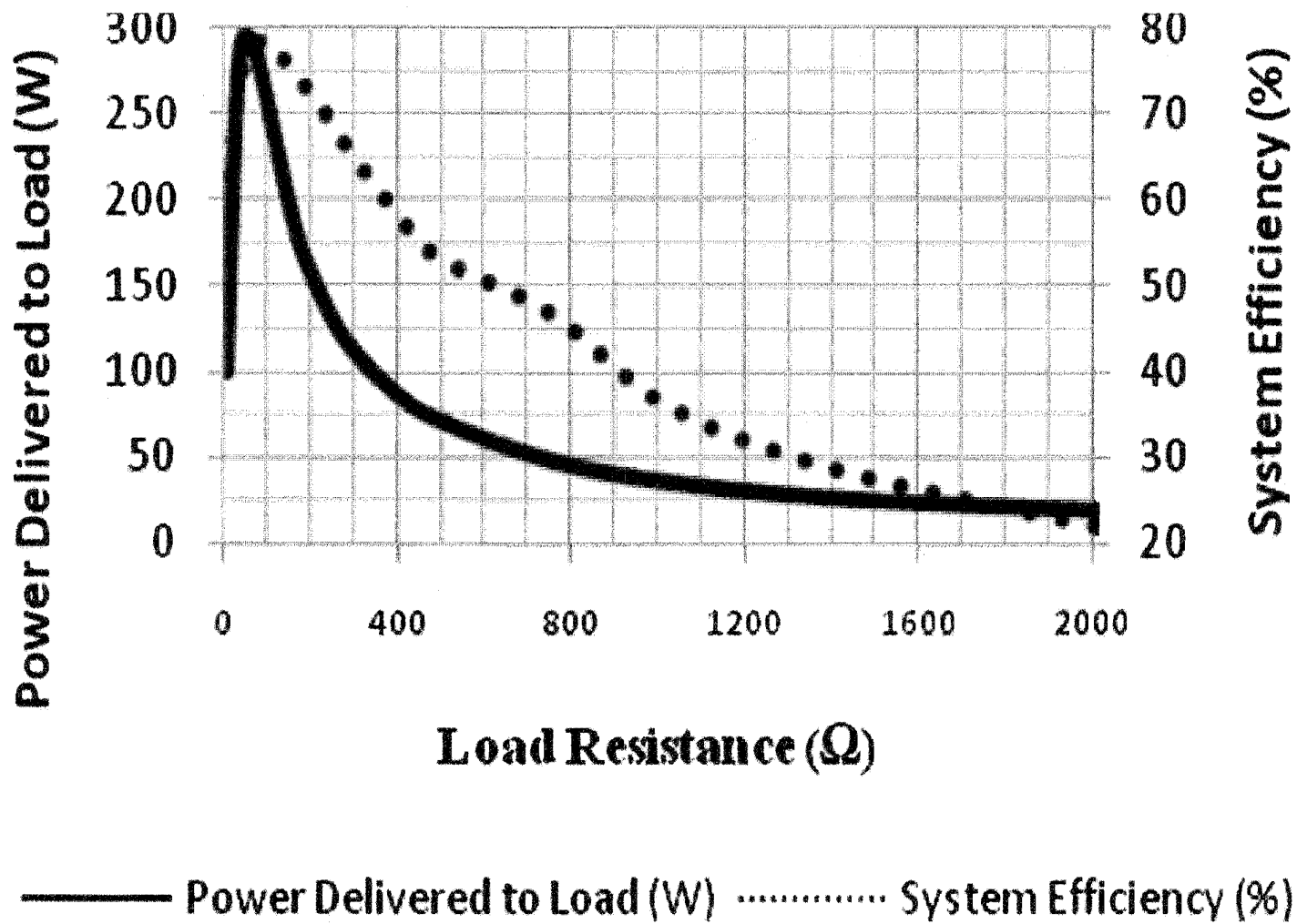
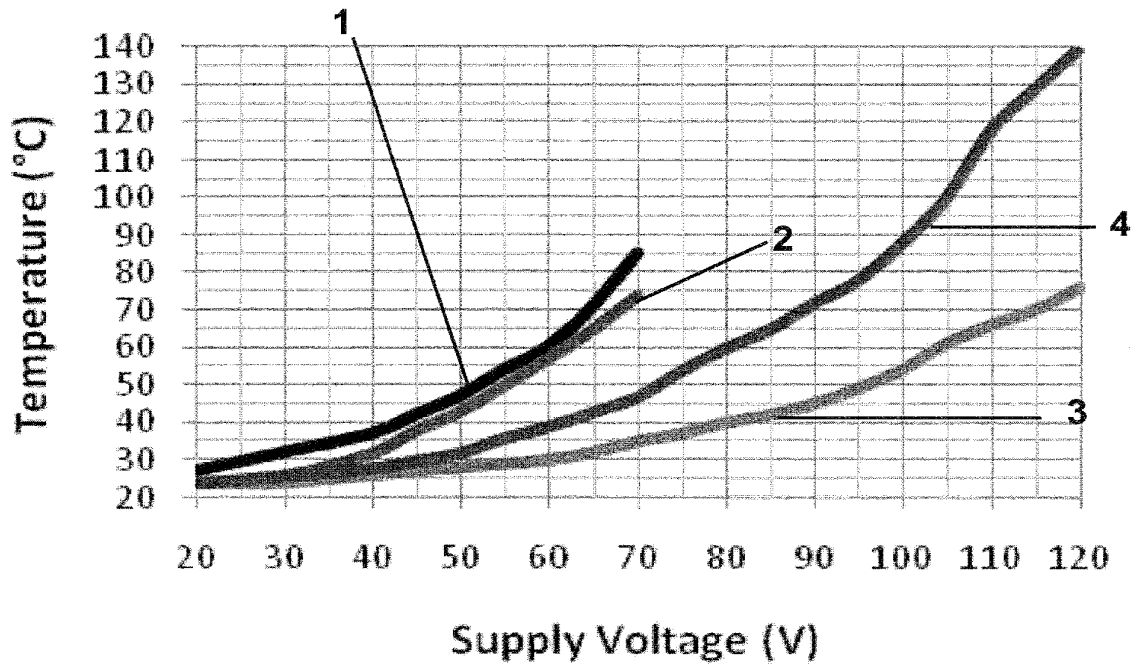


FIG. 58



60/84



- 1 — Transistor Temperature (natural convection cooling)
- 2 — Inductor Temperature (natural convection cooling)
- 3 — Transistor Temperature (forced cooling)
- 4 — Inductor Temperature (forced cooling)

FIG. 59

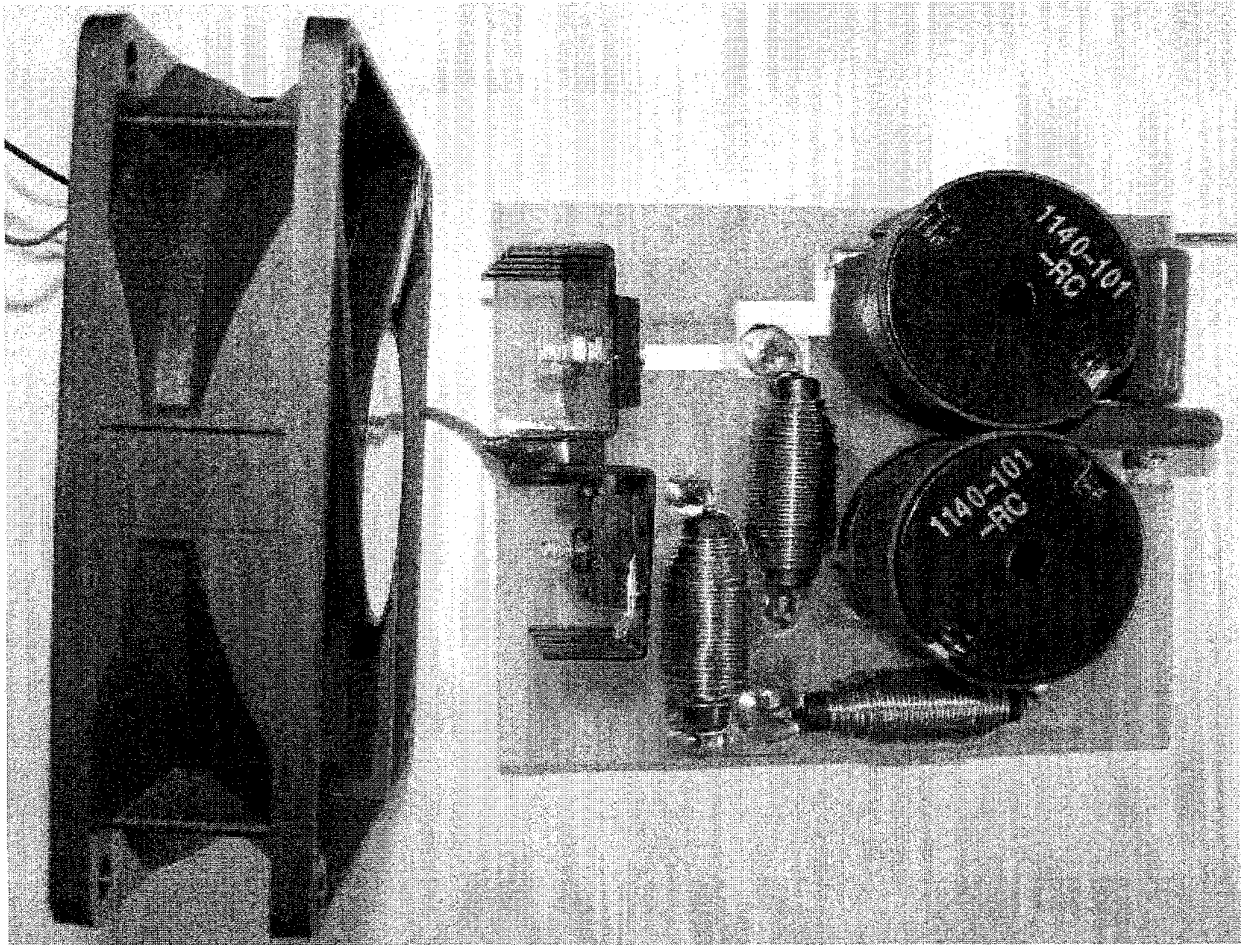


FIG. 60

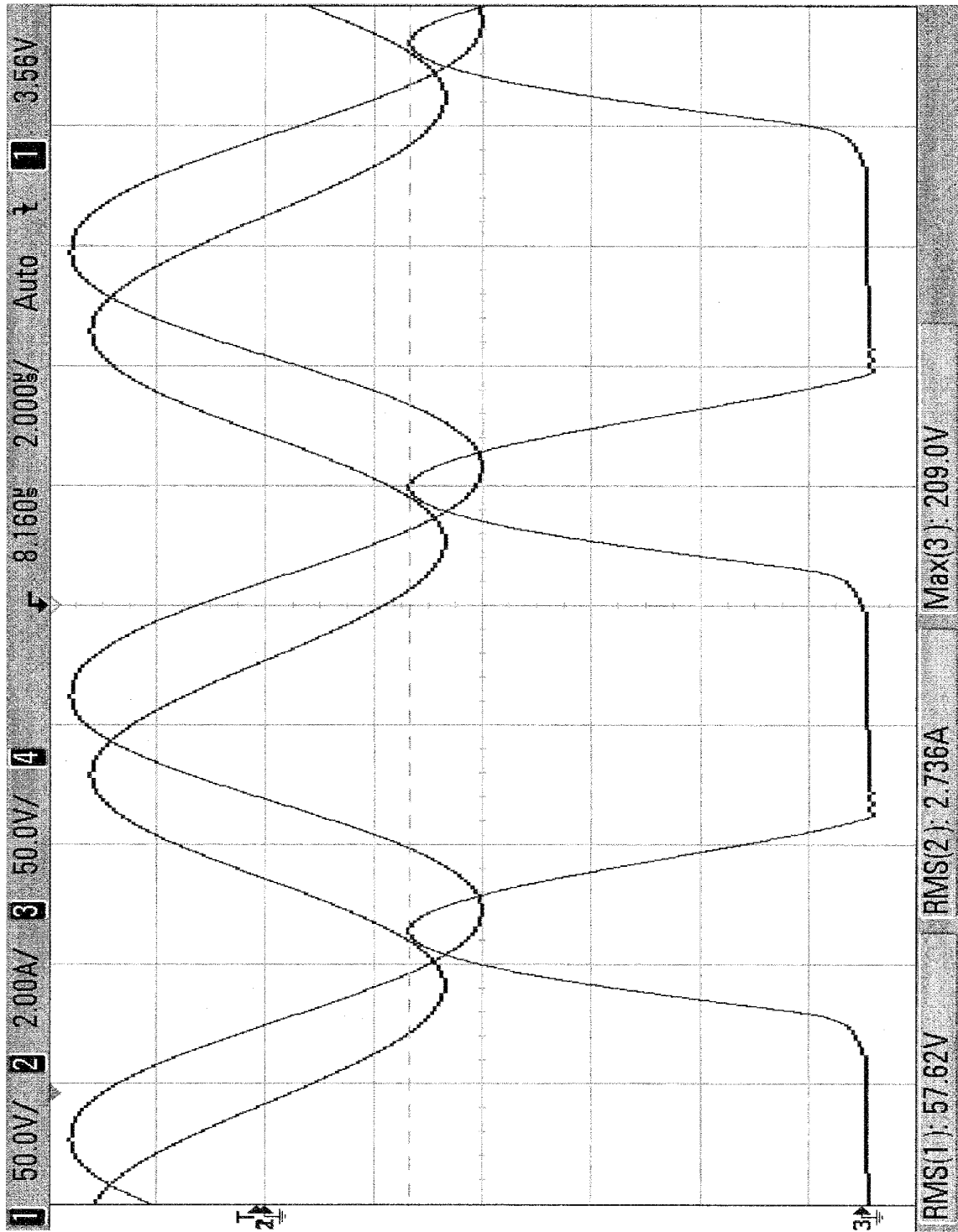


FIG. 61

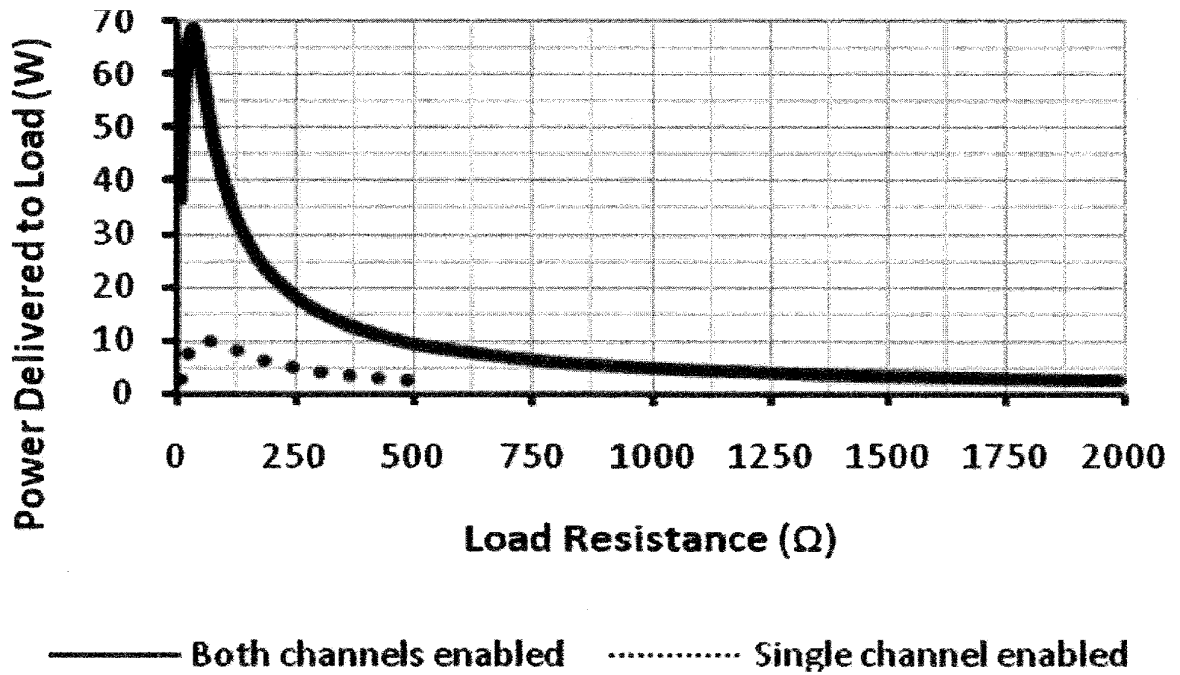


FIG. 62A

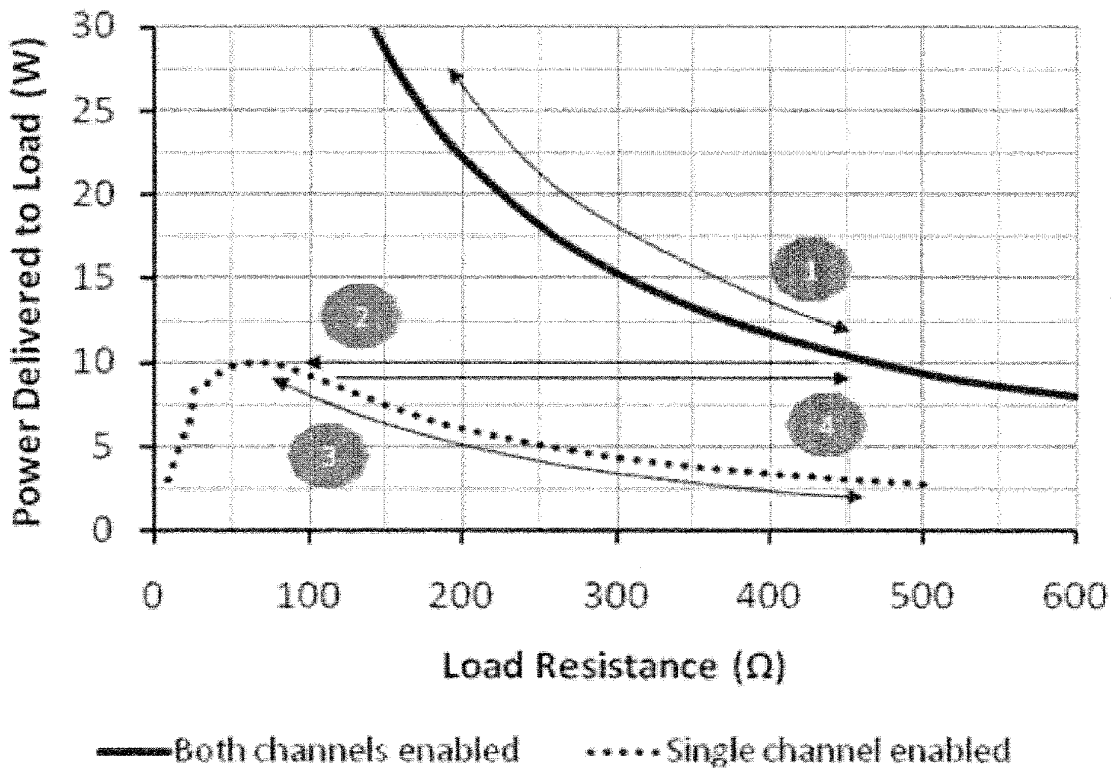


FIG. 62B

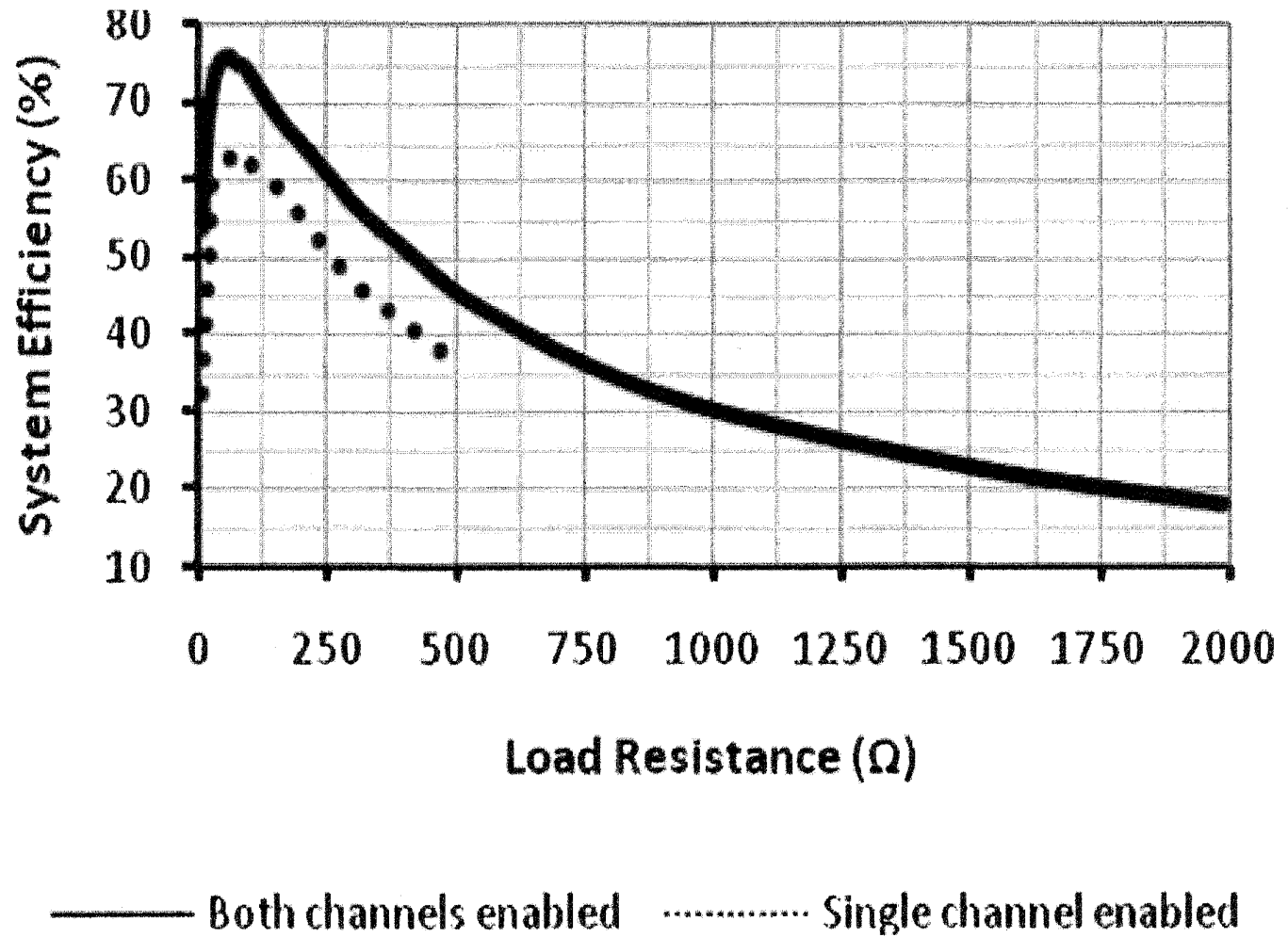
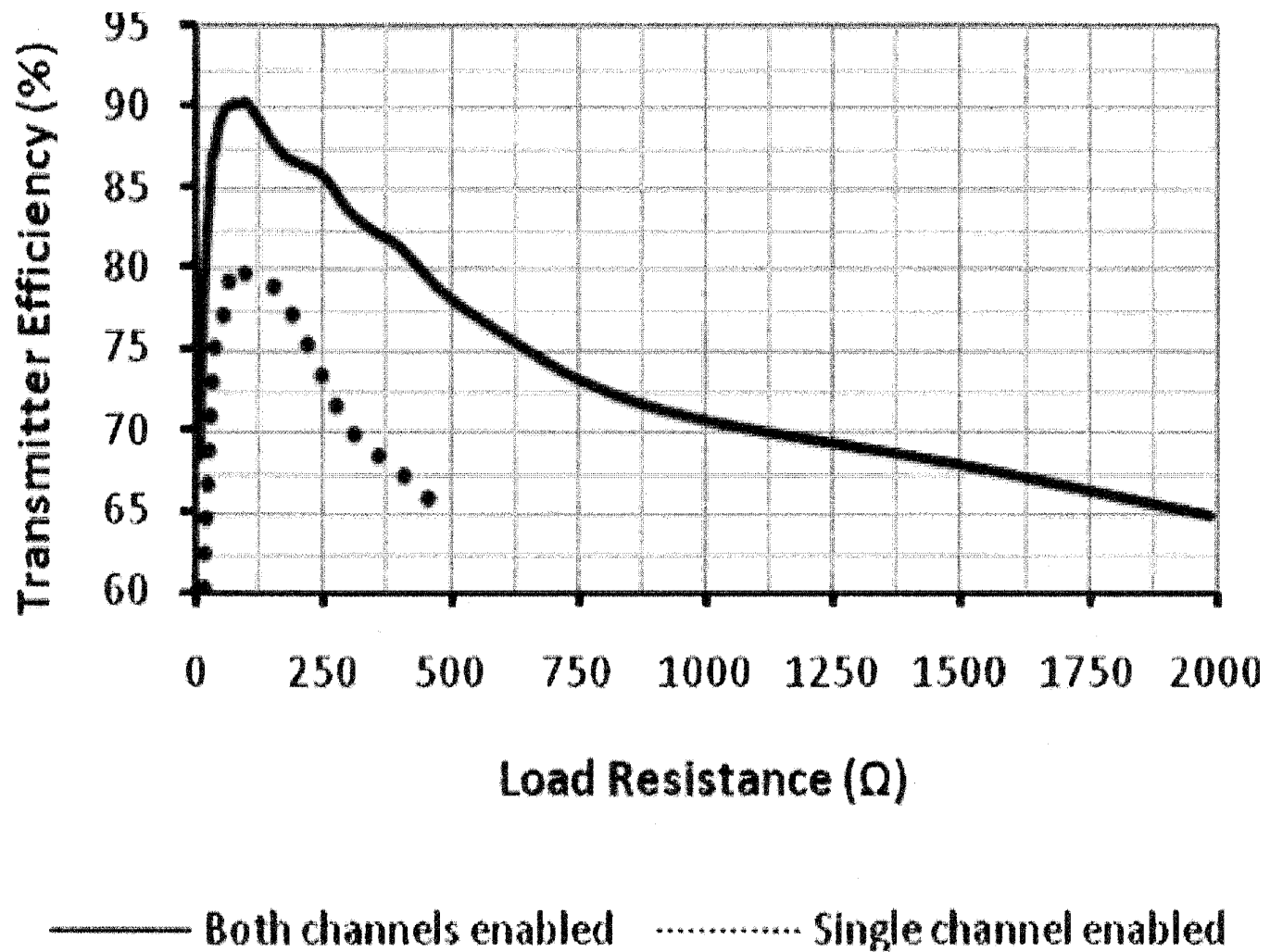
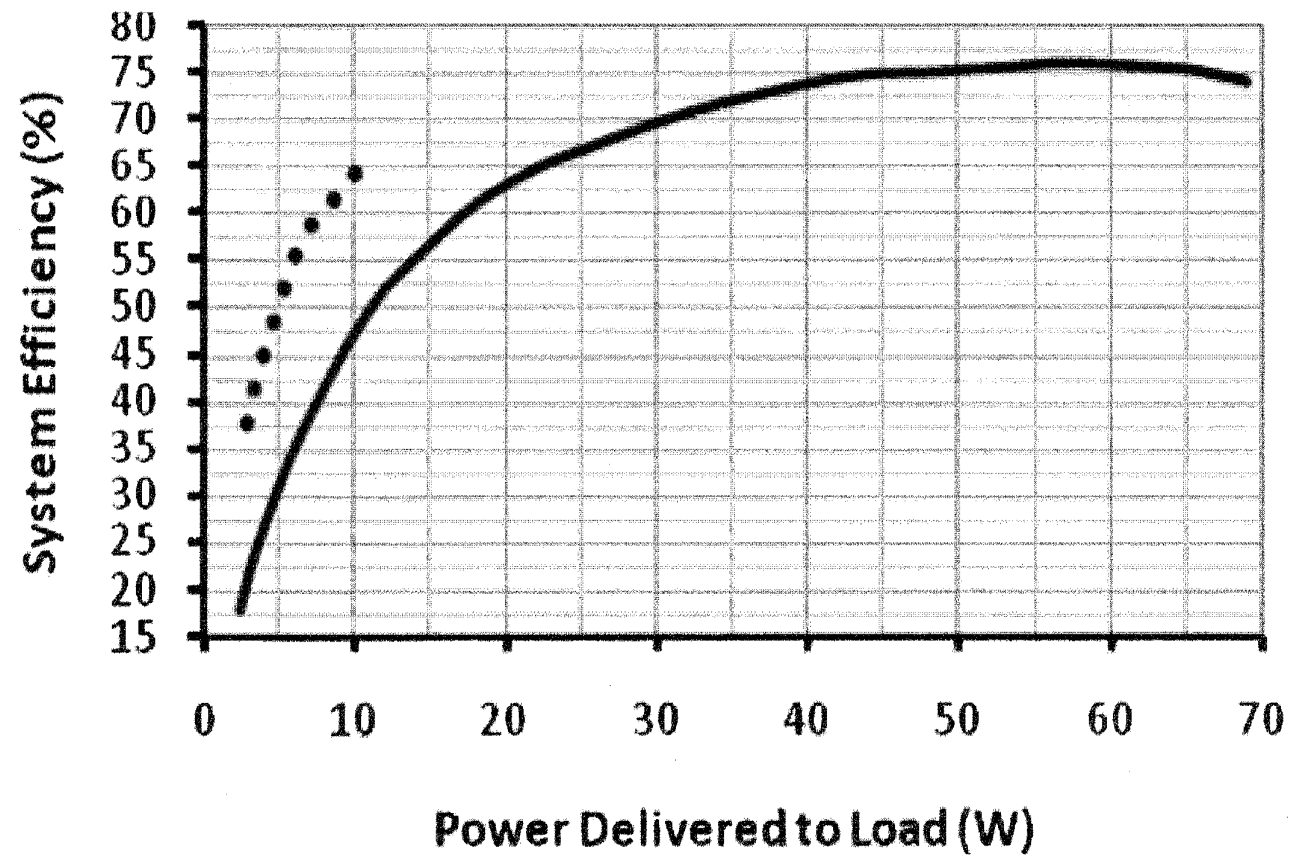


FIG. 63



65/84

FIG. 64



Both channels enabled
  Single channel enabled

FIG. 65

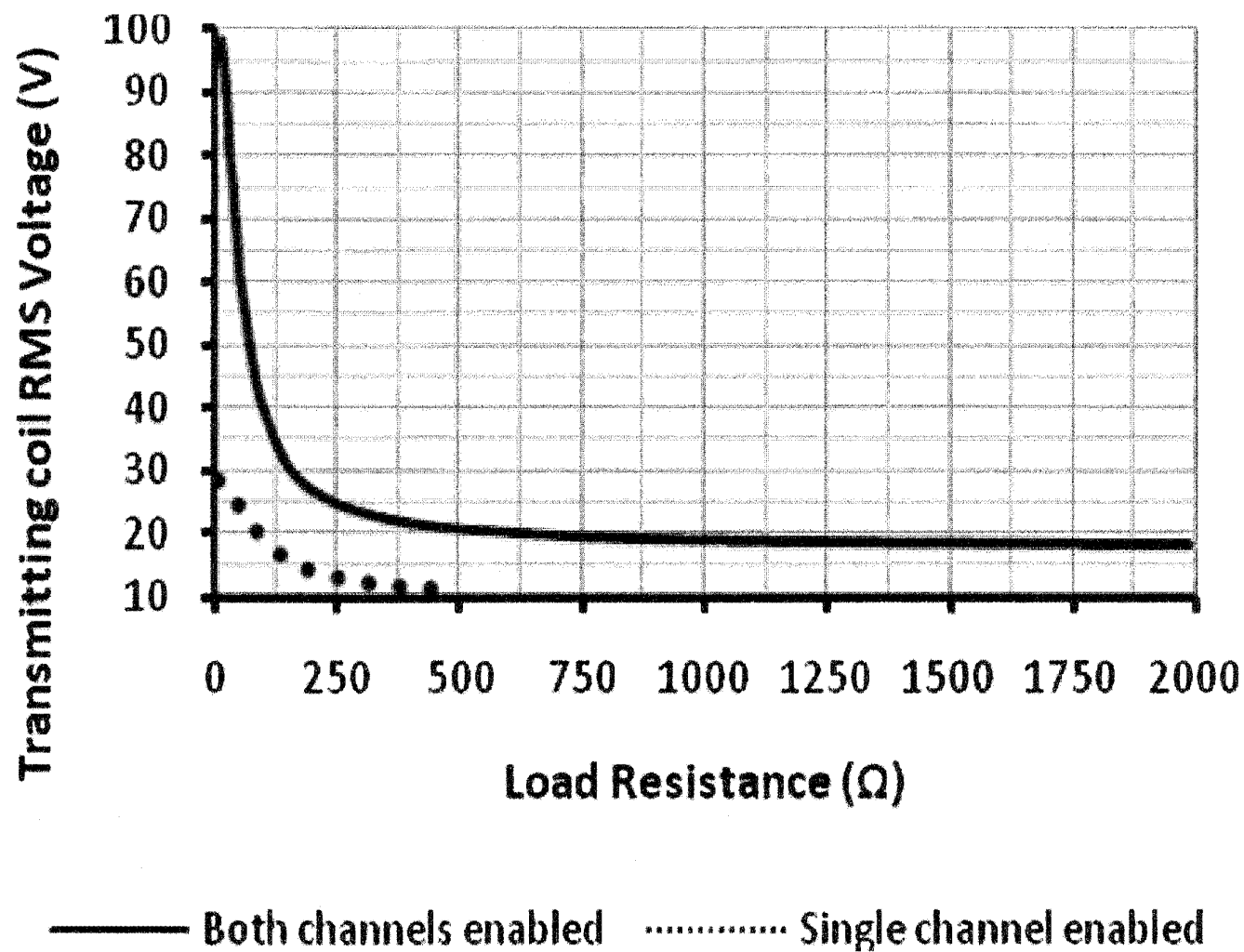
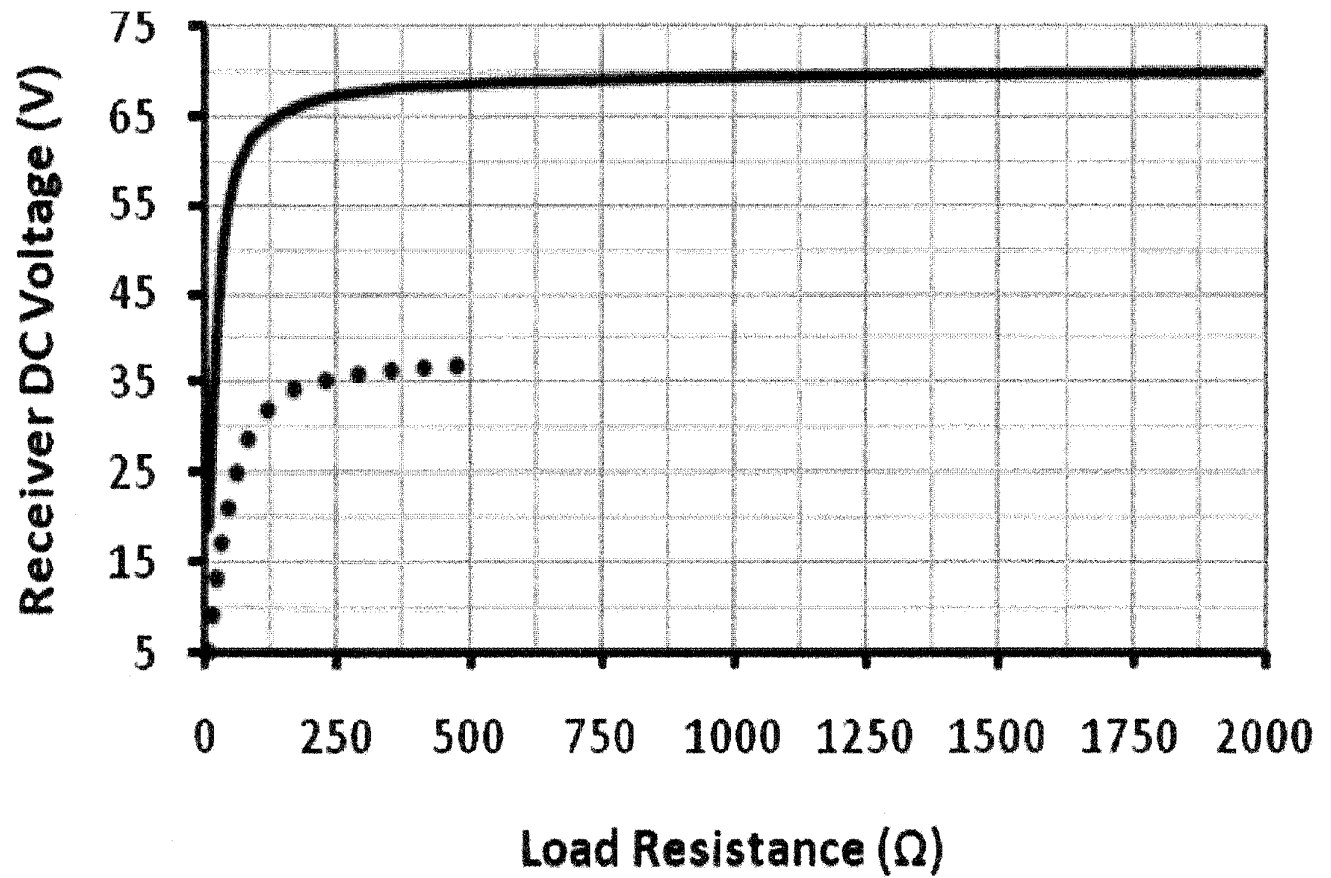


FIG. 66





— Both channels enabled      ..... Single channel enabled

FIG. 67

Generalized single-transistor power amplifier

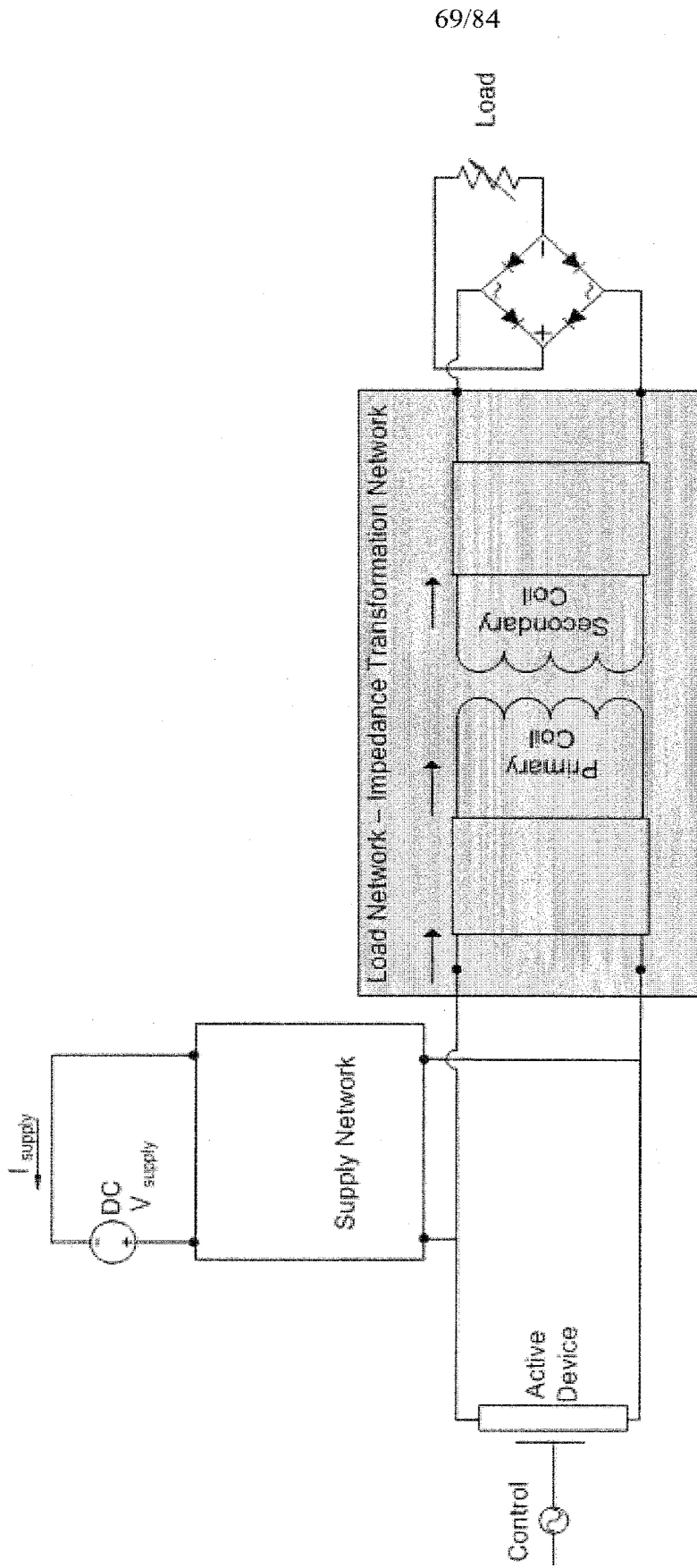


FIG. 68

70/84

Generalized single-transistor amplifiers in a push-pull configuration

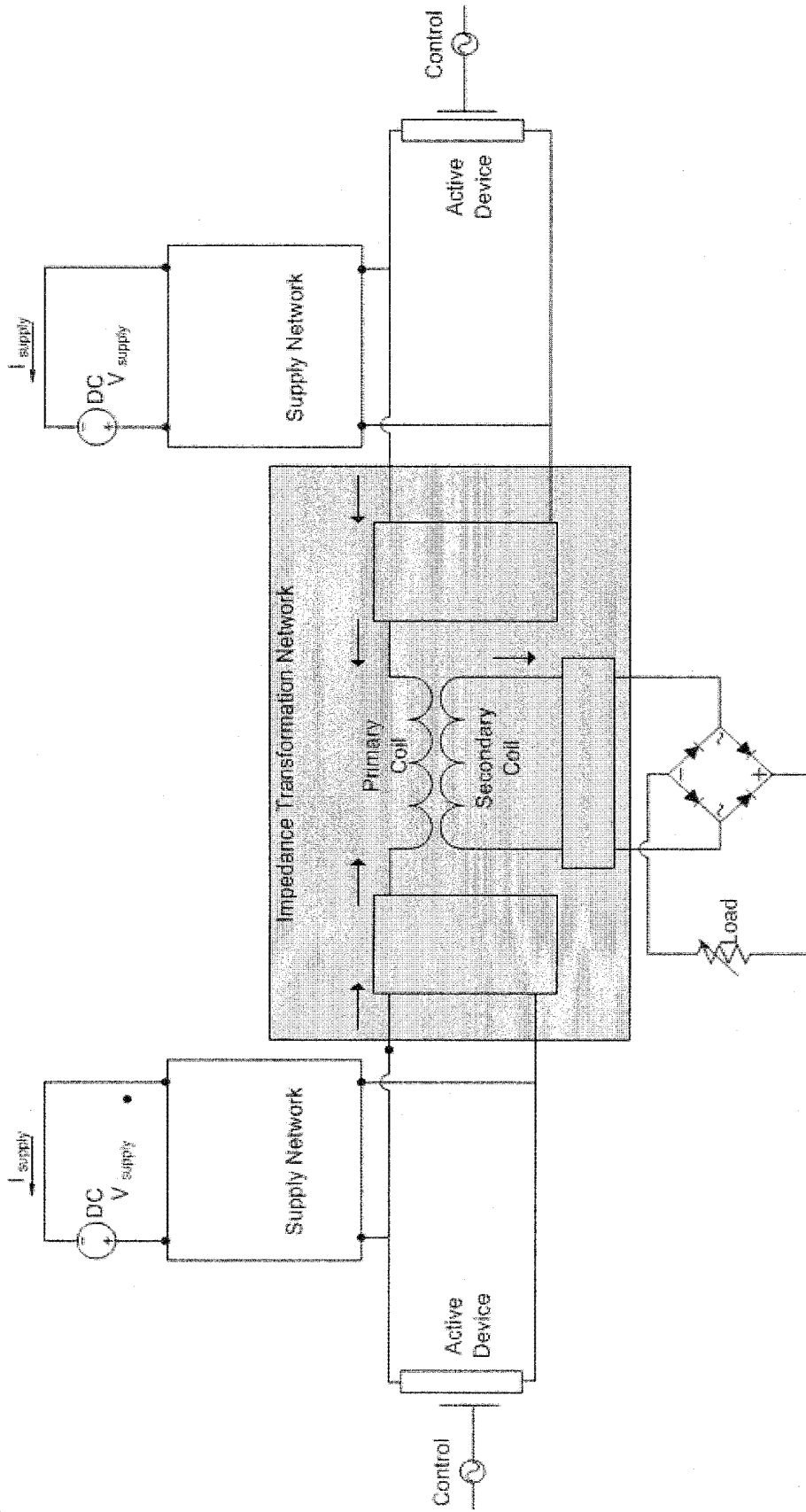


FIG. 69

Generalized Form – Class D, DE and Variants

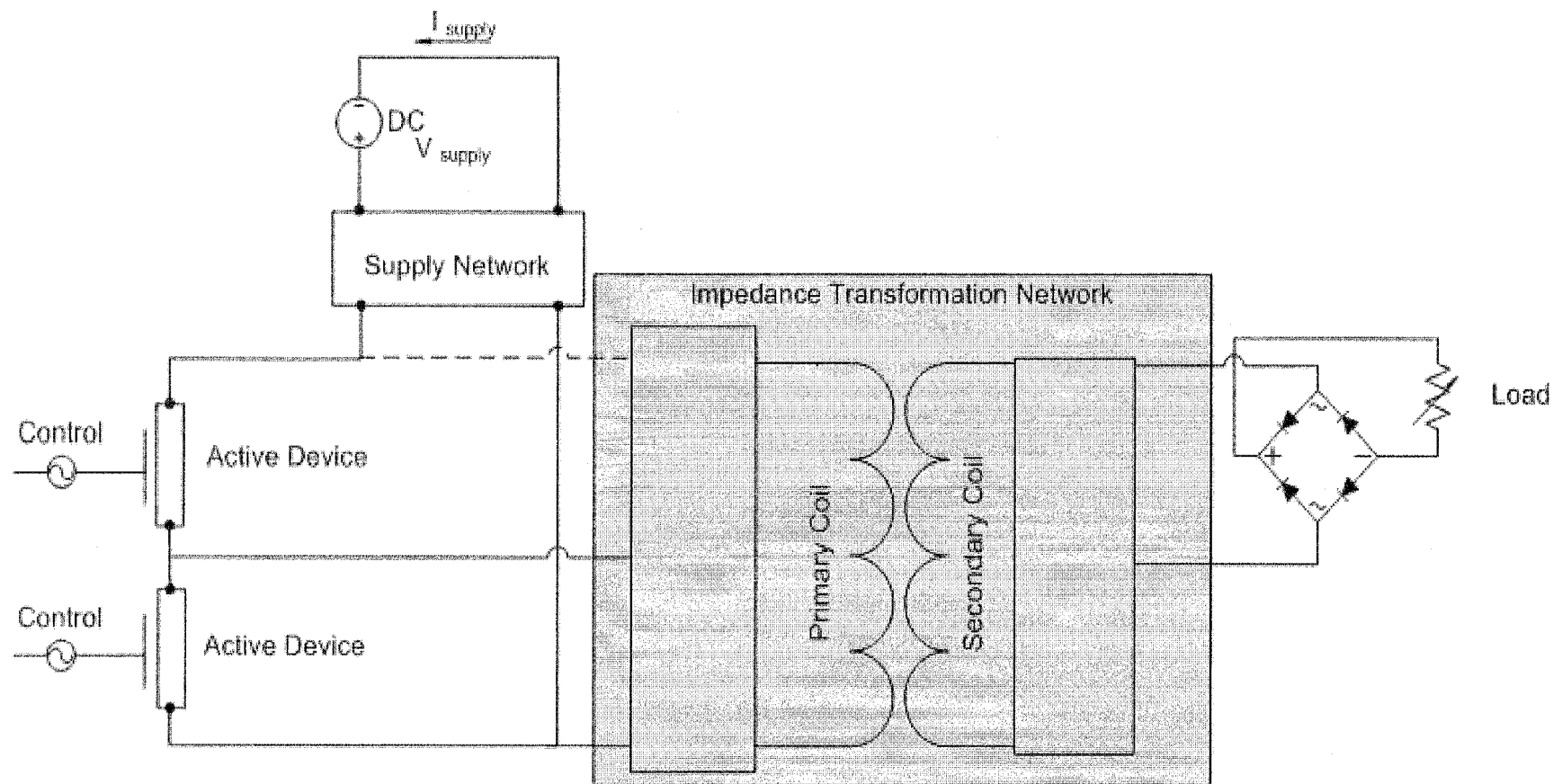
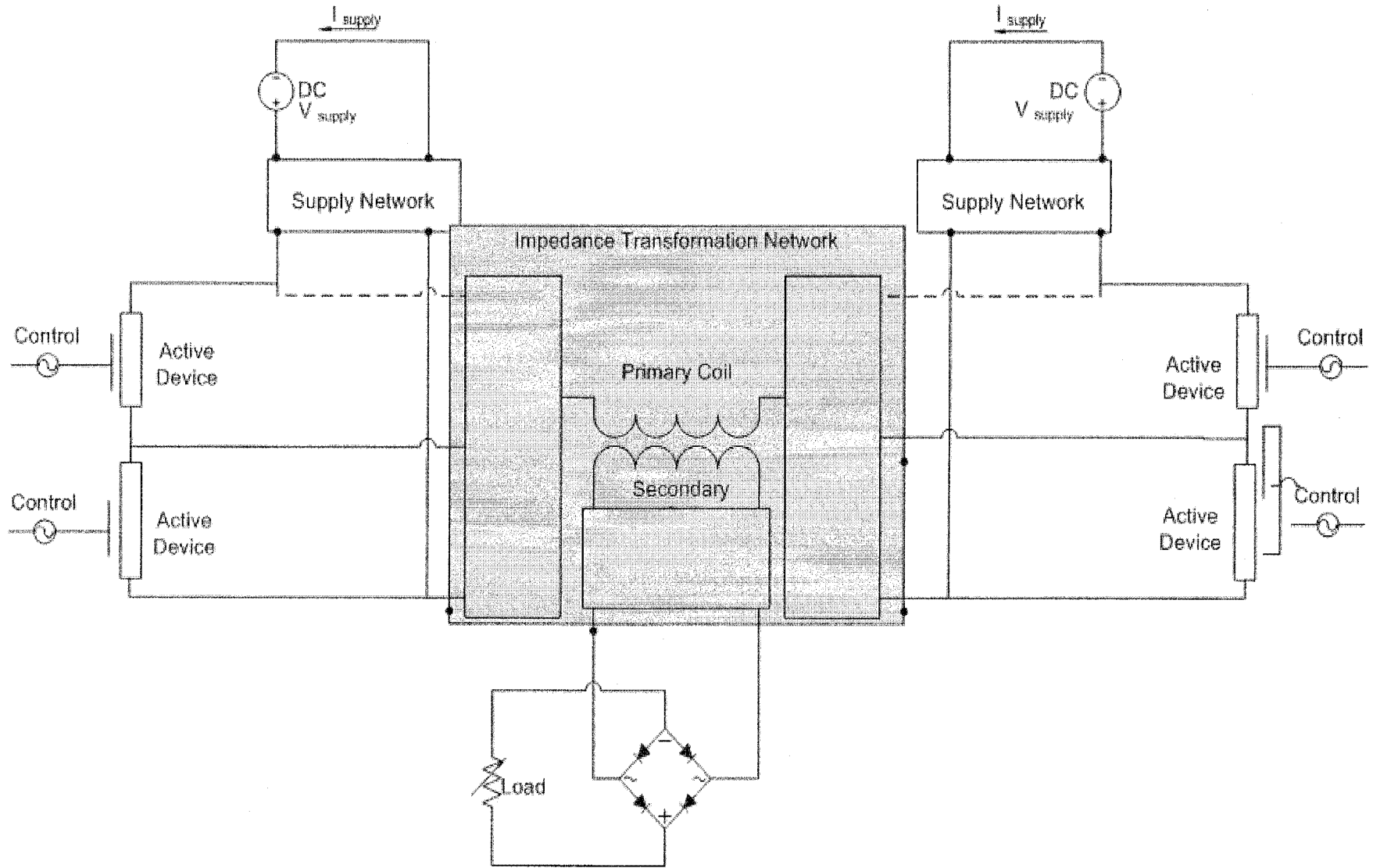


FIG. 70

Generalized Form – Class D, DE and Variants in a push-pull configuration

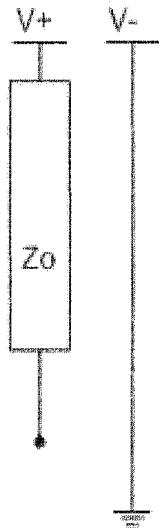


72/84

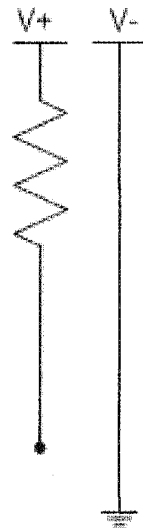
FIG. 71

Supply network configurations

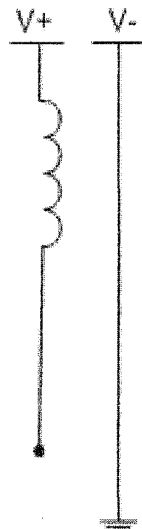
Generalized supply network



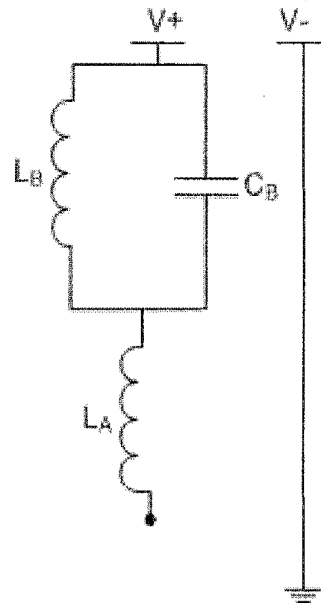
Example: Class A amplifier



Example: Class E or F amplifier



Example: Class E/F amplifier



Example: Class Phi amplifier

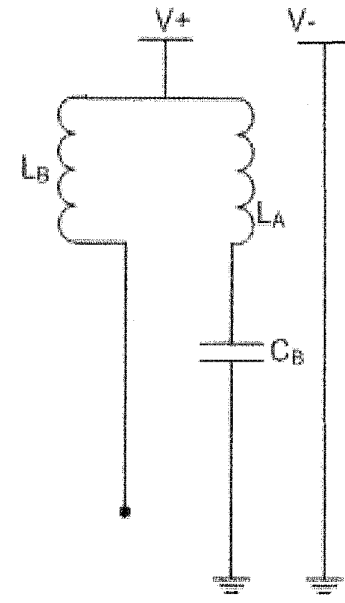


FIG. 72

73/84

Load network functions – Impedance Transformation Network

Generalized form - single-end drive

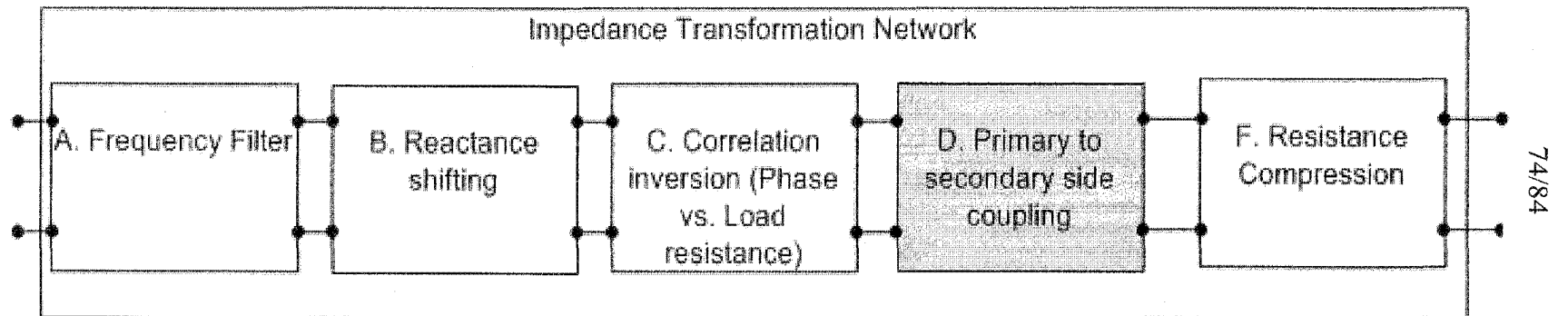
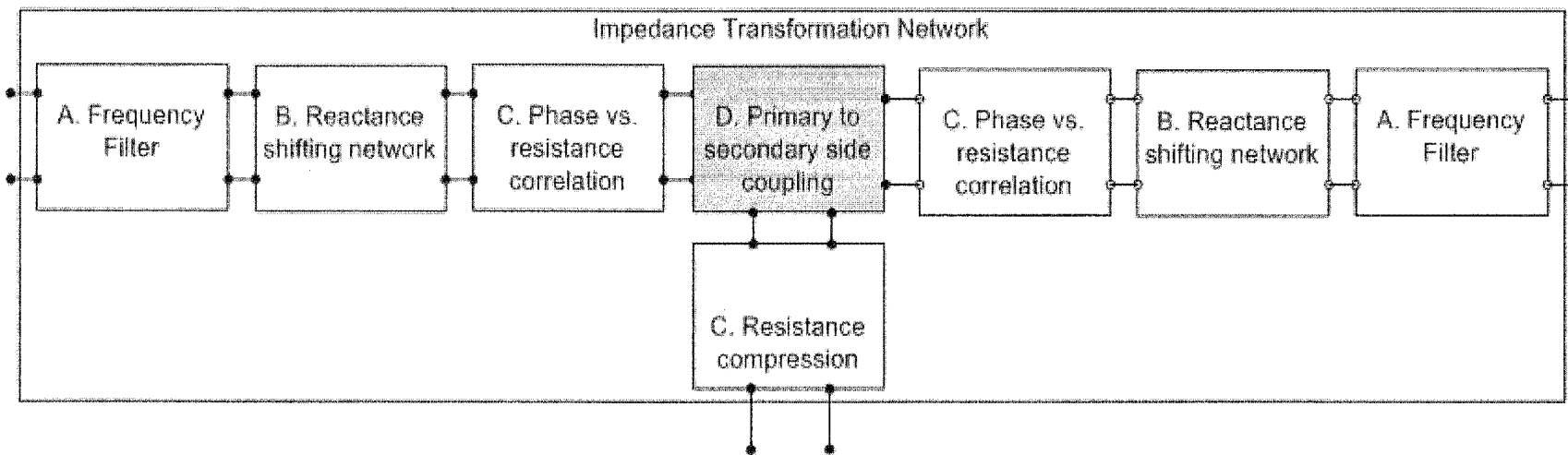


FIG. 73

Generalized form – push-pull drive



75/84

FIG. 74

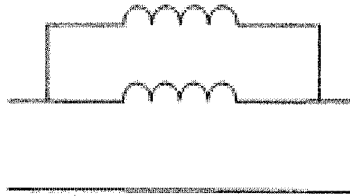


A. Reactance shifting network

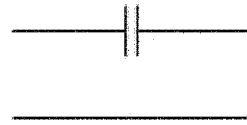
Reactance shift –  
positive shift



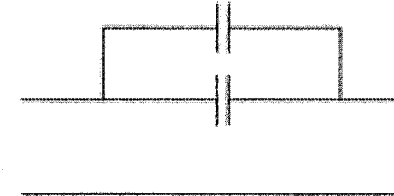
Reactance shift –  
positive shift



Reactance shift –  
negative shift



Reactance shift –  
negative shift



76/84

FIG. 75

B. Notch Filter

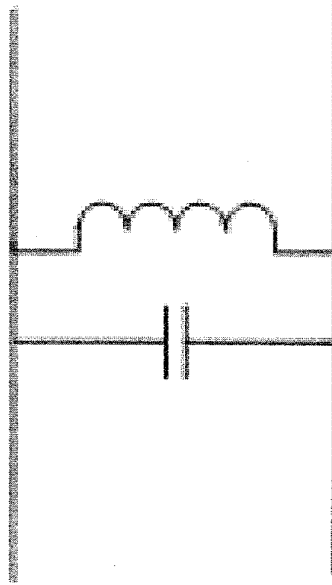
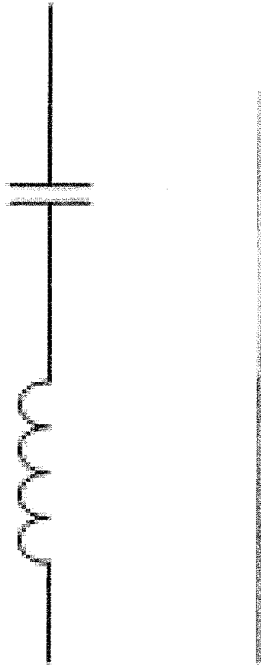


FIG. 76

78/84

C. Phase vs. resistance correlation



FIG. 77

D. Primary to Secondary Side Coupling

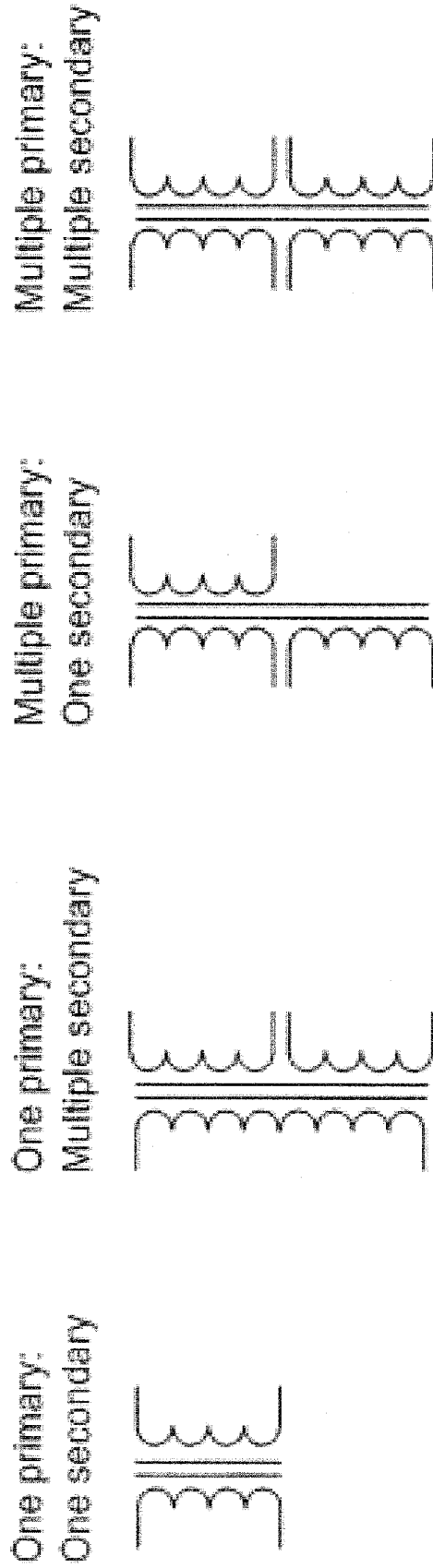


FIG. 78

E. Resistance compression

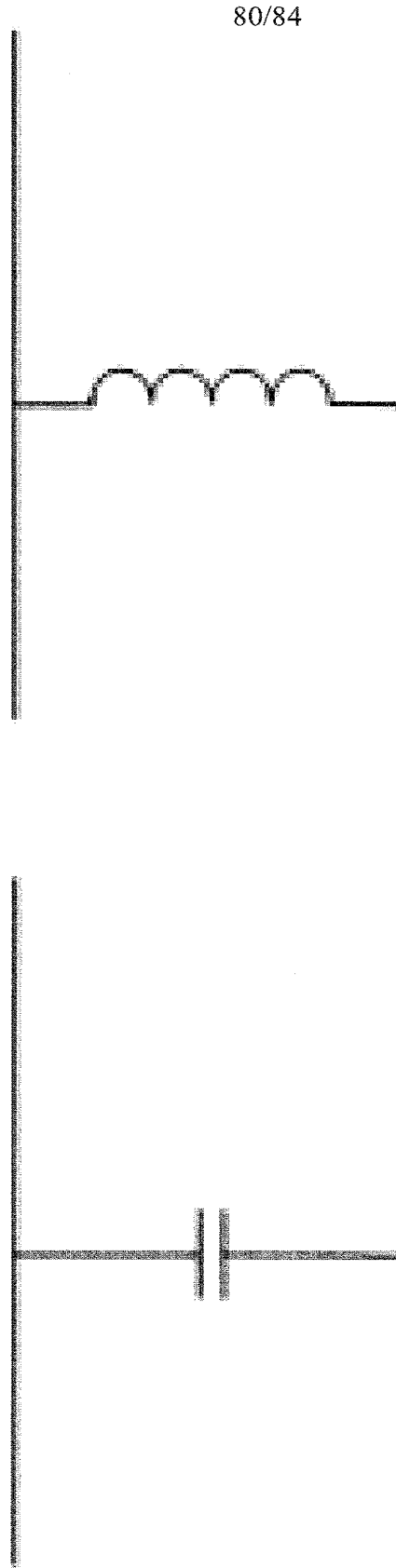


FIG. 79

81/84

Typical configuration A

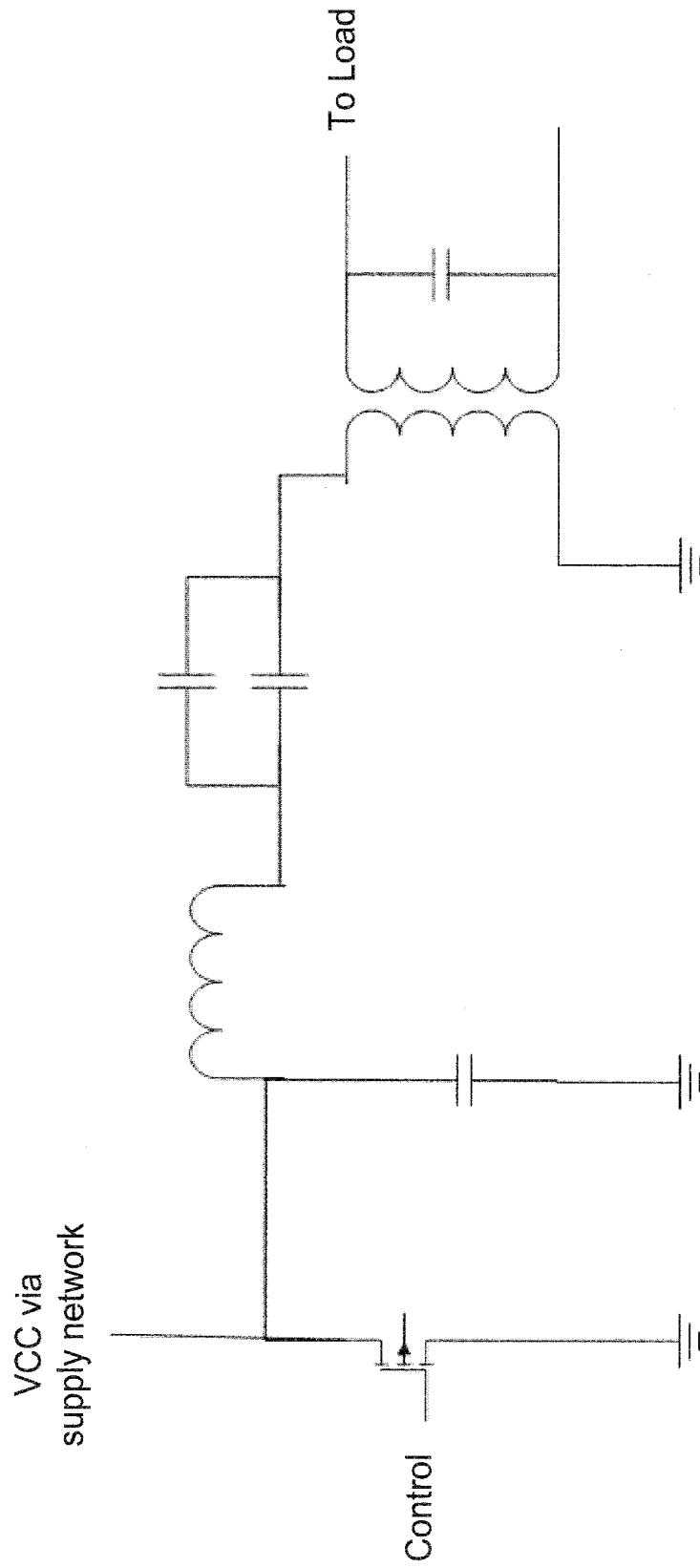


FIG. 80

Typical configuration B

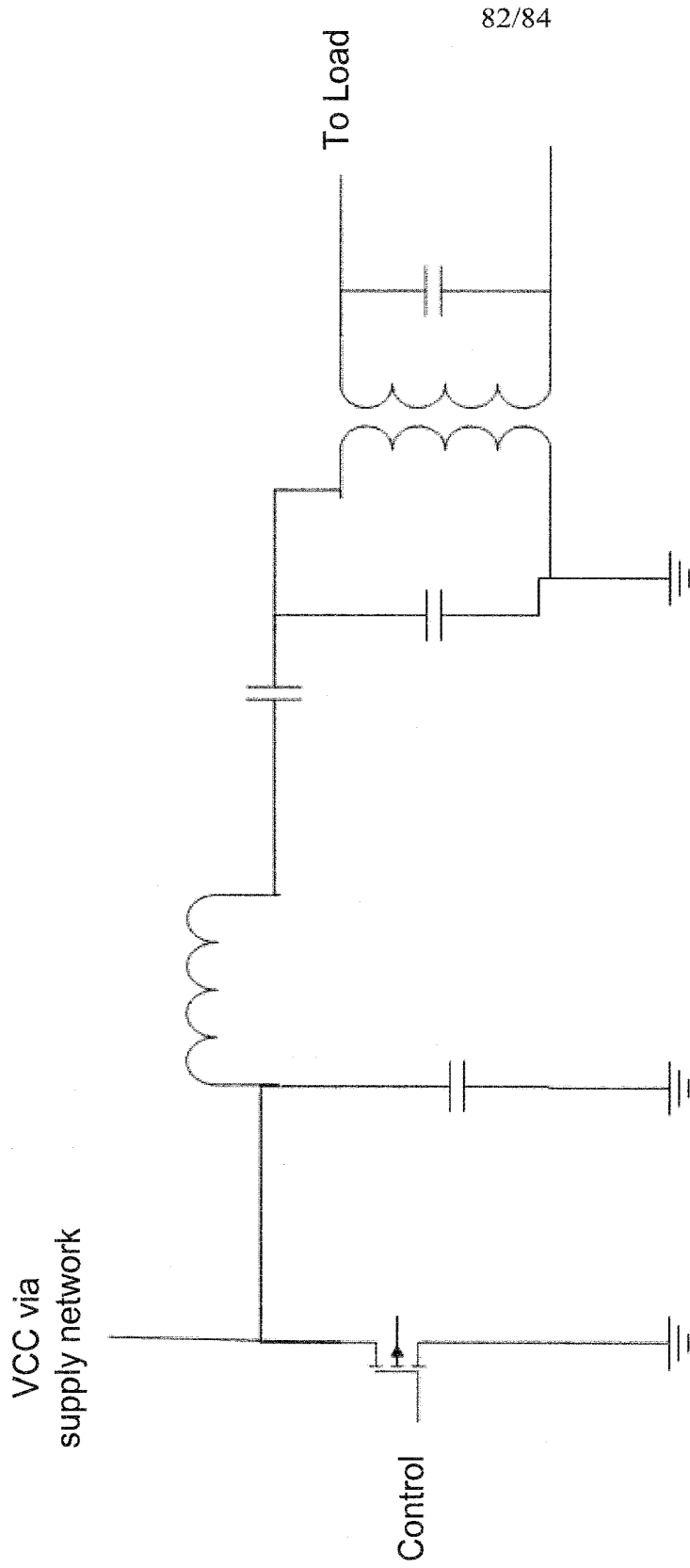


FIG. 81

Typical configuration C

VCC via supply network

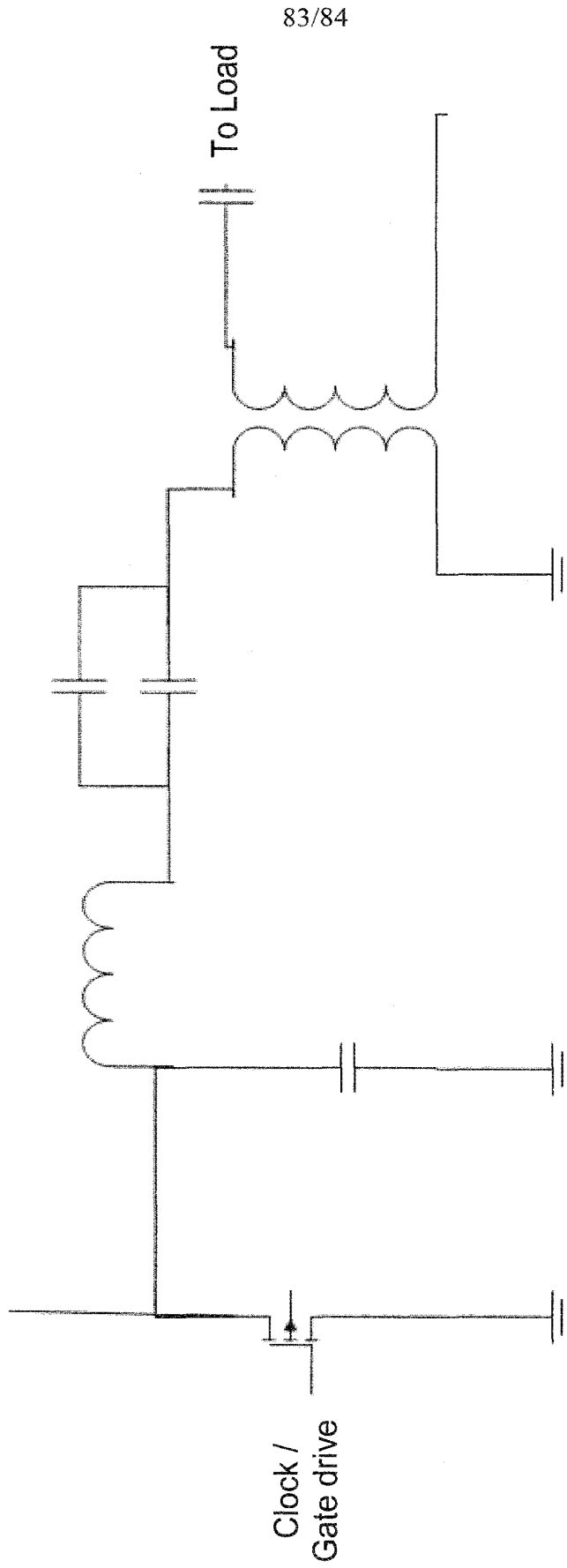


FIG. 82



84/84

Typical configuration D

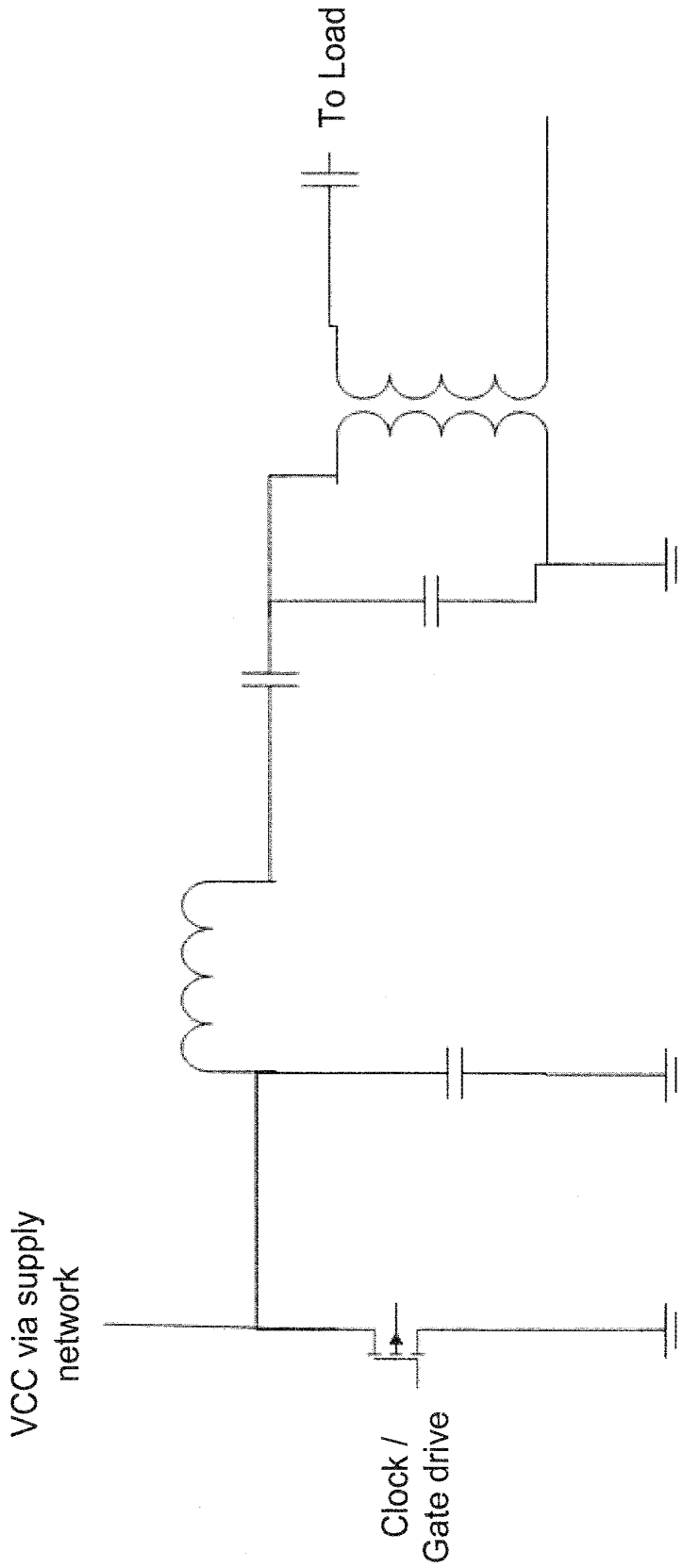


FIG. 83

(19) World Intellectual Property Organization  
International Bureau



(43) International Publication Date  
23 December 2009 (23.12.2009)

(10) International Publication Number  
**WO 2009/155000 A2**

- (51) International Patent Classification:  
*H02J 7/00* (2006.01)      *H02J 17/00* (2006.01)
- (21) International Application Number:  
PCT/US2009/045339
- (22) International Filing Date:  
27 May 2009 (27.05.2009)
- (25) Filing Language: English
- (26) Publication Language: English
- (30) Priority Data:  
61/056,354      27 May 2008 (27.05.2008)      US
- (71) Applicant (for all designated States except US): **UNIVERSITY OF FLORIDA RESEARCH FOUNDATION, INC.** [US/US]; 223 Grinter Hall, Gainesville, FL 32611 (US).
- (72) Inventor; and
- (75) Inventor/Applicant (for US only): **LIN, Jenshan** [US/US]; 910 S.W. 105th Terrace, Gainesville, FL 32607 (US).
- (74) Agent: **PARKER, James, S.**; Saliwanchik, Lloyd, Saliwanchik, P.O. Box 142950, Gainesville, FL 32614-2950 (US).
- (81) Designated States (unless otherwise indicated, for every kind of national protection available): AE, AG, AL, AM, AO, AT, AU, AZ, BA, BB, BG, BH, BR, BW, BY, BZ, CA, CH, CN, CO, CR, CU, CZ, DE, DK, DM, DO, DZ, EC, EE, EG, ES, FI, GB, GD, GE, GH, GM, GT, HN, HR, HU, ID, IL, IN, IS, JP, KE, KG, KM, KN, KP, KR, KZ, LA, LC, LK, LR, LS, LT, LU, LY, MA, MD, ME, MG, MK, MN, MW, MX, MY, MZ, NA, NG, NI, NO, NZ, OM, PG, PH, PL, PT, RO, RS, RU, SC, SD, SE, SG, SK, SL, SM, ST, SV, SY, TJ, TM, TN, TR, TT, TZ, UA, UG, US, UZ, VC, VN, ZA, ZM, ZW.
- (84) Designated States (unless otherwise indicated, for every kind of regional protection available): ARIPO (BW, GH, GM, KE, LS, MW, MZ, NA, SD, SL, SZ, TZ, UG, ZM, ZW), Eurasian (AM, AZ, BY, KG, KZ, MD, RU, TJ, TM), European (AT, BE, BG, CH, CY, CZ, DE, DK, EE, ES, FI, FR, GB, GR, HR, HU, IE, IS, IT, LT, LU, LV, MC, MK, MT, NL, NO, PL, PT, RO, SE, SI, SK, TR), OAPI (BF, BJ, CF, CG, CI, CM, GA, GN, GQ, GW, ML, MR, NE, SN, TD, TG).

[Continued on next page]

(54) Title: METHOD AND APPARATUS FOR PRODUCING SUBSTANTIALLY UNIFORM MAGNETIC FIELD

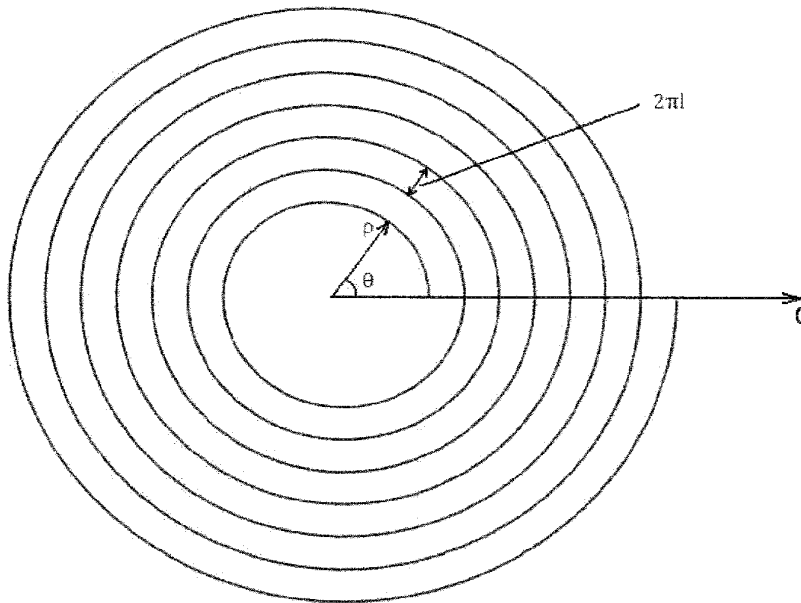


**FIG. 1**

(57) Abstract: A planar wireless power transmitter coil design and method are provided. A single spiral coil can be used to provide a uniform magnetic field across its surface area for location-independent planar wireless power charging. The spiral coil can be designed to have a non-constant gap between adjacent loops such that the gap between adjacent loops decreases towards the outer loops.

WO 2009/155000 A2



---

**Published:**

- *without international search report and to be republished upon receipt of that report (Rule 48.2(g))*

## DESCRIPTION

METHOD AND APPARATUS FOR PRODUCING SUBSTANTIALLY  
UNIFORM MAGNETIC FIELD

5

## CROSS-REFERENCE TO RELATED APPLICATION

The present application claims the benefit of U.S. Provisional Application Serial No. 61/056,354, filed May 27, 2008, which is hereby incorporated by reference herein in its entirety, including any figures, tables, or drawings.

10

## BACKGROUND OF INVENTION

In recent years, consumer electronics devices such as cell phones, personal digital assistants (PDAs), and laptops are using more wireless components such as a Bluetooth headset, wireless mouse, and wireless LAN. However, the wired power line remains to impair wireless freedom. Many designs and research has been conducted to provide solutions to get rid of this wire. Inductive wireless power transmission appears to be the most promising solution to this problem.

15

In wireless power charging, AC current passes through a transmitter coil, inducing magnetic flux on and/or above the surface of a power platform. A receiver coil generates voltage when magnetic flux passing through the receiver coil's loop(s) changes. In many cases, the transmitter coil and the receiver coil are not of the same size.

20

However, when the transmitter coil and receiver coil have significantly different sizes, the voltage generated on the receiving side can be greatly affected by the receiver coil's placement on the surface of the transmitter coil.

25

Specifically, a typical transmitter coil has a non-uniform magnetic field across its surface area, which may cause voltage variation and impedance matching difficulty.

A normal spiral coil as shown in Figure 1 usually has constant gap between adjacent loops. For example, the circular spiral coil of Figure 1 follows the equation of

30

$$\rho = \rho_0 + l\theta . \quad (1)$$

where  $\rho$  is the radius,  $\theta$  is the angle,  $\rho_0$  is the initial radius and  $l$  is a constant. In Figure 1, the distance between adjacent wires is a constant  $2pl$ .

The magnetic field near the surface for the coil shown in Figure 1 is shown in Figure 2, which illustrates a high magnetic field strength at the center of the coil. Each loop of the coil contributes magnetic field in the area it encloses, and the magnetic field in the center is the superposition of magnetic field contributions from all the loops.

5 For a regular coil, the density of magnetic flux generated in the coil has a maximum value at a position closest to the coil, and has a minimum value at a position at the center of the coil. Thus, the charging efficiency may be abruptly deteriorated leading to significant variation in charging efficiency.

10 One approach to solve this problem is discussed in WO2007/013725A1 (Gwon *et al.*), which discloses a wireless charger having decreased variation of charging efficiency. According to Gwon *et al.*, a smaller coil is placed in the center of an outer coil, which reinforces the magnetic flux density in the center of the outer and inner coils. Thus the entire magnetic flux density is flattened as a whole in comparison to the magnetic flux density formed by only the outer coil. Though the design disclosed in Gwon *et al.* reduces the effect  
15 of variation of the magnetic flux density of the outer coil, the variation can still be significant. In addition, when the receiver coil is much smaller than the transmitter coil, the location of the receiver coil can often affect its performance.

In a similar approach, WO2007/019806A1 (Hui *et al.*) provides a design of an auxiliary winding for improved performance of a planar inductive charging platform.  
20 According to Hui *et al.* an auxiliary winding is introduced to compensate the magnetic field generated by a principle winding. The design taught by Hui *et al.* uses a similar mechanism as that taught by Gwon *et al.* in that separate coils are used to improve charging efficiency.

Thus, there exists in the art a need for improved inductive wireless power transmission.

25

#### BRIEF SUMMARY

Embodiments of the subject invention relate to a method and apparatus for providing a planar spiral transmitter coil that produces a substantially uniform magnetic field over a region of interest near the surface of the coil. Embodiments of the invention provide a planar  
30 inductive wireless power transmission system incorporating a planar spiral transmitter coil and a receiver coil.

According to embodiments of the invention, a single coil design can provide improved charging efficiency to a wireless power transmission apparatus.

Coils in accordance with embodiments of the invention can provide for a system that uses near-field coupling to transfer power. Advantageously, embodiments of the invention do not require the alignment of the two axes of two coils. Certain embodiments of the invention provide improved robustness for wireless power transfer.

5 According to an embodiment of the invention, a single spiral coil can be used to provide a uniform magnetic field across the coil's surface area for location-independent planar wireless power charging. Embodiments of the invention generate a uniform magnetic field across an area that enables uniform wireless power transfer insensitive to the location of the device being charged.

10 In one embodiment, a circular spiral coil can be used. In another embodiment, a rectangular spiral coil can be used. Other shapes can also be utilized for the coil, such as elliptical, rectangular, hexagonal, and other polygonal shapes. The spiral coil can be designed to have a non-constant gap between adjacent loops such that the gap between adjacent loops decreases towards the outer loops.

15

#### BRIEF DESCRIPTION OF DRAWINGS

**Figure 1** shows a normal spiral coil having a constant gap between adjacent loops.

**Figure 2** shows a plot of the magnetic field of the normal spiral coil shown in Figure 1.

20 **Figure 3** shows a spiral coil according to an embodiment of the invention.

**Figure 4** shows a plot of the magnetic field of the spiral coil shown in Figure 3.

**Figure 5** shows a rectangular spiral coil according to an embodiment of the invention.

**Figure 6** shows a plot of the magnetic field of the rectangular spiral coil shown in Figure 5.

25

#### DETAILED DISCLOSURE

Embodiments of the subject invention relate to a spiral coil that can generate a substantially uniform magnetic field near the surface of the coil, across at least a portion of the surface area of the coil. Embodiments provide a location-independent planar wireless power charging system. Embodiments of the spiral coil can generate a substantially uniform magnetic field near the surface of the coil, across a portion of the surface area of the coil. A wireless power transmission system in accordance with an embodiment of the invention can have performance insensitive to the placement of the receiver coil within the substantially

uniform magnetic field. The transmitter coil can be driven by a driver. In specific embodiments, the driver is a current source or a voltage source.

Specific embodiments can provide magnetic fields where the magnitude of the magnetic field in a direction perpendicular to the plane of the coil is substantially uniform over the region of interest such that  $\frac{MAX - MIN}{AVERAGE}$  is less than or equal to 0.2 over the region of interest, where MAX and MIN are the maximum magnitude, and minimum magnitude, of the magnet field over the region of interest, respectively, and AVERAGE is  $\frac{MAX + MIN}{2}$ .

Further specific embodiments can have the  $\frac{MAX - MIN}{AVERAGE}$  of less than or equal to 0.1 over the region of interest and the  $\frac{MAX - MIN}{AVERAGE}$  is less than or equal to 0.05 over the region of interest.

In an embodiment of a wireless power charging system, AC current passes through a transmitter coil, inducing magnetic flux on the surface of a power platform. In a specific embodiment, the frequency of the transmitter is between 1kHz and 10MHz. In a preferred embodiment, the frequency of the transmitter is in the range 100 kHz to 400 kHz, and in another embodiment, less than 1MHz. In specific embodiments, the region of interest can be a plane parallel to the plane of the coil offset from the plane of the coil by less than R, less than 30 cm, and/or less than 10 cm. The region of interest can cover a portion of, or all of the area of the coil. A receiver coil generates voltage when magnetic flux passing through the loop of the receiver coil changes. In specific embodiments, the transmitter coil and the receiver coil are not of the same size. A normal coil in accordance with an embodiment of the subject charging system can have a uniform magnetic field across its surface area, which reduces voltage variation and improves impedance matching. In a specific embodiment, the uniformity of the magnetic field can be less than 10% across the surface area of the coil, where the surface of the coil is the area enclosed by the outermost turn of the coil.

According to embodiments of the invention, to generate a more uniform field near the surface of the spiral coil, the distance between two adjacent loops can be adjusted. To reduce the magnetic field density at the center, the density of the inner loops should be less than the outer loops. In a specific embodiment, the gap between two adjacent coils decreases continuously toward the outer loops of the coil. A formula that describes the curve of a

circular spiral inductor according to an embodiment of the invention is

$$\rho(\theta) = \rho_0 + l(\theta)\theta \quad (2)$$

5 where  $l(\theta)$  is a function of  $\theta$ .  $\theta$  can vary from 0 to  $2\pi N$ , where  $N$  is the number of turns of the coil. In an embodiment, the derivative of  $l(\theta)$  is positive and decreases as  $\theta$  increases. Specific functions allow  $l(\theta)$ , the distance between adjacent loops, to be adjusted, and can allow the field across the surface of the coil to be substantially uniform. In another  
10 embodiment, the derivative of  $l(\theta)$  is such that the spacing between adjacent loops can decrease or remain the same as  $\theta$  increases such that as the coil moves from the innermost radius to the outermost radius the spacing decreases.

According to an embodiment of the invention, a circular spiral coil, which can be used to obtain the formula for  $l(\theta)$ , is

$$15 \quad \rho(\theta) = r + \left(1 - \left(1 - \frac{\theta}{2\pi N}\right)^4\right)(R - r) \quad (3)$$

where  $R$  is the outermost radius,  $r$  is the innermost radius, and  $N$  is the total turns of the coil.  $l(\theta)$  can be obtained by setting the right side of equation (2) equal to the right side of equation (3) and solving  $l(\theta)$ , where  $r$  has the same meaning as  $\rho_0$ . According to one embodiment,  $r$   
20 is 1/4 to 1/3 of  $R$ . In another embodiment, the coil can be elliptical with appropriate modifications to equations (2) and (3).

Figure 3 shows a coil with non-constant gap between adjacent loops, in accordance with an embodiment of the subject invention. The curvature of the spiral coil of Figure 3 follows equation 3, in which  $R = 200$  mm,  $r = 50$  mm, and  $N = 8$ . Figure 4 shows the  
25 magnetic field strength in a perpendicular direction across the surface area of the coil of Figure 3. As shown in Figure 4, the uniformity of the magnetic field for the coil of Figure 3 is significantly improved over the uniformity of the magnetic field for the coil of Figure 1.

For a rectangular spiral inductor, narrower gaps can be used between adjacent loops as the loops become farther from the center. According to an embodiment of the present  
30 invention, the gap between adjacent loops can be derived from

$$\rho(2n\pi) - \rho[2(n-1)\pi], n=1, 2, \dots, N. \quad (4)$$



where  $\rho$  is the same function as Equation 3. Figure 5 shows a rectangular spiral coil according to an embodiment of the invention. The design of the coil of Figure 5 follows equation 4, in which  $R = 200$  mm,  $r = 50$  mm, and  $N = 8$ mm. The magnetic field strength in a perpendicular direction for the coil of Figure 5 is shown in Figure 6.

5 The results, as shown in Figures 4 and 6, demonstrate that a substantially uniform magnetic field of spiral coil can be generated in accordance with embodiments of the invention.

Additional embodiments utilize polygonal coils, such as rectangles, squares, hexagons, and other multisided shapes, to produce the magnetic fields. The spacing between  
10 adjacent coils can decrease or stay the same at each corner of the polygon such that the spacing decreases as the coil goes from the innermost radius to the outermost radius. In specific embodiments, the spacing can continuously decrease, the spacing can be the same between two corners (along one side of the polygonal) and decrease from before each corner to after each corner, the spacing can remain the same for a portion or all of a loop (as shown  
15 in Figure 5) and have decreases as the coil moves outward, and/or combinations of these changes.

In specific embodiments, a receiver coil can be inductively coupled to the transmitter coil so as to transfer power to the receiver coil. Embodiments can use receiver coils that have areas such that the transmitter coil area is 2 to 12 times as large, 2 to 8 times as large, or 2 to  
20 4 times as large as the receiver coil area.

All patents, patent applications, provisional applications, and publications referred to or cited herein are incorporated by reference in their entirety, including all figures and tables, to the extent they are not inconsistent with the explicit teachings of this specification.

It should be understood that the examples and embodiments described herein are for  
25 illustrative purposes only and that various modifications or changes in light thereof will be suggested to persons skilled in the art and are to be included within the spirit and purview of this application.

## CLAIMS

What is claimed is:

1. An apparatus for producing a magnetic field, comprising:  
a coil, wherein the coil is a planar spiral coil, where the coil has at least two loops, wherein a spacing between adjacent loops decreases continuously from an inner loop toward an outer loop of the coil, and  
a driver, wherein the driver drives the coil to produce a magnetic field, wherein a magnitude of the magnetic field in a direction perpendicular to a plane of the coil is substantially uniform over a region of interest.
2. The apparatus according to claim 1, wherein the magnitude of the magnetic field in a direction perpendicular to the plane of the coil is substantially uniform over the region of interest such that  $\frac{MAX - MIN}{AVERAGE}$  is less than or equal to 0.2 over the region of interest, where MAX and MIN are the maximum magnitude, and minimum magnitude, of the magnet field over the region of interest, respectively, and AVERAGE is  $\frac{MAX + MIN}{2}$ .
3. The apparatus according to claim 2, wherein the  $\frac{MAX - MIN}{AVERAGE}$  is less than or equal to 0.1 over the region of interest.
4. The apparatus according to claim 2, wherein the  $\frac{MAX - MIN}{AVERAGE}$  is less than or equal to 0.05 over the region of interest.
5. The apparatus according to claim 1, wherein the magnetic field is time-varying.
6. The apparatus according to claim 5, wherein the time-varying magnetic field has a frequency in the range 1 kHz to 10 MHz.

7. The apparatus according to claim 5, wherein the time-varying magnetic field has a frequency in the range 100 kHz to 400 kHz.

8. The apparatus according to claim 5, wherein the time varying magnetic field has a frequency less than or equal to 1 MHz.

9. An apparatus according to claim 1, wherein the coil is a planar elliptical spiral coil.

10. The apparatus according to claim 1, wherein the coil is a planar circular spiral coil, wherein the coil follows the equation:

$$\rho(\theta) = \rho_0 + l(\theta)\theta$$

where  $\rho(\theta)$  is the radius of the coil,  $\rho_0$  is the initial radius of the coil,  $\theta$  is the angle with respect to the initial radius of the coil, and  $l(\theta)$  is a function of  $\theta$ .

11. The apparatus according to claim 10, wherein a derivative of  $l(\theta)$  is positive.

12. The apparatus according to claim 11, wherein the derivative of  $l(\theta)$  decreases as  $\theta$  increases over at least a portion of the coil.

13. The apparatus according to claim 12, wherein the derivative of  $l(\theta)$  decreases as  $\theta$  increases over the coil.

14. The apparatus according to claim 1, wherein the spiral coil further follows the equation:

$$\rho(\theta) = r + \left(1 - \left(1 - \frac{\theta}{2\pi N}\right)^4\right)(R - r)$$

where  $R$  is an outermost radius of the coil,  $r$  is the initial radius of the coil, and  $N$  is a number of loops of the coil.

15. The apparatus according to claim 1, wherein the region of interest is a second plane parallel to a plane of the coil.

16. The apparatus according to claim 15, wherein the second plane is offset from the plane of the coil by a distance  $d$ .

17. The apparatus according to claim 16, wherein  $d$  is less than 30 cm.

18. The apparatus according to claim 16, wherein  $d$  is less than 10 cm.

19. The apparatus according to claim 16, wherein  $d$  is less than  $R$ , where  $R$  is an outermost radius of the coil.

20. The apparatus according to claim 15, wherein the region of interest is a region covering at least a portion of an area of the coil.

21. The apparatus according to claim 15, wherein the region of interest is a region covering an area of the coil.

22. The apparatus according to claim 1, wherein the coil is a polygonal spiral coil.

23. The apparatus according to claim 1, wherein the coil is a rectangular spiral coil.

24. An apparatus for producing a magnetic field, comprising:

a coil, wherein the coil is a planer polygonal spiral coil wherein the coil has at least two loops, wherein a spacing between adjacent loops either stays the same or decreases at each corner of the polygonal going from an inner loop toward an outer loop of the coil; and

a driver, wherein the driver drives the coil to produce a magnetic field, wherein a magnitude of the magnetic field in a direction perpendicular to a plane of the coil substantially is uniform over a region of interest.

25. The apparatus according to claim 24, wherein the magnitude of the magnetic field in a direction perpendicular to the plane of the coil is substantially uniform over the region of

interest such that  $\frac{MAX - MIN}{AVERAGE}$  is less than or equal to 0.2 over the region of interest, where MAX and MIN are the maximum magnitude, and minimum magnitude, of the magnet field over the region of interest, respectively, and AVERAGE is  $\frac{MAX + MIN}{2}$ .

26. The apparatus according to claim 25, wherein the  $\frac{MAX - MIN}{AVERAGE}$  is less than or equal to 0.1 over the region of interest.

27. The apparatus according to claim 25, wherein the  $\frac{MAX - MIN}{AVERAGE}$  is less than or equal to 0.05 over the region of interest.

28. The apparatus according to claim 24, wherein the magnetic field is time-varying.

29. The apparatus according to claim 28, wherein the time-varying magnetic field has a frequency in the range 1 kHz to 10 MHz.

30. The apparatus according to claim 25, wherein the time-varying magnetic field has a frequency in the range 100 kHz to 400 kHz.

31. The apparatus according to claim 25, wherein the time varying magnetic field has a frequency less than or equal to 1 MHz.

32. The apparatus according to claim 24, wherein the spacing between adjacent loops follows the equation:

$\rho(2n\pi) - \rho[2(n-1)\pi]$ ,  $n = 1, 2, \dots, N$ , where  $\rho$  is the function

$$\rho(\theta) = r + (1 - (1 - \frac{\theta}{2\pi N})^4)(R - r),$$

where  $R$  is an outermost radius of the coil,  $r$  is an innermost radius of the coil, and  $N$  is a number of loops of the coil.

33. The apparatus according to claim 24, wherein the region of interest is a second plane parallel to the plane of the coil.

34. The apparatus according to claim 33, wherein the second plane is offset from the plane of the coil by a distance  $d$ .

35. The apparatus according to claim 34, wherein  $d$  is less than 30 cm.

36. The apparatus according to claim 34, wherein  $d$  is less than 10 cm.

37. The apparatus according to claim 34, wherein  $d$  is less than  $R$ , where  $R$  is an outermost radius of the coil.

38. The apparatus according to claim 33, wherein the region of interest is a region covering at least a portion of an area of the coil.

39. The apparatus according to claim 33, wherein the region of interest is a region covering an area of the coil.

40. The apparatus according to claim 24, wherein the polygonal coil is a square coil.

41. The apparatus according to claim 24, wherein the polygonal coil is a hexagonal coil.

42. An apparatus for producing a magnetic field, comprising:

a coil, wherein the coil is a planar spiral coil, where the coil has at least two loops, wherein a spacing between starting points of adjacent loops decreases from an inner loop toward an outer loop of the coil, and

a driver, wherein the driver drives the coil to produce a magnetic field, wherein a magnitude of the magnetic field in a direction perpendicular to the plane of the coil is substantially uniform over the region of interest such that  $\frac{MAX - MIN}{AVERAGE}$  is less than or equal

to 0.2 over the region of interest, where MAX and MIN are the maximum magnitude, and minimum magnitude, of the magnet field over the region of interest, respectively, and AVERAGE is  $\frac{MAX + MIN}{2}$ , wherein a magnitude of the magnetic field in a direction perpendicular to a plane of the coil is substantially uniform over a region of interest.

43. A method for producing a magnetic field, comprising:

providing a coil, wherein the coil is a planar spiral coil, where the coil has at least two loops, wherein a spacing between adjacent loops decreases continuously from an inner loop toward an outer loop of the coil, and

driving the coil to produce a magnetic field, wherein a magnitude of the magnetic field in a direction perpendicular to a plane of the coil is substantially uniform over a region of interest.

44. The method according to claim 43, wherein the magnitude of the magnetic field in a direction perpendicular to the plane of the coil is substantially uniform over the region of interest such that  $\frac{MAX - MIN}{AVERAGE}$  is less than or equal to 0.2 over the region of interest, where MAX and MIN are the maximum magnitude, and minimum magnitude, of the magnet field over the region of interest, respectively, and AVERAGE is  $\frac{MAX + MIN}{2}$ .

45. The method according to claim 44, wherein the  $\frac{MAX - MIN}{AVERAGE}$  is less than or equal to 0.1 over the region of interest.

46. The method according to claim 44, wherein the  $\frac{MAX - MIN}{AVERAGE}$  is less than or equal to 0.05 over the region of interest.

47. The method according to claim 44, wherein the magnetic field is time-varying.

48. The method according to claim 47, wherein the time-varying magnetic field has a frequency in the range 1 kHz to 10 MHz.

49. The method according to claim 47, wherein the time-varying magnetic field has a frequency in the range 100 kHz to 400 kHz.

50. The method according to claim 47, wherein the time varying magnetic field has a frequency less than or equal to 1 MHz.

51. An method according to claim 43, wherein the coil is a planar elliptical spiral coil.

52. The method according to claim 43, wherein the coil is a planar circular spiral coil, wherein the coil follows the equation:

$$\rho(\theta) = \rho_0 + l(\theta)\theta$$

where  $\rho(\theta)$  is the radius of the coil,  $\rho_0$  is the initial radius of the coil,  $\theta$  is the angle with respect to the initial radius of the coil, and  $l(\theta)$  is a function of  $\theta$ .

53. The method according to claim 52, wherein a derivative of  $l(\theta)$  is positive.

54. The method according to claim 53, wherein the derivative of  $l(\theta)$  decreases as  $\theta$  increases over at least a portion of the coil.

55. The method according to claim 54, wherein the derivative of  $l(\theta)$  decreases as  $\theta$  increases over the coil.

56. The method according to claim 43, wherein the spiral coil further follows the equation:

$$\rho(\theta) = r + (1 - (1 - \frac{\theta}{2\pi N})^4)(R - r)$$



where  $R$  is an outermost radius of the coil,  $r$  is the initial radius of the coil, and  $N$  is a number of loops of the coil.

57. The method according to claim 43, wherein the region of interest is a second plane parallel to a plane of the coil.

58. The method according to claim 57, wherein the second plane is offset from the plane of the coil by a distance  $d$ .

59. The method according to claim 58, wherein  $d$  is less than 30 cm.

60. The method according to claim 58, wherein  $d$  is less than 10 cm.

61. The method according to claim 58, wherein  $d$  is less than  $R$ , where  $R$  is an outermost radius of the coil.

62. The method according to claim 57, wherein the region of interest is a region covering at least a portion of an area of the coil.

63. The method according to claim 57, wherein the region of interest is a region covering an area of the coil.

64. The method according to claim 43, wherein the coil is a polygonal spiral coil.

65. The method according to claim 43, wherein the coil is a rectangular spiral coil.

66. An method for producing a magnetic field, comprising:

producing a coil, wherein the coil is a planer polygonal spiral coil wherein the coil has at least two loops, wherein a spacing between adjacent loops either stays the same or decreases at each corner of the polygonal going from an inner loop toward an outer loop of the coil; and

driving the coil to produce a magnetic field, wherein a magnitude of the magnetic field in a direction perpendicular to a plane of the coil substantially is uniform over a region of interest.

67. The method according to claim 66, wherein the magnitude of the magnetic field in a direction perpendicular to the plane of the coil is substantially uniform over the region of interest such that  $\frac{MAX - MIN}{AVERAGE}$  is less than or equal to 0.2 over the region of interest, where MAX and MIN are the maximum magnitude, and minimum magnitude, of the magnet field over the region of interest, respectively, and AVERAGE is  $\frac{MAX + MIN}{2}$ .

68. The method according to claim 67, wherein the  $\frac{MAX - MIN}{AVERAGE}$  is less than or equal to 0.1 over the region of interest.

69. The method according to claim 67, wherein the  $\frac{MAX - MIN}{AVERAGE}$  is less than or equal to 0.05 over the region of interest.

70. The method according to claim 66, wherein the magnetic field is time-varying.

71. The method according to claim 70, wherein the time-varying magnetic field has a frequency in the range 1 kHz to 10 MHz.

72. The method according to claim 67, wherein the time-varying magnetic field has a frequency in the range 100 kHz to 400 kHz.

73. The method according to claim 67, wherein the time varying magnetic field has a frequency less than or equal to 1 MHz.

74. The method according to claim 66, wherein the spacing between adjacent loops follows the equation:

$\rho(2n\pi) - \rho[2(n-1)\pi]$ ,  $n = 1, 2, \dots, N$ , where  $\rho$  is the function

$$\rho(\theta) = r + \left(1 - \left(1 - \frac{\theta}{2\pi N}\right)^4\right)(R - r),$$

where  $R$  is an outermost radius of the coil,  $r$  is an innermost radius of the coil, and  $N$  is a number of loops of the coil.

75. The method according to claim 66, wherein the region of interest is a second plane parallel to the plane of the coil.

76. The method according to claim 75, wherein the second plane is offset from the plane of the coil by a distance  $d$ .

77. The method according to claim 76, wherein  $d$  is less than 30 cm.

78. The method according to claim 76, wherein  $d$  is less than 10 cm.

79. The method according to claim 76, wherein  $d$  is less than  $R$ , where  $R$  is an outermost radius of the coil.

80. The method according to claim 75, wherein the region of interest is a region covering at least a portion of an area of the coil.

81. The method according to claim 75, wherein the region of interest is a region covering an area of the coil.

82. The method according to claim 66, wherein the polygonal coil is a square coil.

83. The method according to claim 66, wherein the polygonal coil is a hexagonal coil.

84. A method for producing a magnetic field, comprising:

providing a coil, wherein the coil is a planar spiral coil, where the coil has at least two loops, wherein a spacing between starting points of adjacent loops decreases from an inner loop toward an outer loop of the coil, and

driving the coil to produce a magnetic field, wherein a magnitude of the magnetic field in a direction perpendicular to the plane of the coil is substantially uniform over the region of interest such that  $\frac{MAX - MIN}{AVERAGE}$  is less than or equal to 0.2 over the region of interest, where MAX and MIN are the maximum magnitude, and minimum magnitude, of the magnet field over the region of interest, respectively, and AVERAGE is  $\frac{MAX + MIN}{2}$ , wherein a magnitude of the magnetic field in a direction perpendicular to a plane of the coil is substantially uniform over a region of interest.

85. A system for inductive power transfer, comprising:

an apparatus for producing a magnetic field according to any of claims 1-42; and  
a receiver coil, wherein when the receiver coil is positioned proximate the apparatus for producing the magnetic field, power is inductively transfer to the receiver coil.

86. The system according to claim 85, wherein the coil has an area in the range of 2 to 12 times as large as an area of the receiver coil.

87. A method for inductively transferring power, comprising:

implementing the method according to any of claims 43-84; and  
providing a receiver coil proximate to the coil such that power is inductively coupled to the receiver coil.

88. The method according to claim 87, wherein the coil has an area in the range of 2 to 12 times as large as an area of the receiver coil.

1/3

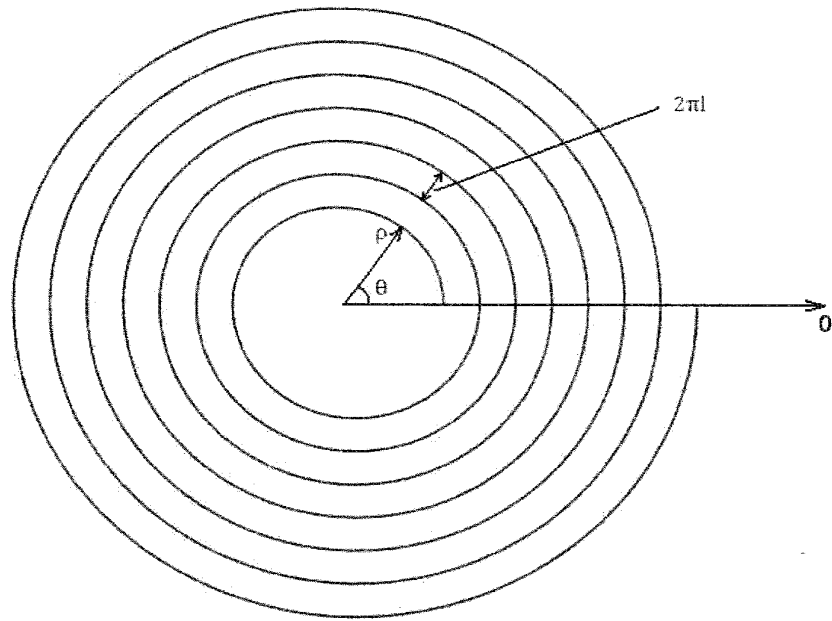


FIG. 1

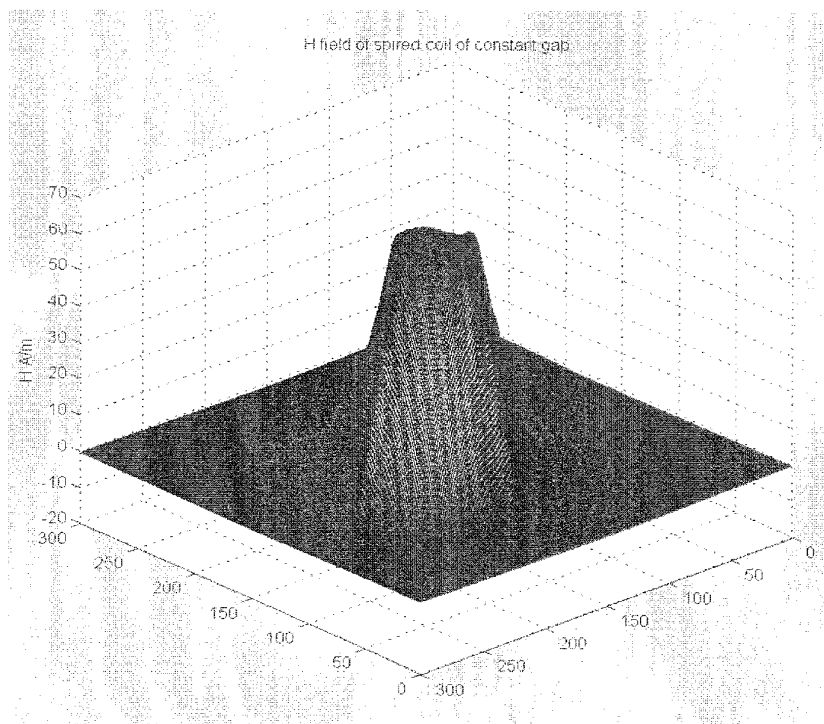


FIG. 2

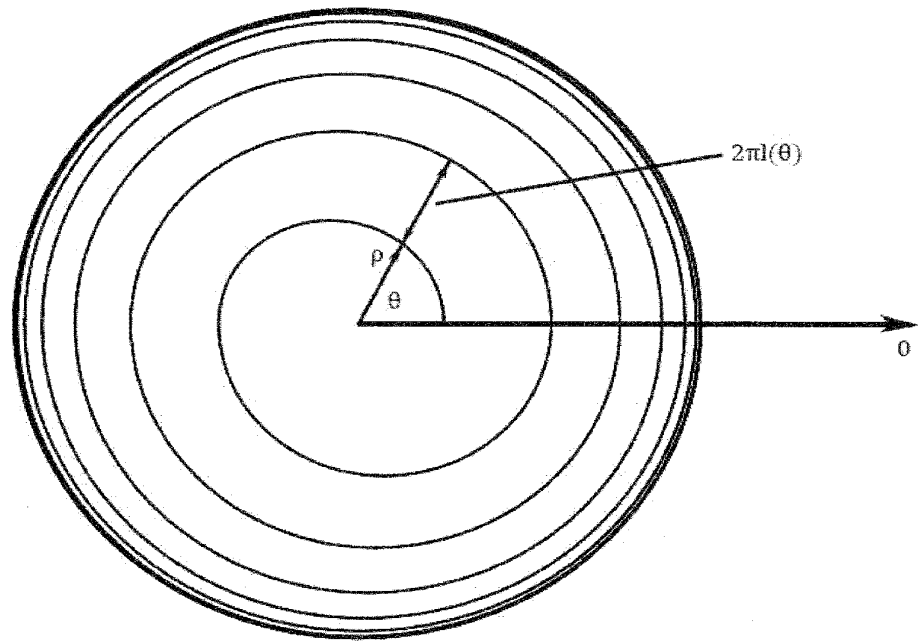


FIG. 3

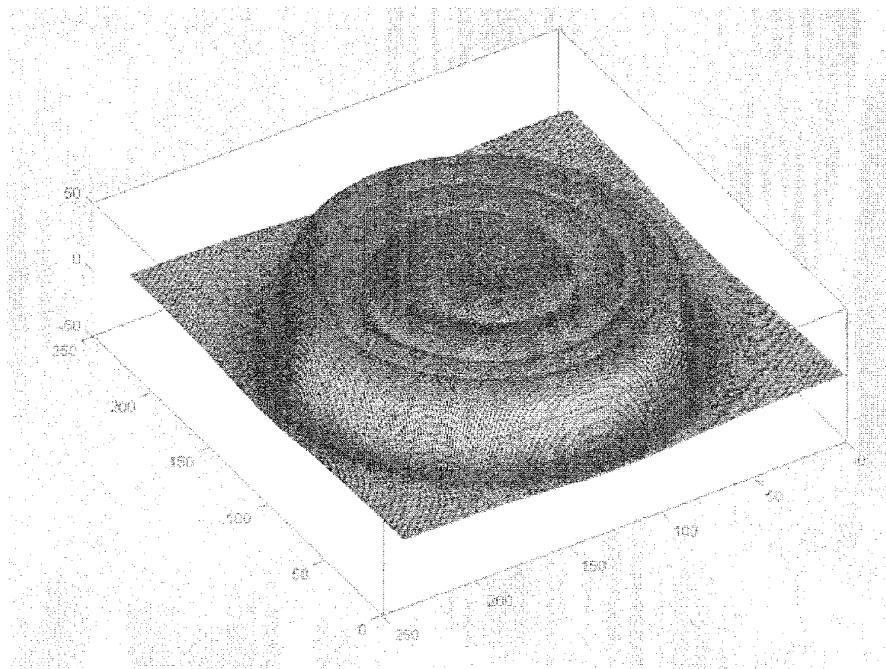


FIG. 4

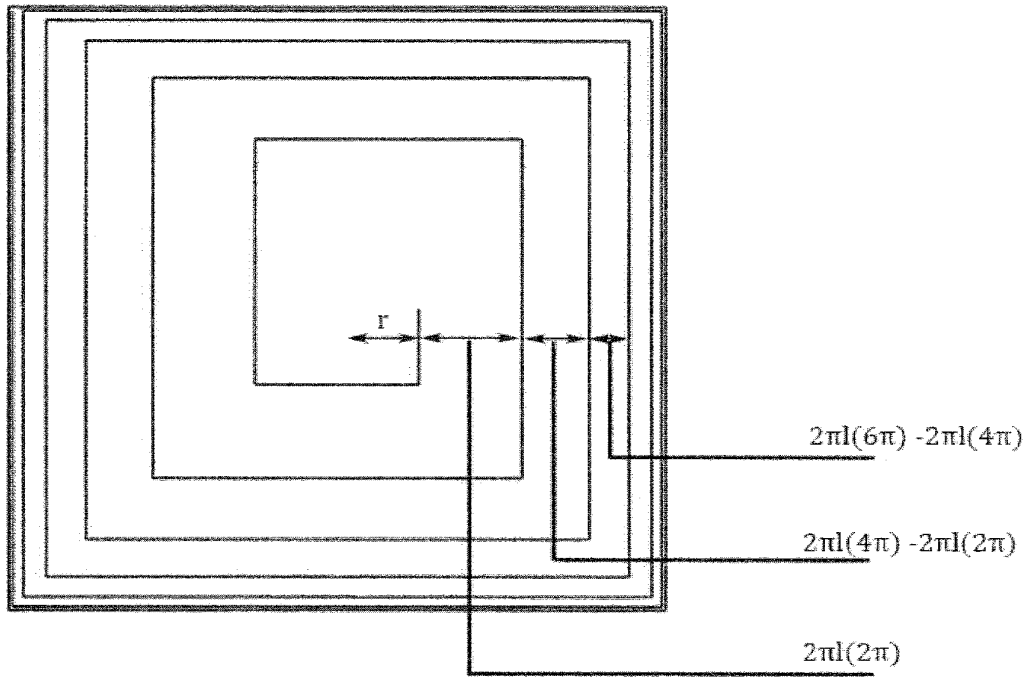


FIG. 5

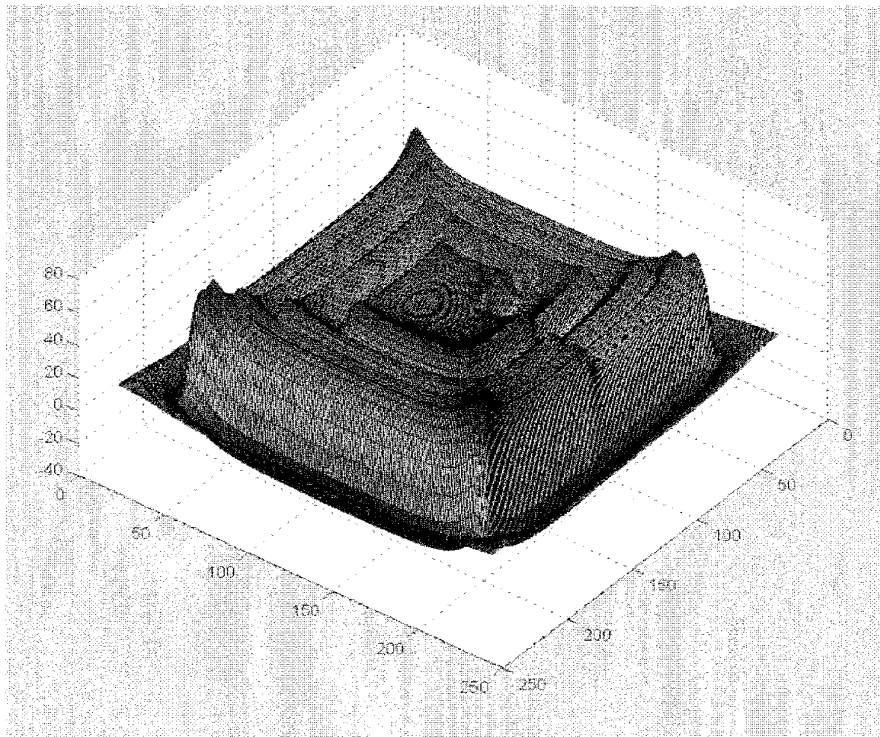


FIG. 6



(43) International Publication Date  
18 March 2010 (18.03.2010)

(10) International Publication Number  
**WO 2010/030977 A2**

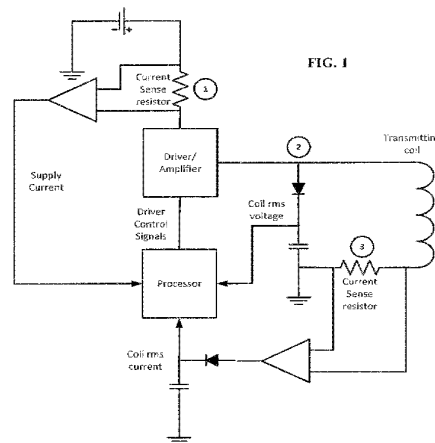
- (51) International Patent Classification:  
G01R 29/00 (2006.01) G01R 27/00 (2006.01)
- (21) International Application Number:  
PCT/US2009/056804
- (22) International Filing Date:  
14 September 2009 (14.09.2009)
- (25) Filing Language: English
- (26) Publication Language: English
- (30) Priority Data:  
12/209,784 12 September 2008 (12.09.2008) US
- (71) Applicant (for all designated States except US): **UNIVERSITY OF FLORIDA RESEARCH FOUNDATION, INC.** [US/US]; 223 Grinter Hall, Gainesville, FL 32611 (US).
- (72) Inventors; and
- (75) Inventors/Applicants (for US only): **LIN, Jenshan** [US/US]; 910 S.W. 105th Terrace, Gainesville, FL 32607 (US). **LOW, Zhen, Ning** [SG/US]; 712 S.W. 16th Avenue, #311, Gainesville, FL 32601 (US).
- (74) Agents: **PARKER, James, S.** et al.; Saliwanchik, Lloyd, Saliwanchik, P.O. Box 142950, Gainesville, FL 32614-2950 (US).

- (81) Designated States (unless otherwise indicated, for every kind of national protection available): AE, AG, AL, AM, AO, AT, AU, AZ, BA, BB, BG, BH, BR, BW, BY, BZ, CA, CH, CL, CN, CO, CR, CU, CZ, DE, DK, DM, DO, DZ, EC, EE, EG, ES, FI, GB, GD, GE, GH, GM, GT, HN, HR, HU, ID, IL, IN, IS, JP, KE, KG, KM, KN, KP, KR, KZ, LA, LC, LK, LR, LS, LT, LU, LY, MA, MD, ME, MG, MK, MN, MW, MX, MY, MZ, NA, NG, NI, NO, NZ, OM, PE, PG, PH, PL, PT, RO, RS, RU, SC, SD, SE, SG, SK, SL, SM, ST, SV, SY, TJ, TM, TN, TR, TT, TZ, UA, UG, US, UZ, VC, VN, ZA, ZM, ZW.
- (84) Designated States (unless otherwise indicated, for every kind of regional protection available): ARIPO (BW, GH, GM, KE, LS, MW, MZ, NA, SD, SL, SZ, TZ, UG, ZM, ZW), Eurasian (AM, AZ, BY, KG, KZ, MD, RU, TJ, TM), European (AT, BE, BG, CH, CY, CZ, DE, DK, EE, ES, FI, FR, GB, GR, HR, HU, IE, IS, IT, LT, LU, LV, MC, MK, MT, NL, NO, PL, PT, RO, SE, SI, SK, SM, TR), OAPI (BF, BJ, CF, CG, CI, CM, GA, GN, GQ, GW, ML, MR, NE, SN, TD, TG).

**Published:**

- without international search report and to be republished upon receipt of that report (Rule 48.2(g))

(54) Title: METHOD AND APPARATUS FOR LOAD DETECTION FOR A PLANAR WIRELESS POWER SYSTEM



(57) **Abstract:** Embodiments of the subject invention relate to a method and apparatus for determining information regarding a load in a planar wireless power transfer system by extracting system operating parameters from one or more test points in the transmitter circuit. As shown in Figure 1, a specific embodiment showing three test points in the transmitter circuit from which operating parameters can be extracted. The transmitter circuit is designed to produce a magnetic field, by driving the transmitter coil, which inductively couples to a receiver coil such that power is provided to a receiver. By extracting operating parameters from the transmitter circuit, the receiver does not need to incorporate sophisticated signal processing and can be manufactured with low cost.

WO 2010/030977 A2



## DESCRIPTION

METHOD AND APPARATUS FOR LOAD DETECTION FOR A PLANAR WIRELESS  
POWER SYSTEM

## CROSS-REFERENCE TO RELATED APPLICATION

The present application claims the benefit of U.S. Application Serial No. 12/209,784, filed September 12, 2008, which is hereby incorporated by reference herein in its entirety, including any figures, tables, or drawings.

## BACKGROUND OF INVENTION

Portable electronic devices such as laptop computers, LCD digital photo frames, mobile phones, and mp3 players require power to operate. Often, these devices use rechargeable batteries to provide power. The batteries are typically recharged by plugging a charger into the portable device or by removing the battery from the portable device and separately recharging the battery using a wired charger.

The cables that once restricted electronic devices are gradually being rendered unnecessary by wireless communication technology, and as the circuits that constitute the electronic devices shrink, only the power cords and batteries continue to restrict the portability of mobile electronic devices.

Current trends are leading towards going completely wireless. This means that portable devices can remain portable and can avoid having to 'plug-in' for power charging. Electro-magnetic inductive charging uses a coil to create an electromagnetic field across a charging station surface. The device then converts power from the electromagnetic field back into usable electricity, which is put to work charging the battery. Two coils are brought close to each other and when current is passed through one, the generated magnetic flux causes electromotive force to be generated in the other.

In order to reduce unnecessary generation of magnetic flux, for example when no receiver is positioned to receive the magnetic flux or when the battery associated with the receiver is already charged, techniques to determine whether a valid load is placed in position with respect to the transmitting coil and to determine the charging status of the load have been developed. In order to determine if a valid load is placed on the transmitting coil and to determine the charging status, a communication link is often used between the transmitting

unit and the receiving unit. Such a link is often also used to determine whether multiple loads are placed on the transmitter. However, a communication link adds cost and size to the system, which is not desirable for a compact receiving unit to be integrated inside a portable device. Alternatively to a communication system, such as a complex DSP system, can be used to extract system operating parameters from the transmitter to determine the operating status of the system. However, such systems are typically complicated and consume large amounts of power which reduce system efficiency and increase system cost.

Accordingly, there still exists a need in the art for an efficient method and apparatus to determine whether a valid load is positioned to be charged and the charging status of the load.

#### BRIEF SUMMARY

Embodiments of the subject invention relate to a method and apparatus for determining information regarding a load in a planar wireless power transfer system by extracting system operating parameters from one or more test points in the transmitter circuit. As shown in Figure 1, a specific embodiment showing three test points in the transmitter circuit from which operating parameters can be extracted. The transmitter circuit is designed to produce a magnetic field, by driving the transmitter coil, which inductively couples to a receiver coil such that power is provided to a receiver. By extracting operating parameters from the transmitter circuit, the receiver does not need to incorporate sophisticated signal processing and can be manufactured with low cost.

Test point 1 in Figure 1 shows where the supply current of the system can be measured. The embodiment shown in Figure 1 is to use a current sense resistor and a differential amplifier located on the high side of the power supply to measure the transmitter supply current. In an alternative embodiment, the transmitter supply current can be measured on the low side of the power supply. Other techniques can also be used. The output voltage of the differential amplifier, which is proportional to the supply current, is then fed into the analog-to-digital conversion (ADC) port of a processor.

Test point 2 in Figure 1 shows where the RMS coil voltage can be measured. The embodiment shown in Figure 1 extracts the RMS coil voltage by rectifying the coil voltage across a diode and holding the charge using a charge holding capacitor. A resistor can be added in parallel to the capacitor to control the response time of the circuit. Other techniques can also be used to extract the RMS coil voltage. The rectified DC voltage is then fed into

the ADC port of a processor.

Test point 3 in Figure 1 shows where the RMS coil current of the coil can be measured. The RMS coil current can be extracted before or after the coil. The embodiment shown in Figure 1, which is positioned after the coil, transforms the coil current to its voltage equivalent by using a current sense resistor and a differential amplifier. A diode charge holding capacitor is then used to further extract the RMS coil current. A resistor can be added in parallel to the capacitor to control the response time of the circuit. The rectified DC voltage is then fed into the ADC port of a processor. Other techniques can also be used to extract the RMS coil current.

#### BRIEF DESCRIPTION OF DRAWINGS

**Figure 1** shows a system block diagram for system operating parameters extraction in accordance with an embodiment of the subject invention.

**Figure 2** shows measurement results of RMS coil voltage and supply current space diagram in accordance with an embodiment of the subject invention.

**Figure 3** shows measurement results of RMS coil current and supply current space diagram in accordance with an embodiment of the subject invention.

**Figure 4** shows simulation results of system operation for different number of loads in accordance with an embodiment of the subject invention.

**Figure 5** shows power delivery versus transmitting coil voltage in accordance with an embodiment of the subject invention.

#### DETAILED DISCLOSURE

Embodiments of the subject invention relate to a method and apparatus for determining information regarding a load in a planar wireless transfer system by extracting system operating parameters from one or more test points in the transmitter circuit. As shown in Figure 1, a specific embodiment showing three test points in the transmitter circuit from which operating parameters can be extracted. The transmitter circuit is designed to produce a magnetic field, by driving the transmitter coil, which inductively couples to a receiver coil such that power is provided to a receiver. By extracting operating parameters from the transmitter circuit, the receiver does not need to incorporate sophisticated signal processing and can be manufactured with low cost.

Test point 1 in Figure 1 shows where the supply current of the system can be

measured. The embodiment shown in Figure 1 is to use a current sense resistor and a differential amplifier located on the high side of the power supply to measure the transmitter supply current. In an alternative embodiment, the transmitter supply current can be measured on the low side of the power supply. Other techniques can also be used. The output voltage of the differential amplifier, which is proportional to the supply current, is then fed into the analog-to-digital conversion (ADC) port of a processor.

Test point 2 in Figure 1 shows where the RMS coil voltage can be measured. The embodiment shown in Figure 1 extracts the RMS coil voltage by rectifying the coil voltage across a diode and holding the charge using a charge holding capacitor. A resistor can be added in parallel to the capacitor to control the response time of the circuit. Other techniques can also be used to extract the RMS coil voltage. As an example, the real time AC voltage can be measured with a fast enough ADC. The rectified DC voltage is then fed into the ADC port of a processor.

Test point 3 in Figure 1 shows where the RMS coil current of the coil can be measured. The RMS coil current can be extracted before or after the coil. The embodiment shown in Figure 1, which is positioned after the coil, transforms the coil current to its voltage equivalent by using a current sense resistor and a differential amplifier. A diode charge holding capacitor is then used to further extract the RMS coil current. The diode can be removed by using a fast ADC. A resistor can be added in parallel to the capacitor to control the response time of the circuit. The rectified DC voltage is then fed into the ADC port of a processor. Other techniques can also be used to extract the RMS coil current. As an example, a loop can be used to measure the AC current.

Figure 2 shows the coil RMS voltage and supply current space diagram of the operation of an embodiment of a planar wireless power transfer system measured in accordance with an embodiment of the invention. Figure 3 shows the coil RMS current and supply current space diagram of the operation of the wireless power transfer system measured in accordance with an embodiment of the invention. As the threshold and location of the various regions in the space diagrams of Figure 2 and Figure 3 depend primarily on the size of the transmitter coil and supply voltage of the transmitter, each transmitter can have different thresholds and locations of regions. In a specific embodiment, the coil voltage or the coil current can be used to track the charge status of the load and/or whether the load is operation properly. The method and system are able to determine invalid load conditions such as no load and metal sheet, and distinguish them clearly from normal operation with

valid load. This is because the distance between the invalid load conditions and valid load conditions is large in either the coil RMS voltage and supply current space diagram or coil RMS current and supply current space diagram. In one embodiment, the system extracts supply current and coil RMS voltage. In another embodiment, the system extracts supply current and coil RMS current. In a further embodiment, the system extracts all three of the parameters. Measurements of these parameters at a point in time can be used to determine whether there is a valid load or not proximate the transmitter coil, or whether there is a fault conditioning by comparing the measurements to a known space diagram such as in Figure 2 or Figure 3.

In addition, it is possible to differentiate the number of loads being placed on the transmitting pad by comparing with either space diagram. An example is shown in Figure 4. It should be noted that there are overlaps of certain load conditions but they occur at very light loads (low current). Light load operation does not occur during the power-up state. Therefore, the system is able to easily detect the number of loads on the transmitting coil when powering up. Adding or removing a receiver from the transmitting coil can also be detected by observing any sharp transitions in either space diagram. The direction of the transition can be used to determine if a receiver is added or removed from the transmitting coil.

Power delivered and other system operating parameters can be determined by the coil RMS voltage. Figure 5 shows the direct correlation between the coil RMS voltage and the power delivered to the load. Figure 5 was produced by using a variable resistor as the load, which models the behavior of a battery charging for the portion of the curve below about 70V. As the battery begins charging the space diagram would read about 70V, 6W and would tend to go down and to the left as charging proceeded. In this way, measuring the coil voltage over a period of time and comparing with a curve such as shown in Figure 5 for the receiver, a determination of the charging status of the load, and/or type of load, can be made. In another embodiment, a plot of transmitter coil current versus power delivered to load (W) can be used to also determine the charge status of a load, and/or the type of load, based on the measurement of coil current over a period of time. In this way, having prior knowledge of the coil voltage versus power delivered, or the coil current versus power delivered, for a receiver can allow the determination of the charging status for the receiver by measuring coil voltage, or coil current, respectively.

In a further embodiment, power delivered can be determined by measuring the coil voltage or the coil current and using, for example, a look up table and microprocessor to determine power delivered, and charge status from following power delivered.

The information regarding the load can be used to modify the behavior of the transmitter. As examples, if a faulty load is determined the transmitter can be shut off to prevent damage, if a charged load is determined, the transmitter can shut off and come on in intervals to check for new loads, if no load is determined then the transmitter can be shut off until a load is determined.

All patents, patent applications, provisional applications, and publications referred to or cited herein are incorporated by reference in their entirety, including all figures and tables, to the extent they are not inconsistent with the explicit teachings of this specification.

It should be understood that the examples and embodiments described herein are for illustrative purposes only and that various modifications or changes in light thereof will be suggested to persons skilled in the art and are to be included within the spirit and purview of this application.

## CLAIMS

1. A method of determining information regarding a load for a planar wireless power transfer system, comprising:
  - driving a transmitter coil of a planar wireless power transfer system with a drive amplifier;
  - measuring a transmitter coil voltage provided to the transmitter coil by the drive amplifier; and
  - determining information regarding a load positioned proximate the transmitter coil.
  
2. A method of determining information regarding a load for planar wireless power transfer system, comprising:
  - driving a transmitter coil of a planar wireless power transfer system with a drive amplifier;
  - measuring a transmitter coil current passing through the transmitter coil; and
  - determining information regarding a load positioned proximate the transmitter coil.
  
3. The method according to claim 1, wherein determining information regarding the load proximate the transmitter coil comprises comparing the transmitter coil voltage over a period of time with an *a priori* curve in the transmitter coil voltage and power delivered to load space.
  
4. The method according to claim 2, wherein determining information regarding the load proximate the transmitter coil comprises comparing the transmitter coil current over a period of time with *a priori* curve in the transmitter coil current and power delivered to load space.
  
5. The method according to claim 1, further comprising:
  - measuring a transmitter supply current provided to the drive amplifier.

6. The method according to claim 2, further comprising:  
measuring a transmitter supply current provided to the drive amplifier.
7. The method according to claim 1, wherein the information regarding the load is the charging status of the load.
8. The method according to claim 5, wherein the transmitter supply current is measured on a high side of a power supply, wherein the power supply supplies power to the drive amplifier.
9. The method according to claim 8, wherein the transmitter supply current is measured via a current sensing resistor.
10. The method according to claim 9, wherein the transmitter supply current is measured via an amplifier across the current sensing resistor.
11. The method according to claim 5, wherein the transmitter supply current is measured on a low side of a power supply, wherein the power supply supplies power to the driver amplifier.
12. The method according to claim 11, wherein the transmitter supply current is measured via a current sensing resistor.
13. The method according to claim 12, wherein the transmitter supply current is measured via an amplifier across the current sensing resistor.
14. The method according to claim 6, wherein the transmitter coil current is measured on high side of the transmitting coil.
15. The coil method according to claim 14, wherein the transmitter coil current is measured via a current sensing resistor.



16. The method according to claim 15, wherein the transmitter coil current is measured via an amplifier across the current sensing resistor.

17. The method according to claim 16, wherein an output of the amplifier is input into a rectification circuit.

18. The method according to claim 17, wherein the rectification circuit comprises a diode and a charge holding capacitor.

19. The method according to claim 6, wherein the transmitter coil current is measured at a low side of the transmitting coil.

20. The method according to claim 19, wherein the transmitter coil current is measured via a current sensing resistor.

21. The method according to claim 20, wherein the transmitter coil current is measured via an amplifier across the current sensing resistor.

22. The method according to claim 21, wherein an output of the amplifier is input to a rectification circuit.

23. The method according to claim 22, wherein the rectification circuit comprises a diode and a charge holding capacitor.

24. The method according to claim 5, wherein the transmitter coil voltage is measured at a high side of the transmitter coil.

25. The coil method according to claim 24, wherein the transmitter coil voltage is measured via a rectification circuit.

26. The method according to claim 25, wherein the rectification circuit comprises a diode and a charge holding capacitor.

27. The method according to claim 5, wherein information regarding the load is determined via analysis of the transmitter supply current and the transmitter coil voltage space.

28. The method according to claim 6, wherein information regarding the load is determined via analysis of the transmitter supply current and the transmitter coil current space.

29. The method according to claim 5, further comprising:  
measuring a transmitter coil current passing through the transmitter coil.

30. The method according to claim 29, wherein information regarding the load is determined via analysis of the transmitter supply current, the transmitter coil voltage, and the transmitter coil current space.

31. The method according to claim 5, wherein the transmitter supply current is measured over a period of time, wherein the transmitter coil voltage is measured over the period of time.

32. The method according to claim 6, wherein the transmitter supply current is measured over a period of time, wherein the transmitter coil current is measured over a period of time.

33. The method according to claim 5, wherein the information regarding the load comprises the charge status of the load.

34. The method according to claim 6, wherein the information regarding the load comprises the charge status of the load.

35. The method according to claim 5, wherein the information regarding the load comprises whether load operating properly.

36. The method according to claim 6, wherein the information regarding the load comprises whether the load is operating properly.

37. The method according to claim 5, wherein the information regarding the load comprises whether a valid load is proximate the transmitter coil.

38. The method according to claim 6, wherein the information regarding the load comprises whether a valid load is proximate the transmitter coil.

39. The method according to claim 5, wherein the transmitter supply current and the transmitter coil voltage are measured at a point in time, wherein the information regarding the load is whether there is no load, a valid load, or a faulty load.

40. The method according to claim 6, wherein the transmitter supply current and the transmitter coil current are measured at a point in time, wherein the information regarding the load is whether there is no load, a valid load, or a faulty load.

41. The method according to claim 5, wherein the transmitter supply current and the transmitter coil voltage are measured at a point in time, wherein the information regarding the load is whether the load is operating properly.

42. The method according to claim 6, wherein the transmitter supply current and the transmitter coil current are measured at a point in time, wherein the information regarding the load is whether the load is operating properly.

43. The method according to claim 31, wherein the information regarding the load comprises the charge status of the load.

44. The method according to claim 32, wherein the information regarding the load comprises the charge status of the load.

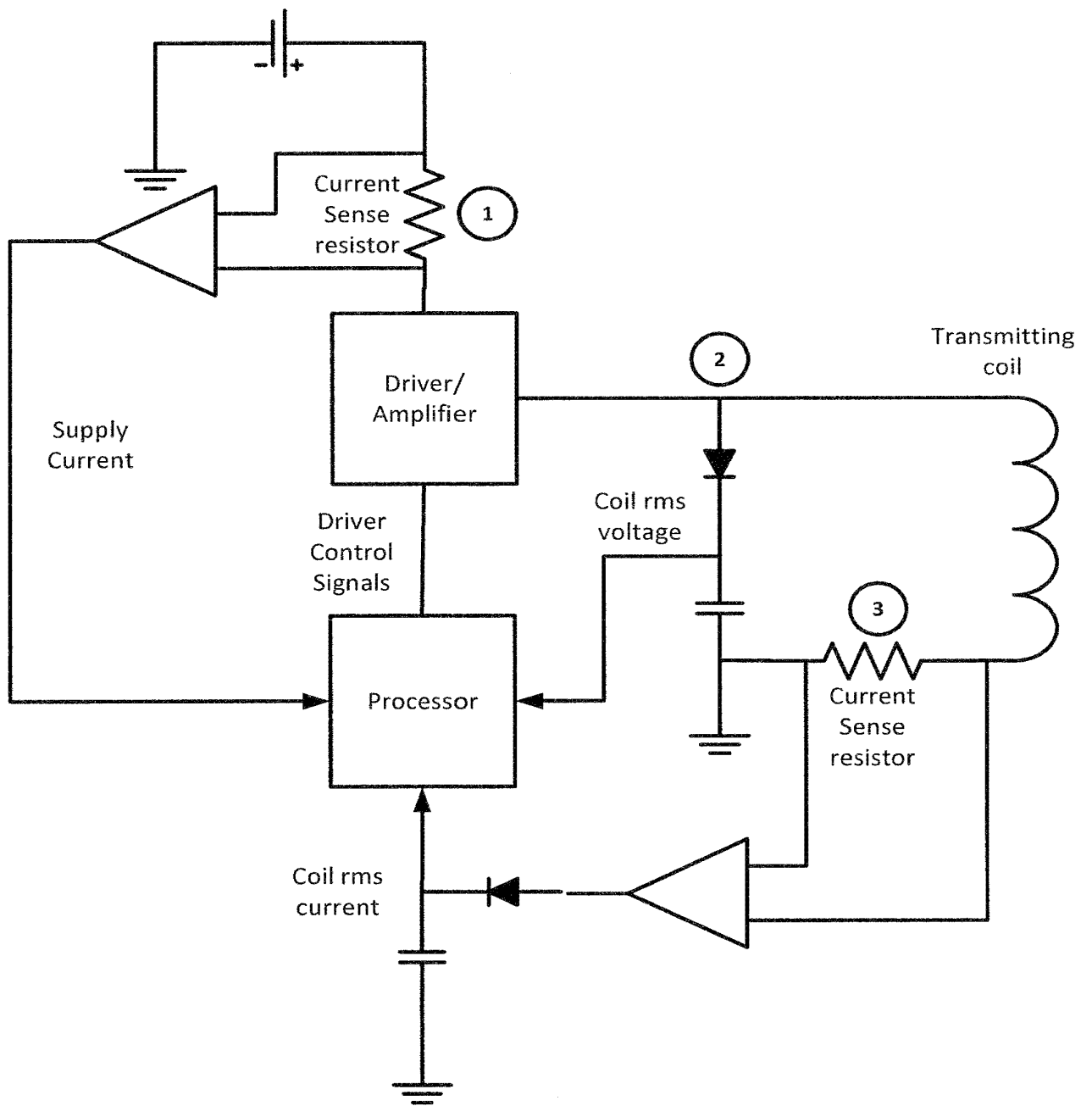


FIG. 1

SUBSTITUTE SHEET (RULE 26)

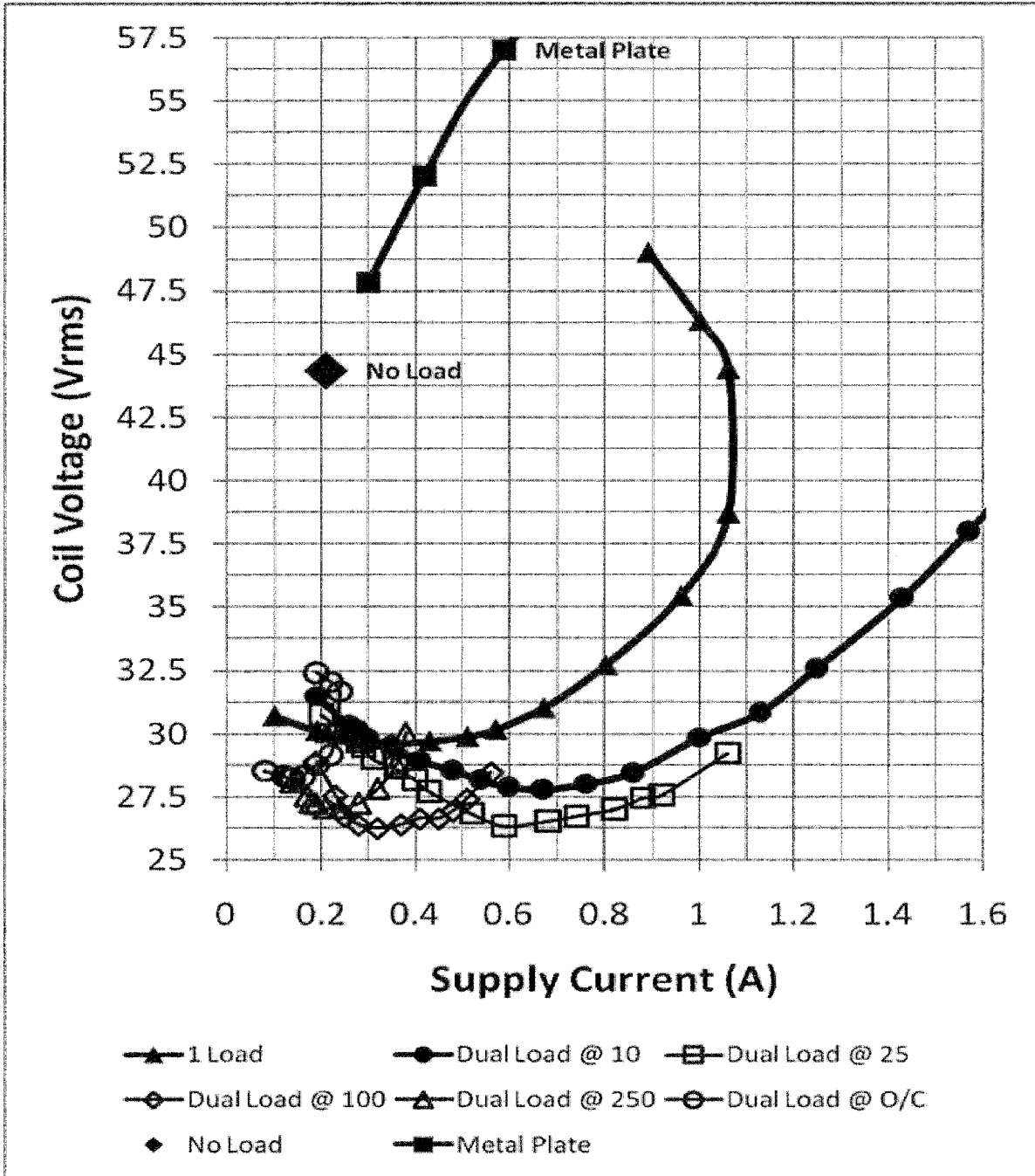


FIG. 2

SUBSTITUTE SHEET (RULE 26)

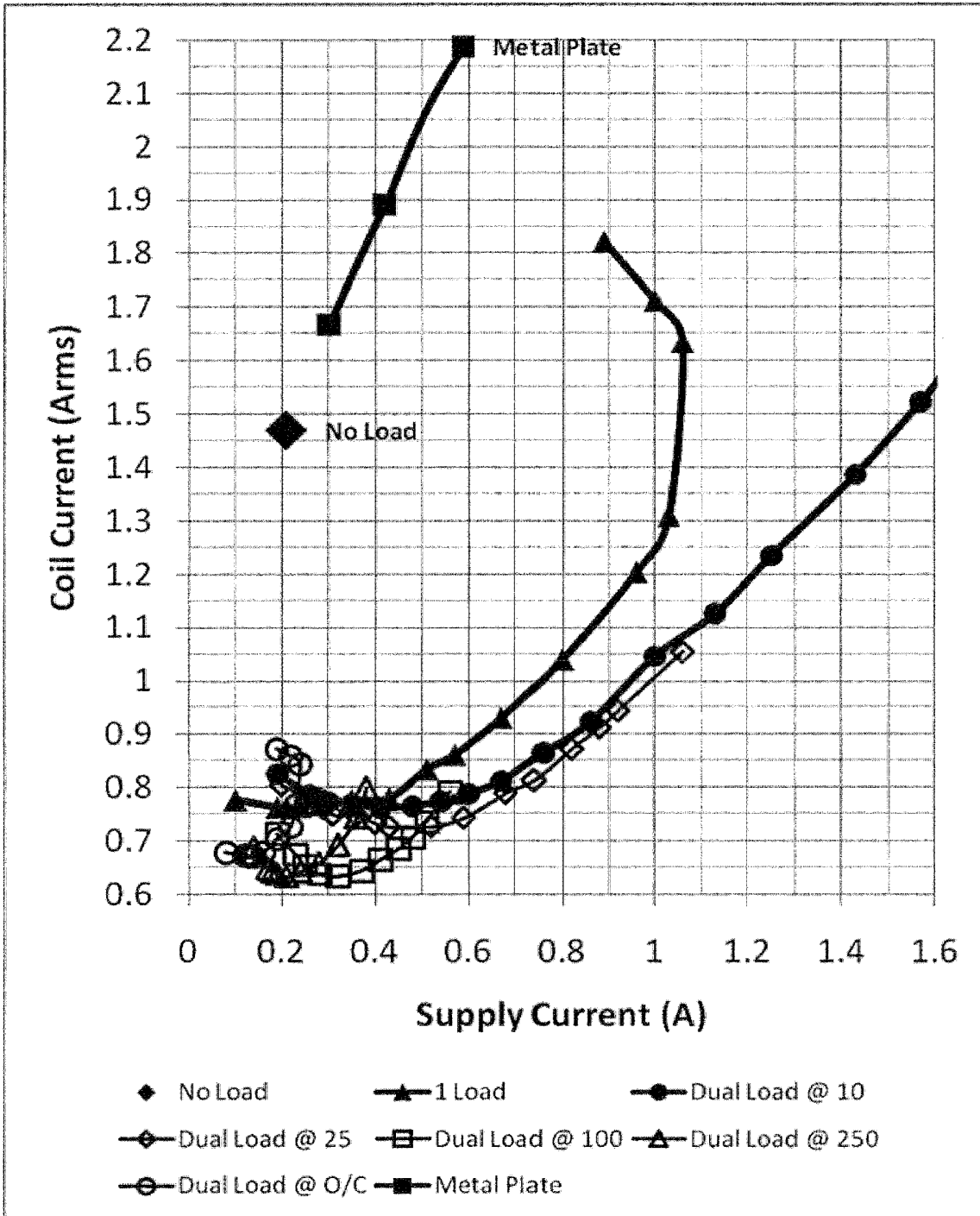


FIG. 3

SUBSTITUTE SHEET (RULE 26)

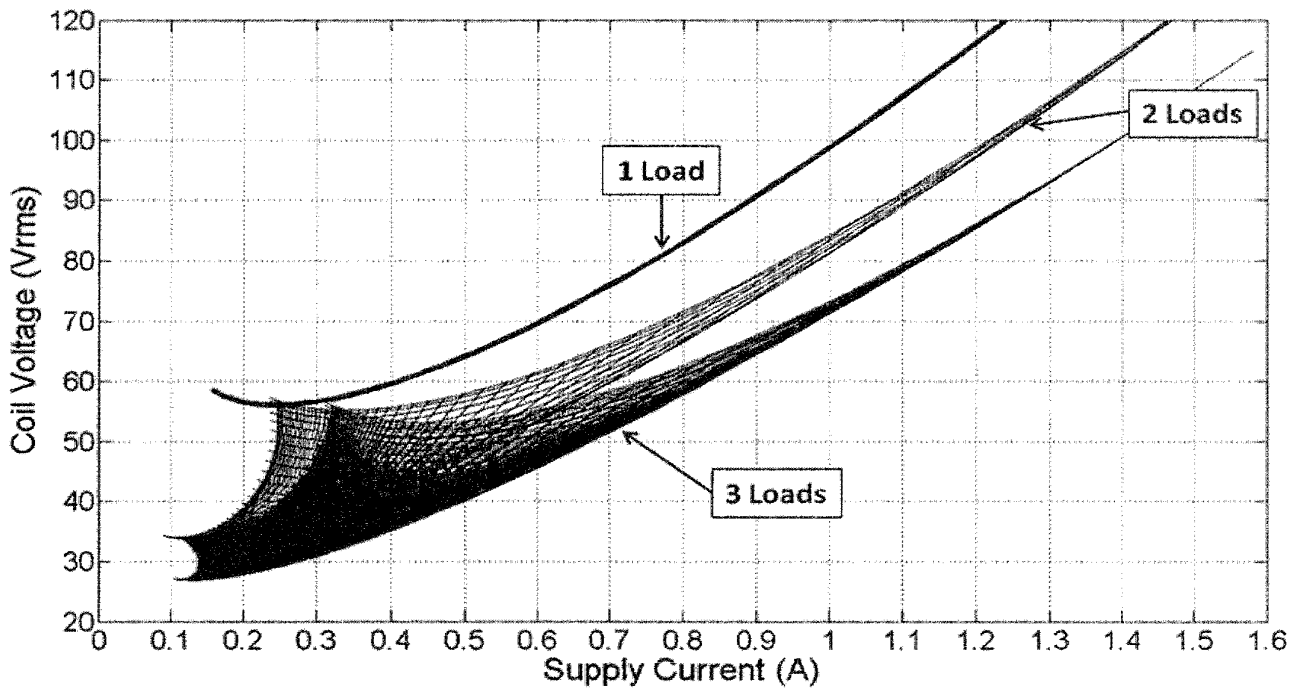


FIG. 4

SUBSTITUTE SHEET (RULE 26)

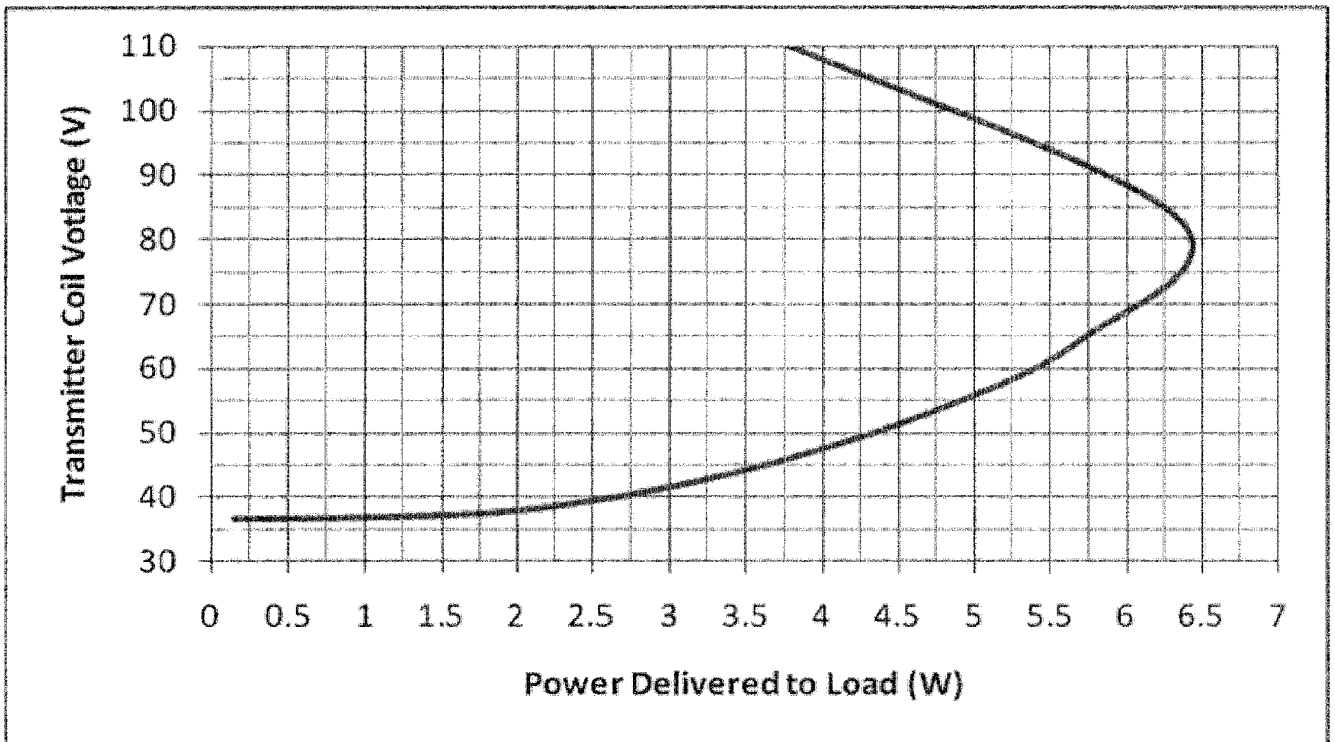


FIG. 5

SUBSTITUTE SHEET (RULE 26)





- (51) International Patent Classification:  
*H03B 19/00* (2006.01)
- (21) International Application Number:  
PCT/US2009/058499
- (22) International Filing Date:  
25 September 2009 (25.09.2009)
- (25) Filing Language: English
- (26) Publication Language: English
- (30) Priority Data:
 

61/100,721	27 September 2008 (27.09.2008)	US
61/108,743	27 October 2008 (27.10.2008)	US
61/121,159	9 December 2008 (09.12.2008)	US
61/142,887	6 January 2009 (06.01.2009)	US
61/142,796	6 January 2009 (06.01.2009)	US
61/142,889	6 January 2009 (06.01.2009)	US
61/142,885	6 January 2009 (06.01.2009)	US
61/142,880	6 January 2009 (06.01.2009)	US
61/142,818	6 January 2009 (06.01.2009)	US
61/142,977	7 January 2009 (07.01.2009)	US
61/143,058	7 January 2009 (07.01.2009)	US
61/147,386	26 January 2009 (26.01.2009)	US
61/152,086	12 February 2009 (12.02.2009)	US
61/152,390	13 February 2009 (13.02.2009)	US
61/156,764	2 March 2009 (02.03.2009)	US
61/163,695	26 March 2009 (26.03.2009)	US
61/169,240	14 April 2009 (14.04.2009)	US
61/172,633	24 April 2009 (24.04.2009)	US
61/173,747	29 April 2009 (29.04.2009)	US
61/178,508	15 May 2009 (15.05.2009)	US
61/182,768	1 June 2009 (01.06.2009)	US

- (72) Inventors; and
- (75) Inventors/Applicants (for US only): **KESLER, Morris, P.** [US/US]; 95 Hancock Street, Bedford, MA 01730 (US). **KARALIS, Aristeidis** [GR/US]; 151 Tremont Street, Apartment 21F, Boston, MA 02111 (US). **KURS, Andre, B.** [BR/US]; 250 Hammond Pond Parkway, Apartment 1203S, Chestnut Hill, MA 02467 (US). **CAMPANELLA, Andrew, J.** [US/US]; 30 Orange Street, Waltham, MA 02453 (US). **FIGIELLO, Ron** [US/US]; 20 Scotland Drive, Tewksbury, MA 01876 (US). **LI, Qiang** [CN/US]; 654 Main Street, Malden, MA 02148 (US). **KULIKOWSKI, Konrad** [US/US]; 91 Pearson Avenue, Apartment 1, Somerville, MA 02144 (US). **GILER, Eric, R.** [US/US]; 105 Benvenue Street, Wellesley, MA 02482 (US). **PERGAL, Frank, J.** [US/US]; 14 Norrock Road, Gloucester, MA 01930 (US). **SCHATZ, David, A.** [US/US]; 37 White Pine Rd., Needham, MA 02492 (US). **HALL, Katherine, L.** [US/US]; 21 Griffin Road, Westford, MA 01886 (US). **SOLJACIC, Marin** [HR/US]; 44 Westlund Road, Belmont, MA 02478 (US).
- (74) Agents: **MAZZARESE, Robert, A.** et al.; Strategic Patents, P.C., C/o Intellevate, P.O. Box 52050, Minneapolis, MN 55402 (US).

- (81) Designated States (unless otherwise indicated, for every kind of national protection available): AE, AG, AL, AM, AO, AT, AU, AZ, BA, BB, BG, BH, BR, BW, BY, BZ, CA, CH, CL, CN, CO, CR, CU, CZ, DE, DK, DM, DO, DZ, EC, EE, EG, ES, FI, GB, GD, GE, GH, GM, GT, HN, HR, HU, ID, IL, IN, IS, JP, KE, KG, KM, KN, KP, KR, KZ, LA, LC, LK, LR, LS, LT, LU, LY, MA, MD, ME, MG, MK, MN, MW, MX, MY, MZ, NA, NG, NI, NO, NZ, OM, PE, PG, PH, PL, PT, RO, RS, RU, SC, SD, SE, SG, SK, SL, SM, ST, SV, SY, TJ, TM, TN, TR, TT, TZ, UA, UG, US, UZ, VC, VN, ZA, ZM, ZW.

- (71) Applicant (for all designated States except US): **WITRICITY CORPORATION** [US/US]; 80 Coolidge Hill Road, Watertown, MA 02472 (US).

[Continued on next page]

(54) Title: WIRELESS ENERGY TRANSFER SYSTEMS

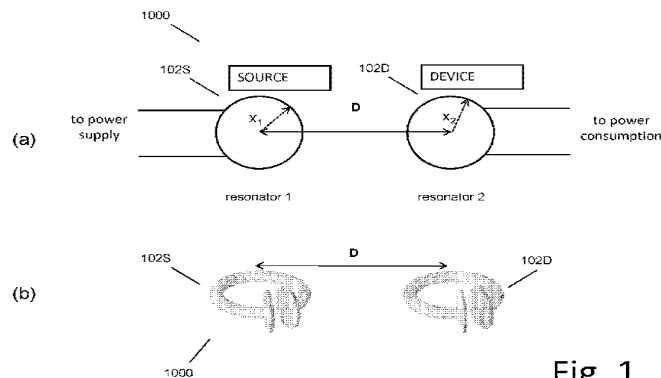


Fig. 1

(57) Abstract: Described herein are improved capabilities for a source resonator having a Q-factor  $Q_1 > 100$  and a characteristic size  $x_1$  coupled to an energy source, and a second resonator having a Q-factor  $Q_2 > 100$  and a characteristic size  $x_2$  coupled to an energy drain located a distance  $D$  from the source resonator, where the source resonator and the second resonator are coupled to exchange energy wirelessly among the source resonator and the second resonator.

WO 2010/036980 A1



(84) **Designated States** (unless otherwise indicated, for every kind of regional protection available): ARIPO (BW, GH, GM, KE, LS, MW, MZ, NA, SD, SL, SZ, TZ, UG, ZM, ZW), Eurasian (AM, AZ, BY, KG, KZ, MD, RU, TJ, TM), European (AT, BE, BG, CH, CY, CZ, DE, DK, EE, ES, FI, FR, GB, GR, HR, HU, IE, IS, IT, LT, LU, LV, MC, MK, MT, NL, NO, PL, PT, RO, SE, SI, SK, SM,

TR), OAPI (BF, BJ, CF, CG, CI, CM, GA, GN, GQ, GW, ML, MR, NE, SN, TD, TG).

**Published:**

— with international search report (Art. 21(3))

## WIRELESS ENERGY TRANSFER SYSTEMS

### CROSS-REFERENCE TO RELATED APPLICATIONS

[0001] This application claims priority to the following U.S. patent applications, each of which is hereby incorporated by reference in its entirety:

[0002] U.S. App. No. 61/100,721 filed September 27, 2008; U.S. App. No. 61/108,743 filed October 27, 2008; U.S. App. No. 61/147,386 filed January 26, 2009; U.S. App. No. 61/152,086 filed February 12, 2009; U.S. App. No. 61/178,508 filed May 15, 2009; U.S. App. No. 61/182,768 filed June 1, 2009; U.S. App. No. 61/121,159 filed December 9, 2008; U.S. App. No. 61/142,977 filed January 7, 2009; U.S. App. No. 61/142,885 filed January 6, 2009; U.S. App. No. 61/142,796 filed January 6, 2009; U.S. App. No. 61/142,889 filed January 6, 2009; U.S. App. No. 61/142,880 filed January 6, 2009; U.S. App. No. 61/142,818 filed January 6, 2009; U.S. App. No. 61/142,887 filed January 6, 2009; U.S. App. No. 61/156,764 filed March 2, 2009; U.S. App. No. 61/143,058 filed January 7, 2009; U.S. App. No. 61/152,390 filed February 13, 2009; U.S. App. No. 61/163,695 filed March 26, 2009; U.S. App. No. 61/172,633 filed April 24, 2009; U.S. App. No. 61/169,240 filed April 14, 2009, and U.S. App. No. 61/173,747 filed April 29, 2009.

### BACKGROUND

[0003] Field:

[0004] This disclosure relates to wireless energy transfer, also referred to as wireless power transmission.

[0005] Description of the Related Art:

[0006] Energy or power may be transferred wirelessly using a variety of known radiative, or far-field, and non-radiative, or near-field, techniques. For example, radiative wireless information transfer using low-directionality antennas, such as those used in radio and cellular communications systems and home computer networks, may be considered wireless energy transfer. However, this type of radiative transfer is very inefficient because only a tiny portion of the supplied or radiated power, namely, that portion in the direction of, and

overlapping with, the receiver is picked up. The vast majority of the power is radiated away in all the other directions and lost in free space. Such inefficient power transfer may be acceptable for data transmission, but is not practical for transferring useful amounts of electrical energy for the purpose of doing work, such as for powering or charging electrical devices. One way to improve the transfer efficiency of some radiative energy transfer schemes is to use directional antennas to confine and preferentially direct the radiated energy towards a receiver. However, these directed radiation schemes may require an uninterrupted line-of-sight and potentially complicated tracking and steering mechanisms in the case of mobile transmitters and/or receivers. In addition, such schemes may pose hazards to objects or people that cross or intersect the beam when modest to high amounts of power are being transmitted. A known non-radiative, or near-field, wireless energy transfer scheme, often referred to as either induction or traditional induction, does not (intentionally) radiate power, but uses an oscillating current passing through a primary coil, to generate an oscillating magnetic near-field that induces currents in a near-by receiving or secondary coil. Traditional induction schemes have demonstrated the transmission of modest to large amounts of power, however only over very short distances, and with very small offset tolerances between the primary power supply unit and the secondary receiver unit. Electric transformers and proximity chargers are examples of devices that utilize this known short range, near-field energy transfer scheme.

[0007] Therefore a need exists for a wireless power transfer scheme that is capable of transferring useful amounts of electrical power over mid-range distances or alignment offsets. Such a wireless power transfer scheme should enable useful energy transfer over greater distances and alignment offsets than those realized with traditional induction schemes, but without the limitations and risks inherent in radiative transmission schemes.

## **SUMMARY**

[0008] There is disclosed herein a non-radiative or near-field wireless energy transfer scheme that is capable of transmitting useful amounts of power over mid-range distances and alignment offsets. This inventive technique uses coupled electromagnetic resonators with long-lived oscillatory resonant modes to transfer power from a power supply to a power drain. The technique is general and may be applied to a wide range of resonators, even where the specific examples disclosed herein relate to electromagnetic resonators. If the resonators are designed

such that the energy stored by the electric field is primarily confined within the structure and that the energy stored by the magnetic field is primarily in the region surrounding the resonator. Then, the energy exchange is mediated primarily by the resonant magnetic near-field. These types of resonators may be referred to as magnetic resonators. If the resonators are designed such that the energy stored by the magnetic field is primarily confined within the structure and that the energy stored by the electric field is primarily in the region surrounding the resonator. Then, the energy exchange is mediated primarily by the resonant electric near-field. These types of resonators may be referred to as electric resonators. Either type of resonator may also be referred to as an electromagnetic resonator. Both types of resonators are disclosed herein.

**[0009]** The omni-directional but stationary (non-lossy) nature of the near-fields of the resonators we disclose enables efficient wireless energy transfer over mid-range distances, over a wide range of directions and resonator orientations, suitable for charging, powering, or simultaneously powering and charging a variety of electronic devices. As a result, a system may have a wide variety of possible applications where a first resonator, connected to a power source, is in one location, and a second resonator, potentially connected to electrical/electronic devices, batteries, powering or charging circuits, and the like, is at a second location, and where the distance from the first resonator to the second resonator is on the order of centimeters to meters. For example, a first resonator connected to the wired electricity grid could be placed on the ceiling of a room, while other resonators connected to devices, such as robots, vehicles, computers, communication devices, medical devices, and the like, move about within the room, and where these devices are constantly or intermittently receiving power wirelessly from the source resonator. From this one example, one can imagine many applications where the systems and methods disclosed herein could provide wireless power across mid-range distances, including consumer electronics, industrial applications, infrastructure power and lighting, transportation vehicles, electronic games, military applications, and the like.

**[0010]** Energy exchange between two electromagnetic resonators can be optimized when the resonators are tuned to substantially the same frequency and when the losses in the system are minimal. Wireless energy transfer systems may be designed so that the “coupling-time” between resonators is much shorter than the resonators’ “loss-times”. Therefore, the systems and methods described herein may utilize high quality factor (high-Q) resonators with low intrinsic-loss rates. In addition, the systems and methods described herein may use sub-

wavelength resonators with near-fields that extend significantly longer than the characteristic sizes of the resonators, so that the near-fields of the resonators that exchange energy overlap at mid-range distances. This is a regime of operation that has not been practiced before and that differs significantly from traditional induction designs.

**[0011]** It is important to appreciate the difference between the high-Q magnetic resonator scheme disclosed here and the known close-range or proximity inductive schemes, namely, that those known schemes do not conventionally utilize high-Q resonators. Using coupled-mode theory (CMT), (see, for example, *Waves and Fields in Optoelectronics*, H.A. Haus, Prentice Hall, 1984), one may show that a high-Q resonator-coupling mechanism can enable orders of magnitude more efficient power delivery between resonators spaced by mid-range distances than is enabled by traditional inductive schemes. Coupled high-Q resonators have demonstrated efficient energy transfer over mid-range distances and improved efficiencies and offset tolerances in short range energy transfer applications.

**[0012]** The systems and methods described herein may provide for near-field wireless energy transfer via strongly coupled high-Q resonators, a technique with the potential to transfer power levels from picowatts to kilowatts, safely, and over distances much larger than have been achieved using traditional induction techniques. Efficient energy transfer may be realized for a variety of general systems of strongly coupled resonators, such as systems of strongly coupled acoustic resonators, nuclear resonators, mechanical resonators, and the like, as originally described by researchers at M.I.T. in their publications, "Efficient wireless non-radiative mid-range energy transfer", *Annals of Physics*, vol. 323, Issue 1, p. 34 (2008) and "Wireless Power Transfer via Strongly Coupled Magnetic Resonances", *Science*, vol. 317, no. 5834, p. 83, (2007). Disclosed herein are electromagnetic resonators and systems of coupled electromagnetic resonators, also referred to more specifically as coupled magnetic resonators and coupled electric resonators, with operating frequencies below 10 GHz.

**[0013]** This disclosure describes wireless energy transfer technologies, also referred to as wireless power transmission technologies. Throughout this disclosure, we may use the terms wireless energy transfer, wireless power transfer, wireless power transmission, and the like, interchangeably. We may refer to supplying energy or power from a source, an AC or DC source, a battery, a source resonator, a power supply, a generator, a solar panel, and thermal collector, and the like, to a device, a remote device, to multiple remote devices, to a device

resonator or resonators, and the like. We may describe intermediate resonators that extend the range of the wireless energy transfer system by allowing energy to hop, transfer through, be temporarily stored, be partially dissipated, or for the transfer to be mediated in any way, from a source resonator to any combination of other device and intermediate resonators, so that energy transfer networks, or strings, or extended paths may be realized. Device resonators may receive energy from a source resonator, convert a portion of that energy to electric power for powering or charging a device, and simultaneously pass a portion of the received energy onto other device or mobile device resonators. Energy may be transferred from a source resonator to multiple device resonators, significantly extending the distance over which energy may be wirelessly transferred. The wireless power transmission systems may be implemented using a variety of system architectures and resonator designs. The systems may include a single source or multiple sources transmitting power to a single device or multiple devices. The resonators may be designed to be source or device resonators, or they may be designed to be repeaters. In some cases, a resonator may be a device and source resonator simultaneously, or it may be switched from operating as a source to operating as a device or a repeater. One skilled in the art will understand that a variety of system architectures may be supported by the wide range of resonator designs and functionalities described in this application.

**[0014]** In the wireless energy transfer systems we describe, remote devices may be powered directly, using the wirelessly supplied power or energy, or the devices may be coupled to an energy storage unit such as a battery, a super-capacitor, an ultra-capacitor, or the like (or other kind of power drain), where the energy storage unit may be charged or re-charged wirelessly, and/or where the wireless power transfer mechanism is simply supplementary to the main power source of the device. The devices may be powered by hybrid battery/energy storage devices such as batteries with integrated storage capacitors and the like. Furthermore, novel battery and energy storage devices may be designed to take advantage of the operational improvements enabled by wireless power transmission systems.

**[0015]** Other power management scenarios include using wirelessly supplied power to recharge batteries or charge energy storage units while the devices they power are turned off, in an idle state, in a sleep mode, and the like. Batteries or energy storage units may be charged or recharged at high (fast) or low (slow) rates. Batteries or energy storage units may be trickle charged or float charged. Multiple devices may be charged or powered simultaneously in parallel

or power delivery to multiple devices may be serialized such that one or more devices receive power for a period of time after which other power delivery is switched to other devices. Multiple devices may share power from one or more sources with one or more other devices either simultaneously, or in a time multiplexed manner, or in a frequency multiplexed manner, or in a spatially multiplexed manner, or in an orientation multiplexed manner, or in any combination of time and frequency and spatial and orientation multiplexing. Multiple devices may share power with each other, with at least one device being reconfigured continuously, intermittently, periodically, occasionally, or temporarily, to operate as wireless power sources. It would be understood by one of ordinary skill in the art that there are a variety of ways to power and/or charge devices, and the variety of ways could be applied to the technologies and applications described herein.

**[0016]** Wireless energy transfer has a variety of possible applications including for example, placing a source (e.g. one connected to the wired electricity grid) on the ceiling, under the floor, or in the walls of a room, while devices such as robots, vehicles, computers, PDAs or similar are placed or move freely within the room. Other applications may include powering or recharging electric-engine vehicles, such as buses and/or hybrid cars and medical devices, such as wearable or implantable devices. Additional example applications include the ability to power or recharge autonomous electronics (e.g. laptops, cell-phones, portable music players, household robots, GPS navigation systems, displays, etc), sensors, industrial and manufacturing equipment, medical devices and monitors, home appliances and tools (e.g. lights, fans, drills, saws, heaters, displays, televisions, counter-top appliances, etc.), military devices, heated or illuminated clothing, communications and navigation equipment, including equipment built into vehicles, clothing and protective-wear such as helmets, body armor and vests, and the like, and the ability to transmit power to physically isolated devices such as to implanted medical devices, to hidden, buried, implanted or embedded sensors or tags, to and/or from roof-top solar panels to indoor distribution panels, and the like.

**[0017]** In one aspect, a system disclosed herein includes a source resonator having a  $Q$ -factor  $Q_1$  and a characteristic size  $x_1$ , coupled to a power generator, and a second resonator having a  $Q$ -factor  $Q_2$  and a characteristic size  $x_2$ , coupled to a load located a distance  $D$  from the source resonator, wherein the source resonator and the second resonator are coupled to exchange



energy wirelessly among the source resonator and the second resonator, and wherein  $\sqrt{Q_1 Q_2} > 100$ .

**[0018]**  $Q_1$  may be less than 100.  $Q_2$  may be less than 100. The system may include a third resonator having a Q-factor  $Q_3$  configured to transfer energy non-radiatively with the source and second resonators, wherein  $\sqrt{Q_1 Q_3} > 100$  and  $\sqrt{Q_2 Q_3} > 100$ .  $Q_3$  may be less than 100.

**[0019]** The source resonator may be coupled to the power generator with direct electrical connections. The system may include an impedance matching network wherein the source resonator is coupled and impedance matched to the power generator with direct electrical connections. The system may include a tunable circuit wherein the source resonator is coupled to the power generator through the tunable circuit with direct electrical connections. The tunable circuit may include variable capacitors. The tunable circuit may include variable inductors. At least one of the direct electrical connections may be configured to substantially preserve a resonant mode of the source resonator. The source resonator may have a first terminal, a second terminal, and a center terminal, and an impedance between the first terminal and the center terminal and between the second terminal and the center terminal may be substantially equal. The source resonator may include a capacitive loaded loop having a first terminal, a second terminal, and a center terminal, wherein an impedance between the first terminal and the center terminal and between the second terminal and the center terminal are substantially equal. The source resonator may be coupled to an impedance matching network and the impedance matching network further comprises a first terminal, a second terminal, and a center terminal, wherein an impedance between the first terminal and the center terminal and between the second terminal and the center terminal are substantially equal.

**[0020]** The first terminal and the second terminal may be directly coupled to the power generator and driven with oscillating signals that are near 180 degrees out of phase. The source resonator may have a resonant frequency  $\omega_1$  and the first terminal and the second terminal may be directly coupled to the power generator and driven with oscillating signals that are substantially equal to the resonant frequency  $\omega_1$ . The center terminal may be connected to an electrical ground. The source resonator may have a resonant frequency  $\omega_1$  and the first terminal and the second terminal may be directly coupled to the power generator and driven with a

frequency substantially equal to the resonant frequency  $\omega_1$ . The system may include a plurality of capacitors coupled to the power generator and the load. The source resonator and the second resonator may each be enclosed in a low loss tangent material. The system may include a power conversion circuit wherein the second resonator is coupled to the power conversion circuit to deliver DC power to the load. The system may include a power conversion circuit wherein the second resonator is coupled to the power conversion circuit to deliver AC power to the load. The system may include a power conversion circuit, wherein the second resonator is coupled to the power conversion circuit to deliver both AC and DC power to the load. The system may include a power conversion circuit and a plurality of loads, wherein the second resonator is coupled to the power conversion circuit, and the power conversion circuit is coupled to the plurality of loads. The impedance matching network may include capacitors. The impedance matching network may include inductors.

**[0021]** Throughout this disclosure we may refer to the certain circuit components such as capacitors, inductors, resistors, diodes, switches and the like as circuit components or elements. We may also refer to series and parallel combinations of these components as elements, networks, topologies, circuits, and the like. We may describe combinations of capacitors, diodes, varactors, transistors, and/or switches as adjustable impedance networks, tuning networks, matching networks, adjusting elements, and the like. We may also refer to “self-resonant” objects that have both capacitance, and inductance distributed (or partially distributed, as opposed to solely lumped) throughout the entire object. It would be understood by one of ordinary skill in the art that adjusting and controlling variable components within a circuit or network may adjust the performance of that circuit or network and that those adjustments may be described generally as tuning, adjusting, matching, correcting, and the like. Other methods to tune or adjust the operating point of the wireless power transfer system may be used alone, or in addition to adjusting tunable components such as inductors and capacitors, or banks of inductors and capacitors.

**[0022]** Unless otherwise defined, all technical and scientific terms used herein have the same meaning as commonly understood by one of ordinary skill in the art to which this disclosure belongs. In case of conflict with publications, patent applications, patents, and other references mentioned or incorporated herein by reference, the present specification, including definitions, will control.

[0023] Any of the features described above may be used, alone or in combination, without departing from the scope of this disclosure. Other features, objects, and advantages of the systems and methods disclosed herein will be apparent from the following detailed description and figures.

## BRIEF DESCRIPTION OF FIGURES

[0024] Fig. 1 (a) and (b) depict exemplary wireless power systems containing a source resonator 1 and device resonator 2 separated by a distance D.

[0025] Fig. 2 shows an exemplary resonator labeled according to the labeling convention described in this disclosure. Note that there are no extraneous objects or additional resonators shown in the vicinity of resonator 1.

[0026] Fig. 3 shows an exemplary resonator in the presence of a “loading” object, labeled according to the labeling convention described in this disclosure.

[0027] Fig. 4 shows an exemplary resonator in the presence of a “perturbing” object, labeled according to the labeling convention described in this disclosure.

[0028] Fig. 5 shows a plot of efficiency,  $\eta$ , vs. strong coupling factor,  $U = \kappa / \sqrt{\Gamma_s \Gamma_d} = k \sqrt{Q_s Q_d}$ .

[0029] Fig. 6 (a) shows a circuit diagram of one example of a resonator (b) shows a diagram of one example of a capacitively-loaded inductor loop magnetic resonator, (c) shows a drawing of a self-resonant coil with distributed capacitance and inductance, (d) shows a simplified drawing of the electric and magnetic field lines associated with an exemplary magnetic resonator of the current disclosure, and (e) shows a diagram of one example of an electric resonator.

[0030] Fig. 7 shows a plot of the “quality factor”,  $Q$  (solid line), as a function of frequency, of an exemplary resonator that may be used for wireless power transmission at MHz frequencies. The absorptive Q (dashed line) increases with frequency, while the radiative Q (dotted line) decreases with frequency, thus leading the overall Q to peak at a particular frequency.

[0031] Fig. 8 shows a drawing of a resonator structure with its characteristic size, thickness and width indicated.

[0032] Fig. 9 (a) and (b) show drawings of exemplary inductive loop elements.

[0033] Fig. 10 (a) and (b) show two examples of trace structures formed on printed circuit boards and used to realize the inductive element in magnetic resonator structures.

[0034] Fig. 11 (a) shows a perspective view diagram of a planar magnetic resonator, (b) shows a perspective view diagram of a two planar magnetic resonator with various geometries, and c) shows is a perspective view diagram of a two planar magnetic resonators separated by a distance  $D$ .

[0035] Fig. 12 is a perspective view of an example of a planar magnetic resonator.

[0036] Fig. 13 is a perspective view of a planar magnetic resonator arrangement with a circular resonator coil.

[0037] Fig. 14 is a perspective view of an active area of a planar magnetic resonator.

[0038] Fig. 15 is a perspective view of an application of the wireless power transfer system with a source at the center of a table powering several devices placed around the source.

[0039] Fig. 16(a) shows a 3D finite element model of a copper and magnetic material structure driven by a square loop of current around the choke point at its center. In this example, a structure may be composed of two boxes made of a conducting material such as copper, covered by a layer of magnetic material, and connected by a block of magnetic material. The inside of the two conducting boxes in this example would be shielded from AC electromagnetic fields generated outside the boxes and may house lossy objects that might lower the  $Q$  of the resonator or sensitive components that might be adversely affected by the AC electromagnetic fields. Also shown are the calculated magnetic field streamlines generated by this structure, indicating that the magnetic field lines tend to follow the lower reluctance path in the magnetic material. Fig. 16(b) shows interaction, as indicated by the calculated magnetic field streamlines, between two identical structures as shown in (a). Because of symmetry, and to reduce computational complexity, only one half of the system is modeled (but the computation assumes the symmetrical arrangement of the other half).

[0040] Fig. 17 shows an equivalent circuit representation of a magnetic resonator including a conducting wire wrapped  $N$  times around a structure, possibly containing magnetically permeable material. The inductance is realized using conducting loops wrapped around a structure comprising a magnetic material and the resistors represent loss mechanisms in the system ( $R_{\text{wire}}$  for resistive losses in the loop,  $R_{\mu}$  denoting the equivalent series resistance of the structure surrounded by the loop). Losses may be minimized to realize high- $Q$  resonators.

[0041] Fig. 18 shows a Finite Element Method (FEM) simulation of two high conductivity surfaces above and below a disk composed of lossy dielectric material, in an external magnetic field of frequency 6.78 MHz. Note that the magnetic field was uniform before the disk and conducting materials were introduced to the simulated environment. This simulation is performed in cylindrical coordinates. The image is azimuthally symmetric around the  $r=0$  axis. The lossy dielectric disk has  $\epsilon_r = 1$  and  $\sigma = 10$  S/m.

[0042] Fig. 19 shows a drawing of a magnetic resonator with a lossy object in its vicinity completely covered by a high-conductivity surface.

[0043] Fig. 20 shows a drawing of a magnetic resonator with a lossy object in its vicinity partially covered by a high-conductivity surface.

[0044] Fig. 21 shows a drawing of a magnetic resonator with a lossy object in its vicinity placed on top of a high-conductivity surface.

[0045] Fig. 22 shows a diagram of a completely wireless projector.

[0046] Fig. 23 shows the magnitude of the electric and magnetic fields along a line that contains the diameter of the circular loop inductor and along the axis of the loop inductor.

[0047] Fig. 24 shows a drawing of a magnetic resonator and its enclosure along with a necessary but lossy object placed either (a) in the corner of the enclosure, as far away from the resonator structure as possible or (b) in the center of the surface enclosed by the inductive element in the magnetic resonator.

[0048] Fig. 25 shows a drawing of a magnetic resonator with a high-conductivity surface above it and a lossy object, which may be brought into the vicinity of the resonator, but above the high-conductivity sheet.

[0049] Fig. 26(a) shows an axially symmetric FEM simulation of a thin conducting (copper) cylinder or disk (20 cm in diameter, 2 cm in height) exposed to an initially uniform, externally applied magnetic field (gray flux lines) along the z-axis. The axis of symmetry is at  $r=0$ . The magnetic streamlines shown originate at  $z = -\infty$ , where they are spaced from  $r=3$  cm to  $r=10$  cm in intervals of 1 cm. The axes scales are in meters. Fig. 26 (b) shows the same structure and externally applied field as in (a), except that the conducting cylinder has been modified to include a 0.25 mm layer of magnetic material (not visible) with  $\mu_r = 40$ , on its outside surface. Note that the magnetic streamlines are deflected away from the cylinder significantly less than in (a).

[0050] Fig. 27 shows an axi-symmetric view of a variation based on the system shown in Fig. 26. Only one surface of the lossy material is covered by a layered structure of copper and magnetic materials. The inductor loop is placed on the side of the copper and magnetic material structure opposite to the lossy material as shown.

[0051] Fig. 28 (a) depicts a general topology of a matching circuit including an indirect coupling to a high-Q inductive element.

[0052] Fig. 28 (b) shows a block diagram of a magnetic resonator that includes a conductor loop inductor and a tunable impedance network. Physical electrical connections to this resonator may be made to the terminal connections.

[0053] Fig. 28 (c) depicts a general topology of a matching circuit directly coupled to a high-Q inductive element.

[0054] Fig. 28 (d) depicts a general topology of a symmetric matching circuit directly coupled to a high-Q inductive element and driven anti-symmetrically (balanced drive).

[0055] Fig. 28 (e) depicts a general topology of a matching circuit directly coupled to a high-Q inductive element and connected to ground at a point of symmetry of the main resonator (unbalanced drive).

[0056] Figs. 29(a) and 29(b) depict two topologies of matching circuits transformer-coupled (i.e. indirectly or inductively) to a high-Q inductive element. The highlighted portion of the Smith chart in (c) depicts the complex impedances (arising from  $L$  and  $R$  of the inductive element) that may be matched to an arbitrary real impedance  $Z_0$  by the topology of Fig. 31(b) in the case  $\omega L_2 = 1/\omega C_2$ .

[0057] Figs. 30(a),(b),(c),(d),(e),(f) depict six topologies of matching circuits directly coupled to a high-Q inductive element and including capacitors in series with  $Z_0$ . The topologies shown in Figs. 30(a),(b),(c) are driven with a common-mode signal at the input terminals, while the topologies shown in Figs 30(d),(e),(f) are symmetric and receive a balanced drive. The highlighted portion of the Smith chart in 30(g) depicts the complex impedances that may be matched by these topologies. Figs. 30(h),(i),(j),(k),(l),(m) depict six topologies of matching circuits directly coupled to a high-Q inductive element and including inductors in series with  $Z_0$ .

[0058] Figs. 31(a),(b),(c) depict three topologies of matching circuits directly coupled to a high-Q inductive element and including capacitors in series with  $Z_0$ . They are connected to ground at the center point of a capacitor and receive an unbalanced drive. The highlighted

portion of the Smith chart in Fig. 31(d) depicts the complex impedances that may be matched by these topologies. Figs. 31(e),(f),(g) depict three topologies of matching circuits directly coupled to a high-Q inductive element and including inductors in series with  $Z_o$ .

**[0059]** Figs. 32(a),(b),(c) depict three topologies of matching circuits directly coupled to a high-Q inductive element and including capacitors in series with  $Z_o$ . They are connected to ground by tapping at the center point of the inductor loop and receive an unbalanced drive. The highlighted portion of the Smith chart in (d) depicts the complex impedances that may be matched by these topologies, (e),(f),(g) depict three topologies of matching circuits directly coupled to a high-Q inductive element and including inductors in series with  $Z_o$ .

**[0060]** Figs. 33(a),(b),(c),(d),(e),(f) depict six topologies of matching circuits directly coupled to a high-Q inductive element and including capacitors in parallel with  $Z_o$ . The topologies shown in Figs. 33(a),(b),(c) are driven with a common-mode signal at the input terminals, while the topologies shown in Figs 33(d),(e),(f) are symmetric and receive a balanced drive. The highlighted portion of the Smith chart in Fig. 33(g) depicts the complex impedances that may be matched by these topologies. Figs. 33(h),(i),(j),(k),(l),(m) depict six topologies of matching circuits directly coupled to a high-Q inductive element and including inductors in parallel with  $Z_o$ .

**[0061]** Figs. 34(a),(b),(c) depict three topologies of matching circuits directly coupled to a high-Q inductive element and including capacitors in parallel with  $Z_o$ . They are connected to ground at the center point of a capacitor and receive an unbalanced drive. The highlighted portion of the Smith chart in (d) depicts the complex impedances that may be matched by these topologies. Figs. 34(e),(f),(g) depict three topologies of matching circuits directly coupled to a high-Q inductive element and including inductors in parallel with  $Z_o$ .

**[0062]** Figs. 35(a),(b),(c) depict three topologies of matching circuits directly coupled to a high-Q inductive element and including capacitors in parallel with  $Z_o$ . They are connected to ground by tapping at the center point of the inductor loop and receive an unbalanced drive. The highlighted portion of the Smith chart in Figs. 35(d),(e), and (f) depict the complex impedances that may be matched by these topologies.

**[0063]** Figs. 36(a),(b),(c),(d) depict four topologies of networks of fixed and variable capacitors designed to produce an overall variable capacitance with finer tuning resolution and some with reduced voltage on the variable capacitor.

**[0064]** Figs. 37(a) and 37(b) depict two topologies of networks of fixed capacitors and a variable inductor designed to produce an overall variable capacitance.

**[0065]** Fig. 38 depicts a high level block diagram of a wireless power transmission system.

**[0066]** Fig. 39 depicts a block diagram of an exemplary wirelessly powered device.

**[0067]** Fig. 40 depicts a block diagram of the source of an exemplary wireless power transfer system.

**[0068]** Fig. 41 shows an equivalent circuit diagram of a magnetic resonator. The slash through the capacitor symbol indicates that the represented capacitor may be fixed or variable. The port parameter measurement circuitry may be configured to measure certain electrical signals and may measure the magnitude and phase of signals.

**[0069]** Fig. 42 shows a circuit diagram of a magnetic resonator where the tunable impedance network is realized with voltage controlled capacitors. Such an implementation may be adjusted, tuned or controlled by electrical circuits including programmable or controllable voltage sources and/or computer processors. The voltage controlled capacitors may be adjusted in response to data measured by the port parameter measurement circuitry and processed by measurement analysis and control algorithms and hardware. The voltage controlled capacitors may be a switched bank of capacitors.

**[0070]** Fig. 43 shows an end-to-end wireless power transmission system. In this example, both the source and the device contain port measurement circuitry and a processor. The box labeled "coupler/switch" indicates that the port measurement circuitry may be connected to the resonator by a directional coupler or a switch, enabling the measurement, adjustment and control of the source and device resonators to take place in conjunction with, or separate from, the power transfer functionality.

**[0071]** Fig. 44 shows an end-to-end wireless power transmission system. In this example, only the source contains port measurement circuitry and a processor. In this case, the device resonator operating characteristics may be fixed or may be adjusted by analog control circuitry and without the need for control signals generated by a processor.

**[0072]** Fig. 45 shows an end-to-end wireless power transmission system. In this example, both the source and the device contain port measurement circuitry but only the source contains a processor. Data from the device is transmitted through a wireless communication



channel, which could be implemented either with a separate antenna, or through some modulation of the source drive signal.

[0073] Fig. 46 shows an end-to-end wireless power transmission system. In this example, only the source contains port measurement circuitry and a processor. Data from the device is transmitted through a wireless communication channel, which could be implemented either with a separate antenna, or through some modulation of the source drive signal.

[0074] Fig. 47 shows coupled magnetic resonators whose frequency and impedance may be automatically adjusted using algorithms implemented using a processor or a computer.

[0075] Fig. 48 shows a varactor array.

[0076] Fig. 49 shows a device (laptop computer) being wirelessly powered or charged by a source, where both the source and device resonator are physically separated from, but electrically connected to, the source and device.

[0077] Fig. 50 (a) is an illustration of a wirelessly powered or charged laptop application where the device resonator is inside the laptop case and is not visible.

[0078] Fig. 50 (b) is an illustration of a wirelessly powered or charged laptop application where the resonator is underneath the laptop base and is electrically connected to the laptop power input by an electrical cable.

[0079] Fig. 50 (c) is an illustration of a wirelessly powered or charged laptop application where the resonator is attached to the laptop base.

[0080] Fig. 50 (d) is an illustration of a wirelessly powered or charged laptop application where the resonator is attached to the laptop display.

[0081] Fig. 51 is a diagram of rooftop PV panels with wireless power transfer.

## **DETAILED DESCRIPTION**

[0082] As described above, this disclosure relates to coupled electromagnetic resonators with long-lived oscillatory resonant modes that may wirelessly transfer power from a power supply to a power drain. However, the technique is not restricted to electromagnetic resonators, but is general and may be applied to a wide variety of resonators and resonant objects. Therefore, we first describe the general technique, and then disclose electromagnetic examples for wireless energy transfer.

### **[0083] Resonators**

**[0084]** A resonator may be defined as a system that can store energy in at least two different forms, and where the stored energy is oscillating between the two forms. The resonance has a specific oscillation mode with a resonant (modal) frequency,  $f$ , and a resonant (modal) field. The angular resonant frequency,  $\omega$ , may be defined as  $\omega = 2\pi f$ , the resonant wavelength,  $\lambda$ , may be defined as  $\lambda = c/f$ , where  $c$  is the speed of light, and the resonant period,  $T$ , may be defined as  $T = 1/f = 2\pi/\omega$ . In the absence of loss mechanisms, coupling mechanisms or external energy supplying or draining mechanisms, the total resonator stored energy,  $W$ , would stay fixed and the two forms of energy would oscillate, wherein one would be maximum when the other is minimum and vice versa.

**[0085]** In the absence of extraneous materials or objects, the energy in the resonator 102 shown in Fig. 1 may decay or be lost by intrinsic losses. The resonator fields then obey the following linear equation:

$$\frac{da(t)}{dt} = -i(\omega - i\Gamma)a(t),$$

where the variable  $a(t)$  is the resonant field amplitude, defined so that the energy contained within the resonator is given by  $|a(t)|^2$ .  $\Gamma$  is the intrinsic energy decay or loss rate (e.g. due to absorption and radiation losses).

**[0086]** The Quality Factor, or  $Q$ -factor, or  $Q$ , of the resonator, which characterizes the energy decay, is inversely proportional to these energy losses. It may be defined as  $Q = \omega * W/P$ , where  $P$  is the time-averaged power lost at steady state. That is, a resonator 102 with a high- $Q$  has relatively low intrinsic losses and can store energy for a relatively long time. Since the resonator loses energy at its intrinsic decay rate,  $2\Gamma$ , its  $Q$ , also referred to as its intrinsic  $Q$ , is given by  $Q = \omega/2\Gamma$ . The quality factor also represents the number of oscillation periods,  $T$ , it takes for the energy in the resonator to decay by a factor of  $e$ .

**[0087]** As described above, we define the quality factor or  $Q$  of the resonator as that due only to intrinsic loss mechanisms. A subscript index such as  $Q_i$ , indicates the resonator (resonator 1 in this case) to which the  $Q$  refers. Fig. 2 shows an electromagnetic resonator 102 labeled according to this convention. Note that in this figure, there are no extraneous objects or additional resonators in the vicinity of resonator 1.

**[0088]** Extraneous objects and/or additional resonators in the vicinity of a first resonator may perturb or load the first resonator, thereby perturbing or loading the  $Q$  of the first resonator, depending on a variety of factors such as the distance between the resonator and object or other resonator, the material composition of the object or other resonator, the structure of the first resonator, the power in the first resonator, and the like. Unintended external energy losses or coupling mechanisms to extraneous materials and objects in the vicinity of the resonators may be referred to as “perturbing” the  $Q$  of a resonator, and may be indicated by a subscript within rounded parentheses, (). Intended external energy losses, associated with energy transfer via coupling to other resonators and to generators and loads in the wireless energy transfer system may be referred to as “loading” the  $Q$  of the resonator, and may be indicated by a subscript within square brackets, [].

**[0089]** The  $Q$  of a resonator 102 connected or coupled to a power generator,  $g$ , or load 302,  $l$ , may be called the “loaded quality factor” or the “loaded  $Q$ ” and may be denoted by  $Q_{[g]}$  or  $Q_{[l]}$ , as illustrated in Fig. 3. In general, there may be more than one generator or load 302 connected to a resonator 102. However, we do not list those generators or loads separately but rather use “ $g$ ” and “ $l$ ” to refer to the equivalent circuit loading imposed by the combinations of generators and loads. In general descriptions, we may use the subscript “ $l$ ” to refer to either generators or loads connected to the resonators.

**[0090]** In some of the discussion herein, we define the “loading quality factor” or the “loading  $Q$ ” due to a power generator or load connected to the resonator, as  $\delta Q_{[l]}$ , where,  $1/\delta Q_{[l]} \equiv 1/Q_{[l]} - 1/Q$ . Note that the larger the loading  $Q$ ,  $\delta Q_{[l]}$ , of a generator or load, the less the loaded  $Q$ ,  $Q_{[l]}$ , deviates from the unloaded  $Q$  of the resonator.

**[0091]** The  $Q$  of a resonator in the presence of an extraneous object 402,  $p$ , that is not intended to be part of the energy transfer system may be called the “perturbed quality factor” or the “perturbed  $Q$ ” and may be denoted by  $Q_{(p)}$ , as illustrated in Fig. 4. In general, there may be many extraneous objects, denoted as  $p1$ ,  $p2$ , etc., or a set of extraneous objects  $\{p\}$ , that perturb the  $Q$  of the resonator 102. In this case, the perturbed  $Q$  may be denoted  $Q_{(p1+p2+\dots)}$  or  $Q_{(\{p\})}$ . For example,  $Q_{1(\text{brick+wood})}$  may denote the perturbed quality factor of a first resonator in a system for wireless power exchange in the presence of a brick and a piece of wood, and  $Q_{2(\{\text{office}\})}$  may

denote the perturbed quality factor of a second resonator in a system for wireless power exchange in an office environment.

**[0092]** In some of the discussion herein, we define the “perturbing quality factor” or the “perturbing  $Q$ ” due to an extraneous object,  $p$ , as  $\delta Q_{(p)}$ , where  $1/\delta Q_{(p)} \equiv 1/Q_{(p)} - 1/Q$ . As stated before, the perturbing quality factor may be due to multiple extraneous objects,  $p1, p2$ , etc. or a set of extraneous objects,  $\{p\}$ . The larger the perturbing  $Q$ ,  $\delta Q_{(p)}$ , of an object, the less the perturbed  $Q$ ,  $Q_{(p)}$ , deviates from the unperturbed  $Q$  of the resonator.

**[0093]** In some of the discussion herein, we also define  $\Theta_{(p)} \equiv Q_{(p)} / Q$  and call it the “quality factor insensitivity” or the “Q-insensitivity” of the resonator in the presence of an extraneous object. A subscript index, such as  $\Theta_{1(p)}$ , indicates the resonator to which the perturbed and unperturbed quality factors are referring, namely,  $\Theta_{1(p)} \equiv Q_{1(p)} / Q_1$ .

**[0094]** Note that the quality factor,  $Q$ , may also be characterized as “unperturbed”, when necessary to distinguish it from the perturbed quality factor,  $Q_{(p)}$ , and “unloaded”, when necessary to distinguish it from the loaded quality factor,  $Q_{[l]}$ . Similarly, the perturbed quality factor,  $Q_{(p)}$ , may also be characterized as “unloaded”, when necessary to distinguish them from the loaded perturbed quality factor,  $Q_{(p)[l]}$ .

**[0095] Coupled Resonators**

**[0096]** Resonators having substantially the same resonant frequency, coupled through any portion of their near-fields may interact and exchange energy. There are a variety of physical pictures and models that may be employed to understand, design, optimize and characterize this energy exchange. One way to describe and model the energy exchange between two coupled resonators is using coupled mode theory (CMT).

**[0097]** In coupled mode theory, the resonator fields obey the following set of linear equations:

$$\frac{da_m(t)}{dt} = -i(\omega_m - i\Gamma_m)a_m(t) + i \sum_{n \neq m} \kappa_{mn} a_n(t)$$

where the indices denote different resonators and  $\kappa_{mn}$  are the coupling coefficients between the resonators. For a reciprocal system, the coupling coefficients may obey the relation  $\kappa_{mn} = \kappa_{nm}$ . Note that, for the purposes of the present specification, far-field radiation interference effects

will be ignored and thus the coupling coefficients will be considered real. Furthermore, since in all subsequent calculations of system performance in this specification the coupling coefficients appear only with their square,  $\kappa_{mn}^2$ , we use  $\kappa_{mn}$  to denote the absolute value of the real coupling coefficients.

**[0098]** Note that the coupling coefficient,  $\kappa_{mn}$ , from the CMT described above is related to the so-called coupling factor,  $k_{mn}$ , between resonators  $m$  and  $n$  by  $k_{mn} = 2\kappa_{mn} / \sqrt{\omega_m \omega_n}$ . We define a “strong-coupling factor”,  $U_{mn}$ , as the ratio of the coupling and loss rates between resonators  $m$  and  $n$ , by  $U_{mn} = \kappa_{mn} / \sqrt{\Gamma_m \Gamma_n} = k_{mn} \sqrt{Q_m Q_n}$ .

**[0099]** The quality factor of a resonator  $m$ , in the presence of a similar frequency resonator  $n$  or additional resonators, may be loaded by that resonator  $n$  or additional resonators, in a fashion similar to the resonator being loaded by a connected power generating or consuming device. The fact that resonator  $m$  may be loaded by resonator  $n$  and vice versa is simply a different way to see that the resonators are coupled.

**[00100]** The loaded  $Q$ 's of the resonators in these cases may be denoted as  $Q_{m[n]}$  and  $Q_{n[m]}$ . For multiple resonators or loading supplies or devices, the total loading of a resonator may be determined by modeling each load as a resistive loss, and adding the multiple loads in the appropriate parallel and/or series combination to determine the equivalent load of the ensemble.

**[00101]** In some of the discussion herein, we define the “loading quality factor” or the “loading  $Q_m$ ” of resonator  $m$  due to resonator  $n$  as  $\delta Q_{m[n]}$ , where  $1/\delta Q_{m[n]} \equiv 1/Q_{m[n]} - 1/Q_m$ . Note that resonator  $n$  is also loaded by resonator  $m$  and its “loading  $Q_n$ ” is given by  $1/\delta Q_{n[m]} \equiv 1/Q_{n[m]} - 1/Q_n$ .

**[00102]** When one or more of the resonators are connected to power generators or loads, the set of linear equations is modified to:

$$\frac{da_m(t)}{dt} = -i(\omega_m - i\Gamma_m)a_m(t) + i \sum_{n \neq m} \kappa_{mn} a_n(t) - \kappa_m a_m(t) + \sqrt{2\kappa_m} s_{+m}(t)$$

$$s_{-m}(t) = \sqrt{2\kappa_m} a_m(t) - s_{+m}(t) ,$$

where  $s_{+m}(t)$  and  $s_{-m}(t)$  are respectively the amplitudes of the fields coming from a generator into the resonator  $m$  and going out of the resonator  $m$  either back towards the generator or into a load, defined so that the power they carry is given by  $|s_{+m}(t)|^2$  and  $|s_{-m}(t)|^2$ . The loading coefficients

$\kappa_m$  relate to the rate at which energy is exchanged between the resonator  $m$  and the generator or load connected to it.

**[00103]** Note that the loading coefficient,  $\kappa_m$ , from the CMT described above is related to the loading quality factor,  $\delta Q_{m[l]}$ , defined earlier, by  $\delta Q_{m[l]} = \omega_m / 2\kappa_m$ .

**[00104]** We define a “strong-loading factor”,  $U_{m[l]}$ , as the ratio of the loading and loss rates of resonator  $m$ ,  $U_{m[l]} = \kappa_m / \Gamma_m = Q_m / \delta Q_{m[l]}$ .

**[00105]** Fig. 1(a) shows an example of two coupled resonators 1000, a first resonator 102S, configured as a source resonator and a second resonator 102D, configured as a device resonator. Energy may be transferred over a distance  $D$  between the resonators. The source resonator 102S may be driven by a power supply or generator (not shown). Work may be extracted from the device resonator 102D by a power consuming drain or load (e.g. a load resistor, not shown). Let us use the subscripts “s” for the source, “d” for the device, “g” for the generator, and “l” for the load, and, since in this example there are only two resonators and  $\kappa_{sd} = \kappa_{ds}$ , let us drop the indices on  $\kappa_{sd}$ ,  $k_{sd}$ , and  $U_{sd}$ , and denote them as  $\kappa$ ,  $k$ , and  $U$ , respectively.

**[00106]** The power generator may be constantly driving the source resonator at a constant driving frequency,  $f$ , corresponding to an angular driving frequency,  $\omega$ , where  $\omega = 2\pi f$ .

**[00107]** In this case, the efficiency,  $\eta = |s_{-d}|^2 / |s_{+s}|^2$ , of the power transmission from the generator to the load (via the source and device resonators) is maximized under the following conditions: The source resonant frequency, the device resonant frequency and the generator driving frequency have to be matched, namely

$$\omega_s = \omega_d = \omega.$$

Furthermore, the loading  $Q$  of the source resonator due to the generator,  $\delta Q_{s[g]}$ , has to be matched (equal) to the loaded  $Q$  of the source resonator due to the device resonator and the load,  $Q_{s[dl]}$ , and inversely the loading  $Q$  of the device resonator due to the load,  $\delta Q_{d[l]}$ , has to be matched (equal) to the loaded  $Q$  of the device resonator due to the source resonator and the generator,  $Q_{d[sg]}$ , namely

$$\delta Q_{s[g]} = Q_{s[dl]} \quad \text{and} \quad \delta Q_{d[l]} = Q_{d[sg]}.$$

These equations determine the optimal loading rates of the source resonator by the generator and of the device resonator by the load as

$$U_{d[l]} = \kappa_d / \Gamma_d = Q_d / \delta Q_{d[l]} = \sqrt{1+U^2} = \sqrt{1 + \left( \kappa / \sqrt{\Gamma_s \Gamma_d} \right)^2} = Q_s / \delta Q_{s[g]} = \kappa_s / \Gamma_s = U_{s[g]}.$$

Note that the above frequency matching and  $Q$  matching conditions are together known as “impedance matching” in electrical engineering.

**[00108]** Under the above conditions, the maximized efficiency is a monotonically increasing function of only the strong-coupling factor,  $U = \kappa / \sqrt{\Gamma_s \Gamma_d} = k \sqrt{Q_s Q_d}$ , between the source and device resonators and is given by,  $\eta = U^2 / \left( 1 + \sqrt{1+U^2} \right)^2$ , as shown in Fig. 5. Note that the coupling efficiency,  $\eta$ , is greater than 1% when  $U$  is greater than 0.2, is greater than 10% when  $U$  is greater than 0.7, is greater than 17% when  $U$  is greater than 1, is greater than 52% when  $U$  is greater than 3, is greater than 80% when  $U$  is greater than 9, is greater than 90% when  $U$  is greater than 19, and is greater than 95% when  $U$  is greater than 45. In some applications, the regime of operation where  $U > 1$  may be referred to as the “strong-coupling” regime.

**[00109]** Since a large  $U = \kappa / \sqrt{\Gamma_s \Gamma_d} = \left( 2\kappa / \sqrt{\omega_s \omega_d} \right) \sqrt{Q_s Q_d}$  is desired in certain circumstances, resonators may be used that are high- $Q$ . The  $Q$  of each resonator may be high. The geometric mean of the resonator  $Q$ 's,  $\sqrt{Q_s Q_d}$  may also or instead be high.

**[00110]** The coupling factor,  $k$ , is a number between  $0 \leq k \leq 1$ , and it may be independent (or nearly independent) of the resonant frequencies of the source and device resonators, rather it may be determined mostly by their relative geometry and the physical decay-law of the field mediating their coupling. In contrast, the coupling coefficient,  $\kappa = k \sqrt{\omega_s \omega_d} / 2$ , may be a strong function of the resonant frequencies. The resonant frequencies of the resonators may be chosen preferably to achieve a high  $Q$  rather than to achieve a low  $\Gamma$ , as these two goals may be achievable at two separate resonant frequency regimes.

**[00111]** A high- $Q$  resonator may be defined as one with  $Q > 100$ . Two coupled resonators may be referred to as a system of high- $Q$  resonators when each resonator has a  $Q$  greater than 100,  $Q_s > 100$  and  $Q_d > 100$ . In other implementations, two coupled resonators may be referred to as a system of high- $Q$  resonators when the geometric mean of the resonator  $Q$ 's is greater than 100,  $\sqrt{Q_s Q_d} > 100$ .

[00112] The resonators may be named or numbered. They may be referred to as source resonators, device resonators, first resonators, second resonators, repeater resonators, and the like. It is to be understood that while two resonators are shown in Fig. 1, and in many of the examples below, other implementations may include three (3) or more resonators. For example, a single source resonator 102S may transfer energy to multiple device resonators 102D or multiple devices. Energy may be transferred from a first device to a second, and then from the second device to the third, and so forth. Multiple sources may transfer energy to a single device or to multiple devices connected to a single device resonator or to multiple devices connected to multiple device resonators. Resonators 102 may serve alternately or simultaneously as sources, devices, or they may be used to relay power from a source in one location to a device in another location. Intermediate electromagnetic resonators 102 may be used to extend the distance range of wireless energy transfer systems. Multiple resonators 102 may be daisy chained together, exchanging energy over extended distances and with a wide range of sources and devices. High power levels may be split between multiple sources 102S, transferred to multiple devices and recombined at a distant location.

[00113] The analysis of a single source and a single device resonator may be extended to multiple source resonators and/or multiple device resonators and/or multiple intermediate resonators. In such an analysis, the conclusion may be that large strong-coupling factors,  $U_{mn}$ , between at least some or all of the multiple resonators is preferred for a high system efficiency in the wireless energy transfer. Again, implementations may use source, device and intermediate resonators that have a high  $Q$ . The  $Q$  of each resonator may be high. The geometric mean  $\sqrt{Q_m Q_n}$  of the  $Q$ 's for pairs of resonators  $m$  and  $n$ , for which a large  $U_{mn}$  is desired, may also or instead be high.

[00114] Note that since the strong-coupling factor of two resonators may be determined by the relative magnitudes of the loss mechanisms of each resonator and the coupling mechanism between the two resonators, the strength of any or all of these mechanisms may be perturbed in the presence of extraneous objects in the vicinity of the resonators as described above.

[00115] Continuing the conventions for labeling from the previous sections, we describe  $k$  as the coupling factor in the absence of extraneous objects or materials. We denote the



coupling factor in the presence of an extraneous object,  $p$ , as  $k_{(p)}$ , and call it the “perturbed coupling factor” or the “perturbed  $k$ ”. Note that the coupling factor,  $k$ , may also be characterized as “unperturbed”, when necessary to distinguish from the perturbed coupling factor  $k_{(p)}$ .

**[00116]** We define  $\delta k_{(p)} \equiv k_{(p)} - k$  and we call it the “perturbation on the coupling factor” or the “perturbation on  $k$ ” due to an extraneous object,  $p$ .

**[00117]** We also define  $\beta_{(p)} \equiv k_{(p)}/k$  and we call it the “coupling factor insensitivity” or the “ $k$ -insensitivity”. Lower indices, such as  $\beta_{12(p)}$ , indicate the resonators to which the perturbed and unperturbed coupling factor is referred to, namely  $\beta_{12(p)} \equiv k_{12(p)}/k_{12}$ .

**[00118]** Similarly, we describe  $U$  as the strong-coupling factor in the absence of extraneous objects. We denote the strong-coupling factor in the presence of an extraneous object,  $p$ , as  $U_{(p)}$ ,  $U_{(p)} = k_{(p)} \sqrt{Q_{1(p)} Q_{2(p)}}$ , and call it the “perturbed strong-coupling factor” or the “perturbed  $U$ ”. Note that the strong-coupling factor  $U$  may also be characterized as “unperturbed”, when necessary to distinguish from the perturbed strong-coupling factor  $U_{(p)}$ . Note that the strong-coupling factor  $U$  may also be characterized as “unperturbed”, when necessary to distinguish from the perturbed strong-coupling factor  $U_{(p)}$ .

**[00119]** We define  $\delta U_{(p)} \equiv U_{(p)} - U$  and call it the “perturbation on the strong-coupling factor” or the “perturbation on  $U$ ” due to an extraneous object,  $p$ .

**[00120]** We also define  $\Xi_{(p)} \equiv U_{(p)}/U$  and call it the “strong-coupling factor insensitivity” or the “ $U$ -insensitivity”. Lower indices, such as  $\Xi_{12(p)}$ , indicate the resonators to which the perturbed and unperturbed coupling factor refers, namely  $\Xi_{12(p)} \equiv U_{12(p)}/U_{12}$ .

**[00121]** The efficiency of the energy exchange in a perturbed system may be given by the same formula giving the efficiency of the unperturbed system, where all parameters such as strong-coupling factors, coupling factors, and quality factors are replaced by their perturbed equivalents. For example, in a system of wireless energy transfer including one source and one device resonator, the optimal efficiency may be calculated as

$$\eta_{(p)} = \left[ \frac{U_{(p)}}{1 + \sqrt{1 + U_{(p)}^2}} \right]^2.$$

Therefore, in a system of wireless energy exchange which is perturbed by extraneous objects, large perturbed strong-coupling factors,  $U_{m(p)}$ , between at least some or all of the multiple resonators may be desired for a high system efficiency in the wireless energy transfer. Source, device and/or intermediate resonators may have a high  $Q_{(p)}$ .

[00122] Some extraneous perturbations may sometimes be detrimental for the perturbed strong-coupling factors (via large perturbations on the coupling factors or the quality factors). Therefore, techniques may be used to reduce the effect of extraneous perturbations on the system and preserve large strong-coupling factor insensitivities.

[00123] **Efficiency of Energy Exchange**

[00124] The so-called “useful” energy in a useful energy exchange is the energy or power that must be delivered to a device (or devices) in order to power or charge the device. The transfer efficiency that corresponds to a useful energy exchange may be system or application dependent. For example, high power vehicle charging applications that transfer kilowatts of power may need to be at least 80% efficient in order to supply useful amounts of power resulting in a useful energy exchange sufficient to recharge a vehicle battery, without significantly heating up various components of the transfer system. In some consumer electronics applications, a useful energy exchange may include any energy transfer efficiencies greater than 10%, or any other amount acceptable to keep rechargeable batteries “topped off” and running for long periods of time. For some wireless sensor applications, transfer efficiencies that are much less than 1% may be adequate for powering multiple low power sensors from a single source located a significant distance from the sensors. For still other applications, where wired power transfer is either impossible or impractical, a wide range of transfer efficiencies may be acceptable for a useful energy exchange and may be said to supply useful power to devices in those applications. In general, an operating distance is any distance over which a useful energy exchange is or can be maintained according to the principles disclosed herein.

[00125] A useful energy exchange for a wireless energy transfer in a powering or recharging application may be efficient, highly efficient, or efficient enough, as long as the wasted energy levels, heat dissipation, and associated field strengths are within tolerable limits. The tolerable limits may depend on the application, the environment and the system location. Wireless energy transfer for powering or recharging applications may be efficient, highly efficient, or efficient enough, as long as the desired system performance may be attained for the reasonable cost restrictions, weight restrictions, size restrictions, and the like. Efficient energy transfer may be determined relative to that which could be achieved using traditional inductive techniques that are not high-Q systems. Then, the energy transfer may be defined as being efficient, highly efficient, or efficient enough, if more energy is delivered than could be delivered

by similarly sized coil structures in traditional inductive schemes over similar distances or alignment offsets.

**[00126]** Note that, even though certain frequency and  $Q$  matching conditions may optimize the system efficiency of energy transfer, these conditions may not need to be exactly met in order to have efficient enough energy transfer for a useful energy exchange. Efficient energy exchange may be realized so long as the relative offset of the resonant frequencies ( $|\omega_m - \omega_n| / \sqrt{\omega_m \omega_n}$ ) is less than approximately the maximum among  $1/Q_{m(p)}$ ,  $1/Q_{n(p)}$  and  $k_{mn(p)}$ . The  $Q$  matching condition may be less critical than the frequency matching condition for efficient energy exchange. The degree by which the strong-loading factors,  $U_{m[i]}$ , of the resonators due to generators and/or loads may be away from their optimal values and still have efficient enough energy exchange depends on the particular system, whether all or some of the generators and/or loads are  $Q$ -mismatched and so on.

**[00127]** Therefore, the resonant frequencies of the resonators may not be exactly matched, but may be matched within the above tolerances. The strong-loading factors of at least some of the resonators due to generators and/or loads may not be exactly matched to their optimal value. The voltage levels, current levels, impedance values, material parameters, and the like may not be at the exact values described in the disclosure but will be within some acceptable tolerance of those values. The system optimization may include cost, size, weight, complexity, and the like, considerations, in addition to efficiency,  $Q$ , frequency, strong coupling factor, and the like, considerations. Some system performance parameters, specifications, and designs may be far from optimal in order to optimize other system performance parameters, specifications and designs.

**[00128]** In some applications, at least some of the system parameters may be varying in time, for example because components, such as sources or devices, may be mobile or aging or because the loads may be variable or because the perturbations or the environmental conditions are changing etc. In these cases, in order to achieve acceptable matching conditions, at least some of the system parameters may need to be dynamically adjustable or tunable. All the system parameters may be dynamically adjustable or tunable to achieve approximately the optimal operating conditions. However, based on the discussion above, efficient enough energy exchange may be realized even if some system parameters are not variable. In some examples, at least

some of the devices may not be dynamically adjusted. In some examples, at least some of the sources may not be dynamically adjusted. In some examples, at least some of the intermediate resonators may not be dynamically adjusted. In some examples, none of the system parameters may be dynamically adjusted.

**[00129] Electromagnetic Resonators**

**[00130]** The resonators used to exchange energy may be electromagnetic resonators. In such resonators, the intrinsic energy decay rates,  $\Gamma_m$ , are given by the absorption (or resistive) losses and the radiation losses of the resonator.

**[00131]** The resonator may be constructed such that the energy stored by the electric field is primarily confined within the structure and that the energy stored by the magnetic field is primarily in the region surrounding the resonator. Then, the energy exchange is mediated primarily by the resonant magnetic near-field. These types of resonators may be referred to as magnetic resonators.

**[00132]** The resonator may be constructed such that the energy stored by the magnetic field is primarily confined within the structure and that the energy stored by the electric field is primarily in the region surrounding the resonator. Then, the energy exchange is mediated primarily by the resonant electric near-field. These types of resonators may be referred to as electric resonators.

**[00133]** Note that the total electric and magnetic energies stored by the resonator have to be equal, but their localizations may be quite different. In some cases, the ratio of the average electric field energy to the average magnetic field energy specified at a distance from a resonator may be used to characterize or describe the resonator.

**[00134]** Electromagnetic resonators may include an inductive element, a distributed inductance, or a combination of inductances with inductance,  $L$ , and a capacitive element, a distributed capacitance, or a combination of capacitances, with capacitance,  $C$ . A minimal circuit model of an electromagnetic resonator 102 is shown in Fig. 6a. The resonator may include an inductive element 108 and a capacitive element 104. Provided with initial energy, such as electric field energy stored in the capacitor 104, the system will oscillate as the capacitor discharges transferring energy into magnetic field energy stored in the inductor 108 which in turn transfers energy back into electric field energy stored in the capacitor 104.

[00135] The resonators 102 shown in Figs. 6(b)(c)(d) may be referred to as magnetic resonators. Magnetic resonators may be preferred for wireless energy transfer applications in populated environments because most everyday materials including animals, plants, and humans are non-magnetic (i.e.,  $\mu_r \approx 1$ ), so their interaction with magnetic fields is minimal and due primarily to eddy currents induced by the time-variation of the magnetic fields, which is a second-order effect. This characteristic is important both for safety reasons and because it reduces the potential for interactions with extraneous environmental objects and materials that could alter system performance.

[00136] Fig. 6d shows a simplified drawing of some of the electric and magnetic field lines associated with an exemplary magnetic resonator 102B. The magnetic resonator 102B may include a loop of conductor acting as an inductive element 108 and a capacitive element 104 at the ends of the conductor loop. Note that this drawing depicts most of the energy in the region surrounding the resonator being stored in the magnetic field, and most of the energy in the resonator (between the capacitor plates) stored in the electric field. Some electric field, owing to fringing fields, free charges, and the time varying magnetic field, may be stored in the region around the resonator, but the magnetic resonator may be designed to confine the electric fields to be close to or within the resonator itself, as much as possible.

[00137] The inductor 108 and capacitor 104 of an electromagnetic resonator 102 may be bulk circuit elements, or the inductance and capacitance may be distributed and may result from the way the conductors are formed, shaped, or positioned, in the structure. For example, the inductor 108 may be realized by shaping a conductor to enclose a surface area, as shown in Figs. 6(b)(c)(d). This type of resonator 102 may be referred to as a capacitively-loaded loop inductor. Note that we may use the terms “loop” or “coil” to indicate generally a conducting structure (wire, tube, strip, etc.), enclosing a surface of any shape and dimension, with any number of turns. In Fig. 6b, the enclosed surface area is circular, but the surface may be any of a wide variety of other shapes and sizes and may be designed to achieve certain system performance specifications. As an example to indicate how inductance scales with physical dimensions, the inductance for a length of circular conductor arranged to form a circular single-turn loop is approximately,

$$L = \mu_0 x \left( \ln \frac{8x}{a} - 2 \right),$$

where  $\mu_0$  is the magnetic permeability of free space,  $x$ , is the radius of the enclosed circular surface area and,  $a$ , is the radius of the conductor used to form the inductor loop. A more precise value of the inductance of the loop may be calculated analytically or numerically.

[00138] The inductance for other cross-section conductors, arranged to form other enclosed surface shapes, areas, sizes, and the like, and of any number of wire turns, may be calculated analytically, numerically or it may be determined by measurement. The inductance may be realized using inductor elements, distributed inductance, networks, arrays, series and parallel combinations of inductors and inductances, and the like. The inductance may be fixed or variable and may be used to vary impedance matching as well as resonant frequency operating conditions.

[00139] There are a variety of ways to realize the capacitance required to achieve the desired resonant frequency for a resonator structure. Capacitor plates 110 may be formed and utilized as shown in Fig. 6b, or the capacitance may be distributed and be realized between adjacent windings of a multi-loop conductor 114, as shown in Fig. 6c. The capacitance may be realized using capacitor elements, distributed capacitance, networks, arrays, series and parallel combinations of capacitances, and the like. The capacitance may be fixed or variable and may be used to vary impedance matching as well as resonant frequency operating conditions.

[00140] It is to be understood that the inductance and capacitance in an electromagnetic resonator 102 may be lumped, distributed, or a combination of lumped and distributed inductance and capacitance and that electromagnetic resonators may be realized by combinations of the various elements, techniques and effects described herein.

[00141] Electromagnetic resonators 102 may include inductors, inductances, capacitors, capacitances, as well as additional circuit elements such as resistors, diodes, switches, amplifiers, diodes, transistors, transformers, conductors, connectors and the like.

[00142] **Resonant Frequency of an Electromagnetic Resonator**

[00143] An electromagnetic resonator 102 may have a characteristic, natural, or resonant frequency determined by its physical properties. This resonant frequency is the frequency at which the energy stored by the resonator oscillates between that stored by the electric field,  $W_E$ , ( $W_E=q^2/2C$ , where  $q$  is the charge on the capacitor,  $C$ ) and that stored by the magnetic field,  $W_B$ , ( $W_B=Li^2/2$ , where  $i$  is the current through the inductor,  $L$ ) of the resonator. In the absence of any losses in the system, energy would continually be exchanged between the

electric field in the capacitor 104 and the magnetic field in the inductor 108. The frequency at which this energy is exchanged may be called the characteristic frequency, the natural frequency, or the resonant frequency of the resonator, and is given by  $\omega$ ,

$$\omega = 2\pi f = \sqrt{\frac{1}{LC}}.$$

**[00144]** The resonant frequency of the resonator may be changed by tuning the inductance,  $L$ , and/or the capacitance,  $C$ , of the resonator. The resonator frequency may be design to operate at the so-called ISM (Industrial, Scientific and Medical) frequencies as specified by the FCC. The resonator frequency may be chosen to meet certain field limit specifications, specific absorption rate (SAR) limit specifications, electromagnetic compatibility (EMC) specifications, electromagnetic interference (EMI) specifications, component size, cost or performance specifications, and the like.

**[00145] Quality Factor of an Electromagnetic Resonator**

**[00146]** The energy in the resonators 102 shown in Fig. 6 may decay or be lost by intrinsic losses including absorptive losses (also called ohmic or resistive losses) and/or radiative losses. The Quality Factor, or  $Q$ , of the resonator, which characterizes the energy decay, is inversely proportional to these losses. Absorptive losses may be caused by the finite conductivity of the conductor used to form the inductor as well as by losses in other elements, components, connectors, and the like, in the resonator. An inductor formed from low loss materials may be referred to as a “high- $Q$  inductive element” and elements, components, connectors and the like with low losses may be referred to as having “high resistive  $Q$ ’s”. In general, the total absorptive loss for a resonator may be calculated as the appropriate series and/or parallel combination of resistive losses for the various elements and components that make up the resonator. That is, in the absence of any significant radiative or component/connection losses, the  $Q$  of the resonator may be given by,  $Q_{abs}$ ,

$$Q_{abs} = \frac{\omega L}{R_{abs}},$$

where  $\omega$ , is the resonant frequency,  $L$ , is the total inductance of the resonator and the resistance for the conductor used to form the inductor, for example, may be given by  $R_{abs} = l\rho/A$ , ( $l$  is the length of the wire,  $\rho$  is the resistivity of the conductor material, and  $A$  is the cross-sectional area over which current flows in the wire). For alternating currents, the cross-sectional area over

which current flows may be less than the physical cross-sectional area of the conductor owing to the skin effect. Therefore, high- $Q$  magnetic resonators may be composed of conductors with high conductivity, relatively large surface areas and/or with specially designed profiles (e.g. Litz wire) to minimize proximity effects and reduce the AC resistance.

**[00147]** The magnetic resonator structures may include high- $Q$  inductive elements composed of high conductivity wire, coated wire, Litz wire, ribbon, strapping or plates, tubing, paint, gels, traces, and the like. The magnetic resonators may be self-resonant, or they may include external coupled elements such as capacitors, inductors, switches, diodes, transistors, transformers, and the like. The magnetic resonators may include distributed and lumped capacitance and inductance. In general, the  $Q$  of the resonators will be determined by the  $Q$ 's of all the individual components of the resonator.

**[00148]** Because  $Q$  is proportional to inductance,  $L$ , resonators may be designed to increase  $L$ , within certain other constraints. One way to increase  $L$ , for example, is to use more than one turn of the conductor to form the inductor in the resonator. Design techniques and trade-offs may depend on the application, and a wide variety of structures, conductors, components, and resonant frequencies may be chosen in the design of high- $Q$  magnetic resonators.

**[00149]** In the absence of significant absorption losses, the  $Q$  of the resonator may be determined primarily by the radiation losses, and given by,  $Q_{rad} = \omega L / R_{rad}$ , where  $R_{rad}$  is the radiative loss of the resonator and may depend on the size of the resonator relative to the frequency,  $\omega$ , or wavelength,  $\lambda$ , of operation. For the magnetic resonators discussed above, radiative losses may scale as  $R_{rad} \sim (x/\lambda)^4$  (characteristic of magnetic dipole radiation), where  $x$  is a characteristic dimension of the resonator, such as the radius of the inductive element shown in Fig. 6b, and where  $\lambda = c / f$ , where  $c$  is the speed of light and  $f$  is as defined above. The size of the magnetic resonator may be much less than the wavelength of operation so radiation losses may be very small. Such structures may be referred to as sub-wavelength resonators. Radiation may be a loss mechanism for non-radiative wireless energy transfer systems and designs may be chosen to reduce or minimize  $R_{rad}$ . Note that a high- $Q_{rad}$  may be desirable for non-radiative wireless energy transfer schemes.

**[00150]** Note too that the design of resonators for non-radiative wireless energy transfer differs from antennas designed for communication or far-field energy transmission



purposes. Specifically, capacitively-loaded conductive loops may be used as resonant antennas (for example in cell phones), but those operate in the far-field regime where the radiation  $Q$ 's are intentionally designed to be small to make the antenna efficient at radiating energy. Such designs are not appropriate for the efficient near-field wireless energy transfer technique disclosed in this application.

[00151] The quality factor of a resonator including both radiative and absorption losses is  $Q = \omega L / (R_{abs} + R_{rad})$ . Note that there may be a maximum  $Q$  value for a particular resonator and that resonators may be designed with special consideration given to the size of the resonator, the materials and elements used to construct the resonator, the operating frequency, the connection mechanisms, and the like, in order to achieve a high- $Q$  resonator. Fig. 7 shows a plot of  $Q$  of an exemplary magnetic resonator (in this case a coil with a diameter of 60 cm made of copper pipe with an outside diameter (OD) of 4 cm) that may be used for wireless power transmission at MHz frequencies. The absorptive  $Q$  (dashed line) 702 increases with frequency, while the radiative  $Q$  (dotted line) 704 decreases with frequency, thus leading the overall  $Q$  to peak 708 at a particular frequency. Note that the  $Q$  of this exemplary resonator is greater than 100 over a wide frequency range. Magnetic resonators may be designed to have high- $Q$  over a range of frequencies and system operating frequency may set to any frequency in that range.

[00152] When the resonator is being described in terms of loss rates, the  $Q$  may be defined using the intrinsic decay rate,  $2\Gamma$ , as described previously. The intrinsic decay rate is the rate at which an uncoupled and undriven resonator loses energy. For the magnetic resonators described above, the intrinsic loss rate may be given by  $\Gamma = (R_{abs} + R_{rad}) / 2L$ , and the quality factor,  $Q$ , of the resonator is given by  $Q = \omega / 2\Gamma$ .

[00153] Note that a quality factor related only to a specific loss mechanism may be denoted as  $Q_{mechanism}$ , if the resonator is not specified, or as  $Q_{1,mechanism}$ , if the resonator is specified (e.g. resonator 1). For example,  $Q_{1,rad}$  is the quality factor for resonator 1 related to its radiation losses.

[00154] **Electromagnetic Resonator Near-Fields**

[00155] The high- $Q$  electromagnetic resonators used in the near-field wireless energy transfer system disclosed here may be sub-wavelength objects. That is, the physical dimensions of the resonator may be much smaller than the wavelength corresponding to the resonant

frequency. Sub-wavelength magnetic resonators may have most of the energy in the region surrounding the resonator stored in their magnetic near-fields, and these fields may also be described as stationary or non-propagating because they do not radiate away from the resonator. The extent of the near-field in the area surrounding the resonator is typically set by the wavelength, so it may extend well beyond the resonator itself for a sub-wavelength resonator. The limiting surface, where the field behavior changes from near-field behavior to far-field behavior may be called the “radiation caustic”.

**[00156]** The strength of the near-field is reduced the farther one gets away from the resonator. While the field strength of the resonator near-fields decays away from the resonator, the fields may still interact with objects brought into the general vicinity of the resonator. The degree to which the fields interact depends on a variety of factors, some of which may be controlled and designed, and some of which may not. The wireless energy transfer schemes described herein may be realized when the distance between coupled resonators is such that one resonator lies within the radiation caustic of the other.

**[00157]** The near-field profiles of the electromagnetic resonators may be similar to those commonly associated with dipole resonators or oscillators. Such field profiles may be described as omni-directional, meaning the magnitudes of the fields are non-zero in all directions away from the object.

**[00158]** Characteristic Size of An Electromagnetic Resonator

**[00159]** Spatially separated and/or offset magnetic resonators of sufficient  $Q$  may achieve efficient wireless energy transfer over distances that are much larger than have been seen in the prior art, even if the sizes and shapes of the resonator structures are different. Such resonators may also be operated to achieve more efficient energy transfer than was achievable with previous techniques over shorter range distances. We describe such resonators as being capable of mid-range energy transfer.

**[00160]** Mid-range distances may be defined as distances that are larger than the characteristic dimension of the smallest of the resonators involved in the transfer, where the distance is measured from the center of one resonator structure to the center of a spatially separated second resonator structure. In this definition, two-dimensional resonators are spatially separated when the areas circumscribed by their inductive elements do not intersect and three-dimensional resonators are spatially separated when their volumes do not intersect. A two-

dimensional resonator is spatially separated from a three-dimensional resonator when the area circumscribed by the former is outside the volume of the latter.

[00161] Fig. 8 shows some example resonators with their characteristic dimensions labeled. It is to be understood that the characteristic sizes 802 of resonators 102 may be defined in terms of the size of the conductor and the area circumscribed or enclosed by the inductive element in a magnetic resonator and the length of the conductor forming the capacitive element of an electric resonator. Then, the characteristic size 802 of a resonator 102,  $x_{char}$ , may be equal to the radius of the smallest sphere that can fit around the inductive or capacitive element of the magnetic or electric resonator respectively, and the center of the resonator structure is the center of the sphere. The characteristic thickness 804,  $t_{char}$ , of a resonator 102 may be the smallest possible height of the highest point of the inductive or capacitive element in the magnetic or capacitive resonator respectively, measured from a flat surface on which it is placed. The characteristic width 808 of a resonator 102,  $w_{char}$ , may be the radius of the smallest possible circle through which the inductive or capacitive element of the magnetic or electric resonator respectively, may pass while traveling in a straight line. For example, the characteristic width 808 of a cylindrical resonator may be the radius of the cylinder.

[00162] In this inventive wireless energy transfer technique, energy may be exchanged efficiently over a wide range of distances, but the technique is distinguished by the ability to exchange useful energy for powering or recharging devices over mid-range distances and between resonators with different physical dimensions, components and orientations. Note that while  $k$  may be small in these circumstances, strong coupling and efficient energy transfer may be realized by using high- $Q$  resonators to achieve a high  $U$ ,  $U = k\sqrt{Q_s Q_d}$ . That is, increases in  $Q$  may be used to at least partially overcome decreases in  $k$ , to maintain useful energy transfer efficiencies.

[00163] Note too that while the near-field of a single resonator may be described as omni-directional, the efficiency of the energy exchange between two resonators may depend on the relative position and orientation of the resonators. That is, the efficiency of the energy exchange may be maximized for particular relative orientations of the resonators. The sensitivity of the transfer efficiency to the relative position and orientation of two uncompensated resonators may be captured in the calculation of either  $k$  or  $\kappa$ . While coupling may be achieved between resonators that are offset and/or rotated relative to each other, the efficiency of the

exchange may depend on the details of the positioning and on any feedback, tuning, and compensation techniques implemented during operation.

**[00164] High-Q Magnetic Resonators**

**[00165]** In the near-field regime of a sub-wavelength capacitively-loaded loop magnetic resonator ( $x \ll \lambda$ ), the resistances associated with a circular conducting loop inductor composed of  $N$  turns of wire whose radius is larger than the skin depth, are approximately  $R_{abs} = \sqrt{\mu_o \rho \omega / 2} \cdot Nx / a$  and  $R_{rad} = \pi / 6 \cdot \eta_o N^2 (\omega x / c)^4$ , where  $\rho$  is the resistivity of the conductor material and  $\eta_o \approx 120\pi \Omega$  is the impedance of free space. The inductance,  $L$ , for such a  $N$ -turn loop is approximately  $N^2$  times the inductance of a single-turn loop given previously. The quality factor of such a resonator,  $Q = \omega L / (R_{abs} + R_{rad})$ , is highest for a particular frequency determined by the system parameters (Fig. 4). As described previously, at lower frequencies the  $Q$  is determined primarily by absorption losses and at higher frequencies the  $Q$  is determined primarily by radiation losses.

**[00166]** Note that the formulas given above are approximate and intended to illustrate the functional dependence of  $R_{abs}$ ,  $R_{rad}$  and  $L$  on the physical parameters of the structure. More accurate numerical calculations of these parameters that take into account deviations from the strict quasi-static limit, for example a non-uniform current/charge distribution along the conductor, may be useful for the precise design of a resonator structure.

**[00167]** Note that the absorptive losses may be minimized by using low loss conductors to form the inductive elements. The loss of the conductors may be minimized by using large surface area conductors such as conductive tubing, strapping, strips, machined objects, plates, and the like, by using specially designed conductors such as Litz wire, braided wires, wires of any cross-section, and other conductors with low proximity losses, in which case the frequency scaled behavior described above may be different, and by using low resistivity materials such as high-purity copper and silver, for example. One advantage of using conductive tubing as the conductor at higher operating frequencies is that it may be cheaper and lighter than a similar diameter solid conductor, and may have similar resistance because most of the current is traveling along the outer surface of the conductor owing to the skin effect.

**[00168]** To get a rough estimate of achievable resonator designs made from copper wire or copper tubing and appropriate for operation in the microwave regime, one may calculate

the optimum  $Q$  and resonant frequency for a resonator composed of one circular inductive element ( $N=1$ ) of copper wire ( $\rho=1.69 \cdot 10^{-8} \Omega m$ ) with various cross sections. Then for an inductive element with characteristic size  $x=1 \text{ cm}$  and conductor diameter  $a=1 \text{ mm}$ , appropriate for a cell phone for example, the quality factor peaks at  $Q=1225$  when  $f=380 \text{ MHz}$ . For  $x=30 \text{ cm}$  and  $a=2 \text{ mm}$ , an inductive element size that might be appropriate for a laptop or a household robot,  $Q=1103$  at  $f=17 \text{ MHz}$ . For a larger source inductive element that might be located in the ceiling for example,  $x=1 \text{ m}$  and  $a=4 \text{ mm}$ ,  $Q$  may be as high as  $Q=1315$  at  $f=5 \text{ MHz}$ . Note that a number of practical examples yield expected quality factors of  $Q \approx 1000-1500$  at  $\lambda/x \approx 50-80$ . Measurements of a wider variety of coil shapes, sizes, materials and operating frequencies than described above show that  $Q$ 's  $>100$  may be realized for a variety of magnetic resonator structures using commonly available materials.

**[00169]** As described above, the rate for energy transfer between two resonators of characteristic size  $x_1$  and  $x_2$ , and separated by a distance  $D$  between their centers, may be given by  $\kappa$ . To give an example of how the defined parameters scale, consider the cell phone, laptop, and ceiling resonator examples from above, at three (3) distances;  $D/x=10, 8, 6$ . In the examples considered here, the source and device resonators are the same size,  $x_1=x_2$ , and shape, and are oriented as shown in Fig. 1(b). In the cell phone example,  $\omega/2\kappa=3033, 1553, 655$  respectively. In the laptop example,  $\omega/2\kappa=7131, 3651, 1540$  respectively and for the ceiling resonator example,  $\omega/2\kappa=6481, 3318, 1400$ . The corresponding coupling-to-loss ratios peak at the frequency where the inductive element  $Q$  peaks and are  $\kappa/\Gamma=0.4, 0.79, 1.97$  and  $0.15, 0.3, 0.72$  and  $0.2, 0.4, 0.94$  for the three inductive element sizes and distances described above. An example using different sized inductive elements is that of an  $x_1=1 \text{ m}$  inductor (e.g. source in the ceiling) and an  $x_2=30 \text{ cm}$  inductor (e.g. household robot on the floor) at a distance  $D=3 \text{ m}$  apart (e.g. room height). In this example, the strong-coupling figure of merit,  $U = \kappa / \sqrt{\Gamma_1 \Gamma_2} = 0.88$ , for an efficiency of approximately 14%, at the optimal operating frequency of  $f=6.4 \text{ MHz}$ . Here, the optimal system operating frequency lies between the peaks of the individual resonator  $Q$ 's.

**[00170]** Inductive elements may be formed for use in high- $Q$  magnetic resonators. We have demonstrated a variety of high- $Q$  magnetic resonators based on copper conductors that are formed into inductive elements that enclose a surface. Inductive elements may be formed using a variety of conductors arranged in a variety of shapes, enclosing any size or shaped area, and they may be single turn or multiple turn elements. Drawings of exemplary inductive elements 900A-B

are shown in Fig. 9. The inductive elements may be formed to enclose a circle, a rectangle, a square, a triangle, a shape with rounded corners, a shape that follows the contour of a particular structure or device, a shape that follows, fills, or utilizes, a dedicated space within a structure or device, and the like. The designs may be optimized for size, cost, weight, appearance, performance, and the like.

[00171] These conductors may be bent or formed into the desired size, shape, and number of turns. However, it may be difficult to accurately reproduce conductor shapes and sizes using manual techniques. In addition, it may be difficult to maintain uniform or desired center-to-center spacings between the conductor segments in adjacent turns of the inductive elements. Accurate or uniform spacing may be important in determining the self capacitance of the structure as well as any proximity effect induced increases in AC resistance, for example.

[00172] Molds may be used to replicate inductor elements for high- $Q$  resonator designs. In addition, molds may be used to accurately shape conductors into any kind of shape without creating kinks, buckles or other potentially deleterious effects in the conductor. Molds may be used to form the inductor elements and then the inductor elements may be removed from the forms. Once removed, these inductive elements may be built into enclosures or devices that may house the high- $Q$  magnetic resonator. The formed elements may also or instead remain in the mold used to form them.

[00173] The molds may be formed using standard CNC (computer numerical control) routing or milling tools or any other known techniques for cutting or forming grooves in blocks. The molds may also or instead be formed using machining techniques, injection molding techniques, casting techniques, pouring techniques, vacuum techniques, thermoforming techniques, cut-in-place techniques, compression forming techniques and the like.

[00174] The formed element may be removed from the mold or it may remain in the mold. The mold may be altered with the inductive element inside. The mold may be covered, machined, attached, painted and the like. The mold and conductor combination may be integrated into another housing, structure or device. The grooves cut into the molds may be any dimension and may be designed to form conducting tubing, wire, strapping, strips, blocks, and the like into the desired inductor shapes and sizes.

[00175] The inductive elements used in magnetic resonators may contain more than one loop and may spiral inward or outward or up or down or in some combination of directions.

In general, the magnetic resonators may have a variety of shapes, sizes and number of turns and they may be composed of a variety of conducting materials.

[00176] The magnetic resonators may be free standing or they may be enclosed in an enclosure, container, sleeve or housing. The magnetic resonators may include the form used to make the inductive element. These various forms and enclosures may be composed of almost any kind of material. Low loss materials such as Teflon, REXOLITE, styrene, and the like may be preferable for some applications. These enclosures may contain fixtures that hold the inductive elements.

[00177] Magnetic resonators may be composed of self-resonant coils of copper wire or copper tubing. Magnetic resonators composed of self resonant conductive wire coils may include a wire of length  $l$ , and cross section radius  $a$ , wound into a helical coil of radius  $x$ , height  $h$ , and number of turns  $N$ , which may for example be characterized as  $N = \sqrt{l^2 - h^2} / 2\pi x$ .

[00178] A magnetic resonator structure may be configured so that  $x$  is about 30 cm,  $h$  is about 20 cm,  $a$  is about 3 mm and  $N$  is about 5.25, and, during operation, a power source coupled to the magnetic resonator may drive the resonator at a resonant frequency,  $f$ , where  $f$  is about 10.6 MHz. Where  $x$  is about 30 cm,  $h$  is about 20 cm,  $a$  is about 1 cm and  $N$  is about 4, the resonator may be driven at a frequency,  $f$ , where  $f$  is about 13.4 MHz. Where  $x$  is about 10 cm,  $h$  is about 3 cm,  $a$  is about 2 mm and  $N$  is about 6, the resonator may be driven at a frequency,  $f$ , where  $f$  is about 21.4 MHz.

[00179] High-Q inductive elements may be designed using printed circuit board traces. Printed circuit board traces may have a variety of advantages compared to mechanically formed inductive elements including that they may be accurately reproduced and easily integrated using established printed circuit board fabrication techniques, that their AC resistance may be lowered using custom designed conductor traces, and that the cost of mass-producing them may be significantly reduced.

[00180] High-Q inductive elements may be fabricated using standard PCB techniques on any PCB material such as FR-4 (epoxy E-glass), multi-functional epoxy, high performance epoxy, bismalimide triazine/epoxy, polyimide, Cyanate Ester, polytetraflouroethylene (Teflon), FR-2, FR-3, CEM-1, CEM-2, Rogers, Resolute, and the like. The conductor traces may be formed on printed circuit board materials with lower loss tangents.

[00181] The conducting traces may be composed of copper, silver, gold, aluminum, nickel and the like, and they may be composed of paints, inks, or other cured materials. The circuit board may be flexible and it may be a flex-circuit. The conducting traces may be formed by chemical deposition, etching, lithography, spray deposition, cutting, and the like. The conducting traces may be applied to form the desired patterns and they may be formed using crystal and structure growth techniques.

[00182] The dimensions of the conducting traces, as well as the number of layers containing conducting traces, the position, size and shape of those traces and the architecture for interconnecting them may be designed to achieve or optimize certain system specifications such as resonator  $Q$ ,  $Q_{(p)}$ , resonator size, resonator material and fabrication costs,  $U$ ,  $U_{(p)}$ , and the like.

[00183] As an example, a three-turn high- $Q$  inductive element 1001A was fabricated on a four-layer printed circuit board using the rectangular copper trace pattern as shown in Fig. 10(a). The copper trace is shown in black and the PCB in white. The width and thickness of the copper traces in this example was approximately 1 cm (400 mils) and 43  $\mu$  m (1.7 mils) respectively. The edge-to-edge spacing between turns of the conducting trace on a single layer was approximately 0.75 cm (300 mils) and each board layer thickness was approximately 100  $\mu$  m (4 mils). The pattern shown in Fig. 10(a) was repeated on each layer of the board and the conductors were connected in parallel. The outer dimensions of the 3-loop structure were approximately 30 cm by 20 cm. The measured inductance of this PCB loop was 5.3  $\mu$  H. A magnetic resonator using this inductor element and tunable capacitors had a quality factor,  $Q$ , of 550 at its designed resonance frequency of 6.78 MHz. The resonant frequency could be tuned by changing the inductance and capacitance values in the magnetic resonator.

[00184] As another example, a two-turn inductor 1001B was fabricated on a four-layer printed circuit board using the rectangular copper trace pattern shown in Fig. 10(b). The copper trace is shown in black and the PCB in white. The width and height of the copper traces in this example were approximately 0.75 cm (300 mils) and 43  $\mu$  m (1.7 mils) respectively. The edge-to-edge spacing between turns of the conducting trace on a single layer was approximately 0.635 cm (250 mils) and each board layer thickness was approximately 100  $\mu$  m (4 mils). The pattern shown in Fig. 10(b) was repeated on each layer of the board and the conductors were connected in parallel. The outer dimensions of the two-loop structure were approximately 7.62 cm by 26.7



cm. The measured inductance of this PCB loop was  $1.3 \mu\text{H}$ . Stacking two boards together with a vertical separation of approximately 0.635 cm (250 mils) and connecting the two boards in series produced a PCB inductor with an inductance of approximately  $3.4 \mu\text{H}$ . A magnetic resonator using this stacked inductor loop and tunable capacitors had a quality factor,  $Q$ , of 390 at its designed resonance frequency of 6.78 MHz. The resonant frequency could be tuned by changing the inductance and capacitance values in the magnetic resonator.

[00185] The inductive elements may be formed using magnetic materials of any size, shape thickness, and the like, and of materials with a wide range of permeability and loss values. These magnetic materials may be solid blocks, they may enclose hollow volumes, they may be formed from many smaller pieces of magnetic material tiled and or stacked together, and they may be integrated with conducting sheets or enclosures made from highly conducting materials. Wires may be wrapped around the magnetic materials to generate the magnetic near-field. These wires may be wrapped around one or more than one axis of the structure. Multiple wires may be wrapped around the magnetic materials and combined in parallel, or in series, or via a switch to form customized near-field patterns.

[00186] The magnetic resonator may include 15 turns of Litz wire wound around a 19.2 cm x 10 cm x 5 mm tiled block of 3F3 ferrite material. The Litz wire may be wound around the ferrite material in any direction or combination of directions to achieve the desire resonator performance. The number of turns of wire, the spacing between the turns, the type of wire, the size and shape of the magnetic materials and the type of magnetic material are all design parameters that may be varied or optimized for different application scenarios.

[00187] **High- $Q$  Magnetic resonators using magnetic material structures**

[00188] It may be possible to use magnetic materials assembled to form an open magnetic circuit, albeit one with an air gap on the order of the size of the whole structure, to realize a magnetic resonator structure. In these structures, high conductivity materials are wound around a structure made from magnetic material to form the inductive element of the magnetic resonator. Capacitive elements may be connected to the high conductivity materials, with the resonant frequency then determined as described above. These magnetic resonators have their dipole moment in the plane of the two dimensional resonator structures, rather than perpendicular to it, as is the case for the capacitively-loaded inductor loop resonators.

**[00189]** A diagram of a single planar resonator structure is shown in Fig. 11(a). The planar resonator structure is constructed of a core of magnetic material 1121, such as ferrite with a loop or loops of conducting material 1122 wrapped around the core 1121. The structure may be used as the source resonator that transfers power and the device resonator that captures energy. When used as a source, the ends of the conductor may be coupled to a power source. Alternating electrical current flowing through the conductor loops excites alternating magnetic fields. When the structure is being used to receive power, the ends of the conductor may be coupled to a power drain or load. Changing magnetic fields induce an electromotive force in the loop or loops of the conductor wound around the core magnetic material. The dipole moment of these types of structures is in the plane of the structures and is, for example, directed along the Y axis for the structure in Figure 11(a). Two such structures have strong coupling when placed substantially in the same plane (i.e. the X,Y plane of Figure 11). The structures of Figure 11(a) have the most favorable orientation when the resonators are aligned in the same plane along their Y axis.

**[00190]** The geometry and the coupling orientations of the described planar resonators may be preferable for some applications. The planar or flat resonator shape may be easier to integrate into many electronic devices that are relatively flat and planar. The planar resonators may be integrated into the whole back or side of a device without requiring a change in geometry of the device. Due to the flat shape of many devices, the natural position of the devices when placed on a surface is to lay with their largest dimension being parallel to the surface they are placed on. A planar resonator integrated into a flat device is naturally parallel to the plane of the surface and is in a favorable coupling orientation relative to the resonators of other devices or planar resonator sources placed on a flat surface.

**[00191]** As mentioned, the geometry of the planar resonators may allow easier integration into devices. Their low profile may allow a resonator to be integrated into or as part of a complete side of a device. When a whole side of a device is covered by the resonator, magnetic flux can flow through the resonator core without being obstructed by lossy material that may be part of the device or device circuitry.

**[00192]** The core of the planar resonator structure may be of a variety of shapes and thicknesses and may be flat or planar such that the minimum dimension does not exceed 30% of the largest dimension of the structure. The core may have complex geometries and may have indentations, notches, ridges, and the like. Geometric enhancements may be used to reduce the

coupling dependence on orientation and they may be used to facilitate integration into devices, packaging, packages, enclosures, covers, skins, and the like. Two exemplary variations of core geometries are shown in Figure 11(b). For example, the planar core 1131 may be shaped such that the ends are substantially wider than the middle of the structure to create an indentation for the conductor winding. The core material may be of varying thickness with ends that are thicker and wider than the middle. The core material 1132 may have any number of notches or cutouts 1133 of various depths, width, and shapes to accommodate conductor loops, housing, packaging, and the like.

**[00193]** The shape and dimensions of the core may be further dictated by the dimensions and characteristics of the device that they are integrated into. The core material may curve to follow the contours of the device, or may require non-symmetric notches or cutouts to allow clearance for parts of the device. The core structure may be a single monolithic piece of magnetic material or may be composed of a plurality of tiles, blocks, or pieces that are arranged together to form the larger structure. The different layers, tiles, blocks, or pieces of the structure may be of similar or may be of different materials. It may be desirable to use materials with different magnetic permeability in different locations of the structure. Core structures with different magnetic permeability may be useful for guiding the magnetic flux, improving coupling, and affecting the shape or extent of the active area of a system.

**[00194]** The conductor of the planar resonator structure may be wound at least once around the core. In certain circumstances, it may be preferred to wind at least three loops. The conductor can be any good conductor including conducting wire, Litz wire, conducting tubing, sheets, strips, gels, inks, traces and the like.

**[00195]** The size, shape, or dimensions of the active area of source may be further enhanced, altered, or modified with the use of materials that block, shield, or guide magnetic fields. To create non-symmetric active area around a source one side of the source may be covered with a magnetic shield to reduce the strength of the magnetic fields in a specific direction. The shield may be a conductor or a layered combination of conductor and magnetic material which can be used to guide magnetic fields away from a specific direction. Structures composed of layers of conductors and magnetic materials may be used to reduce energy losses that may occur due to shielding of the source.

[00196] The plurality of planar resonators may be integrated or combined into one planar resonator structure. A conductor or conductors may be wound around a core structure such that the loops formed by the two conductors are not coaxial. An example of such a structure is shown in Figure 12 where two conductors 1201,1202 are wrapped around a planar rectangular core 1203 at orthogonal angles. The core may be rectangular or it may have various geometries with several extensions or protrusions. The protrusions may be useful for wrapping of a conductor, reducing the weight, size, or mass of the core, or may be used to enhance the directionality or omni-directionality of the resonator. A multi wrapped planar resonator with four protrusions is shown by the inner structure 1310 in Figure 13, where four conductors 1301, 1302, 1303, 1304 are wrapped around the core. The core may have extensions 1305,1306,1307,1308 with one or more conductor loops. A single conductor may be wrapped around a core to form loops that are not coaxial. The four conductor loops of Figure 13, for example, may be formed with one continuous piece of conductor, or using two conductors where a single conductor is used to make all coaxial loops.

[00197] Non-uniform or asymmetric field profiles around the resonator comprising a plurality of conductor loops may be generated by driving some conductor loops with non-identical parameters. Some conductor loops of a source resonator with a plurality of conductor loops may be driven by a power source with a different frequency, voltage, power level, duty cycle, and the like all of which may be used to affect the strength of the magnetic field generated by each conductor.

[00198] The planar resonator structures may be combined with a capacitively-loaded inductor resonator coil to provide an omni-directional active area all around, including above and below the source while maintaining a flat resonator structure. As shown in Figure 13, an additional resonator loop coil 1309 comprising of a loop or loops of a conductor, may be placed in a common plane as the planar resonator structure 1310. The outer resonator coil provides an active area that is substantially above and below the source. The resonator coil can be arranged with any number of planar resonator structures and arrangements described herein.

[00199] The planar resonator structures may be enclosed in magnetically permeable packaging or integrated into other devices. The planar profile of the resonators within a single, common plane allows packaging and integration into flat devices. A diagram illustrating the application of the resonators is shown in Figure 14. A flat source 1411 comprising one or more

planar resonators 1414 each with one or more conductor loops may transfer power to devices 1412,1413 that are integrated with other planar resonators 1415,1416 and placed within an active area 1417 of the source. The devices may comprise a plurality of planar resonators such that regardless of the orientation of the device with respect to the source the active area of the source does not change. In addition to invariance to rotational misalignment, a flat device comprising of planar resonators may be turned upside down without substantially affecting the active area since the planar resonator is still in the plane of the source.

**[00200]** Another diagram illustrating a possible use of a power transfer system using the planar resonator structures is shown in Figure 15. A planar source 1521 placed on top of a surface 1525 may create an active area that covers a substantial surface area creating an “energized surface” area. Devices such as computers 1524, mobile handsets 1522, games, and other electronics 1523 that are coupled to their respective planar device resonators may receive energy from the source when placed within the active area of the source, which may be anywhere on top of the surface. Several devices with different dimensions may be placed in the active area and used normally while charging or being powered from the source without having strict placement or alignment constraints. The source may be placed under the surface of a table, countertop, desk, cabinet, and the like, allowing it to be completely hidden while energizing the top surface of the table, countertop, desk, cabinet and the like, creating an active area on the surface that is much larger than the source.

**[00201]** The source may include a display or other visual, auditory, or vibration indicators to show the direction of charging devices or what devices are being charged, error or problems with charging, power levels, charging time, and the like.

**[00202]** The source resonators and circuitry may be integrated into any number of other devices. The source may be integrated into devices such as clocks, keyboards, monitors, picture frames, and the like. For example, a keyboard integrated with the planar resonators and appropriate power and control circuitry may be used as a source for devices placed around the keyboard such as computer mice, webcams, mobile handsets, and the like without occupying any additional desk space.

**[00203]** While the planar resonator structures have been described in the context of mobile devices it should be clear to those skilled in the art that a flat planar source for wireless power transfer with an active area that extends beyond its physical dimensions has many other

consumer and industrial applications. The structures and configuration may be useful for a large number of applications where electronic or electric devices and a power source are typically located, positioned, or manipulated in substantially the same plane and alignment. Some of the possible application scenarios include devices on walls, floor, ceilings or any other substantially planar surfaces.

**[00204]** Flat source resonators may be integrated into a picture frame or hung on a wall thereby providing an active area within the plane of the wall where other electronic devices such as digital picture frames, televisions, lights, and the like can be mounted and powered without wires. Planar resonators may be integrated into a floor resulting in an energized floor or active area on the floor on which devices can be placed to receive power. Audio speakers, lamps, heaters, and the like can be placed within the active area and receive power wirelessly.

**[00205]** The planar resonator may have additional components coupled to the conductor. Components such as capacitors, inductors, resistors, diodes, and the like may be coupled to the conductor and may be used to adjust or tune the resonant frequency and the impedance matching for the resonators.

**[00206]** A planar resonator structure of the type described above and shown in Fig. 11(a), may be created, for example, with a quality factor,  $Q$ , of 100 or higher and even  $Q$  of 1,000 or higher. Energy may be wirelessly transferred from one planar resonator structure to another over a distance larger than the characteristic size of the resonators, as shown in Fig. 11(c).

**[00207]** In addition to utilizing magnetic materials to realize a structure with properties similar to the inductive element in the magnetic resonators, it may be possible to use a combination of good conductor materials and magnetic material to realize such inductive structures. Fig. 16(a) shows a magnetic resonator structure 1602 that may include one or more enclosures made of high-conductivity materials (the inside of which would be shielded from AC electromagnetic fields generated outside) surrounded by at least one layer of magnetic material and linked by blocks of magnetic material 1604.

A structure may include a high-conductivity sheet of material covered on one side by a layer of magnetic material. The layered structure may instead be applied conformally to an electronic device, so that parts of the device may be covered by the high-conductivity and magnetic material layers, while other parts that need to be easily accessed (such as buttons or

screens) may be left uncovered. The structure may also or instead include only layers or bulk pieces of magnetic material. Thus, a magnetic resonator may be incorporated into an existing device without significantly interfering with its existing functions and with little or no need for extensive redesign. Moreover, the layers of good conductor and/or magnetic material may be made thin enough (of the order of a millimeter or less) that they would add little extra weight and volume to the completed device. An oscillating current applied to a length of conductor wound around the structure, as shown by the square loop in the center of the structure in Figure 16 may be used to excite the electromagnetic fields associated with this structure.

**[00208]**    Quality factor of the structure

**[00209]**    A structure of the type described above may be created with a quality factor,  $Q$ , of the order of 1,000 or higher. This high- $Q$  is possible even if the losses in the magnetic material are high, if the fraction of magnetic energy within the magnetic material is small compared to the total magnetic energy associated with the object. For structures composed of layers conducting materials and magnetic materials, the losses in the conducting materials may be reduced by the presence of the magnetic materials as described previously. In structures where the magnetic material layer's thickness is of the order of 1/100 of the largest dimension of the system (e.g., the magnetic material may be of the order of 1 mm thick, while the area of the structure is of the order of 10 cm x 10 cm), and the relative permeability is of the order of 1,000, it is possible to make the fraction of magnetic energy contained within the magnetic material only a few hundredths of the total magnetic energy associated with the object or resonator. To see how that comes about, note that the expression for the magnetic energy contained in a volume is  $U_m = \int_V \mathbf{dr} \mathbf{B}(\mathbf{r})^2 / (2\mu_r \mu_0)$ , so as long as  $\mathbf{B}$  (rather than  $\mathbf{H}$ ) is the main field conserved across the magnetic material-air interface (which is typically the case in open magnetic circuits), the fraction of magnetic energy contained in the high- $\mu_r$  region may be significantly reduced compared to what it is in air.

**[00210]**    If the fraction of magnetic energy in the magnetic material is denoted by  $frac$ , and the loss tangent of the material is  $\tan\delta$ , then the  $Q$  of the resonator, assuming the magnetic material is the only source of losses, is  $Q=1/(frac \times \tan\delta)$ . Thus, even for loss tangents as high as 0.1, it is possible to achieve  $Q$ 's of the order of 1,000 for these types of resonator structures.

[00211] If the structure is driven with  $N$  turns of wire wound around it, the losses in the excitation inductor loop can be ignored if  $N$  is sufficiently high. Fig. 17 shows an equivalent circuit 1700 schematic for these structures and the scaling of the loss mechanisms and inductance with the number of turns,  $N$ , wound around a structure made of conducting and magnetic material. If proximity effects can be neglected (by using an appropriate winding, or a wire designed to minimize proximity effects, such as Litz wire and the like), the resistance 1702 due to the wire in the looped conductor scales linearly with the length of the loop, which is in turn proportional to the number of turns. On the other hand, both the equivalent resistance 1708 and equivalent inductance 1704 of these special structures are proportional to the square of the magnetic field inside the structure. Since this magnetic field is proportional to  $N$ , the equivalent resistance 1708 and equivalent inductance 1704 are both proportional to  $N^2$ . Thus, for large enough  $N$ , the resistance 1702 of the wire is much smaller than the equivalent resistance 1708 of the magnetic structure, and the  $Q$  of the resonator asymptotes to  $Q_{max} = \omega L_{\mu} / R_{\mu}$ .

[00212] Fig. 16 (a) shows a drawing of a copper and magnetic material structure 1602 driven by a square loop of current around the narrowed segment at the center of the structure 1604 and the magnetic field streamlines generated by this structure 1608. This exemplary structure includes two 20 cm x 8 cm x 2 cm hollow regions enclosed with copper and then completely covered with a 2 mm layer of magnetic material having the properties  $\mu_r' = 1,400$ ,  $\mu_r'' = 5$ , and  $\sigma = 0.5$  S/m. These two parallelepipeds are spaced 4 cm apart and are connected by a 2 cm x 4 cm x 2 cm block of the same magnetic material. The excitation loop is wound around the center of this block. At a frequency of 300 kHz, this structure has a calculated  $Q$  of 890. The conductor and magnetic material structure may be shaped to optimize certain system parameters. For example, the size of the structure enclosed by the excitation loop may be small to reduce the resistance of the excitation loop, or it may be large to mitigate losses in the magnetic material associated with large magnetic fields. Note that the magnetic streamlines and  $Q$ 's associated with the same structure composed of magnetic material only would be similar to the layer conductor and magnetic material design shown here.

[00213] **Electromagnetic Resonators Interacting with Other Objects**

[00214] For electromagnetic resonators, extrinsic loss mechanisms that perturb the intrinsic  $Q$  may include absorption losses inside the materials of nearby extraneous objects and



radiation losses related to scattering of the resonant fields from nearby extraneous objects. Absorption losses may be associated with materials that, over the frequency range of interest, have non-zero, but finite, conductivity,  $\sigma$ , (or equivalently a non-zero and finite imaginary part of the dielectric permittivity), such that electromagnetic fields can penetrate it and induce currents in it, which then dissipate energy through resistive losses. An object may be described as lossy if it at least partly includes lossy materials.

**[00215]** Consider an object including a homogeneous isotropic material of conductivity,  $\sigma$  and magnetic permeability,  $\mu$ . The penetration depth of electromagnetic fields inside this object is given by the skin depth,  $\delta = \sqrt{2/\omega\mu\sigma}$ . The power dissipated inside the object,  $P_d$ , can be determined from  $P_d = \int_V d\mathbf{r} \sigma |\mathbf{E}|^2 = \int_V d\mathbf{r} |\mathbf{J}|^2 / \sigma$  where we made use of Ohm's law,  $\mathbf{J} = \sigma\mathbf{E}$ , and where  $\mathbf{E}$  is the electric field and  $\mathbf{J}$  is the current density.

**[00216]** If over the frequency range of interest, the conductivity,  $\sigma$ , of the material that composes the object is low enough that the material's skin depth,  $\delta$ , may be considered long, (i.e.  $\delta$  is longer than the objects' characteristic size, or  $\delta$  is longer than the characteristic size of the portion of the object that is lossy) then the electromagnetic fields,  $\mathbf{E}$  and  $\mathbf{H}$ , where  $\mathbf{H}$  is the magnetic field, may penetrate significantly into the object. Then, these finite-valued fields may give rise to a dissipated power that scales as  $P_d \sim \sigma V_{ol} \langle |\mathbf{E}|^2 \rangle$ , where  $V_{ol}$  is the volume of the object that is lossy and  $\langle |\mathbf{E}|^2 \rangle$  is the spatial average of the electric-field squared, in the volume under consideration. Therefore, in the low-conductivity limit, the dissipated power scales proportionally to the conductivity and goes to zero in the limit of a non-conducting (purely dielectric) material.

**[00217]** If over the frequency range of interest, the conductivity,  $\sigma$ , of the material that composes the object is high enough that the material's skin depth may be considered short, then the electromagnetic fields,  $\mathbf{E}$  and  $\mathbf{H}$ , may penetrate only a short distance into the object (namely they stay close to the 'skin' of the material, where  $\delta$  is smaller than the characteristic thickness of the portion of the object that is lossy). In this case, the currents induced inside the material may be concentrated very close to the material surface, approximately within a skin depth, and their magnitude may be approximated by the product of a surface current density (mostly determined by the shape of the incident electromagnetic fields and, as long as the

thickness of the conductor is much larger than the skin-depth, independent of frequency and conductivity to first order)  $K(x, y)$  (where  $x$  and  $y$  are coordinates parameterizing the surface) and a function decaying exponentially into the surface:  $\exp(-z/\delta)/\delta$  (where  $z$  denotes the coordinate locally normal to the surface):  $J(x, y, z) = K(x, y)\exp(-z/\delta)/\delta$ . Then, the dissipated power,  $P_d$ , may be estimated by,

$$P_d = \int_V d\mathbf{r} |\mathbf{J}(\mathbf{r})|^2 / \sigma \approx \left( \int_S d\mathbf{x} d\mathbf{y} |\mathbf{K}(\mathbf{x}, \mathbf{y})|^2 \right) \left( \int_0^\infty dz \exp(2z/\delta) / (\sigma\delta^2) \right) = \sqrt{\mu\omega / 8\sigma} \left( \int_S d\mathbf{x} d\mathbf{y} |\mathbf{K}(\mathbf{x}, \mathbf{y})|^2 \right)$$

**[00218]** Therefore, in the high-conductivity limit, the dissipated power scales inverse proportionally to the square-root of the conductivity and goes to zero in the limit of a perfectly-conducting material.

**[00219]** If over the frequency range of interest, the conductivity,  $\sigma$ , of the material that composes the object is finite, then the material's skin depth,  $\delta$ , may penetrate some distance into the object and some amount of power may be dissipated inside the object, depending also on the size of the object and the strength of the electromagnetic fields. This description can be generalized to also describe the general case of an object including multiple different materials with different properties and conductivities, such as an object with an arbitrary inhomogeneous and anisotropic distribution of the conductivity inside the object.

**[00220]** Note that the magnitude of the loss mechanisms described above may depend on the location and orientation of the extraneous objects relative to the resonator fields as well as the material composition of the extraneous objects. For example, high-conductivity materials may shift the resonant frequency of a resonator and detune it from other resonant objects. This frequency shift may be fixed by applying a feedback mechanism to a resonator that corrects its frequency, such as through changes in the inductance and/or capacitance of the resonator. These changes may be realized using variable capacitors and inductors, in some cases achieved by changes in the geometry of components in the resonators. Other novel tuning mechanisms, described below, may also be used to change the resonator frequency.

**[00221]** Where external losses are high, the perturbed  $Q$  may be low and steps may be taken to limit the absorption of resonator energy inside such extraneous objects and materials. Because of the functional dependence of the dissipated power on the strength of the electric and

magnetic fields, one might optimize system performance by designing a system so that the desired coupling is achieved with shorter evanescent resonant field tails at the source resonator and longer at the device resonator, so that the perturbed  $Q$  of the source in the presence of other objects is optimized (or vice versa if the perturbed  $Q$  of the device needs to be optimized).

[00222] Note that many common extraneous materials and objects such as people, animals, plants, building materials, and the like, may have low conductivities and therefore may have little impact on the wireless energy transfer scheme disclosed here. An important fact related to the magnetic resonator designs we describe is that their electric fields may be confined primarily within the resonator structure itself, so it should be possible to operate within the commonly accepted guidelines for human safety while providing wireless power exchange over mid range distances.

[00223] **Electromagnetic Resonators with Reduced Interactions**

[00224] One frequency range of interest for near-field wireless power transmission is between 10 kHz and 100 MHz. In this frequency range, a large variety of ordinary non-metallic materials, such as for example several types of wood and plastic may have relatively low conductivity, such that only small amounts of power may be dissipated inside them. In addition, materials with low loss tangents,  $\tan \Delta$ , where  $\tan \Delta = \epsilon'' / \epsilon'$ , and  $\epsilon''$  and  $\epsilon'$  are the imaginary and real parts of the permittivity respectively, may also have only small amounts of power dissipated inside them. Metallic materials, such as copper, silver, gold, and the like, with relatively high conductivity, may also have little power dissipated in them, because electromagnetic fields are not able to significantly penetrate these materials, as discussed earlier. These very high and very low conductivity materials, and low loss tangent materials and objects may have a negligible impact on the losses of a magnetic resonator.

[00225] However, in the frequency range of interest, there are materials and objects such as some electronic circuits and some lower-conductivity metals, which may have moderate (in general inhomogeneous and anisotropic) conductivity, and/or moderate to high loss tangents, and which may have relatively high dissipative losses. Relatively larger amounts of power may be dissipated inside them. These materials and objects may dissipate enough energy to reduce  $Q_{(p)}$  by non-trivial amounts, and may be referred to as “lossy objects”.

[00226] One way to reduce the impact of lossy materials on the  $Q_{(p)}$  of a resonator is to use high-conductivity materials to shape the resonator fields such that they avoid the lossy

objects. The process of using high-conductivity materials to tailor electromagnetic fields so that they avoid lossy objects in their vicinity may be understood by visualizing high-conductivity materials as materials that deflect or reshape the fields. This picture is qualitatively correct as long as the thickness of the conductor is larger than the skin-depth because the boundary conditions for electromagnetic fields at the surface of a good conductor force the electric field to be nearly completely perpendicular to, and the magnetic field to be nearly completely tangential to, the conductor surface. Therefore, a perpendicular magnetic field or a tangential electric field will be “deflected away” from the conducting surface. Furthermore, even a tangential magnetic field or a perpendicular electric field may be forced to decrease in magnitude on one side and/or in particular locations of the conducting surface, depending on the relative position of the sources of the fields and the conductive surface.

[00227] As an example, Fig. 18 shows a finite element method (FEM) simulation of two high conductivity surfaces 1802 above and below a lossy dielectric material 1804 in an external, initially uniform, magnetic field of frequency  $f=6.78$  MHz. The system is azimuthally symmetric around the  $r=0$  axis. In this simulation, the lossy dielectric material 1804 is sandwiched between two conductors 1802, shown as the white lines at approximately  $z = \pm 0.01$  m. In the absence of the conducting surfaces above and below the dielectric disk, the magnetic field (represented by the drawn magnetic field lines) would have remained essentially uniform (field lines straight and parallel with the z-axis), indicating that the magnetic field would have passed straight through the lossy dielectric material. In this case, power would have been dissipated in the lossy dielectric disk. In the presence of conducting surfaces, however, this simulation shows the magnetic field is reshaped. The magnetic field is forced to be tangential to surface of the conductor and so is deflected around those conducting surfaces 1802, minimizing the amount of power that may be dissipated in the lossy dielectric material 1804 behind or between the conducting surfaces. As used herein, an axis of electrical symmetry refers to any axis about which a fixed or time-varying electrical or magnetic field is substantially symmetric during an exchange of energy as disclosed herein.

[00228] A similar effect is observed even if only one conducting surface, above or below, the dielectric disk, is used. If the dielectric disk is thin, the fact that the electric field is essentially zero at the surface, and continuous and smooth close to it, means that the electric field is very low everywhere close to the surface (i.e. within the dielectric disk). A single surface

implementation for deflecting resonator fields away from lossy objects may be preferred for applications where one is not allowed to cover both sides of the lossy material or object (e.g. an LCD screen). Note that even a very thin surface of conducting material, on the order of a few skin-depths, may be sufficient (the skin depth in pure copper at 6.78 MHz is  $\sim 20 \mu\text{m}$ , and at 250 kHz is  $\sim 100 \mu\text{m}$ ) to significantly improve the  $Q_{(p)}$  of a resonator in the presence of lossy materials.

**[00229]** Lossy extraneous materials and objects may be parts of an apparatus, in which a high- $Q$  resonator is to be integrated. The dissipation of energy in these lossy materials and objects may be reduced by a number of techniques including:

- by positioning the lossy materials and objects away from the resonator, or, in special positions and orientations relative to the resonator.
- by using a high conductivity material or structure to partly or entirely cover lossy materials and objects in the vicinity of a resonator
- by placing a closed surface (such as a sheet or a mesh) of high-conductivity material around a lossy object to completely cover the lossy object and shape the resonator fields such that they avoid the lossy object.
- by placing a surface (such as a sheet or a mesh) of a high-conductivity material around only a portion of a lossy object, such as along the top, the bottom, along the side, and the like, of an object or material.
- by placing even a single surface (such as a sheet or a mesh) of high-conductivity material above or below or on one side of a lossy object to reduce the strength of the fields at the location of the lossy object.

**[00230]** Fig. 19 shows a capacitively-loaded loop inductor forming a magnetic resonator 102 and a disk-shaped surface of high-conductivity material 1802 that completely surrounds a lossy object 1804 placed inside the loop inductor. Note that some lossy objects may be components, such as electronic circuits, that may need to interact with, communicate with, or be connected to the outside environment and thus cannot be completely electromagnetically isolated. Partially covering a lossy material with high conductivity materials may still reduce extraneous losses while enabling the lossy material or object to function properly.

[00231] Fig. 20 shows a capacitively-loaded loop inductor that is used as the resonator 102 and a surface of high-conductivity material 1802, surrounding only a portion of a lossy object 1804, that is placed inside the inductor loop.

[00232] Extraneous losses may be reduced, but may not be completely eliminated, by placing a single surface of high-conductivity material above, below, on the side, and the like, of a lossy object or material. An example is shown in Fig. 21, where a capacitively-loaded loop inductor is used as the resonator 102 and a surface of high-conductivity material 1802 is placed inside the inductor loop under a lossy object 1804 to reduce the strength of the fields at the location of the lossy object. It may be preferable to cover only one side of a material or object because of considerations of cost, weight, assembly complications, air flow, visual access, physical access, and the like.

[00233] A single surface of high-conductivity material may be used to avoid objects that cannot or should not be covered from both sides (e.g. LCD or plasma screens). Such lossy objects may be avoided using optically transparent conductors. High-conductivity optically opaque materials may instead be placed on only a portion of the lossy object, instead of, or in addition to, optically transparent conductors. The adequacy of single-sided vs. multi-sided covering implementations, and the design trade-offs inherent therein may depend on the details of the wireless energy transfer scenario and the properties of the lossy materials and objects.

[00234] Below we describe an example using high-conductivity surfaces to improve the  $Q$ -insensitivity,  $\Theta_{(p)}$ , of an integrated magnetic resonator used in a wireless energy-transfer system. Fig. 22 shows a wireless projector 2200. The wireless projector may include a device resonator 102C, a projector 2202, a wireless network/video adapter 2204, and power conversion circuits 2208, arranged as shown. The device resonator 102C may include a three-turn conductor loop, arranged to enclose a surface, and a capacitor network 2210. The conductor loop may be designed so that the device resonator 102C has a high  $Q$  (e.g.,  $>100$ ) at its operating resonant frequency. Prior to integration in the completely wireless projector 2200, this device resonator 102C has a  $Q$  of approximately 477 at the designed operating resonant frequency of 6.78 MHz. Upon integration, and placing the wireless network/video adapter card 2204 in the center of the resonator loop inductor, the resonator  $Q_{(integrated)}$  was decreased to approximately 347. At least some of the reduction from  $Q$  to  $Q_{(integrated)}$  was attributed to losses in the perturbing wireless network/video adapter card. As described above, electromagnetic fields associated with the

magnetic resonator 102C may induce currents in and on the wireless network/video adapter card 2204, which may be dissipated in resistive losses in the lossy materials that compose the card. We observed that  $Q_{(integrated)}$  of the resonator may be impacted differently depending on the composition, position, and orientation, of objects and materials placed in its vicinity.

**[00235]** In a completely wireless projector example, covering the network/video adapter card with a thin copper pocket (a folded sheet of copper that covered the top and the bottom of the wireless network/video adapter card, but not the communication antenna) improved the  $Q_{(integrated)}$  of the magnetic resonator to a  $Q_{(integrated + copper\ pocket)}$  of approximately 444. In other words, most of the reduction in  $Q_{(integrated)}$  due to the perturbation caused by the extraneous network/video adapter card could be eliminated using a copper pocket to deflect the resonator fields away from the lossy materials.

**[00236]** In another completely wireless projector example, covering the network/video adapter card with a single copper sheet placed beneath the card provided a  $Q_{(integrated + copper\ sheet)}$  approximately equal to  $Q_{(integrated + copper\ pocket)}$ . In that example, the high perturbed  $Q$  of the system could be maintained with a single high-conductivity sheet used to deflect the resonator fields away from the lossy adapter card.

**[00237]** It may be advantageous to position or orient lossy materials or objects, which are part of an apparatus including a high-Q electromagnetic resonator, in places where the fields produced by the resonator are relatively weak, so that little or no power may be dissipated in these objects and so that the Q-insensitivity,  $\Theta_{(p)}$ , may be large. As was shown earlier, materials of different conductivity may respond differently to electric versus magnetic fields. Therefore, according to the conductivity of the extraneous object, the positioning technique may be specialized to one or the other field.

**[00238]** Fig. 23 shows the magnitude of the electric 2312 and magnetic fields 2314 along a line that contains the diameter of the circular loop inductor and the electric 2318 and magnetic fields 2320 along the axis of the loop inductor for a capacitively-loaded circular loop inductor of wire of radius 30 cm, resonant at 10 MHz. It can be seen that the amplitude of the resonant near-fields reach their maxima close to the wire and decay away from the loop, 2312 , 2314 . In the plane of the loop inductor 2318, 2320, the fields reach a local minimum at the center of the loop. Therefore, given the finite size of the apparatus, it may be that the fields are weakest at the extrema of the apparatus or it may be that the field magnitudes have local minima

somewhere within the apparatus. This argument holds for any other type of electromagnetic resonator 102 and any type of apparatus. Examples are shown in Figs. 24a and 24b, where a capacitively-loaded inductor loop forms a magnetic resonator 102 and an extraneous lossy object 1804 is positioned where the electromagnetic fields have minimum magnitude.

**[00239]** In a demonstration example, a magnetic resonator was formed using a three-turn conductor loop, arranged to enclose a square surface (with rounded corners), and a capacitor network. The  $Q$  of the resonator was approximately 619 at the designed operating resonant frequency of 6.78 MHz. The perturbed  $Q$  of this resonator depended on the placement of the perturbing object, in this case a pocket projector, relative to the resonator. When the perturbing projector was located inside the inductor loop and at its center or on top of the inductor wire turns,  $Q_{(projector)}$  was approximately 96, lower than when the perturbing projector was placed outside of the resonator, in which case  $Q_{(projector)}$  was approximately 513. These measurements support the analysis that shows the fields inside the inductor loop may be larger than those outside it, so lossy objects placed inside such a loop inductor may yield lower perturbed  $Q$ 's for the system than when the lossy object is placed outside the loop inductor. Depending on the resonator designs and the material composition and orientation of the lossy object, the arrangement shown in Fig. 24b may yield a higher  $Q$ -insensitivity,  $\Theta_{(projector)}$ , than the arrangement shown in Fig. 24a.

**[00240]** High- $Q$  resonators may be integrated inside an apparatus. Extraneous materials and objects of high dielectric permittivity, magnetic permeability, or electric conductivity may be part of the apparatus into which a high- $Q$  resonator is to be integrated. For these extraneous materials and objects in the vicinity of a high- $Q$  electromagnetic resonator, depending on their size, position and orientation relative to the resonator, the resonator field-profile may be distorted and deviate significantly from the original unperturbed field-profile of the resonator. Such a distortion of the unperturbed fields of the resonator may significantly decrease the  $Q$  to a lower  $Q_{(p)}$ , even if the extraneous objects and materials are lossless.

**[00241]** It may be advantageous to position high-conductivity objects, which are part of an apparatus including a high- $Q$  electromagnetic resonator, at orientations such that the surfaces of these objects are, as much as possible, perpendicular to the electric field lines produced by the unperturbed resonator and parallel to the magnetic field lines produced by the unperturbed resonator, thus distorting the resonant field profiles by the smallest amount possible.



Other common objects that may be positioned perpendicular to the plane of a magnetic resonator loop include screens (LCD, plasma, etc), batteries, cases, connectors, radiative antennas, and the like. The Q-insensitivity,  $\Theta_{(p)}$ , of the resonator may be much larger than if the objects were positioned at a different orientation with respect to the resonator fields.

**[00242]** Lossy extraneous materials and objects, which are not part of the integrated apparatus including a high-Q resonator, may be located or brought in the vicinity of the resonator, for example, during the use of the apparatus. It may be advantageous in certain circumstances to use high conductivity materials to tailor the resonator fields so that they avoid the regions where lossy extraneous objects may be located or introduced to reduce power dissipation in these materials and objects and to increase Q-insensitivity,  $\Theta_{(p)}$ . An example is shown in Fig. 25, where a capacitively-loaded loop inductor and capacitor are used as the resonator 102 and a surface of high-conductivity material 1802 is placed above the inductor loop to reduce the magnitude of the fields in the region above the resonator, where lossy extraneous objects 1804 may be located or introduced.

**[00243]** Note that a high-conductivity surface brought in the vicinity of a resonator to reshape the fields may also lead to  $Q_{(cond. surface)} < Q$ . The reduction in the perturbed  $Q$  may be due to the dissipation of energy inside the lossy conductor or to the distortion of the unperturbed resonator field profiles associated with matching the field boundary conditions at the surface of the conductor. Therefore, while a high-conductivity surface may be used to reduce the extraneous losses due to dissipation inside an extraneous lossy object, in some cases, especially in some of those where this is achieved by significantly reshaping the electromagnetic fields, using such a high-conductivity surface so that the fields avoid the lossy object may result effectively in  $Q_{(p + cond. surface)} < Q_{(p)}$  rather than the desired result  $Q_{(p + cond. surface)} > Q_{(p)}$ .

**[00244]** As described above, in the presence of loss inducing objects, the perturbed quality factor of a magnetic resonator may be improved if the electromagnetic fields associated with the magnetic resonator are reshaped to avoid the loss inducing objects. Another way to reshape the unperturbed resonator fields is to use high permeability materials to completely or partially enclose or cover the loss inducing objects, thereby reducing the interaction of the magnetic field with the loss inducing objects.

**[00245]** Magnetic field shielding has been described previously, for example in *Electrodynamics 3<sup>rd</sup> Ed.*, Jackson, pp. 201-203. There, a spherical shell of magnetically

permeable material was shown to shield its interior from external magnetic fields. For example, if a shell of inner radius  $a$ , outer radius  $b$ , and relative permeability  $\mu_r$ , is placed in an initially uniform magnetic field  $H_0$ , then the field inside the shell will have a constant magnitude,  $9\mu_r H_0 / \left[ (2\mu_r + 1)(\mu_r + 2) - 2(a/b)^3 (\mu_r - 1)^2 \right]$ , which tends to  $9H_0 / 2\mu_r (1 - (a/b)^3)$  if  $\mu_r \gg 1$ . This result shows that an incident magnetic field (but not necessarily an incident electric field) may be greatly attenuated inside the shell, even if the shell is quite thin, provided the magnetic permeability is high enough. It may be advantageous in certain circumstances to use high permeability materials to partly or entirely cover lossy materials and objects so that they are avoided by the resonator magnetic fields and so that little or no power is dissipated in these materials and objects. In such an approach, the Q-insensitivity,  $\Theta_{(p)}$ , may be larger than if the materials and objects were not covered, possibly larger than 1.

**[00246]** It may be desirable to keep both the electric and magnetic fields away from loss inducing objects. As described above, one way to shape the fields in such a manner is to use high-conductivity surfaces to either completely or partially enclose or cover the loss inducing objects. A layer of magnetically permeable material, also referred to as magnetic material, (any material or meta-material having a non-trivial magnetic permeability), may be placed on or around the high-conductivity surfaces. The additional layer of magnetic material may present a lower reluctance path (compared to free space) for the deflected magnetic field to follow and may partially shield the electric conductor underneath it from the incident magnetic flux. This arrangement may reduce the losses due to induced currents in the high-conductivity surface. Under some circumstances the lower reluctance path presented by the magnetic material may improve the perturbed  $Q$  of the structure.

**[00247]** Fig. 26a shows an axially symmetric FEM simulation of a thin conducting 2604 (copper) disk (20 cm in diameter, 2 cm in height) exposed to an initially uniform, externally applied magnetic field (gray flux lines) along the z-axis. The axis of symmetry is at  $r=0$ . The magnetic streamlines shown originate at  $z = -\infty$ , where they are spaced from  $r=3$  cm to  $r=10$  cm in intervals of 1 cm. The axes scales are in meters. Imagine, for example, that this conducting cylinder encloses loss-inducing objects within an area circumscribed by a magnetic resonator in a wireless energy transfer system such as shown in Fig. 19.

[00248] This high-conductivity enclosure may increase the perturbing  $Q$  of the lossy objects and therefore the overall perturbed  $Q$  of the system, but the perturbed  $Q$  may still be less than the unperturbed  $Q$  because of induced losses in the conducting surface and changes to the profile of the electromagnetic fields. Decreases in the perturbed  $Q$  associated with the high-conductivity enclosure may be at least partially recovered by including a layer of magnetic material along the outer surface or surfaces of the high-conductivity enclosure. Fig. 26b shows an axially symmetric FEM simulation of the thin conducting 2604A (copper) disk (20 cm in diameter, 2 cm in height) from Fig. 26a, but with an additional layer of magnetic material placed directly on the outer surface of the high-conductivity enclosure. Note that the presence of the magnetic material may provide a lower reluctance path for the magnetic field, thereby at least partially shielding the underlying conductor and reducing losses due to induced eddy currents in the conductor.

[00249] Fig. 27 depicts a variation (in axi-symmetric view) to the system shown in Fig. 26 where not all of the lossy material 2708 may be covered by a high-conductivity surface 2706. In certain circumstances it may be useful to cover only one side of a material or object, such as due to considerations of cost, weight, assembly complications, air flow, visual access, physical access, and the like. In the exemplary arrangement shown in Fig. 27, only one surface of the lossy material 2708 is covered and the resonator inductor loop is placed on the opposite side of the high-conductivity surface.

[00250] Mathematical models were used to simulate a high-conductivity enclosure made of copper and shaped like a 20 cm diameter by 2 cm high cylindrical disk placed within an area circumscribed by a magnetic resonator whose inductive element was a single-turn wire loop with loop radius  $r=11$  cm and wire radius  $a=1$  mm. Simulations for an applied 6.78 MHz electromagnetic field suggest that the perturbing quality factor of this high-conductivity enclosure,  $\delta Q_{(enclosure)}$ , is 1,870. When the high-conductivity enclosure was modified to include a 0.25 cm-thick layer of magnetic material with real relative permeability,  $\mu'_r = 40$ , and imaginary relative permeability,  $\mu''_r = 10^{-2}$ , simulations suggest the perturbing quality factor is increased to  $\delta Q_{(enclosure+magnetic\ material)}=5,060$ .

[00251] The improvement in performance due to the addition of thin layers of magnetic material 2702 may be even more dramatic if the high-conductivity enclosure fills a

larger portion of the area circumscribed by the resonator's loop inductor 2704. In the example above, if the radius of the inductor loop 2704 is reduced so that it is only 3 mm away from the surface of the high-conductivity enclosure, the perturbing quality factor may be improved from 670 (conducting enclosure only) to 2,730 (conducting enclosure with a thin layer of magnetic material) by the addition of a thin layer of magnetic material 2702 around the outside of the enclosure.

**[00252]** The resonator structure may be designed to have highly confined electric fields, using shielding, or distributed capacitors, for example, which may yield high, even when the resonator is very close to materials that would typically induce loss.

**[00253] Coupled Electromagnetic Resonators**

**[00254]** The efficiency of energy transfer between two resonators may be determined by the strong-coupling figure-of-merit,  $U = \kappa / \sqrt{\Gamma_s \Gamma_d} = (2\kappa / \sqrt{\omega_s \omega_d}) \sqrt{Q_s Q_d}$ . In magnetic resonator implementations the coupling factor between the two resonators may be related to the inductance of the inductive elements in each of the resonators,  $L_1$  and  $L_2$ , and the mutual inductance,  $M$ , between them by  $\kappa_{12} = \omega M / 2\sqrt{L_1 L_2}$ . Note that this expression assumes there is negligible coupling through electric-dipole coupling. For capacitively-loaded inductor loop resonators where the inductor loops are formed by circular conducting loops with  $N$  turns, separated by a distance  $D$ , and oriented as shown in Fig. 1(b), the mutual inductance is

$M = \pi / 4 \cdot \mu_0 N_1 N_2 (x_1 x_2)^2 / D^3$  where  $x_1$ ,  $N_1$  and  $x_2$ ,  $N_2$  are the characteristic size and number of turns of the conductor loop of the first and second resonators respectively. Note that this is a quasi-static result, and so assumes that the resonator's size is much smaller than the wavelength and the resonators' distance is much smaller than the wavelength, but also that their distance is at least a few times their size. For these circular resonators operated in the quasi-static limit and at mid-range distances, as described above,  $k = 2\kappa / \sqrt{\omega_1 \omega_2} \sim (\sqrt{x_1 x_2} / D)^3$ . Strong coupling (a large  $U$ ) between resonators at mid-range distances may be established when the quality factors of the resonators are large enough to compensate for the small  $k$  at mid-range distances

**[00255]** For electromagnetic resonators, if the two resonators include conducting parts, the coupling mechanism may be that currents are induced on one resonator due to electric and magnetic fields generated from the other. The coupling factor may be proportional to the flux of

the magnetic field produced from the high-Q inductive element in one resonator crossing a closed area of the high-Q inductive element of the second resonator.

**[00256] Coupled Electromagnetic Resonators with Reduced Interactions**

**[00257]** As described earlier, a high-conductivity material surface may be used to shape resonator fields such that they avoid lossy objects,  $p$ , in the vicinity of a resonator, thereby reducing the overall extraneous losses and maintaining a high Q-insensitivity  $\Theta_{(p + \text{cond. surface})}$  of the resonator. However, such a surface may also lead to a perturbed coupling factor,  $k_{(p + \text{cond. surface})}$ , between resonators that is smaller than the perturbed coupling factor,  $k_{(p)}$  and depends on the size, position, and orientation of the high-conductivity material relative to the resonators. For example, if high-conductivity materials are placed in the plane and within the area circumscribed by the inductive element of at least one of the magnetic resonators in a wireless energy transfer system, some of the magnetic flux through the area of the resonator, mediating the coupling, may be blocked and  $k$  may be reduced.

**[00258]** Consider again the example of Fig. 19. In the absence of the high-conductivity disk enclosure, a certain amount of the external magnetic flux may cross the circumscribed area of the loop. In the presence of the high-conductivity disk enclosure, some of this magnetic flux may be deflected or blocked and may no longer cross the area of the loop, thus leading to a smaller perturbed coupling factor  $k_{12(p + \text{cond. surfaces})}$ . However, because the deflected magnetic-field lines may follow the edges of the high-conductivity surfaces closely, the reduction in the flux through the loop circumscribing the disk may be less than the ratio of the areas of the face of the disk to the area of the loop.

**[00259]** One may use high-conductivity material structures, either alone, or combined with magnetic materials to optimize perturbed quality factors, perturbed coupling factors, or perturbed efficiencies.

**[00260]** Consider the example of Fig. 21. Let the lossy object have a size equal to the size of the capacitively-loaded inductor loop resonator, thus filling its area  $A_{2102}$ . A high-conductivity surface 1802 may be placed under the lossy object 1804. Let this be resonator 1 in a system of two coupled resonators 1 and 2, and let us consider how  $U_{12(\text{object} + \text{cond. surface})}$  scales compared to  $U_{12}$  as the area  $A_s$  2104 of the conducting surface increases. Without the conducting surface 1802 below the lossy object 1804, the  $k$ -insensitivity,  $\beta_{12(\text{object})}$ , may be approximately one, but the Q-insensitivity,  $\Theta_{1(\text{object})}$ , may be small, so the U-insensitivity  $\Xi_{12(\text{object})}$  may be small.

[00261] Where the high-conductivity surface below the lossy object covers the entire area of the inductor loop resonator ( $A_s=A$ ),  $k_{12(object + cond. surface)}$  may approach zero, because little flux is allowed to cross the inductor loop, so  $U_{12(object + cond. surface)}$  may approach zero. For intermediate sizes of the high-conductivity surface, the suppression of extrinsic losses and the associated Q-insensitivity,  $\Theta_{1(object + cond. surface)}$ , may be large enough compared to  $\Theta_{1(object)}$ , while the reduction in coupling may not be significant and the associated  $k$ -insensitivity,  $\beta_{12(object + cond. surface)}$ , may be not much smaller than  $\beta_{12(object)}$ , so that the overall  $U_{12(object + cond. surface)}$  may be increased compared to  $U_{12(object)}$ . The optimal degree of avoiding of extraneous lossy objects via high-conductivity surfaces in a system of wireless energy transfer may depend on the details of the system configuration and the application.

[00262] We describe using high-conductivity materials to either completely or partially enclose or cover loss inducing objects in the vicinity of high-Q resonators as one potential method to achieve high perturbed  $Q$ 's for a system. However, using a good conductor alone to cover the objects may reduce the coupling of the resonators as described above, thereby reducing the efficiency of wireless power transfer. As the area of the conducting surface approaches the area of the magnetic resonator, for example, the perturbed coupling factor,  $k_{(p)}$ , may approach zero, making the use of the conducting surface incompatible with efficient wireless power transfer.

[00263] One approach to addressing the aforementioned problem is to place a layer of magnetic material around the high-conductivity materials because the additional layer of permeable material may present a lower reluctance path (compared to free space) for the deflected magnetic field to follow and may partially shield the electric conductor underneath it from incident magnetic flux. Under some circumstances the lower reluctance path presented by the magnetic material may improve the electromagnetic coupling of the resonator to other resonators. Decreases in the perturbed coupling factor associated with using conducting materials to tailor resonator fields so that they avoid lossy objects in and around high- $Q$  magnetic resonators may be at least partially recovered by including a layer of magnetic material along the outer surface or surfaces of the conducting materials. The magnetic materials may increase the perturbed coupling factor relative to its initial unperturbed value.

[00264] Note that the simulation results in Fig. 26 show that an incident magnetic field may be deflected less by a layered magnetic material and conducting structure than by a

conducting structure alone. If a magnetic resonator loop with a radius only slightly larger than that of the disks shown in Figs. 26(a) and 26(b) circumscribed the disks, it is clear that more flux lines would be captured in the case illustrated in Fig. 26(b) than in Fig. 26(a), and therefore  $k_{(disk)}$  would be larger for the case illustrated in Fig. 26(b). Therefore, including a layer of magnetic material on the conducting material may improve the overall system performance. System analyses may be performed to determine whether these materials should be partially, totally, or minimally integrated into the resonator.

**[00265]** As described above, Fig. 27 depicts a layered conductor 2706 and magnetic material 2702 structure that may be appropriate for use when not all of a lossy material 2708 may be covered by a conductor and/or magnetic material structure. It was shown earlier that for a copper conductor disk with a 20 cm diameter and a 2 cm height, circumscribed by a resonator with an inductor loop radius of 11 cm and a wire radius  $a=1$  mm, the calculated perturbing  $Q$  for the copper cylinder was 1,870. If the resonator and the conducting disk shell are placed in a uniform magnetic field (aligned along the axis of symmetry of the inductor loop), we calculate that the copper conductor has an associated coupling factor insensitivity of 0.34. For comparison, we model the same arrangement but include a 0.25 cm-thick layer of magnetic material with a real relative permeability,  $\mu_r' = 40$ , and an imaginary relative permeability,  $\mu_r'' = 10^{-2}$ . Using the same model and parameters described above, we find that the coupling factor insensitivity is improved to 0.64 by the addition of the magnetic material to the surface of the conductor.

**[00266]** Magnetic materials may be placed within the area circumscribed by the magnetic resonator to increase the coupling in wireless energy transfer systems. Consider a solid sphere of a magnetic material with relative permeability,  $\mu_r$ , placed in an initially uniform magnetic field. In this example, the lower reluctance path offered by the magnetic material may cause the magnetic field to concentrate in the volume of the sphere. We find that the magnetic flux through the area circumscribed by the equator of the sphere is enhanced by a factor of  $3\mu_r/(\mu_r + 2)$ , by the addition of the magnetic material. If  $\mu_r \gg 1$ , this enhancement factor may be close to 3.

**[00267]** One can also show that the dipole moment of a system comprising the magnetic sphere circumscribed by the inductive element in a magnetic resonator would have its magnetic dipole enhanced by the same factor. Thus, the magnetic sphere with high permeability practically triples the dipole magnetic coupling of the resonator. It is possible to keep most of

this increase in coupling if we use a spherical shell of magnetic material with inner radius  $a$ , and outer radius  $b$ , even if this shell is on top of block or enclosure made from highly conducting materials. In this case, the enhancement in the flux through the equator is

$$\frac{3\mu_r \left(1 - \left(\frac{a}{b}\right)^3\right)}{\mu_r \left(1 - \left(\frac{a}{b}\right)^3\right) + 2 \left(1 + \frac{1}{2} \left(\frac{a}{b}\right)^3\right)}$$

For  $\mu_r=1,000$  and  $(a/b)=0.99$ , this enhancement factor is still 2.73, so it possible to significantly improve the coupling even with thin layers of magnetic material.

**[00268]** As described above, structures containing magnetic materials may be used to realize magnetic resonators. Fig. 16(a) shows a 3 dimensional model of a copper and magnetic material structure 1600 driven by a square loop of current around the choke point at its center. Fig. 16(b) shows the interaction, indicated by magnetic field streamlines, between two identical structures 1600A-B with the same properties as the one shown in Fig. 16(a). Because of symmetry, and to reduce computational complexity, only one half of the system is modeled. If we fix the relative orientation between the two objects and vary their center-to-center distance (the image shown is at a relative separation of 50 cm), we find that, at 300 kHz, the coupling efficiency varies from 87% to 55% as the separation between the structures varies from 30 cm to 60 cm. Each of the example structures shown 1600 A-B includes two 20 cm x 8 cm x 2cm parallelepipeds made of copper joined by a 4 cm x 4 cm x 2 cm block of magnetic material and entirely covered with a 2 mm layer of the same magnetic material (assumed to have  $\mu_r=1,400+j5$ ). Resistive losses in the driving loop are ignored. Each structure has a calculated  $Q$  of 815.

**[00269]** ELECTROMAGNETIC RESONATORS AND IMPEDANCE MATCHING

**[00270]** Impedance Matching Architectures for Low-Loss Inductive Elements

**[00271]** For purposes of the present discussion, an inductive element may be any coil or loop structure (the 'loop') of any conducting material, with or without a (gapped or ungapped) core made of magnetic material, which may also be coupled inductively or in any other contactless way to other systems. The element is inductive because its impedance, including both



the impedance of the loop and the so-called 'reflected' impedances of any potentially coupled systems, has positive reactance,  $X$ , and resistance,  $R$ .

**[00272]** Consider an external circuit, such as a driving circuit or a driven load or a transmission line, to which an inductive element may be connected. The external circuit (e.g. a driving circuit) may be delivering power to the inductive element and the inductive element may be delivering power to the external circuit (e.g. a driven load). The efficiency and amount of power delivered between the inductive element and the external circuit at a desired frequency may depend on the impedance of the inductive element relative to the properties of the external circuit. Impedance-matching networks and external circuit control techniques may be used to regulate the power delivery between the external circuit and the inductive element, at a desired frequency,  $f$ .

**[00273]** The external circuit may be a driving circuit configured to form an amplifier of class A, B, C, D, DE, E, F and the like, and may deliver power at maximum efficiency (namely with minimum losses within the driving circuit) when it is driving a resonant network with specific impedance  $Z_o^*$ , where  $Z_o$  may be complex and  $*$  denotes complex conjugation. The external circuit may be a driven load configured to form a rectifier of class A, B, C, D, DE, E, F and the like, and may receive power at maximum efficiency (namely with minimum losses within the driven load) when it is driven by a resonant network with specific impedance  $Z_o^*$ , where  $Z_o$  may be complex. The external circuit may be a transmission line with characteristic impedance,  $Z_o$ , and may exchange power at maximum efficiency (namely with zero reflections) when connected to an impedance  $Z_o^*$ . We will call the characteristic impedance  $Z_o$  of an external circuit the complex conjugate of the impedance that may be connected to it for power exchange at maximum efficiency.

**[00274]** Typically the impedance of an inductive element,  $R+jX$ , may be much different from  $Z_o^*$ . For example, if the inductive element has low loss (a high  $X/R$ ), its resistance,  $R$ , may be much lower than the real part of the characteristic impedance,  $Z_o$ , of the external circuit. Furthermore, an inductive element by itself may not be a resonant network. An impedance-matching network connected to an inductive element may typically create a resonant network, whose impedance may be regulated.

[00275] Therefore, an impedance-matching network may be designed to maximize the efficiency of the power delivered between the external circuit and the inductive element (including the reflected impedances of any coupled systems). The efficiency of delivered power may be maximized by matching the impedance of the combination of an impedance-matching network and an inductive element to the characteristic impedance of an external circuit (or transmission line) at the desired frequency.

[00276] An impedance-matching network may be designed to deliver a specified amount of power between the external circuit and the inductive element (including the reflected impedances of any coupled systems). The delivered power may be determined by adjusting the complex ratio of the impedance of the combination of the impedance-matching network and the inductive element to the impedance of the external circuit (or transmission line) at the desired frequency.

[00277] Impedance-matching networks connected to inductive elements may create magnetic resonators. For some applications, such as wireless power transmission using strongly-coupled magnetic resonators, a high  $Q$  may be desired for the resonators. Therefore, the inductive element may be chosen to have low losses (high  $X/R$ ).

[00278] Since the matching circuit may typically include additional sources of loss inside the resonator, the components of the matching circuit may also be chosen to have low losses. Furthermore, in high-power applications and/or due to the high resonator  $Q$ , large currents may run in parts of the resonator circuit and large voltages may be present across some circuit elements within the resonator. Such currents and voltages may exceed the specified tolerances for particular circuit elements and may be too high for particular components to withstand. In some cases, it may be difficult to find or implement components, such as tunable capacitors for example, with size, cost and performance (loss and current/voltage-rating) specifications sufficient to realize high- $Q$  and high-power resonator designs for certain applications. We disclose matching circuit designs, methods, implementations and techniques that may preserve the high  $Q$  for magnetic resonators, while reducing the component requirements for low loss and/or high current/voltage-rating.

[00279] Matching-circuit topologies may be designed that minimize the loss and current-rating requirements on some of the elements of the matching circuit. The topology of a circuit matching a low-loss inductive element to an impedance,  $Z_0$ , may be chosen so that some

of its components lie outside the associated high-Q resonator by being in series with the external circuit. The requirements for low series loss or high current-ratings for these components may be reduced. Relieving the low series loss and/or high-current-rating requirement on a circuit element may be particularly useful when the element needs to be variable and/or to have a large voltage-rating and/or low parallel loss.

**[00280]** Matching-circuit topologies may be designed that minimize the voltage rating requirements on some of the elements of the matching circuit. The topology of a circuit matching a low-loss inductive element to an impedance,  $Z_0$ , may be chosen so that some of its components lie outside the associated high-Q resonator by being in parallel with  $Z_0$ . The requirements for low parallel loss or high voltage-rating for these components may be reduced. Relieving the low parallel loss and/or high-voltage requirement on a circuit element may be particularly useful when the element needs to be variable and/or to have a large current-rating and/or low series loss.

**[00281]** The topology of the circuit matching a low-loss inductive element to an external characteristic impedance,  $Z_0$ , may be chosen so that the field pattern of the associated resonant mode and thus its high  $Q$  are preserved upon coupling of the resonator to the external impedance. Otherwise inefficient coupling to the desired resonant mode may occur (potentially due to coupling to other undesired resonant modes), resulting in an effective lowering of the resonator  $Q$ .

**[00282]** For applications where the low-loss inductive element or the external circuit, may exhibit variations, the matching circuit may need to be adjusted dynamically to match the inductive element to the external circuit impedance,  $Z_0$ , at the desired frequency,  $f$ . Since there may typically be two tuning objectives, matching or controlling both the real and imaginary part of the impedance level,  $Z_0$ , at the desired frequency,  $f$ , there may be two variable elements in the matching circuit. For inductive elements, the matching circuit may need to include at least one variable capacitive element.

**[00283]** A low-loss inductive element may be matched by topologies using two variable capacitors, or two networks of variable capacitors. A variable capacitor may, for example, be a tunable butterfly-type capacitor having, e.g., a center terminal for connection to a ground or other lead of a power source or load, and at least one other terminal across which a

capacitance of the tunable butterfly-type capacitor can be varied or tuned, or any other capacitor having a user-configurable, variable capacitance.

**[00284]** A low-loss inductive element may be matched by topologies using one, or a network of, variable capacitor(s) and one, or a network of, variable inductor(s).

**[00285]** A low-loss inductive element may be matched by topologies using one, or a network of, variable capacitor(s) and one, or a network of, variable mutual inductance(s), which transformer-couple the inductive element either to an external circuit or to other systems.

**[00286]** In some cases, it may be difficult to find or implement tunable lumped elements with size, cost and performance specifications sufficient to realize high- $Q$ , high-power, and potentially high-speed, tunable resonator designs. The topology of the circuit matching a variable inductive element to an external circuit may be designed so that some of the variability is assigned to the external circuit by varying the frequency, amplitude, phase, waveform, duty cycle, and the like, of the drive signals applied to transistors, diodes, switches and the like, in the external circuit.

**[00287]** The variations in resistance,  $R$ , and inductance,  $L$ , of an inductive element at the resonant frequency may be only partially compensated or not compensated at all. Adequate system performance may thus be preserved by tolerances designed into other system components or specifications. Partial adjustments, realized using fewer tunable components or less capable tunable components, may be sufficient.

**[00288]** Matching-circuit architectures may be designed that achieve the desired variability of the impedance matching circuit under high-power conditions, while minimizing the voltage/current rating requirements on its tunable elements and achieving a finer (i.e. more precise, with higher resolution) overall tunability. The topology of the circuit matching a variable inductive element to an impedance,  $Z_0$ , may include appropriate combinations and placements of fixed and variable elements, so that the voltage/current requirements for the variable components may be reduced and the desired tuning range may be covered with finer tuning resolution. The voltage/current requirements may be reduced on components that are not variable.

**[00289]** The disclosed impedance matching architectures and techniques may be used to achieve the following:

- To maximize the power delivered to, or to minimize impedance mismatches between, the source low-loss inductive elements (and any other systems wirelessly coupled to them) from the power driving generators.
- To maximize the power delivered from, or to minimize impedance mismatches between, the device low-loss inductive elements (and any other systems wirelessly coupled to them) to the power driven loads.
- To deliver a controlled amount of power to, or to achieve a certain impedance relationship between, the source low-loss inductive elements (and any other systems wirelessly coupled to them) from the power driving generators.
- To deliver a controlled amount of power from, or to achieve a certain impedance relationship between, the device low-loss inductive elements (and any other systems wirelessly coupled to them) to the power driven loads.

**[00290]** TOPOLOGIES FOR PRESERVATION OF MODE PROFILE (HIGH- $Q$ )

**[00291]** The resonator structure may be designed to be connected to the generator or the load wirelessly (indirectly) or with a hard-wired connection (directly).

**[00292]** Consider a general indirectly coupled matching topology such as that shown by the block diagram in Fig. 28(a). There, an inductive element 2802, labeled as  $(R,L)$  and represented by the circuit symbol for an inductor, may be any of the inductive elements discussed in this disclosure or in the references provided herein, and where an impedance-matching circuit 2402 includes or consists of parts A and B. B may be the part of the matching circuit that connects the impedance 2804,  $Z_0$ , to the rest of the circuit (the combination of A and the inductive element  $(A+(R,L))$ ) via a wireless connection (an inductive or capacitive coupling mechanism).

**[00293]** The combination of A and the inductive element 2802 may form a resonator 102, which in isolation may support a high- $Q$  resonator electromagnetic mode, with an associated current and charge distribution. The lack of a wired connection between the external circuit,  $Z_0$  and B, and the resonator,  $A + (R,L)$ , may ensure that the high- $Q$  resonator electromagnetic mode and its current/charge distributions may take the form of its intrinsic (in-isolation) profile, so long as the degree of wireless coupling is not too large. That is, the electromagnetic mode, current/charge distributions, and thus the high- $Q$  of the resonator may be automatically maintained using an indirectly coupled matching topology.

[00294] This matching topology may be referred to as indirectly coupled, or transformer-coupled, or inductively-coupled, in the case where inductive coupling is used between the external circuit and the inductor loop. This type of coupling scenario was used to couple the power supply to the source resonator and the device resonator to the light bulb in the demonstration of wireless energy transfer over mid-range distances described in the referenced *Science* article.

[00295] Next consider examples in which the inductive element may include the inductive element and any indirectly coupled systems. In this case, as disclosed above, and again because of the lack of a wired connection between the external circuit or the coupled systems and the resonator, the coupled systems may not, with good approximation for not-too-large degree of indirect coupling, affect the resonator electromagnetic mode profile and the current/charge distributions of the resonator. Therefore, an indirectly-coupled matching circuit may work equally well for any general inductive element as part of a resonator as well as for inductive elements wirelessly-coupled to other systems, as defined herein. Throughout this disclosure, the matching topologies we disclose refer to matching topologies for a general inductive element of this type, that is, where any additional systems may be indirectly coupled to the low-loss inductive element, and it is to be understood that those additional systems do not greatly affect the resonator electromagnetic mode profile and the current/charge distributions of the resonator.

[00296] Based on the argument above, in a wireless power transmission system of any number of coupled source resonators, device resonators and intermediate resonators the wireless magnetic (inductive) coupling between resonators does not affect the electromagnetic mode profile and the current/charge distributions of each one of the resonators. Therefore, when these resonators have a high (unloaded and unperturbed)  $Q$ , their (unloaded and unperturbed)  $Q$  may be preserved in the presence of the wireless coupling. (Note that the loaded  $Q$  of a resonator may be reduced in the presence of wireless coupling to another resonator, but we may be interested in preserving the unloaded  $Q$ , which relates only to loss mechanisms and not to coupling/loading mechanisms.)

[00297] Consider a matching topology such as is shown in Fig. 28(b). The capacitors shown in Fig. 28(b) may represent capacitor circuits or networks. The capacitors shown may be used to form the resonator 102 and to adjust the frequency and/or impedance of the source and device resonators. This resonator 102 may be directly coupled to an impedance,  $Z_0$ , using the

ports labeled “terminal connections” 2808. Fig. 28(c) shows a generalized directly coupled matching topology, where the impedance-matching circuit 2602 includes or consists of parts A, B and C. Here, circuit elements in A, B and C may be considered part of the resonator 102 as well as part of the impedance matching 2402 (and frequency tuning) topology. B and C may be the parts of the matching circuit 2402 that connect the impedance  $Z_0$  2804 (or the network terminals) to the rest of the circuit (A and the inductive element) via a single wire connection each. Note that B and C could be empty (short-circuits). If we disconnect or open circuit parts B and C (namely those single wire connections), then, the combination of A and the inductive element (R,L) may form the resonator.

**[00298]** The high- $Q$  resonator electromagnetic mode may be such that the profile of the voltage distribution along the inductive element has nodes, namely positions where the voltage is zero. One node may be approximately at the center of the length of the inductive element, such as the center of the conductor used to form the inductive element, (with or without magnetic materials) and at least one other node may be within A. The voltage distribution may be approximately anti-symmetric along the inductive element with respect to its voltage node. A high  $Q$  may be maintained by designing the matching topology (A, B, C) and/or the terminal voltages ( $V_1$ ,  $V_2$ ) so that this high- $Q$  resonator electromagnetic mode distribution may be approximately preserved on the inductive element. This high- $Q$  resonator electromagnetic mode distribution may be approximately preserved on the inductive element by preserving the voltage node (approximately at the center) of the inductive element. Examples that achieve these design goals are provided herein.

**[00299]** A, B, and C may be arbitrary (namely not having any special symmetry), and  $V_1$  and  $V_2$  may be chosen so that the voltage across the inductive element is symmetric (voltage node at the center inductive). These results may be achieved using simple matching circuits but potentially complicated terminal voltages, because a topology-dependent common-mode signal  $(V_1+V_2)/2$  may be required on both terminals.

**[00300]** Consider an ‘axis’ that connects all the voltage nodes of the resonator, where again one node is approximately at the center of the length of the inductive element and the others within A. (Note that the ‘axis’ is really a set of points (the voltage nodes) within the electric-circuit topology and may not necessarily correspond to a linear axis of the actual physical structure. The ‘axis’ may align with a physical axis in cases where the physical structure

has symmetry.) Two points of the resonator are electrically symmetric with respect to the 'axis', if the impedances seen between each of the two points and a point on the 'axis', namely a voltage-node point of the resonator, are the same.

**[00301]** B and C may be the same ( $C=B$ ), and the two terminals may be connected to any two points of the resonator ( $A + (R,L)$ ) that are electrically symmetric with respect to the 'axis' defined above and driven with opposite voltages ( $V_2=-V_1$ ) as shown in Fig. 28(d). The two electrically symmetric points of the resonator 102 may be two electrically symmetric points on the inductor loop. The two electrically symmetric points of the resonator may be two electrically symmetric points inside A. If the two electrically symmetric points, (to which each of the equal parts B and C is connected), are inside A, A may need to be designed so that these electrically-symmetric points are accessible as connection points within the circuit. This topology may be referred to as a 'balanced drive' topology. These balanced-drive examples may have the advantage that any common-mode signal that may be present on the ground line, due to perturbations at the external circuitry or the power network, for example, may be automatically rejected (and may not reach the resonator). In some balanced-drive examples, this topology may require more components than other topologies.

**[00302]** In other examples, C may be chosen to be a short-circuit and the corresponding terminal to be connected to ground ( $V=0$ ) and to any point on the electric-symmetry (zero-voltage) 'axis' of the resonator, and B to be connected to any other point of the resonator not on the electric-symmetry 'axis', as shown in Fig. 28(e). The ground-connected point on the electric-symmetry 'axis' may be the voltage node on the inductive element, approximately at the center of its conductor length. The ground-connected point on the electric-symmetry 'axis' may be inside the circuit A. Where the ground-connected point on the electric-symmetry 'axis' is inside A, A may need to be designed to include one such point on the electrical-symmetric 'axis' that is electrically accessible, namely where connection is possible.

**[00303]** This topology may be referred to as an 'unbalanced drive' topology. The approximately anti-symmetric voltage distribution of the electromagnetic mode along the inductive element may be approximately preserved, even though the resonator may not be driven exactly symmetrically. The reason is that the high  $Q$  and the large associated R-vs.- $Z_0$  mismatch necessitate that a small current may run through B and ground, compared to the much larger current that may flow inside the resonator, ( $A+(R,L)$ ). In this scenario, the perturbation on the



resonator mode may be weak and the location of the voltage node may stay at approximately the center location of the inductive element. These unbalanced-drive examples may have the advantage that they may be achieved using simple matching circuits and that there is no restriction on the driving voltage at the V1 terminal. In some unbalanced-drive examples, additional designs may be required to reduce common-mode signals that may appear at the ground terminal.

**[00304]** The directly-coupled impedance-matching circuit, generally including or consisting of parts A, B and C, as shown in Fig. 28(c), may be designed so that the wires and components of the circuit do not perturb the electric and magnetic field profiles of the electromagnetic mode of the inductive element and/or the resonator and thus preserve the high resonator  $Q$ . The wires and metallic components of the circuit may be oriented to be perpendicular to the electric field lines of the electromagnetic mode. The wires and components of the circuit may be placed in regions where the electric and magnetic field of the electromagnetic mode are weak.

**[00305]** TOPOLOGIES FOR ALLEVIATING LOW-SERIES-LOSS AND HIGH-CURRENT-RATING REQUIREMENTS ON ELEMENTS

**[00306]** If the matching circuit used to match a small resistance,  $R$ , of a low-loss inductive element to a larger characteristic impedance,  $Z_0$ , of an external circuit may be considered lossless, then  $I_{Z_0}^2 Z_0 = I_R^2 R \leftrightarrow I_{Z_0} / I_R = \sqrt{R / Z_0}$  and the current flowing through the terminals is much smaller than the current flowing through the inductive element. Therefore, elements connected immediately in series with the terminals (such as in directly-coupled B, C (Fig. 28(c))) may not carry high currents. Then, even if the matching circuit has lossy elements, the resistive loss present in the elements in series with the terminals may not result in a significant reduction in the high- $Q$  of the resonator. That is, resistive loss in those series elements may not significantly reduce the efficiency of power transmission from  $Z_0$  to the inductive element or vice versa. Therefore, strict requirements for low-series-loss and/or high current-ratings may not be necessary for these components. In general, such reduced requirements may lead to a wider selection of components that may be designed into the high- $Q$  and/or high-power impedance matching and resonator topologies. These reduced requirements may be especially helpful in expanding the variety of variable and/or high voltage and/or low-parallel-loss components that may be used in these high- $Q$  and/or high-power impedance-matching circuits.

**[00307]** TOPOLOGIES FOR ALLEVIATING LOW-PARALLEL-LOSS AND HIGH-VOLTAGE-RATING REQUIREMENTS ON ELEMENTS

**[00308]** If, as above, the matching circuit used to match a small resistance,  $R$ , of a low-loss inductive element to a larger characteristic impedance,  $Z_0$ , of an external circuit is lossless, then using the previous analysis,

$$|V_{Z_0} / V_{load}| = |I_{Z_0} Z_0 / I_R (R + jX)| \approx \sqrt{R / Z_0} \cdot Z_0 / X = \sqrt{Z_0 / R} / (X / R),$$

and, for a low-loss (high- $X/R$ ) inductive element, the voltage across the terminals may be typically much smaller than the voltage across the inductive element. Therefore, elements connected immediately in parallel to the terminals may not need to withstand high voltages. Then, even if the matching circuit has lossy elements, the resistive loss present in the elements in parallel with the terminals may not result in a significant reduction in the high- $Q$  of the resonator. That is, resistive loss in those parallel elements may not significantly reduce the efficiency of power transmission from  $Z_0$  to the inductive element or vice versa. Therefore, strict requirements for low-parallel-loss and/or high voltage-ratings may not be necessary for these components. In general, such reduced requirements may lead to a wider selection of components that may be designed into the high- $Q$  and/or high-power impedance matching and resonator topologies. These reduced requirements may be especially helpful in expanding the variety of variable and/or high current and/or low-series-loss components that may be used in these high- $Q$  and/or high-power impedance-matching and resonator circuits.

**[00309]** Note that the design principles above may reduce currents and voltages on various elements differently, as they variously suggest the use of networks in series with  $Z_0$  (such as directly-coupled B, C) or the use of networks in parallel with  $Z_0$ . The preferred topology for a given application may depend on the availability of low-series-loss/high-current-rating or low-parallel-loss/high-voltage-rating elements.

**[00310]** COMBINATIONS OF FIXED AND VARIABLE ELEMENTS FOR ACHIEVING FINE TUNABILITY AND ALLEVIATING HIGH-RATING REQUIREMENTS ON VARIABLE ELEMENTS

**[00311]** Circuit topologies

**[00312]** Variable circuit elements with satisfactory low-loss and high-voltage or current ratings may be difficult or expensive to obtain. In this disclosure, we describe impedance-matching topologies that may incorporate combinations of fixed and variable elements, such that large voltages or currents may be assigned to fixed elements in the circuit,

which may be more likely to have adequate voltage and current ratings, and alleviating the voltage and current rating requirements on the variable elements in the circuit.

**[00313]** Variable circuit elements may have tuning ranges larger than those required by a given impedance-matching application and, in those cases, fine tuning resolution may be difficult to obtain using only such large-range elements. In this disclosure, we describe impedance-matching topologies that incorporate combinations of both fixed and variable elements, such that finer tuning resolution may be accomplished with the same variable elements.

**[00314]** Therefore, topologies using combinations of both fixed and variable elements may bring two kinds of advantages simultaneously: reduced voltage across, or current through, sensitive tuning components in the circuit and finer tuning resolution. Note that the maximum achievable tuning range may be related to the maximum reduction in voltage across, or current through, the tunable components in the circuit designs.

**[00315] Element topologies**

**[00316]** A single variable circuit-element (as opposed to the network of elements discussed above) may be implemented by a topology using a combination of fixed and variable components, connected in series or in parallel, to achieve a reduction in the rating requirements of the variable components and a finer tuning resolution. This can be demonstrated mathematically by the fact that:

$$\begin{aligned} \text{If } x_{|total|} &= x_{|fixed|} + x_{|variable|}, \\ \text{then } \Delta x_{|total|} / x_{|total|} &= \Delta x_{|variable|} / (x_{|fixed|} + x_{|variable|}), \\ \text{and } X_{variable} / X_{total} &= X_{variable} / (X_{fixed} + X_{variable}), \end{aligned}$$

where  $x_{|subscript|}$  is any element value (e.g. capacitance, inductance),  $X$  is voltage or current, and the “+ sign” denotes the appropriate (series-addition or parallel-addition) combination of elements. Note that the subscript format for  $x_{|subscript|}$ , is chosen to easily distinguish it from the radius of the area enclosed by a circular inductive element (e.g.  $x$ ,  $x_f$ , etc.).

**[00317]** Furthermore, this principle may be used to implement a variable electric element of a certain type (e.g. a capacitance or inductance) by using a variable element of a different type, if the latter is combined appropriately with other fixed elements.

**[00318]** In conclusion, one may apply a topology optimization algorithm that decides on the required number, placement, type and values of fixed and variable elements with the required tunable range as an optimization constraint and the minimization of the currents and/or voltages on the variable elements as the optimization objective.

**[00319] EXAMPLES**

**[00320]** In the following schematics, we show different specific topology implementations for impedance matching to and resonator designs for a low-loss inductive element. In addition, we indicate for each topology: which of the principles described above are used, the equations giving the values of the variable elements that may be used to achieve the matching, and the range of the complex impedances that may be matched (using both inequalities and a Smith-chart description). For these examples, we assume that  $Z_0$  is real, but an extension to a characteristic impedance with a non-zero imaginary part is straightforward, as it implies only a small adjustment in the required values of the components of the matching network. We will use the convention that the subscript,  $n$ , on a quantity implies normalization to (division by)  $Z_0$ .

**[00321]** Fig. 29 shows two examples of a transformer-coupled impedance-matching circuit, where the two tunable elements are a capacitor and the mutual inductance between two inductive elements. If we define respectively  $X_2 = \omega L_2$  for Fig. 29(a) and  $X_2 = \omega L_2 - 1/\omega C_2$  for Fig. 29(b), and  $X \equiv \omega L$ , then the required values of the tunable elements are:

$$\omega C_1 = \frac{1}{X + R X_{2n}}$$

$$\omega M = \sqrt{Z_0 R (1 + X_{2n}^2)}.$$

For the topology of Fig. 29(b), an especially straightforward design may be to choose  $X_2 = 0$ . In that case, these topologies may match the impedances satisfying the inequalities:

$$R_n > 0, X_n > 0,$$

which are shown by the area enclosed by the bold lines on the Smith chart of Fig. 29(c).

**[00322]** Given a well pre-chosen fixed  $M$ , one can also use the above matching topologies with a tunable  $C_2$  instead.

**[00323]** Fig. 30 shows six examples (a)-(f) of directly-coupled impedance-matching circuits, where the two tunable elements are capacitors, and six examples (h)-(m) of directly-coupled impedance-matching circuits, where the two tunable elements are one capacitor and one inductor. For the topologies of Figs. 30(a),(b),(c),(h),(i),(j), a common-mode signal may be required at the two terminals to preserve the voltage node of the resonator at the center of the inductive element and thus the high  $Q$ . Note that these examples may be described as implementations of the general topology shown in Fig. 28(c). For the symmetric topologies of Figs. 30(d),(e),(f),(k),(l),(m), the two terminals may need to be driven anti-symmetrically (balanced drive) to preserve the voltage node of the resonator at the center of the inductive element and thus the high  $Q$ . Note that these examples may be described as implementations of the general topology shown in Fig. 28(d). It will be appreciated that a network of capacitors, as used herein, may in general refer to any circuit topology including one or more capacitors, including without limitation any of the circuits specifically disclosed herein using capacitors, or any other equivalent or different circuit structure(s), unless another meaning is explicitly provided or otherwise clear from the context.

**[00324]** Let us define respectively  $Z=R+j\omega L$  for Figs. 30(a),(d),(h),(k),  $Z=R+j\omega L+1/j\omega C_3$  for Figs. 30(b),(e),(i),(l), and  $Z=(R+j\omega L)\|(1/j\omega C_3)$  for Figs. 30(c),(f),(j),(m), where the symbol “ $\|$ ” means “the parallel combination of”, and then  $R \equiv \text{Re}\{Z\}$ ,  $X \equiv \text{Im}\{Z\}$ . Then, for Figs.30(a)-(f) the required values of the tunable elements may be given by:

$$\omega C_1 = \frac{X - \sqrt{X^2 R_n - R^2 (1 - R_n)}}{X^2 + R^2},$$

$$\omega C_2 = \frac{R_n \omega C_1}{1 - X \omega C_1 - R_n},$$

and these topologies can match the impedances satisfying the inequalities:

$$R_n \leq 1, X_n \geq \sqrt{R_n (1 - R_n)}$$

which are shown by the area enclosed by the bold lines on the Smith chart of Fig. 30(g). For Figs.30(h)-(m) the required values of the tunable elements may be given by:

$$\omega C_1 = \frac{X + \sqrt{X^2 R_n - R^2 (1 - R_n)}}{X^2 + R^2},$$

$$\omega L_2 = -\frac{1 - X \omega C_1 - R_n}{R_n \omega C_1}.$$

[00325] Fig. 31 shows three examples (a)-(c) of directly-coupled impedance-matching circuits, where the two tunable elements are capacitors, and three examples (e)-(g) of directly-coupled impedance-matching circuits, where the two tunable elements are one capacitor and one inductor. For the topologies of Figs. 31(a),(b),(c),(e),(f),(g), the ground terminal is connected between two equal-value capacitors,  $2C_1$ , (namely on the axis of symmetry of the main resonator) to preserve the voltage node of the resonator at the center of the inductive element and thus the high  $Q$ . Note that these examples may be described as implementations of the general topology shown in Fig. 28(e).

[00326] Let us define respectively  $Z=R+j\omega L$  for Figs. 31(a),(e),  $Z=R+j\omega L+1/j\omega C_3$  for Figs. 31(b),(f), and  $Z=(R+j\omega L)\|(1/j\omega C_3)$  for Fig. 31(c),(g), and then  $R \equiv \text{Re}\{Z\}$ ,  $X \equiv \text{Im}\{Z\}$ . Then, for Figs.31(a)-(c) the required values of the tunable elements may be given by:

$$\omega C_1 = \frac{X - \frac{1}{2}\sqrt{X^2 R_n - R^2 (4 - R_n)}}{X^2 + R^2},$$

$$\omega C_2 = \frac{R_n \omega C_1}{1 - X \omega C_1 - \frac{R_n}{2}},$$

and these topologies can match the impedances satisfying the inequalities:

$$R_n \leq 1, \quad X_n \geq \sqrt{\frac{R_n}{1 - R_n}} (2 - R_n)$$

which are shown by the area enclosed by the bold lines on the Smith chart of Fig. 31(d). For Figs.31(e)-(g) the required values of the tunable elements may be given by:

$$\omega C_1 = \frac{X + \frac{1}{2} \sqrt{X^2 R_n - R^2 (4 - R_n)}}{X^2 + R^2},$$

$$\omega L_2 = -\frac{1 - X \omega C_1 - \frac{R_n}{2}}{R_n \omega C_1}.$$

[00327] Fig. 32 shows three examples (a)-(c) of directly-coupled impedance-matching circuits, where the two tunable elements are capacitors, and three examples (e)-(g) of directly-coupled impedance-matching circuits, where the two tunable elements are one capacitor and one inductor. For the topologies of Figs. 32(a),(b),(c),(e),(f),(g), the ground terminal may be connected at the center of the inductive element to preserve the voltage node of the resonator at that point and thus the high  $Q$ . Note that these example may be described as implementations of the general topology shown in Fig. 28(e).

[00328] Let us define respectively  $Z=R+j\omega L$  for Fig. 32(a),  $Z=R+j\omega L+1/j\omega C_3$  for Fig. 32(b), and  $Z=(R+j\omega L)\|(1/j\omega C_3)$  for Fig. 32(c), and then  $R \equiv \text{Re}\{Z\}$ ,  $X \equiv \text{Im}\{Z\}$ . Then, for Figs.32(a)-(c) the required values of the tunable elements may be given by:

$$\omega C_1 = \frac{X - \sqrt{X^2 R_n - 2R^2 (2 - R_n)}}{X^2 + R^2},$$

$$\omega C_2 = \frac{R_n \omega C_1}{1 - X \omega C_1 - \frac{R_n}{2} + \frac{R_n X \omega C_1}{2(1+k)}},$$

where  $k$  is defined by  $M' = -kL'$ , where  $L'$  is the inductance of each half of the inductor loop and  $M'$  is the mutual inductance between the two halves, and these topologies can match the impedances satisfying the inequalities:

$$R_n \leq 2, \quad X_n \geq \sqrt{2R_n(2 - R_n)}$$

which are shown by the area enclosed by the bold lines on the Smith chart of Fig. 32(d).

For Figs.32(e)-(g) the required values of the tunable elements may be given by:

$$\omega C_1 = \frac{X + \sqrt{\frac{X^2 R_n - 2R^2(2 - R_n)}{4 - R_n}}}{X^2 + R^2},$$

**[00329]** In the circuits of Figs. 30, 31, 32, the capacitor,  $C_2$ , or the inductor,  $L_2$ , is (or the two capacitors,  $2C_2$ , or the two inductors,  $L_2/2$ , are) in series with the terminals and may not need to have very low series-loss or withstand a large current.

**[00330]** Fig. 33 shows six examples (a)-(f) of directly-coupled impedance-matching circuits, where the two tunable elements are capacitors, and six examples (h)-(m) of directly-coupled impedance-matching circuits, where the two tunable elements are one capacitor and one inductor. For the topologies of Figs. 33(a),(b),(c),(h),(i),(j), a common-mode signal may be required at the two terminals to preserve the voltage node of the resonator at the center of the inductive element and thus the high  $Q$ . Note that these examples may be described as implementations of the general topology shown in Fig. 28(c), where B and C are short-circuits and A is not balanced. For the symmetric topologies of Figs. 33(d),(e),(f),(k),(l),(m), the two terminals may need to be driven anti-symmetrically (balanced drive) to preserve the voltage node of the resonator at the center of the inductive element and thus the high  $Q$ . Note that these examples may be described as implementations of the general topology shown in Fig. 28(d), where B and C are short-circuits and A is balanced.

**[00331]** Let us define respectively  $Z=R+j\omega L$  for Figs. 33(a),(d),(h),(k),  $Z=R+j\omega L+1/j\omega C_3$  for Figs. 33(b),(e),(i),(l), and  $Z=(R+j\omega L)\|(1/j\omega C_3)$  for Figs. 33(c),(f),(j),(m), and then  $R \equiv \text{Re}\{Z\}$ ,  $X \equiv \text{Im}\{Z\}$ . Then, for Figs.33(a)-(f) the required values of the tunable elements may be given by:

$$\omega C_1 = \frac{1}{X - Z_o \sqrt{R_n(1 - R_n)}},$$

$$\omega C_2 = \frac{1}{Z_o} \sqrt{\frac{1}{R_n} - 1},$$

and these topologies can match the impedances satisfying the inequalities:



$$R_n \leq 1, \quad X_n \geq \sqrt{R_n(1-R_n)}$$

which are shown by the area enclosed by the bold lines on the Smith chart of Fig. 33(g). For Figs.35(h)-(m) the required values of the tunable elements may be given by:

$$\omega C_1 = \frac{1}{X + Z_o \sqrt{R_n(1-R_n)}},$$

$$\omega L_2 = \frac{Z_o}{\sqrt{\frac{1}{R_n} - 1}}.$$

**[00332]** Fig. 34 shows three examples (a)-(c) of directly-coupled impedance-matching circuits, where the two tunable elements are capacitors, and three examples (e)-(g) of directly-coupled impedance-matching circuits, where the two tunable elements are one capacitor and one inductor. For the topologies of Figs. 34(a),(b),(c),(e),(f),(g), the ground terminal is connected between two equal-value capacitors,  $2C_2$ , (namely on the axis of symmetry of the main resonator) to preserve the voltage node of the resonator at the center of the inductive element and thus the high  $Q$ . Note that these examples may be described as implementations of the general topology shown in Fig. 28(e).

**[00333]** Let us define respectively  $Z=R+j\omega L$  for Fig. 34(a),(e),  $Z=R+j\omega L+1/j\omega C_3$  for Fig. 34(b),(f), and  $Z=(R+j\omega L)\|(1/j\omega C_3)$  for Fig. 34(c),(g), and then  $R \equiv \text{Re}\{Z\}$ ,  $X \equiv \text{Im}\{Z\}$ . Then, for Figs.34(a)-(c) the required values of the tunable elements may be given by:

$$\omega C_1 = \frac{1}{X - Z_o \sqrt{\frac{1-R_n}{R_n}}(2-R_n)},$$

$$\omega C_2 = \frac{1}{2Z_o} \sqrt{\frac{1}{R_n} - 1},$$

and these topologies can match the impedances satisfying the inequalities:

$$R_n \leq 1, X_n \geq \sqrt{\frac{R_n}{1-R_n}}(2-R_n)$$

which are shown by the area enclosed by the bold lines on the Smith chart of Fig. 34(d). For Figs.34(e)-(g) the required values of the tunable elements may be given by:

$$\omega C_1 = \frac{1}{X + Z_o \sqrt{\frac{1-R_n}{R_n}}(2-R_n)},$$

$$\omega L_2 = \frac{2Z_o}{\sqrt{\frac{1}{R_n}-1}}.$$

**[00334]** Fig. 35 shows three examples of directly-coupled impedance-matching circuits, where the two tunable elements are capacitors. For the topologies of Figs. 35, the ground terminal may be connected at the center of the inductive element to preserve the voltage node of the resonator at that point and thus the high  $Q$ . Note that these examples may be described as implementations of the general topology shown in Fig. 28(e).

**[00335]** Let us define respectively  $Z=R+j\omega L$  for Fig. 35(a),  $Z=R+j\omega L+1/j\omega C_3$  for Fig. 35(b), and  $Z=(R+j\omega L)\|(1/j\omega C_3)$  for Fig. 35(c), and then  $R \equiv \text{Re}\{Z\}$ ,  $X \equiv \text{Im}\{Z\}$ . Then, the required values of the tunable elements may be given by:

$$\omega C_1 = \frac{2}{X(1+a) - \sqrt{Z_o R(4-R_n)(1+a^2)}},$$

$$\omega C_2 = \frac{2}{X(1+a) + \sqrt{Z_o R(4-R_n)(1+a^2)}},$$

where  $a = \frac{R}{2Z_o - R} \cdot \frac{k}{1+k}$  and  $k$  is defined by  $M' = -kL'$ , where  $L'$  is the inductance of each half of the inductive element and  $M'$  is the mutual inductance between the two halves. These topologies can match the impedances satisfying the inequalities:

$$R_n \leq 2 \& \frac{2}{\gamma} \leq R_n \leq 4,$$

$$X_n \geq \sqrt{\frac{R_n(4-R_n)(2-R_n)}{2-\gamma R_n}},$$

where

$$\gamma = \frac{1-6k+k^2}{1+2k+k^2} \leq 1$$

which are shown by the area enclosed by the bold lines on the three Smith charts shown in Fig. 35(d) for  $k=0$ , Fig. 35(e) for  $k=0.05$ , and Fig. 35(f) for  $k=1$ . Note that for  $0 < k < 1$  there are two disconnected regions of the Smith chart that this topology can match.

**[00336]** In the circuits of Figs. 33, 34, 35, the capacitor,  $C_2$ , or the inductor,  $L_2$ , is (or one of the two capacitors,  $2C_2$ , or one of the two inductors,  $2L_2$ , are) in parallel with the terminals and thus may not need to have a high voltage-rating. In the case of two capacitors,  $2C_2$ , or two inductors,  $2L_2$ , both may not need to have a high voltage-rating, since approximately the same current flows through them and thus they experience approximately the same voltage across them.

**[00337]** For the topologies of Figs. 30-35, where a capacitor,  $C_3$ , is used, the use of the capacitor,  $C_3$ , may lead to finer tuning of the frequency and the impedance. For the topologies of Figs. 30-35, the use of the fixed capacitor,  $C_3$ , in series with the inductive element may ensure that a large percentage of the high inductive-element voltage will be across this fixed capacitor,  $C_3$ , thus potentially alleviating the voltage rating requirements for the other elements of the impedance matching circuit, some of which may be variable. Whether or not such topologies are preferred depends on the availability, cost and specifications of appropriate fixed and tunable components.

**[00338]** In all the above examples, a pair of equal-value variable capacitors without a common terminal may be implemented using ganged-type capacitors or groups or arrays of varactors or diodes biased and controlled to tune their values as an ensemble. A pair of equal-value variable capacitors with one common terminal can be implemented using a tunable butterfly-type capacitor or any other tunable or variable capacitor or group or array of varactors or diodes biased and controlled to tune their capacitance values as an ensemble.

**[00339]** Another criterion which may be considered upon the choice of the impedance matching network is the response of the network to different frequencies than the desired

operating frequency. The signals generated in the external circuit, to which the inductive element is coupled, may not be monochromatic at the desired frequency but periodic with the desired frequency, as for example the driving signal of a switching amplifier or the reflected signal of a switching rectifier. In some such cases, it may be desirable to suppress the amount of higher-order harmonics that enter the inductive element (for example, to reduce radiation of these harmonics from this element). Then the choice of impedance matching network may be one that sufficiently suppresses the amount of such harmonics that enters the inductive element.

**[00340]** The impedance matching network may be such that the impedance seen by the external circuit at frequencies higher than the fundamental harmonic is high, when the external periodic signal is a signal that can be considered to behave as a voltage-source signal (such as the driving signal of a class-D amplifier with a series resonant load), so that little current flows through the inductive element at higher frequencies. Among the topologies of Figs. 30-35, those which use an inductor,  $L_2$ , may then be preferable, as this inductor presents a high impedance at high frequencies.

**[00341]** The impedance matching network may be such that the impedance seen by the external circuit at frequencies higher than the fundamental harmonic is low, when the external periodic signal is a signal that can be considered to behave as a current-source signal, so that little voltage is induced across the inductive element at higher frequencies. Among the topologies of Figs. 30-35, those which use a capacitor,  $C_2$ , are then preferable, as this capacitor presents a low impedance at high frequencies.

**[00342]** Fig. 36 shows four examples of a variable capacitance, using networks of one variable capacitor and the rest fixed capacitors. Using these network topologies, fine tunability of the total capacitance value may be achieved. Furthermore, the topologies of Figs. 36(a),(c),(d), may be used to reduce the voltage across the variable capacitor, since most of the voltage may be assigned across the fixed capacitors.

**[00343]** Fig. 37 shows two examples of a variable capacitance, using networks of one variable inductor and fixed capacitors. In particular, these networks may provide implementations for a variable reactance, and, at the frequency of interest, values for the variable inductor may be used such that each network corresponds to a net negative variable reactance, which may be effectively a variable capacitance.

**[00344]** Tunable elements such as tunable capacitors and tunable inductors may be mechanically-tunable, electrically-tunable, thermally-tunable and the like. The tunable elements may be variable capacitors or inductors, varactors, diodes, Schottky diodes, reverse-biased PN diodes, varactor arrays, diode arrays, Schottky diode arrays and the like. The diodes may be Si diodes, GaN diodes, SiC diodes, and the like. GaN and SiC diodes may be particularly attractive for high power applications. The tunable elements may be electrically switched capacitor banks, electrically-switched mechanically-tunable capacitor banks, electrically-switched varactor-array banks, electrically-switched transformer-coupled inductor banks, and the like. The tunable elements may be combinations of the elements listed above.

**[00345]** As described above, the efficiency of the power transmission between coupled high-Q magnetic resonators may be impacted by how closely matched the resonators are in resonant frequency and how well their impedances are matched to the power supplies and power consumers in the system. Because a variety of external factors including the relative position of extraneous objects or other resonators in the system, or the changing of those relative positions, may alter the resonant frequency and/or input impedance of a high-Q magnetic resonator, tunable impedance networks may be required to maintain sufficient levels of power transmission in various environments or operating scenarios.

**[00346]** The capacitance values of the capacitors shown may be adjusted to adjust the resonant frequency and/or the impedance of the magnetic resonator. The capacitors may be adjusted electrically, mechanically, thermally, or by any other known methods. They may be adjusted manually or automatically, such as in response to a feedback signal. They may be adjusted to achieve certain power transmission efficiencies or other operating characteristics between the power supply and the power consumer.

**[00347]** The inductance values of the inductors and inductive elements in the resonator may be adjusted to adjust the frequency and/or impedance of the magnetic resonator. The inductance may be adjusted using coupled circuits that include adjustable components such as tunable capacitors, inductors and switches. The inductance may be adjusted using transformer coupled tuning circuits. The inductance may be adjusted by switching in and out different sections of conductor in the inductive elements and/or using ferro-magnetic tuning and/or mu-tuning, and the like.

[00348] The resonant frequency of the resonators may be adjusted to or may be allowed to change to lower or higher frequencies. The input impedance of the resonator may be adjusted to or may be allowed to change to lower or higher impedance values. The amount of power delivered by the source and/or received by the devices may be adjusted to or may be allowed to change to lower or higher levels of power. The amount of power delivered to the source and/or received by the devices from the device resonator may be adjusted to or may be allowed to change to lower or higher levels of power. The resonator input impedances, resonant frequencies, and power levels may be adjusted depending on the power consumer or consumers in the system and depending on the objects or materials in the vicinity of the resonators. The resonator input impedances, frequencies, and power levels may be adjusted manually or automatically, and may be adjusted in response to feedback or control signals or algorithms.

[00349] Circuit elements may be connected directly to the resonator, that is, by physical electrical contact, for example to the ends of the conductor that forms the inductive element and/or the terminal connectors. The circuit elements may be soldered to, welded to, crimped to, glued to, pinched to, or closely position to the conductor or attached using a variety of electrical components, connectors or connection techniques. The power supplies and the power consumers may be connected to magnetic resonators directly or indirectly or inductively. Electrical signals may be supplied to, or taken from, the resonators through the terminal connections.

[00350] It is to be understood by one of ordinary skill in the art that in real implementations of the principles described herein, there may be an associated tolerance, or acceptable variation, to the values of real components (capacitors, inductors, resistors and the like) from the values calculated via the herein stated equations, to the values of real signals (voltages, currents and the like) from the values suggested by symmetry or anti-symmetry or otherwise, and to the values of real geometric locations of points (such as the point of connection of the ground terminal close to the center of the inductive element or the 'axis' points and the like) from the locations suggested by symmetry or otherwise.

[00351] **Examples**

[00352] **SYSTEM BLOCK DIAGRAMS**

[00353] We disclose examples of high-Q resonators for wireless power transmission systems that may wirelessly power or charge devices at mid-range distances. High-Q resonator

wireless power transmission systems also may wirelessly power or charge devices with magnetic resonators that are different in size, shape, composition, arrangement, and the like, from any source resonators in the system.

**[00354]** Fig. 1(a)(b) shows high level diagrams of two exemplary two-resonator systems. These exemplary systems each have a single source resonator 102S or 104S and a single device resonator 102D or 104D. Fig. 38 shows a high level block diagram of a system with a few more features highlighted. The wirelessly powered or charged device 2310 may include or consist of a device resonator 102D, device power and control circuitry 2304, and the like, along with the device 2308 or devices, to which either DC or AC or both AC and DC power is transferred. The energy or power source for a system may include the source power and control circuitry 2302, a source resonator 102S, and the like. The device 2308 or devices that receive power from the device resonator 102D and power and control circuitry 2304 may be any kind of device 2308 or devices as described previously. The device resonator 102D and circuitry 2304 delivers power to the device/devices 2308 that may be used to recharge the battery of the device/devices, power the device/devices directly, or both when in the vicinity of the source resonator 102S.

**[00355]** The source and device resonators may be separated by many meters or they may be very close to each other or they may be separated by any distance in between. The source and device resonators may be offset from each other laterally or axially. The source and device resonators may be directly aligned (no lateral offset), or they may be offset by meters, or anything in between. The source and device resonators may be oriented so that the surface areas enclosed by their inductive elements are approximately parallel to each other. The source and device resonators may be oriented so that the surface areas enclosed by their inductive elements are approximately perpendicular to each other, or they may be oriented for any relative angle (0 to 360 degrees) between them.

**[00356]** The source and device resonators may be free standing or they may be enclosed in an enclosure, container, sleeve or housing. These various enclosures may be composed of almost any kind of material. Low loss tangent materials such as Teflon, REXOLITE, styrene, and the like may be preferable for some applications. The source and device resonators may be integrated in the power supplies and power consumers. For example, the source and device resonators may be integrated into keyboards, computer mice, displays, cell

phones, etc. so that they are not visible outside these devices. The source and device resonators may be separate from the power supplies and power consumers in the system and may be connected by a standard or custom wires, cables, connectors or plugs.

**[00357]** The source 102S may be powered from a number of DC or AC voltage, current or power sources including a USB port of a computer. The source 102S may be powered from the electric grid, from a wall plug, from a battery, from a power supply, from an engine, from a solar cell, from a generator, from another source resonator, and the like. The source power and control circuitry 2302 may include circuits and components to isolate the source electronics from the power source, so that any reflected power or signals are not coupled out through the source input terminals. The source power and control circuits 2302 may include power factor correction circuits and may be configured to monitor power usage for monitoring accounting, billing, control, and like functionalities.

**[00358]** The system may be operated bi-directionally. That is, energy or power that is generated or stored in a device resonator may be fed back to a power source including the electric grid, a battery, any kind of energy storage unit, and the like. The source power and control circuits may include power factor correction circuits and may be configured to monitor power usage for monitoring accounting, billing, control, and like functionalities for bi-directional energy flow. Wireless energy transfer systems may enable or promote vehicle-to-grid (V2G) applications.

**[00359]** The source and the device may have tuning capabilities that allow adjustment of operating points to compensate for changing environmental conditions, perturbations, and loading conditions that can affect the operation of the source and device resonators and the efficiency of the energy exchange. The tuning capability may also be used to multiplex power delivery to multiple devices, from multiple sources, to multiple systems, to multiple repeaters or relays, and the like. The tuning capability may be manually controlled, or automatically controlled and may be performed continuously, periodically, intermittently or at scheduled times or intervals.

**[00360]** The device resonator and the device power and control circuitry may be integrated into any portion of the device, such as a battery compartment, or a device cover or sleeve, or on a mother board, for example, and may be integrated alongside standard rechargeable batteries or other energy storage units. The device resonator may include a device



field reshaper which may shield any combination of the device resonator elements and the device power and control electronics from the electromagnetic fields used for the power transfer and which may deflect the resonator fields away from the lossy device resonator elements as well as the device power and control electronics. A magnetic material and/or high-conductivity field reshaper may be used to increase the perturbed quality factor  $Q$  of the resonator and increase the perturbed coupling factor of the source and device resonators.

[00361] The source resonator and the source power and control circuitry may be integrated into any type of furniture, structure, mat, rug, picture frame (including digital picture frames, electronic frames), plug-in modules, electronic devices, vehicles, and the like. The source resonator may include a source field reshaper which may shield any combination of the source resonator elements and the source power and control electronics from the electromagnetic fields used for the power transfer and which may deflect the resonator fields away from the lossy source resonator elements as well as the source power and control electronics. A magnetic material and/or high-conductivity field reshaper may be used to increase the perturbed quality factor  $Q$  of the resonator and increase the perturbed coupling factor of the source and device resonators.

[00362] A block diagram of the subsystems in an example of a wirelessly powered device is shown in Fig. 39. The power and control circuitry may be designed to transform the alternating current power from the device resonator 102D and convert it to stable direct current power suitable for powering or charging a device. The power and control circuitry may be designed to transform an alternating current power at one frequency from the device resonator to alternating current power at a different frequency suitable for powering or charging a device. The power and control circuitry may include or consist of impedance matching circuitry 2402D, rectification circuitry 2404, voltage limiting circuitry (not shown), current limiting circuitry (not shown), AC-to-DC converter 2408 circuitry, DC-to-DC converter 2408 circuitry, DC-to-AC converter 2408 circuitry, AC-to-AC converter 2408 circuitry, battery charge control circuitry (not shown), and the like.

[00363] The impedance-matching 2402D network may be designed to maximize the power delivered between the device resonator 102D and the device power and control circuitry 2304 at the desired frequency. The impedance matching elements may be chosen and connected such that the high- $Q$  of the resonators is preserved. Depending on the operating conditions, the

impedance matching circuitry 2402D may be varied or tuned to control the power delivered from the source to the device, from the source to the device resonator, between the device resonator and the device power and control circuitry, and the like. The power, current and voltage signals may be monitored at any point in the device circuitry and feedback algorithms circuits, and techniques, may be used to control components to achieve desired signal levels and system operation. The feedback algorithms may be implemented using analog or digital circuit techniques and the circuits may include a microprocessor, a digital signal processor, a field programmable gate array processor and the like.

**[00364]** The third block of Fig. 39 shows a rectifier circuit 2404 that may rectify the AC voltage power from the device resonator into a DC voltage. In this configuration, the output of the rectifier 2404 may be the input to a voltage clamp circuit. The voltage clamp circuit (not shown) may limit the maximum voltage at the input to the DC-to-DC converter 2408D or DC-to-AC converter 2408D. In general, it may be desirable to use a DC-to-DC/AC converter with a large input voltage dynamic range so that large variations in device position and operation may be tolerated while adequate power is delivered to the device. For example, the voltage level at the output of the rectifier may fluctuate and reach high levels as the power input and load characteristics of the device change. As the device performs different tasks it may have varying power demands. The changing power demands can cause high voltages at the output of the rectifier as the load characteristics change. Likewise as the device and the device resonator are brought closer and further away from the source, the power delivered to the device resonator may vary and cause changes in the voltage levels at the output of the rectifier. A voltage clamp circuit may prevent the voltage output from the rectifier circuit from exceeding a predetermined value which is within the operating range of the DC-to-DC/AC converter. The voltage clamp circuitry may be used to extend the operating modes and ranges of a wireless energy transfer system.

**[00365]** The next block of the power and control circuitry of the device is the DC-to-DC converter 2408D that may produce a stable DC output voltage. The DC-to-DC converter may be a boost converter, buck converter, boost-buck converter, single ended primary inductance converter (SEPIC), or any other DC-DC topology that fits the requirements of the particular application. If the device requires AC power, a DC-to-AC converter may be substituted for the DC-to-DC converter, or the DC-to-DC converter may be followed by a DC-

to-AC converter. If the device contains a rechargeable battery, the final block of the device power and control circuitry may be a battery charge control unit which may manage the charging and maintenance of the battery in battery powered devices.

**[00366]** The device power and control circuitry 2304 may contain a processor 2410D, such as a microcontroller, a digital signal processor, a field programmable gate array processor, a microprocessor, or any other type of processor. The processor may be used to read or detect the state or the operating point of the power and control circuitry and the device resonator. The processor may implement algorithms to interpret and adjust the operating point of the circuits, elements, components, subsystems and resonator. The processor may be used to adjust the impedance matching, the resonator, the DC to DC converters, the DC to AC converters, the battery charging unit, the rectifier, and the like of the wirelessly powered device.

**[00367]** The processor may have wireless or wired data communication links to other devices or sources and may transmit or receive data that can be used to adjust the operating point of the system. Any combination of power, voltage, and current signals at a single, or over a range of frequencies, may be monitored at any point in the device circuitry. These signals may be monitored using analog or digital or combined analog and digital techniques. These monitored signals may be used in feedback loops or may be reported to the user in a variety of known ways or they may be stored and retrieved at later times. These signals may be used to alert a user of system failures, to indicate performance, or to provide audio, visual, vibrational, and the like, feedback to a user of the system.

**[00368]** Fig. 40 shows components of source power and control circuitry 2302 of an exemplary wireless power transfer system configured to supply power to a single or multiple devices. The source power and control circuitry 2302 of the exemplary system may be powered from an AC voltage source 2502 such as a home electrical outlet, a DC voltage source such as a battery, a USB port of a computer, a solar cell, another wireless power source, and the like. The source power and control circuitry 2302 may drive the source resonator 102S with alternating current, such as with a frequency greater than 10 kHz and less than 100 MHz. The source power and control circuitry 2302 may drive the source resonator 102S with alternating current of frequency less than less than 10 GHz. The source power and control circuitry 2302 may include a DC-to-DC converter 2408S, an AC-to-DC converter 2408S, or both an AC-to-DC converter

2408S and a DC-to-DC 2408S converter, an oscillator 2508, a power amplifier 2504, an impedance matching network 2402S, and the like.

[00369] The source power and control circuitry 2302 may be powered from multiple AC-or-DC voltage sources 2502 and may contain AC-to-DC and DC-to-DC converters 2408S to provide necessary voltage levels for the circuit components as well as DC voltages for the power amplifiers that may be used to drive the source resonator. The DC voltages may be adjustable and may be used to control the output power level of the power amplifier. The source may contain power factor correction circuitry.

[00370] The oscillator 2508 output may be used as the input to a power amplifier 2504 that drives the source resonator 102S. The oscillator frequency may be tunable and the amplitude of the oscillator signal may be varied as one means to control the output power level from the power amplifier. The frequency, amplitude, phase, waveform, and duty cycle of the oscillator signal may be controlled by analog circuitry, by digital circuitry or by a combination of analog and digital circuitry. The control circuitry may include a processor 2410S, such as a microprocessor, a digital signal processor, a field programmable gate array processor, and the like.

[00371] The impedance matching blocks 2402 of the source and device resonators may be used to tune the power and control circuits and the source and device resonators. For example, tuning of these circuits may adjust for perturbation of the quality factor  $Q$  of the source or device resonators due to extraneous objects or changes in distance between the source and device in a system. Tuning of these circuits may also be used to sense the operating environment, control power flow to one or more devices, to control power to a wireless power network, to reduce power when unsafe or failure mode conditions are detected, and the like.

[00372] Any combination of power, voltage, and current signals may be monitored at any point in the source circuitry. These signals may be monitored using analog or digital or combined analog and digital techniques. These monitored signals may be used in feedback circuits or may be reported to the user in a variety of known ways or they may be stored and retrieved at later times. These signals may be used to alert a user to system failures, to alert a user to exceeded safety thresholds, to indicate performance, or to provide audio, visual, vibrational, and the like, feedback to a user of the system.

**[00373]** The source power and control circuitry may contain a processor. The processor may be used to read the state or the operating point of the power and control circuitry and the source resonator. The processor may implement algorithms to interpret and adjust the operating point of the circuits, elements, components, subsystems and resonator. The processor may be used to adjust the impedance matching, the resonator, the DC-to-DC converters, the AC-to-DC converters, the oscillator, the power amplifier of the source, and the like. The processor and adjustable components of the system may be used to implement frequency and/or time power delivery multiplexing schemes. The processor may have wireless or wired data communication links to devices and other sources and may transmit or receive data that can be used to adjust the operating point of the system.

**[00374]** Although detailed and specific designs are shown in these block diagrams, it should be clear to those skilled in the art that many different modifications and rearrangements of the components and building blocks are possible within the spirit of the exemplary system. The division of the circuitry was outlined for illustrative purposes and it should be clear to those skilled in the art that the components of each block may be further divided into smaller blocks or merged or shared. In equivalent examples the power and control circuitry may be composed of individual discrete components or larger integrated circuits. For example, the rectifier circuitry may be composed of discrete diodes, or use diodes integrated on a single chip. A multitude of other circuits and integrated devices can be substituted in the design depending on design criteria such as power or size or cost or application. The whole of the power and control circuitry or any portion of the source or device circuitry may be integrated into one chip.

**[00375]** The impedance matching network of the device and or source may include a capacitor or networks of capacitors, an inductor or networks of inductors, or any combination of capacitors, inductors, diodes, switches, resistors, and the like. The components of the impedance matching network may be adjustable and variable and may be controlled to affect the efficiency and operating point of the system. The impedance matching may be performed by controlling the connection point of the resonator, adjusting the permeability of a magnetic material, controlling a bias field, adjusting the frequency of excitation, and the like. The impedance matching may use or include any number or combination of varactors, varactor arrays, switched elements, capacitor banks, switched and tunable elements, reverse bias diodes, air gap capacitors, compression capacitors, BZT electrically tuned capacitors, MEMS-tunable capacitors, voltage variable

dielectrics, transformer coupled tuning circuits, and the like. The variable components may be mechanically tuned, thermally tuned, electrically tuned, piezo-electrically tuned, and the like. Elements of the impedance matching may be silicon devices, gallium nitride devices, silicon carbide devices and the like. The elements may be chosen to withstand high currents, high voltages, high powers, or any combination of current, voltage and power. The elements may be chosen to be high- $Q$  elements.

[00376] The matching and tuning calculations of the source may be performed on an external device through a USB port that powers the device. The device may be a computer a PDA or other computational platform.

[00377] A demonstration system used a source resonator, coupled to a device resonator, to wirelessly power/recharge multiple electronic consumer devices including, but not limited to, a laptop, a DVD player, a projector, a cell-phone, a display, a television, a projector, a digital picture frame, a light, a TV/DVD player, a portable music player, a circuit breaker, a hand-held tool, a personal digital assistant, an external battery charger, a mouse, a keyboard, a camera, an active load, and the like. A variety of devices may be powered simultaneously from a single device resonator. Device resonators may be operated simultaneously as source resonators. The power supplied to a device resonator may pass through additional resonators before being delivered to its intended device resonator.

[00378] *Monitoring, Feedback and Control*

[00379] So-called port parameter measurement circuitry may measure or monitor certain power, voltage, and current, signals in the system and processors or control circuits may adjust certain settings or operating parameters based on those measurements. In addition to these port parameter measurements, the magnitude and phase of voltage and current signals, and the magnitude of the power signals, throughout the system may be accessed to measure or monitor the system performance. The measured signals referred to throughout this disclosure may be any combination of the port parameter signals, as well as voltage signals, current signals, power signals, and the like. These parameters may be measured using analog or digital signals, they may be sampled and processed, and they may be digitized or converted using a number of known analog and digital processing techniques. Measured or monitored signals may be used in feedback circuits or systems to control the operation of the resonators and/or the system. In general, we refer to these monitored or measured signals as reference signals, or port parameter

measurements or signals, although they are sometimes also referred to as error signals, monitor signals, feedback signals, and the like. We will refer to the signals that are used to control circuit elements such as the voltages used to drive voltage controlled capacitors as the control signals.

**[00380]** In some cases the circuit elements may be adjusted to achieve a specified or predetermined impedance value for the source and device resonators. In other cases the impedance may be adjusted to achieve a desired impedance value for the source and device resonators when the device resonator is connected to a power consumer or consumers. In other cases the impedance may be adjusted to mitigate changes in the resonant frequency, or impedance or power level changes owing to movement of the source and/or device resonators, or changes in the environment (such as the movement of interacting materials or objects) in the vicinity of the resonators. In other cases the impedance of the source and device resonators may be adjusted to different impedance values.

**[00381]** The coupled resonators may be made of different materials and may include different circuits, components and structural designs or they may be the same. The coupled resonators may include performance monitoring and measurement circuitry, signal processing and control circuitry or a combination of measurement and control circuitry. Some or all of the high- $Q$  magnetic resonators may include tunable impedance circuits. Some or all of the high- $Q$  magnetic resonators may include automatically controlled tunable impedance circuits.

**[00382]** Fig. 41 shows a magnetic resonator with port parameter measurement circuitry 3802 configured to measure certain parameters of the resonator. The port parameter measurement circuitry may measure the input impedance of the structure, or the reflected power. Port parameter measurement circuits may be included in the source and/or device resonator designs and may be used to measure two port circuit parameters such as S-parameters (scattering parameters), Z-parameters (impedance parameters), Y-parameters (admittance parameters), T-parameters (transmission parameters), H-parameters (hybrid parameters), ABCD-parameters (chain, cascade or transmission parameters), and the like. These parameters may be used to describe the electrical behavior of linear electrical networks when various types of signals are applied.

**[00383]** Different parameters may be used to characterize the electrical network under different operating or coupling scenarios. For example, S-parameters may be used to measure matched and unmatched loads. In addition, the magnitude and phase of voltage and current

signals within the magnetic resonators and/or within the sources and devices themselves may be monitored at a variety of points to yield system performance information. This information may be presented to users of the system via a user interface such as a light, a read-out, a beep, a noise, a vibration or the like, or it may be presented as a digital signal or it may be provided to a processor in the system and used in the automatic control of the system. This information may be logged, stored, or may be used by higher level monitoring and control systems.

**[00384]** Fig. 42 shows a circuit diagram of a magnetic resonator where the tunable impedance network may be realized with voltage controlled capacitors 3902 or capacitor networks. Such an implementation may be adjusted, tuned or controlled by electrical circuits and/or computer processors, such as a programmable voltage source 3908, and the like. For example, the voltage controlled capacitors may be adjusted in response to data acquired by the port parameter measurement circuitry 3802 and processed by a measurement analysis and control algorithm subsystem 3904. Reference signals may be derived from the port parameter measurement circuitry or other monitoring circuitry designed to measure the degree of deviation from a desired system operating point. The measured reference signals may include voltage, current, complex-impedance, reflection coefficient, power levels and the like, at one or several points in the system and at a single frequency or at multiple frequencies.

**[00385]** The reference signals may be fed to measurement analysis and control algorithm subsystem modules that may generate control signals to change the values of various components in a tunable impedance matching network. The control signals may vary the resonant frequency and/or the input impedance of the magnetic resonator, or the power level supplied by the source, or the power level drawn by the device, to achieve the desired power exchange between power supplies/generators and power drains/loads.

**[00386]** Adjustment algorithms may be used to adjust the frequency and/or impedance of the magnetic resonators. The algorithms may take in reference signals related to the degree of deviation from a desired operating point for the system and output correction or control signals related to that deviation that control variable or tunable elements of the system to bring the system back towards the desired operating point or points. The reference signals for the magnetic resonators may be acquired while the resonators are exchanging power in a wireless power transmission system, or they may be switched out of the circuit during system operation.



Corrections to the system may be applied or performed continuously, periodically, upon a threshold crossing, digitally, using analog methods, and the like.

**[00387]** Fig. 43 shows an end-to-end wireless power transmission system. Both the source and the device may include port measurement circuitry 3802 and a processor 2410. The box labeled “coupler/switch” 4002 indicates that the port measurement circuitry 3802 may be connected to the resonator 102 by a directional coupler or a switch, enabling the measurement, adjustment and control of the source and device resonators to take place in conjunction with, or separate from, the power transfer functionality.

**[00388]** The port parameter measurement and/or processing circuitry may reside with some, any, or all resonators in a system. The port parameter measurement circuitry may utilize portions of the power transmission signal or may utilize excitation signals over a range of frequencies to measure the source/device resonator response (i.e. transmission and reflection between any two ports in the system), and may contain amplitude and/or phase information. Such measurements may be achieved with a swept single frequency signal or a multi-frequency signal. The signals used to measure and monitor the resonators and the wireless power transmission system may be generated by a processor or processors and standard input/output (I/O) circuitry including digital to analog converters (DACs), analog to digital converters (ADCs), amplifiers, signal generation chips, passive components and the like. Measurements may be achieved using test equipment such as a network analyzer or using customized circuitry. The measured reference signals may be digitized by ADCs and processed using customized algorithms running on a computer, a microprocessor, a DSP chip, an ASIC, and the like. The measured reference signals may be processed in an analog control loop.

**[00389]** The measurement circuitry may measure any set of two port parameters such as S-parameters, Y-parameters, Z-parameters, H-parameters, G-parameters, T-parameters, ABCD-parameters, and the like. Measurement circuitry may be used to characterize current and voltage signals at various points in the drive and resonator circuitry, the impedance and/or admittance of the source and device resonators at opposite ends of the system, i.e. looking into the source resonator matching network (“port 1” in Fig. 43) towards the device and vice versa.

**[00390]** The device may measure relevant signals and/or port parameters, interpret the measurement data, and adjust its matching network to optimize the impedance looking into the coupled system independently of the actions of the source. The source may measure relevant port

parameters, interpret the measurement data, and adjust its matching network to optimize the impedance looking into the coupled system independently of the actions of the device.

[00391] Fig. 43 shows a block diagram of a source and device in a wireless power transmission system. The system may be configured to execute a control algorithm that actively adjusts the tuning/matching networks in either of or both the source and device resonators to optimize performance in the coupled system. Port measurement circuitry 3802S may measure signals in the source and communicate those signals to a processor 2410. A processor 2410 may use the measured signals in a performance optimization or stabilization algorithm and generate control signals based on the outputs of those algorithms. Control signals may be applied to variable circuit elements in the tuning/impedance matching circuits 2402S to adjust the source's operating characteristics, such as power in the resonator and coupling to devices. Control signals may be applied to the power supply or generator to turn the supply on or off, to increase or decrease the power level, to modulate the supply signal and the like.

[00392] The power exchanged between sources and devices may depend on a variety of factors. These factors may include the effective impedance of the sources and devices, the  $Q$ 's of the sources and devices, the resonant frequencies of the sources and devices, the distances between sources and devices, the interaction of materials and objects in the vicinity of sources and devices and the like. The port measurement circuitry and processing algorithms may work in concert to adjust the resonator parameters to maximize power transfer, to hold the power transfer constant, to controllably adjust the power transfer, and the like, under both dynamic and steady state operating conditions.

[00393] Some, all or none of the sources and devices in a system implementation may include port measurement circuitry 3802S and processing 2410 capabilities. Fig. 44 shows an end-to-end wireless power transmission system in which only the source 102S contains port measurement circuitry 3802 and a processor 2410S. In this case, the device resonator 102D operating characteristics may be fixed or may be adjusted by analog control circuitry and without the need for control signals generated by a processor.

[00394] Fig. 45 shows an end-to-end wireless power transmission system. Both the source and the device may include port measurement circuitry 3802 but in the system of Fig. 45, only the source contains a processor 2410S. The source and device may be in communication with each other and the adjustment of certain system parameters may be in response to control

signals that have been wirelessly communicated, such as through wireless communications circuitry 4202, between the source and the device. The wireless communication channel 4204 may be separate from the wireless power transfer channel 4208, or it may be the same. That is, the resonators 102 used for power exchange may also be used to exchange information. In some cases, information may be exchanged by modulating a component a source or device circuit and sensing that change with port parameter or other monitoring equipment.

[00395] Implementations where only the source contains a processor 2410 may be beneficial for multi-device systems where the source can handle all of the tuning and adjustment “decisions” and simply communicate the control signals back to the device(s). This implementation may make the device smaller and cheaper because it may eliminate the need for, or reduce the required functionality of, a processor in the device. A portion of or an entire data set from each port measurement at each device may be sent back to the source microprocessor for analysis, and the control instructions may be sent back to the devices. These communications may be wireless communications.

[00396] Fig. 46 shows an end-to-end wireless power transmission system. In this example, only the source contains port measurement circuitry 3802 and a processor 2410S. The source and device may be in communication, such as via wireless communication circuitry 4202, with each other and the adjustment of certain system parameters may be in response to control signals that have been wirelessly communicated between the source and the device.

[00397] Fig. 47 shows coupled electromagnetic resonators 102 whose frequency and impedance may be automatically adjusted using a processor or a computer. Resonant frequency tuning and continuous impedance adjustment of the source and device resonators may be implemented with reverse biased diodes, Schottky diodes and/or varactor elements contained within the capacitor networks shown as C1, C2, and C3 in Fig. 47. The circuit topology that was built and demonstrated and is described here is exemplary and is not meant to limit the discussion of automatic system tuning and control in any way. Other circuit topologies could be utilized with the measurement and control architectures discussed in this disclosure.

[00398] Device and source resonator impedances and resonant frequencies may be measured with a network analyzer 4402A-B, or by other means described above, and implemented with a controller, such as with Lab View 4404. The measurement circuitry or

equipment may output data to a computer or a processor that implements feedback algorithms and dynamically adjusts the frequencies and impedances via a programmable DC voltage source.

**[00399]** In one arrangement, the reverse biased diodes (Schottky, semiconductor junction, and the like) used to realize the tunable capacitance drew very little DC current and could be reverse biased by amplifiers having large series output resistances. This implementation may enable DC control signals to be applied directly to the controllable circuit elements in the resonator circuit while maintaining a very high- $Q$  in the magnetic resonator.

**[00400]** C2 biasing signals may be isolated from C1 and/or C3 biasing signals with a DC blocking capacitor as shown in Fig. 47, if the required DC biasing voltages are different. The output of the biasing amplifiers may be bypassed to circuit ground to isolate RF voltages from the biasing amplifiers, and to keep non-fundamental RF voltages from being injected into the resonator. The reverse bias voltages for some of the capacitors may instead be applied through the inductive element in the resonator itself, because the inductive element acts as a short circuit at DC.

**[00401]** The port parameter measurement circuitry may exchange signals with a processor (including any required ADCs and DACs) as part of a feedback or control system that is used to automatically adjust the resonant frequency, input impedance, energy stored or captured by the resonator or power delivered by a source or to a device load. The processor may also send control signals to tuning or adjustment circuitry in or attached to the magnetic resonator.

**[00402]** When utilizing varactors or diodes as tunable capacitors, it may be beneficial to place fixed capacitors in parallel and in series with the tunable capacitors operating at high reverse bias voltages in the tuning/matching circuits. This arrangement may yield improvements in circuit and system stability and in power handling capability by optimizing the operating voltages on the tunable capacitors.

**[00403]** Varactors or other reverse biased diodes may be used as a voltage controlled capacitor. Arrays of varactors may be used when higher voltage compliance or different capacitance is required than that of a single varactor component. Varactors may be arranged in an N by M array connected serially and in parallel and treated as a single two terminal component with different characteristics than the individual varactors in the array. For example, an N by N array of equal varactors where components in each row are connected in parallel and

components in each column are connected in series may be used as a two terminal device with the same capacitance as any single varactor in the array but with a voltage compliance that is  $N$  times that of a single varactor in the array. Depending on the variability and differences of parameters of the individual varactors in the array additional biasing circuits composed of resistors, inductors, and the like may be needed. A schematic of a four by four array of unbiased varactors 4502 that may be suitable for magnetic resonator applications is shown in Fig. 48.

**[00404]** Further improvements in system performance may be realized by careful selection of the fixed value capacitor(s) that are placed in parallel and/or in series with the tunable (varactor/diode/capacitor) elements. Multiple fixed capacitors that are switched in or out of the circuit may be able to compensate for changes in resonator  $Q$ 's, impedances, resonant frequencies, power levels, coupling strengths, and the like, that might be encountered in test, development and operational wireless power transfer systems. Switched capacitor banks and other switched element banks may be used to assure the convergence to the operating frequencies and impedance values required by the system design.

**[00405]** An exemplary control algorithm for isolated and coupled magnetic resonators may be described for the circuit and system elements shown in Fig. 47. One control algorithm first adjusts each of the source and device resonator loops "in isolation", that is, with the other resonators in the system "shorted out" or "removed" from the system. For practical purposes, a resonator can be "shorted out" by making it resonant at a much lower frequency such as by maximizing the value of  $C1$  and/or  $C3$ . This step effectively reduces the coupling between the resonators, thereby effectively reducing the system to a single resonator at a particular frequency and impedance.

**[00406]** Tuning a magnetic resonator in isolation includes varying the tunable elements in the tuning and matching circuits until the values measured by the port parameter measurement circuitry are at their predetermined, calculated or measured relative values. The desired values for the quantities measured by the port parameter measurement circuitry may be chosen based on the desired matching impedance, frequency, strong coupling parameter, and the like. For the exemplary algorithms disclosed below, the port parameter measurement circuitry measures S-parameters over a range of frequencies. The range of frequencies used to characterize the resonators may be a compromise between the system performance information

obtained and computation/measurement speed. For the algorithms described below the frequency range may be approximately +/- 20% of the operating resonant frequency.

**[00407]** Each isolated resonator may be tuned as follows. First, short out the resonator not being adjusted. Next minimize C1, C2, and C3, in the resonator that is being characterized and adjusted. In most cases there will be fixed circuit elements in parallel with C1, C2, and C3, so this step does not reduce the capacitance values to zero. Next, start increasing C2 until the resonator impedance is matched to the "target" real impedance at any frequency in the range of measurement frequencies described above. The initial "target" impedance may be less than the expected operating impedance for the coupled system.

**[00408]** C2 may be adjusted until the initial "target" impedance is realized for a frequency in the measurement range. Then C1 and/or C3 may be adjusted until the loop is resonant at the desired operating frequency.

**[00409]** Each resonator may be adjusted according to the above algorithm. After tuning each resonator in isolation, a second feedback algorithm may be applied to optimize the resonant frequencies and/or input impedances for wirelessly transferring power in the coupled system.

**[00410]** The required adjustments to C1 and/or C2 and/or C3 in each resonator in the coupled system may be determined by measuring and processing the values of the real and imaginary parts of the input impedance from either and/or both "port(s)" shown in Fig. 43. For coupled resonators, changing the input impedance of one resonator may change the input impedance of the other resonator. Control and tracking algorithms may adjust one port to a desired operating point based on measurements at that port, and then adjust the other port based on measurements at that other port. These steps may be repeated until both sides converge to the desired operating point.

**[00411]** S-parameters may be measured at both the source and device ports and the following series of measurements and adjustments may be made. In the description that follows,  $Z_0$  is an input impedance and may be the target impedance. In some cases  $Z_0$  is 50 ohms or is near 50 ohms.  $Z_1$  and  $Z_2$  are intermediate impedance values that may be the same value as  $Z_0$  or may be different than  $Z_0$ .  $\text{Re}\{\text{value}\}$  means the real part of a value and  $\text{Im}\{\text{value}\}$  means the imaginary part of a value.

**[00412]** An algorithm that may be used to adjust the input impedance and resonant frequency of two coupled resonators is set forth below:

- 1) Adjust each resonator “in isolation” as described above.
- 2) Adjust source C1/C3 until, at  $\omega_o$ ,  $\text{Re}\{S11\} = (Z_1 +/- \epsilon_{Re})$  as follows:
  - If  $\text{Re}\{S11 @ \omega_o\} > (Z_1 + \epsilon_{Re})$ , decrease C1/C3. If  $\text{Re}\{S11 @ \omega_o\} < (Z_0 - \epsilon_{Re})$ , increase C1/C3.
- 3) Adjust source C2 until, at  $\omega_o$ ,  $\text{Im}\{S11\} = (+/- \epsilon_{Im})$  as follows:
  - If  $\text{Im}\{S11 @ \omega_o\} > \epsilon_{Im}$ , decrease C2. If  $\text{Im}\{S11 @ \omega_o\} < -\epsilon_{Im}$ , increase C2.
- 4) Adjust device C1/C3 until, at  $\omega_o$ ,  $\text{Re}\{S22\} = (Z_2 +/- \epsilon_{Re})$  as follows:
  - If  $\text{Re}\{S22 @ \omega_o\} > (Z_2 + \epsilon_{Re})$ , decrease C1/C3. If  $\text{Re}\{S22 @ \omega_o\} < (Z_0 - \epsilon_{Re})$ , increase C1/C3.
- 5) Adjust device C2 until, at  $\omega_o$ ,  $\text{Im}\{S22\} = 0$  as follows:
  - If  $\text{Im}\{S22 @ \omega_o\} > \epsilon_{Im}$ , decrease C2. If  $\text{Im}\{S22 @ \omega_o\} < -\epsilon_{Im}$ , increase C2.

**[00413]** We have achieved a working system by repeating steps 1-4 until both  $(\text{Re}\{S11\}, \text{Im}\{S11\})$  and  $(\text{Re}\{S22\}, \text{Im}\{S22\})$  converge to  $((Z_0 +/- \epsilon_{Re}), (+/- \epsilon_{Im}))$  at  $\omega_o$ , where  $Z_0$  is the desired matching impedance and  $\omega_o$  is the desired operating frequency. Here,  $\epsilon_{Im}$  represents the maximum deviation of the imaginary part, at  $\omega_o$ , from the desired value of 0, and  $\epsilon_{Re}$  represents the maximum deviation of the real part from the desired value of  $Z_0$ . It is understood that  $\epsilon_{Im}$  and  $\epsilon_{Re}$  can be adjusted to increase or decrease the number of steps to convergence at the potential cost of system performance (efficiency). It is also understood that steps 1-4 can be performed in a variety of sequences and a variety of ways other than that outlined above (i.e. first adjust the source imaginary part, then the source real part; or first adjust the device real part, then the device imaginary part, etc.) The intermediate impedances  $Z_1$  and  $Z_2$  may be adjusted during steps 1-4 to reduce the number of steps required for convergence. The desire or target impedance value may be complex, and may vary in time or under different operating scenarios.

**[00414]** Steps 1-4 may be performed in any order, in any combination and any number of times. Having described the above algorithm, variations to the steps or the described implementation may be apparent to one of ordinary skill in the art. The algorithm outlined above may be implemented with any equivalent linear network port parameter measurements (i.e., Z-parameters, Y-parameters, T-parameters, H-parameters, ABCD-parameters, etc.) or other monitor signals described above, in the same way that impedance or admittance can be alternatively used to analyze a linear circuit to derive the same result.

**[00415]** The resonators may need to be retuned owing to changes in the “loaded” resistances,  $R_s$  and  $R_d$ , caused by changes in the mutual inductance  $M$  (coupling) between the source and device resonators. Changes in the inductances,  $L_s$  and  $L_d$ , of the inductive elements themselves may be caused by the influence of external objects, as discussed earlier, and may also require compensation. Such variations may be mitigated by the adjustment algorithm described above.

**[00416]** A directional coupler or a switch may be used to connect the port parameter measurement circuitry to the source resonator and tuning/adjustment circuitry. The port parameter measurement circuitry may measure properties of the magnetic resonator while it is exchanging power in a wireless power transmission system, or it may be switched out of the circuit during system operation. The port parameter measurement circuitry may measure the parameters and the processor may control certain tunable elements of the magnetic resonator at start-up, or at certain intervals, or in response to changes in certain system operating parameters.

**[00417]** A wireless power transmission system may include circuitry to vary or tune the impedance and/or resonant frequency of source and device resonators. Note that while tuning circuitry is shown in both the source and device resonators, the circuitry may instead be included in only the source or the device resonators, or the circuitry may be included in only some of the source and/or device resonators. Note too that while we may refer to the circuitry as “tuning” the impedance and or resonant frequency of the resonators, this tuning operation simply means that various electrical parameters such as the inductance or capacitance of the structure are being varied. In some cases, these parameters may be varied to achieve a specific predetermined value, in other cases they may be varied in response to a control algorithm or to stabilize a target performance value that is changing. In some cases, the parameters are varied as a function of temperature, of other sources or devices in the area, of the environment, at the like.



**[00418] Applications**

**[00419]** For each listed application, it will be understood by one of ordinary skill-in-the-art that there are a variety of ways that the resonator structures used to enable wireless power transmission may be connected or integrated with the objects that are supplying or being powered. The resonator may be physically separate from the source and device objects. The resonator may supply or remove power from an object using traditional inductive techniques or through direct electrical connection, with a wire or cable for example. The electrical connection may be from the resonator output to the AC or DC power input port on the object. The electrical connection may be from the output power port of an object to the resonator input.

**[00420]** FIG. 49 shows a source resonator 4904 that is physically separated from a power supply and a device resonator 4902 that is physically separated from the device 4900, in this illustration a laptop computer. Power may be supplied to the source resonator, and power may be taken from the device resonator directly, by an electrical connection. One of ordinary skill in the art will understand from the materials incorporated by reference that the shape, size, material composition, arrangement, position and orientation of the resonators above are provided by way of non-limiting example, and that a wide variation in any and all of these parameters could be supported by the disclosed technology for a variety of applications.

**[00421]** Continuing with the example of the laptop, and without limitation, the device resonator may be physically connected to the device it is powering or charging. For example, as shown in FIG. 50a and FIG. 50b, the device resonator 5002 may be (a) integrated into the housing of the device 5000 or (b) it may be attached by an adapter. The resonator 5002 may (FIG. 50b-d) or may not (FIG. 50a) be visible on the device. The resonator may be affixed to the device, integrated into the device, plugged into the device, and the like.

**[00422]** The source resonator may be physically connected to the source supplying the power to the system. As described above for the devices and device resonators, there are a variety of ways the resonators may be attached to, connected to or integrated with the power supply. One of ordinary skill in the art will understand that there are a variety of ways the resonators may be integrated in the wireless power transmission system, and that the sources and devices may utilize similar or different integration techniques.

**[00423]** Continuing again with the example of the laptop computer, and without limitation, the laptop computer may be powered, charged or recharged by a wireless power

transmission system. A source resonator may be used to supply wireless power and a device resonator may be used to capture the wireless power. A device resonator 5002 may be integrated into the edge of the screen (display) as illustrated in FIG. 50d, and/or into the base of the laptop as illustrated in FIG. 50c. The source resonator 5002 may be integrated into the base of the laptop and the device resonator may be integrated into the edge of the screen. The resonators may also or instead be affixed to the power source and/or the laptop. The source and device resonators may also or instead be physically separated from the power supply and the laptop and may be electrically connected by a cable. The source and device resonators may also or instead be physically separated from the power supply and the laptop and may be electrically coupled using a traditional inductive technique. One of ordinary skill in the art will understand that, while the preceding examples relate to wireless power transmission to a laptop, that the methods and systems disclosed for this application may be suitably adapted for use with other electrical or electronic devices. In general, the source resonator may be external to the source and supplying power to a device resonator that in turn supplies power the device, or the source resonator may be connected to the source and supplying power to a device resonator that in turn supplies power to a portion of the device, or the source resonator may internal to the source and supplying power to a device resonator that in turn supplies power to a portion of the device, as well as any combination of these.

**[00424]** A system or method disclosed herein may provide power to an electrical or electronics device, such as, and not limited to, phones, cell phones, cordless phones, smart phones, PDAs, audio devices, music players, MP3 players, radios, portable radios and players, wireless headphones, wireless headsets, computers, laptop computers, wireless keyboards, wireless mouse, televisions, displays, flat screen displays, computer displays, displays embedded in furniture, digital picture frames, electronic books, (e.g. the Kindle, e-ink books, magazines, and the like), remote control units (also referred to as controllers, game controllers, commanders, clickers, and the like, and used for the remote control of a plurality of electronics devices, such as televisions, video games, displays, computers, audio visual equipment, lights, and the like), lighting devices, cooling devices, air circulation devices, purification devices, personal hearing aids, power tools, security systems, alarms, bells, flashing lights, sirens, sensors, loudspeakers, electronic locks, electronic keypads, light switches, other electrical switches, and the like. Here the term electronic lock is used to indicate a door lock which operates electronically (e.g. with

electronic combo-key, magnetic card, RFID card, and the like) which is placed on a door instead of a mechanical key-lock. Such locks are often battery operated, risking the possibility that the lock might stop working when a battery dies, leaving the user locked-out. This may be avoided where the battery is either charged or completely replaced by a wireless power transmission implementation as described herein.

**[00425]** Here, the term light switch (or other electrical switch) is meant to indicate any switch (e.g. on a wall of a room) in one part of the room that turns on/off a device (e.g. light fixture at the center of the ceiling) in another part of the room. To install such a switch by direct connection, one would have to run a wire all the way from the device to the switch. Once such a switch is installed at a particular spot, it may be very difficult to move. Alternately, one can envision a 'wireless switch', where "wireless" means the switching (on/off) commands are communicated wirelessly, but such a switch has traditionally required a battery for operation. In general, having too many battery operated switches around a house may be impractical, because those many batteries will need to be replaced periodically. So, a wirelessly communicating switch may be more convenient, provided it is also wirelessly powered. For example, there already exist communications wireless door-bells that are battery powered, but where one still has to replace the battery in them periodically. The remote doorbell button may be made to be completely wireless, where there may be no need to ever replace the battery again. Note that here, the term 'cordless' or 'wireless' or 'communications wireless' is used to indicate that there is a cordless or wireless communications facility between the device and another electrical component, such as the base station for a cordless phone, the computer for a wireless keyboard, and the like. One skilled in the art will recognize that any electrical or electronics device may include a wireless communications facility, and that the systems and methods described herein may be used to add wireless power transmission to the device. As described herein, power to the electrical or electronics device may be delivered from an external or internal source resonator, and to the device or portion of the device. Wireless power transmission may significantly reduce the need to charge and/or replace batteries for devices that enter the near vicinity of the source resonator and thereby may reduce the downtime, cost and disposal issues often associated with batteries.

**[00426]** The systems and methods described herein may provide power to lights without the need for either wired power or batteries. That is, the systems and methods described

herein may provide power to lights without wired connection to any power source, and provide the energy to the light non-radiatively across mid-range distances, such as across a distance of a quarter of a meter, one meter, three meters, and the like. A 'light' as used herein may refer to the light source itself, such as an incandescent light bulb, florescent light bulb lamps, Halogen lamps, gas discharge lamps, fluorescent lamps, neon lamps, high-intensity discharge lamps, sodium vapor lamps, Mercury-vapor lamps, electroluminescent lamps, light emitting diodes (LED) lamps, and the like; the light as part of a light fixture, such as a table lamp, a floor lamp, a ceiling lamp, track lighting, recessed light fixtures, and the like; light fixtures integrated with other functions, such as a light/ceiling fan fixture, and illuminated picture frame, and the like. As such, the systems and methods described herein may reduce the complexity for installing a light, such as by minimizing the installation of electrical wiring, and allowing the user to place or mount the light with minimal regard to sources of wired power. For instance, a light may be placed anywhere in the vicinity of a source resonator, where the source resonator may be mounted in a plurality of different places with respect to the location of the light, such as on the floor of the room above, (e.g. as in the case of a ceiling light and especially when the room above is the attic); on the wall of the next room, on the ceiling of the room below, (e.g. as in the case of a floor lamp); in a component within the room or in the infrastructure of the room as described herein; and the like. For example, a light/ceiling fan combination is often installed in a master bedroom, and the master bedroom often has the attic above it. In this instance a user may more easily install the light/ceiling fan combination in the master bedroom, such as by simply mounting the light/ceiling fan combination to the ceiling, and placing a source coil (plugged into the house wired AC power) in the attic above the mounted fixture. In another example, the light may be an external light, such as a flood light or security light, and the source resonator mounted inside the structure. This way of installing lighting may be particularly beneficial to users who rent their homes, because now they may be able to mount lights and such other electrical components without the need to install new electrical wiring. The control for the light may also be communicated by near-field communications as described herein, or by traditional wireless communications methods.

**[00427]** The systems and methods described herein may provide power from a source resonator to a device resonator that is either embedded into the device component, or outside the device component, such that the device component may be a traditional electrical component or

fixture. For instance, a ceiling lamp may be designed or retrofitted with a device resonator integrated into the fixture, or the ceiling lamp may be a traditional wired fixture, and plugged into a separate electrical facility equipped with the device resonator. In an example, the electrical facility may be a wireless junction box designed to have a device resonator for receiving wireless power, say from a source resonator placed on the floor of the room above (e.g. the attic), and which contains a number of traditional outlets that are powered from the device resonator. The wireless junction box, mounted on the ceiling, may now provide power to traditional wired electrical components on the ceiling (e.g. a ceiling light, track lighting, a ceiling fan). Thus, the ceiling lamp may now be mounted to the ceiling without the need to run wires through the infrastructure of the building. This type of device resonator to traditional outlet junction box may be used in a plurality of applications, including being designed for the interior or exterior of a building, to be made portable, made for a vehicle, and the like. Wireless power may be transferred through common building materials, such as wood, wall board, insulation, glass, brick, stone, concrete, and the like. The benefits of reduced installation cost, re-configurability, and increased application flexibility may provide the user significant benefits over traditional wired installations. The device resonator for a traditional outlet junction box may include a plurality of electrical components for facilitating the transfer of power from the device resonator to the traditional outlets, such as power source electronics which convert the specific frequencies needed to implement efficient power transfer to line voltage, power capture electronics which may convert high frequency AC to usable voltage and frequencies (AC and/or DC), controls which synchronize the capture device and the power output and which ensure consistent, safe, and maximally efficient power transfer, and the like.

**[00428]** The systems and methods described herein may provide advantages to lights or electrical components that operate in environments that are wet, harsh, controlled, and the like, such as outside and exposed to the rain, in a pool/sauna/shower, in a maritime application, in hermetically sealed components, in an explosive-proof room, on outside signage, a harsh industrial environment in a volatile environment (e.g. from volatile vapors or airborne organics, such as in a grain silo or bakery) , and the like. For example, a light mounted under the water level of a pool is normally difficult to wire up, and is required to be water-sealed despite the need for external wires. But a pool light using the principles disclosed herein may more easily be made water sealed, as there may be no external wires needed. In another example, an explosion

proof room, such as containing volatile vapors, may not only need to be hermetically sealed, but may need to have all electrical contacts (that could create a spark) sealed. Again, the principles disclosed herein may provide a convenient way to supply sealed electrical components for such applications.

**[00429]** The systems and methods disclosed herein may provide power to game controller applications, such as to a remote handheld game controller. These game controllers may have been traditionally powered solely by batteries, where the game controller's use and power profile caused frequent changing of the battery, battery pack, rechargeable batteries, and the like, that may not have been ideal for the consistent use to the game controller, such as during extended game play. A device resonator may be placed into the game controller, and a source resonator, connected to a power source, may be placed in the vicinity. Further, the device resonator in the game controller may provide power directly to the game controller electronics without a battery; provide power to a battery, battery pack, rechargeable battery, and the like, which then provides power to the game controller electronics; and the like. The game controller may utilize multiple battery packs, where each battery pack is equipped with a device resonator, and thus may be constantly recharging while in the vicinity of the source resonator, whether plugged into the game controller or not. The source resonator may be resident in a main game controller facility for the game, where the main game controller facility and source resonator are supplied power from AC 'house' power; resident in an extension facility form AC power, such as in a source resonator integrated into an 'extension cord'; resident in a game chair, which is at least one of plugged into the wall AC, plugged into the main game controller facility, powered by a battery pack in the game chair; and the like. The source resonator may be placed and implemented in any of the configurations described herein.

**[00430]** The systems and methods disclosed herein may integrate device resonators into battery packs, such as battery packs that are interchangeable with other battery packs. For instance, some portable devices may use up electrical energy at a high rate such that a user may need to have multiple interchangeable battery packs on hand for use, or the user may operate the device out of range of a source resonator and need additional battery packs to continue operation, such as for power tools, portable lights, remote control vehicles, and the like. The use of the principles disclosed herein may not only provide a way for device resonator enabled battery packs to be recharged while in use and in range, but also for the recharging of battery packs not

currently in use and placed in range of a source resonator. In this way, battery packs may always be ready to use when a user runs down the charge of a battery pack being used. For example, a user may be working with a wireless power tool, where the current requirements may be greater than can be realized through direct powering from a source resonator. In this case, despite the fact that the systems and methods described herein may be providing charging power to the in-use battery pack while in range, the battery pack may still run down, as the power usage may have exceeded the recharge rate. Further, the user may simply be moving in and out of range, or be completely out of range while using the device. However, the user may have placed additional battery packs in the vicinity of the source resonator, which have been recharged while not in use, and are now charged sufficiently for use. In another example, the user may be working with the power tool away from the vicinity of the source resonator, but leave the supplemental battery packs to charge in the vicinity of the source resonator, such as in a room with a portable source resonator or extension cord source resonator, in the user's vehicle, in user's tool box, and the like. In this way, the user may not have to worry about taking the time to, and/or remembering to plug in their battery packs for future use. The user may only have to change out the used battery pack for the charged battery pack and place the used one in the vicinity of the source resonator for recharging. Device resonators may be built into enclosures with known battery form factors and footprints and may replace traditional chemical batteries in known devices and applications. For example, device resonators may be built into enclosures with mechanical dimensions equivalent to AA batteries, AAA batteries, D batteries, 9V batteries, laptop batteries, cell phone batteries, and the like. The enclosures may include a smaller "button battery" in addition to the device resonator to store charge and provide extended operation, either in terms of time or distance. Other energy storage devices in addition to or instead of button batteries may be integrated with the device resonators and any associated power conversion circuitry. These new energy packs may provide similar voltage and current levels as provided by traditional batteries, but may be composed of device resonators, power conversion electronics, a small battery, and the like. These new energy packs may last longer than traditional batteries because they may be more easily recharged and may be recharging constantly when they are located in a wireless power zone. In addition, such energy packs may be lighter than traditional batteries, may be safer to use and store, may operate over wider temperature and humidity ranges, may be less harmful

to the environment when thrown away, and the like. As described herein, these energy packs may last beyond the life of the product when used in wireless power zones as described herein.

[00431] The systems and methods described herein may be used to power visual displays, such as in the case of the laptop screen, but more generally to include the great variety and diversity of displays utilized in today's electrical and electronics components, such as in televisions, computer monitors, desktop monitors, laptop displays, digital photo frames, electronic books, mobile device displays (e.g. on phones, PDAs, games, navigation devices, DVD players), and the like. Displays that may be powered through one or more of the wireless power transmission systems described herein may also include embedded displays, such as embedded in electronic components (e.g. audio equipment, home appliances, automotive displays, entertainment devices, cash registers, remote controls), in furniture, in building infrastructure, in a vehicle, on the surface of an object (e.g. on the surface of a vehicle, building, clothing, signs, transportation), and the like. Displays may be very small with tiny resonant devices, such as in a smart card as described herein, or very large, such as in an advertisement sign. Displays powered using the principles disclosed herein may also be any one of a plurality of imaging technologies, such as liquid crystal display (LCD), thin film transistor LCD, passive LCD, cathode ray tube (CRT), plasma display, projector display (e.g. LCD, DLP, LCOS), surface-conduction electron-emitter display (SED), organic light-emitting diode (OLED), and the like. Source coil configurations may include attaching to a primary power source, such as building power, vehicle power, from a wireless extension cord as described herein, and the like; attached to component power, such as the base of an electrical component (e.g. the base of a computer, a cable box for a TV); an intermediate relay source coil; and the like. For example, hanging a digital display on the wall may be very appealing, such as in the case of a digital photo frame that receives its information signals wirelessly or through a portable memory device, but the need for an unsightly power cord may make it aesthetically unpleasant. However, with a device coil embedded in the digital photo frame, such as wrapped within the frame portion, may allow the digital photo frame to be hung with no wires at all. The source resonator may then be placed in the vicinity of the digital photo frame, such as in the next room on the other side of the wall, plugged directly into a traditional power outlet, from a wireless extension cord as described herein, from a central source resonator for the room, and the like.



**[00432]** The systems and methods described herein may provide wireless power transmission between different portions of an electronics facility. Continuing with the example of the laptop computer, and without limitation, the screen of the laptop computer may require power from the base of the laptop. In this instance, the electrical power has been traditionally routed via direct electrical connection from the base of the laptop to the screen over a hinged portion of the laptop between the screen and the base. When a wired connection is utilized, the wired connection may tend to wear out and break, the design functionality of the laptop computer may be limited by the required direct electrical connection, the design aesthetics of the laptop computer may be limited by the required direct electrical connection, and the like. However, a wireless connection may be made between the base and the screen. In this instance, the device resonator may be placed in the screen portion to power the display, and the base may be either powered by a second device resonator, by traditional wired connections, by a hybrid of resonator-battery- direct electrical connection, and the like. This may not only improve the reliability of the power connection due to the removal of the physical wired connection, but may also allow designers to improve the functional and/or aesthetic design of the hinge portion of the laptop in light of the absence of physical wires associated with the hinge. Again, the laptop computer has been used here to illustrate how the principles disclosed herein may improve the design of an electric or electronic device, and should not be taken as limiting in any way. For instance, many other electrical devices with separated physical portions could benefit from the systems and methods described herein, such as a refrigerator with electrical functions on the door, including an ice maker, a sensor system, a light, and the like; a robot with movable portions, separated by joints; a car's power system and a component in the car's door; and the like. The ability to provide power to a device via a device resonator from an external source resonator, or to a portion of the device via a device resonator from either external or internal source resonators, will be recognized by someone skilled in the art to be widely applicable across the range of electric and electronic devices.

**[00433]** The systems and methods disclosed herein may provide for a sharing of electrical power between devices, such as between charged devices and uncharged devices. For instance a charged up device or appliance may act like a source and send a predetermined amount of energy, dialed in amount of energy, requested and approved amount of energy, and the like, to a nearby device or appliance. For example, a user may have a cell phone and a digital

camera that are both capable of transmitting and receiving power through embedded source and device resonators, and one of the devices, say the cell phone, is found to be low on charge. The user may then transfer charge from the digital camera to the cell phone. The source and device resonators in these devices may utilize the same physical resonator for both transmission and reception, utilize separate source and device resonators, one device may be designed to receive and transmit while the other is designed to receive only, one device may be designed to transmit only and the other to receive only, and the like.

**[00434]** To prevent complete draining the battery of a device it may have a setting allowing a user to specify how much of the power resource the receiving device is entitled to. It may be useful, for example, to put a limit on the amount of power available to external devices and to have the ability to shut down power transmission when battery power falls below a threshold.

**[00435]** The systems and methods described herein may provide wireless power transfer to a nearby electrical or electronics component in association with an electrical facility, where the source resonator is in the electrical facility and the device resonator is in the electronics component. The source resonator may also be connected to, plugged into, attached to the electrical facility, such as through a universal interface (e.g. a USB interface, PC card interface), supplemental electrical outlet, universal attachment point, and the like, of the electrical facility. For example, the source resonator may be inside the structure of a computer on a desk, or be integrated into some object, pad, and the like, that is connected to the computer, such as into one of the computer's USB interfaces. In the example of the source resonator embedded in the object, pad, and the like, and powered through a USB interface, the source resonator may then be easily added to a user's desktop without the need for being integrated into any other electronics device, thus conveniently providing a wireless energy zone around which a plurality of electric and/or electronics devices may be powered. The electrical facility may be a computer, a light fixture, a dedicated source resonator electrical facility, and the like, and the nearby components may be computer peripherals, surrounding electronics components, infrastructure devices, and the like, such as computer keyboards, computer mouse, fax machine, printer, speaker system, cell phone, audio device, intercom, music player, PDA, lights, electric pencil sharpener, fan, digital picture frame, calculator, electronic games, and the like. For example, a computer system may be the electrical facility with an integrated source resonator

that utilizes a 'wireless keyboard' and 'wireless mouse', where the use of the term wireless here is meant to indicate that there is wireless communication facility between each device and the computer, and where each device must still contain a separate battery power source. As a result, batteries would need to be replaced periodically, and in a large company, may result in a substantial burden for support personnel for replacement of batteries, cost of batteries, and proper disposal of batteries. Alternatively, the systems and methods described herein may provide wireless power transmission from the main body of the computer to each of these peripheral devices, including not only power to the keyboard and mouse, but to other peripheral components such as a fax, printer, speaker system, and the like, as described herein. A source resonator integrated into the electrical facility may provide wireless power transmission to a plurality of peripheral devices, user devices, and the like, such that there is a significant reduction in the need to charge and/or replace batteries for devices in the near vicinity of the source resonator integrated electrical facility. The electrical facility may also provide tuning or auto-tuning software, algorithms, facilities, and the like, for adjusting the power transfer parameters between the electrical facility and the wirelessly powered device. For example, the electrical facility may be a computer on a user's desktop, and the source resonator may be either integrated into the computer or plugged into the computer (e.g. through a USB connection), where the computer provides a facility for providing the tuning algorithm (e.g. through a software program running on the computer).

**[00436]** The systems and methods disclosed herein may provide wireless power transfer to a nearby electrical or electronics component in association with a facility infrastructure component, where the source resonator is in, or mounted on, the facility infrastructure component and the device resonator is in the electronics component. For instance, the facility infrastructure component may be a piece of furniture, a fixed wall, a movable wall or partition, the ceiling, the floor, and the source resonator attached or integrated into a table or desk (e.g. just below/above the surface, on the side, integrated into a table top or table leg), a mat placed on the floor (e.g. below a desk, placed on a desk), a mat on the garage floor (e.g. to charge the car and/or devices in the car), in a parking lot/garage (e.g. on a post near where the car is parked), a television (e.g. for charging a remote control), a computer monitor (e.g. to power/charge a wireless keyboard, wireless mouse, cell phone), a chair (e.g. for powering electric blankets, medical devices, personal health monitors), a painting, office furniture,

common household appliances, and the like. For example, the facility infrastructure component may be a lighting fixture in an office cubical, where the source resonator and light within the lighting fixture are both directly connected to the facility's wired electrical power. However, with the source resonator now provided in the lighting fixture, there would be no need to have any additional wired connections for those nearby electrical or electronics components that are connected to, or integrated with, a device resonator. In addition, there may be a reduced need for the replacement of batteries for devices with device resonators, as described herein.

**[00437]** The use of the systems and methods described herein to supply power to electrical and electronic devices from a central location, such as from a source resonator in an electrical facility, from a facility infrastructure component and the like, may minimize the electrical wiring infrastructure of the surrounding work area. For example, in an enterprise office space there are typically a great number of electrical and electronic devices that need to be powered by wired connections. With utilization of the systems and methods described herein, much of this wiring may be eliminated, saving the enterprise the cost of installation, decreasing the physical limitations associated with office walls having electrical wiring, minimizing the need for power outlets and power strips, and the like. The systems and methods described herein may save money for the enterprise through a reduction in electrical infrastructure associated with installation, re-installation (e.g., reconfiguring office space), maintenance, and the like. In another example, the principles disclosed herein may allow the wireless placement of an electrical outlet in the middle of a room. Here, the source could be placed on the ceiling of a basement below the location on the floor above where one desires to put an outlet. The device resonator could be placed on the floor of the room right above it. Installing a new lighting fixture (or any other electric device for that matter, e.g. camera, sensor, etc., in the center of the ceiling may now be substantially easier for the same reason).

**[00438]** In another example, the systems and methods described herein may provide power "through" walls. For instance, suppose one has an electric outlet in one room (e.g. on a wall), but one would like to have an outlet in the next room, but without the need to call an electrician, or drill through a wall, or drag a wire around the wall, or the like. Then one might put a source resonator on the wall in one room, and a device resonator outlet/pickup on the other side of the wall. This may power a flat-screen TV or stereo system or the like (e.g. one may not want to have an ugly wire climbing up the wall in the living room, but doesn't mind having a similar

wire going up the wall in the next room, e.g. storage room or closet, or a room with furniture that blocks view of wires running along the wall). The systems and methods described herein may be used to transfer power from an indoor source to various electric devices outside of homes or buildings without requiring holes to be drilled through, or conduits installed in, these outside walls. In this case, devices could be wirelessly powered outside the building without the aesthetic or structural damage or risks associated with drilling holes through walls and siding. In addition, the systems and methods described herein may provide for a placement sensor to assist in placing an interior source resonator for an exterior device resonator equipped electrical component. For example, a home owner may place a security light on the outside of their home which includes a wireless device resonator, and now needs to adequately or optimally position the source resonator inside the home. A placement sensor acting between the source and device resonators may better enable that placement by indicating when placement is good, or to a degree of good, such as in a visual indication, an audio indication, a display indication, and the like. In another example, and in a similar way, the systems and methods described herein may provide for the installation of equipment on the roof of a home or building, such as radio transmitters and receivers, solar panels and the like. In the case of the solar panel, the source resonator may be associated with the panel, and power may be wirelessly transferred to a distribution panel inside the building without the need for drilling through the roof. The systems and methods described herein may allow for the mounting of electric or electrical components across the walls of vehicles (such as through the roof) without the need to drill holes, such as for automobiles, water craft, planes, trains, and the like. In this way, the vehicle's walls may be left intact without holes being drilled, thus maintaining the value of the vehicle, maintaining watertightness, eliminating the need to route wires, and the like. For example, mounting a siren or light to the roof of a police car decreases the future resale of the car, but with the systems and methods described herein, any light, horn, siren, and the like, may be attached to the roof without the need to drill a hole.

**[00439]** The systems and methods described herein may be used for wireless transfer of power from solar photovoltaic (PV) panels. PV panels with wireless power transfer capability may have several benefits including simpler installation, more flexible, reliable, and weatherproof design. Wireless power transfer may be used to transfer power from the PV panels to a device, house, vehicle, and the like. Solar PV panels may have a wireless source resonator

allowing the PV panel to directly power a device that is enabled to receive the wireless power. For example, a solar PV panel may be mounted directly onto the roof of a vehicle, building, and the like. The energy captured by the PV panel may be wirelessly transferred directly to devices inside the vehicle or under the roof of a building. Devices that have resonators can wirelessly receive power from the PV panel. Wireless power transfer from PV panels may be used to transfer energy to a resonator that is coupled to the wired electrical system of a house, vehicle, and the like allowing traditional power distribution and powering of conventional devices without requiring any direct contact between the exterior PV panels and the internal electrical system.

**[00440]** With wireless power transfer significantly simpler installation of rooftop PV panels is possible because power may be transmitted wirelessly from the panel to a capture resonator in the house, eliminating all outside wiring, connectors, and conduits, and any holes through the roof or walls of the structure. Wireless power transfer used with solar cells may have a benefit in that it can reduced roof danger since it eliminates the need for electricians to work on the roof to interconnect panels, strings, and junction boxes. Installation of solar panels integrated with wireless power transfer may require less skilled labor since fewer electrical contacts need to be made. Less site specific design may be required with wireless power transfer since the technology gives the installer the ability to individually optimize and position each solar PV panel, significantly reducing the need for expensive engineering and panel layout services. There may not be need to carefully balance the solar load on every panel and no need for specialized DC wiring layout and interconnections.

**[00441]** For rooftop or on-wall installations of PV panels, the capture resonator may be mounted on the underside of the roof, inside the wall, or in any other easily accessible inside space within a foot or two of the solar PV panel. A diagram showing a possible general rooftop PV panel installation is shown in Figure 51. Various PV solar collectors may be mounted in top of a roof with wireless power capture coils mounted inside the building under the roof. The resonator coils in the PV panels can transfer their energy wirelessly through the roof to the wireless capture coils. The captured energy from the PV cells may be collected and coupled to the electrical system of the house to power electric and electronic devices or coupled to the power grid when more power than needed is generated. Energy is captured from the PV cells without requiring holes or wires that penetrate the roof or the walls of the building. Each PV

panel may have a resonator that is coupled to a corresponding resonator on the interior of the vehicle or building. Multiple panels may utilize wireless power transfer between each other to transfer or collect power to one or a couple of designated panels that are coupled to resonators on the interior of the vehicle or house. Panels may have wireless power resonators on their sides or in their perimeter that can couple to resonators located in other like panels allowing transfer of power from panel to panel. An additional bus or connection structure may be provided that wirelessly couples the power from multiple panels on the exterior of a building or vehicle and transfers power to one or a more resonators on the interior of building or vehicle.

**[00442]** For example, as shown in Fig. 51, a source resonator 5102 may be coupled to a PV cell 5100 mounted on top of roof 5104 of a building. A corresponding capture resonator 5106 is placed inside the building. The solar energy captured by the PV cells can then be transferred between the source resonators 5102 outside to the device resonators 5106 inside the building without having direct holes and connections through the building.

**[00443]** Each solar PV panel with wireless power transfer may have its own inverter, significantly improving the economics of these solar systems by individually optimizing the power production efficiency of each panel, supporting a mix of panel sizes and types in a single installation, including single panel “pay-as-you-grow” system expansions. Reduction of installation costs may make a single panel economical for installation. Eliminating the need for panel string designs and careful positioning and orienting of multiple panels, and eliminating a single point of failure for the system.

**[00444]** Wireless power transfer in PV solar panels may enable more solar deployment scenarios because the weather-sealed solar PV panels eliminate the need to drill holes for wiring through sealed surfaces such as car roofs and ship decks, and eliminate the requirement that the panels be installed in fixed locations. With wireless power transfer, PV panels may be deployed temporarily, and then moved or removed, without leaving behind permanent alterations to the surrounding structures. They may be placed out in a yard on sunny days, and moved around to follow the sun, or brought inside for cleaning or storage, for example. For backyard or mobile solar PV applications, an extension cord with a wireless energy capture device may be thrown on the ground or placed near the solar unit. The capture extension cord can be completely sealed from the elements and electrically isolated, so that it may be used in any indoor or outdoor environment.

**[00445]** With wireless power transfer no wires or external connections may be necessary and the PV solar panels can be completely weather sealed. Significantly improved reliability and lifetime of electrical components in the solar PV power generation and transmission circuitry can be expected since the weather-sealed enclosures can protect components from UV radiation, humidity, weather, and the like. With wireless power transfer and weather-sealed enclosures it may be possible to use less expensive components since they will no longer be directly exposed to external factors and weather elements and it may reduce the cost of PV panels.

**[00446]** Power transfer between the PV panels and the capture resonators inside a building or a vehicle may be bidirectional. Energy may be transmitted from the house grid to the PV panels to provide power when the panels do not have enough energy to perform certain tasks such. Reverse power flow can be used to melt snow from the panels, or power motors that will position the panels in a more favorable positions with respect to the sun energy. Once the snow is melted or the panels are repositioned and the PV panels can generate their own energy the direction of power transfer can be returned to normal delivering power from the PV panels to buildings, vehicles, or devices.

**[00447]** PV panels with wireless power transfer may include auto-tuning on installation to ensure maximum and efficient power transfer to the wireless collector. Variations in roofing materials or variations in distances between the PV panels and the wireless power collector in different installations may affect the performance or perturb the properties of the resonators of the wireless power transfer. To reduce the installation complexity the wireless power transfer components may include a tuning capability to automatically adjust their operating point to compensate for any effects due to materials or distance. Frequency, impedance, capacitance, inductance, duty cycle, voltage levels and the like may be adjusted to ensure efficient and safe power transfer

**[00448]** The systems and methods described herein may be used to provide a wireless power zone on a temporary basis or in extension of traditional electrical outlets to wireless power zones, such as through the use of a wireless power extension cord. For example, a wireless power extension cord may be configured as a plug for connecting into a traditional power outlet, a long wire such as in a traditional power extension cord, and a resonant source coil on the other end (e.g. in place of, or in addition to, the traditional socket end of the extension The wireless



extension cord may also be configured where there are source resonators at a plurality of locations along the wireless extension cord. This configuration may then replace any traditional extension cord where there are wireless power configured devices, such as providing wireless power to a location where there is no convenient power outlet (e.g. a location in the living room where there's no outlet), for temporary wireless power where there is no wired power infrastructure (e.g. a construction site), out into the yard where there are no outlets (e.g. for parties or for yard grooming equipment that is wirelessly powered to decrease the chances of cutting the traditional electrical cord), and the like. The wireless extension cord may also be used as a drop within a wall or structure to provide wireless power zones within the vicinity of the drop. For example, a wireless extension cord could be run within a wall of a new or renovated room to provide wireless power zones without the need for the installation of traditional electrical wiring and outlets.

**[00449]** The systems and methods described herein may be utilized to provide power between moving parts or rotating assemblies of a vehicle, a robot, a mechanical device, a wind turbine, or any other type of rotating device or structure with moving parts such as robot arms, construction vehicles, movable platforms and the like. Traditionally, power in such systems may have been provided by slip rings or by rotary joints for example. Using wireless power transfer as described herein, the design simplicity, reliability and longevity of these devices may be significantly improved because power can be transferred over a range of distances without any physical connections or contact points that may wear down or out with time. In particular, the preferred coaxial and parallel alignment of the source and device coils may provide wireless power transmission that is not severely modulated by the relative rotational motion of the two coils.

**[00450]** The systems and methods described herein may be utilized to extend power needs beyond the reach of a single source resonator by providing a series of source-device-source-device resonators. For instance, suppose an existing detached garage has no electrical power and the owner now wants to install a new power service. However, the owner may not want to run wires all over the garage, or have to break into the walls to wire electrical outlets throughout the structure. In this instance, the owner may elect to connect a source resonator to the new power service, enabling wireless power to be supplied to device resonator outlets throughout the back of the garage. The owner may then install a device-source 'relay' to supply

wireless power to device resonator outlets in the front of the garage. That is, the power relay may now receive wireless power from the primary source resonator, and then supply available power to a second source resonator to supply power to a second set of device resonators in the front of the garage. This configuration may be repeated again and again to extend the effective range of the supplied wireless power.

**[00451]** Multiple resonators may be used to extend power needs around an energy blocking material. For instance, it may be desirable to integrate a source resonator into a computer or computer monitor such that the resonator may power devices placed around and especially in front of the monitor or computer such as keyboards, computer mice, telephones, and the like. Due to aesthetics, space constraints, and the like an energy source that may be used for the source resonator may only be located or connected to in the back of the monitor or computer. In many designs of computer or monitors metal components and metal containing circuits are used in the design and packaging which may limit and prevent power transfer from source resonator in the back of the monitor or computer to the front of the monitor or computer. An additional repeater resonator may be integrated into the base or pedestal of the monitor or computer that couples to the source resonator in the back of the monitor or computer and allows power transfer to the space in front of the monitor or computer. The intermediate resonator integrated into the base or pedestal of the monitor or computer does not require an additional power source, it captures power from the source resonator and transfers power to the front around the blocking or power shielding metal components of the monitor or computer.

**[00452]** The systems and methods described herein may be built-into, placed on, hung from, embedded into, integrated into, and the like, the structural portions of a space, such as a vehicle, office, home, room, building, outdoor structure, road infrastructure, and the like. For instance, one or more sources may be built into, placed on, hung from, embedded or integrated into a wall, a ceiling or ceiling panel, a floor, a divider, a doorway, a stairwell, a compartment, a road surface, a sidewalk, a ramp, a fence, an exterior structure, and the like. One or more sources may be built into an entity within or around a structure, for instance a bed, a desk, a chair, a rug, a mirror, a clock, a display, a television, an electronic device, a counter, a table, a piece of furniture, a piece of artwork, an enclosure, a compartment, a ceiling panel, a floor or door panel, a dashboard, a trunk, a wheel well, a post, a beam, a support or any like entity. For example, a source resonator may be integrated into the dashboard of a user's car so that any device that is

equipped with or connected to a device resonator may be supplied with power from the dashboard source resonator. In this way, devices brought into or integrated into the car may be constantly charged or powered while in the car.

**[00453]** The systems and methods described herein may provide power through the walls of vehicles, such as boats, cars, trucks, busses, trains, planes, satellites and the like. For instance, a user may not want to drill through the wall of the vehicle in order to provide power to an electric device on the outside of the vehicle. A source resonator may be placed inside the vehicle and a device resonator may be placed outside the vehicle (e.g. on the opposite side of a window, wall or structure). In this way the user may achieve greater flexibility in optimizing the placement, positioning and attachment of the external device to the vehicle, (such as without regard to supplying or routing electrical connections to the device). In addition, with the electrical power supplied wirelessly, the external device may be sealed such that it is water tight, making it safe if the electric device is exposed to weather (e.g. rain), or even submerged under water. Similar techniques may be employed in a variety of applications, such as in charging or powering hybrid vehicles, navigation and communications equipment, construction equipment, remote controlled or robotic equipment and the like, where electrical risks exist because of exposed conductors. The systems and methods described herein may provide power through the walls of vacuum chambers or other enclosed spaces such as those used in semiconductor growth and processing, material coating systems, aquariums, hazardous materials handling systems and the like. Power may be provided to translation stages, robotic arms, rotating stages, manipulation and collection devices, cleaning devices and the like.

**[00454]** The systems and methods described herein may provide wireless power to a kitchen environment, such as to counter-top appliances, including mixers, coffee makers, toasters, toaster ovens, grills, griddles, electric skillets, electric pots, electric woks, waffle makers, blenders, food processors, crock pots, warming trays, induction cooktops, lights, computers, displays, and the like. This technology may improve the mobility and/or positioning flexibility of devices, reduce the number of power cords stored on and strewn across the counter-top, improve the washability of the devices, and the like. For example, an electric skillet may traditionally have separate portions, such as one that is submersible for washing and one that is not submersible because it includes an external electrical connection (e.g. a cord or a socket for a removable cord). However, with a device resonator integrated into the unit, all electrical

connections may be sealed, and so the entire device may now be submersed for cleaning. In addition, the absence of an external cord may eliminate the need for an available electrical wall outlet, and there is no longer a need for a power cord to be placed across the counter or for the location of the electric griddle to be limited to the location of an available electrical wall outlet.

**[00455]** The systems and methods described herein may provide continuous power/charging to devices equipped with a device resonator because the device doesn't leave the proximity of a source resonator, such as fixed electrical devices, personal computers, intercom systems, security systems, household robots, lighting, remote control units, televisions, cordless phones, and the like. For example, a household robot (e.g. ROOMBA) could be powered/charged via wireless power, and thus work arbitrarily long without recharging. In this way, the power supply design for the household robot may be changed to take advantage of this continuous source of wireless power, such as to design the robot to only use power from the source resonator without the need for batteries, use power from the source resonator to recharge the robot's batteries, use the power from the source resonator to trickle charge the robot's batteries, use the power from the source resonator to charge a capacitive energy storage unit, and the like. Similar optimizations of the power supplies and power circuits may be enabled, designed, and realized, for any and all of the devices disclosed herein.

**[00456]** The systems and methods described herein may be able to provide wireless power to electrically heated blankets, heating pads/patches, and the like. These electrically heated devices may find a variety of indoor and outdoor uses. For example, hand and foot warmers supplied to outdoor workers such as guards, policemen, construction workers and the like might be remotely powered from a source resonator associated with or built into a nearby vehicle, building, utility pole, traffic light, portable power unit, and the like.

**[00457]** The systems and methods described herein may be used to power a portable information device that contains a device resonator and that may be powered up when the information device is near an information source containing a source resonator. For instance, the information device may be a card (e.g. credit card, smart card, electronic card, and the like) carried in a user's pocket, wallet, purse, vehicle, bike, and the like. The portable information device may be powered up when it is in the vicinity of an information source that then transmits information to the portable information device that may contain electronic logic, electronic processors, memory, a display, an LCD display, LEDs, RFID tags, and the like. For example, the

portable information device may be a credit card with a display that "turns on" when it is near an information source, and provide the user with some information such as, "You just received a coupon for 50% off your next Coca Cola purchase". The information device may store information such as coupon or discount information that could be used on subsequent purchases. The portable information device may be programmed by the user to contain tasks, calendar appointments, to-do lists, alarms and reminders, and the like. The information device may receive up-to-date price information and inform the user of the location and price of previously selected or identified items.

**[00458]** The systems and methods described herein may provide wireless power transmission to directly power or recharge the batteries in sensors, such as environmental sensors, security sensors, agriculture sensors, appliance sensors, food spoilage sensors, power sensors, and the like, which may be mounted internal to a structure, external to a structure, buried underground, installed in walls, and the like. For example, this capability may replace the need to dig out old sensors to physically replace the battery, or to bury a new sensor because the old sensor is out of power and no longer operational. These sensors may be charged up periodically through the use of a portable sensor source resonator charging unit. For instance, a truck carrying a source resonator equipped power source, say providing ~kW of power, may provide enough power to a ~mW sensor in a few minutes to extend the duration of operation of the sensor for more than a year. Sensors may also be directly powered, such as powering sensors that are in places where it is difficult to connect to them with a wire but they are still within the vicinity of a source resonator, such as devices outside of a house (security camera), on the other side of a wall, on an electric lock on a door, and the like. In another example, sensors that may need to be otherwise supplied with a wired power connection may be powered through the systems and methods described herein. For example, a ground fault interrupter breaker combines residual current and over-current protection in one device for installation into a service panel. However, the sensor traditionally has to be independently wired for power, and this may complicate the installation. However, with the systems and methods described herein the sensor may be powered with a device resonator, where a single source resonator is provided within the service panel, thus simplifying the installation and wiring configuration within the service panel. In addition, the single source resonator may power device resonators mounted on either side of the source resonator mounted within the service panel, throughout the service panel, to additional

nearby service panels, and the like. The systems and methods described herein may be employed to provide wireless power to any electrical component associated with electrical panels, electrical rooms, power distribution and the like, such as in electric switchboards, distribution boards, circuit breakers, transformers, backup batteries, fire alarm control panels, and the like. Through the use of the systems and methods described herein, it may be easier to install, maintain, and modify electrical distribution and protection components and system installations.

**[00459]** In another example, sensors that are powered by batteries may run continuously, without the need to change the batteries, because wireless power may be supplied to periodically or continuously recharge or trickle charge the battery. In such applications, even low levels of power may adequately recharge or maintain the charge in batteries, significantly extending their lifetime and usefulness. In some cases, the battery life may be extended to be longer than the lifetime of the device it is powering, making it essentially a battery that “lasts forever”.

**[00460]** The systems and methods described herein may be used for charging implanted medical device batteries, such as in an artificial heart, pacemaker, heart pump, insulin pump, implanted coils for nerve or acupuncture/acupressure/acupuncture point stimulation, and the like. For instance, it may not be convenient or safe to have wires sticking out of a patient because the wires may be a constant source of possible infection and may generally be very unpleasant for the patient. The systems and methods described herein may also be used to charge or power medical devices in or on a patient from an external source, such as from a bed or a hospital wall or ceiling with a source resonator. Such medical devices may be easier to attach, read, use and monitor the patient. The systems and methods described herein may ease the need for attaching wires to the patient and the patient’s bed or bedside, making it more convenient for the patient to move around and get up out of bed without the risk of inadvertently disconnecting a medical device. This may, for example, be usefully employed with patients that have multiple sensors monitoring them, such as for measuring pulse, blood pressure, glucose, and the like. For medical and monitoring devices that utilize batteries, the batteries may need to be replaced quite often, perhaps multiple times a week. This may present risks associated with people forgetting to replace batteries, not noticing that the devices or monitors are not working because the batteries have died, infection associated with improper cleaning of the battery covers and compartments, and the like.

[00461] The systems and methods described herein may reduce the risk and complexity of medical device implantation procedures. Today many implantable medical devices such as ventricular assist devices, pacemakers, defibrillators and the like, require surgical implantation due to their device form factor, which is heavily influenced by the volume and shape of the long-life battery that is integrated in the device. In one aspect, there is described herein a non-invasive method of recharging the batteries so that the battery size may be dramatically reduced, and the entire device may be implanted, such as via a catheter. A catheter implantable device may include an integrated capture or device coil. A catheter implantable capture or device coil may be designed so that it may be wired internally, such as after implantation. The capture or device coil may be deployed via a catheter as a rolled up flexible coil (e.g. rolled up like two scrolls, easily unrolled internally with a simple spreader mechanism). The power source coil may be worn in a vest or article of clothing that is tailored to fit in such a way that places the source in proper position, may be placed in a chair cushion or bed cushion, may be integrated into a bed or piece of furniture, and the like.

[00462] The systems and methods described herein may enable patients to have a 'sensor vest', sensor patch, and the like, that may include at least one of a plurality of medical sensors and a device resonator that may be powered or charged when it is in the vicinity of a source resonator. Traditionally, this type of medical monitoring facility may have required batteries, thus making the vest, patch, and the like, heavy, and potentially impractical. But using the principles disclosed herein, no batteries (or a lighter rechargeable battery) may be required, thus making such a device more convenient and practical, especially in the case where such a medical device could be held in place without straps, such as by adhesive, in the absence of batteries or with substantially lighter batteries. A medical facility may be able to read the sensor data remotely with the aim of anticipating (e.g. a few minutes ahead of) a stroke, a heart-attack, or the like. When the vest is used by a person in a location remote from the medical facility, such as in their home, the vest may then be integrated with a cell-phone or communications device to call an ambulance in case of an accident or a medical event. The systems and methods described herein may be of particular value in the instance when the vest is to be used by an elderly person, where traditional non-wireless recharging practices (e.g. replacing batteries, plugging in at night, and the like) may not be followed as required. The systems and methods described herein may also be used for charging devices that are used by or that aid handicapped or disabled people

who may have difficulty replacing or recharging batteries, or reliably supplying power to devices they enjoy or rely on.

**[00463]** The systems and methods described herein may be used for the charging and powering of artificial limbs. Artificial limbs have become very capable in terms of replacing the functionality of original limbs, such as arms, legs, hands and feet. However, an electrically powered artificial limb may require substantial power, (such as 10-20W) which may translate into a substantial battery. In that case, the amputee may be left with a choice between a light battery that doesn't last very long, and a heavy battery that lasts much longer, but is more difficult to 'carry' around. The systems and methods described herein may enable the artificial limb to be powered with a device resonator, where the source resonator is either carried by the user and attached to a part of the body that may more easily support the weight (such as on a belt around the waist, for example) or located in an external location where the user will spend an adequate amount of time to keep the device charged or powered, such as at their desk, in their car, in their bed, and the like.

**[00464]** The systems and methods described herein may be used for charging and powering of electrically powered exo-skeletons, such as those used in industrial and military applications, and for elderly/weak/sick people. An electrically powered exo-skeleton may provide up to a 10-to-20 times increase in "strength" to a person, enabling the person to perform physically strenuous tasks repeatedly without much fatigue. However, exo-skeletons may require more than 100W of power under certain use scenarios, so battery powered operation may be limited to 30 minutes or less. The delivery of wireless power as described herein may provide a user of an exo-skeleton with a continuous supply of power both for powering the structural movements of the exo-skeleton and for powering various monitors and sensors distributed throughout the structure. For instance, an exo-skeleton with an embedded device resonator(s) may be supplied with power from a local source resonator. For an industrial exo-skeleton, the source resonator may be placed in the walls of the facility. For a military exo-skeleton, the source resonator may be carried by an armored vehicle. For an exo-skeleton employed to assist a caretaker of the elderly, the source resonator(s) may be installed or placed in or the room(s) of a person's home.

**[00465]** The systems and methods described herein may be used for the powering/charging of portable medical equipment, such as oxygen systems, ventilators,



defibrillators, medication pumps, monitors, and equipment in ambulances or mobile medical units, and the like. Being able to transport a patient from an accident scene to the hospital, or to move patients in their beds to other rooms or areas, and bring all the equipment that is attached with them and have it powered the whole time offers great benefits to the patients' health and eventual well-being. Certainly one can understand the risks and problems caused by medical devices that stop working because their battery dies or because they must be unplugged while a patient is transported or moved in any way. For example, an emergency medical team on the scene of an automotive accident might need to utilize portable medical equipment in the emergency care of patients in the field. Such portable medical equipment must be properly maintained so that there is sufficient battery life to power the equipment for the duration of the emergency. However, it is too often the case that the equipment is not properly maintained so that batteries are not fully charged and in some cases, necessary equipment is not available to the first responders. The systems and methods described herein may provide for wireless power to portable medical equipment (and associated sensor inputs on the patient) in such a way that the charging and maintaining of batteries and power packs is provided automatically and without human intervention. Such a system also benefits from the improved mobility of a patient unencumbered by a variety of power cords attached to the many medical monitors and devices used in their treatment.

**[00466]** The systems and methods described herein may be used to for the powering/charging of personal hearing aids. Personal hearing aids need to be small and light to fit into or around the ear of a person. The size and weight restrictions limit the size of batteries that can be used. Likewise, the size and weight restrictions of the device make battery replacement difficult due to the delicacy of the components. The dimensions of the devices and hygiene concerns make it difficult to integrate additional charging ports to allow recharging of the batteries. The systems and methods described herein may be integrated into the hearing aid and may reduce the size of the necessary batteries which may allow even smaller hearing aids. Using the principles disclosed herein, the batteries of the hearing aid may be recharged without requiring external connections or charging ports. Charging and device circuitry and a small rechargeable battery may be integrated into a form factor of a conventional hearing aid battery allowing retrofit into existing hearing aids. The hearing aid may be recharged while it is used and worn by a person. The energy source may be integrated into a pad or a cup allowing recharging

when the hearing is placed on such a structure. The charging source may be integrated into a hearing aid dryer box allowing wireless recharging while the hearing aid is drying or being sterilized. The source and device resonator may be used to also heat the device reducing or eliminating the need for an additional heating element. Portable charging cases powered by batteries or AC adaptors may be used as storage and charging stations.

**[00467]** The source resonator for the medical systems described above may be in the main body of some or all of the medical equipment, with device resonators on the patient's sensors and devices; the source resonator may be in the ambulance with device resonators on the patient's sensors and the main body of some or all of the equipment; a primary source resonator may be in the ambulance for transferring wireless power to a device resonator on the medical equipment while the medical equipment is in the ambulance and a second source resonator is in the main body of the medical equipment and a second device resonator on the patient sensors when the equipment is away from the ambulance; and the like. The systems and methods described herein may significantly improve the ease with which medical personnel are able to transport patients from one location to another, where power wires and the need to replace or manually charge associated batteries may now be reduced.

**[00468]** The systems and methods described herein may be used for the charging of devices inside a military vehicle or facility, such as a tank, armored carrier, mobile shelter, and the like. For instance, when soldiers come back into a vehicle after "action" or a mission, they may typically start charging their electronic devices. If their electronic devices were equipped with device resonators, and there was a source resonator inside the vehicle, (e.g. integrated in the seats or on the ceiling of the vehicle), their devices would start charging immediately. In fact, the same vehicle could provide power to soldiers/robots (e.g. packbot from iRobot) standing outside or walking beside the vehicle. This capability may be useful in minimizing accidental battery-swapping with someone else (this may be a significant issue, as soldiers tend to trust only their own batteries); in enabling quicker exits from a vehicle under attack; in powering or charging laptops or other electronic devices inside a tank, as too many wires inside the tank may present a hazard in terms of reduced ability to move around fast in case of "trouble" and/or decreased visibility; and the like. The systems and methods described herein may provide a significant improvement in association with powering portable power equipment in a military environment.

**[00469]** The systems and methods described herein may provide wireless powering or charging capabilities to mobile vehicles such as golf carts or other types of carts, all-terrain vehicles, electric bikes, scooters, cars, mowers, bobcats and other vehicles typically used for construction and landscaping and the like. The systems and methods described herein may provide wireless powering or charging capabilities to miniature mobile vehicles, such as mini-helicopters, airborne drones, remote control planes, remote control boats, remote controlled or robotic rovers, remote controlled or robotic lawn mowers or equipment, bomb detection robots, and the like. For instance, mini-helicopter flying above a military vehicle to increase its field of view can fly for a few minutes on standard batteries. If these mini-helicopters were fitted with a device resonator, and the control vehicle had a source resonator, the mini-helicopter might be able to fly indefinitely. The systems and methods described herein may provide an effective alternative to recharging or replacing the batteries for use in miniature mobile vehicles. In addition, the systems and methods described herein may provide power/charging to even smaller devices, such as microelectromechanical systems (MEMS), nano-robots, nano devices, and the like. In addition, the systems and methods described herein may be implemented by installing a source device in a mobile vehicle or flying device to enable it to serve as an in-field or in-flight re-charger, that may position itself autonomously in proximity to a mobile vehicle that is equipped with a device resonator.

**[00470]** The systems and methods described herein may be used to provide power networks for temporary facilities, such as military camps, oil drilling setups, remote filming locations, and the like, where electrical power is required, such as for power generators, and where power cables are typically run around the temporary facility. There are many instances when it is necessary to set up temporary facilities that require power. The systems and methods described herein may enable a more efficient way to rapidly set up and tear down these facilities, and may reduce the number of wires that must be run throughout the facilities to supply power. For instance, when Special Forces move into an area, they may erect tents and drag many wires around the camp to provide the required electricity. Instead, the systems and methods described herein may enable an army vehicle, outfitted with a power supply and a source resonator, to park in the center of the camp, and provide all the power to nearby tents where the device resonator may be integrated into the tents, or some other piece of equipment associated with each tent or area. A series of source-device-source-device resonators may be used to extend the power to

tents that are farther away. That is, the tents closest to the vehicle could then provide power to tents behind them. The systems and methods described herein may provide a significant improvement to the efficiency with which temporary installations may be set up and torn down, thus improving the mobility of the associated facility.

**[00471]** The systems and methods described herein may be used in vehicles, such as for replacing wires, installing new equipment, powering devices brought into the vehicle, charging the battery of a vehicle (e.g. for a traditional gas powered engine, for a hybrid car, for an electric car, and the like), powering devices mounted to the interior or exterior of the vehicle, powering devices in the vicinity of the vehicle, and the like. For example, the systems and methods described herein may be used to replace wires such as those are used to power lights, fans and sensors distributed throughout a vehicle. As an example, a typical car may have 50kg of wires associated with it, and the use of the systems and methods described herein may enable the elimination of a substantial amount of this wiring. The performance of larger and more weight sensitive vehicles such as airplanes or satellites could benefit greatly from having the number of cables that must be run throughout the vehicle reduced. The systems and methods described herein may allow the accommodation of removable or supplemental portions of a vehicle with electric and electrical devices without the need for electrical harnessing. For example, a motorcycle may have removable side boxes that act as a temporary trunk space for when the cyclist is going on a long trip. These side boxes may have exterior lights, interior lights, sensors, auto equipment, and the like, and if not for being equipped with the systems and methods described herein might require electrical connections and harnessing.

**[00472]** An in-vehicle wireless power transmission system may charge or power one or more mobile devices used in a car: mobile phone handset, Bluetooth headset, blue tooth hands free speaker phone, GPS, MP3 player, wireless audio transceiver for streaming MP3 audio through car stereo via FM, Bluetooth, and the like. The in vehicle wireless power source may utilize source resonators that are arranged in any of several possible configurations including charging pad on dash, charging pad otherwise mounted on floor, or between seat and center console, charging “cup” or receptacle that fits in cup holder or on dash, and the like.

**[00473]** The wireless power transmission source may utilize a rechargeable battery system such that said supply battery gets charged whenever the vehicle power is on such that

when the vehicle is turned off the wireless supply can draw power from the supply battery and can continue to wirelessly charge or power mobile devices that are still in the car.

[00474] The plug-in electric cars, hybrid cars, and the like, of the future need to be charged, and the user may need to plug in to an electrical supply when they get home or to a charging station. Based on a single over-night recharging, the user may be able to drive up to 50 miles the next day. Therefore, in the instance of a hybrid car, if a person drives less than 50 miles on most days, they will be driving mostly on electricity. However, it would be beneficial if they didn't have to remember to plug in the car at night. That is, it would be nice to simply drive into a garage, and have the car take care of its own charging. To this end, a source resonator may be built into the garage floor and/or garage side-wall, and the device resonator may be built into the bottom (or side) of the car. Even a few kW transfer may be sufficient to recharge the car over-night. The in-vehicle device resonator may measure magnetic field properties to provide feedback to assist in vehicle (or any similar device) alignment to a stationary resonating source. The vehicle may use this positional feedback to automatically position itself to achieve optimum alignment, thus optimum power transmission efficiency. Another method may be to use the positional feedback to help the human operator to properly position the vehicle or device, such as by making LED's light up, providing noises, and the like when it is well positioned. In such cases where the amount of power being transmitted could present a safety hazard to a person or animal that intrudes into the active field volume, the source or receiver device may be equipped with an active light curtain or some other external device capable of sensing intrusion into the active field volume, and capable of shutting off the source device and alert a human operator. In addition, the source device may be equipped with self-sensing capability such that it may detect that its expected power transmission rate has been interrupted by an intruding element, and in such case shut off the source device and alert a human operator. Physical or mechanical structures such as hinged doors or inflatable bladder shields may be incorporated as a physical barrier to prevent unwanted intrusions. Sensors such as optical, magnetic, capacitive, inductive, and the like may also be used to detect foreign structures or interference between the source and device resonators. The shape of the source resonator may be shaped such to prevent water or debris accumulation. The source resonator may be placed in a cone shaped enclosure or may have an enclosure with an angled top to allow water and debris to roll off. The source of the

system may use battery power of the vehicle or its own battery power to transmit its presence to the source to initiate power transmission.

[00475] The source resonator may be mounted on an embedded or hanging post, on a wall, on a stand, and the like for coupling to a device resonator mounted on the bumper, hood, body panel, and the like, of an electric vehicle. The source resonator may be enclosed or embedded into a flexible enclosure such as a pillow, a pad, a bellows, a spring loaded enclosure and the like so that the electric vehicle may make contact with the structure containing the source coil without damaging the car in any way. The structure containing the source may prevent objects from getting between the source and device resonators. Because the wireless power transfer may be relatively insensitive to misalignments between the source and device coils, a variety of flexible source structures and parking procedures may be appropriate for this application.

[00476] The systems and methods described herein may be used to trickle charge batteries of electric, hybrid or combustion engine vehicles. Vehicles may require small amounts of power to maintain or replenish battery power. The power may be transferred wirelessly from a source to a device resonator that may be incorporated into the front grill, roof, bottom, or other parts of the vehicle. The device resonator may be designed to fit into a shape of a logo on the front of a vehicle or around the grill as not to obstruct air flow through the radiator. The device or source resonator may have additional modes of operation that allow the resonator to be used as a heating element which can be used to melt of snow or ice from the vehicle.

[00477] An electric vehicle or hybrid vehicle may require multiple device resonators, such as to increase the ease with which the vehicle may come in proximity with a source resonator for charging (i.e. the greater the number and varied position of device resonators are, the greater the chances that the vehicle can pull in and interface with a diversity of charging stations), to increase the amount of power that can be delivered in a period of time (e.g. additional device resonators may be required to keep the local heating due to charging currents to acceptable levels), to aid in automatic parking/docking the vehicle with the charging station, and the like. For example, the vehicle may have multiple resonators (or a single resonator) with a feedback system that provides guidance to either the driver or an automated parking/docking facility in the parking of the vehicle for optimized charging conditions (i.e., the optimum positioning of the vehicle's device resonator to the charging station's source resonator may

provide greater power transfer efficiency). An automated parking/docking facility may allow for the automatic parking of the vehicle based on how well the vehicle is coupled.

**[00478]** The power transmission system may be used to power devices and peripherals of a vehicle. Power to peripherals may be provided while a vehicle is charging, or while not charging, or power may be delivered to conventional vehicles that do not need charging. For example, power may be transferred wirelessly to conventional non-electric cars to power air conditioning, refrigeration units, heaters, lights, and the like while parked to avoid running the engine which may be important to avoid exhaust build up in garage parking lots or loading docks. Power may for example be wirelessly transferred to a bus while it is parked to allow powering of lights, peripherals, passenger devices, and the like avoiding the use of onboard engines or power sources. Power may be wirelessly transferred to an airplane while parked on the tarmac or in a hanger to power instrumentation, climate control, de-icing equipment, and the like without having to use onboard engines or power sources.

**[00479]** Wireless power transmission on vehicles may be used to enable the concept of Vehicle to Grid (V2G). Vehicle to grid is based on utilizing electric vehicles and plug-in hybrid electric vehicles (PHEV) as distributed energy storage devices, charged at night when the electric grid is underutilized, and available to discharge back into the grid during episodes of peak demand that occur during the day. The wireless power transmission system on a vehicle and the respective infrastructure may be implemented in such a way as to enable bidirectional energy flow—so that energy can flow back into the grid from the vehicle—without requiring a plug in connection. Vast fleets of vehicles, parked at factories, offices, parking lots, can be viewed as “peaking power capacity” by the smart grid. Wireless power transmission on vehicles can make such a V2G vision a reality. By simplifying the process of connecting a vehicle to the grid, (i.e. by simply parking it in a wireless charging enabled parking spot), it becomes much more likely that a certain number of vehicles will be “dispatchable” when the grid needs to tap their power. Without wireless charging, electric and PHEV owners will likely charge their vehicles at home, and park them at work in conventional parking spots. Who will want to plug their vehicle in at work, if they do not need charging? With wireless charging systems capable of handling 3 kW, 100,000 vehicles can provide 300 Megawatts back to the grid—using energy generated the night before by cost effective base load generating capacity. It is the streamlined ergonomics of the cordless self charging PHEV and electric vehicles that make it a viable V2G energy source.

**[00480]** The systems and methods described herein may be used to power sensors on the vehicle, such as sensors in tires to measure air-pressure, or to run peripheral devices in the vehicle, such as cell phones, GPS devices, navigation devices, game players, audio or video players, DVD players, wireless routers, communications equipment, anti-theft devices, radar devices, and the like. For example, source resonators described herein may be built into the main compartment of the car in order to supply power to a variety of devices located both inside and outside of the main compartment of the car. Where the vehicle is a motorcycle or the like, devices described herein may be integrated into the body of the motorcycle, such as under the seat, and device resonators may be provided in a user's helmet, such as for communications, entertainment, signaling, and the like, or device resonators may be provided in the user's jacket, such as for displaying signals to other drivers for safety, and the like.

**[00481]** The systems and methods described herein may be used in conjunction with transportation infrastructure, such as roads, trains, planes, shipping, and the like. For example, source resonators may be built into roads, parking lots, rail-lines, and the like. Source resonators may be built into traffic lights, signs, and the like. For example, with source resonators embedded into a road, and device resonators built into vehicles, the vehicles may be provided power as they drive along the road or as they are parked in lots or on the side of the road. The systems and methods described herein may provide an effective way for electrical systems in vehicles to be powered and/or charged while the vehicle traverses a road network, or a portion of a road network. In this way, the systems and methods described herein may contribute to the powering/charging of autonomous vehicles, automatic guided vehicles, and the like. The systems and methods described herein may provide power to vehicles in places where they typically idle or stop, such as in the vicinity of traffic lights or signs, on highway ramps, or in parking lots.

**[00482]** The systems and methods described herein may be used in an industrial environment, such as inside a factory for powering machinery, powering/charging robots, powering and/or charging wireless sensors on robot arms, powering/charging tools and the like. For example, using the systems and methods described herein to supply power to devices on the arms of robots may help eliminate direct wire connections across the joints of the robot arm. In this way, the wearing out of such direct wire connections may be reduced, and the reliability of the robot increased. In this case, the device resonator may be out on the arm of the robot, and the source resonator may be at the base of the robot, in a central location near the robot, integrated



into the industrial facility in which the robot is providing service, and the like. The use of the systems and methods described herein may help eliminate wiring otherwise associated with power distribution within the industrial facility, and thus benefit the overall reliability of the facility.

**[00483]** The systems and methods described herein may be used for underground applications, such as drilling, mining, digging, and the like. For example, electrical components and sensors associated with drilling or excavation may utilize the systems and methods described herein to eliminate cabling associated with a digging mechanism, a drilling bit, and the like, thus eliminating or minimizing cabling near the excavation point. In another example, the systems and methods described herein may be used to provide power to excavation equipment in a mining application where the power requirements for the equipment may be high and the distances large, but where there are no people to be subjected to the associated required fields. For instance, the excavation area may have device resonator powered digging equipment that has high power requirements and may be digging relatively far from the source resonator. As a result the source resonator may need to provide high field intensities to satisfy these requirements, but personnel are far enough away to be outside these high intensity fields. This high power, no personnel, scenario may be applicable to a plurality of industrial applications.

**[00484]** The systems and methods described herein may also use the near-field non-radiative resonant scheme for information transfer rather than, or in addition to, power transfer. For instance, information being transferred by near-field non-radiative resonance techniques may not be susceptible to eavesdropping and so may provide an increased level of security compared to traditional wireless communication schemes. In addition, information being transferred by near-field non-radiative resonance techniques may not interfere with the EM radiative spectrum and so may not be a source of EM interference, thereby allowing communications in an extended frequency range and well within the limits set by any regulatory bodies. Communication services may be provided between remote, inaccessible or hard-to-reach places such as between remote sensors, between sections of a device or vehicle, in tunnels, caves and wells (e.g. oil wells, other drill sites) and between underwater or underground devices, and the like. Communications services may be provided in places where magnetic fields experience less loss than electric fields.

[00485] The systems and methods described herein may enable the simultaneous transmission of power and communication signals between sources and devices in wireless power transmission systems, or it may enable the transmission of power and communication signals during different time periods or at different frequencies. The performance characteristics of the resonator may be controllably varied to preferentially support or limit the efficiency or range of either energy or information transfer. The performance characteristics of the resonators may be controlled to improve the security by reducing the range of information transfer, for example. The performance characteristics of the resonators may be varied continuously, periodically, or according to a predetermined, computed or automatically adjusted algorithm. For example, the power and information transfer enabled by the systems and methods described herein may be provided in a time multiplexed or frequency multiplexed manner. A source and device may signal each other by tuning, changing, varying, dithering, and the like, the resonator impedance which may affect the reflected impedance of other resonators that can be detected. The information transferred as described herein may include information regarding device identification, device power requirements, handshaking protocols, and the like.

[00486] The source and device may sense, transmit, process and utilize position and location information on any other sources and/or devices in a power network. The source and device may capture or use information such as elevation, tilt, latitude and longitude, and the like from a variety of sensors and sources that may be built into the source and device or may be part of a component the source or device connect. The positioning and orientation information may include sources such as global positioning sensors (GPS), compasses, accelerometers, pressure sensors, atmospheric barometric sensors, positioning systems which use Wi-Fi or cellular network signals, and the like. The source and device may use the position and location information to find nearby wireless power transmission sources. A source may broadcast or communicate with a central station or database identifying its location. A device may obtain the source location information from the central station or database or from the local broadcast and guide a user or an operator to the source with the aid of visual, vibrational, or auditory signals. Sources and devices may be nodes in a power network, in a communications network, in a sensor network, in a navigational network, and the like or in kind of combined functionality network.

[00487] The position and location information may also be used to optimize or coordinate power delivery. Additional information about the relative position of a source and a

device may be used to optimize magnetic field direction and resonator alignment. The orientation of a device and a source which may be obtained from accelerometers and magnetic sensors, and the like, for example, may be used to identify the orientation of resonators and the most favorable direction of a magnetic field such that the magnetic flux is not blocked by the device circuitry. With such information a source with the most favorable orientation, or a combination of sources, may be used. Likewise, position and orientation information may be used to move or provide feedback to a user or operator of a device to place a device in a favorable orientation or location to maximize power transmission efficiency, minimize losses, and the like.

**[00488]** The source and device may include power metering and measuring circuitry and capability. The power metering may be used to track how much power was delivered to a device or how much power was transferred by a source. The power metering and power usage information may be used in fee based power delivery arrangements for billing purposes. Power metering may be also be used to enable power delivery policies to ensure power is distributed to multiple devices according to specific criteria. For example, the power metering may be used to categorize devices based on the amount of power they received and priority in power delivery may be given to those having received the least power. Power metering may be used to provide tiered delivery services such as “guaranteed power” and “best effort power” which may be billed at separate rates. Power metering may be used to institute and enforce hierarchical power delivery structures and may enable priority devices to demand and receive- more power under certain circumstances or use scenarios.

**[00489]** Power metering may be used to optimize power delivery efficiency and minimize absorption and radiation losses. Information related to the power received by devices may be used by a source in conjunction with information about the power output of the source to identify unfavorable operating environments or frequencies. For example, a source may compare the amount of power which was received by the devices and the amount of power which it transmitted to determine if the transmission losses may be unusually or unacceptably large. Large transmission losses may be due to an unauthorized device receiving power from the source and the source and other devices may initiate frequency hopping of the resonance frequency or other defensive measures to prevent or deter unauthorized use. Large transmission losses may be due to absorption losses for example, and the device and source may tune to alternate resonance frequencies to minimize such losses. Large transmission losses may also indicate the presence of

unwanted or unknown objects or materials and the source may turn down or off its power level until the unwanted or unknown object is removed or identified, at which point the source may resume powering remote devices.

**[00490]** The source and device may include authentication capability. Authentication may be used to ensure that only compatible sources and devices are able to transmit and receive power. Authentication may be used to ensure that only authentic devices that are of a specific manufacturer and not clones or devices and sources from other manufacturers, or only devices that are part of a specific subscription or plan, are able to receive power from a source. Authentication may be based on cryptographic request and respond protocols or it may be based on the unique signatures of perturbations of specific devices allowing them to be used and authenticated based on properties similar to physically unclonable functions. Authentication may be performed locally between each source and device with local communication or it may be used with third person authentication methods where the source and device authenticate with communications to a central authority. Authentication protocols may use position information to alert a local source or sources of a genuine device.

**[00491]** The source and device may use frequency hopping techniques to prevent unauthorized use of a wireless power source. The source may continuously adjust or change the resonant frequency of power delivery. The changes in frequency may be performed in a pseudorandom or predetermined manner that is known, reproducible, or communicated to authorized device but difficult to predict. The rate of frequency hopping and the number of various frequencies used may be large and frequent enough to ensure that unauthorized use is difficult or impractical. Frequency hopping may be implemented by tuning the impedance network, tuning any of the driving circuits, using a plurality of resonators tuned or tunable to multiple resonant frequencies, and the like.

**[00492]** The source may have a user notification capability to show the status of the source as to whether it is coupled to a device resonator and transmitting power, if it is in standby mode, or if the source resonator is detuned or perturbed by an external object. The notification capability may include visual, auditory, and vibrational methods. The notification may be as simple as three color lights, one for each state, and optionally a speaker to provide notification in case of an error in operation. Alternatively, the notification capability may involve an interactive

display that shows the status of the source and optionally provides instructions on how to fix or solve any errors or problems identified.

**[00493]** As another example, wireless power transfer may be used to improve the safety of electronic explosive detonators. Explosive devices are detonated with an electronic detonator, electric detonator, or shock tube detonator. The electronic detonator utilizes stored electrical energy (usually in a capacitor) to activate the igniter charge, with a low energy trigger signal transmitted conductively or by radio. The electric detonator utilizes a high energy conductive trigger signal to provide both the signal and the energy required to activate the igniter charge. A shock tube sends a controlled explosion through a hollow tube coated with explosive from the generator to the igniter charge. There are safety issues associated with the electric and electronic detonators, as there are cases of stray electromagnetic energy causing unintended activation. Wireless power transfer via sharply resonant magnetic coupling can improve the safety of such systems.

**[00494]** Using the wireless power transfer methods disclosed herein, one can build an electronic detonation system that has no locally stored energy, thus reducing the risk of unintended activation. A wireless power source can be placed in proximity (within a few meters) of the detonator. The detonator can be equipped with a resonant capture coil. The activation energy can be transferred when the wireless power source has been triggered. The triggering of the wireless power source can be initiated by any number of mechanisms: radio, magnetic near field radio, conductive signaling, ultrasonics, laser light. Wireless power transfer based on resonant magnetic coupling also has the benefit of being able to transfer power through materials such as rock, soil, concrete, water, and other dense materials. The use of very high Q coils as receivers and sources, having very narrow band response and sharply tuned to proprietary frequencies, further ensure that the detonator circuits cannot capture stray EMI and activate unintentionally.

**[00495]** The resonator of a wirelessly powered device may be external, or outside of the device, and wired to the battery of the device. The battery of the device may be modified to include appropriate rectification and control circuitry to receive the alternating currents of the device resonator. This can enable configurations with larger external coils, such as might be built into a battery door of a keyboard or mouse, or digital still camera, or even larger coils that are attached to the device but wired back to the battery/converter with ribbon cable. The battery door

can be modified to provide interconnection from the external coil to the battery/converter (which will need an exposed contact that can touch the battery door contacts.

[00496] While the invention has been described in connection with certain preferred embodiments, other embodiments will be understood by one of ordinary skill in the art and are intended to fall within the scope of this disclosure, which is to be interpreted in the broadest sense allowable by law.

[00497] All documents referenced herein are hereby incorporated by reference.

## CLAIMS

What is claimed is:

1. A system, comprising:  
a source resonator having a  $Q$ -factor  $Q_1$  and a characteristic size  $x_1$ , coupled to a power generator, and a second resonator having a  $Q$ -factor  $Q_2$  and a characteristic size  $x_2$ , coupled to a load located a distance  $D$  from the source resonator, wherein the source resonator and the second resonator are coupled to exchange energy wirelessly among the source resonator and the second resonator, and wherein  $\sqrt{Q_1 Q_2} > 100$ .
2. The system of claim 1, wherein  $Q_1 < 100$ .
3. The system of claim 1, wherein  $Q_2 < 100$ .
4. The system of claim 1 further comprising, a third resonator having a  $Q$ -factor  $Q_3$  configured to transfer energy non-radiatively with the source and second resonators, wherein  $\sqrt{Q_1 Q_3} > 100$  and  $\sqrt{Q_2 Q_3} > 100$ .
5. The system of claim 4, wherein  $Q_3 < 100$ .
6. The system of claim 1, wherein the source resonator is coupled to the power generator with direct electrical connections.
7. The system of claim 1, further comprising an impedance matching network wherein the source resonator is coupled and impedance matched to the power generator with direct electrical connections.

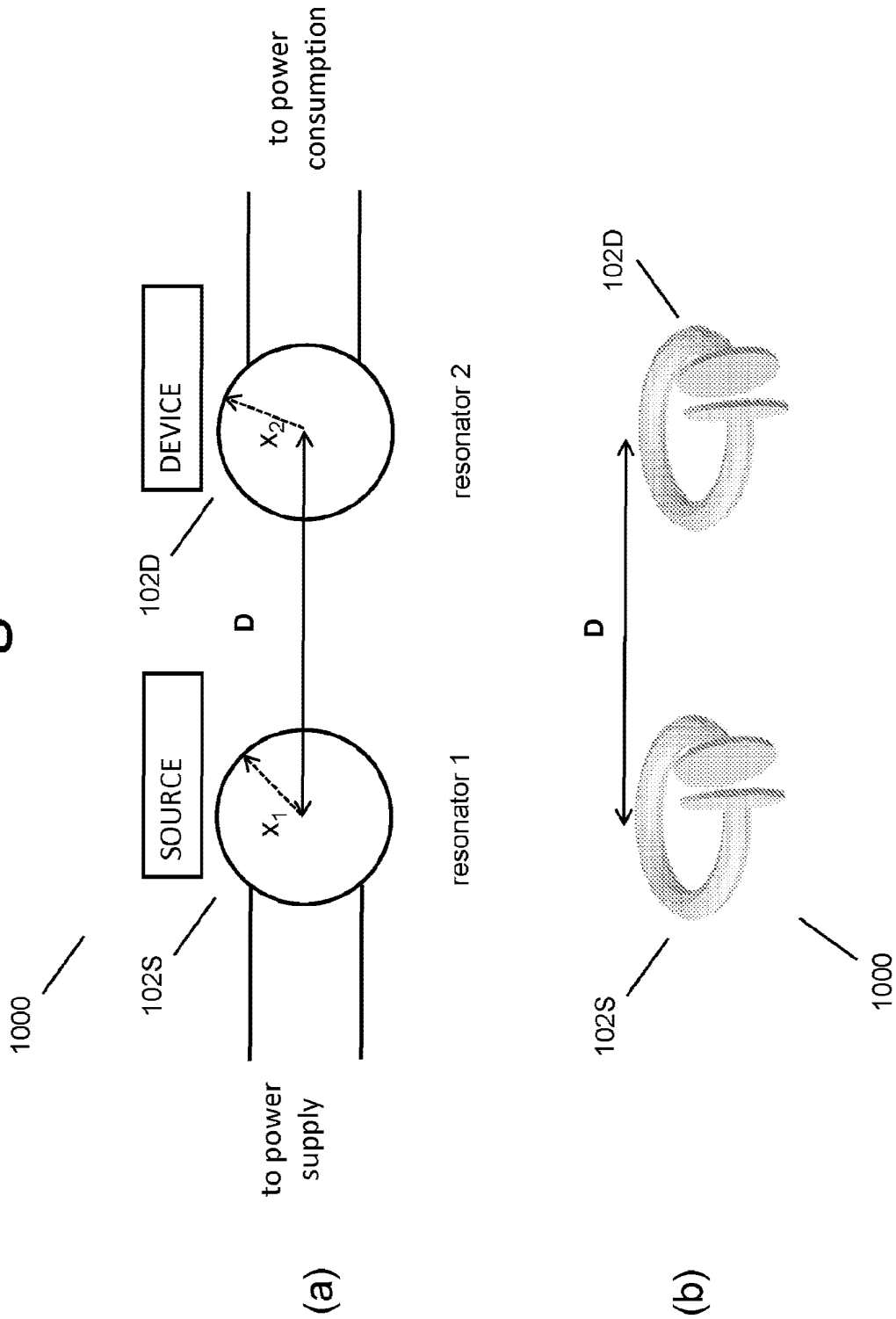
8. The system of claim 1, further comprising a tunable circuit wherein the source resonator is coupled to the power generator through the tunable circuit with direct electrical connections.
9. The system of claim 6, 7, or 8 where at least one of the direct electrical connections is configured to substantially preserve a resonant mode of the source resonator.
10. The system of claim 6, wherein the source resonator has a first terminal, a second terminal, and a center terminal, and wherein an impedance between the first terminal and the center terminal and between the second terminal and the center terminal are substantially equal.
11. The system of claim 6, wherein the source resonator includes a capacitive loaded loop having a first terminal, a second terminal, and a center terminal, and wherein an impedance between the first terminal and the center terminal and between the second terminal and the center terminal are substantially equal.
12. The system of claim 6, wherein the source resonator is coupled to an impedance matching network and the impedance matching network further comprises a first terminal, a second terminal, and a center terminal, and wherein an impedance between the first terminal and the center terminal and between the second terminal and the center terminal are substantially equal.
13. The system of claim 10, 11, or 12, wherein the first terminal and the second terminal are directly coupled to the power generator and driven with oscillating signals that are near 180 degrees out of phase.
14. The system of claim 10, 11, or 12, wherein the source resonator has a resonant frequency  $\omega_1$  and the first terminal and the second terminal are directly coupled to the power generator and driven with oscillating signals that are substantially equal to the resonant frequency  $\omega_1$ .



15. The system of claim 10, 11, or 12, wherein the center terminal is connected to an electrical ground.
16. The system of claim 15, wherein the source resonator has a resonant frequency  $\omega_1$  and the first terminal and the second terminal are directly coupled to the power generator and driven with a frequency substantially equal to the resonant frequency  $\omega_1$ .
17. The system of claim 2, including a plurality of capacitors coupled to the power generator and the load.
18. The system of claim 1, wherein the source resonator and the second resonator are each enclosed in a low loss tangent material.
19. The system of claim 1, further comprising a power conversion circuit wherein the second resonator is coupled to the power conversion circuit to deliver DC power to the load.
20. The system of claim 1, further comprising a power conversion circuit wherein the second resonator is coupled to the power conversion circuit to deliver AC power to the load.
21. The system of claim 1, further comprising a power conversion circuit, wherein the second resonator is coupled to the power conversion circuit to deliver both AC and DC power to the load.
22. The system of claim 1, further comprising a power conversion circuit and a plurality of loads, wherein the second resonator is coupled to the power conversion circuit, and the power conversion circuit is coupled to the plurality of loads.
23. The system of claim 7, wherein the impedance matching network comprises capacitors.

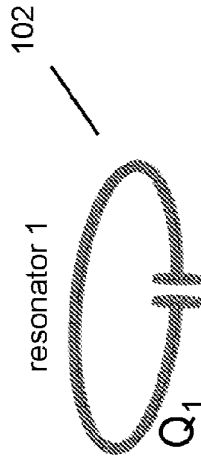
24. The system of claim 7, wherein the impedance matching network comprises inductors.
25. The system of claim 8, wherein the tunable circuit comprises variable capacitors.
26. The system of claim 8, wherein the tunable circuit comprises variable inductors.

Fig. 1



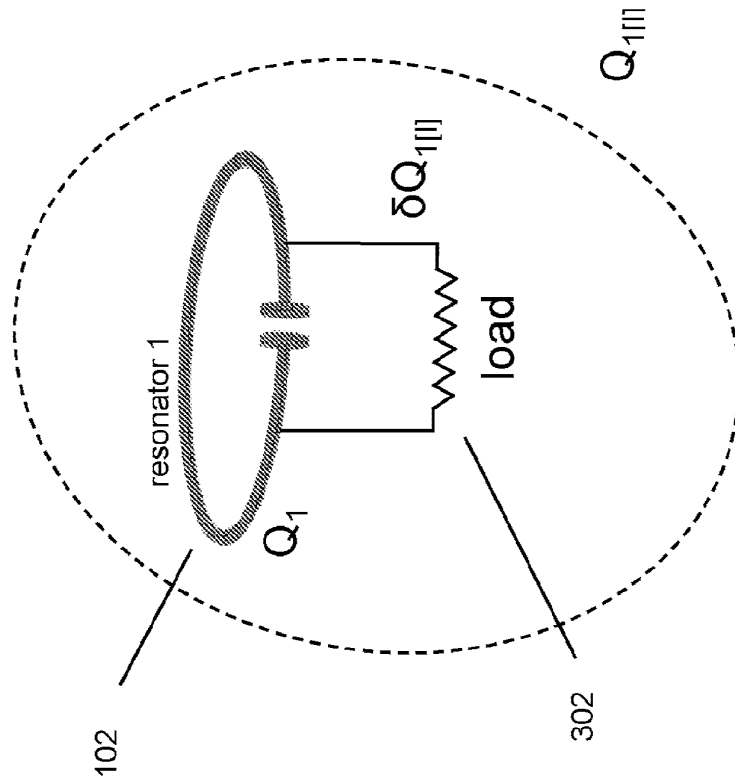
SUBSTITUTE SHEET (RULE 26)

Fig. 2



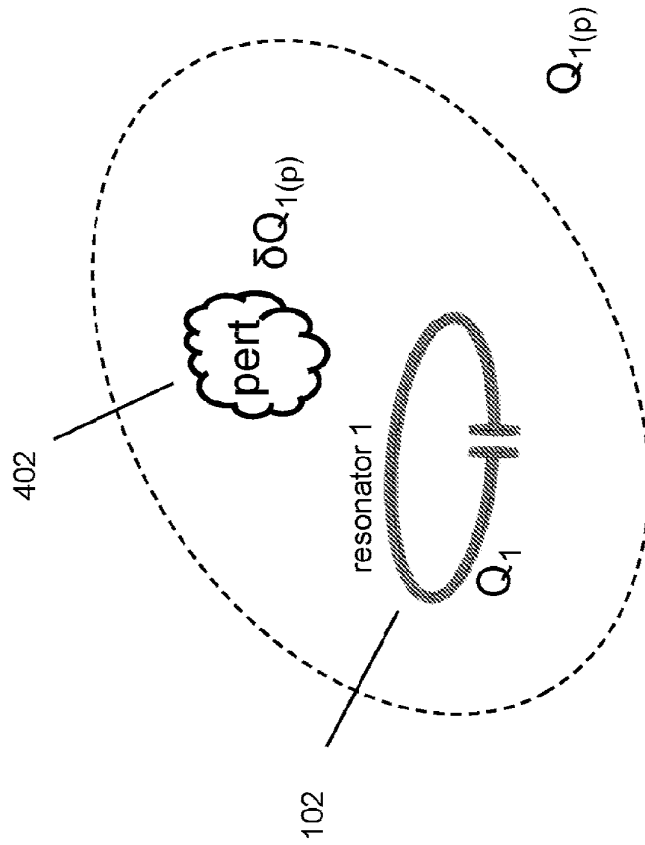
**SUBSTITUTE SHEET (RULE 26)**

Fig. 3



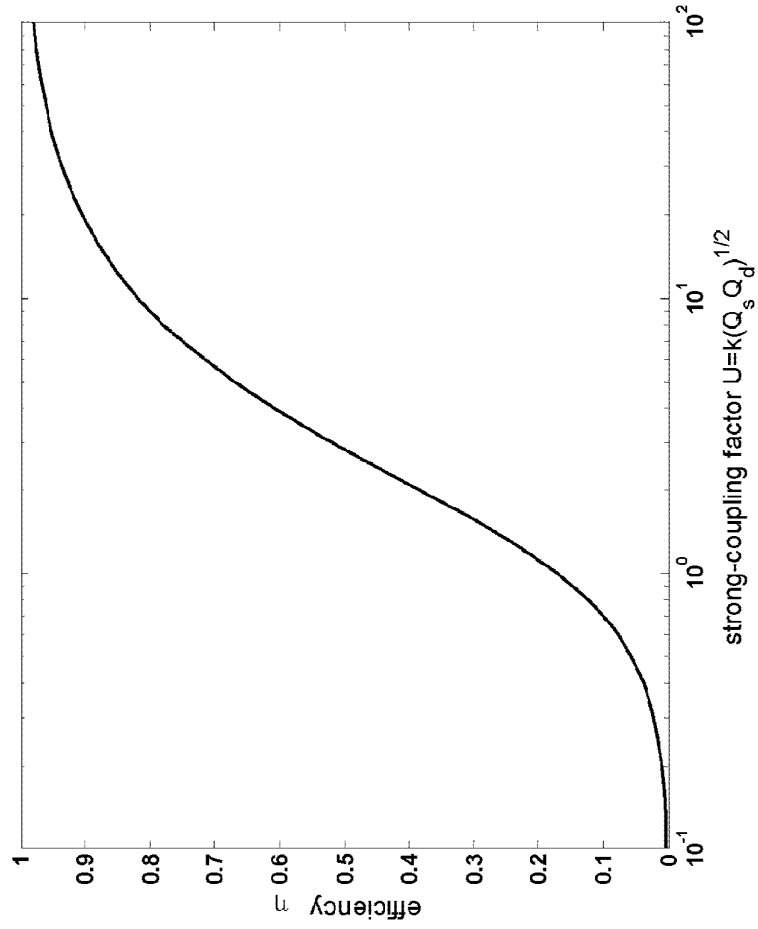
SUBSTITUTE SHEET (RULE 26)

Fig. 4



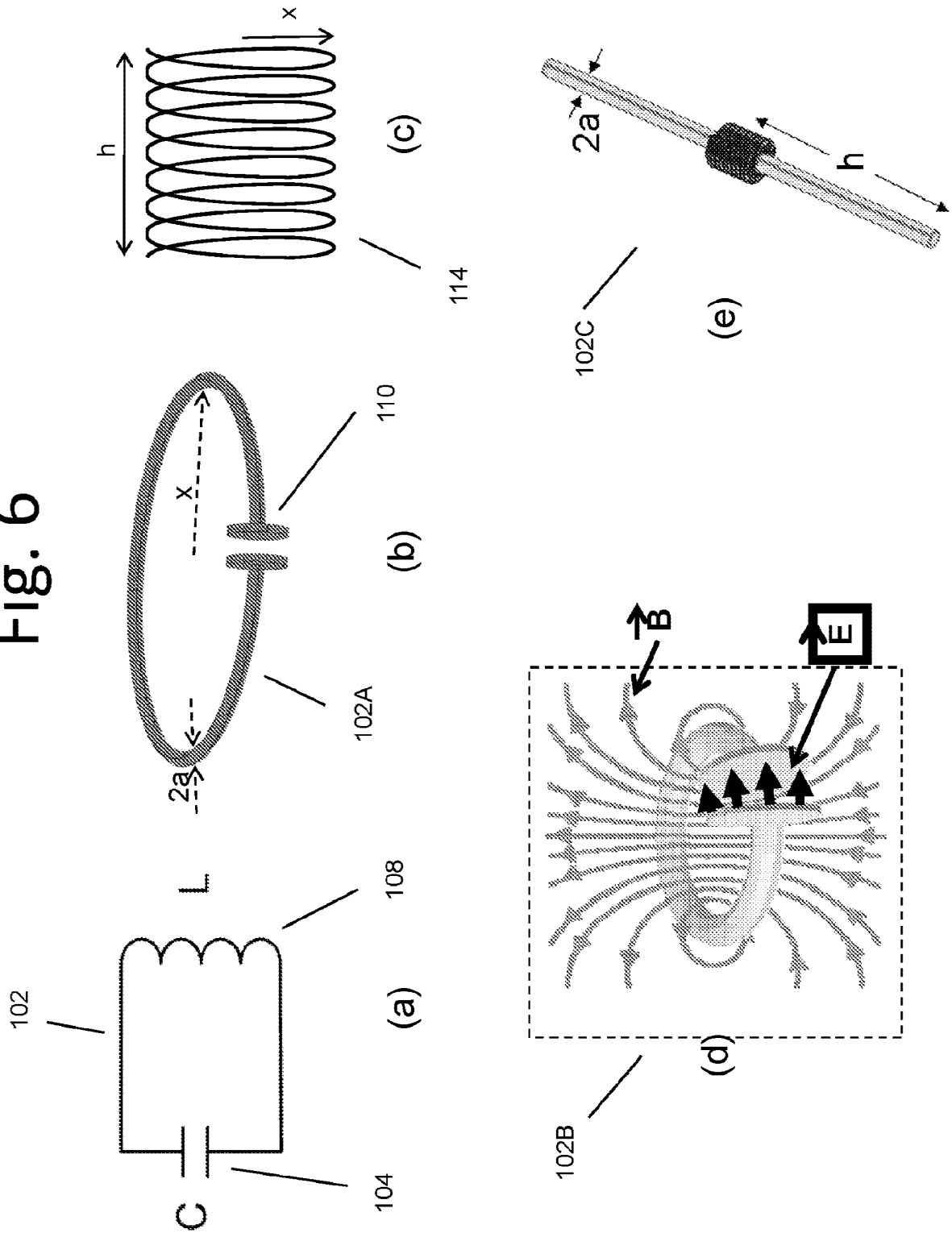
SUBSTITUTE SHEET (RULE 26)

Fig. 5



SUBSTITUTE SHEET (RULE 26)

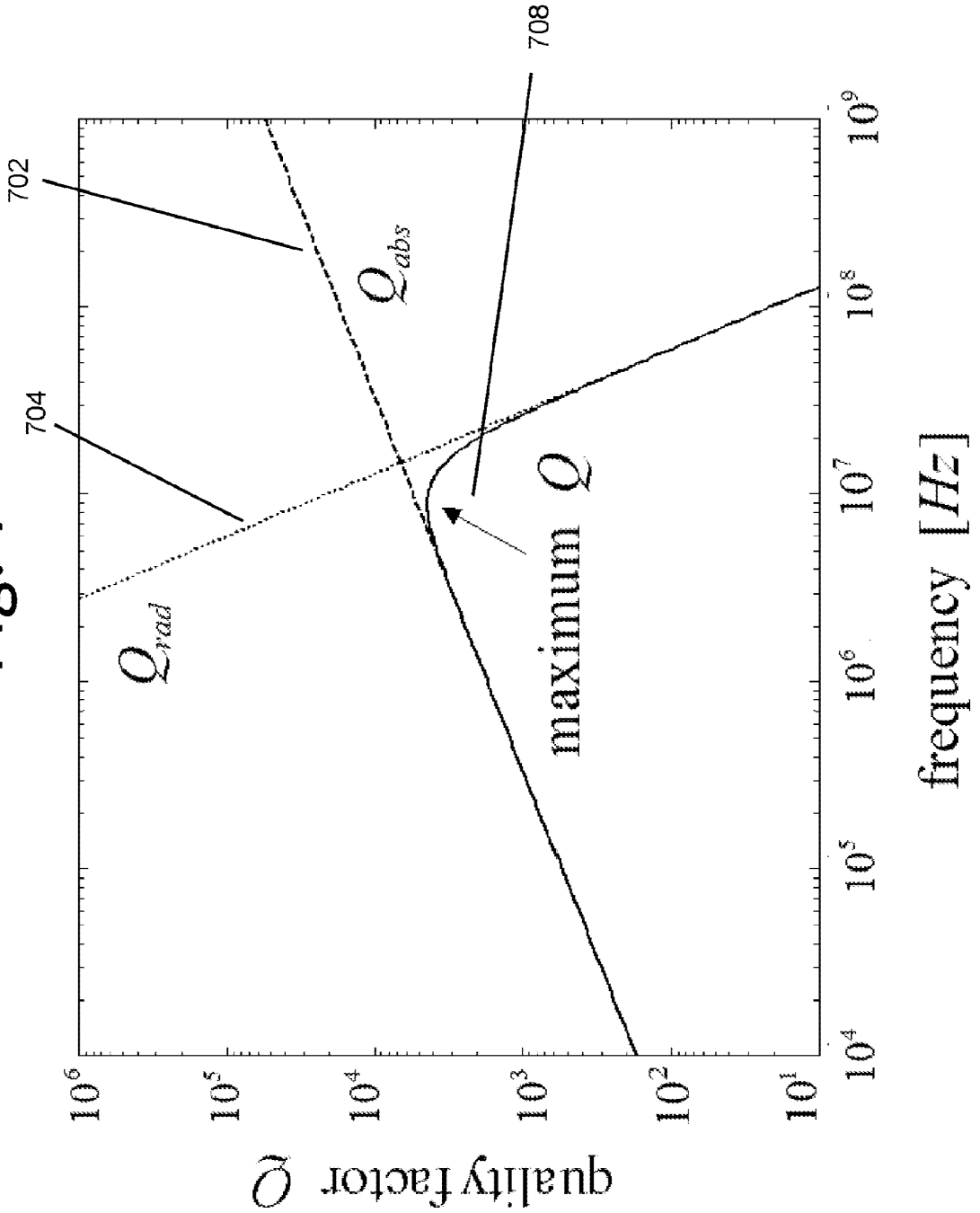
Fig. 6



SUBSTITUTE SHEET (RULE 26)

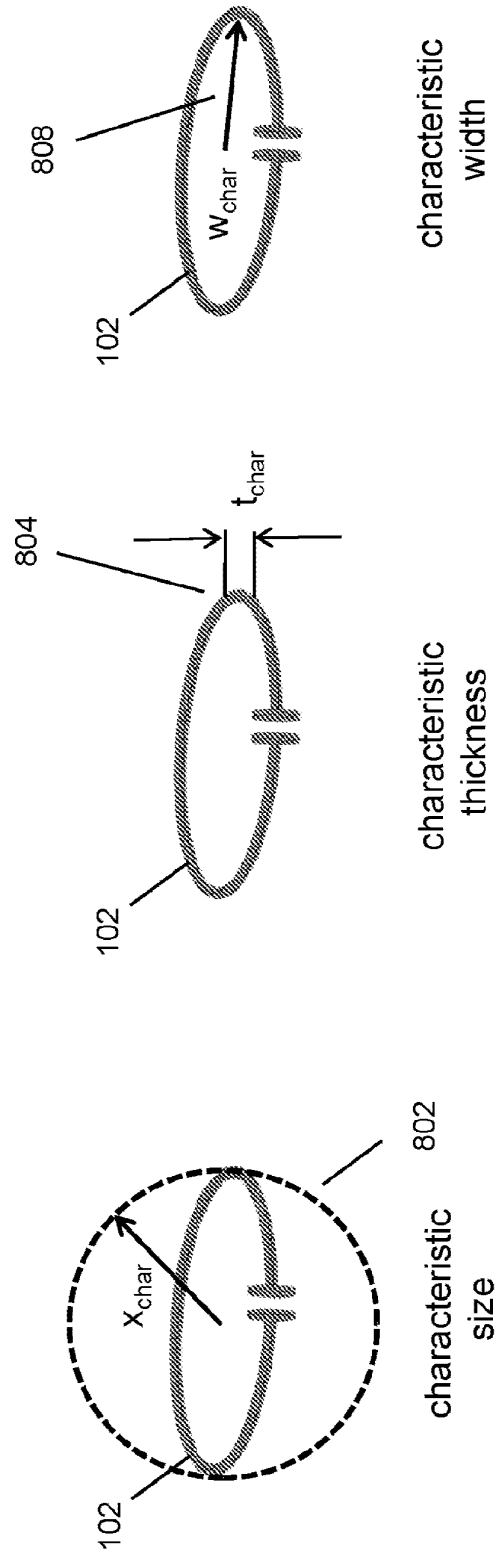


Fig. 7



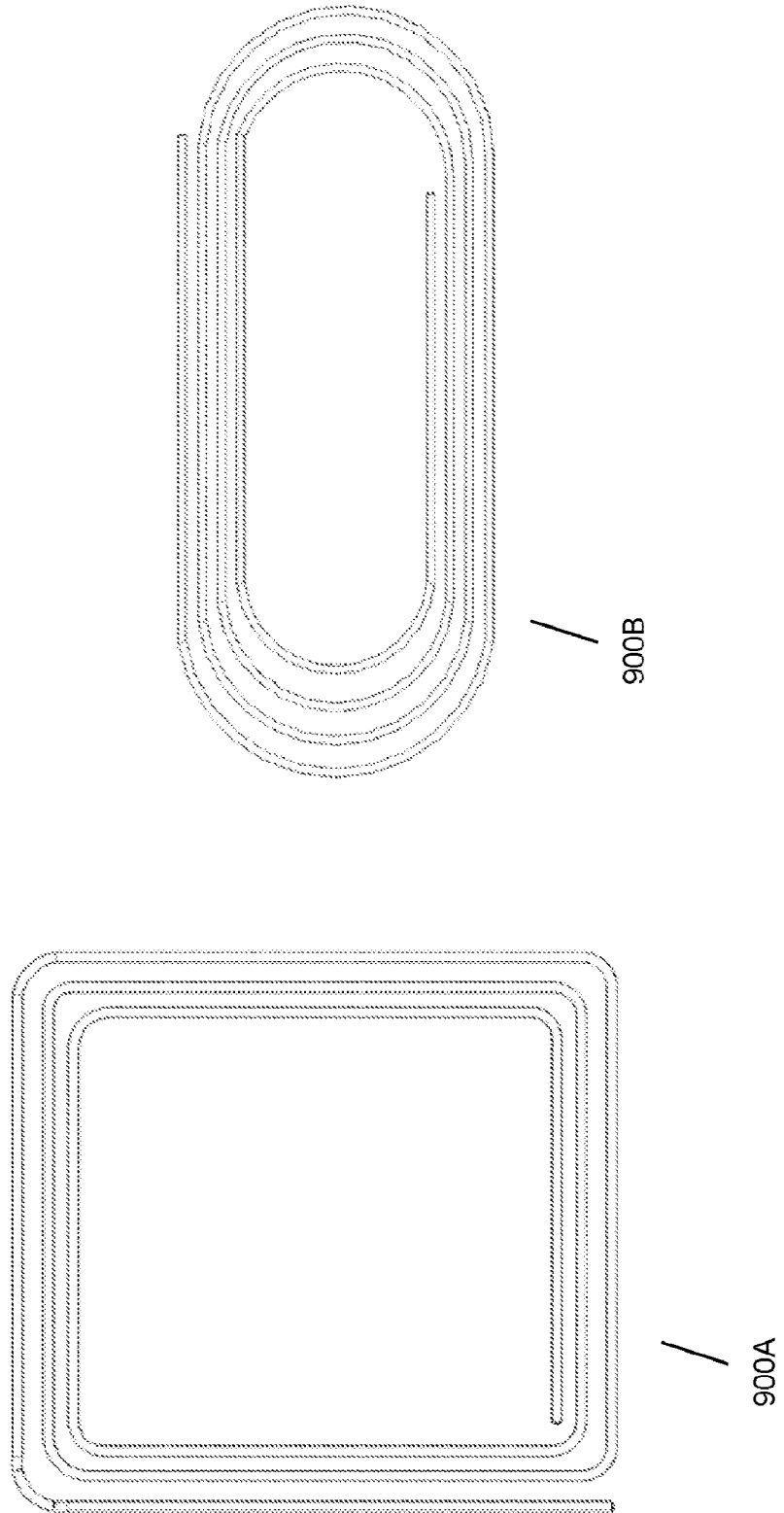
SUBSTITUTE SHEET (RULE 26)

Fig. 8



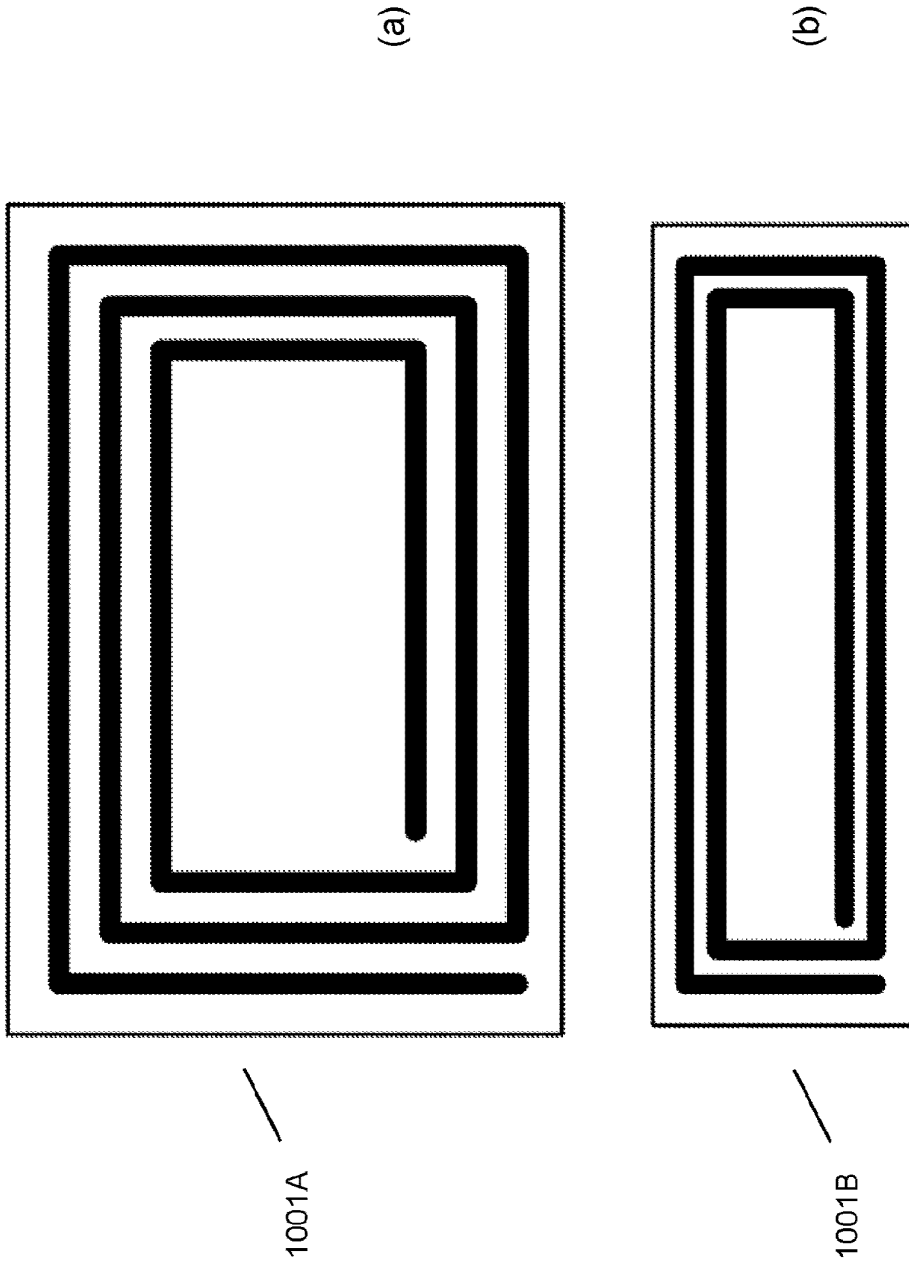
SUBSTITUTE SHEET (RULE 26)

Fig. 9



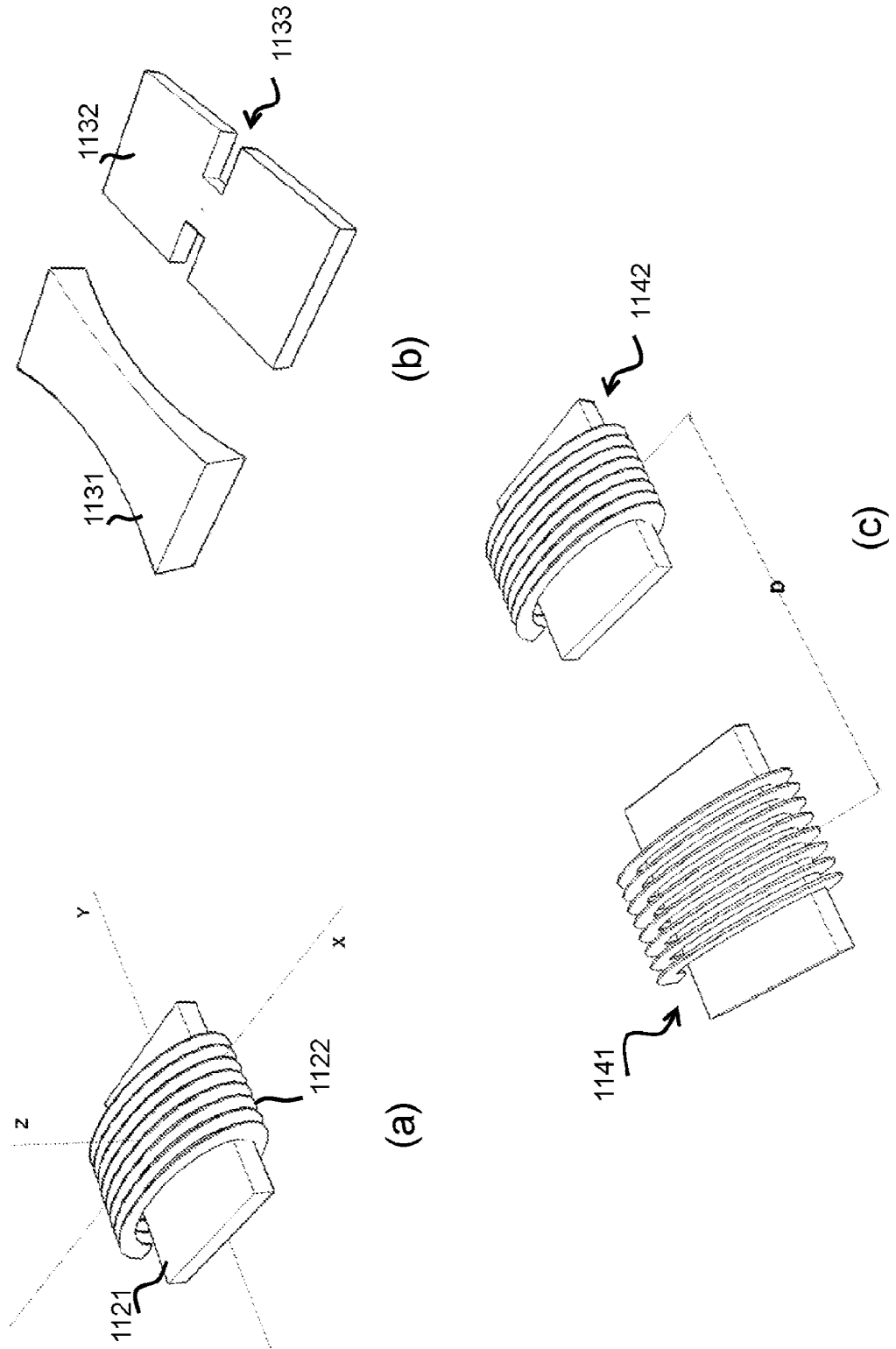
**SUBSTITUTE SHEET (RULE 26)**

Fig. 10



SUBSTITUTE SHEET (RULE 26)

Fig. 11



SUBSTITUTE SHEET (RULE 26)

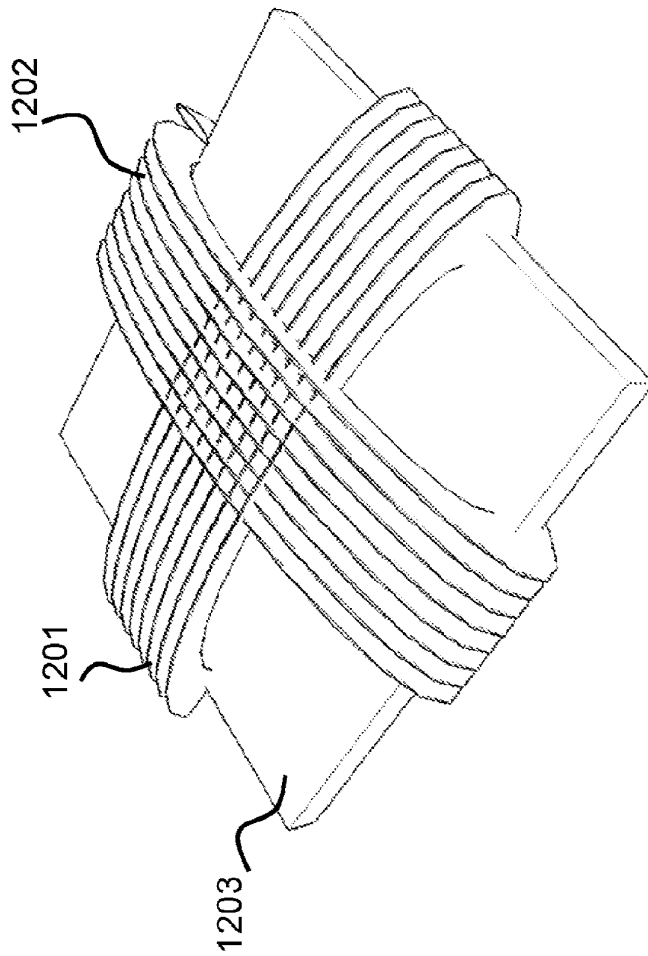


Fig. 12

SUBSTITUTE SHEET (RULE 26)

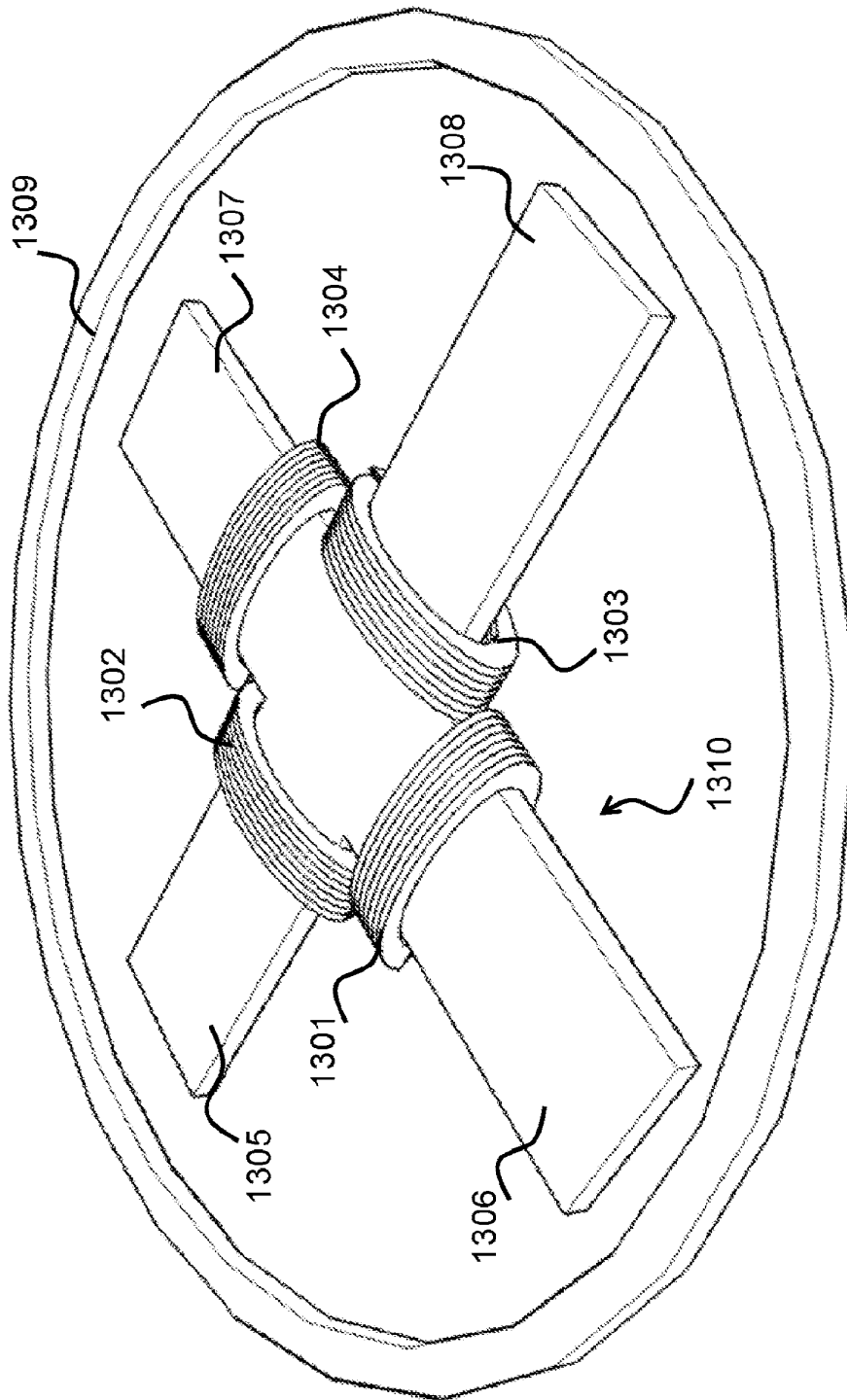


Fig. 13

SUBSTITUTE SHEET (RULE 26)

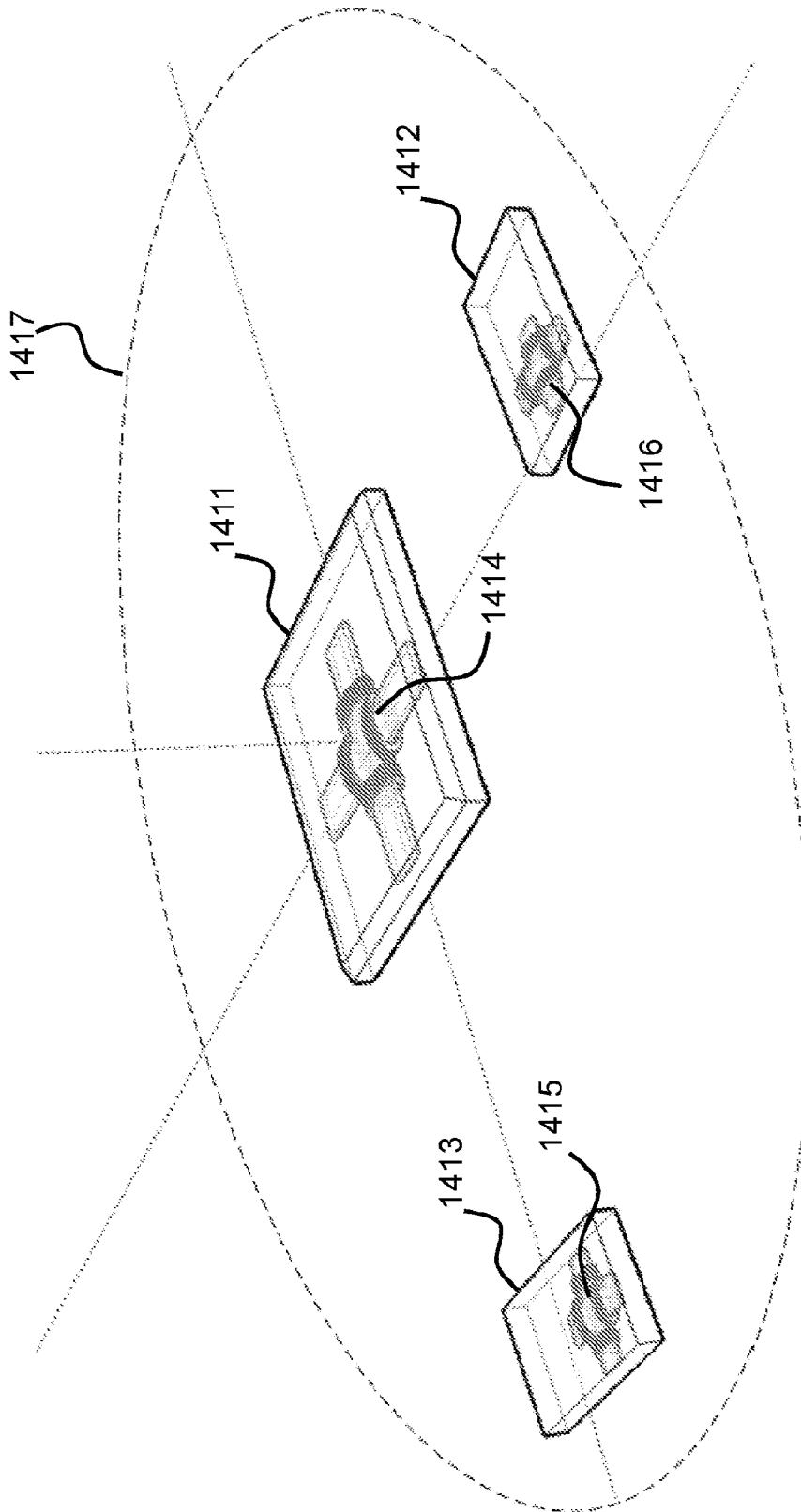


Fig. 14

SUBSTITUTE SHEET (RULE 26)



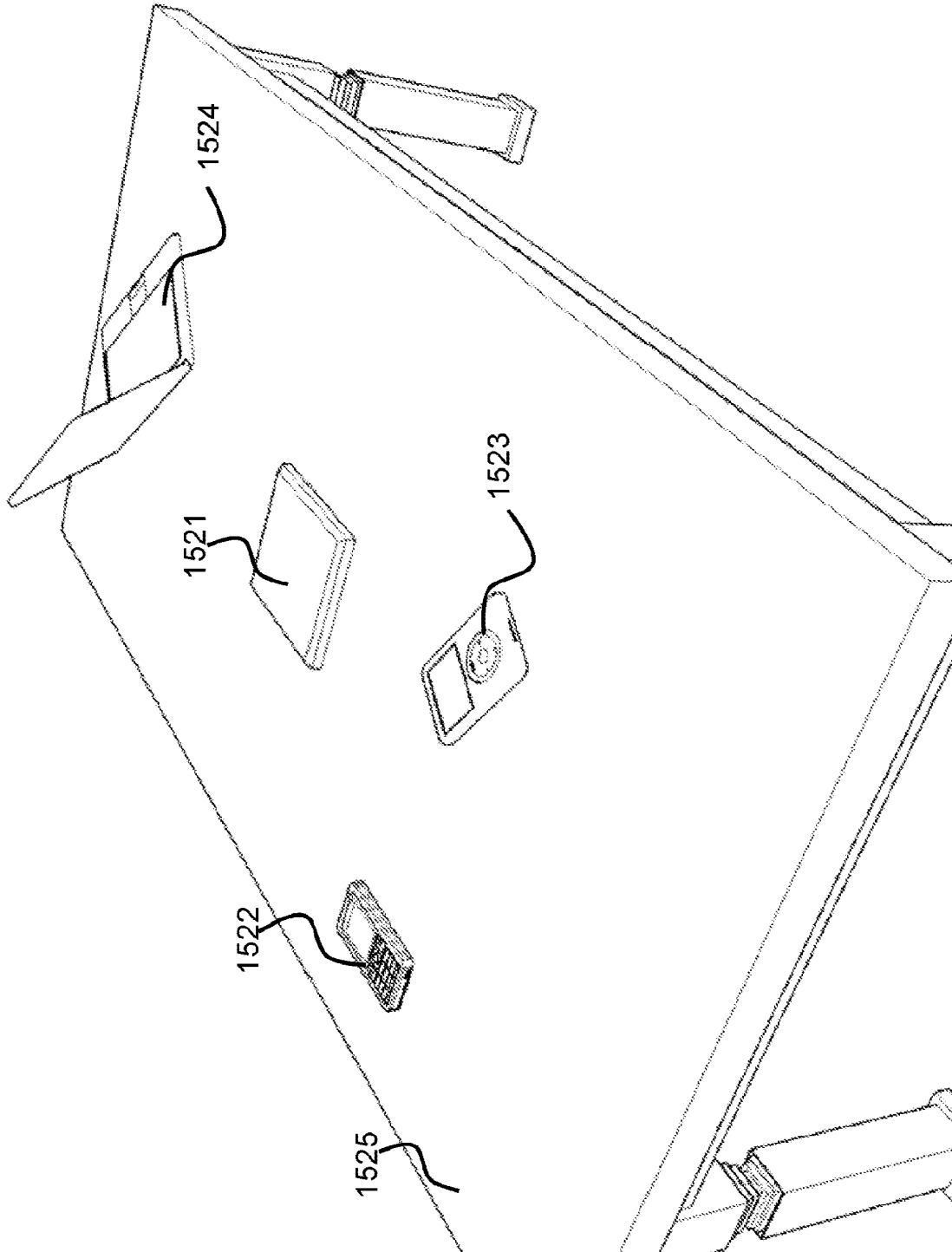
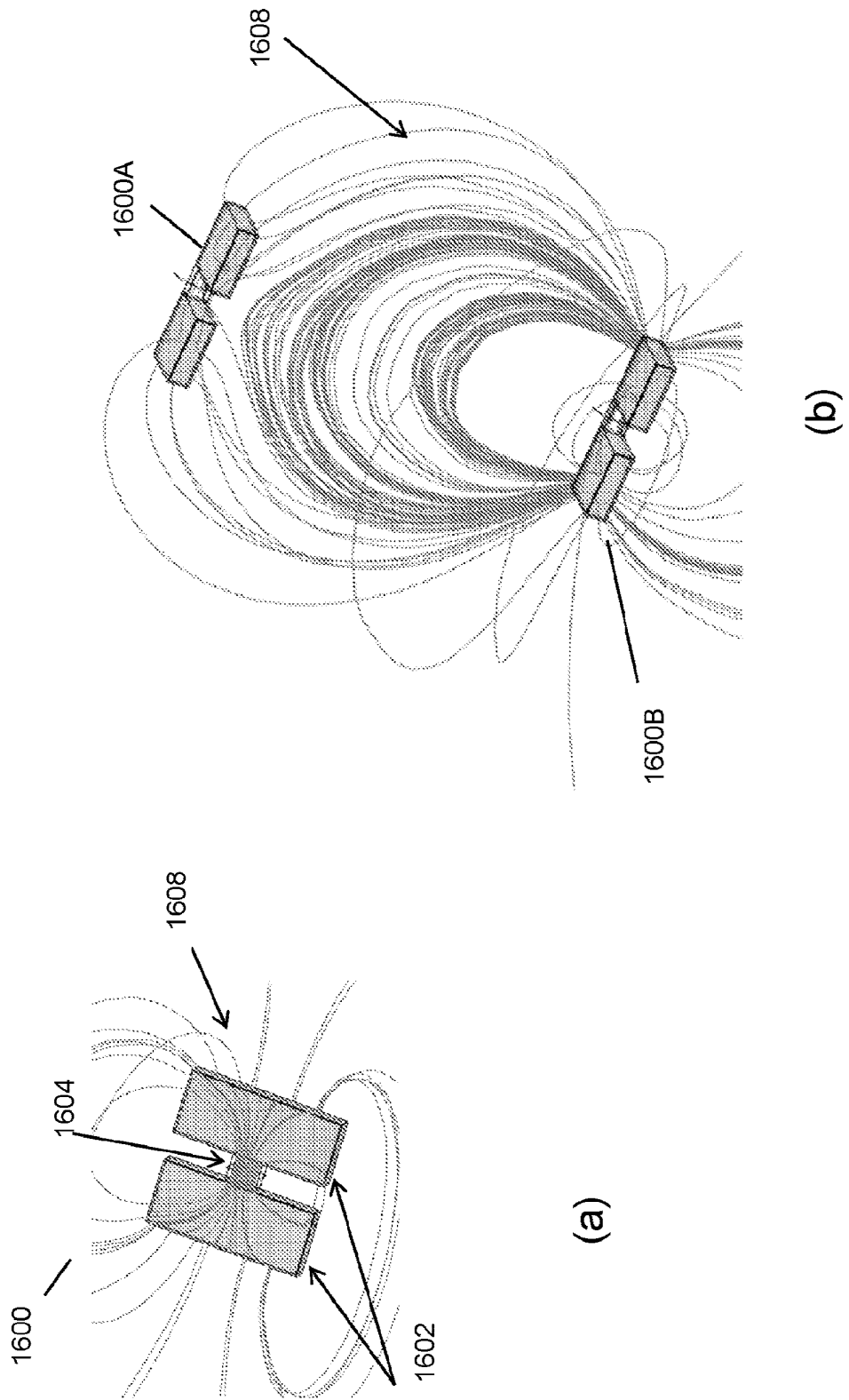


Fig. 15

SUBSTITUTE SHEET (RULE 26)

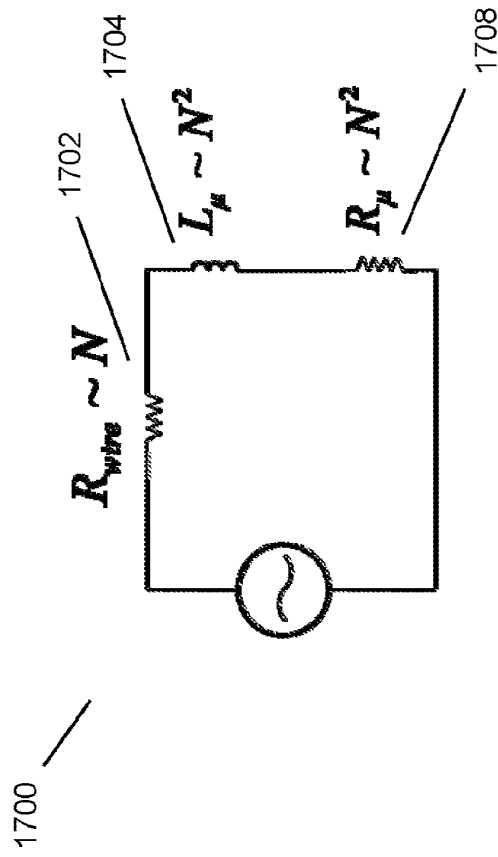
16/51

Fig. 16



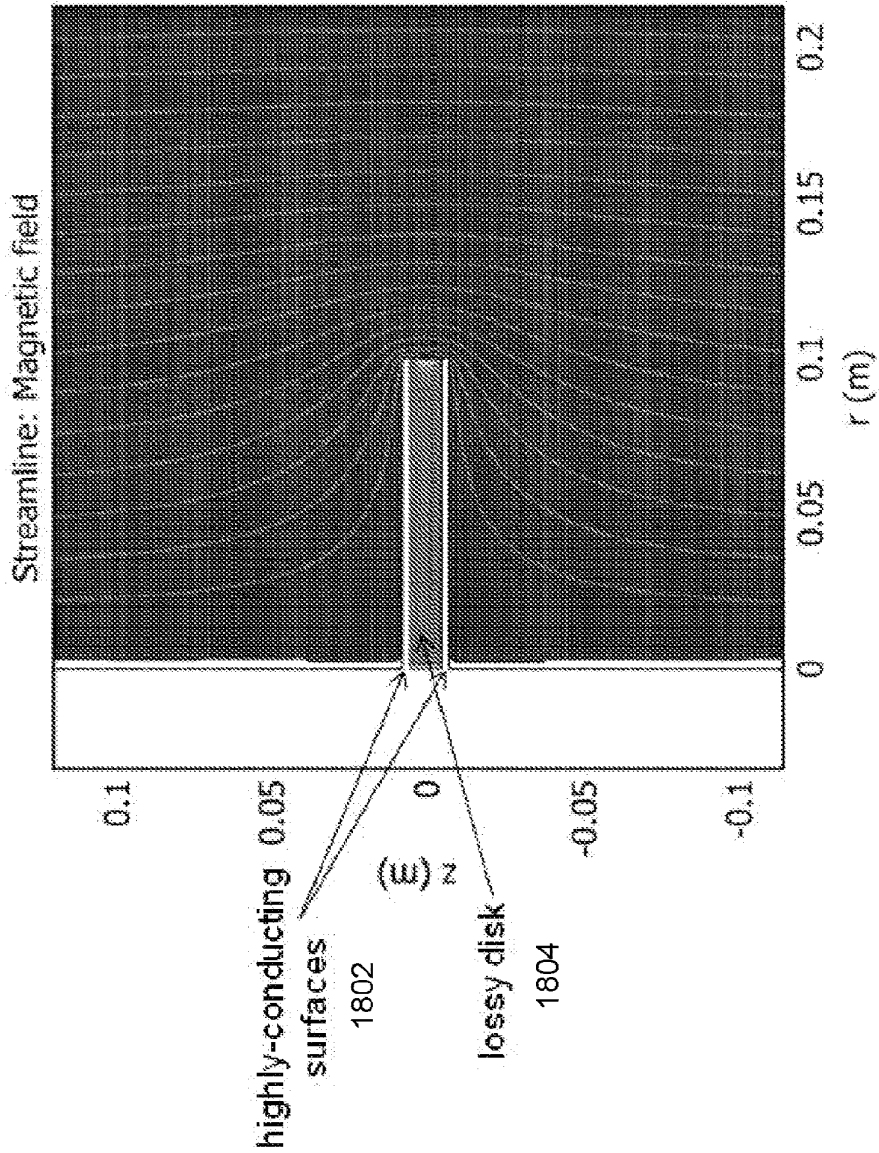
SUBSTITUTE SHEET (RULE 26)

Fig. 17



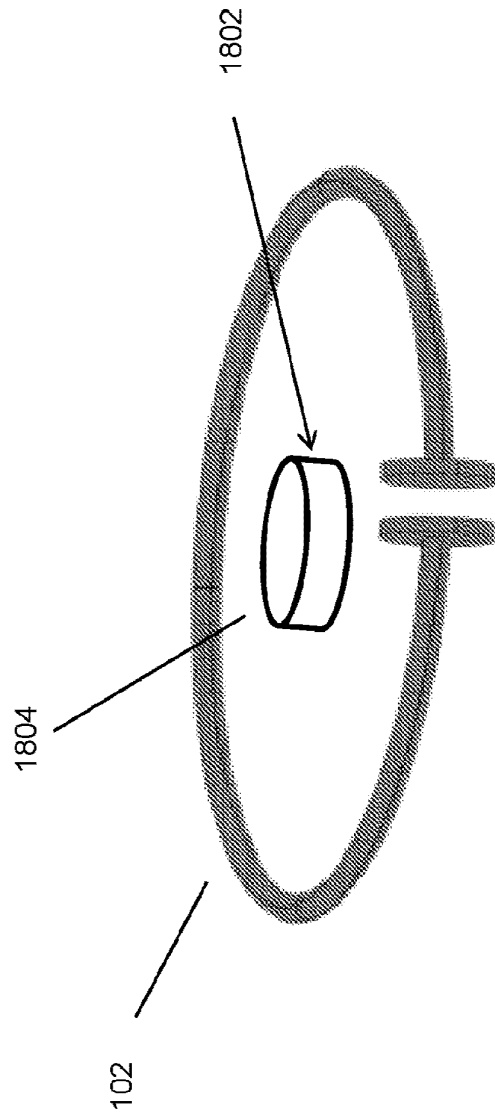
SUBSTITUTE SHEET (RULE 26)

Fig. 18



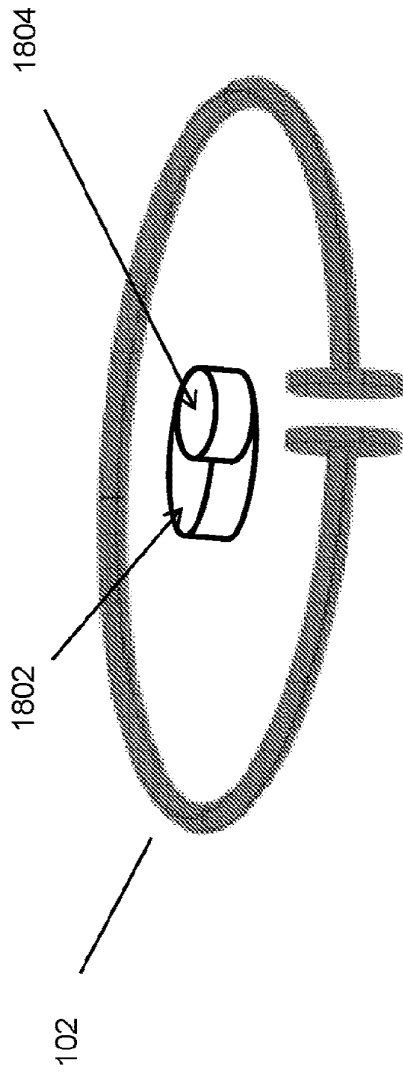
SUBSTITUTE SHEET (RULE 26)

Fig. 19



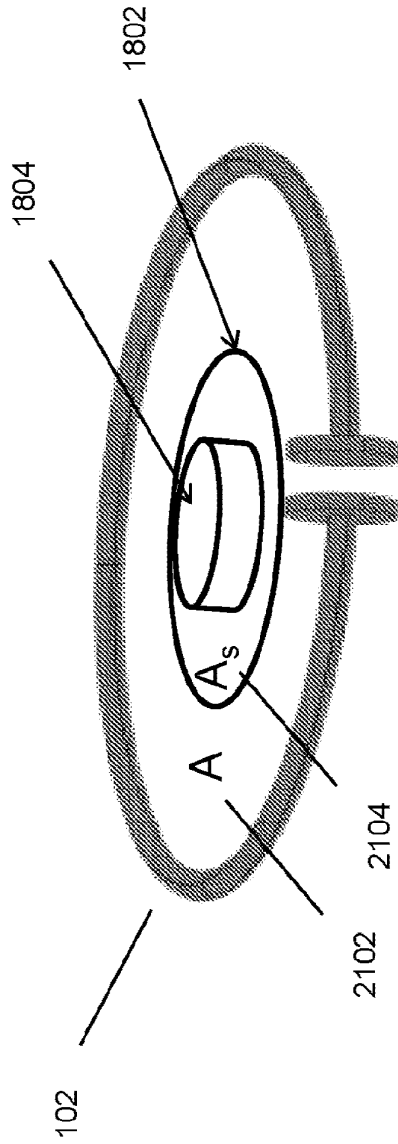
SUBSTITUTE SHEET (RULE 26)

Fig. 20



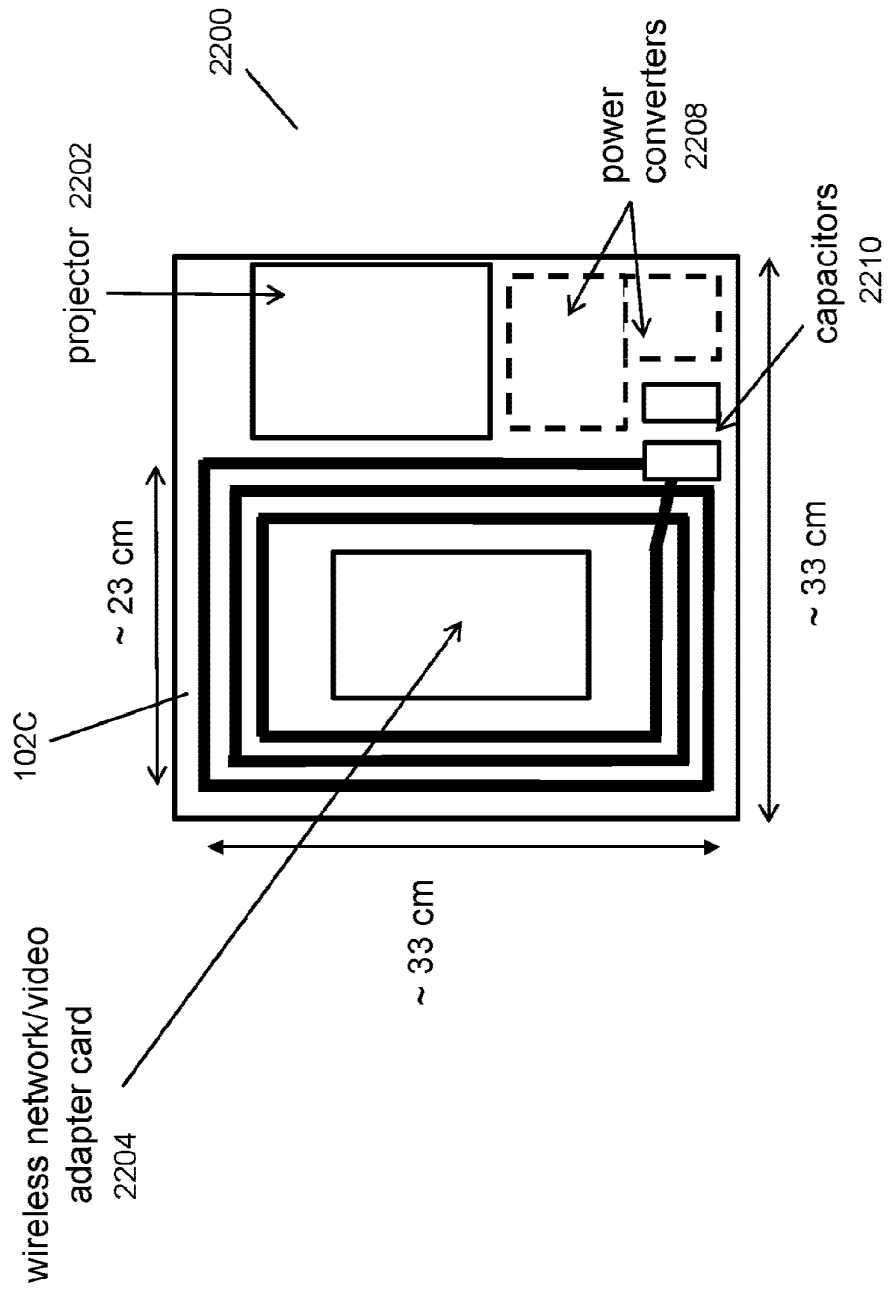
SUBSTITUTE SHEET (RULE 26)

Fig. 21



SUBSTITUTE SHEET (RULE 26)

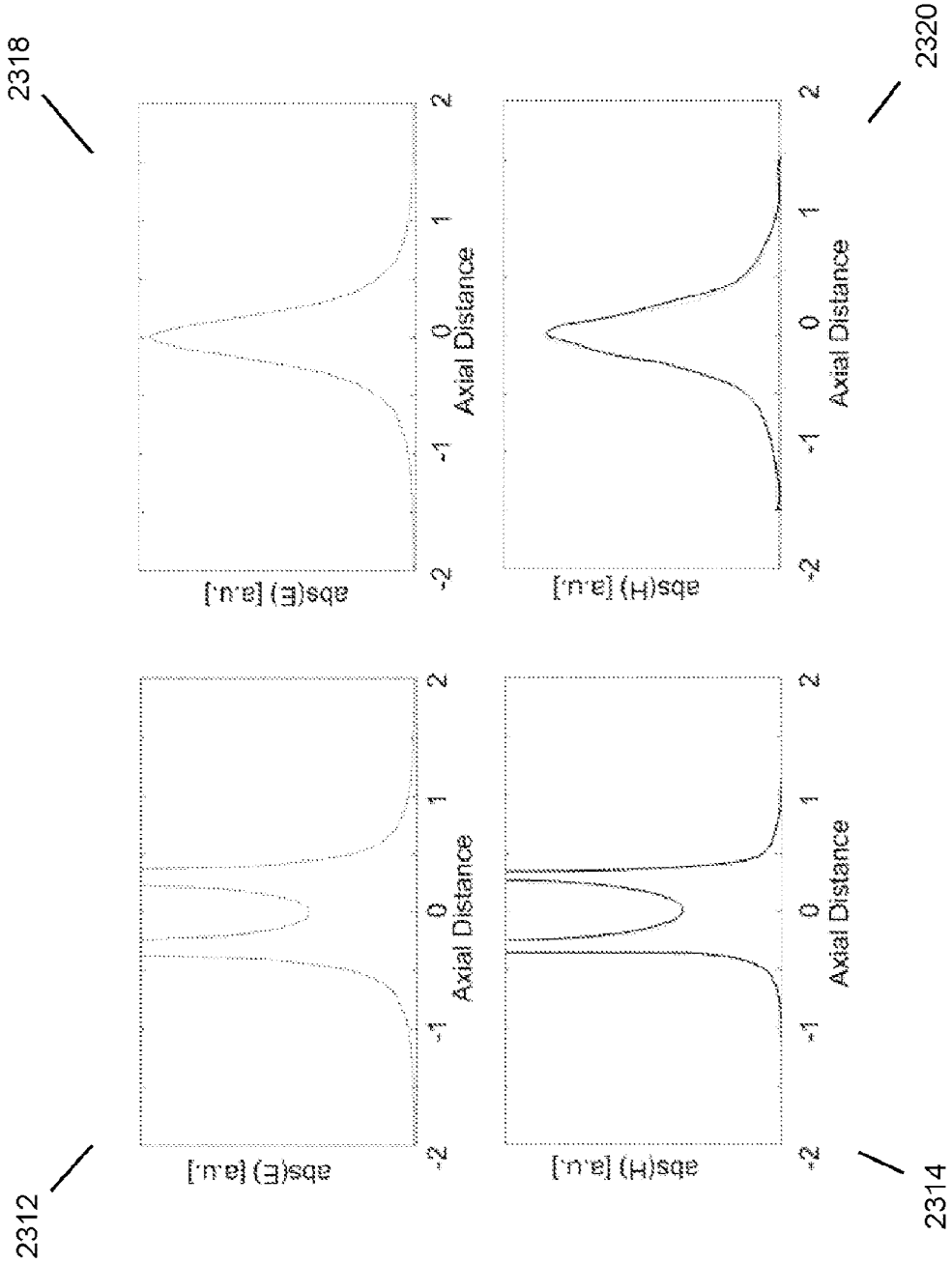
Fig. 22



SUBSTITUTE SHEET (RULE 26)

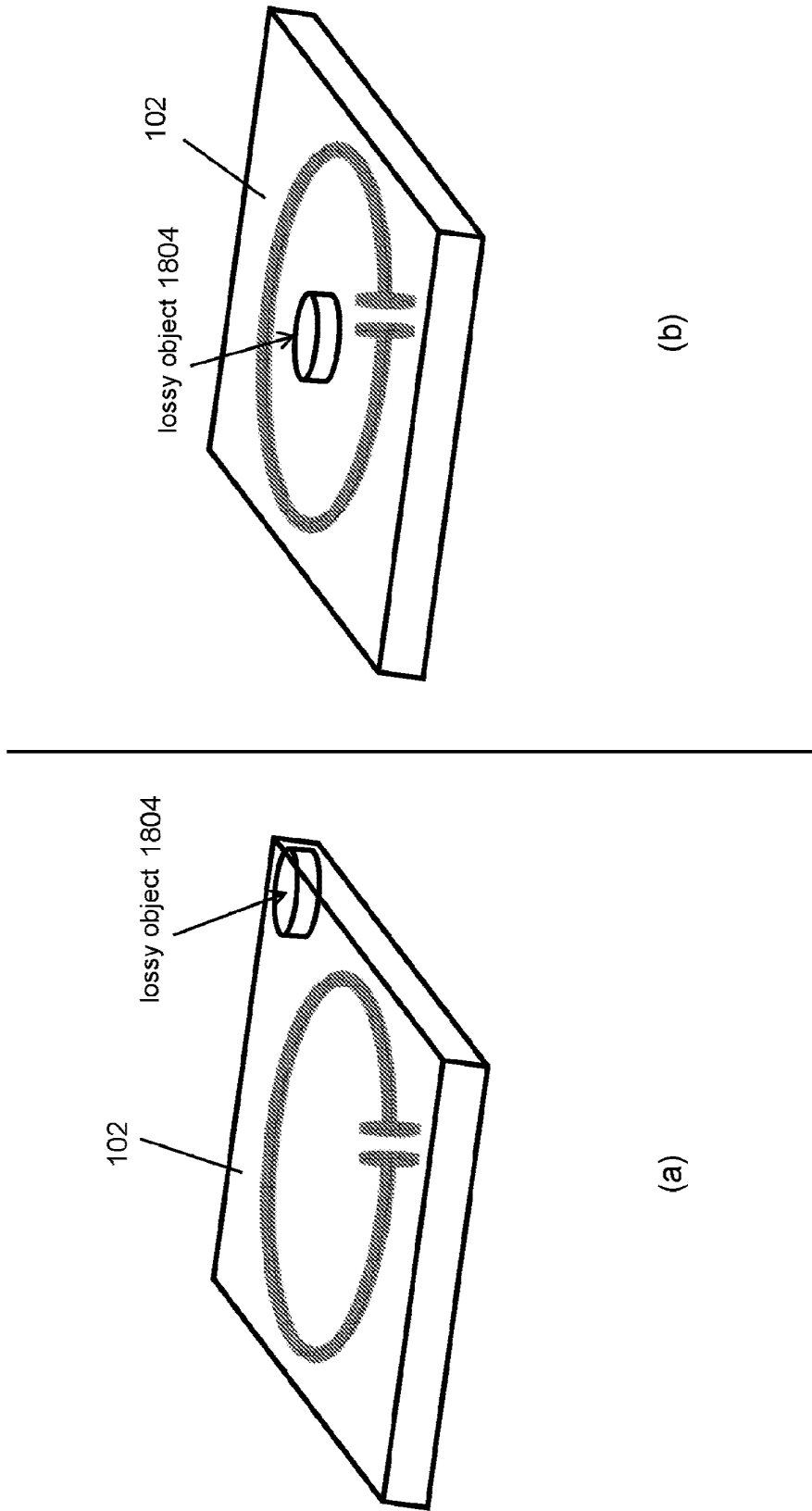


Fig. 23



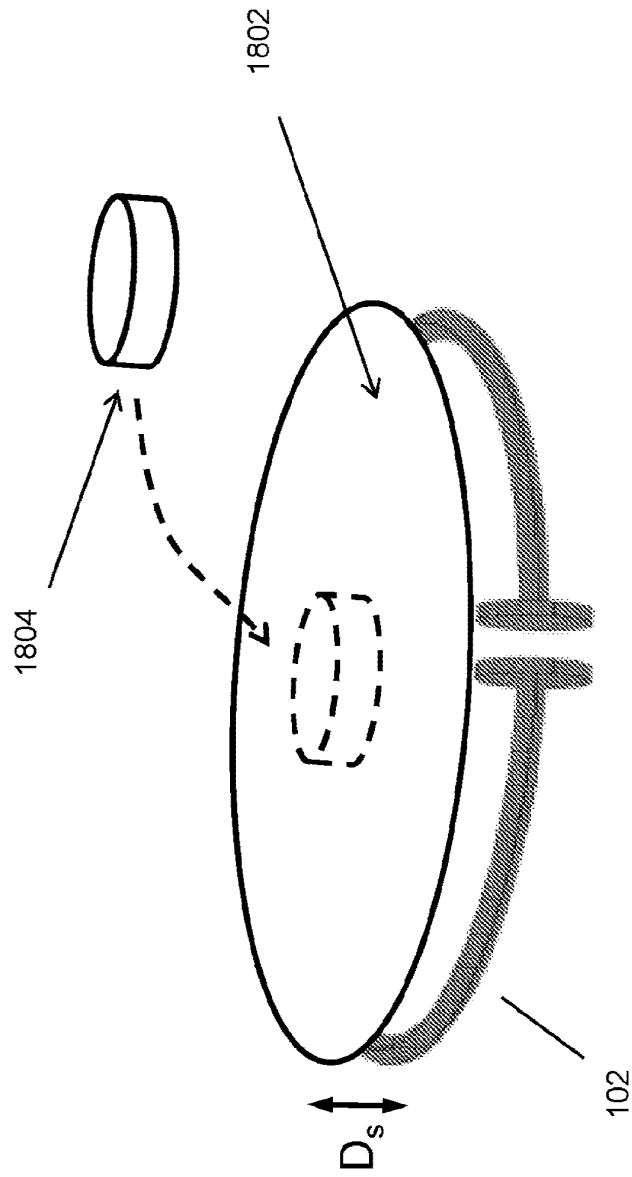
SUBSTITUTE SHEET (RULE 26)

Fig. 24



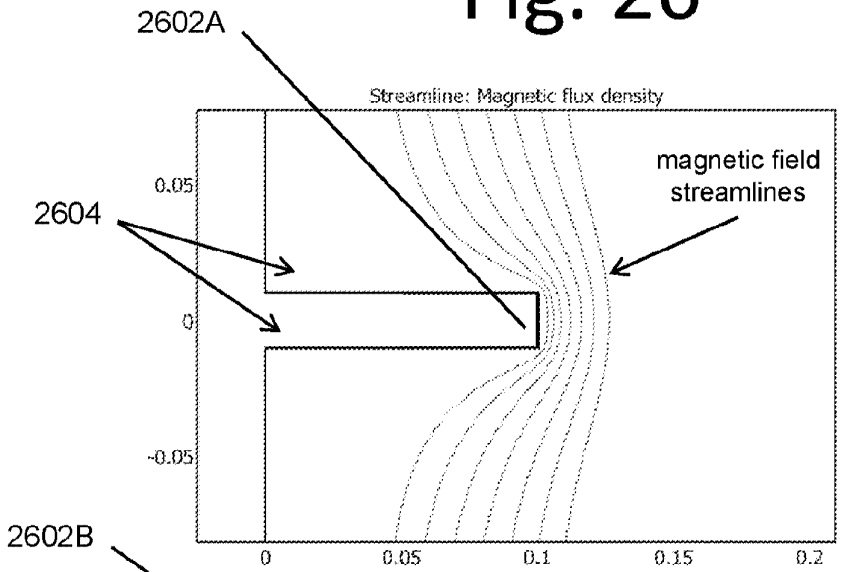
SUBSTITUTE SHEET (RULE 26)

Fig. 25

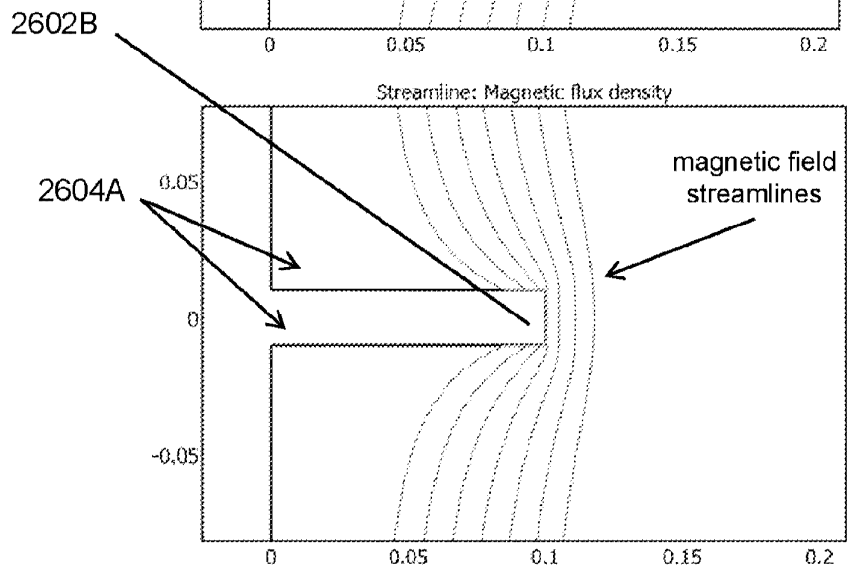


SUBSTITUTE SHEET (RULE 26)

# Fig. 26



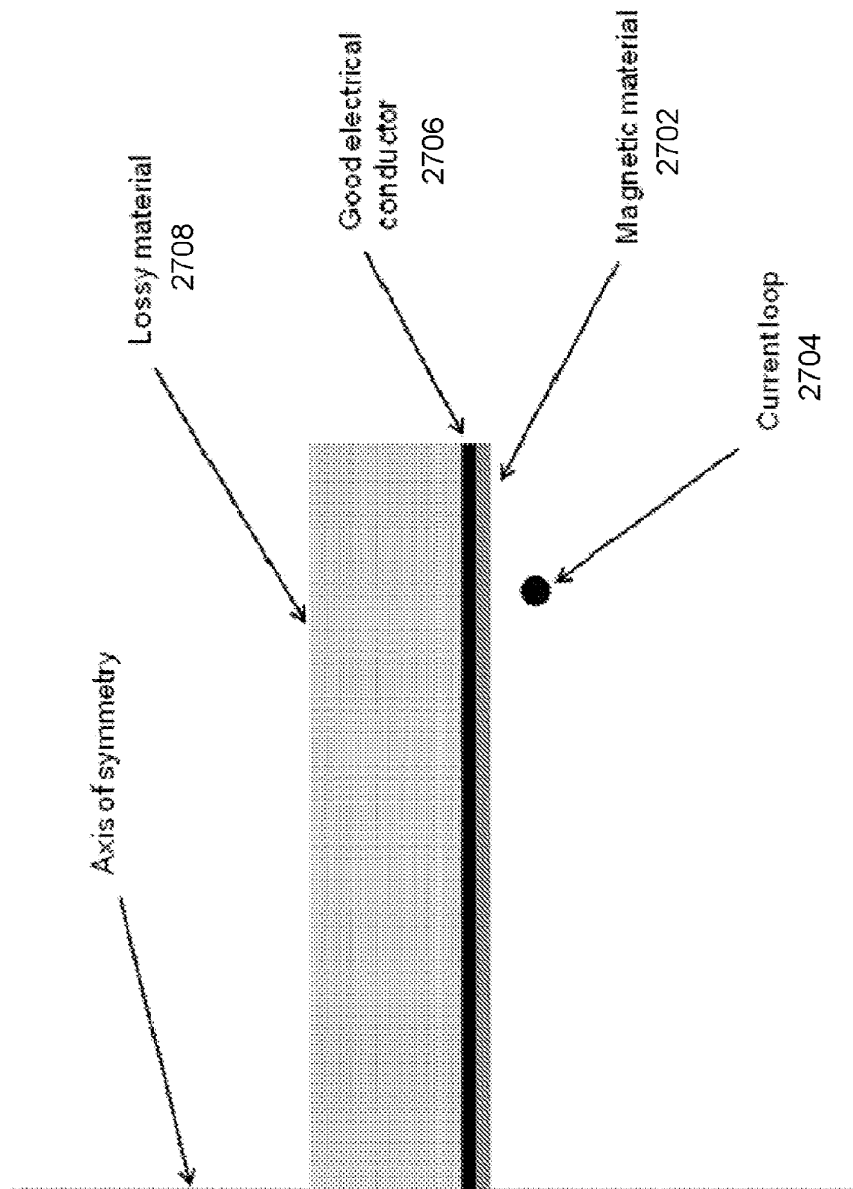
(a)



(b)

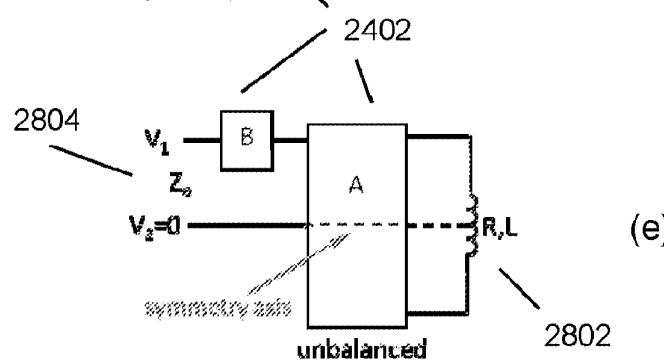
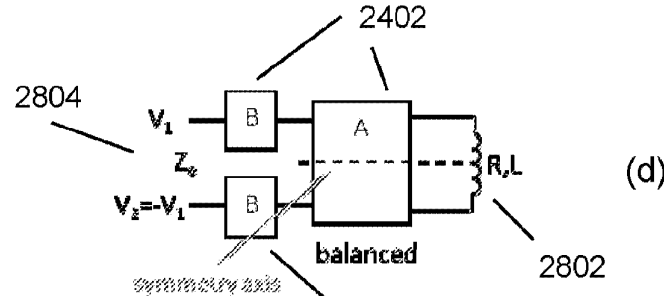
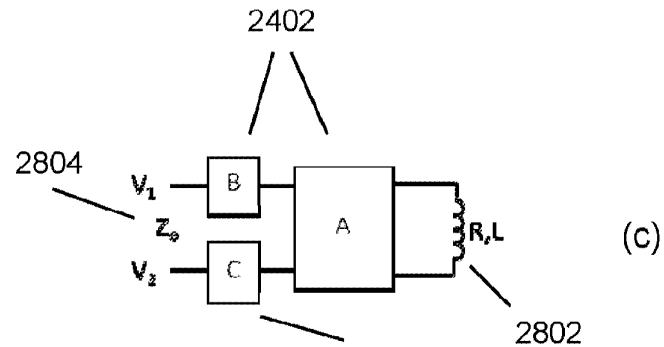
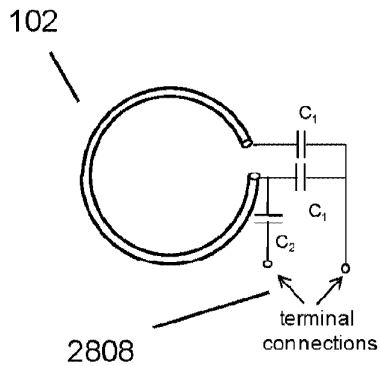
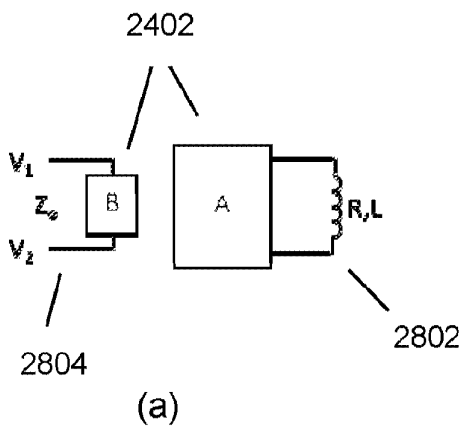
SUBSTITUTE SHEET (RULE 26)

Fig. 27



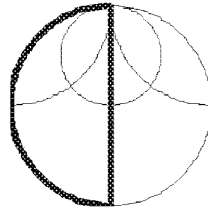
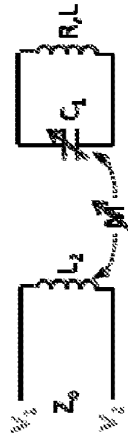
SUBSTITUTE SHEET (RULE 26)

# Fig. 28



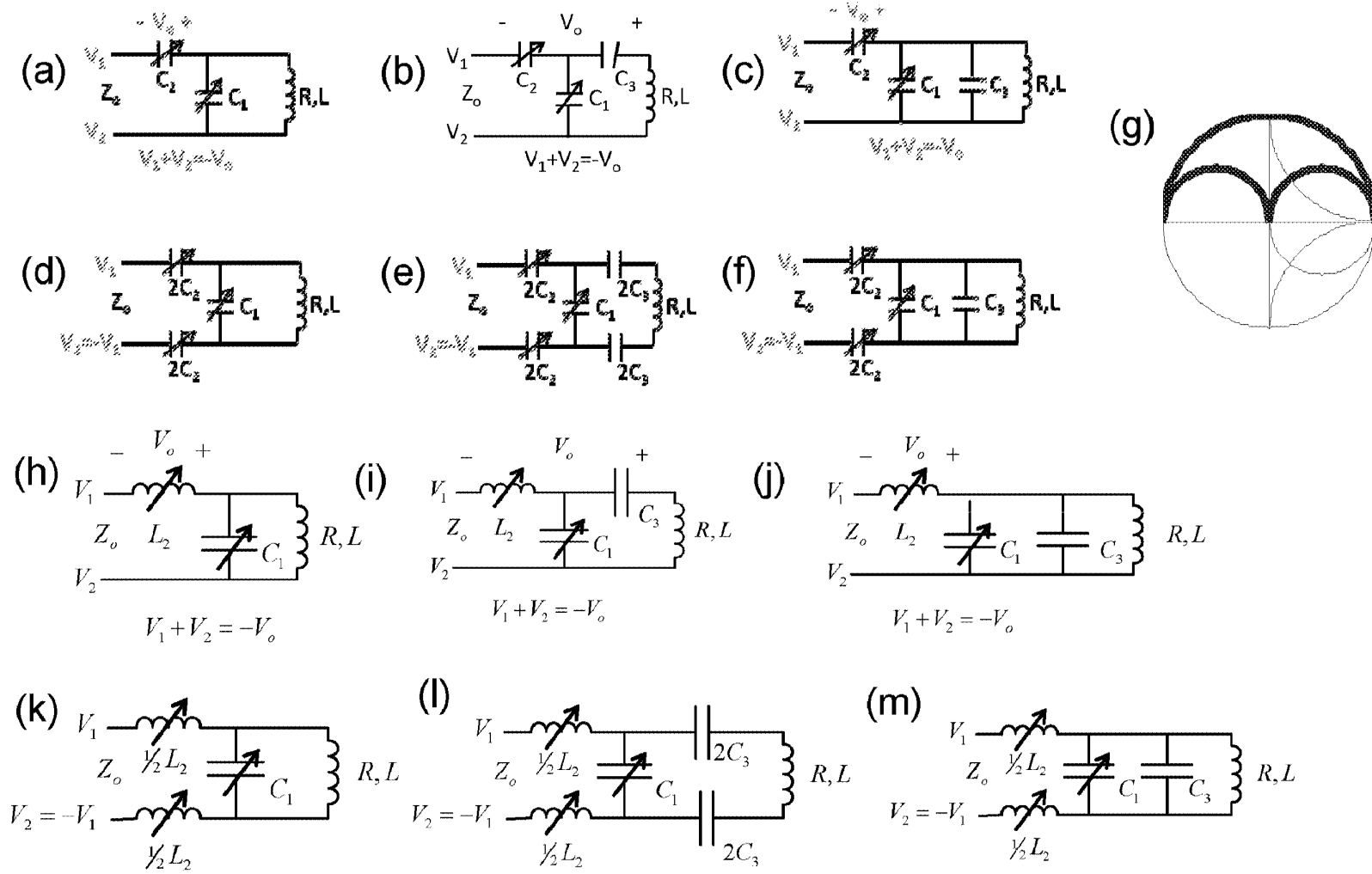
SUBSTITUTE SHEET (RULE 26)

Fig. 29



SUBSTITUTE SHEET (RULE 26)

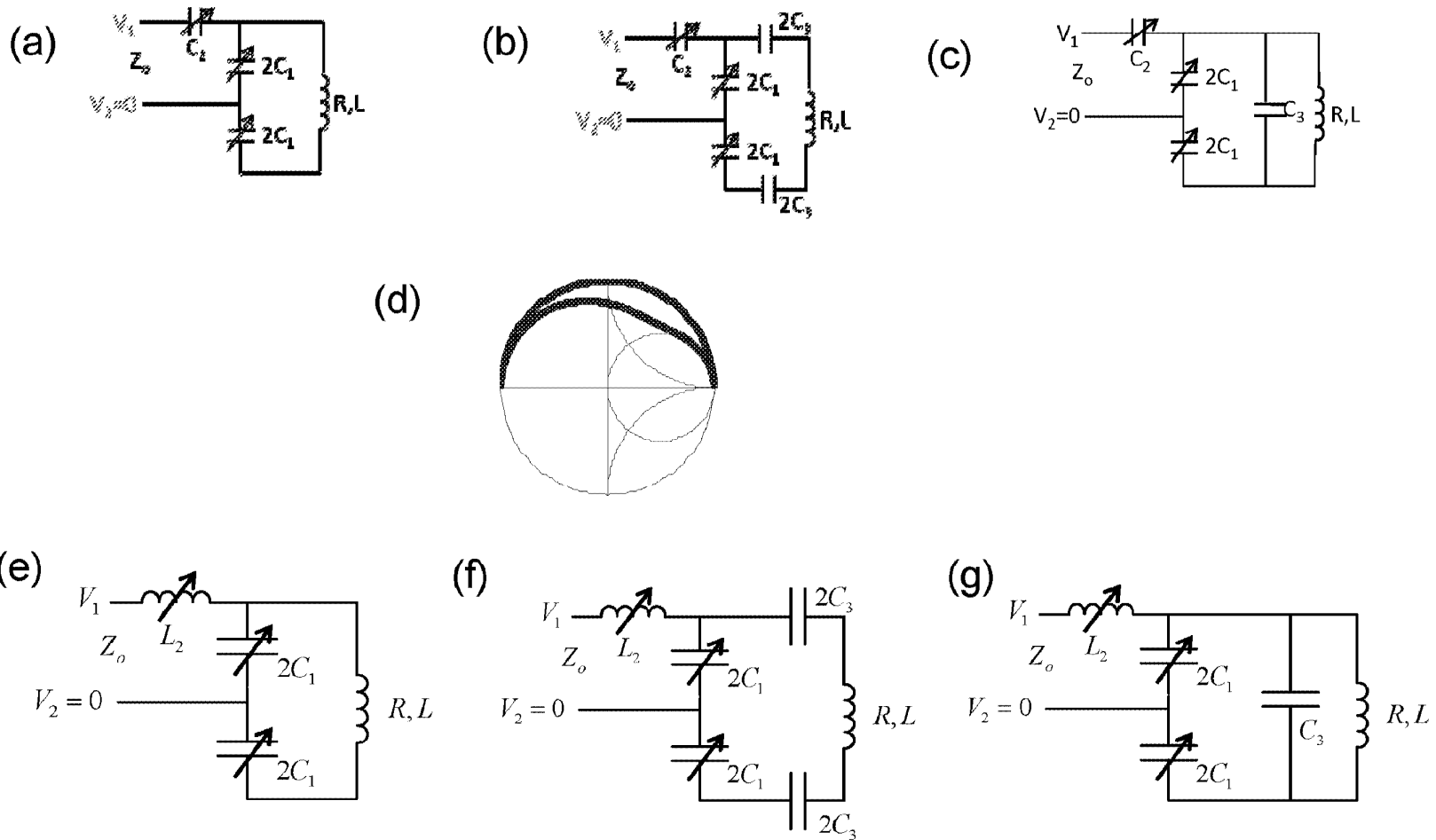
Fig. 30



SUBSTITUTE SHEET (RULE 26)

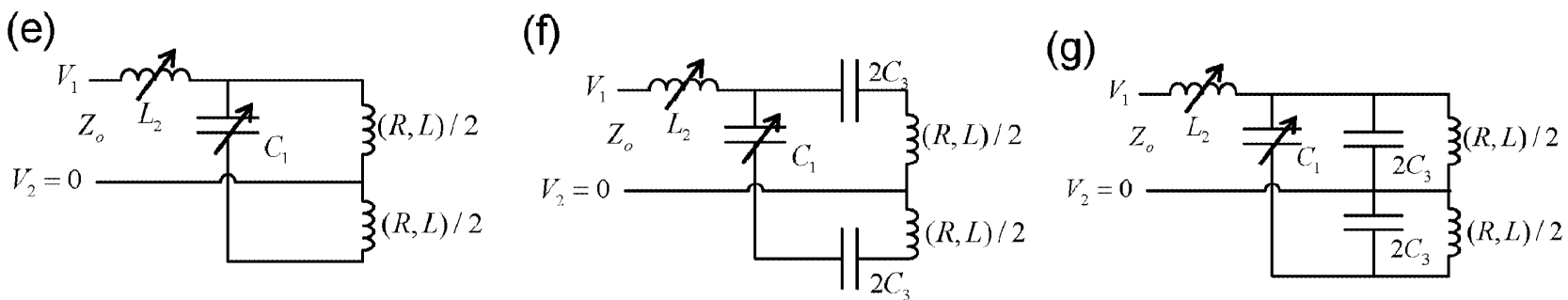
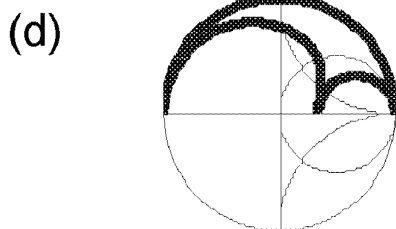
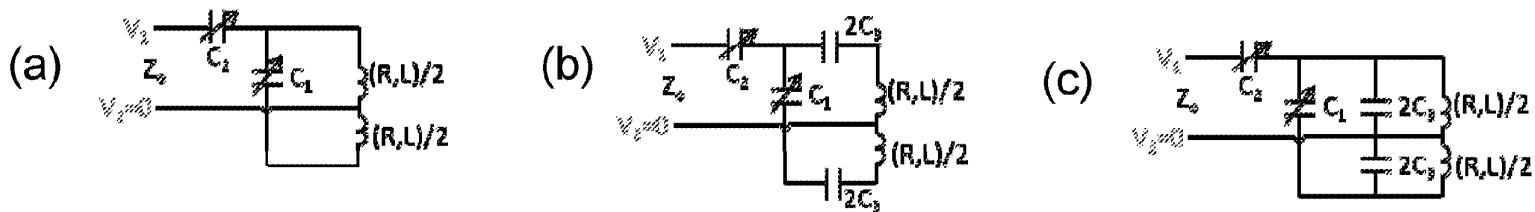


# Fig. 31



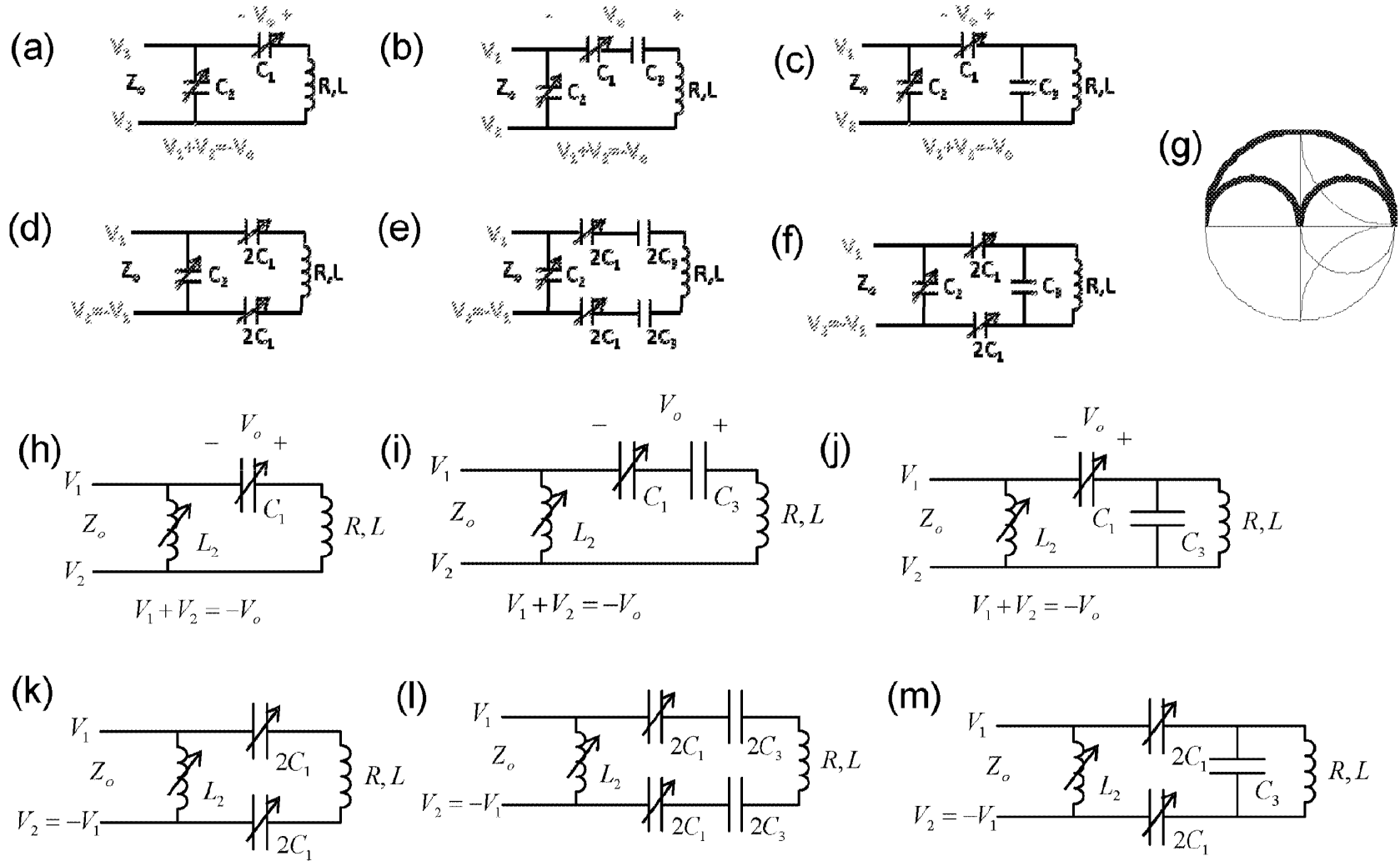
SUBSTITUTE SHEET (RULE 26)

Fig. 32



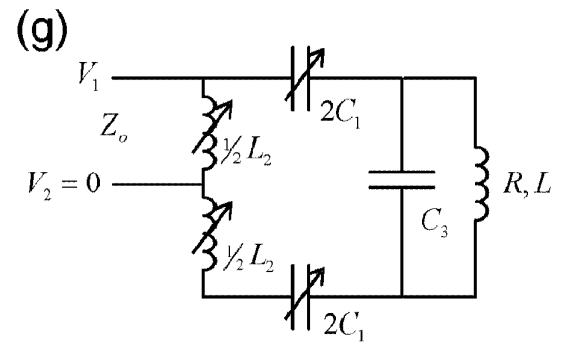
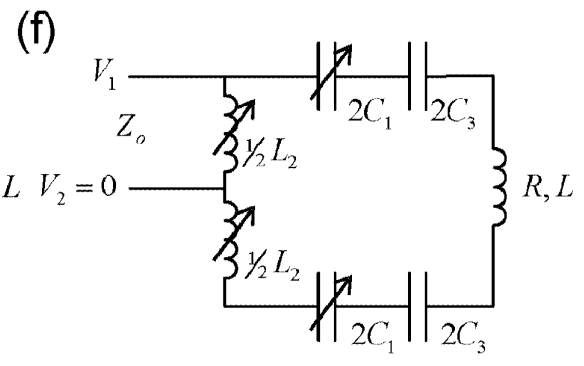
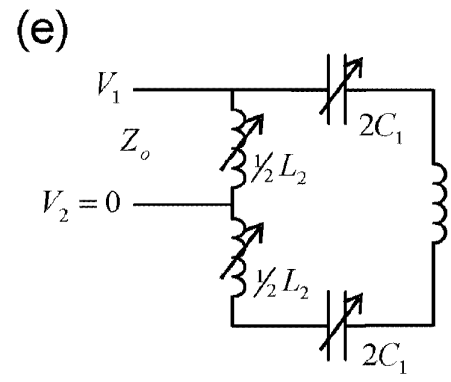
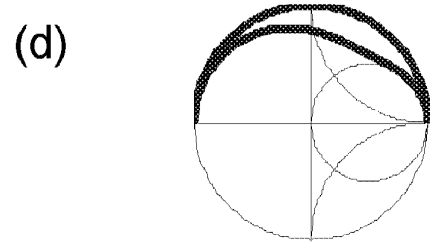
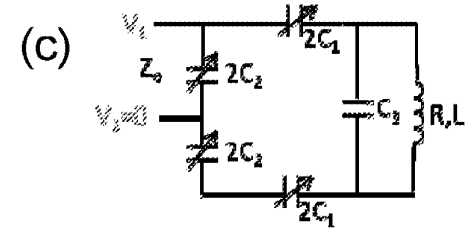
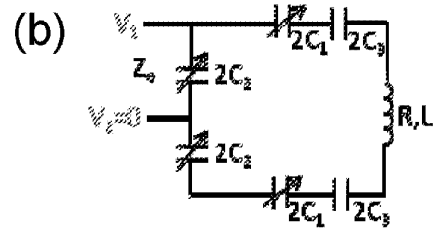
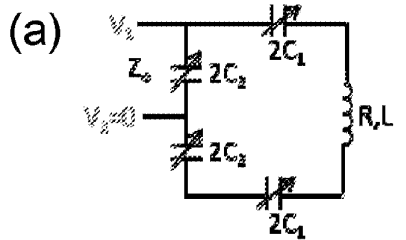
SUBSTITUTE SHEET (RULE 26)

# Fig. 33



SUBSTITUTE SHEET (RULE 26)

# Fig. 34



SUBSTITUTE SHEET (RULE 26)